# DESIGN AND SYNTHESIS OF π-STACKED CONJUGATED OLIGOMERS AND POLYMERS

A Dissertation
Presented to
The Academic Faculty

by

Subodh P. Jagtap

In Partial Fulfillment
of the Requirements for the Degree
Doctor of Philosophy in the
School of Chemistry and Biochemistry

Georgia Institute of Technology

May 2012

**DESIGN AND SYNTHESIS OF π-STACKED CONJUGATED OLIGOMERS AND POLYMERS**

Approved by:

Dr. David Collard, Advisor
School of Chemistry
and Biochemistry
*Georgia Institute of Technology*

Dr. Stefan France
School of Chemistry
and Biochemistry
*Georgia Institute of Technology*

Dr. Laren Tolbert
School of Chemistry
and Biochemistry
*Georgia Institute of Technology*

Dr. Haskell Beckham
Material Science
and Engineering
*Georgia Institute of Technology*

Dr. Mohan Srinivasarao
Material Science and Engineering
*Georgia Institute of Technology*

Date Approved: May 2012

*To my Grandparents, my Mom (Dr. Anjali), my Dad (Dr. Prakash) and my Wife (Dr. Sayali)*

## ACKNOWLEDGEMENTS

I am very grateful to my advisor Dr. David M. Collard, for his guidance and immense support throughout my research. I really appreciate his dedication towards science. I would like to thank my committee members Drs. Laren Tolbert, Mohan Srinivasarao, Haskell Beckham, and Stefan France for their support at Georgia Tech.

I would like to thank persons who have helped support my research including Dr. Glen Brizius (Post-Doc), Dr. Leslie Gelbaum (NMR lab), Mr. David Bostwick (mass spec lab), Dr. Kenneth Hardcastle (X-ray crystal measurements), Dr. Vladimir Tsukruk (UV-Vis and Fluorescence spectroscopy), and Dr Sukrit Mukhopadhyay, Dr. Veaceslav Coropceanu Veaceslav, Dr Jean-Luc Brédas (Computational work).

I would also like to issue thanks to former and current members of Team Collard for just being such great people to work around, including: Dr. David Noga, Dr. Jenny Raynor, Dr. Rakesh Nambiar, Dr. Cianan Russell, Dr. Kathy Woody, Guillermo Alas, Stephen Zappitello, Katelyn Thomas, and Alma Castaneda.

I would also like to thank all my friends especially Amalraj Jayapalan, Rishiraj Bheda, Daulatrao Mahadik, Vishal Patil and Dadasaheb Patil for their continued friendship, support and laughter and help me remember that life exists outside of lab.

I would like to give a special thanks to my family for their endless support in graduate school: my parents, sister, aunts, grandparents for their encouragement and love throughout my education and career. I would like to thank my wife, Sayali, for her love and support especially when I felt overwhelmed in my studies.

Thank you everyone for their wishes.

## TABLE OF CONTENTS

## LIST OF TABLES

## LIST OF FIGURES

## LIST OF SYMBOLS AND ABBREVIATION

| | |
|---|---|
| δ | Chemical shift |
| λ | Wavelength |
| ε | Molar Absorptivity |
| *J* | Coupling constant |
| Hz | Hertz |
| ppm | Parts per million |
| d | Doublet |
| dd | Doublet of doublets |
| t | Triplet |
| s | Singlet |
| b s | Broad singlet |
| m.p. | Melting point |
| RT | Room temperature |
| DPV | Differential pulse voltammometry |
| IR | Infrared |
| NMR | Nuclear magnetic resonance |
| ESR | Electron spin resonance |
| OLED | Organic light emitting diode |
| OFET | Organic field effect transistor |
| OPC | Organic photovoltaic cell |
| DMF | Dimethyl formamide |

| | |
|---|---|
| THF | Tetrahydrofuran |
| NBS | N-Bromosuccinimide |
| HOMO | Highest occupied molecular orbital |
| LUMO | Lowest unoccupied molecular orbital |
| HRMS | High resolution mass spectrometry |
| *p*-TSA | Para-toluene sulfonic acid |
| *pg* | Pseudo-geminal |
| *po* | Pseudo-ortho |
| *pp* | Pseudo-para |
| Cp | Cyclophane |
| PE | Phenylene ethynylene |
| PV | Phenylene vinylene |

## SUMMARY

Conjugated oligomers and polymers are very attractive materials for organic electronic devices by virtue of their semiconducting properties. The transport of charge carriers along π-conjugated chains in one dimension does not provide a complete understanding of the semiconducting behavior of these materials. The electronic structure of conjugated organic materials depends on both the molecular structure and the three-dimensional packing of the conjugated chains with one another. To explore the effect of interchain interaction on optoelectronic properties of conjugated oligomers, we chose to explore benzo-fused bicyclo[4.4.1]undecane and pseudo-geminal [2.2]paracyclophane as convenient scaffolds to prepare oligomers that are held in a π-stacked manner. These scaffolds provide the opportunity to control the distance and orientation of conjugated segments and to study their electro-optical properties.

We have installed conjugated oligomers on the benzo-fused bicyclo[4.4.1]undecane core to prepare a series of stacked oligo(phenylene ethynylene)s and compare their spectroscopy and electrochemistry with their linear unstacked counterparts. In another approach, we explored the pseudo-geminal [2.2]paracyclophane as a scaffold to prepare the stacked oligo(phenylene vinylene)s. A combined experimental and theoretical study of well-defined stacked oligomers provided very useful insights into the effect of π-π interactions on the electronic structure of closely packed conjugated chains. The significantly large Stokes shifts associated with our stacked compounds are due to the formation of an extended excimer-like state arising from stacking of entire length of the conjugated chains.

To extend the utility of pseudo-geminal (*pg*) cyclophane as a scaffold, we chose to explore the use of (*pg*) cyclophanes bearing alkyne, alkene and halogen substituents as monomers in the preparation of π-stacked conjugated polymers. The U-turn provided by the pseudo-geminal [2.2]paracyclophane core is useful to build ladder-type polymers consisting of conjugated units that are stacked over their entire length. The multilayered polymers exhibit the effect of extensive π-π interactions between the stacked conjugated tiers. This is most pronounced in the excited state with the formation of a phane state by virtue of the extended overlap along the entire length of the stacked chromophores.

Thus, the π-stacked arctitectures (conjugated oligomers and polymers) serve as suitable platforms to develop an understanding of the interactions between stacked conjugated chains, since they more closely resemble the arrangement of the π-systems of semiconducting organic oligomers and polymers in thin-film organic electronic devices.

# CHAPTER 1

# INTRODUCTION TO CONJUGATED POLYMERS

## 1.7. π-Conjugated Materials

Conjugated oligomers and polymers are very attractive materials for organic electronic devices such as light emitting diodes (LEDs),[1] organic photovoltaic cells (OPCs),[2] field effect transistors (FETs),[3-7] lasers,[8,9] and supercapacitors[10] by virtue of their unique optoelectronic properties. They have potential benefits over the use of inorganic semiconductors, including: flexibility, large scale processibility and low cost of production. These materials became a point of interest when Heeger, MacDiarmid, and Shirakawa discovered the conducting behavior of doped polyacetylenes in 1977.[11, 12] They were awarded the Nobel Prize in Chemistry in 2000 in recognition of their efforts and contribution to the field.

Over the last three decades, the science of semiconducting polymers has advanced rapidly. New classes of π-conjugated polymers such as polythiophenes,[4] poly(phenylene vinylene)s,[13] and poly(phenylene ethynylene)s[14] have been synthesized and studied for their intrinsic semiconducting properties, Figure 1.1. The semiconducting behavior of these polymers arises from the presence of a delocalized π-electron cloud along the polymer backbone. It is possible to tune the properties of these materials by simple modifications of their molecular structures.

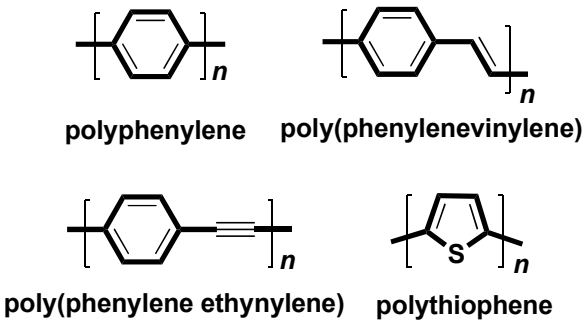


**Figure 1.1.** Examples of some π-conjugated polymers.

## 1.8. Charge Carriers in Organic Conjugated Semiconducting Materials

For a small molecule such as ethylene, the energy difference between highest occupied molecular orbital (HOMO) and lowest unoccupied molecular orbital (LUMO) is considerably high, Figure 1.2. Hence, the promotion of an electron from HOMO to LUMO is very difficult. In a longer conjugated molecule such as hexatriene, the energy levels further split to create an equal number of molecular orbitals which reduces the effective energy difference between HOMO and LUMO. When it reaches a very high conjugation length (ca. polyacetylene), the energy levels are closely spaced to each other and can be considered as energy bands. The energy band formed by bonding molecular orbitals is termed as the valence band because it contains electrons. Whereas, the antibonding molecular orbitals constitute an energy band which is empty and termed as the conduction band. Due to such a small bandgap between these bands, an electron can be promoted from the valence band to the conduction band by either thermal or photo excitation to create an exciton.[15] The exciton is formed when an electron and hole are coupled to each other by the Coulombic force of attraction.[16]

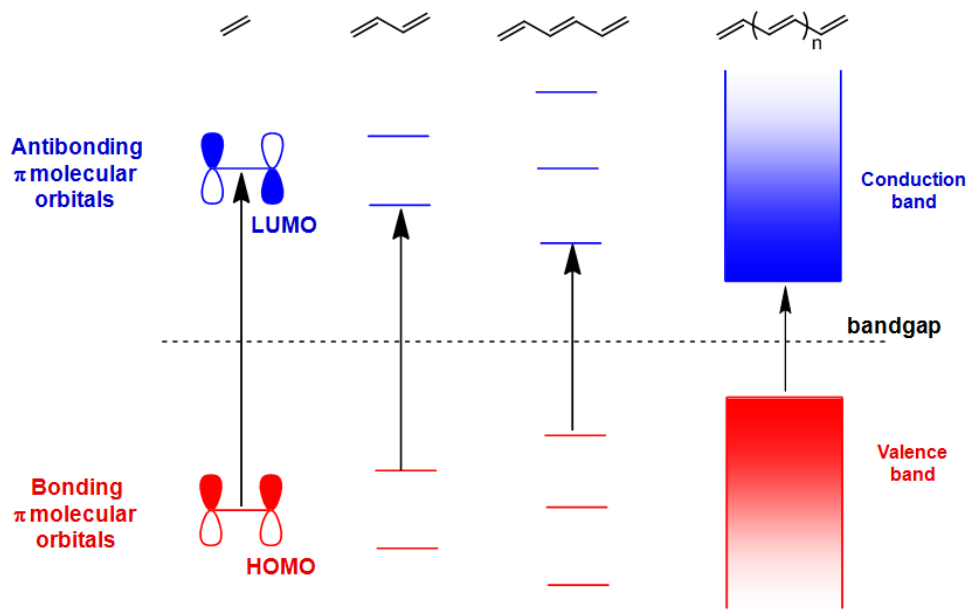


**Figure 1.2.** Formation of valence and conduction band in the conjugated polymers.

Typically, chemical oxidation or reduction (known as doping) of conjugated polymers increases their conductivity by a number of orders of magnitude. Oxidation of a conjugated chain would provide a radical cation. A low level of oxidation of conjugated material leads to a formation of polaron-like charge carrier which is delocalized over the conjugated chain and gives rise to new optical transitions and is ESR active. This creates a new localized electronic state in the bandgap, with the lower energy state being occupied by a single unpaired electron. It was evident from the fact that both UV-Vis-NIR and ESR signals were observed which confirmed the formation of a radical cation by oxidation of polythiophene.[17]

Further oxidation of a single conjugated chain would lead to the formation of bis(radical cation). However, combination of two radical cations on a single chain would create a spinless dication which is ESR silent. A high level of oxidation of conjugated materials creates a spinless

bipolaron-like charge carrier. Electrochemical characterization of fused thiophene oligomers showed the existence of such dicationic species.[18]

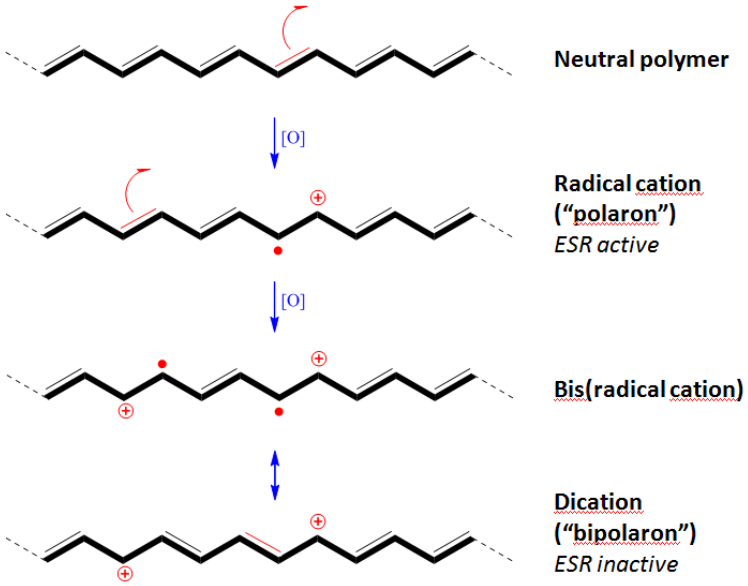


**Figure 1.3.** Charge carriers in the conjugated polymer.

The reversible π-dimerization of radical cations may also be possible as a mechanism to form charge carriers in conjugated materials.[19] Miller and coworkers studied the oxidation of alkylated oligothiophenes in solution to form radical cations which show ESR signals.[20, 21] Upon addition of a poor solvent to a solution of these oxidized oligothiophenes, they observed a new absorption band in the near IR region of the spectrum and a decrease in the strength of the ESR signal.[22] They concluded that addition of poor solvent leads to the aggregation of these oxidized oligomers which undergo reversible π-dimerizarion, Figure 1.4.[20] These are similar to a bipolaron-like species and could be considered as a model for the charge carriers in oxidized conjugated materials.

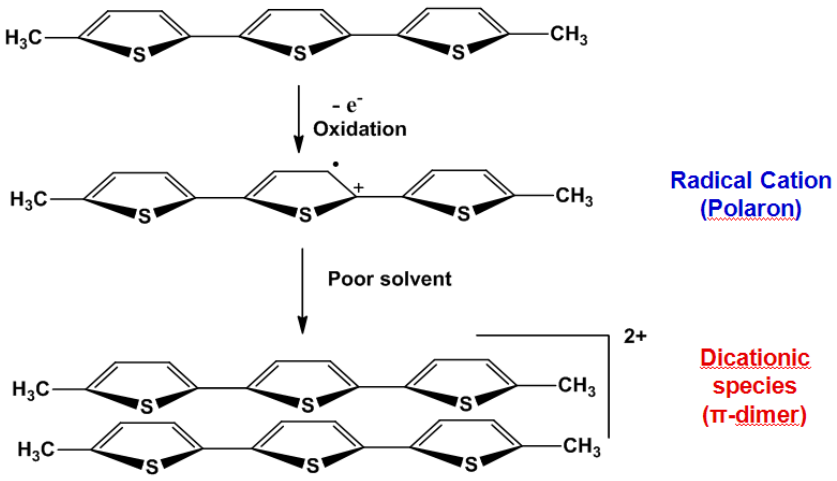


**Figure 1.4.** π-Dimer formation by aggregation of radical cations.

Such charge carriers delocalize along the conjugation length of polymer chain and possibly over multiple chains to provide the material with semiconducting properties. Recent work by Knoblock in the Collard group probed the electronic interactions between oxidized oligothiophenes that were held in a permanently stacked fashion using a molecular scaffold.[23] Such molecular scaffold provides an opportunity to control the orientation and degree of interaction between conjugated units. The optical and electrochemical characterization of these stacked molecules provides insights into the nature of interchain interaction between the conjugated chains. This reinforces the understanding of charge carriers and the development of new functional materials.

## 1.9. Excitons in Conjugated Organic Materials

An exciton is formed when an electron and hole are attracted to each other by Coulombic force.[16] When a light is absorbed by a molecule, the transition of an electron from one molecular orbital to another molecular orbital occurs. Usually absorption promotes an electron from the highest occupied molecular orbital (HOMO) to the lowest unoccupied molecular orbital (LUMO) creating a hole in the HOMO and promotes the electron in LUMO. The electron in the conduction band remains associated with the hole by Coulombic attraction (binding energy). The relaxation of the electron to a lower energy orbital is responsible for the fluorescence (emission). The exciton may transfer from one molecule to another if there is energy match absorbance of the second molecule.[24] This phenomenon depends on the intermolecular distance and is useful for applications such as sensors and light emitting diodes. In the context of Knoblock's stacked oligomers,[23] such process can be probed in detail by performing optical studies where we can control the distance between the conjugated units.

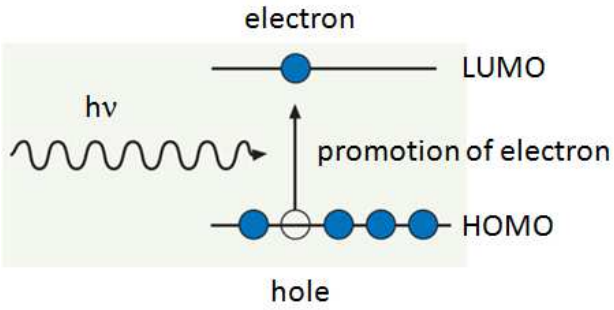


**Figure 1.5.** Formation of an exciton.

## 1.10. Two-dimensional π-Stacked Compounds

The transport of charge carriers along π-conjugated chains in one dimension does not provide a complete understanding of the semiconducting behavior of conjugated materials. The electronic structure of conjugated organic materials also depends on the molecular structure and the three-dimensional packing of the conjugated chains with one another. While the supramolecular architecture of conjugated chains is itself a function of molecular structure, and varies between a herringbone arrangement (common for unsubstituted oligoacenes) and face-to-face packing which is often observed for substituted chains; gaining an understanding of the evolution of electronic structure with variation of molecular structure remains a significant challenge. Computational studies[25] and experimental methods[26] show that three-dimensional interactions between the conjugated units influence the electronic structure of the polymer chains and exert a strong influence on the material properties.

To explore the effect of π-π interactions on optoelectronic properties, various scaffolds such as macrocyclic oligothiophenes,[27] calix[4]arene,[28] arene-annelated bicyclo[4.4.1]undecane, [23,29,16,22] [2.2]paracyclophane,[30-34] 4,5-disubstituted xanthene,[35] *m*-terphenyl oxacyclophane[36] have been designed to hold pairs of conjugated units atop one another, Figure 1.6. Otsubo prepared the oligothiophenophane which upon oxidation readily showed formation of spinless π-dimer like dicationic species at ambient temperature.[27] Swager demonstrated the conformational change in the structure of calix[4]arene upon oxidation in a solvent which leads to the formation of a stable dicationic species which are ESR silent.[28] Arene-annelated bicyclo[4.4.1]undecanes provide the compounds in which fused-arenes are held in stacks. This can be extended to triple-layered and quadruple-layered orthonaphthophanes.[37] This scaffold can also be used to prepare the triple and quadruple layered π-stacked conjugated oligomers. Bazan explored the through-

space interactions between pairs of stilbenes[30] or phenylene ethynylenes[31] by using a pseudo-para disubstituted [2.2]paracyclophane scaffold to hold the chromophores in a stacked arrangement. Collard et al. have previously synthesized oligothienyl-substituted [2.2]paracyclophanes and illustrated the effect of interchain delocalization of charges between the conjugated units.[34] Other studies demonstrate the electronic communication of oligothiophenes through the paracyclophane subunit with shorter oligomers. On the other hand, Knoblock et al. explored the through-space interactions between pairs of terthiophene and pentathiophene oligomers by using a dithieno-fused bicyclo[4.4.1]undecane scaffold to hold these chromophores in a stacked arrangement over their entire length.[23] This study explored the effect of stacking on the formation of cationic species and provided further evidence for the stabilization of π-dimers of radical cations. Such stabilization of cationic species on these stacked compounds compared to those of unstacked models arises from through-space interaction between the stacked π-systems.

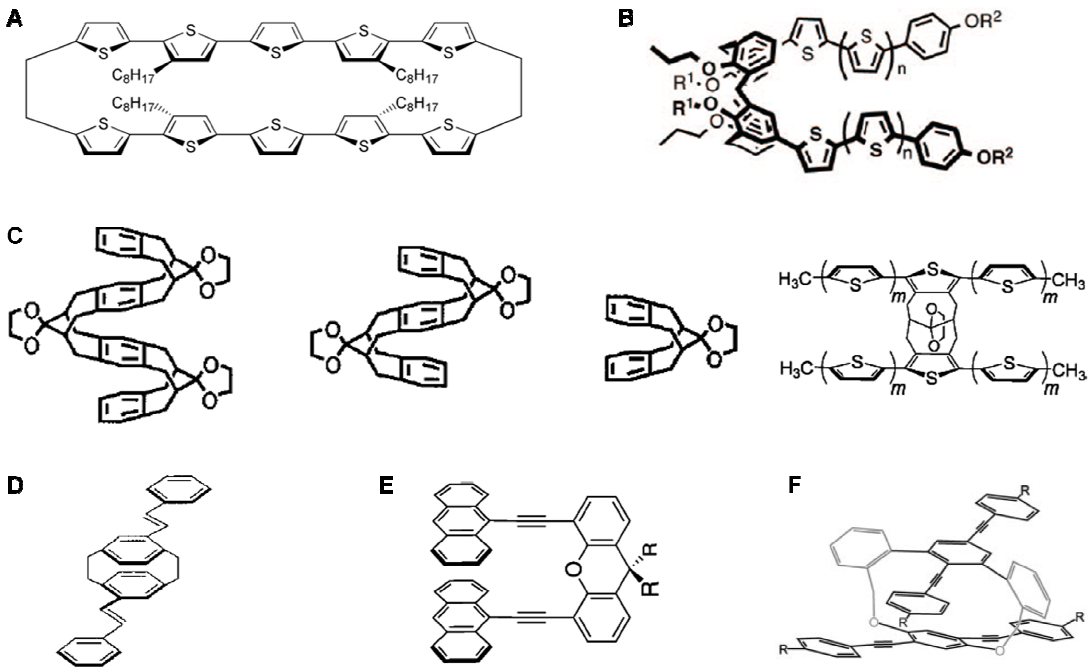


**Figure 1.6.** π-Stacked compounds based on scaffolds: A, macrocylic oligothiophenes[27]; B, calix[4]arene[28]; C, arene-annelated bicycle[4.4.1]undecane[23,29,37]; D, [2.2]paracyclophane[30]; E, 4,5-disubstituted xanthenes[38]; and F, *m*-terphenyl oxacyclophane.[36]

The electrochemistry and photophysics of conjugated oligomers continues to be a field of interest as models for the development of new functional materials. While the interaction of pairs of conjugated chains held in defined geometries can be determined through computational studies, there are few model compounds that mimic these geometries to allow for correlation of results from theoretical treatments with spectroscopic characteristics.[39] A combined approach which includes the experimental and computational studies would be the ideal strategy to examine the electronic structure of conjugated materials.

## 1.11. Scope of work

To achieve a more extensive overlap of conjugated units and thereby develop a greater understanding of inter-chain communication in closely packed conjugated chains, we proposed the design of molecular scaffolds which can hold conjugated units stacked atop one another, Figure 1.7. These structures could be extended further by preparation of polymeric analogs. The optical and electrochemical properties of such stacked compounds could be compared to the linear unstacked models to study the effect of π-π interactions on the electronic structure of these materials. Chapter 2 describes general experimental methods, which includes the synthesis, and structural, optical and electrochemical characterization of the stacked compounds described in the following chapters.

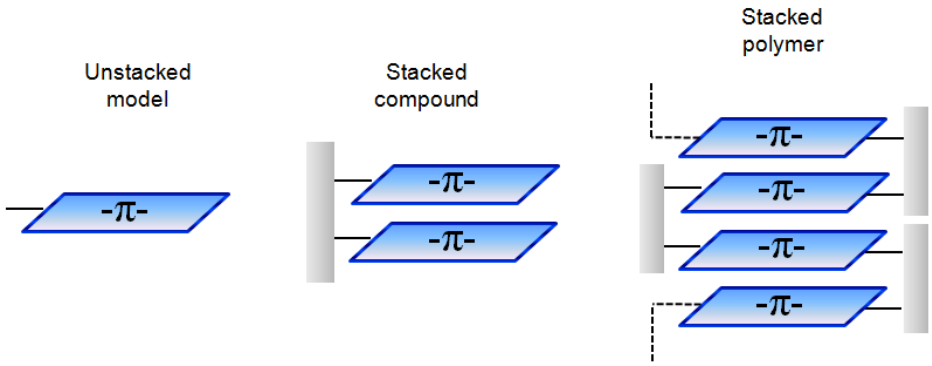


**Figure 1.7.** Unstacked linear model (left), π-stacked compound (middle), and π-stacked polymer (right).

In Chapter 3, we report use of a molecular scaffold consisting of the benzo-fused bicyclo[4.4.1]undecane[29] reported by Mataka to prepare π-stacked compounds, Figure 1.8. We explored various bulky and electron rich groups to achieve a pseudo chair-pesudo chair conformation of the bicyclic core in which the benzene units are stacked atop one another.

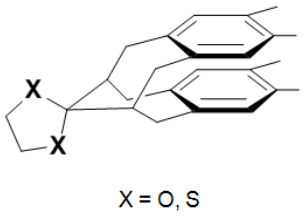


**Figure 1.8.** Benzo-fused bicyclo[4.4.1]undecane scaffold.

We have prepared and studied oligo(phenylene ethynylene)s held in a π-stacked arrangement by a bicyclo[4.4.1]undecane scaffold to achieve a highly planer chromophore with an extended overlap of conjugated units, Chapter 4, Figure 1.9. With the help of computational analysis conducted by the Brédas research group, we have provided an explanation for the differences between the photophysics of these stacked compounds and their linear models.

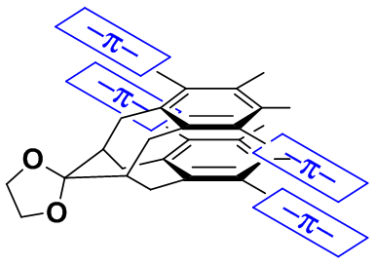


**Figure 1.9.** π-Stacked conjugated oligomers based on benzo-fused bicyclo[4.1.1]undecane scaffold.

In Chapter 5, we have used another scaffold, [2.2]paracyclophane to prepare π-stacked oligo(phenylene vinylene)s, Figure 1.10. In particular, we focuses on a pseudo-geminal (*pg*) substitution pattern of the [2.2][paracyclophane core.[40] The optical and electrochemical properties of these stacked compounds are compared with their unstacked counterparts and the observed results are supported by computational analysis performed on these compounds.

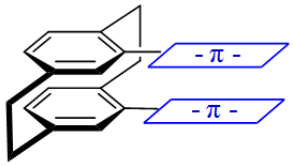


**Figure 1.10.** π-Stacked conjugated oligomers based on pseudo-geminal [2.2]paracyclophane.

To achieve a π-stacked polymeric architecture, we made use of the *pg* disubstituted [2.2]paracyclophane scaffold to provide a U-turn and thereby hold the conjugated oligomers in a multilayered arrangement. In Chapter 6, we report the synthesis of various *pg* paracyclophanes (diethynyl,[40] diethenyl,[40] dibromo,[41] and diiodo[41]), as potential monomers to prepare π-stacked conjugated polymers. These monomers were prepared according to literature methods with minor modifications.

In Chapter 7, we explore the use of monomers reported in Chapter 6 to prepare π-stacked conjugated polymers, Figure 1.11.[42] We also prepared the linear model compounds which resemble a single unstacked tier of the polymeric structure. The optical and electrochemical properties of these polymers are compared to their linear unstacked counterpart to study the effect of extensive π-π interactions between the conjugated chains. We also prepared the extended conjugated monomers to lengthen the tier of these π-stacked polymers in Chapter 8, Figure 1.11.

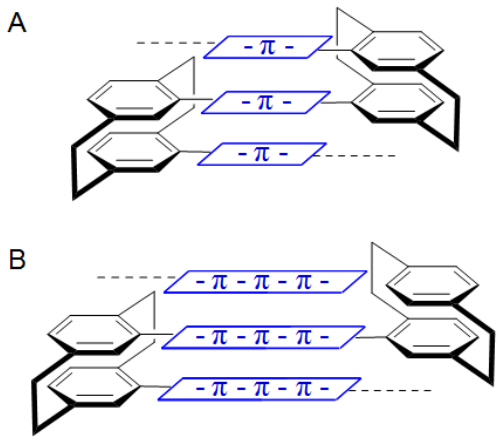


**Figure 1.11.** Multilayered π-stacked conjugated polymers: A, chromophoric tier with short length of conjugation; and B, chromophoric tier with extended length of conjugation.

## 1.12. References


1. Burroughes, J. H.; Bradley, D. D. C.; Brown, A. R.; Marks, R. N.; Mackay, K.; Friend, R. H.; Burns, P. L.; Holmes, A. B., *Nature* **1990,** *347* (6293), 539.
2. Liu, J. S.; Tanaka, T.; Sivula, K.; Alivisatos, A. P.; Frechet, J. M. J., *Journal of the American Chemical Society* **2004,** *126* (21), 6550.
3. Drury, C. J.; Mutsaers, C. M. J.; Hart, C. M.; Matters, M.; de Leeuw, D. M., *Applied Physics Letters* **1998,** *73* (1), 108.
4. Katz, H. E.; Dodabalapur, A.; Z, B.; Fichou, D., *Handbook of Oligo- and Polythiophene* **1998**.
5. Tsumura, A.; Koezuka, H.; Ando, T., *Applied Physics Letters* **1986,** *49* (18), 1210.
6. Garnier, F.; Horowitz, G.; Peng, X. H.; Fichou, D., *Advanced Materials* **1990,** *2* (12), 592.
7. Garnier, F.; Hajlaoui, R.; Yassar, A.; Srivastava, P., *Science* **1994,** *265* (5179), 1684.
8. McGehee, M. D.; Heeger, A. J., *Advanced Materials* **2000,** *12* (22), 1655.
9. Tessler, N.; Denton, G. J.; Friend, R. H., *Nature* **1996,** *382* (6593), 695.
10. Zhou, C. F.; Kumar, S.; Doyle, C. D.; Tour, J. M., *Chemistry of Materials* **2005,** *17* (8), 1997.
11. Shirakawa, H., *Angewandte Chemie-International Edition* **2001,** *40* (14), 2575.
12. Stenger-Smith, J. D., *Progress in Polymer Science* **1998,** *23* (1), 57.
13. Granier, T.; Thomas, E. L.; Gagnon, D. R.; Karasz, F. E.; Lenz, R. W., *Journal of Polymer Science Part B-Polymer Physics* **1986,** *24* (12), 2793.
14. Bunz, U. H. F., *Chemical Reviews* **2000,** *100* (4), 1605.
15. Bredas, J. L.; Street, G. B., *Accounts of Chemical Research* **1985,** *18* (10), 309.

16. Liang, W. Y., *Physics Education* **1970**, 226.

17. Frere, P.; Raimundo, J. M.; Blanchard, P.; Delaunay, J.; Richomme, P.; Sauvajol, J. L.; Orduna, J.; Garin, J.; Roncali, J., *Journal of Organic Chemistry* **2003,** *68* (19), 7254.

18. Guay, J.; Diaz, A.; Wu, R. L.; Tour, J. M., *Journal of the American Chemical Society* **1993,** *115* (5), 1869.

19. Tenhoeve, W.; Wynberg, H.; Havinga, E. E.; Meijer, E. W., *Journal of the American Chemical Society* **1991,** *113* (15), 5887.

20. Miller, L. L.; Mann, K. R., *Accounts of Chemical Research* **1996,** *29* (9), 417.

21. Zotti, G.; Schiavon, G.; Berlin, A.; Pagani, G., *Synthetic Metals* **1993,** *61* (1-2), 81.

22. Hong, Y. L.; Yu, Y.; Miller, L. L., *Synthetic Metals* **1995,** *74* (2), 133.

23. Knoblock, K. M.; Silvestri, C. J.; Collard, D. M., *Journal of the American Chemical Society* **2006,** *128* (42), 13680.

24. Scharber, M. C.; Wuhlbacher, D.; Koppe, M.; Denk, P.; Waldauf, C.; Heeger, A. J.; Brabec, C. L., *Advanced Materials* **2006,** *18* (6), 789.

25. Bredas, J. L.; Beljonne, D.; Coropceanu, V.; Cornil, J., *Chemical Reviews* **2004,** *104* (11), 4971.

26. Tan, C. Y.; Alas, E.; Muller, J. G.; Pinto, M. R.; Kleiman, V. D.; Schanze, K. S., *Journal of the American Chemical Society* **2004,** *126* (42), 13685.

27. Kaikawa, T.; Takimiya, K.; Aso, Y.; Otsubo, T., *Organic Letters* **2000,** *2* (26), 4197.

28. Song, C.; Swager, T. M., *Organic Letters* **2008,** *10* (16), 3575.

29. Mataka, S.; Takahashi, K.; Mimura, T.; Hirota, T.; Takuma, K.; Kobayashi, H.; Tashiro, M.; Imada, K.; Kuniyoshi, M., *Journal of Organic Chemistry* **1987,** *52* (13), 2653.

30. Bazan, G. C.; Oldham, W. J.; Lachicotte, R. J.; Tretiak, S.; Chernyak, V.; Mukamel, S., *Journal of the American Chemical Society* **1998,** *120* (36), 9188.

31. Bartholomew, G. P.; Bazan, G. C., *Accounts of Chemical Research* **2001,** *34* (1), 30.

32. Hong, J. W.; Gaylord, B. S.; Bazan, G. C., *Journal of the American Chemical Society* **2002,** *124* (40), 11868.

33. Hong, J. W.; Benmansour, H.; Bazan, G. C., *Chemistry A European Journal* **2003,** *9* (14), 3186.

34. Salhi, F.; Lee, B.; Metz, C.; Bottomley, L. A.; Collard, D. M., *Organic Letters* **2002,** *4* (19), 3195.

35. Morisaki, Y.; Imoto, H.; Miyake, J.; Chujo, Y., *Macromolecular Rapid Communications* **2009,** *30* (13), 1094.

36. Smith, R. C., *Macromolecular Rapid Communications* **2009,** *30* (24), 2067.

37. Mataka, S.; Shigaki, K.; Sawada, T.; Mitoma, Y.; Taniguchi, M.; Thiemann, T.; Ohga, K.; Egashira, N., *Angewandte Chemie-International Edition* **1998,** *37* (18), 2532.

38. Morisaki, Y.; Sawamura, T.; Murakami, T.; Chujo, Y., *Organic Letters* **2010,** *12* (14), 3188.

39. Hutchison, G. R.; Ratner, M. A.; Marks, T. J., *Journal of the American Chemical Society* **2005,** *127* (48), 16866.

40. Bondarenko, L.; Hentschel, S.; Greiving, H.; Grunenberg, J.; Hopf, H.; Dix, I.; Jones, P. G.; Ernst, L., *Chemistry A European Journal* **2007,** *13* (14), 3950.

41. El Shaieb, K.; Narayanan, V.; Hopf, H.; Dix, I.; Fischer, A.; Jones, P. G.; Ernst, L.; Ibrom, K., *European Journal of Organic Chemistry* **2003,** (3), 567.

42. Jagtap, S. P.; Collard, D. M., *Journal of the American Chemical Society* **2010,** *132* (35), 12208.

# CHAPTER 2

# GENERAL EXPERIMENTAL METHODS

## 2.1. Synthesis

All reagents and catalysts were purchased from Aldrich, TCI, Alfa Aesar, or Strem Chemicals and used without further purification. THF and diethyl ether were distilled from benzophenone-sodium ketyl. Dichloromethane was distilled from calcium hydride and anhydrous DMF, triethylamine, toluene, diisopropylamine, dioxane were purchased from Aldrich. Most of the reactions were performed under inert atmosphere (argon, nitrogen). Column chromatography was performed on flash grade silica (32-60 Å, Sorbent Technologies and Dynamic Adsorbant, Atlanta, GA). Thin-layer chromatography was performed on 3 ×5 cm silica gel plates (0.2 mm thick, 60 F254) on an aluminum support (Sorbent Technologies). TLC plates were visualized by a UV lamp or iodine vapor.

## 2.2. Structural Characterization

Melting points were determined on a MELT-TEMP-II, Laboratory Devices, USA. $^{1}H$ and $^{13}C$ NMR spectra were recorded from a 300 or 400 MHz Varian Mercury spectrophotometer. Chemical shifts are reported relative to internal tetramethylsilane. IR analyses were performed on a Nicolet 4700 FTIR with an ATR attachment from SmartOrbit Thermoelectronic Corporation. Mass spectra were collected on a VG-70SE instrument. Elemental analyses were performed by Atlantic Microlab, Inc. (Norcross, GA). X-ray crystal structure analysis was

performed on a Bruker D8 SMART APEX CCD sealed tube diffractometer with graphite monochromated MoKα (0.71073 Å) radiation by Dr. Hardcastle at Emory university.

## 2.3. Electronic Characterization

Ultraviolet-visible analysis was performed on a Shimadzu UV-2401PC spectrometer, and fluorescence spectroscopy was performed on a Shimadzu RF-5301PC spectrofluorophotometer. Electrochemical measurements were carried out under nitrogen and recorded on a BAS 100B Electrochemical Analyzer with a three electrode cell equipped with a 2 mm gold working electrode, a platinum counter electrode, and a $Ag/Ag^+$ reference electrode with 3M NaCl solution end capped with a vycor tip. Substrates (1-2 mM) were dissolved in a dry $CH_2Cl_2$ containing 0.1 M *n*-$Bu_4NPF_6$ electrolyte.

# CHAPTER 3

# SYNTHESIS AND STRUCTURAL CHARACTERIZATION OF BENZO-FUSED BICYCLO[4.4.1]UNDECANE

## 3.1. Introduction

The design of π-stacked conjugated oligomers requires a suitable molecular scaffold then can hold conjugated units stacked atop one another. Shuntaro Mataka of Kyushu University prepared various arene-fused bicyclo[4.4.1]undecanes that provide the ability to control cofacial interaction between arene units.[1-10] To prepared stacked conjugated oligomers, we chose to use a benzo-fused bicyclo[4.4.1]undecane scaffold that can be has already been prepared using methods described by Mataka. Incorporation of methyl groups on to the fused arenes provides control over the position at which the core undergoes functionalization.

Mataka previously reported the synthesis and conformational analysis of a series of arene-fused bicyclic compounds.[8] Dibenzo[3,4;8,9]bicyclo[4.4.1]undeca-3,8-dienes, Figure 3.1B, and corresponding arene-fused bicycle[4.4.1]undecane, Figure 3.1A, undergo rapid interconversion between different conformations as shown by $^{1}H$ and $^{13}C$ NMR spectroscopy. The benzylic methylene groups of these compounds give a broad signal in the $^{1}H$ NMR spectrum due to coalescence of signals is from the three conformations of the bicyclic core pseudo chair-pseudo boat, pseudo chair-pseudo chair and pseudo boat-pseudo boat, Figure 3.1B.[8]

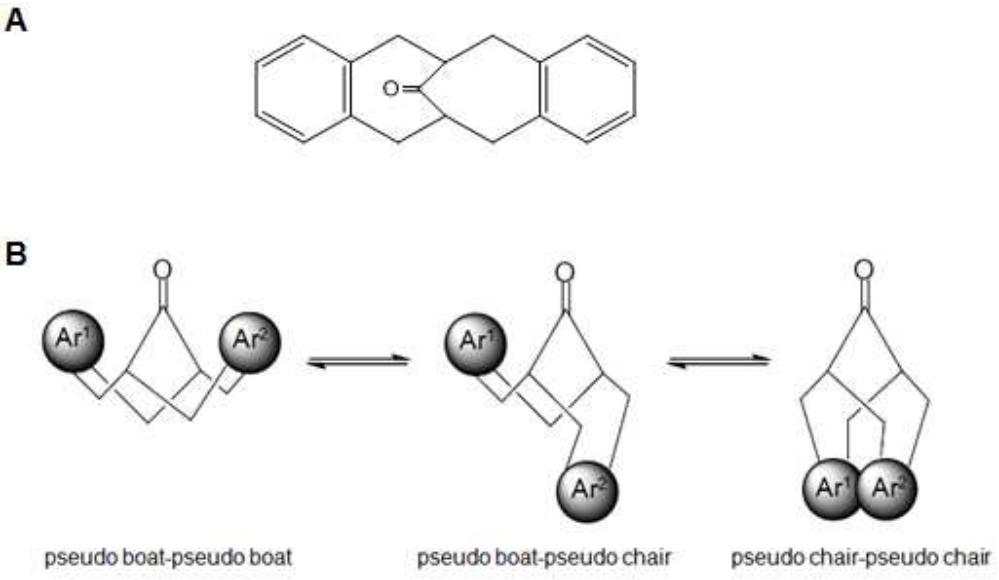


**Figure 3.1.** A, Dibenzo-fused bicycloundecane; and B, Possible conformations of bicyclic ketone (from reference 8).

Mataka showed that conversion of the ketone to the ketal locks the bicyclic core in a single pseudo chair-pseudo chair conformation which provides the stacked arrangement of the fused-arenes, Figure 3.2.[9] This stacking of arenes in close proximity leads to the upfield shift of the aromatic protons in the $^{1}$H NMR spectrum of ketal compared to the ketone. The benzylic protons of the ketal appear as a pair of doublet of doublets for the ketal instead of broad signal exhibited for the ketone, consistent with the pseudo chair-pseudo chair conformation. The X-ray crystal structure of the ketal confirmed the stacked orientation of the arene units, which are separated by distance of 3.03 to 4.10 Å.

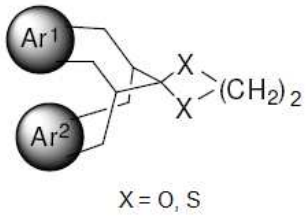


**Figure 3.2.** Single pseudo chair-pseudo chair conformation of ketal (from reference 9).

Here we report a synthetic strategy to prepare π-stacked conjugated oligomers using tetramethyl benzo-fused bicyclo[4.4.1]undecane as a scaffold to study effect of stacking on the optoelectronic properties of π-conjugated materials. We also explored the effect of the presence of a more bulky group in place of the simple acetal on the distance and angle between the pair of stacked arenes. Structural characterization was performed using NMR and X-ray crystal structure analysis.

## 3.2. Synthesis

General procedures and methods are described in Chapter 2**.**

### 3.2.1. 4,5-Dimethylcyclohexa-1,4-diene-1,2-dicarboxylate

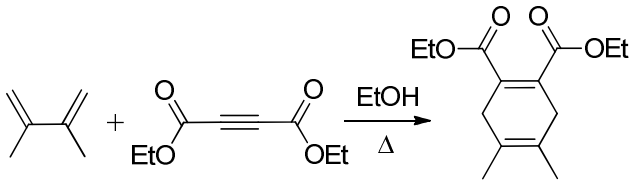


**III-1**

A solution of 2,3-dimethyl-1,2-butadiene (14.4 g, 176 mmol) and diethyl acetylenedicarboxylate (25.0 g, 147 mmol) in EtOH (150 mL) was heated at reflux in a sealed thick-glass pressure vessel for 24 h. The reaction mixture was cooled and the solvent was removed under reduced pressure. The residue was subjected to flash chromatography (10% ethyl acetate/90% hexane) to yield the title compound as clear yellow oil (35.8 g, 98%). $^{1}$H NMR (300 Hz, $CDCl_3$): δ 4.1 (quartet, $J$ = 6 Hz, 4H, $OCH_2$), 2.78 (s, 4H, cyclic-$CH_2$), 1.53 (s, 6H, cyclic-$CH_3$), 1.18 (t, $J$ = 6 Hz, 6H, ester $CH_3$). $^{13}$C NMR (75 MHz, $CDCl_3$): δ 167.5 (carbonyl), 132.2, 121.2 (vinylic), 60.6 (ester $CH_2$), 33.8 (cyclic-$CH_2$), 17.5 (cyclic-$CH_3$), 13.6 (ester $CH_3$). IR (ATR): 2980, 2934, 2905, 2864, 1716, 1661, 1219, 1067, 1025, 765 $cm^{-1}$. MS (EI), m/z (%) = 252.1 ($M^+$, 4), 206.1 (75), 191.1.1 (50). 163.0 (100), 133.1 (25).

### 3.2.2. Diethyl 3,4-dimethylphthalate

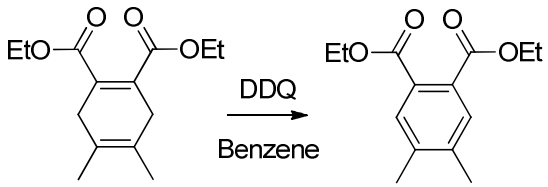


III-1 III-2

DDQ (35.4 g, 156 mmol) was added slowly to a solution of diethyl 4,5-dimethylcyclohexa-1,4-diene-1,2-dicarboxylate (35.7 g, 142 mmol) in benzene (500 mL), and the mixture was stirred for 24 h. Ethyl acetate (200 mL) was added and the mixture was washed with 10% aqueous NaOH solution (100 mL). The solvent was removed under reduced pressure and the residue was subjected to a plug of silica gel (20% ethyl acetate/70% hexane) to afford the title compound as a clear yellow oil (34.0 g, 93%). $^{1}$H NMR (300 Hz, $CDCl_3$): δ 7.44 (s, 2H, Ar-H), 4.30 (quartet, *J* = 6 Hz, 4H, ester $CH_2$), 2.26 (s, 6H, Ar-$CH_3$), 1.31 (t, *J* = 6 Hz, 6H, ester $CH_3$). $^{13}$C NMR (75 MHz, $CDCl_3$): δ 167.7 (carbonyl), 139.9, 129.8, 129.6 (Ar-C), 61.1 (ester $CH_2$), 19.3 (Ar-$CH_3$), 13.9 (ester $CH_3$). IR (ATR): 2977, 2360, 2338, 1686, 1368, 1294, 1131, 1035 $cm^{-1}$. MS (EI), m/z (%) = 250.0 ($M^+$, 16), 205.1 (42), 177.01 (100), 133.0 (5). HRMS calculated for $C_{14}H_{18}O_4$, 250.12051; Found, 250.12064, Δ = 0.5 ppm.

### 3.2.3. 1,2-Bis(hydroxymethyl)-4,5-dimethylbenzene

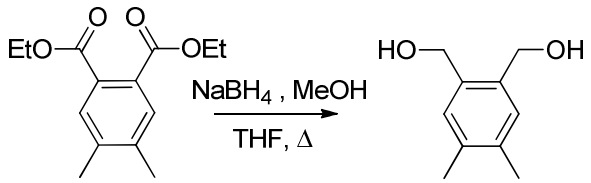


III-2 III-3

$NaBH_4$ (59.7 g, 1.58 mol) was added to a solution of diethyl 3,4-dimethylphthallate (30.0 g, 120 mmol) in dry THF (150 mL) and the mixture was heated to reflux. Methanol (150 mL) was added dropwise over 15 min, and heating was continued for 18 h. The mixture was cooled to 0 °C and a saturated solution of $NH_4Cl$ (100 mL) was added dropwise over 45 min. The organic layer was separated and the aqueous layer was extracted with $CH_2Cl_2$ (3 × 50 mL). The combined organic layers were washed with $H_2O$ (100 mL), and the solvent was removed under reduced pressure to afford the title compound as a white solid (18.5 g, 92%) m.p. = 82-84 °C. $^1H$ NMR (300 Hz, $CDCl_3$): δ 7.08 (s, 2H, Ar-H), 4.60 (s, 4H, benzylic), 2.23 (s, 6H, Ar-$CH_3$). $^{13}C$ NMR (75 MHz, $CDCl_3$): δ 136.8, 134.2, 131.3 (Ar-C), 63.9 (benzylic), 19.3 (Ar-$CH_3$). IR (ATR): 3372, 2957, 2917, 2857, 1459, 1266, 1084, 1001, 891 $cm^{-1}$.

### 3.2.4. 1,2-Bis(bromomethyl)-4,5-dimethylbenzene

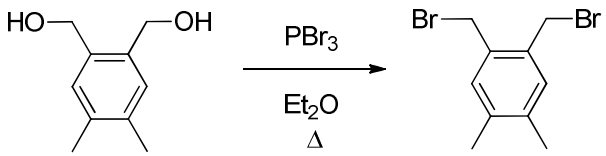


III-3 III-4

$PBr_3$ (4.22 mL, 44.4 mmol) was added dropwise to the solution of 1,2-bis(hydroxymethyl)-4,5-dimethylbenzene (4.8 g, 29 mmol) in $Et_2O$ (150 mL). After complete dissolution of all of the solid, the solution was heated to reflux for 12 h followed by addition of an equal amount of $PBr_3$. The reaction mixture was heated at reflux for 12h and the resulting mixture was poured onto crushed ice (200 g). The aqueous layer was extracted with $Et_2O$ (2 × 100 mL). The combined organic extracts were dried over $MgSO_4$. The solvent was removed under reduced pressure to afford 1,2-bis(bromomethyl)-4,5-dimethylbenzene as a white crystalline solid (6.5 g, 76%) that was used without further purification. m.p. = 68-70 °C. $^1$H NMR (300 Hz, $CDCl_3$): δ 7.13 (s, 2H, Ar-H), 4.63 (s, 4H, benzylic), 2.22 (s, 6H, Ar-$CH_3$). $^{13}$C NMR (75 MHz, $CDCl_3$): δ 138.1, 133.7, 132.3(Ar-C), 30.3 (benzylic), 19.3 (Ar-$CH_3$). IR (ATR): 3046, 2759, 2360, 1520, 1261, 1111, 1084, 947, 778 $cm^{-1}$. MS (EI), m/z (%) = 289.9 ($M^+$, 9), 211.1 ($M^+$-Br, 75), 132.1 ($M^+$-2Br, 100). HRMS (EI), m/z = Calcd. For $C_{10}H_{12}Br_2$, 289.93057; Found, 289.93327, Δ = 9.3 ppm.

### 3.2.5. Dimethyl-tetramethyl-11-oxodibenzo[c,h]bicyclo[4.4.1]undeca-3,8-diene-1,6-dicarboxylate

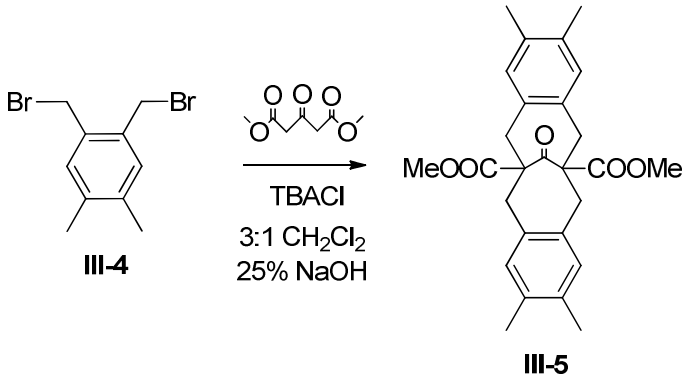


A mixture of dimethyl 1,3-acetonedicarboxylate (6.1 g, 35 mmol) in $CH_2Cl_2$ (27 mL) was added dropwise over 1 h to a vigorously stirred mixture of 1,2-bis(bromomethyl)-4,5-dimethylbenzene (5.9 g, 20 mmol), *n*-$Bu_4NCl$ (3.1 g, 11 mmol), $CH_2Cl_2$ (60 mL) and 25% aqueous NaOH solution (28 mL). The reaction mixture was stirred for 24 h, $CH_2Cl_2$ (100 mL) was added, and the organic layer was separated. The solution was dried over $MgSO_4$ and the solvent was removed under reduced pressure. The residue was subjected to flash chromatography (20% ethyl acetate/70% hexane) to yield the title compound as a white crystalline solid (4.5 g, 60%): m.p. = 183-184 °C. $^1$H NMR (300 Hz, $CDCl_3$): δ 6.98 (br s, 4H, Ar-H), 3.75 (s, 6H, ester $CH_3$), 3.50-3.65 (m, 2H, benzylic), 2.70-3.10 (m, 6H, benzylic), 2.10-2.40 (br d, 12H, Ar-$CH_3$). $^{13}$C NMR (75 MHz, $CDCl_3$): δ 206.8 (ketone C=O), 173.2 (ester C=O), 134.2, 133.2, 131.5 (Ar-C), 64.1 (ester $CH_3$), 52.2 (bridgehead), 39.4, 35.0 (benzylic), 19.2 (Ar-$CH_3$). IR (ATR): 2988, 1717, 1509, 1276, 1260, 878, 770, 759 $cm^{-1}$. MS (EI), m/z (%) = 434.3 ($M^+$, 72), 403.2 (7), 352.2 (10), 325.2 (70), 297.1 (14), 132.1 (100), 91.1 (5). HRMS (EI), m/z = Calcd. For $C_{27}H_{30}O_5$, 434.20932; Found, 434.20871, Δ = 1.4 ppm.

### 3.2.6. Tetramethyl-11-oxodibenzo[c,h]bicyclo[4.4.1]undeca-3,8-diene-1,6-dicarboxylic acid

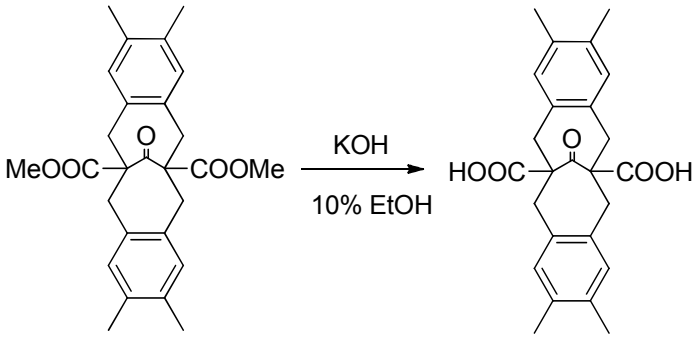


**III-5** **III-6**

A mixture of dimethyl tetramethyl-11-oxodibenzo[*c,h*]bicyclo[4.4.l]undeca-3,8-diene-1,6-dicarboxylate (4.5 g, 10 mmol), KOH (1.2 g, 21 mmol), EtOH (90 mL) and $H_2O$ (10 mL) was heated at reflux for 12 h. The reaction mixture was poured into water (200 mL) and acidified with conc. HCl. The precipitated white solid was collected by filtration and recrystallized from EtOH to give the title compound as a crystalline solid (4.0 g, 95%): m.p. = 298 °C. $^1$H NMR (300 Hz, acetone-$d_6$): δ 6.90-7.10 (br s, 4H, Ar-H), 2.40-3.60 (m, 8H, benzylic), 2.10-2.40 (br s, 12H, Ar-$CH_3$). IR (ATR): 3381, 2574, 2366, 1697, 1456, 1272, 771, 645 cm$^{-1}$. MS (EI), m/z (%) = 406.2 ($M^+$, 65), 344 (25), 132 (100). HRMS (EI), m/z = Calcd. For $C_{25}H_{26}O_5$, 406.1780; Found, 406.1792, Δ = 2.9 ppm.

### 3.2.7. Tetramethyl dibenzo[c,h]bicyclo[4.4.l]undeca-3,8-dien-11-one

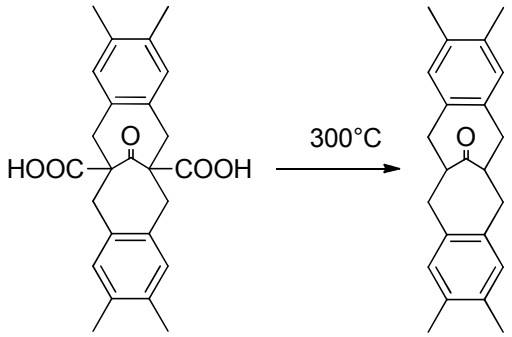


**III-6** **III-7**

A 50-mL round-bottom flask containing tetramethyl-11-oxodibenzo[*c*,*h*]bicyclo[4.4.l]undeca-3,8-diene-1,6-dicarboxylic acid (150 mg, 0.37 mmol) was flushed with argon and heated at 300 °C using a heat gun. When gas evolution ceased (after *ca.* 30 minutes) the flask was cooled to room temperature, $CH_2Cl_2$ (50 mL) was added and the organic layer was washed with 10% aq. NaOH (20 mL). The organic layer was separated and dried over $MgSO_4$. The solvent was removed under reduced pressure and the residue was subjected to a plug of silica gel (30% ethyl acetate / 70% hexane) to give the title compound as a bright white solid (100 mg, 85%). m.p. = 132-134 °C. $^1$H NMR (300 Hz, $CDCl_3$): δ 6.80-6.95 (br s, 4H, Ar-H), 3.00-3.15 (m, 2H, bridgehead), 2.60-2.90 (br m, 8H, benzylic), 2.10-2.25 (br s, 12H, Ar-$CH_3$). $^{13}$C NMR (75 MHz, $CDCl_3$): δ 216.1 (C=O), 135.2, 134.9, 131.8 (Ar-C), 53.7 (bridgehead), 34.7 (benzylic), 19.1 (Ar-$CH_3$). IR (ATR): 2988, 1717, 1509, 1451, 1276, 1260, 878, 770, 723 cm$^{-1}$. MS (EI), m/z (%) = 318.2 ($M^+$, 100), 185.1(63). HRMS (EI), m/z = Calcd. For $C_{23}H_{26}O$, 318.1983; Found, 318.1966, Δ = 4.0 ppm.

### 3.2.8. Ethylene-ketal of dibenzo[c,h]bicyclo[4.4.1]undeca-3,8-dien-11-one

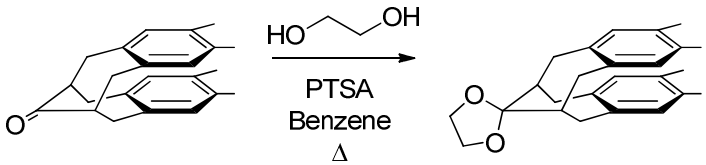


III-7 III-8

A solution of tetramethyl dibenzo[c,h]bicyclo[4.4.1]undeca-3,8-dien-11-one (100 mg, 310 mmol), ethylene glycol (200 mg, 3.23 mmol), *p*-toluenesulfonic acid (1 mg) in benzene (50 mL) was heated at reflux for 48 h with removal of water via a Dean-Stark trap. The solvent was evaporated under reduced pressure, and the residue was subjected to column chromatography ($CH_2Cl_2$) followed by recrystallization from hexanes to give the title compound (95 mg, 84%) as a yellow crystalline solid. m.p. = 221-222 °C. $^1$H NMR (300 Hz, $CDCl_3$): δ 6.40 (s, 4H, Ar-H), 4.05 (s, 4H, $OCH_2CH_2O$), 3.34 (dd, *J* = 15.3, 2.1 Hz, 4H, benzylic), 2.58 (dd, *J* = 15.3, 5.4 Hz, 4H, benzylic), 2.24 (m, 2H, bridgehead), 1.98 (s, 12H, Ar-$CH_3$). $^{13}$C NMR (75 MHz, $CDCl_3$): δ (O-C-C-O), 136.6, 132.8, 132.0 (Ar-C), 64.5 (-$OCH_2$), 42.3 (bridgehead), 35.8 (benzylic), 18.9 (Ar-$CH_3$). IR (ATR): 2997, 2930, 2877, 1439, 1383, 1110, 1040, 891 cm$^{-1}$. MS (EI), m/z (%) = 362.2 ($M^+$, 70), 229.0 (100), 104.9 (75). HRMS (EI), m/z = Calcd. For $C_{25}H_{30}O_2$, 362.2246; Found, 362.2249, Δ = 0.8 ppm.

### 3.2.9. Thio-ketal of dibenzo[c,h]bicyclo[4.4.1]undeca-3,8-dien-11-one

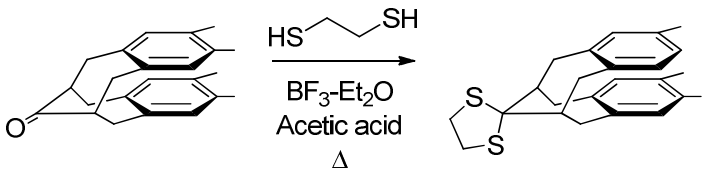


III-7 III-9

A mixture of tetramethyl dibenzo[c,h]bicyclo[4.4.1]undeca-3,8-dien-11-one (100 mg, 310 mmol), 1,2-ethanedithiol (150 mg, 1.59 mmol), $BF_3Et_2O$ (1 mg) in acetic acid (20 mL) was heated at reflux for 48 h. The mixture was cooled and the precipitate was filtered and recrystallized from benzene to give the title compound (96 mg, 77%) as a white crystalline solid. m.p. = 262-263 °C. $^1$H NMR (300 Hz, $CDCl_3$): δ 6.43 (s, 4H, Ar-H), 3.58 (dd, *J* = 15.5, 2.3 Hz, 4H, benzylic), 3.34 (s, 4H, $SCH_2CH_2S$), 2.77 (dd, *J* = 15.2, 5.9 Hz, 4H, benzylic), 2.64 (m, 2H, bridgehead), 1.99 (s, 12H, Ar-$CH_3$). $^{13}$C NMR (75 MHz, $CDCl_3$): δ 136.3, 133.1, 132.1 (Ar-C), 47.6 (bridgehead), 39.9 (-$SCH_2$), 39.2 (benzylic), 18.8 (Ar-$CH_3$). IR (ATR): 3000, 2920, 2887, 1436, 1293, 1014, 941, 881 cm$^{-1}$. MS (EI), m/z (%) = 394.2 ($M^+$, 80), 145.1 (100). HRMS (EI), m/z = Calcd. For $C_{25}H_{30}S_2$, 394.1789; Found, 394.1783, Δ = 1.5 ppm.

### 3.2.10. Sulfone of thio-ketal of dibenzo[c,h]bicyclo[4.4.1]undeca-3,8-dien-11-one

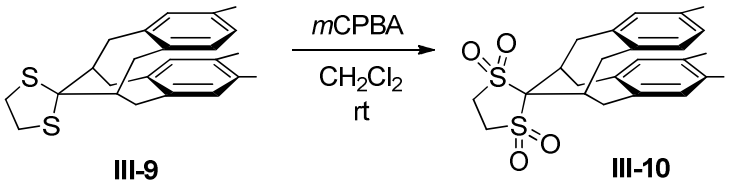


III-9 III-10

A mixture of tetramethyl dibenzo[c,h]bicyclo[4.4.1]undeca-3,8-dien-11-one (100 mg, 310 mmol) and *meta*-chloroperoxybenzoic acid (200 mg, 1.16 mmol) in $CH_2Cl_2$ (20 mL) was stirred at room temperature for 24 h. The solvent was removed under reduced pressure, and the crude residue was subjected to column chromatography ($CH_2Cl_2$) followed by trituration with hot hexanes to give the title compound (120 mg, 83%) as a yellow crystalline solid. m.p. = 296-297 °C (decomposes). $^1$H NMR (300 Hz, $CDCl_3$): δ 6.37 (s, 4H, Ar-H), 4.01 (dd, *J* = 15.5, 2.1 Hz, 4H, benzylic), 3.71 (s, 4H, $SCH_2CH_2S$), 3.23 (m, 2H, bridgehead), 2.82 (dd, *J* = 16.1, 5.3 Hz, 4H, benzylic), 1.97 (s, 12H, Ar-$CH_3$). $^{13}$C NMR (75 MHz, $CDCl_3$): δ 134.7, 133.3, 132.2 (Ar-C), 49.3 (bridgehead), 37.7 (-$SCH_2$), 35.6 (benzylic), 18.7 (Ar-$CH_3$). IR (ATR): 3000, 2914, 2860, 1638, 1323, 1120, 725 cm$^{-1}$. MS (EI), m/z (%) = 458.2 ($M^+$, 100). HRMS (EI), m/z = Calcd. For $C_{25}H_{30}O_4S_2$, 458.1586; Found, 458.1595, Δ = 2.0 ppm.

## 3.3. Results and Discussion

### 3.3.1. Synthesis of Key Intermediate: 1,2-Bis(bromomethyl)-4,5-dimethylbenzene

Our synthetic route to prepare 1,2-bis(bromomethyl)-4,5-dimethylbenzene from commercially available 2,3-dimethyl-1,2-butadiene and diethyl acetylenedicarboxylate is illustrated in Figure 3.3.

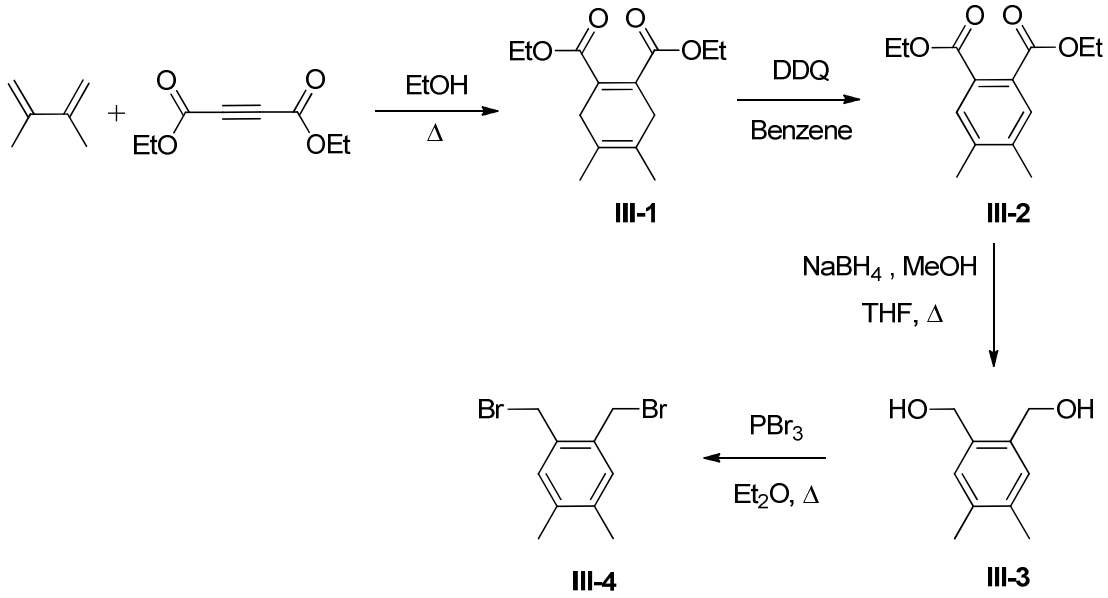


**Figure 3.3.** Synthesis of 1,2-bis(bromomethyl)-4,5-dimethylbenzene.

1,2-Bis(bromomethyl)-4,5-dimethylbenzene is a key intermediate in our multi-step synthesis of the benzo-fused bicycle[4.4.1]undecane core.[8-9] Although this bis(bromomethyl) compound is now commercially available, we chose to prepare it by the reaction of $PBr_3$ with 1,2-bis(hydroxymethyl)-4,5-dimethylbenzene in a similar manner to a literature method for an analogous substrate.[11] This is the first report for the synthesis of 1,2-bis(bromomethyl)-4,5-dimethylbenzene on a multigram scale.

The precursor 1,2-bis(hydroxymethyl)-4,5-dimethylbenzene was prepared by reduction of diethyl 3,4-dimethylphthalate (for which a convenient synthesis is not reported). According to the literature, it was first prepared in the early 1990s from the reaction of 4,5-dimethylphthalic acid with $LiAlH_4$.[12] However the literature reports the synthesis of the diacid in low yields. Accordingly, we decided to explore the utility of its diester analog.

The Diels-Alder reaction between 2,3-dimethyl-1,2-butadiene and diethyl acetylenedicarboxylate in ethanol at reflux provided diethyl 4,5-dimethylcyclohexa-1,4-diene-1,2-dicarboxylate, **III-1**.[13] The cyclohexadiene ring was aromatized by treatment with DDQ in benzene at room temperature to give diethyl 3,4-dimethylphthalate, **III-2**.[14] Upon addition of DDQ, the reaction mixture turned red and eventually dark brown after stirring it for overnight. Purification of **III-2** was accomplished by passing a solution of the crude material through a silica gel plug to remove the DDHQ impurity. The diester **III-2** was subjected to reduction using $NaBH_4$-MeOH[15] in dry THF to provide 1,2-bis(hydroxymethyl)-4,5-dimethylbenzene, **III-3**. Several attempts of reductions using $LiAlH_4$ did not provide pure diol. The size of reaction vessel and rate of addition of methanol are important factors in this step to control the frothing and heat generated during the reduction. Various parameters were modified (concentration, mode of addition, stoichiometry and temperatures) to optimize the yield of diol. 1,2-Bis(bromomethyl)-4,5-dimethylbenzene, **III-4**, was obtained by treatment of the diol with $PBr_3$. $PBr_3$ was added very slowly to a mixture of diol and THF, resulting in the complete dissolution of the diol as the reaction proceeds. After careful workup, leftover starting material was observed. To force reaction to completion, an equal amount of $PBr_3$ was added after overnight stirring and the reaction mixture heated at reflux for another 24 h. This modification led to the isolation of the required dibromide in quantitative yield.

### 3.3.2. Synthesis of Benzo-Fused Bicyclo[4.4.1]undecanone

Once an adequate supply of 1,2-bis(bromomethyl)-4,5-dimethylbenzene was obtained, we used it to alkylate dimethyl 1,3-acetonedicarboxylate under phase transfer conditions.[8] Tetrabutylammonium chloride was used as a phase transfer catalyst in the presence of aq. NaOH in a vigorously stirred solution of dichloromethane. A solution of dimethyl 1,3-acetonedicarboxylate in dichloromethane was added dropwise to a solution of 1,2-bis(bromomethyl)-4,5-dimethylbenzene over 30 min, Figure 3.4. Workup and purification by column chromatography (20% ethyl acetate/70% hexanes) gave the resulting benzo-fused bicycloundecanone diester, **III-5**.

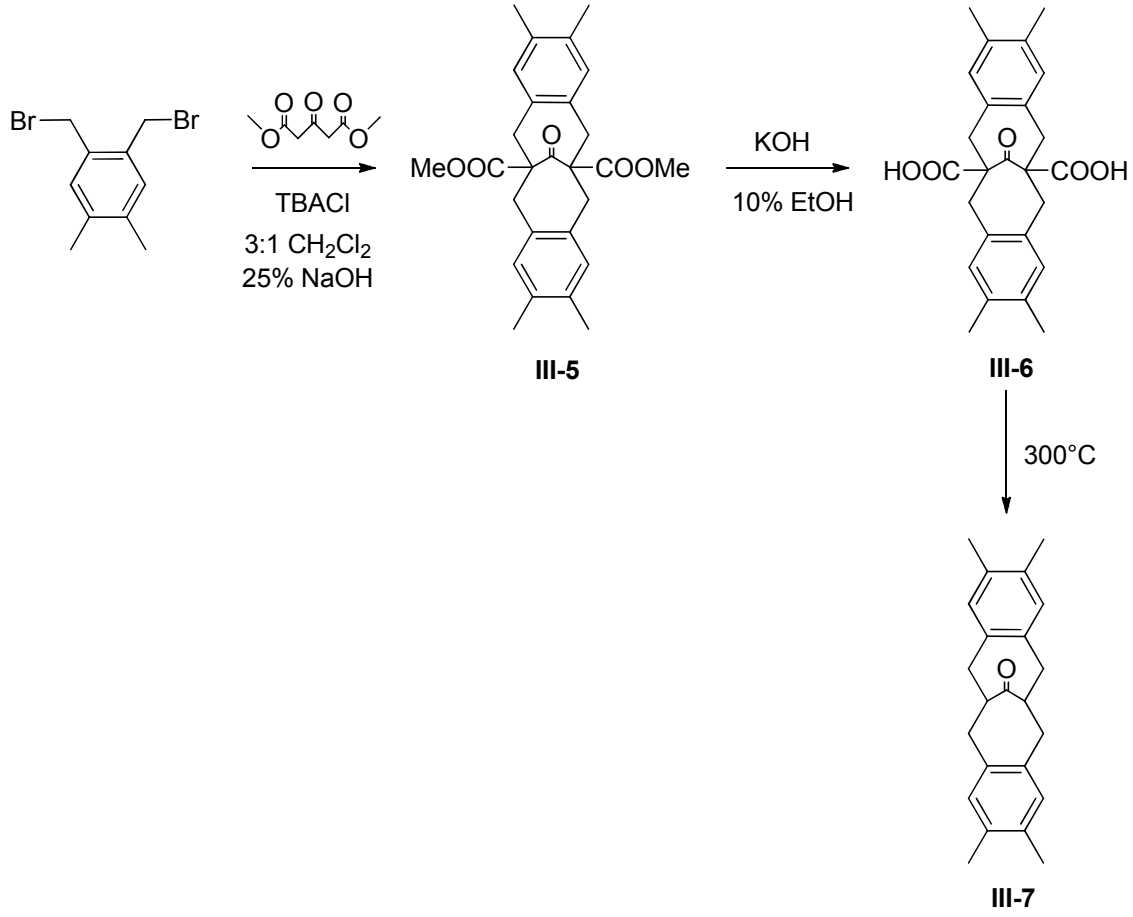


**Figure 3.4.** Synthesis of benzo-fused bicyclo[4.4.1]undecanone.

Saponification of the diester was performed by reaction with excess base (KOH or NaOH) in refluxing aqueous ethanol, Figure 3.4. Addition of water and acidification with conc. HCl resulted in precipitation of the diacid. Filtration and recrystallization from acetone followed by drying under reduced pressure afforded the diacid **III-6** in good yields (90%). In 30% ethyl acetate/hexanes, the $R_f$ value of **III-6** was zero, consistent with the formation of a polar product. The benzo-fused bicyclo[4.4.1]undecanone **III-7** was synthesized by decarboxylation of **III-6** at ca. 300 °C using a heatgun. The pyrolysis on large scale resulted in a large amount of char and lower yields of product, possibly to uneven heating. Performing the reaction on small scale (~100 mg) provided the best results. Purification was performed by passing a solution (30% ethyl acetate/70% hexanes) of crude product in through a short silica plug to afford the desired ketone **III-7** as a white solid in good yields (80-90%).

### 3.3.3. Ketal-Capped Benzo-fused Bicyclo[4.4.1]undecane

The ketalization of the benzo-fused ketone **III-7** provides a suitable scaffold to examine π-π interactions between benzene rings stacked on top one another. Reaction of ketone **III-7** with excess ethylene glycol and *para*-toluenesulfonic acid (*p*-TSA) in benzene afforded the ethylene-ketal **III-8**, Figure 3.5. The ethylene-ketal is acid sensitive and precautions were taken to avoid ring opening of the ketal moiety. The solvent was evaporated under reduced pressure and flushed through short plug of silica gel which was neutralized with 10% triethylamine/90% hexanes. Upon removal of the solvent, pure ethylene-ketal was obtained by recrystallization of the residue from hexanes. NMR analysis of ethylene-ketal was performed in deuterated chloroform which was dried over molecular sieves. The ethylene-ketal decomposes if kept in a chlorinated solvent for a long time. Typical yields for the ketalization were quantitative (>95%).

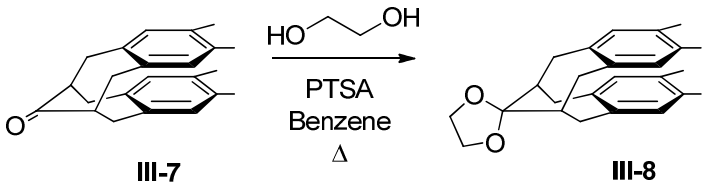


**Figure 3.5.** Synthesis of ethylene ketal-dibenzo[*c*,*h*]bicyclo[4.4.l]undeca-3,8-dien-ll-one.

### 3.3.4. Thioacetal-Capped Benzo-Fused Bicyclo[4.4.1]undecane

Treatment of ketone **III-7** with 1,2-ethanedithiol and boron trifluoride-etherate in acetic acid at room temperature provided thio-ketal, **III-9**, in good yields (>80%), Figure 3.6.[9] Filtration followed by trituration with hot hexanes provided the pure thio-ketal. The thio-ketal was stable to water and acidic conditions.

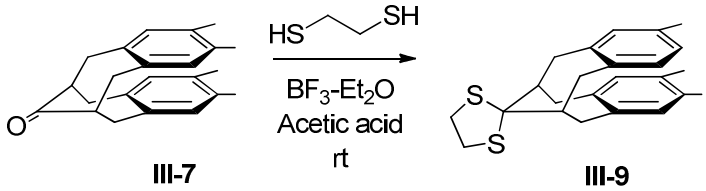


**Figure 3.6.** Synthesis of thio ketal-dibenzo[*c*,*h*]bicyclo[4.4.l]undeca-3,8-dien-ll-one.

### 3.3.5. Sulfone- Capped Benzo-Fused Bicyclo[4.4.1]undecane

The thio-ketal was subjected to oxidation using *meta*-chloroperoxybenzoic acid (*m*CPBA) in $CH_2Cl_2$ at room temperature for to obtain the desired sulfone-ketal, **III-10**, Figure 3.7.[16] Thin layer chromatography showed a distinct $R_f$ value for the sulfone compared to the starting material. Removal of solvent under reduced pressure followed by column chromatography (30% ethyl acetate/70% hexanes) afforded pure sulfone. Typical yields for this oxidation step were ca. 90%.

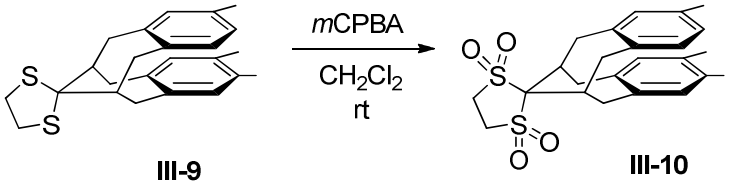


**Figure 3.7.** Synthesis of sulfone ketal-dibenzo[c,h]bicyclo[4.4.l]undeca-3,8-dien-ll-one.

### 3.3.6. Structural Characterization: $^{1}$H NMR and $^{13}$C NMR Spectroscopy

In the $^{1}$H NMR spectrum of ketone **III-7**, the eight benzylic and two bridgehead protons show up as a broad signal which ranges from 2.4-4.0 ppm, Figure 3.8. The twelve methyl protons present on a bicyclic core and four aromatic protons appear as a broad singlet at 2.19 and 6.91 ppm respectively. It confirms that the bicyclic core exhibits conformational flexibility at room temperature due to possible chair or boat conformations.

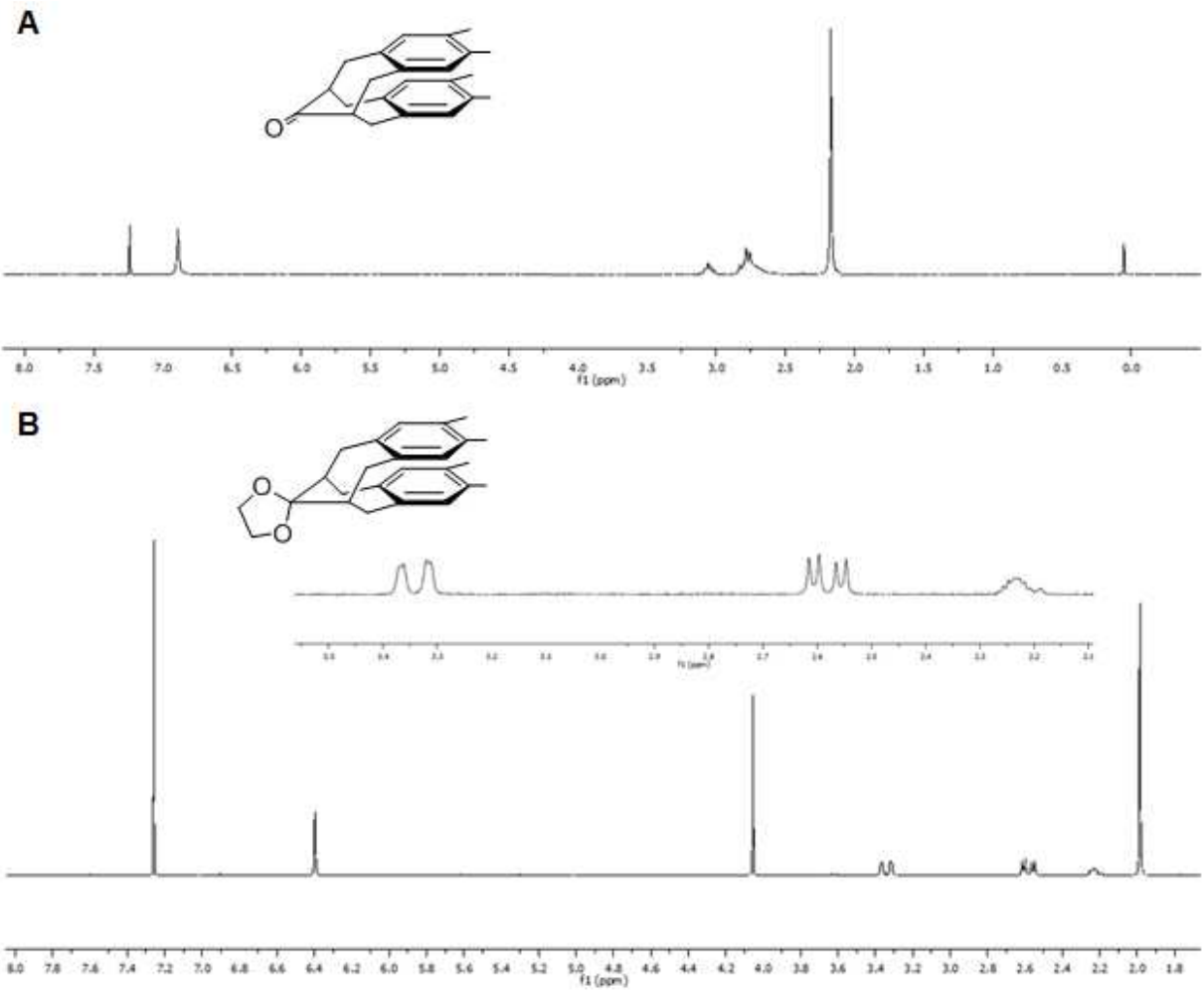


**Figure 3.8.** $^{1}$H NMR (300 MHz, $CDCl_3$): A, ketone **III-7**; and B, ethylene ketal **III-8**.

Upon conversion of ketone **III-7** to ethylene-ketal **III-8**, the $^{1}$H NMR spectrum showed the existence of a single pseudo chair-pseudo chair conformation of bicyclic core. There is an upfield shift for the aromatic protons (6.40 ppm) compared to ketone **III-7** (6.91 ppm). The benzylic protons appear as a pair of doublet of doublets (pseudo-axial: 3.34 ppm, $J$ = 15, 2 Hz; pseudo-equatorial: 2.58 ppm, $J$ = 15, 6 Hz), Figure 3.8. The two bridgehead protons of ethylene-ketal appear as a broad multiplet at 2.22 ppm and are shifted upfield compared to the signal for those protons in ketone **III-7** (3.07 ppm). The twelve methyl protons present on a core are shifted upfield and appear as a sharp singlet at 1.98 ppm. The upfield shift observed for the ethylene-ketal is consistent with π-stacking of the benzene rings leading to chemical shift anisotropy by virtue of ring current effect.

Similar observations were made for the $^{1}$H NMR spectra of thio-ketal and sulfone-ketal which confirms the pseudo chair-pseudo chair conformation of bicyclic core, Figure 3.9.

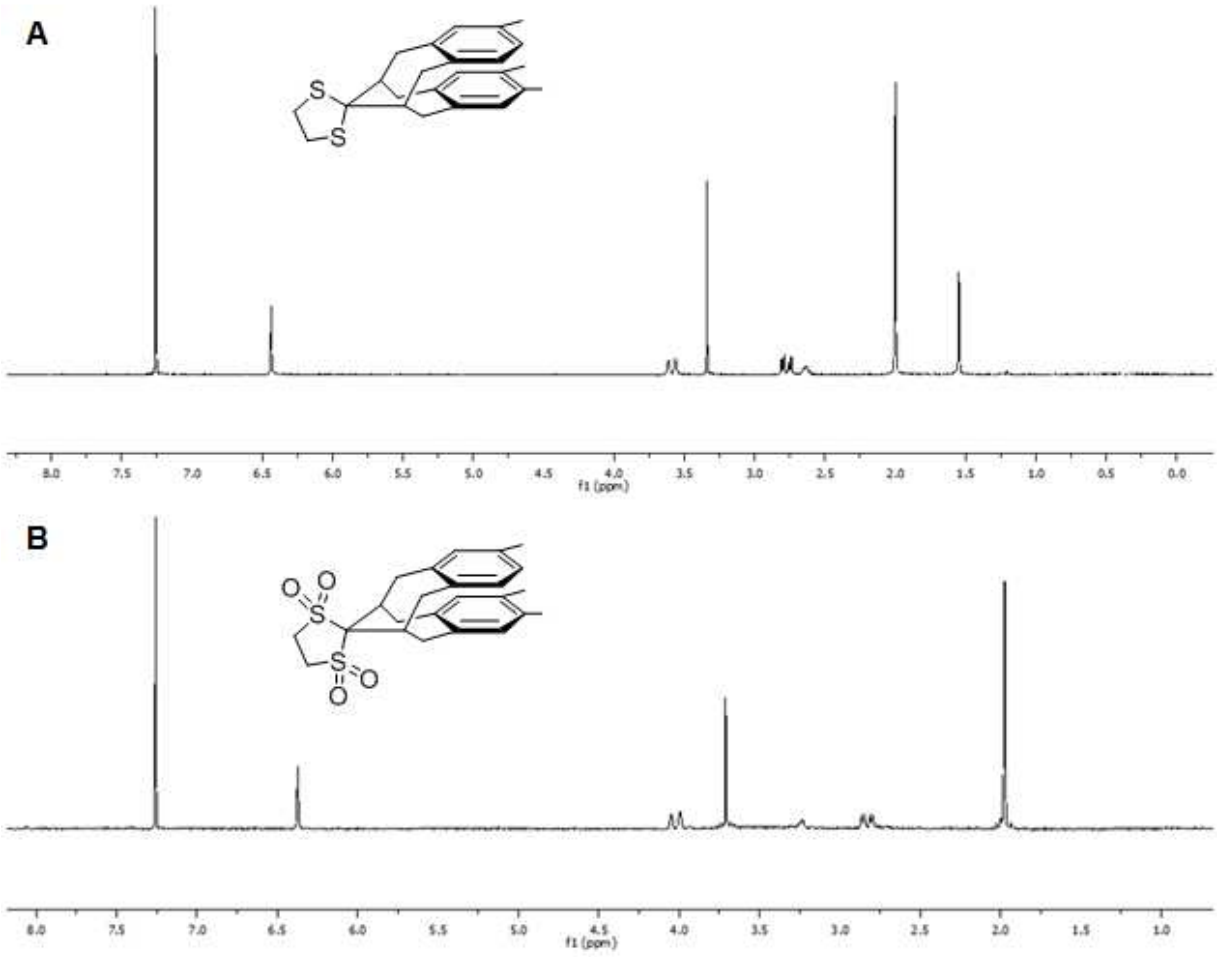


**Figure 3.9.** $^{1}H$ NMR (300 MHz, $CDCl_3$): A, thio-ketal **III-9**; and B, sulfone-ketal **III-10**.

The $^{13}C$ NMR spectrum of ethylene-ketal **III-8** shows the absence of signal from the carbonyl that was present in ketone **III-7** at 216.2 ppm, Figure 3.10. The broad signal for aromatic (131.8 ppm) and benzylic (34.7 ppm) carbons in **III-7** became sharp upon ketalization. In addition, the upfield shift was observed for the bridgehead carbon signal (ethylene-ketal, thio-ketal and sulfone-ketal) due to the presence of a single pseudo chair-pseudo chair conformation of bicyclic core which leads to a stacking between two benzene rings.

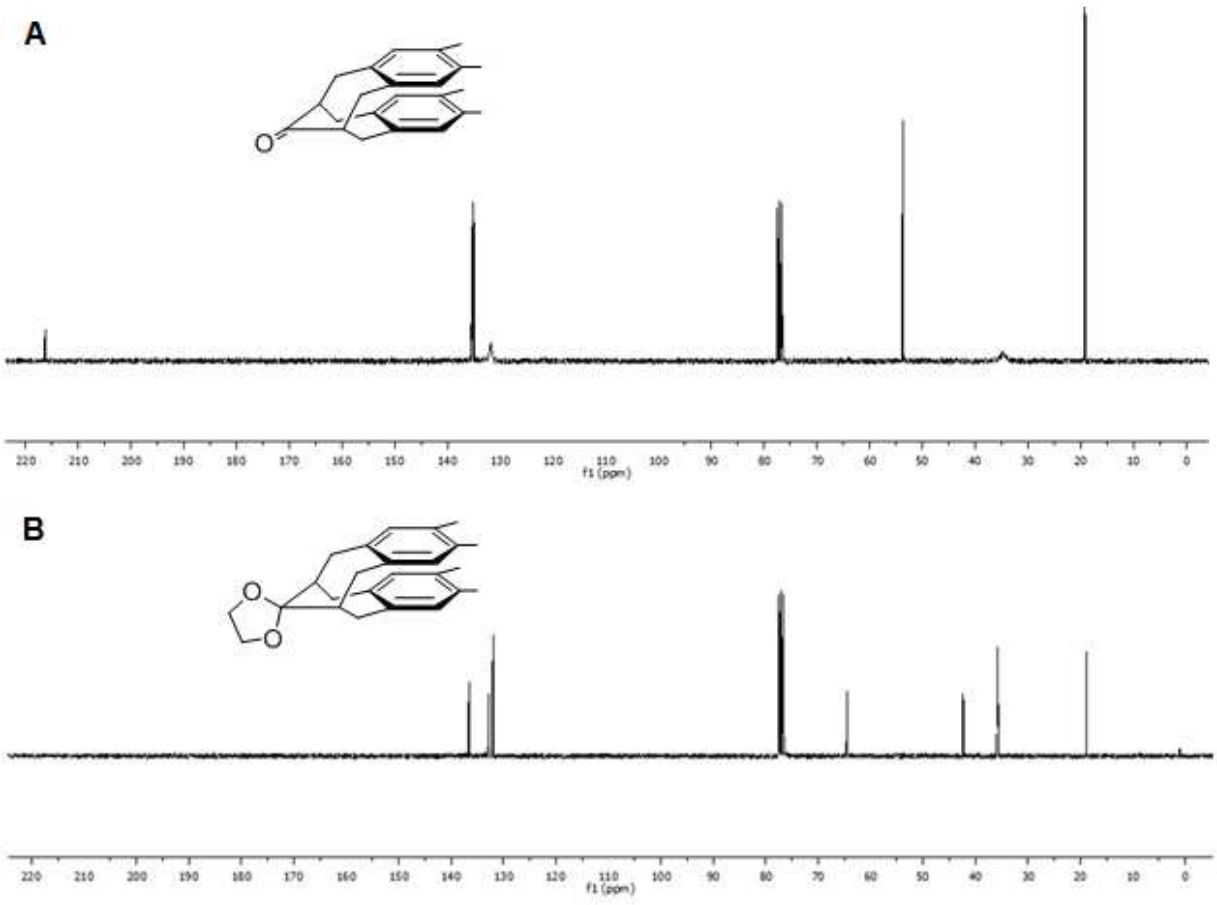


**Figure 3.10.** $^{13}C$ NMR (75 MHz, $CDCl_3$): A, ketone **III-7**; and B, ethylene-ketal **III-8**.

Similar observations were made for the $^{13}C$ NMR spectra of thio-ketal and sulfone-ketal which confirms the pseudo chair-pseudo chair conformation of bicyclic core, Figure 3.11.

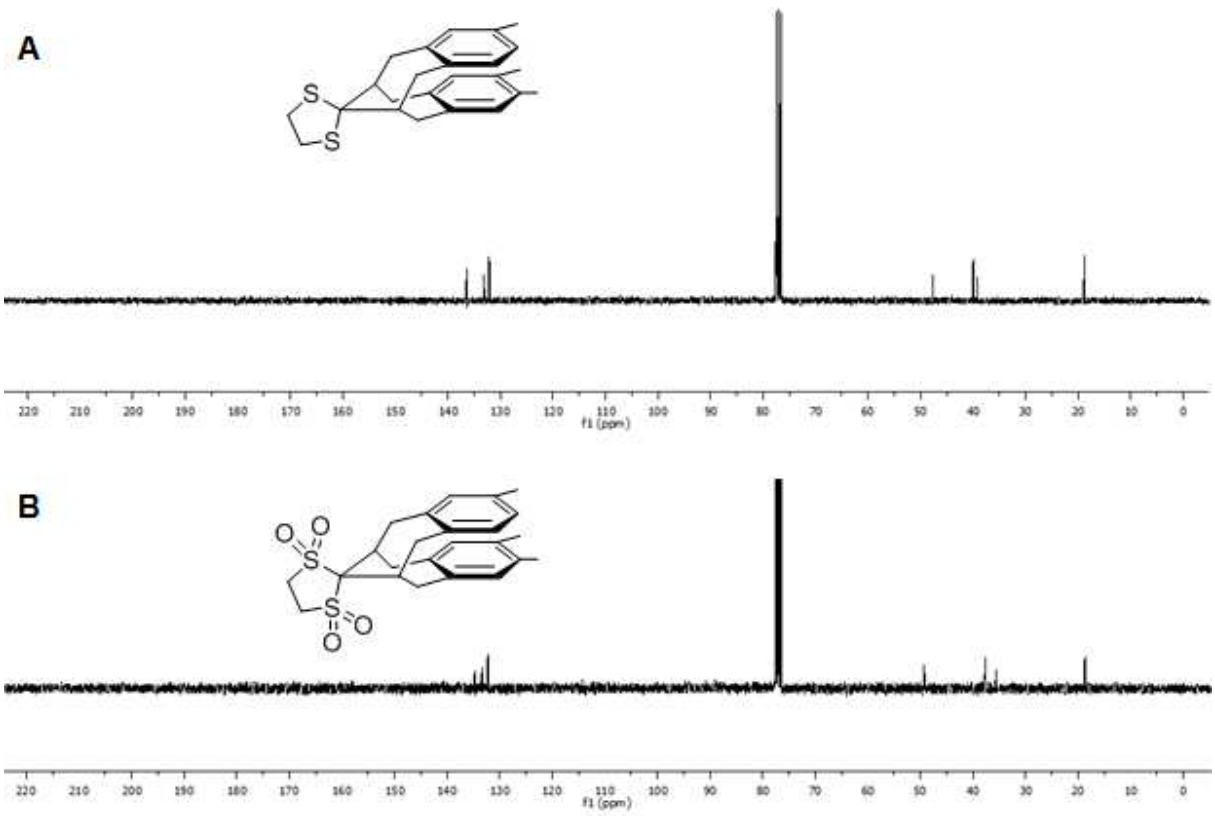


**Figure 3.11.** $^{13}C$ NMR (75 MHz, $CDCl_3$): A, thio-ketal **III-9**; and B, sulfone-ketal **III-10**.

### 3.3.7. X-ray Crystal Structure Analysis

The X-ray crystal structure of ketal **III-8** confirms that bicycloundecanone core adopts a pseudo chair-pseudo chair conformation with a cofacially stacked arrangement of the fused benzene rings. The distance between the centers of the stacked benzene rings ($d_1$) is 3.38 Å, Figure 3.12. The benzene rings are titled at an angle ($\theta_1$) of 16.8° with respect to one another: The inner pairs of aromatic carbon atoms (i.e., those fused to the bicyclic structure) are 3.03 Å apart, whereas the outer pair (methyl substituted) are held at a distance of 3.74 Å. Thus, this conformation is similar to that reported by Mataka for the compound lacking the methyl substituents ($d_1$ = 3.56 Å; $\theta_1 = 25^0$).

The coupling constants for the benzylic protons could be estimated by the Karplus equation:[17]

$$J_{HH'} = A + B \cos \theta + C \cos^2 \theta$$

Where A, B and C are constants a carbon bond and θ is the dihedral angle between the two protons.

The values of coupling constant derived by using Karplus equation are in good agreement with the values obtained by $^1$H NMR analysis. The dihedral angles between bridgehead and benzylic protons determined from the crystallographic data are consistent with the coupling constants obtained from $^1$H NMR analysis of solutions of the ketal: The 6 Hz coupling constant between the bridgehead and equatorial benzylic hydrogens is consistent with dihedral angle of 51°, and the 45° dihedral angle the bridgehead and axial positions results in a 2 Hz coupling.

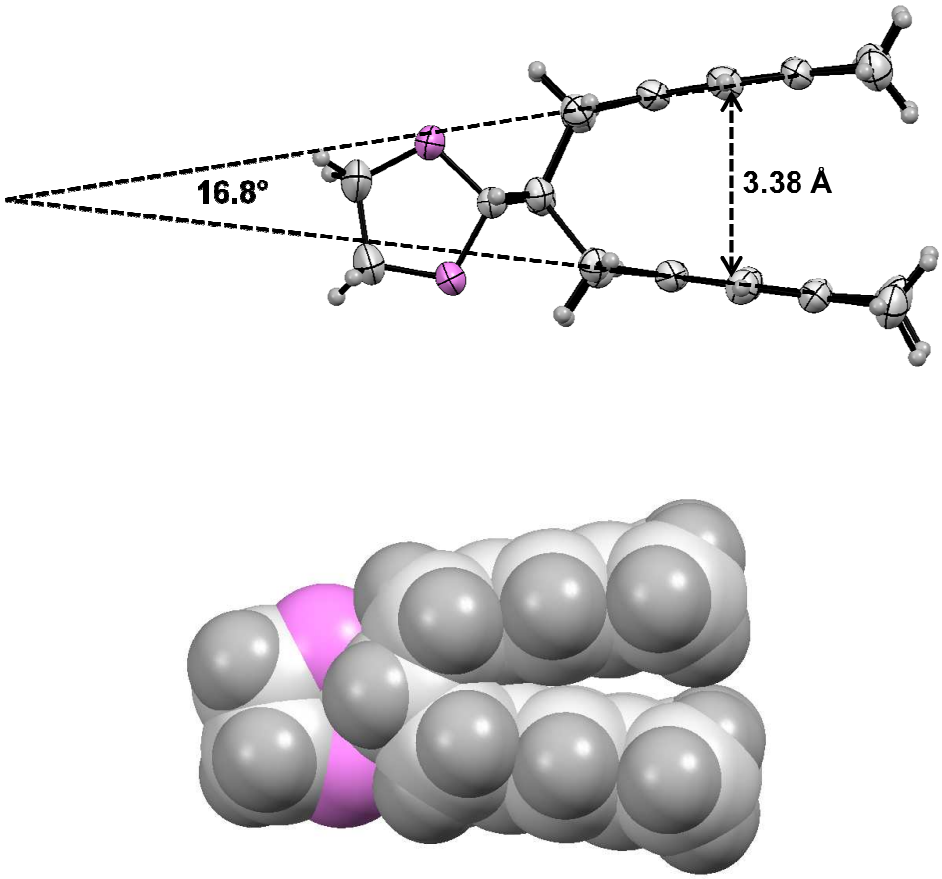


**Figure 3.12.** X-ray crystal structure of ethylene-ketal **III-8** (sideview).

For sulfone-ketal, the distance between the centers of the stacked benzene rings ($d_1$) is 3.41 Å, Figure 3.13. The benzene rings are titled at an angle ($\theta_1$) of 16.8° with respect to one another: The inner pairs of aromatic carbon atoms (i.e., those fused to the bicyclic structure) are 3.03 Å apart, whereas the outer pair (methyl substituted) are held at a distance of 3.81 Å.

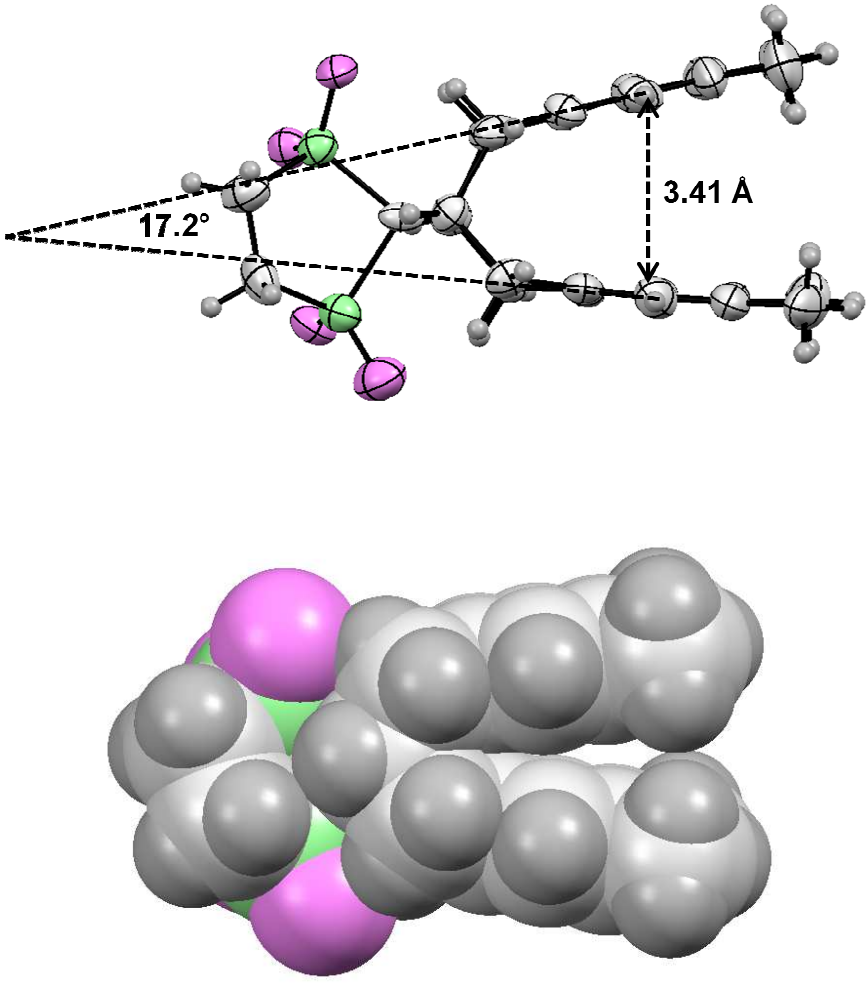


**Figure 3.13.** X-ray crystal structure of sulfone-ketal **III-10** (sideview).

## 3.4. Conclusion

In conclusion, this chapter reported an efficient synthesis of key intermediate 1,2-bis(bromomethyl)-4,5-dimethylbenzene and its utility to prepare the tetramethyl benzo-fused bicyclo[4.4.1]undecane scaffold. The $^{1}$H NMR and X-ray crystal structure analysis confirmed the pseudo chair-pseudo chair conformation of bicyclic core upon ketalization. The distance and angle between two benzene rings of the core remain unaffected irrespective of bulky nature of ketal group. The tetramethyl benzo-fused bicyclo[4.4.1]undecane core will allow us to obtain extended π-stacked compounds by installing suitable conjugated arms on the available unblocked carbons of benzene ring.

### 3.5. References


1. Mataka, S.; Ma, J.; Thiemann, T.; Rudzinski, J. M.; Sawada, T.; Tashiro, M., *Tetrahedron Letters* **1995,** *36* (34), 6105-6108.

2. Mataka, S.; Mimura, T.; Lee, S. T.; Kobayashi, H.; Takahashi, K.; Tashiro, M., *Journal of Organic Chemistry* **1989,** *54* (22), 5237-5241.

3. Mataka, S.; Mitoma, Y.; Sawada, T.; Tashiro, M., *Tetrahedron Letters* **1996,** *37* (1), 65-68.

4. Mataka, S.; Mitoma, Y.; Sawada, T.; Thiemann, T.; Taniguchi, M.; Tashiro, M., *Tetrahedron* **1998,** *54* (20), 5171-5186.

5. Mataka, S.; Mitoma, Y.; Thiemann, T.; Sawada, T.; Taniguchi, M.; Kobuchi, M.; Tashiro, M., *Tetrahedron* **1997,** *53* (9), 3015-3026.

6. Mataka, S.; Shigaki, K.; Sawada, T.; Mitoma, Y.; Taniguchi, M.; Thiemann, T.; Ohga, K.; Egashira, N., *Angewandte Chemie-International Edition* **1998,** *37* (18), 2532-2534.

7. Mataka, S.; Takahashi, K.; Hirota, T.; Takuma, K.; Kobayashi, H.; Tashiro, M., *Journal of the Chemical Society-Chemical Communications* **1985,** (14), 973-973.

8. Mataka, S.; Takahashi, K.; Hirota, T.; Takuma, K.; Kobayashi, H.; Tashiro, M.; Imada, K.; Kuniyoshi, M., *Journal of Organic Chemistry* **1986,** *51* (24), 4618-4622.

9. Mataka, S.; Takahashi, K.; Mimura, T.; Hirota, T.; Takuma, K.; Kobayashi, H.; Tashiro, M.; Imada, K.; Kuniyoshi, M., *Journal of Organic Chemistry* **1987,** *52* (13), 2653-2656.

10. Mataka, S.; Thiemann, T.; Taniguchi, M.; Sawada, T., *Synlett* **2000,** (9), 1211-1227.

11. Helmers, R., *Journal Fur Praktische Chemie* **1972,** *314* (2), 334-&.

12. Farooq, O., *Synthesis-Stuttgart* **1994,** (10), 1035-1036.

13. Lee, S. I.; Park, Y.; Park, J. H.; Jung, G.; Choi, S. Y.; Chung, Y. K.; Lee, B. Y., *Journal of Organic Chemistry* **2006,** *71* (1), 91-96.

14. Kotha, S.; Chavan, A. S., *Journal of Organic Chemistry* **2010,** *75* (12), 4319-4322.

15. da Costa, J. C. S.; Pais, K. C.; Fernandes, E. L.; de Oliveira, P. S. M.; Mendonca, J. S.; de Souza, M. V. N.; Peralta, M. A.; Vasconcelos, T. R. A., *Arkivoc* **2006**, 128-133.

16. Davis, M. A.; Beaulieu, G.; Watson, J. R.; Charest, M. P., *Journal of Medicinal Chemistry* **1966,** *9* (6), 860-&.

17. Karplus, M., *Journal of the American Chemical Society* **1963,** *85* (18), 2870-&.

# CHAPTER 4

# SYNTHESIS AND CHARACTERIZATION OF π-STACKED OLIGO(PHENYLENE ETHYNYLENE)S BASED ON BENZO-FUSED BICYCLO[4.4.1]UNDECANE SCAFFOLD[1]

## 4.1. Introduction

### 4.1.1. Overview

The tetramethyl-dibenzo-fused bicyclo[4.4.1]undecane[1] scaffold explored in Chapter 3 has the potiential to serve as a core to prepare π-stacked conjugated oligomers. In this chapter, we describe the installation of suitable phenylene ethynylene arms onto the core using the Sonogashira cross-coupling condensation reaction[2] to obtain conjugated π-stacked trimer and pentamers. We also prepared the model compounds which resemble a single unstacked tier of the π-stacked compounds. The optical and electrochemical properties of the stacked compounds were compared to that of their unstacked counterparts.

### 4.1.2. Background

To achieve a highly planar chromophore with an extensive overlap of conjugated units and develop a greater understanding of inter-chain communication in tightly packed conjugated chains, we have undertaken a combined experimental and computational study of oligo(phenylene ethynylene)s held in a π-stacked arrangement by a bicyclo[4.4.1]undecane scaffold, e.g., ***st*-[PE$_3$]$_2$**, Figure 4.1. In contrast to the thiophene analogs,[3] these oligo(phenylene

[1] Computational studies described in this chapter were conducted by Dr. Sukrit Mukhopadhyay and Dr. Coropceanu Veaceslav in the group of Dr. Bredas at Georgia Institute of Technology.

ethynylene) chromophores allow conjugated units to have better cofacial overlap over their entire length; this mimics the organization of π-systems in crystals/films of small molecules (e.g., oligoacenes and oligoarylenes) and polymers. This study focuses on the effect of stacking on the electronic properties of planer conjugated oligomers.

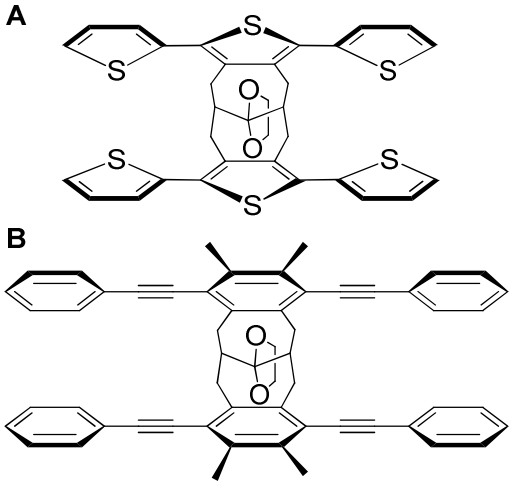


**Figure 4.1.** Stacked conjugated compounds: A, Dithieno-fuzed bicycle[4.4.1]undecane based Stacked oligothiophene, ***st*-[TH$_3$]$_2$** (ref.3); B, Benzo-annelated bicyclo[4.4.1]-undecane based stacked oligo(phenylene ethynylene), ***st*-[PE$_3$]$_2$**.

## 4.2. Experimental procedures

### 4.2.1. General synthetic methods

General procedures and methods are described in Chapter 2.

### 4.2.2. Computational studies were completed by Dr. Sukrit Mukhopadhyay

The geometry optimizations of the unstacked molecules (**$PE_3$** and **$PE_5$**) are performed using both the B3LYP and ωB97X/6-31g* functionals[4] and the 6-31g* basis set. For the stacked molecules, ***st*-$[PE_3]_2$** and ***st*-$[PE_5]_2$**, in order to account for the dispersion interactions between oligomers, the geometries were obtained at the ωB97X-D/6-31g*[5] level of theory. The geometry optimizations have been performed for both gas-phase case and solvent phase case (in $CHCl_3$, using the continuum solvent model). All geometries were confirmed to be minima by additional vibrational frequency calculations. The low-lying excited states (at the gas-phase and solvent phase optimized geometries) have been derived by means of the time dependent density functional theory (TD-DFT) calculations using the ωB97X-D/6-31g* and ωB97X/6-31g* method for the stacked and unstacked molecules, respectively. TD-DFT calculations at the same level of theory as used for the ground state have been also employed to obtain the optimal geometries of the first excited states of both stacked and unstacked systems. All DFT calculations are performed using the Gaussian 09 package.

### 4.2.3. Tetraiodo-dibenzo[*c,h*]bicyclo[4.4.l]undeca-3,8-dien-ll-one

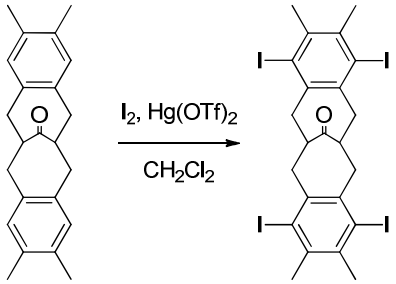


III-7 IV-1

Iodine (0.62 g, 5.0 mmol) was added to a solution of **III-7** (200 mg, 620 μmol) and mercury(II) trifluoromethanesulfonate (1.89 g, 3.72 mmol) in $CH_2Cl_2$ (10 mL) in an oven-dried Shlenk flask. The mixture was stirred for 16 h, and $CH_2Cl_2$ (50 mL) was added. The mixture was filtered and the organic layer was washed with saturated solution of $Na_2S_2O_3$ (50 mL) followed by a saturated solution of KI (50 mL). The organic layer was dried over $MgSO_4$ and the solvent was removed under reduced pressure to give a yellow residue. $^1$H NMR analysis showed the presence of residual hydrogen atoms on aromatic rings. Accordingly, the residue was resubjected to iodination using the same procedure with an additional 0.5 mole equivalent reagents. Following work-up, the residue was triturated with boiling hexane and filtered to give the title compound as a white solid (0.4 g, 74%). m.p. = 216-217 °C. $^1$H NMR (300 MHz, $CDCl_3$): δ 2.40–3.60 (br m, 10H, benzylic and bridgehead), 2.10-2.40 (br s, 12H, Ar–$CH_3$). Low solubility of the product precluded analysis by $^{13}$C NMR spectroscopy. IR (ATR): 2914, 2854, 1711, 1493, 1163, 1007, 881, 738 $cm^{-1}$. MS (MALDI), m/z (%) = 821.8 ($M^+$, 100). HRMS (EI), m/z = Calcd. For $C_{23}H_{24}OI_4$, 821.7802; Found, 821.7810, Δ = 2.4 ppm.

### 4.2.4 1-(4-Iodophenyl)propyn-3-ol

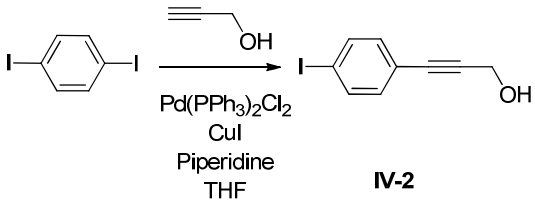


**IV-2**

A solution of 1,4-diiodobenzene (12 g, 36 mmol), $Pd(Ph_3P)Cl_2$ (127 mg, 180 μmol), CuI (69 mg, 0.36 mmol), and propargyl alcohol (1.02 g, 18.2 mmol) in 180 mL (1:1) THF/piperidine solvent mixture under argon were stirred for 12 h. The mixture was diluted with ether (200 mL), washed with sat $NH_4Cl$ (200 mL), and DI water (200 mL). The solvent was removed under reduced pressure and the residue subjected to column chromatography (25% ethyl acetate / 75% hexanes) to afford the title compound as yellow crystals (3.02 g, 64% yield). m.p. = 99-100 ºC. $^1$HNMR (300 MHz, $CDCl_3$): δ 7.40 (dd, *J* = 8.7 Hz, *J* = 161.0, 4H, Ar-H), 4.48 (s, 1H, ≡C-$CH_2$), 4.47 (s, 1H, ≡C-$CH_2$), 1.94 (s, 1H, OH). $^{13}$C NMR (75 MHz, $CDCl_3$): δ 137.4, 133.1, 122.0, 94.5 (Ar-C), 88.6, 84.8 (≡C), 51.6 ($CH_2$); IR (ATR): 3319, 3229, 2917, 2857, 2236, 1575, 1482, 1031, 818 $cm^{-1}$; MS (EI): m/z (%) 257.9 ($M^+$, 100), 103 (60), 77 (35); HRMS calculated for $C_9H_7OI$, 257.95417; found 257.95581, Δ = 6.4 ppm.

### 4.2.5 1-(4-(Phenylethynylene)phenyl)propyn-3-ol

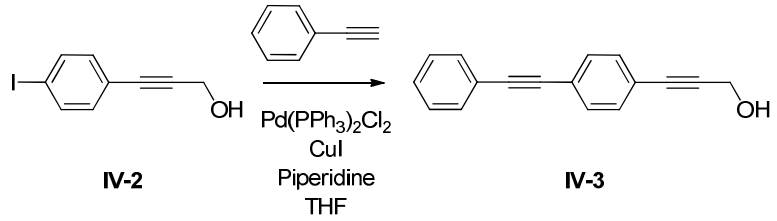


**IV-2** **IV-3**

A solution of 1-(4-iodophenyl)propyn-3-ol (3.58 g, 13.8 mmol), $Pd(Ph_3P)Cl_2$ (97.0 mg, 138 μmol), CuI (26.0 mg, 138 μmol) and phenylacetylene (2.80 g, 27.7 mmol) in 100 mL (1:1) THF/piperidine solvent mixture under argon were stirred for 12 h. The mixture was diluted with $Et_2O$ (100 mL), washed with saturated solution of $NH_4Cl$ (100 mL) and DI water (100 mL). The solvent was removed under reduced pressure and the residue subjected to column chromatography (25% ethyl acetate/75% hexanes) to afford the title compound as yellow crystals (3.1 g, 95% yield). m.p. = 123-124 ºC. $^1$H NMR (300 MHz, $CDCl_3$): δ 7.30-7.55 (m, 9H, Ar-H), 4.5 (s, 2H, $CH_2$). $^{13}$C NMR (75 MHz, $CDCl_3$): δ = 134.4, 133.1, 131.6, 131.3, 123.9, 121.8, 114.7, 114.6 (Ar-C), 91.5, 88.8, 87.6, 85.5 (≡C), 68.1 ($OCH_2$). IR (ATR): 3319, 2953, 2920, 2870, 1605, 1512, 1246, 1027, 835 $cm^{-1}$. MS (EI): m/z (%) 232.0 ($M^+$, 100), 202.0 (55). HRMS calculated for $C_{17}H_{12}O$, 232.0888; found 232.0887, Δ = 0.1 ppm.

### 4.2.6 (4-(Phenylethynyl)phenyl)acetylene[6]

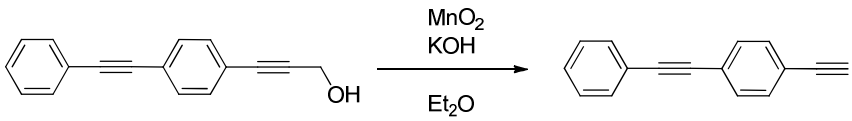


IV-3 IV-4

Manganese dioxide (2.25 g, 25.8 mmol), and potassium hydroxide (1.45 g, 25.8 mmol) were added in four separate portions to 1-(4-(phenylethynylene)phenyl)propyn-3-ol (3.0 g, 12.9 mmol) in $Et_2O$ (100 mL) stirred at room temperature. The reaction was monitored by TLC until no more starting material was observed. The reaction was diluted with $Et_2O$ (300 mL) and filtered through a fritted funnel. The solvent was removed under reduced pressure to afford the title compound as a yellow solid (0.95 g, 48%). m.p. = 97-98 ºC. $^1$H NMR (300 MHz, $CDCl_3$): δ 7.32-7.62 (m, 9H, Ar-H), 3.17 (s, 1H, ≡C-H). $^{13}$C NMR (75 MHz, $CDCl_3$): δ 132.1, 131,6, 131.5, 128.5, 128.4, 123.8, 123.0, 121.4 (Ar-C), 91.5, 88.8, 83.3, 78.9 (≡C). IR (ATR): 3272, 3036, 2927, 2870, 2210, 1605, 1512, 1246, 1027, 838 $cm^{-1}$. MS (EI): m/z (%) 202.0 ($M^+$, 100), 101 (10); HRMS calculated for $C_{16}H_{10}$, 202.0783; found 202.0783, Δ = 0 ppm.

### 4.2.7 2,3,5,6-Tetramethyl-1,4-bis(phenylethynyl)benzene, $PE_3$

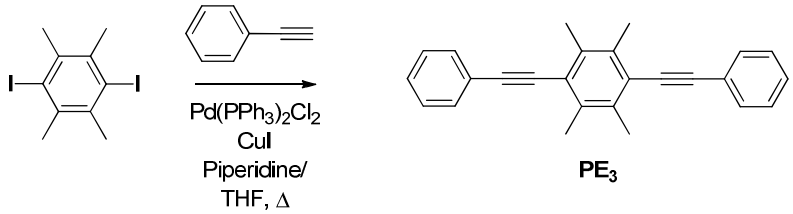


A solution of 2,3,5,6-tetramethyl-1,4-diiodobenzene (500 mg, 1.30 mmol), $Pd(Ph_3P)Cl_2$ (50 mg, 70 μmol), CuI (15 mg, 70 μmol) and phenylacetylene (450 mg, 4.00 mmol) in a 1:1 v/v mixture of THF and piperidine (10 mL) was stirred for 36 h under Ar. $CH_2Cl_2$ (50 mL) was added and the solution was washed with sat. $NH_4Cl$ (100 mL) and $H_2O$ (100 mL). The solvent was removed under reduced pressure and the residue was flushed through a plug of silica gel ($CH_2Cl_2$) followed by trituration from hot hexane to afford the title compound as a yellow solid (400 mg, 93% yield). m.p. = 218-219 ºC. $^1$H NMR (300 MHz, $CDCl_3$): δ 7.53–7.59 (m, 4H, Ar–H), 7.33–7.38 (m, 6H, Ar–H), 2.50 (s, 12H, Ar–$CH_3$). $^{13}$C NMR (75 MHz, $CDCl_3$): δ 135.7, 131.4, 128.4, 128.1, 123.9, 123.3 (aromatic), 98.1, 88.6 (–C≡C–), 18.4 (Ar–$CH_3$). IR (ATR): 3066, 3036, 2927, 1598, 1495, 1017, 752 $cm^{-1}$. MS (EI): m/z (%) 334.1 ($M^+$, 100), 167.1 (20). HRMS calculated for $C_{26}H_{22}$, 334.1722; found 334.1753, Δ = 9.3 ppm.

### 4.2.8 2,3,5,6-Tetramethyl-1,4-(bis(4-phenylethynyl)phenylethynyl)benzene, $PE_5$

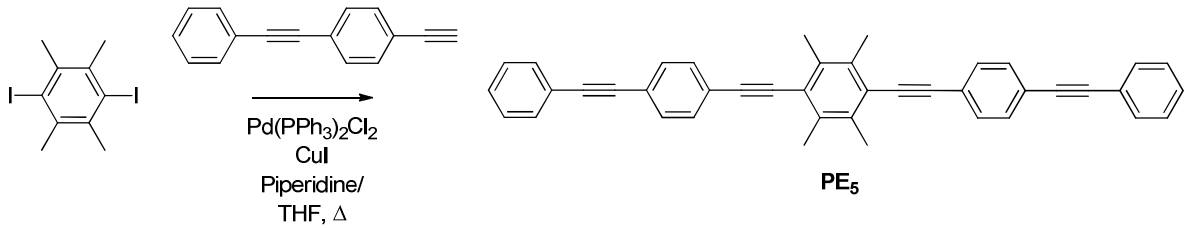


A solution of 1,4-diiodo-2,3,5,6-tetramethylbenzene (250 mg, 650 μmol), $Pd(Ph_3P)Cl_2$ (23 mg, 30 μmol), CuI (6.0 mg, 30 μmol) and (4-(phenylethynyl)phenyl)acetylene (400 mg, 2.00 mmol) was treated according to the procedure provided above for the preparation of **$PE_3$**. The reaction mixture was cooled to room temperature and poured into MeOH (150 mL). The precipitated solid was removed by filtration and recrystallized from THF to afford a yellow solid (330 mg, 96% yield). m.p. = 254-255 ºC. $^1$H NMR ($CDCl_3$): δ 7.50–7.59 (m, 12H, Ar–H), 7.31–7.40 (m, 6H, Ar–H), 2.51 (s, 12H, Ar–$CH_3$). The low solubility of the product precluded analysis by $^{13}$C NMR spectroscopy. IR (ATR, neat): 3072, 3024, 2936, 1585, 1487, 1024, 751 cm$^{-1}$. MS (EI): m/z (%) 534.2 ($M^+$, 100), 267.2 (10). HRMS calculated for $C_{42}H_{30}$, 534.2348; found 534.2340, Δ = 1.5 ppm.

### 4.2.9 Tetra(phenylacetylene)-dibenzo[*c,h*]bicyclo[4.4.1]undeca-3,8-dien-11-one, [$PE_3$]$_2$

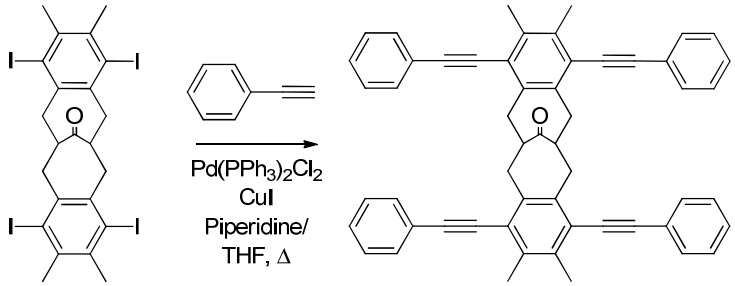


**IV-1** **[$PE_3$]$_2$**

A solution of tetraiodide (350 mg, 420 μmol), $Pd(PPh_3)_2Cl_2$ (56 mg, 80 μmol), CuI (16 mg, 80 μmol) and $PPh_3$ (21 mg, 80 μmol) in a 1:1 v/v mixture of DIPA and THF (5 mL) was degassed using three cycles of freeze-pump-thaw and backpurged with argon. Phenylacetylene (257 mg, 2.52 mmol) was added dropwise and the mixture was heated at reflux for 48 h. $CH_2Cl_2$ (50 mL) was added and the solution was washed sequentially with saturated aqueous $NH_4Cl$ (50 mL) and $H_2O$ (50 mL). The organic layer was dried over $MgSO_4$ and the solvent was removed under reduced pressure. The residue was dissolved in $CH_2Cl_2$ (5 mL) and flushed through a silica gel column with $CH_2Cl_2$. The solvent was removed under reduced pressure and the residue was recrystallized from THF to afford the title compound as a yellow solid (150 mg, 49%). m.p. = 309-310 °C. $^1$H NMR (300 Hz, $CDCl_3$): δ 7.20-7.80 (m, 20H, Ar–H), 2.82-4.30 (br m, 10H, benzylic and bridgehead), 2.40-2.70 (br s, 12H, Ar–$CH_3$). The low solubility of the product precluded analysis by $^{13}$C NMR spectroscopy. IR (ATR): 2997, 2954, 2877, 1736, 1465, 1110, 943 cm$^{-1}$. MS (MALDI), m/z (%) = 718.4 ($M^+$, 80). HRMS (EI), m/z = Calcd. For $C_{55}H_{42}O$, 718.3235; Found, 718.3192, Δ = 6.0 ppm.

### 4.2.10 Ethylene acetal of tetra(phenylethynyl)-dibenzo[*c,h*]bicyclo[4.4.1]undeca-3,8-dien-11-one, *st*-$[PE_3]_2$

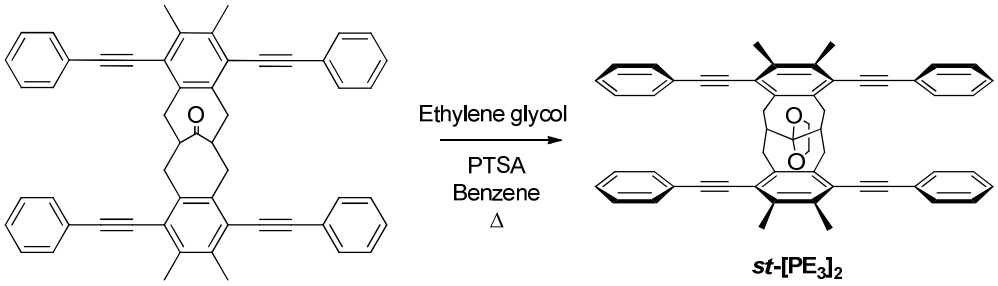


$[PE_3]_2$ *st*-$[PE_3]_2$

A solution of **$[PE_3]_2$** (100 mg, 140 μmol), ethylene glycol (200 mg, 3.23 mmol), *p*-toluenesulfonic acid (1 mg) in benzene (50 mL) was heated at reflux for 48 h with removal of water via a Dean-Stark trap. The solvent was evaporated under reduced pressure, and the residue was subjected to column chromatography ($CH_2Cl_2$) followed by trituration from hot hexanes to give the title compound as a yellow solid (95 mg, 84%). m.p. = 295-296 °C. $^1$H NMR (300 Hz, $CD_2Cl_2$): δ 7.28-7.38 (m, 8H, Ar–H), 7.08-7.24 (m, 12H, Ar–H), 4.10 (s, 4H, –$OCH_2CH_2O$–) 3.79 (dd, 4H, *J* = 16, 6 Hz, equatorial benzylic), 3.30 (dd, 4H, *J* = 15, 2 Hz, axial benzylic), 2.45-2.58 (m, 2H, bridgehead), 2.38 (s, 12 H, Ar–$CH_3$). $^{13}$C NMR (75 MHz, $CDCl_3$): δ 218.1 (C=O), 154.2, 152.1, 139.3, 138.6, 134.2, 133.2, 131.5 (aromatic), 71.1, 70.5 (–$OCH_2$–), 52.2 (bridgehead), 39.4, 35.0 (benzylic), 19.2 (methyl). IR (ATR): 2988, 2938, 2877, 1608, 1502, 1105, 1077, 987 cm$^{-1}$. MS (MALDI), m/z (%) = 762.3 ($M^+$, 80). HRMS (EI), m/z = Calcd. For $C_{57}H_{46}O_2$, 762.34978; Found, 762.3339, Δ = 20.8 ppm.

### 4.2.11 Tetra((4-phenylethynyl)phenylethynyl))-dibenzo[*c*,*h*]bicyclo[4.4.1]undeca-3,8-dien-11-one, $[PE_5]_2$

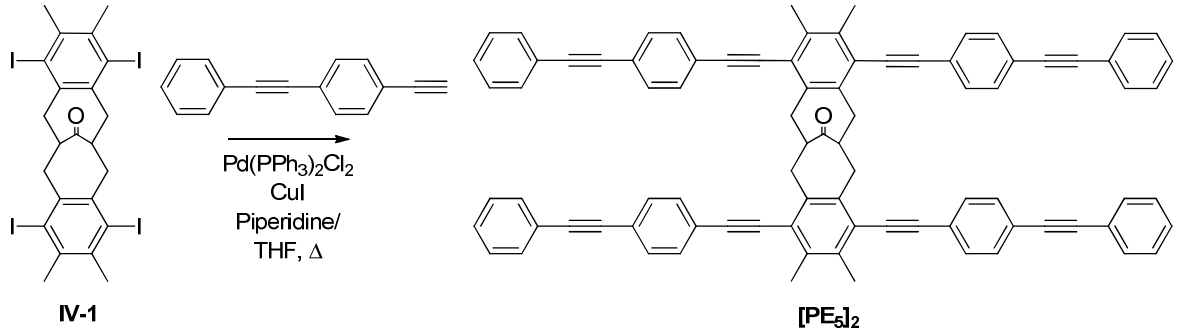


**IV-1** **$[PE_5]_2$**

(4-(Phenylethynyl)phenyl)acetylene (430 mg, 2.20 mmol) was added to a solution of tetraiodide (300 mg, 0.36 mmol), $Pd(PPh_3)_2Cl_2$ (56 mg, 80 μmol), CuI (16 mg, 80 μmol) and $PPh_3$ (21 mg, 80 μmol) in a 1:1 v/v mixture of DIPA/THF (10 mL) according the procedure described above for the preparation of **$[PE_3]_2$**. The reaction mixture was cooled to room temperature and poured into MeOH (200 mL). The precipitated solid was removed by filtration and recrystallized from THF to afford the title product as a green solid (120 mg, 30%). m.p. = 380 °C (decomposes). $^1$H NMR (300 Hz, $C_2D_2Cl_4$, 80°C): δ 7.20–7.70 (m, 36H, Ar-H), 2.82–4.20 (br m, 10H, benzylic and bridgehead), 2.40–2.70 (br s, 12 H, Ar–$CH_3$). The low solubility of the product precluded analysis by $^{13}$C NMR spectroscopy. IR (ATR): 2992, 2958, 2862, 1720, 1475, 1103, 932 cm$^{-1}$. MS (MALDI), m/z (%) = 1118.4 ($M^+$, 80). HRMS (EI), m/z = Calcd. For $C_{87}H_{58}O$, 1118.449; Found, 1118.439, Δ = 9.0 ppm.

### 4.2.12 Ethylene acetal of tetra((4-phenylethynyl)phenylethynyl)) dibenzo[*c*,*h*]bicyclo[4.4.1]undeca-3,8-dien-11-one, *st*-[$PE_5$]$_2$

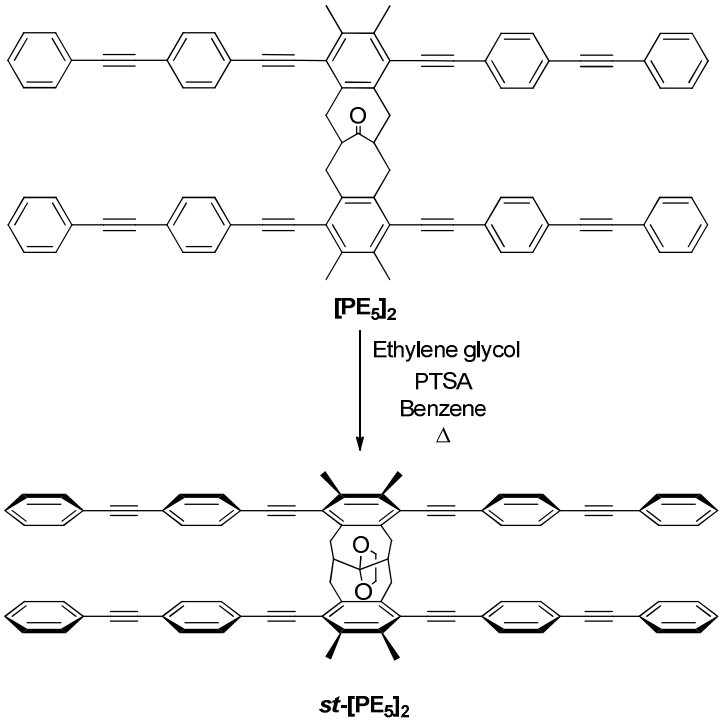


**[$PE_5$]$_2$** (0.10 mg, 90 μmol) was subjected to ketalization with ethylene glycol (200 mg, 3.23 mmol) in the presence of *p*-toluenesulfonic acid (1 mg) in benzene (50 mL) according to the procedure provided above for the preparation of ***st*-[$PE_3$]$_2$** to give the title compound as a green solid (85 mg, 82%). m.p. = 354 °C (decomposes). $^1$H NMR (300 MHz, $CDCl_3$, 60 °C): δ 7.40–7.47 (m, 8H, Ar–H), 7.16–7.34 (m, 28H, Ar–H), 4.18 (s, 4H, –$OCH_2CH_2O$–) 3.84 (dd, 4H, *J* = 15, 6 Hz, equatorial benzylic), 3.30 (dd, 4H, *J* = 15, 2 Hz, axial benzylic), 2.45–2.58 (m, 2 H, bridgehead), 2.38 (s, 12 H, Ar–$CH_3$). The low solubility of the product precluded analysis by $^{13}$C NMR spectroscopy. IR (ATR): 2987, 2934, 2867, 1615, 1510, 1109, 1065, 988 cm$^{-1}$. MS (MALDI), m/z (%) = 1162.4 ($M^+$, 80). HRMS (EI), m/z = Calcd. For $C_{89}H_{62}O_2$, 1162.47498; Found, 1162.4546, Δ = 17.5 ppm.

### 4.2.13 Tetra(hexyloxyphenylacetylene)-dibenzo[*c*,*h*]bicyclo[4.4.1]undeca-3,8-dien-11-one, [$PE_3$-OHex]$_2$

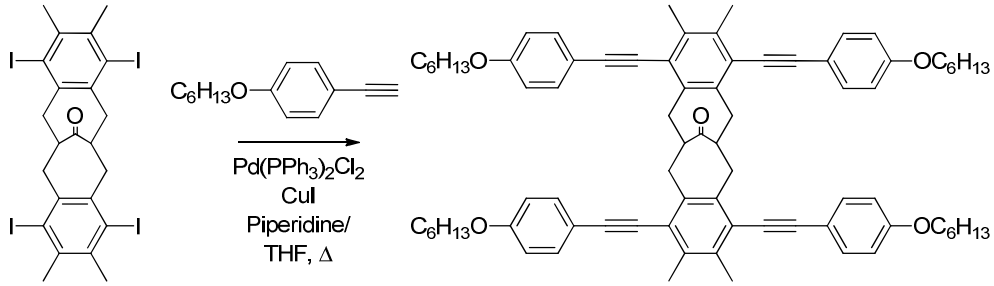


A solution of tetraiodide (300 mg, 420 μmol), $Pd(PPh_3)_2Cl_2$ (60 mg, 80 μmol), CuI (20 mg, 80 μmol) and $PPh_3$ (20 mg, 80 μmol) in a 1:1 v/v mixture of DIPA and THF (8 mL) was degassed using three cycles of freeze-pump-thaw and backpurged with argon. Hexyloxyphenylacetylene (620 mg, 2.88 mmol) was added dropwise and the mixture was heated at reflux for 48 h. The reaction mixture was cooled to room temperature and poured into MeOH (150 mL). The precipitate was filtered, dissolved in $CH_2Cl_2$ (5 mL) and flushed through a silica gel plug with $CH_2Cl_2$. The solvent was removed under reduced pressure and the residue was recrystallized from THF to afford the title compound as a yellow solid (200 mg, 48%). m.p. = 271-272 $^{\circ}$C. $^1$H NMR (300 MHz, $CDCl_3$): δ 7.38 (d, 8H, *J* = 6 Hz Ar–H), 6.79 (d, 8H, *J* = 6 Hz Ar–H), 3.97 (m, 8H, *J* = 3 Hz $OCH_2$), 2.82-3,52 (br m, 10H, benzylic and bridgehead), 2.49 (br s, 12H, Ar–$CH_3$), 1.75-1.85 (m, 8H, $CH_2$), 1.30-1.55 (m, 32H, $CH_2$), 0.85-1.00 (m, 12H, $CH_3$). $^{13}$C NMR (75 MHz, CDCl3): δ 212.2 (carbonyl), 159.4, 137.6, 133.0, 115.6, 114.8 (Ar-C), 86.8 (Alkyne) 68.3 ($OCH_2$), 53.7, 52.3 (bridgehead), 31.9, 29.5 (benzylic), 25.9, 22.8 (methylene), 18.9, 14.3 (methyl). IR (ATR): 2923, 2857, 1701, 1598, 1509, 1256, 1173, 1027, 828 cm$^{-1}$. MS (MALDI), m/z (%) = 1118.7 ($M^+$, 100). HRMS (EI), m/z = Calcd. For $C_{79}H_{90}O_5$, 1118.679; Found, 1118.672, Δ = 6.4 ppm.

### 4.2.14 Ethylene acetal of tetra(hexyloxyphenylacetylene)-dibenzo[*c*,*h*]bicyclo[4.4.1]undeca-3,8-dien-11-one, *st*-[$PE_3$-OHex]$_2$

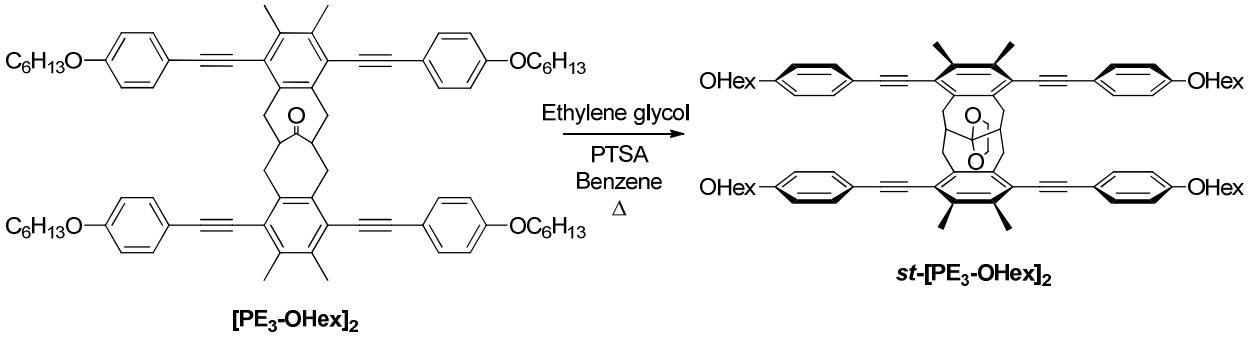


[$PE_3$-OHex]$_2$ *st*-[$PE_3$-OHex]$_2$

**[$PE_3$-OHex]$_2$** (150 mg, 125 μmol) was subjected to ketalization with ethylene glycol (200 mg, 3.23 mmol) in the presence of *p*-toluenesulfonic acid (1 mg) in benzene (50 mL) according to the procedure described above for the synthesis of ***st*-[$PE_3$]$_2$**. The product obtained from column chromatography was triturated with hexanes to give the title compound as a yellow solid. (130 mg, 83%). m.p. = 258-259 °C. $^1$H NMR (300 MHz, $CDCl_3$): δ 7.19 (d, 8H, *J* = 6 Hz Ar–H), 6.60 (d, 8H, *J* = 6 Hz Ar–H), 4.07 (s, 4H, $OCH_2CH_2O$), 3.86 (t, 8H, *J* = 6 Hz $OCH_2$), 3,73 (dd, 4H, *J* = 12, 3 Hz, equatorial benzylic), 3.25 (d, 4H, *J* = 12 Hz, axial benzylic), 2.44 (m, 2H, bridgehead), 2.31 (s, 12H, Ar–$CH_3$), 1.76 (p, *J* = 6 Hz, 8H, $CH_2$), 1.25-1.55 (m, 32H, $CH_2$), 0.91 (t, *J* = 6 Hz, 12H, $CH_3$). $^{13}$C NMR (75 MHz, CDCl3): δ 158.5, 134.9, 132.6, 122.9, 116.3, 114.1, 113.6, (Ar-C), 98.2, 87.9 (Alkyne) 67.9, 64.4 ($OCH_2$), 42.2 (bridgehead), 32.2 (benzylic), 31.6, 29.2, 25.8, 22.6 (methylene), 18.4, 14.1 (methyl). IR (ATR): 2940, 2874, 1602, 1509, 1250, 1170, 1104, 831 cm$^{-1}$. MS (MALDI), m/z (%) = 1162.4 ($M^+$, 100). HRMS (EI), m/z = Calcd. For $C_{57}H_{46}O_2$, 1162.705; Found, 1162.702, Δ = 2.7 ppm.

## 4.3. Results and discussion

### 4.3.1. Synthesis of functional scaffold: Tetraiodo-dibenzo[c,h]bicyclo[4.4.l]undeca-3,8-dien-ll-one

The synthesis and characterization of the tetramethyl-dibenzo-fused bicyclo[4.4.1]undeca-11-one **III-7** was reported in the Chapter 3. It provides an opportunity to prepare π-stacked oligo(phenylene ethynylene)s. We chose to perform electrophilic aromatic iodination to provide the tetraiodinated scaffold on which suitable phenylene ethynylene arms could be installed using Sonogashira reaction. We explored various iodinating agents such as N-iodosuccinimide, benzyltrimethylammonium dichloroiodate, $I_2/AgNO_3$, and $I_2$/mercury(II)trifluoromethanesulfonate to obtain the required tetraiodo-tetramethyl-dibenzo-fused bicycle[4.4.1]undecane **IV-1** scaffold. Of these, only the reaction with mercury(II)trifluoromethanesulfonate provided complete iodination of the ketone, Figure 4.2. To ensure complete iodination, it was necessary to carry out two exposures of the ketone to the iodinating conditions. The yield obtained in this iodination step was satisfactory (~ 70%). The $^1H$ NMR showed disappearance of singlet for the aromatic protons of the starting material and very broad peaks for the bridgehead and benzylic protons of the bicyclic core.

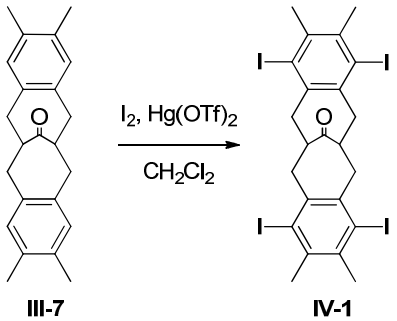


III-7 IV-1

**Figure 4.2.** Synthesis of tetraiodide scaffold, **IV-1**.

### 4.3.2. Synthesis of phenylene ethynylene arms

To prepare the π-stacked trimer, commercially available phenylacetylene was used as a conjugated arm to be installed on tetraiodide scaffold (section 4.3.1). (4-(Phenylethynyl)phenyl)acetylene (**IV-4)**[6] was prepared to extend the conjugated length of the stacked oligomer. 1,4-Diiodobenzene and propargyl alcohol were subjected to Sonagashira coupling in the presence of $Pd(PPh_3)_2Cl_2$ and CuI in dry THF/piperidine to provide 1-(4-iodophenyl)propyn-3-ol **IV-2** in good yields (60%), Figure 4.3. The monopropargyl alcohol was coupled to phenyl acetylene using Sonagashira coupling to provide 1-(4-(phenylethynylene)phenyl)propyn-3-ol (**IV-3)** in high yields (> 95%). The conversion of the propargylic alcohol to the terminal alkyne was conducted under oxidative conditions in the presence $MnO_2$ and KOH in dry $Et_2O$ to provide acetylene, **IV-4**. This deprotection step need not be done in an inert atmosphere.

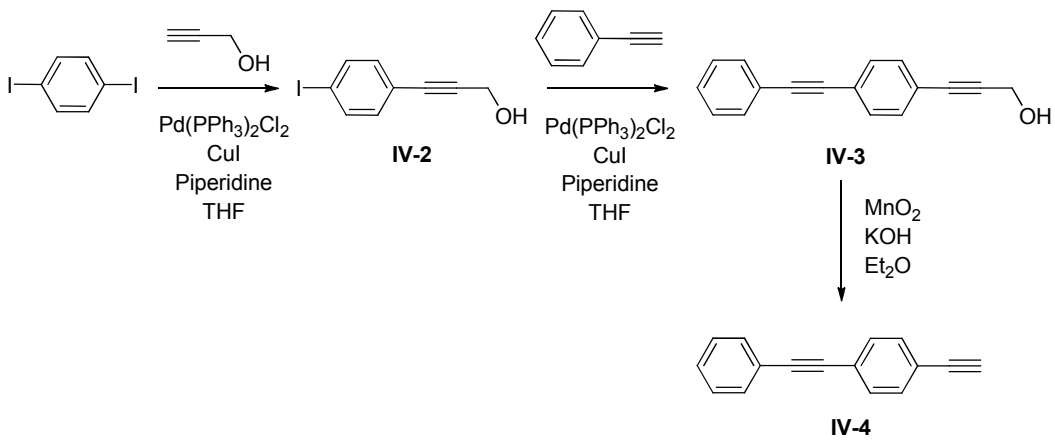


**Figure 4.3.** Synthesis of (4-(phenylethynyl)phenyl)acetylene, **IV-4**.

### 4.3.3. Synthesis of unstacked oligo(phenylene ethynylene)s

Model compounds **$PE_3$** and **$PE_5$** were synthesized by treating commercially available 2,3,5,6-tetramethyl-1,4-diiodobenzene to an excess of the phenylene ethynylene arms using Sonogashira coupling conditions. These model compounds resemble a single unstacked tier of the stacked oligomers.

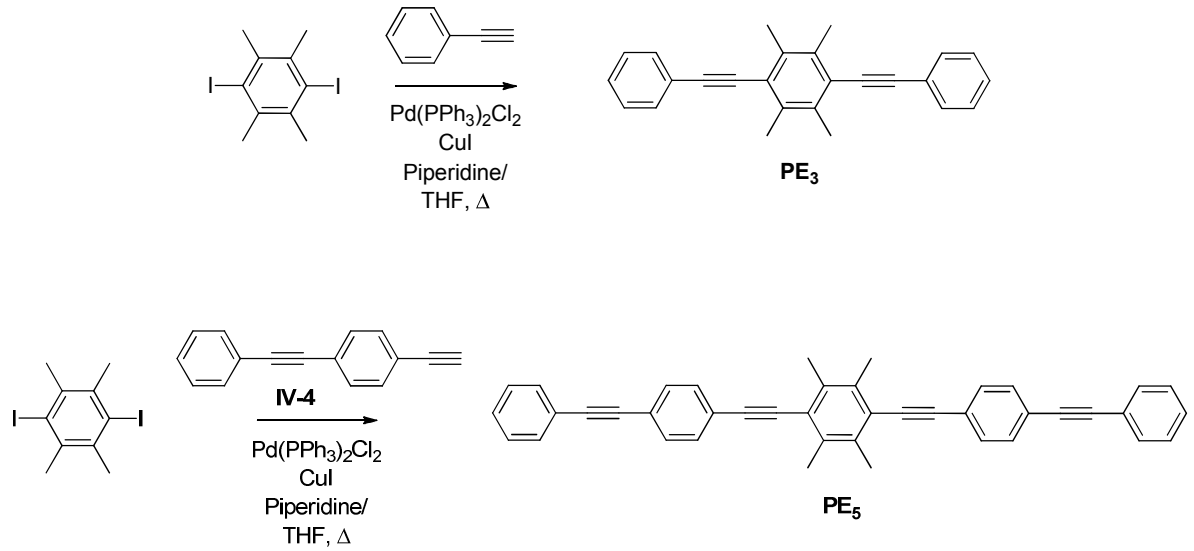


**Figure 4.4.** Synthesis of linear unstacked models **$PE_3$** and **$PE_5$**.

### 4.3.4. Synthesis of π-stacked oligo(phenylene ethynylene)s

The Sonogashira reaction was used to install phenylacetylene on the tetraiodo-tetramethyl-dibenzo-fused bicyclo[4.4.1]undecan-11-one, **IV-1**. Treatment of **IV-1** with large excess (8-12 eq.) of commercially available phenylacetylene in the presence of $Pd(PPh_3)_2Cl_2$ and CuI in dry diisopropylamine/THF at 60 °C for 3 d gave the tetra substituted product in good yield (50%). Attempts to purify the phenylene ethynylene substituted ketone using column chromatography resulted into a poor recovery of material. Accordingly, **$[PE_3]_2$** was purified by passing a solution through a short plug of silica gel followed by recrystallization from THF, provided pure ketone **$[PE_3]_2$** as yellow solid. In order to lock the conformation on the bicyclic core into a pseudo chair-pseudo chair arrangement to bring the conjugated arms into a stacked arrangement, the ketalization with excess of ethylene glycol, in the presence of a catalytic amount of p-toluenesulfonic acid in benzene. A Dean-Stark trap was used to remove water from the reaction. The ketal ***st*-$[PE_3]_2$** was obtained as a yellow solid after removal of the solvent under reduced pressure followed by flushing the crude material through a short plug of silica gel that had been neutralized with triethylamine. Precautions were taken to avoid exposure of the ketal to moisture and chlorinated solvents over a long period of time.

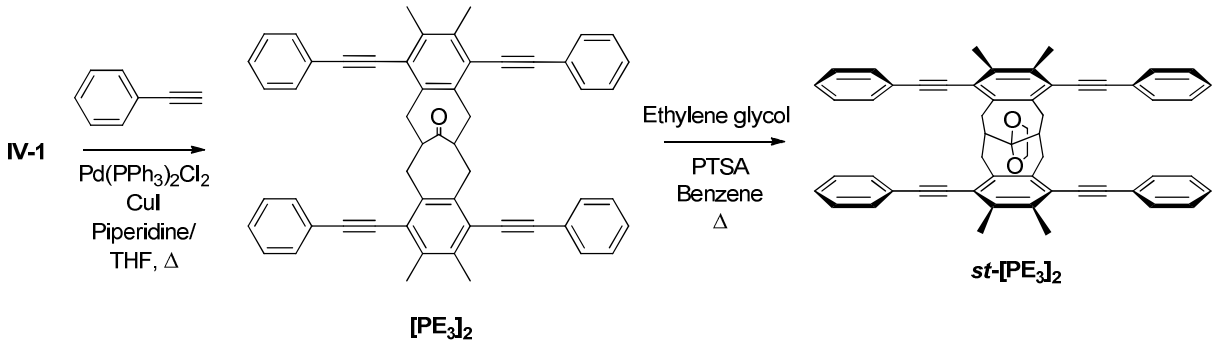


**Figure 4.5.** Synthesis of ketone **$[PE_3]_2$** and ketal ***st*-$[PE_3]_2$**.

The tetraiodide **IV-1** and hexyloxyphenylacetylene were subjected to Sonagashira coupling conditions to give corresponding hexyloxy trimer ketone, **[PE$_3$-OHex]$_2$**. Material obtained by precipitation from methanol was flushed through a short plug of silica gel with solvent. Purification by recrystallization from THF provided the pure ketone in good yield (48%). The ketal ***st*-[PE$_3$-OHex]** was prepared from ketone **[PE$_3$-OHex]$_2$** as per the method illustrated above for preparation of ***st*-[PE$_3$]$_2$**. However, the incorporation of alkoxy groups at the terminus of the oligo(phenylene ethynylene) tiers did not improve the solubility as had been hoped.

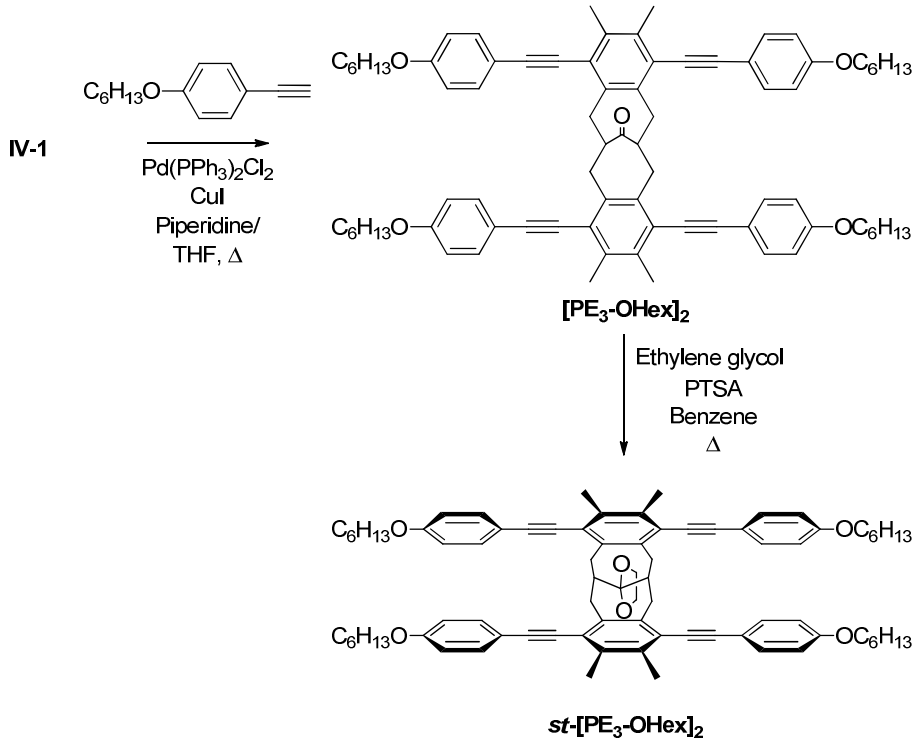


**Figure 4.6.** Synthesis of ketone **[PE$_3$-OHex]$_2$** and ketal ***st*-[PE$_3$-OHex]$_2$.**

Synthesis of the pentamer ketone **[PE$_5$]$_2$** was accomplished by the Sonogashira coupling of tetraiodo ketone **IV-1** to (4-(phenylethynyl)phenyl)acetylene, **IV-4**. Precipitation in MeOH followed by recrystallization from THF provided the substituted ketone as green solid in satisfactory yield (30%), Figure 4.7. Column chromatography or plug of silica gel was avoided because of the low solubility of the **[PE$_5$]$_2$**. Ketalization of ketone **[PE$_5$]$_2$** with ethylene glycol provided the corresponding ketal ***st*-[PE$_5$]$_2$** as green solid. We were unable to perform $^{13}$C NMR and electrochemical measurements of this stacked pentamer ketone and ketal due to poor solubility.

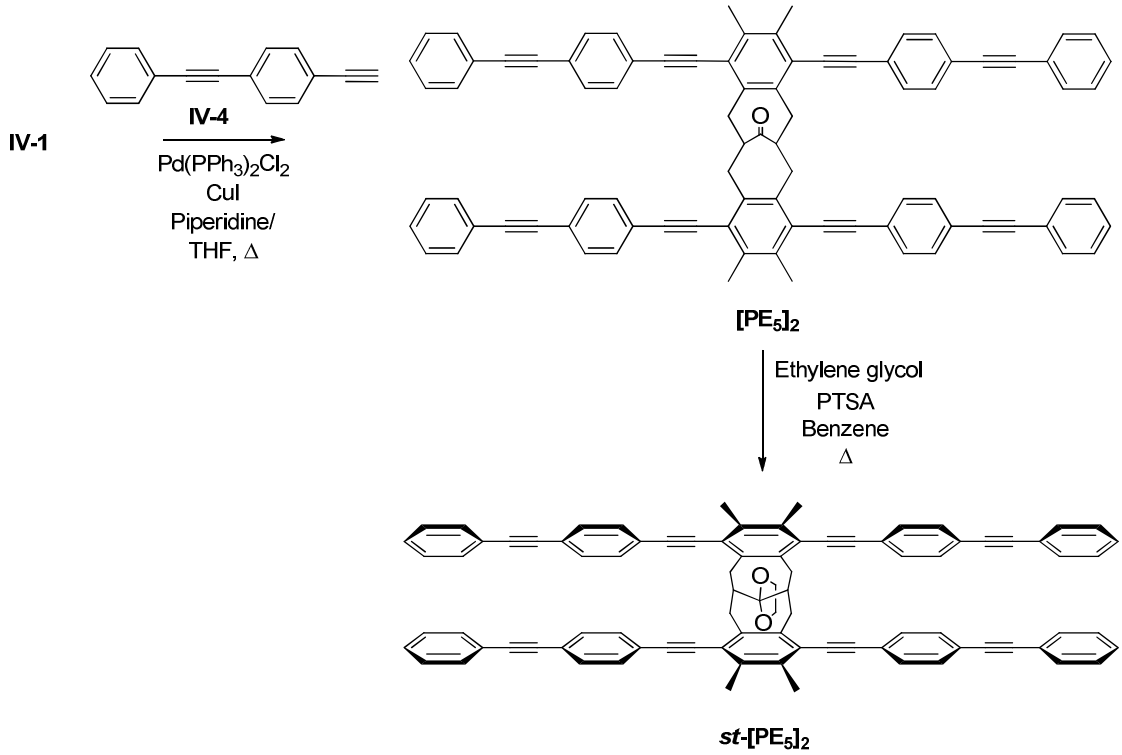


**Figure 4.7.** Synthesis of.ketone **[PE$_5$]$_2$** and ketal ***st*-[PE$_5$]$_2$**.

### 4.3.5. Structural Characterization. $^{1}$H NMR and $^{13}$C NMR Spectroscopy

The $^{1}$H NMR of ketone **[PE$_3$]$_2$** exhibits conformational flexibility and rapid interchange between chair-chair, chair-boat, and boat-boat conformations of the seven-membered rings of the bicyclo[4.4.1]undecane core. This gives rise to a broad coalesced peak at 2.8-3.5 ppm due to signal averaging of the benzylic and bridgehead protons in the different conformations of the bicylic core, Figure 4.8. However, the $^{1}$H NMR spectrum of ketal ***st*-[PE$_3$]$_2$** confirms that the bicyclo[4.4.1]undecane core is fixed in a pseudo chair- pseudo chair conformation with the benzene rings stacked atop one another. The protons of the benzylic methylene groups of ***st*-[PE$_3$]$_2$** give rise to a pair of sharp doublets of doublets at δ 3.79 (dd, $J$ = 16, 6 Hz) and δ 3.30 (dd, $J$ = 15, 2 Hz) corresponding to the two sets of protons (pseudo-axial and pseudo-equatorial) that couple with one another and with the bridgehead proton of the bicycle in the fixed comformation, Figure 4.9. The $^{13}$C NMR spectrum of ketal shows the absence for the signal for the carbonyl which reinforces the formation of ketal, Figure 4.10. The stacking interaction of the arenes causes an upfield shift of the peak for the aromatic protons of ***st*-[PE$_3$]$_2$** (δ = 7.08–7.28 ppm, Figure 4.9) relative to that of the unstacked linear analog **[PE$_3$]$_2$**. (δ = 7.33–7.53 ppm, Appendix #) Accordingly, the phenylene ethynlene arms do not impede the adoption of a stacked conformation of the ketal.

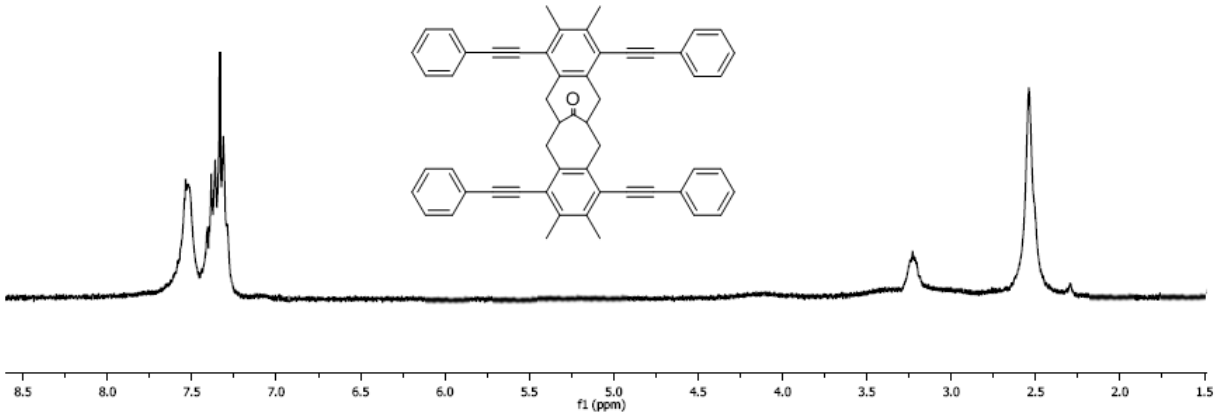


**Figure 4.8.** $^{1}$H NMR of ketone **[PE$_3$]$_2$** (300 MHz, $CDCl_3$, 23 °C). Broadening of peaks indicates structural flexibility of the bicycloundecane core.

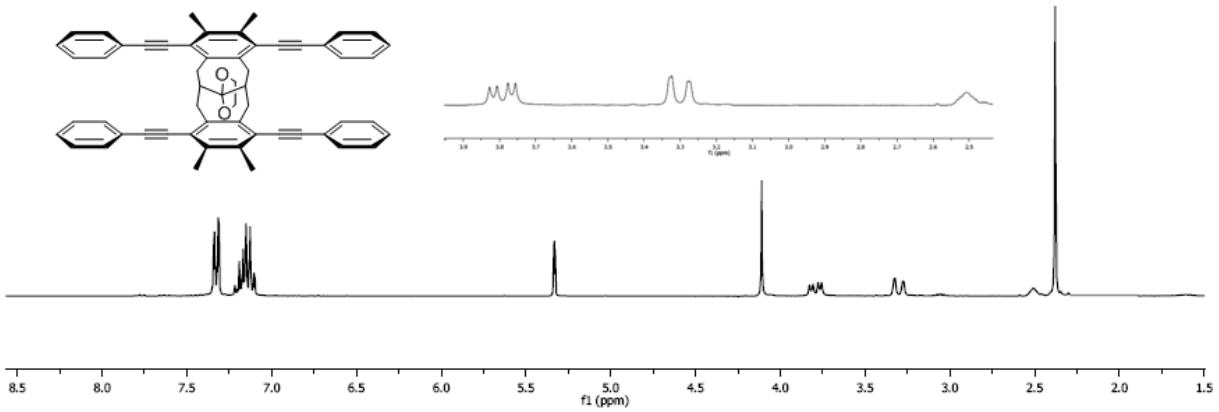


**Figure 4.9.** $^{1}$H NMR of ketal ***st*-[PE$_3$]$_2$** (300 MHz, $CD_2Cl_2$, 23 °C). The distinct set of multiplets for the bridge head positions indicates formation of pseudo chair-pseudo chair conformation.

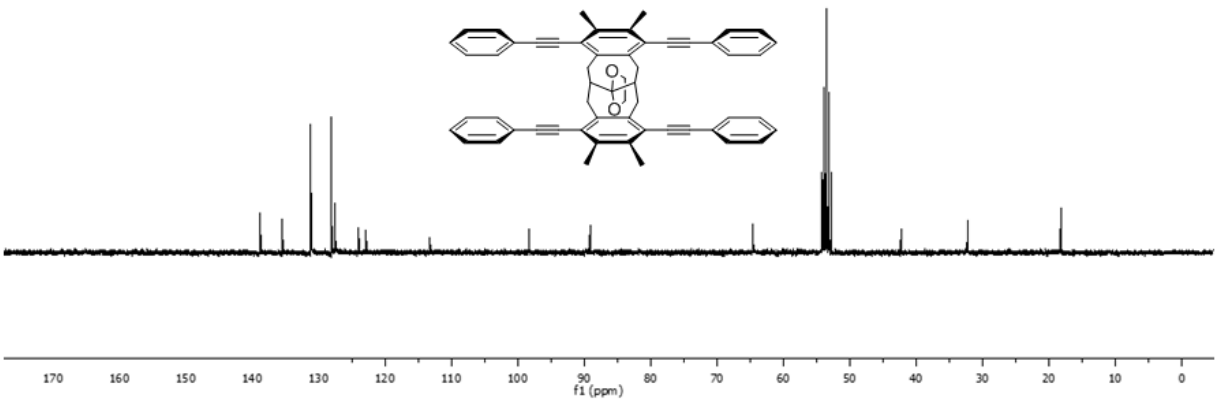


**Figure 4.10.** $^{13}$C NMR of ketal ***st*-[PE$_3$]$_2$** (75 MHz, $CD_2Cl_2$, 23 °C).

The ketone **[PE$_3$-OHex]$_2$** shows the broad peaks for the benzylic and bridgehead protons due to conformational flexibility of the bicyclic core along with all the required peaks for the hexyloxy chain. While, $^1$H NMR analysis of the *p*-hexyloxy-substituted analog ***st*-[PE$_3$-OHex]$_2$** shows a similar pattern of peaks for benzylic and bridgehead protons, which is consistent with the single pseudo chair-pseudo chair conformation of the bicyclic core which provides π-stacked structures, Figure 4.12. Additional evidence of structure was observed in the $^{13}$C NMR analysis of these compounds. The $^{13}$C NMR of ketal (figure 4.13) shows the absence of carbonyl signal which is present in the spectrum of the ketone (δ = 213.2 ppm), Figure 4.14.

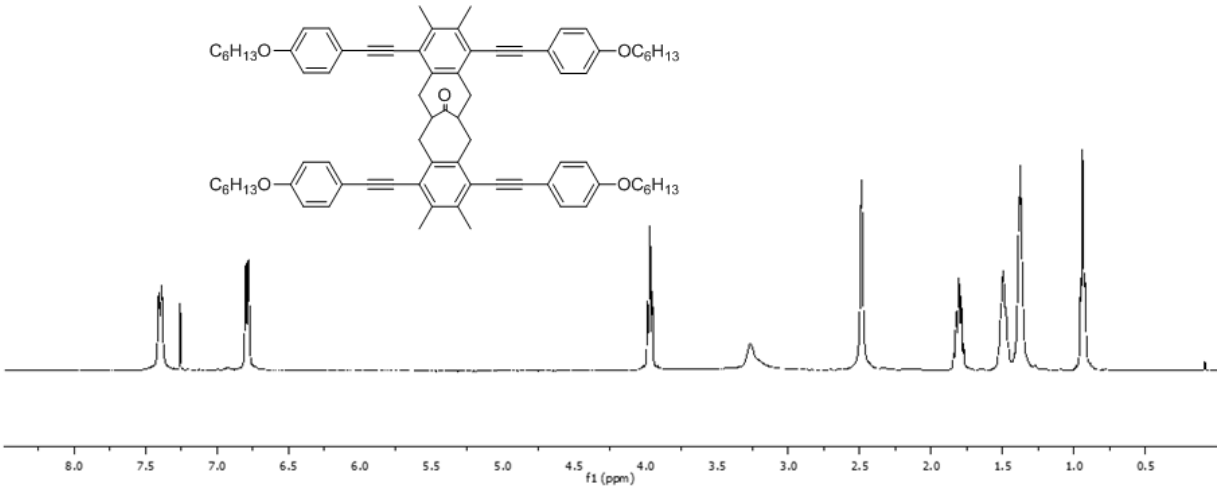


**Figure 4.11.** $^{1}$H NMR of ketone **[PE$_3$-OHex]$_2$** (300 MHz, $CDCl_3$, 23 °C). Broadening of peaks indicates structural flexibility of the bicycloundecane core.

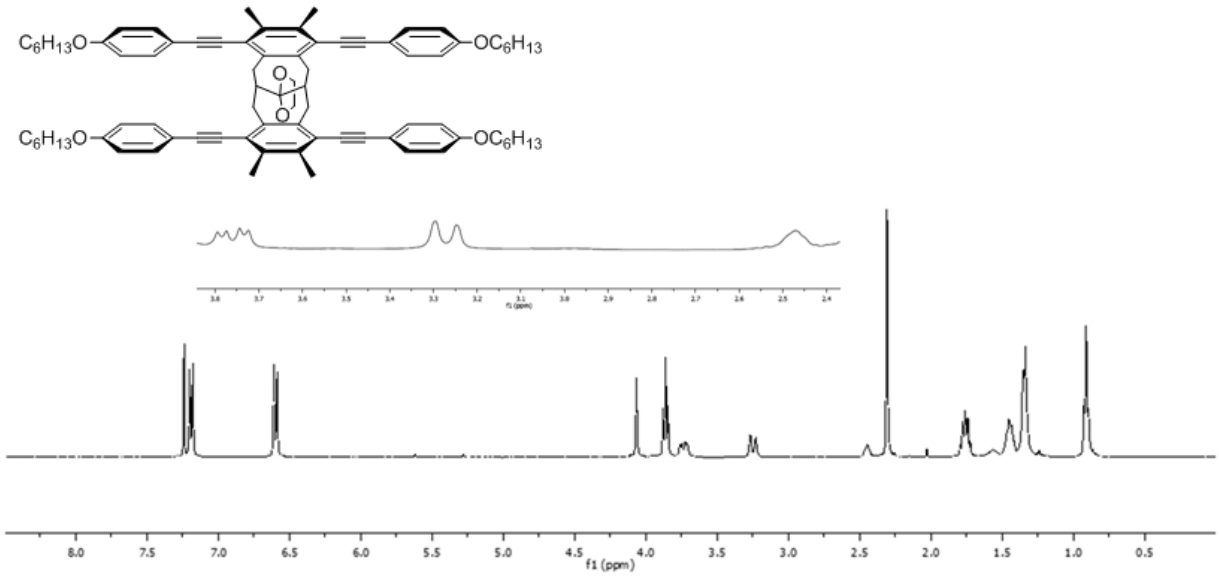


**Figure 4.12.** $^{1}$H NMR of ketal ***st*-[PE$_3$-OHex]$_2$** (300 MHz, $CDCl_3$, 23 °C). The distinct set of multiplets for the bridge head positions indicates formation of pseudo chair-pseudo chair conformation.

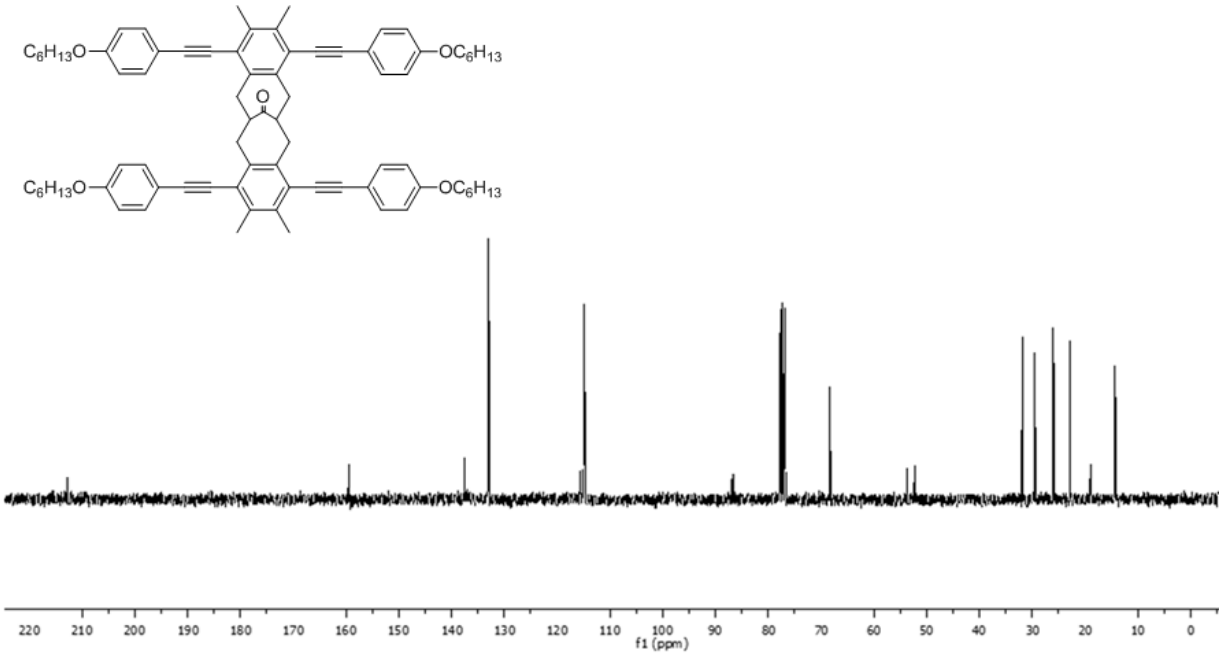


**Figure 4.13.** $^{13}$C NMR of ketone **[PE$_3$-OHex]$_2$** (75 MHz, $CDCl_3$, 23 °C).

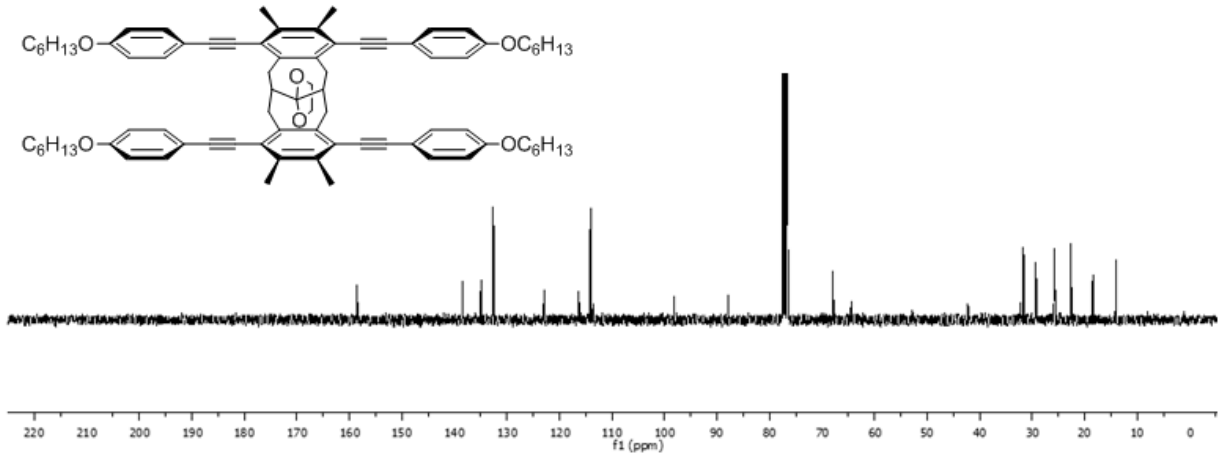


**Figure 4.14.** $^{13}$C NMR of ketal ***st*-[PE$_3$-OHex]$_2$** (75 MHz, $CDCl_3$, 23 °C).

Similar trends and sets of peaks for the benzylic and bridgehead protons were observed for ketone ***st*-[PE$_5$]$_2$** and its stacked analog, Figure 4.16. The $^1$H NMR analysis confirms the chair-chair conformation of bicyclic core. The $^{13}$C NMR for pentamer ketone and ketal were not obtained due to extremely low solubility.

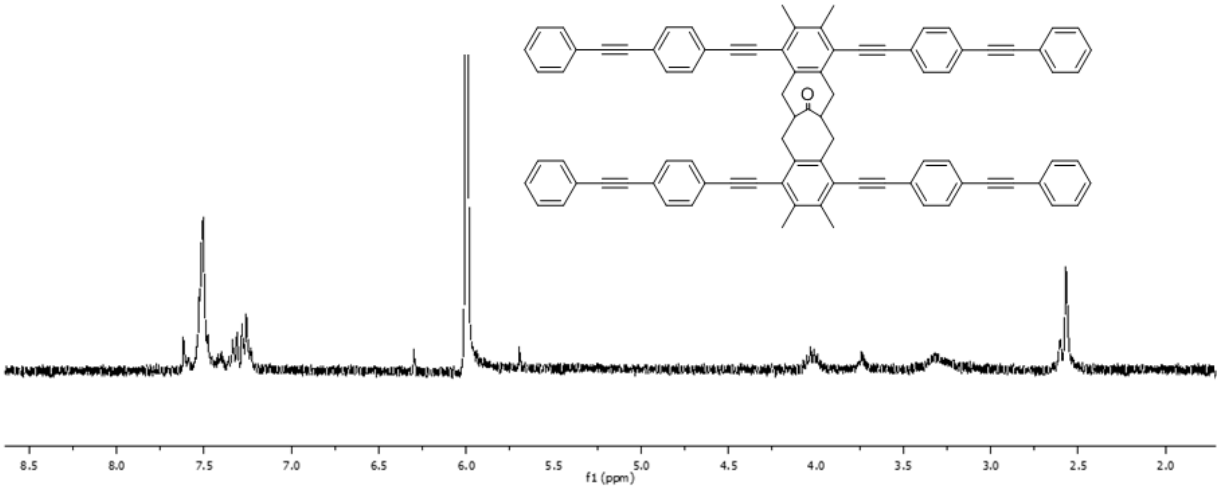


**Figure 4.15.** $^1$H NMR of ketone **[PE$_5$]$_2$** (300 MHz, $C_2D_2Cl_4$, 80 °C). Broadening of peaks indicates structural flexibility of the bicycloundecane core.

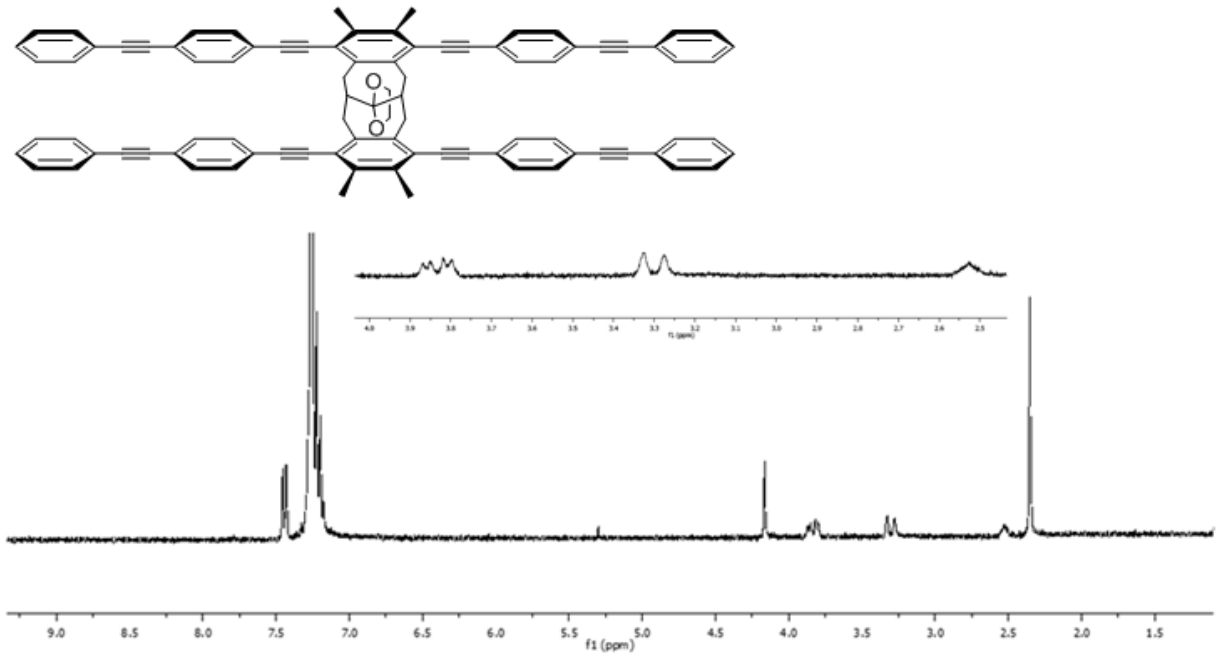


**Figure 4.16.** $^{1}$H NMR of ketal ***st*-[PE$_5$]$_2$** (300 MHz, $CDCl_3$, 50 °C). The distinct set of multiplets for the bridge head positions indicates formation of pseudo chair-pseudo chair conformation.

### 4.3.6. X-Ray Crystal Structural Analysis

The X-ray structure of ketal ***st*-[PE$_3$]$_2$** confirms that bicycloundecanone core adopts a pseudo chair-pseudo chair conformation with a cofacially stacked arrangement of the benzene rings with a distance of 3.42 Å between the central pair of stacked benzene rings, and an angle of 18° between them, Figure 4.17. The optimized geometries of ***st*-[PE$_3$]$_2$** and ***st*-[PE$_3$]$_2$** were obtained using high level of calculations by Dr. Sukrit Mukhopadhyay from Prof. Brédas' research group. The data obtained from calculations confirmed the observed pseudo chair-pseudo chair conformation of the stacked "trimer" in a solution. The results from calculations are in a good agreement with the calculated dihedral angles between bridgehead and benzylic protons, as per the NMR spectra. The dihedral angle between bridgehead and benzylic protons can be calculated using the coupling constants (obtained from $^1$H NMR analysis: bridgehead H and benzylic $H_{equatorial}$ = 6 Hz, bridgehead H and benzylic $H_{axial}$ = 2 Hz) between them by the Karplus Equation. The computed values (dihedral angle between: bridgehead H and benzylic $H_{equatorial}$ = 52°, bridgehead H and benzylic $H_{axial}$ = 85°) are in good agreement with the experimental results (dihedral angle between: bridgehead H and benzylic $H_{equatorial}$ = 47°, bridgehead H and benzylic $H_{axial}$ = 73°) as obtained from x-ray crystal structure analysis. In the X-ray crystal structure, the distances between the pairs of rings on the periphery of the molecule are 3.84 and 4.01 Å, Figure 4.18. The inter-centroid distance and the torsional angle of the central pair of benzene rings in the stacked "trimer" is same compared to ketal ***st*-[PE$_3$]$_2$** which indicates that the incorporation of the four conjugated arms does not cause repulsion between the tiers. The difference in the inter-centroid distance (the difference between $d_2$ and $d_3$ is 0.2 Å) of the peripheral benzene stacks is due to the rotation of one of the benzene rings in the "Stack3", which results in larger $\theta_3$, shown in Table 1. Such a difference in the orientation of the benzene rings in the crystal geometry can

be attributed to the crystal packing forces, which is absent in the ground state optimized geometries irrespective of the presence and absence of solvent. Barring this, the structural parameters of ***st*-[PE$_3$]$_2$** in the ground state optimized geometries (in presence and absence of solvent) compare well with those obtained from the crystal geometry as shown in Table 1. The top view of X-ray crystal structure shows that the conjugated tiers are slightly distorted from planarity, Figure 4.18B. Furthermore, similar to the X-ray crystal structure, individual oligomeric tiers in the ground state geometries of the stacked molecules are twisted with respect to each other. Such a geometry distortion can be quantified by the slip distance ($d_s$) between the benzene stacks. In the ground state optimized geometries (gas-phase), the slip distance of both Stack2 and Stack3 are 1.65 Å. In the X-ray crystal structure of ***st*-[PE$_3$]$_2$**, the slip distance between the benzene rings in Stack2 is 1.33 Å.

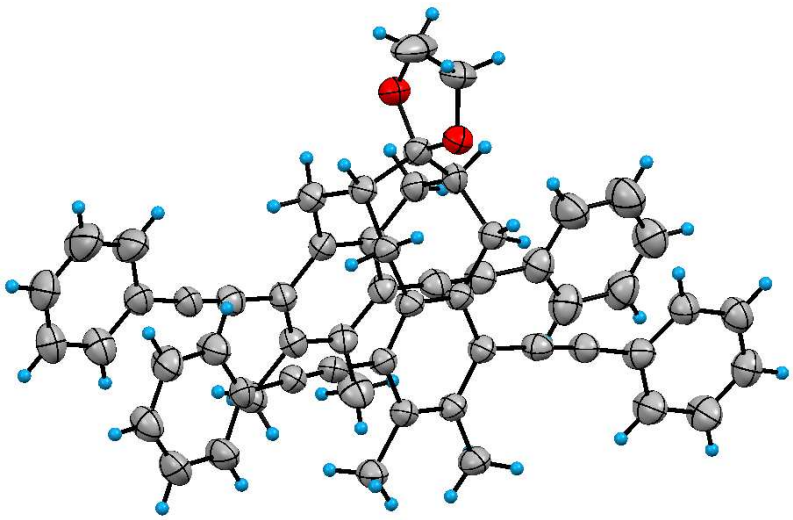

**Figure 4.17.** The molecular structure of ***st*-[PE$_3$]$_2$** with displacement ellipsoids at the 30% probability level.

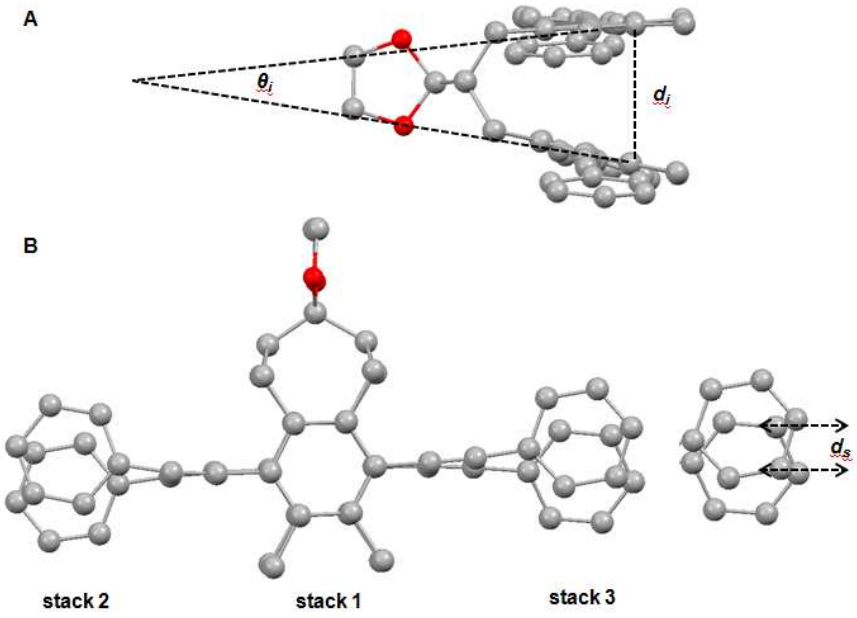


**Figure 4.18.** X-ray crystal structures: A, ***st*-[PE$_3$]$_2$** (side view); B, ***st*-[PE$_3$]$_2$ (**top view). $d_i$ represents the inter-centroid distance, $\theta_i$ represents the inter-planer angle between the two stacked phenyl rings and $d_s$ represents the slip distance between the stacked phenyl rings.

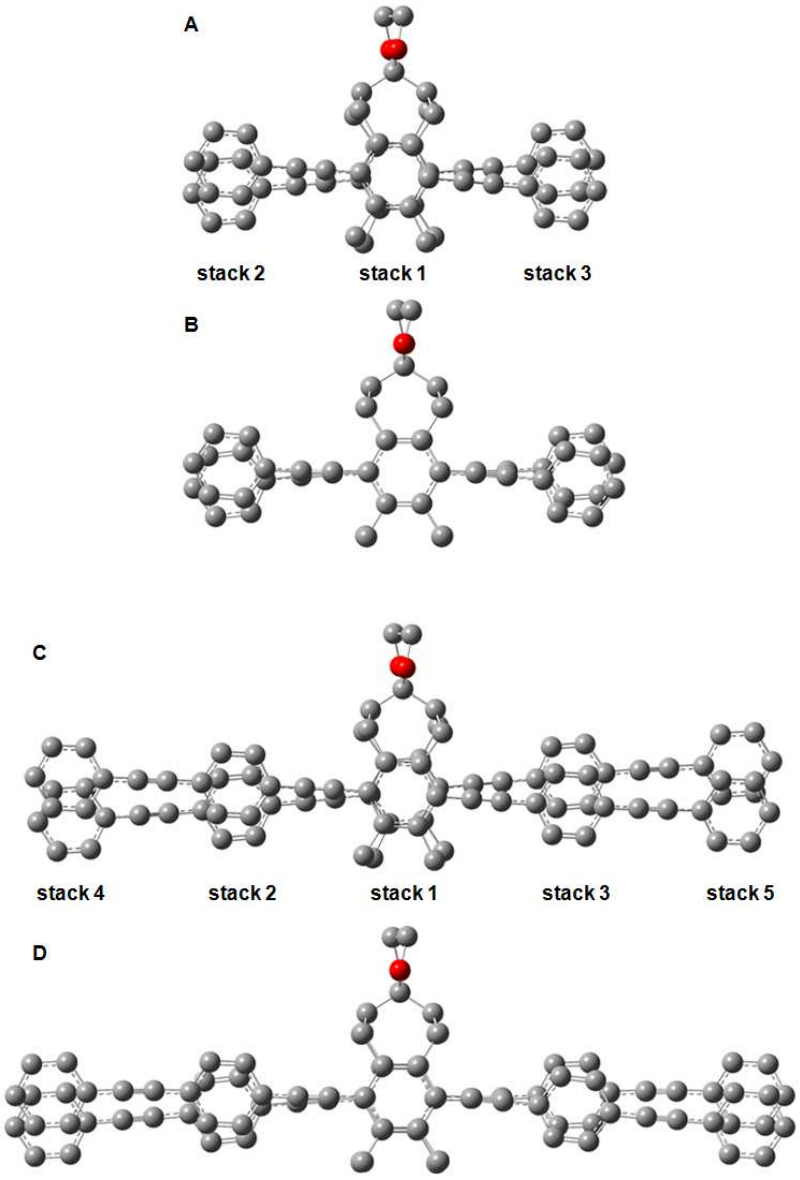


**Figure 4.19.** Optimized geometries of ***st*-[PE$_3$]$_2$** (**A** and **B**) and ***st*-[PE$_5$]$_2$** (**C and D**): Ground state (**A** and **C**) and excited-state (**B** and **D**). The optimizations are performed in gas-phase. For clarity, the hydrogen atoms are not shown in the figure. The inner most pair of benzene rings is marked as **Stack1** for both the stacked molecules and the outermost pair

of ***st*-[PE$_3$]** are marked as **Stack2** and **Stack3**, whereas the same for ***st*-[PE$_5$]** are marked as **Stack4** and **Stack5**.

**Table 1**. Comparison of selected structural parameters (distances, $d_i$, and angles, $\theta_i$) of stacked compounds from X-ray diffraction and calculation of ground state (gs) and excited-state (ex) optimized geometries.

| Geometry | Inter-centroid distance (Å) | | | | | Inter-plane angle (°) | | | | |
|---|---|---|---|---|---|---|---|---|---|---|
| | $d_1$ | $d_2$ | $d_3$ | $d_4$ | $d_5$ | $\theta_1$ | $\theta_2$ | $\theta_3$ | $\theta_4$ | $\theta_5$ |
| *Experimental* | | | | | | | | | | |
| X-ray crystallography | | | | | | | | | | |
| ***st*-[PE$_1$]$_2$** | 3.42 | - | - | - | - | 16.77 | - | - | - | - |
| ***st*-[PE$_3$]$_2$** | 3.42 | 3.81 | 4.00 | - | - | 17.91 | 1.68 | 11.85 | - | - |
| *ωB97X-D/6-31g** | | | | | | | | | | |
| gs | 3.39 | 3.76 | 3.76 | - | - | 15.53 | 1.40 | 1.54 | - | - |
| gs, $CHCl_3$ | 3.39 | 3.78 | 3.78 | - | - | 12.83 | 1.64 | 1.73 | - | - |
| ***st*-[PE$_5$]$_2$** | | | | | | | | | | |
| *ωB97X-D/6-31g** | | | | | | | | | | |
| gs | 3.39 | 3.69 | 3.69 | 3.79 | 3.80 | 13.63 | 0.55 | 1.40 | 1.98 | 2.18 |
| gs, $CHCl_3$ | 3.40 | 3.68 | 3.68 | 3.82 | 3.81 | 12.75 | 0.68 | 1.61 | 1.16 | 1.81 |

Despite the $^{1}$H NMR data for ***st*-[PE$_3$-OHex]$_2$** that indicated the presence of a pseudo chair-pseudo chair conformation in solution, the X-ray crystal structure of this compound shows a pseudo boat-pseudo chair conformation for bicylic core, Figure 4.20. The molecule has planer conjugated oligomers. It is surprising that the ***st*-[PE$_3$-OHex]$_2$** acquires pseudo boat-pseudo chair conformation given that this requires significant steric crowding on one side of the ketal. This could be due to the effect of crystal packing forces which hampers the stacked conformation of the compound

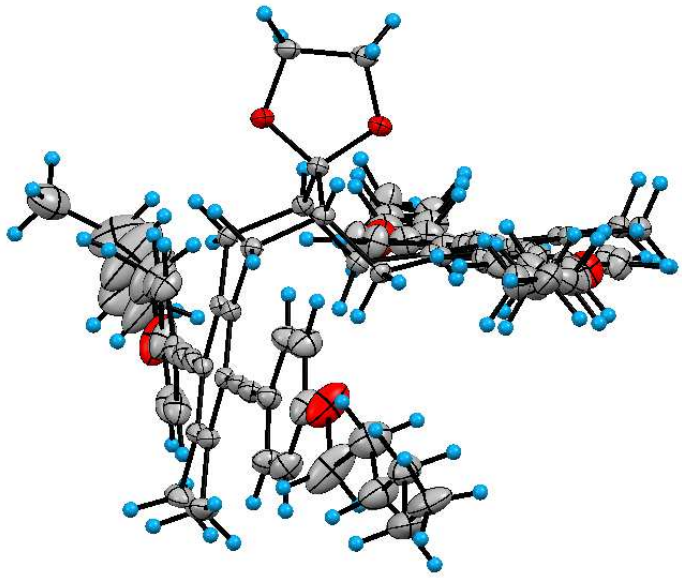

**Figure 4.20.** The molecular structure of ***st*-[PE$_3$-OHex]$_2$** with displacement ellipsoids at the 30% probability level.

### 4.3.7. UV-Vis and Fluorescence spectroscopy

The stacked oligomers and unstacked linear analogues were characterized by UV-Vis and fluorescence spectroscopy to explore the effect of stacking on the electronic structure of the conjugated tiers. The stacked trimer ***st*-[PE$_3$]$_2$** (λmax = 325 nm) shows a small hypsochromic shift (5 nm, 60 meV) in absorbance upon stacking compared to its unstacked model **PE$_3$** (λmax = 330 nm), Figure 4.21. The stacked trimer ***st*-[PE$_3$]$_2$** exhibited the red shifted absorption edge in contrast to that of model **PE$_3$** which suggests that one more weakly optically allowed electronic state contributes to the absorption of the stacked trimer. Also, the stacked compound shows an emission peak at 382 nm which is red shifted from that of the unstacked counterpart (360 nm), Figure 4.22. In addition, the stacked trimer shows a weak emission feature in the low-energy part of the spectrum at about 490 nm (~ 2.5 eV, see inset of Figure 4.22). The absorption and the emission bands of both compounds show well-resolved vibration structures.

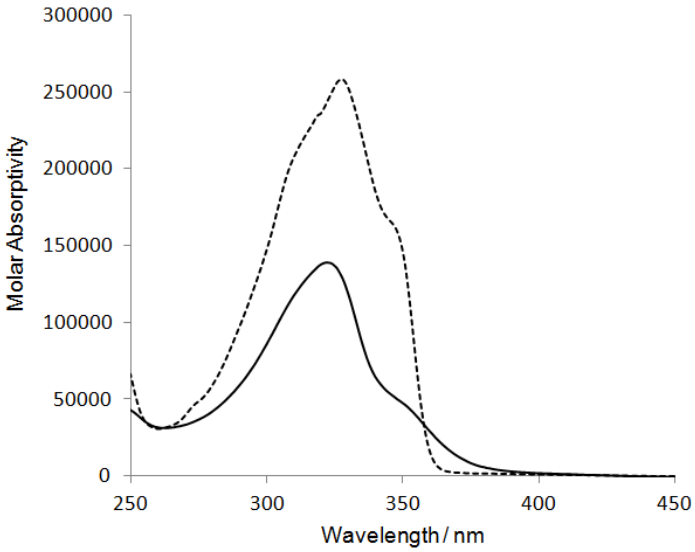


**Figure 4.21.** UV-vis spectra: ***st*-[PE$_3$]$_2$** (solid) and **PE$_3$** (dotted), $c = 3 \times 10^{-6}$ M in $CHCl_3$, T = 23 °C.

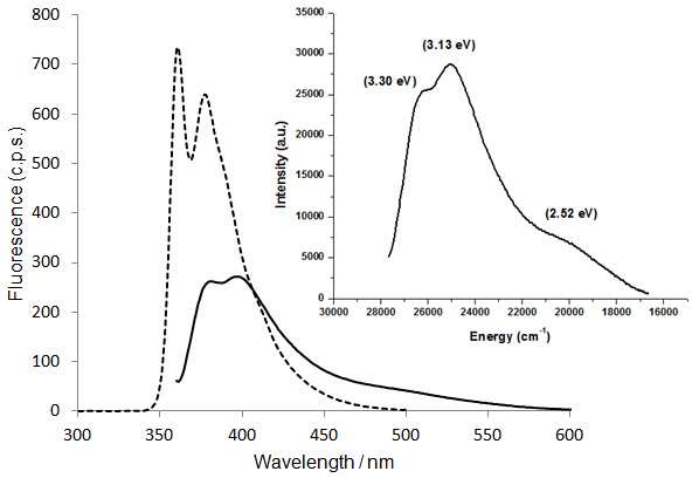


**Figure 4.22.** Fluorescence spectra: ***st*-[PE$_3$]$_2$** (solid) and **PE$_3$** (dotted), $c = 3 \times 10^{-6}$ M in $CHCl_3$, T = 23 °C. The inset depicts the emission spectra of stacked "trimer" in energy scale.

More pronounced differences are observed in the spectra of the pentameric homologs, ***st*-[PE$_5$]$_2$** and **PE$_5$**. The stacked pentamer ***st*-[PE$_5$]$_2$** (λmax = 355 nm) shows a hypsochromic shift (10 nm, 90 meV) in absorbance upon stacking compared to its unstacked model **PE$_5$** (λmax = 365 nm), Figure 4.23. The stacked pentamer also shows the red shifted absorption edge similar to stacked trimer. The emission profile of stacked pentamer is dominated by a broad low-energy transition with a maximum at ca. 495 nm in contrast to that of unstacked model. However, a low-intensity high-energy band (398 nm, 3.1 eV) similar to the emission maximum of the unstacked linear analog **PE$_5$** is also observed, Figure 4.24.

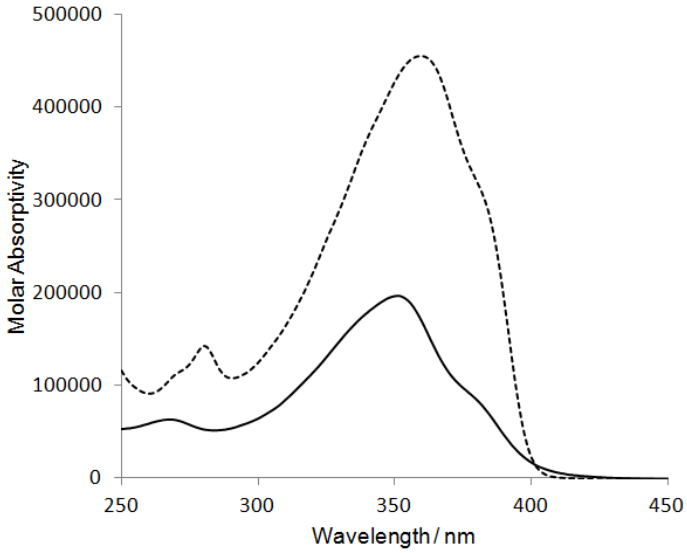


**Figure 4.23.** UV-vis spectra: ***st*-[PE$_5$]$_2$** (solid) and **PE$_5$** (dotted), $c = 1.8 \times 10^{-6}$ M in $CHCl_3$, T = 23 °C.

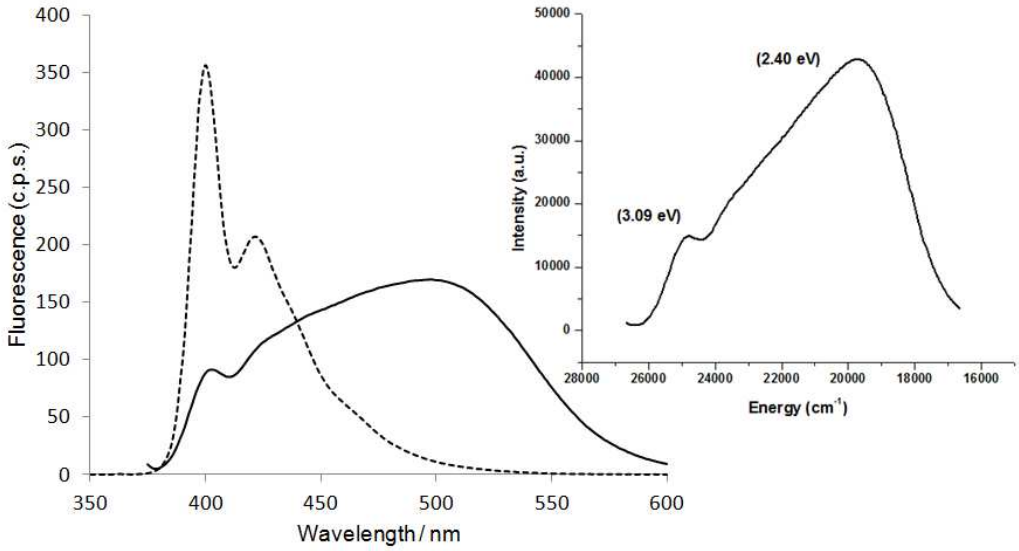


**Figure 4.24.** Fluorescence spectra: ***st*-[PE$_5$]$_2$** (solid) and **PE$_5$** (dotted), $c = 1.8 \times 10^{-6}$ M in $CHCl_3$, T = 23 °C; The inset depicts the emission spectra of stacked “pentamer” in energy scale.

**Table 2.** Absorption and emission maxima.

| | Absorption (nm) | Emission (nm) |
|---|---|---|
| **[PE$_3$]**[a] | 330 | 360, 375 |
| ***st*-[PE$_3$]$_2$**[a] | 325 | 382, 397, 490[c] |
| **[PE$_5$]**[b] | 365 | 399, 418 |
| ***st*-[PE$_5$]$_2$**[b] | 355 | 398, 495 |

[a] [analyte] = 3 x $10^{-6}$ M in $CHCl_3$. [b] [analyte] = 1.8 x $10^{-6}$ M in $CHCl_3$. [c] Shoulder peak.

Analysis of the emission spectra indicates that at least two electronic states contribute to the fluorescence of the stacked systems, Figure 4.25. The similarity between the absorption spectra of the stacked and unstacked analogs, together with the tails seen in the optical band-edge of the stacked compounds, supports this model. Based on this analysis, and a computational study that successfully models the appearance of the spectra, we conclude that a single-tier (local, $S_2$) state is responsible for the absorption and emission of the unstacked systems. This state is also responsible for the main part of the first absorption band and the high-energy emission band of the stacked systems. The low-energy emission band and the absorption edge tail seen in both ***st*-[PE$_3$]$_2$** and ***st*-[PE$_5$]$_2$** is attributed to an inter-oligomer excimer-like state ($S_1$).

The emission profile of the stacked pentamer has a major low energy contribution from an “excimer-like” state, in contrast to that of stacked trimer. This is due to a lower energy of activation $E_a$ for stacked pentamer ***st*-[PE$_5$]$_2$** compared to that of stacked trimer ***st*-[PE$_3$]$_2$**, Figure

3.19. The transition from local state ($S_2$) to a excimer-like state ($S_1$) is governed by the energy of activation barrier.

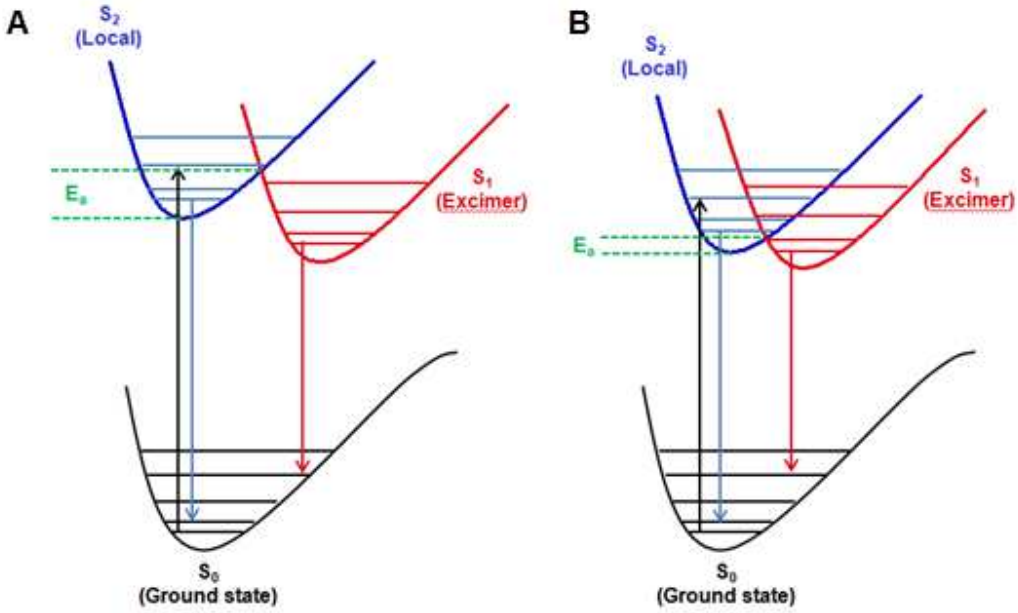


**Figure 4.25.** Local-excited state ($S_2$, blue), excimer-like state ($S_1$, red), and ground state ($S_0$, black); $E_a$, energy required to cross barrier from local state to the excimer-like state; A, ***st*-[PE$_3$]$_2$** and, B, ***st*-[PE$_5$]$_2$**.

### 4.3.8. Cyclic Voltammetry and Differential Pulse Voltammetry

π-π Stacking has significant effect on the electrochemical properties of oligo(phenylene ethynylene)s. Differential pulse voltammetry of the **$PE_3$** and ***st*-$[PE_3]_2$** are shown in Figure 4.26. Both first and second $1e^-$ oxidations (+1.76 and +1.88 V) of the stacked trimer take place at lower potentials than first $1e^-$ oxidation (+2.00 V) of unstacked model, which confirms the stabilization of mono(radical cation) and dication through stacking. This is in accordance with the studies on the thiophene analogs, suggesting that dication leads to formation of π-dimer which overcomes the destabilization expected to arise from Coulombic repulsion through π-stacking. The stacked pentamer ***st*-$[PE_5]_2$** was difficult to characterize due to its poor solubility.

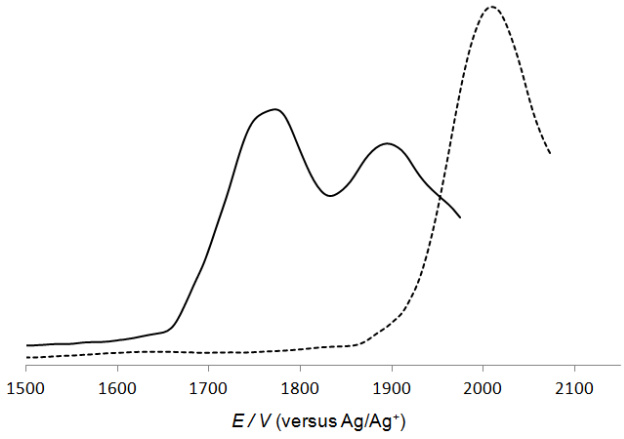


**Figure 4.26.** Differential pulse voltammograms (DPV) of ***st*-$[PE_3]_2$** (solid) and **$PE_3$** (dotted). $c$ = $10^{-5}$ M in $CHCl_3$, $T$ = 23 °C; 0.1 M n-$Bu_4NPF_6$/$CH_2Cl_2$; Au working electrode; Pt auxillary, $Ag/Ag^+$ reference electrode; $v$ = 100 mV/s.

## 4.4. Conclusion

In conclusion, we prepared stacked oligo(phenylene ethynylene)s from the tetraiodo-benzo-annelated bicyclo[4.4.1]undecane (chapter 3). The conjugated arms were installed to the bicyclic core using Sonogashira cross coupling. The identity of the desired compounds was confirmed using NMR spectroscopy and X-ray crystal structure analysis. The emission spectrum showed low energy emission due to the "phane" state formation.[7] The significantly large Stokes shifts associated with the stacked oligomers are due to possible formation of an extended "phane" state arising from stacking of entire conjugated chains. The ease of oxidation of the stacked pentamer is consistent with the formation of a radical cation π-dimer whereby the dicationic species is stabilized by π-stacking. This supports Miller's conjecture that such radical cations in which the charged species is delocalized over the tiers, the synthetic strategy also provides opportunities to build multidecker stacked oligo(phenylene ethynylene)s and thereby study of optoelectronic properties of stacked conjugated oligomers.

## 4.5. References


1. Mataka, S.; Takahashi, K.; Mimura, T.; Hirota, T.; Takuma, K.; Kobayashi, H.; Tashiro, M.; Imada, K.; Kuniyoshi, M., *Journal of Organic Chemistry* **1987**, *52*, 2653.
2. Sonogashira, K.; Tohda, Y.; Hagihara, N., *Tetrahedron Letters* **1975**, 4467.
3. Knoblock, K. M.; Silvestri, C. J.; Collard, D. M., *Journal of the American Chemical Society* **2006**, *128*, 13680.
4. Chai, J. D.; Head-Gordon, M., *Journal of Chemical Physics* **2008**, *128*.
5. Chai, J. D.; Head-Gordon, M., *Physical Chemistry Chemical Physics* **2008**, *10*, 6615.
6. Glimsdal, E.; Carlsson, M.; Kindahl, T.; Lindgren, M.; Lopes, C.; Eliasson, B., *Journal of Physical Chemistry A* **2010**, *114*, 3431.
7. Bazan, G. C.; Oldham, W. J.; Lachicotte, R. J.; Tretiak, S.; Chernyak, V.; Mukamel, S., *Journal of the American Chemical Society* **1998**, *120*, 9188.

# CHAPTER 5

# SYNTHESIS AND CHARACTERIZATION OF π-STACKED OLIGO(PHENYLENE VINYLENE)S[2]

## 5.1. Introduction

In the previous chapter, we showed how benzo-fused bicyclo[4.4.1]undecane can be used as a scaffold to prepare π-stacked oligo(phenylene ethynylene)s. In this chapter, we describe an exploration of [2.2]paracyclophane as another potential scaffold to hold the conjugated units stacked atop one another. The [2.2]paracyclophane scaffold was explored previously to prepare π-stacked conjugated oligomers. For example, the *pseudo-para* (*pp*) [2.2]paracyclophane and *pseudo-ortho* (*po*) [2.2]paracyclophane cores were used to explore the effect of inter-chain interactions between stilbene and distyryl-benzene chromophores held on top of one another, e.g., Figure 1.[1] Unfortunately, these molecules suffer from two significant drawbacks in the context of the analysis of the influence of π-stacking on the properties of conjugated chains: (i) the individual tiers in such stacks are free to adopt various conformations, especially in solution, and (ii) the stacking interactions are restricted to the paracyclophane scaffold itself. Accordingly, the conformational flexibility and restricted amount of overlap do not mimic the arrangement of interacting conjugated chains in thin solid films.

To achieve extended π-stacking over the entire length of chromophoric unit, we chose to explore pseudo-geminal (*pg*) [2.2]paracyclophane[2] as a scaffold to hold oligo(phenylene vinylene)s in a stacked arrangement, Figure 1. The resulting stacking better resembles the solid

[2] Computational studies described in this chapter were conducted by Dr. Sukrit Mukhopadhyay and Dr. Coropceanu Veaceslav in the group of Dr. Brédas at Georgia Institute of Technology.

state packing arrangement of conjugated polymeric chains in thin film devices. Such an extended interaction modifies the electronic structure of the chromophores, which in turn influence their optical properties. The optical properties of these stacked compounds are compared to those of their unstacked linear models to study the effect of interchain interactions. Computational analysis, performed by Dr. Sukrit Mukhopadhyay in Prof. Brédas research group, provided a better understanding of the optoelectronic behavior of these molecules.

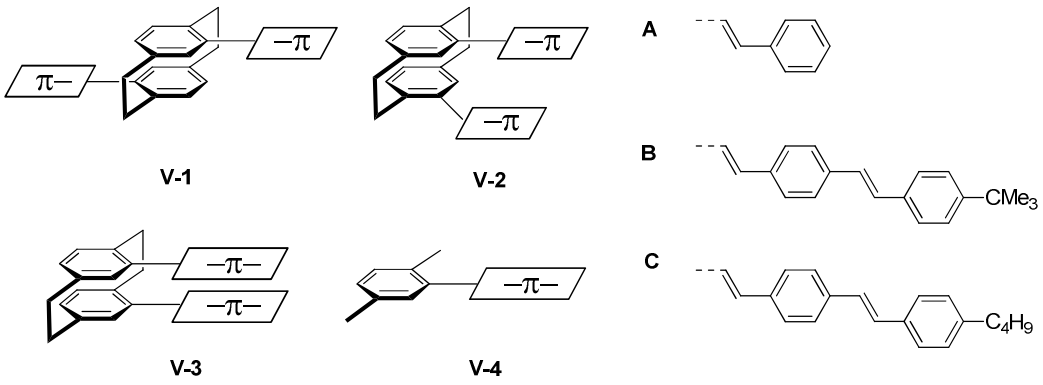


**Figure 5.1.** Molecular structures of [2.2]paracyclophane (CP) stacked oligo(phenylene vinylene)s (OPV)s: *pseudo-para* [2.2]paracyclophane (*pp*) stacked OPVs, **V-1**, *pseudo-ortho* [2.2]paracyclophane (*po*) stacked OPVs,V-**.2**, *pseudo-geminal* [2.2]paracyclophane (*pg*) stacked OPVs, **V-3**, and the model compounds, **V-4.** The molecular structures of individual oligomers are also presented in the figure (**A**, **B**, and **C**).

## 5.2. Experimental Procedures

### 5.2.1. General synthetic methods

General procedures and methods are described in Chapter 2.

### 5.2.2. Computational studies were completed by Dr. Sukrit Mukhopadhyay

The geometry optimizations of the unstacked molecules (**$Me_2PV_2$** and **$Me_2PV_3$**) are performed using both the B3LYP and ωB97X/6-31g* functionals[3] and the 6-31g* basis set. For the stacked molecules, ***pg*-$Cp[PV_2]_2$** and ***pg*-$Cp[PV_3]_2$**, in order to account for the dispersion interactions between oligomers, the geometries were obtained at the ωB97X-D/6-31g*[4] level of theory. The geometry optimizations have been performed for both gas-phase case and solvent phase case (in $CHCl_3$, using the continuum solvent model). All geometries were confirmed to be minima by additional vibrational frequency calculations. The low-lying excited states (at the gas-phase and solvent phase optimized geometries) have been derived by means of the time dependent density functional theory (TD-DFT) calculations using the ωB97X-D/6-31g* and ωB97X/6-31g* method for the stacked and unstacked molecules, respectively. TD-DFT calculations at the same level of theory as used for the ground state have been also employed to obtain the optimal geometries of the first excited states of both stacked and unstacked systems. All DFT calculations are performed using the Gaussian 09 package.

## 5.2.3. [2.2]Paracyclophane-4-glyoxyl chloride[5]

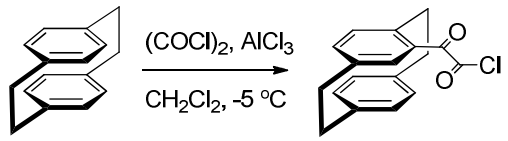


V-5 V-6

A suspension of aluminum trichloride (35.0 g, 262 mmol) in dry $CH_2Cl_2$ (300 mL) was stirred at -10 °C for 10 min. A solution of oxalyl chloride (33.3 g, 262 mmol) in dry $CH_2Cl_2$ (30 mL) was added dropwise to the reaction mixture over 10 min. The reaction mixture was stirred for 10 min followed by addition of [2.2]paracyclophane (31.2 g, 150 mmol) at once. The mixture was then stirred vigorously for 15 min. The reaction mixture was added to ice-cold water (500 mL) and extracted with $CH_2Cl_2$ (3 x 100 mL). The organic layer was separated and dried over $MgSO_4$. The solvent was removed under reduced pressure to afford [2.2]paracyclophane-4-glyoxylchloride as orange solids (43.0 g, 96%). m.p. = 90-91 °C (Lit:[5] 92 °C). $^1$H NMR (300 MHz, $CDCl_3$): δ 6.93 (d, *J* = 1.4 Hz, 1H, Ar-H), 6.83 (dd, *J* = 7.6, 1.8 Hz, 1H, Ar-H), 6.70 (d, *J* = 8.0 Hz, 1H, Ar-H), 6.40-6.60 (m, 4H, Ar-H), 4.07-4.17 (m, 1H, bridge-$CH_2$), 2.88-3.30 (m, 7H, bridge-$CH_2$). $^{13}$C NMR (75 MHz, $CDCl_3$): δ 181.2, 166.9 (carbonyl), 145.5, 140.7, 139.6, 139.5, 137.2, 136.6, 135.4, 133.1, 132.9, 132.3, 131.6, 129.6, (Ar-C), 35.6, 35.0, 34.7, 34.4 (bridge-C). IR (ATR): 2940, 2854, 1788, 1675, 1545, 1253, 1027, 801 cm$^{-1}$. MS (EI), m/z (%) = 298.1 ($M^+$, 1), 270.1 (45), 235.1 (35), 131.1 (50), 104.1 (100).

## 5.2.4. [2.2]Paracyclophane-4-acid chloride[5]

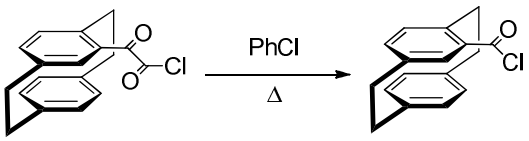


V-6 V-7

A solution of [2.2]paracyclophane-4-glyoxylchloride (40.0 g, 134 mmol) in chlorobenzene (150 mL) was heated at reflux for 6 h. The reaction mixture was then cooled to room temperature and the solvent was removed using vacuum distillation to yield the title compound as yellow powder contaminated with chlorobenzene (36.0 g, 99%). $^{1}$H NMR (300 Hz, $CDCl_3$): δ 7.42 (d, *J* = 1.8 Hz, 1H, Ar-H), 6.77 (dd, *J* = 7.9, 1.8 Hz, 1H, Ar-H), 6.44-6.67 (m, 5H, Ar-H), 3.82-3.99 (m, 1H, bridge-$CH_2$), 2.82-3.36 (m, 7H, bridge-$CH_2$). (The product was used without further purification).

## 5.2.5. Methyl [2.2]paracyclophane-4-carboxylate[5]

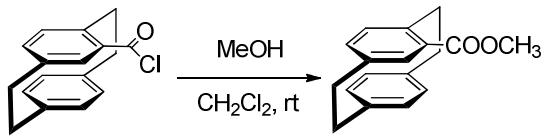


V-7 V-8

A solution of [2.2]paracyclophane-4-acid chloride (36.0 g, 133 mmol) in $CH_2Cl_2$ (100 mL) and MeOH (100 mL) was stirred at 40°C for 12 h. The solvent was removed under reduced pressure to afford methyl [2.2]paracyclophane-4-carboxylate as yellow powder (35 g, 99 %). m.p. = 65-66 °C (lit:[5] 64 °C). $^1$H NMR (300 MHz, $CDCl_3$): δ 7.12 (d, *J* = 1.9 Hz, 1H, Ar-H), 6.64 (dd, *J* = 7.9, 1.8 Hz, 1H, Ar-H), 6.39-6.58 (m, 5H, Ar-H), 4.01-4.14 (m, 1H, bridge-$CH_2$), 3.90 (s, 3H, ester-$CH_3$), 2.80-3.22 (m, 7H, bridge-$CH_2$). $^{13}$C NMR (75 MHz, $CDCl_3$): δ 164.9, (carbonyl), 142.6, 139.9, 139.8, 139.4, 136.4, 136.1, 135.3, 133.1, 132.7, 132.2, 131.6, 130.6 (Ar-C), 52.4 (ester-$CH_3$), 35.5, 35.1, 34.9, 34.6 (bridge-C). IR (ATR): 3010, 2930, 2857, 1711, 1432, 1270, 1193, 1074, 801, 718 $cm^{-1}$. MS (EI), m/z (%) = 294.1 ($M^+$, 24), 104.1 (100).

## 5.2.6. Methyl 15-formyl[2.2]paracyclophane-4-carboxylate[6]

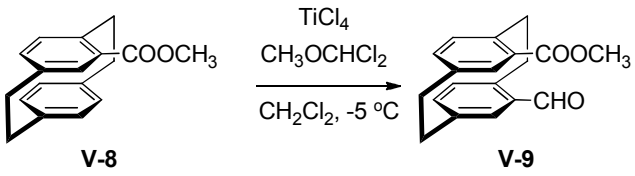


**V-8** **V-9**

A solution of methyl [2.2]paracyclophane-4-carboxylate (20 g, 75 mmol) in dry $CH_2Cl_2$ (300 mL) was stirred at -10°C. Titanium(IV)chloride (53.0 g, 279 mmol) was added dropwise to the solution over 10 min, followed by dropwise addition of α,α-dichloromethyl methyl ether (32.0 g, 279 mmol) while maintaining the reaction mixture at -10°C. The temperature was allowed to rise to room temperature and the mixture was stirred for 24 h. The reaction mixture was poured into ice-cold water (300 mL) and the organic layer was separated. The aqueous layer was repeatedly extracted with $CH_2Cl_2$ (3 x 100 mL). The organic layers were combined and washed with saturated $NaHCO_3$ solution, water, and brine. The organic layer was separated, dried over $MgSO_4$, and the solvent was removed under reduced pressure. The residue was subjected to flash chromatography (100% $CH_2Cl_2$, silica gel) followed by recrystallization from cyclohexane to yield the title compound as a yellow powder (15 g, 68%). m.p. = 168-170 °C (lit:[6] 169 °C). $^1$H NMR (300 Hz, $CDCl_3$): δ 9.91 (s, 1H, aldehyde), 7.08 (m, 2H, Ar-H), 6.58-6.75 (m, 4H, Ar-H), 4.04-4.22 (m, 2H, bridge-$CH_2$), 3.81 (s, 3H, ester-$CH_3$), 2.96-3.20 (m, 6H, bridge-$CH_2$). $^{13}$C NMR (75 MHz, $CDCl_3$): δ 190.6, 167.0 (carbonyl), 143.5, 142.1, 140.1, 139.7, 138.1, 136.5, 136.1, 136.0, 135.7, 134.4, 133.7, 130.8 (Ar-C), 51.9 (ester-$CH_3$), 35.0, 34.7, 34.6, 31.1 (bridge-C). IR (ATR): 3475, 3454, 3026, 2943, 2936, 1711, 1683, 1433, 1290, 1274, 1199, 1074, 983 $cm^{-1}$. MS (EI), m/z (%) = 294.1 ($M^+$, 100), 162.1 (95), 104.1 (75).

## 5.2.7. 4,15-Bis(hydroxymethyl)[2.2]paracyclophane[7]

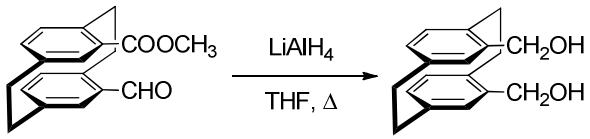


V-9 V-10

$LiAlH_4$ (2.2 g, 58 mmol) was added to a solution of methyl 15-formyl[2.2]paracyclophane-4-carboxylate (6.0 g, mmol) in anhydrous THF (250 mL). The reaction mixture was heated at reflux for 12 h. Water (200 mL) was added and the mixture was acidified with conc. HCl until all of the precipitate was dissolved. $CH_2Cl_2$ (100 mL) was added and the organic layer was separated. The organic layer was washed with saturated aqueous $NaHCO_3$ solution (100 mL) and water (100 mL), and dried over $MgSO_4$. The solvent was removed under reduced pressure to yield 4,15-bis(hydroxymethyl)[2.2]paracyclophane as a white powder (5.0 g, 92%). m.p. = 217-218 °C. $^1$H NMR (300 MHz, $CDCl_3$): 6.60 (d, *J* = 2.0 Hz, 2H, Ar-H), 6.46-6.53 (m, 4H, Ar-H), 4.70 (d, J = 13.5 Hz, 2H, $OCH_2$), 4.56 (d, *J* = 13.5 Hz, 2H, $OCH_2$), 3.34-3.46 (m, 2H, bridge-$CH_2$), 2.92-3.14 (m, 6H, bridge-$CH_2$). $^{13}$C NMR (75 MHz, $CDCl_3$): δ 139.8, 139.1, 135.7, 134.7, 132.4, 129.8 (Ar-C), 62.8 ($OCH_2$), 35.1, 31.4 (bridge-C). IR (ATR): 3186, 2933, 2850, 1595, 1479, 1240, 1090, 1047, 894, 708 cm$^{-1}$. MS (EI), m/z (%) = 268.1 ($M^+$, 25), 105.1 (100). HRMS calculated for $C_{18}H_{20}O_2$, 268.1463; found 268.1472, Δ = 3.4 ppm.

## 5.2.8. 4,15-Diformyl[2.2]paracyclophane[7]

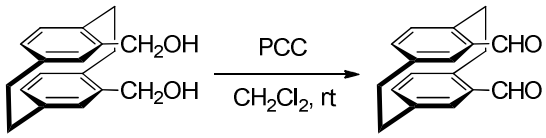


V-10 V-11

Pyridinium chlorochromate (PCC) (2.68 g, 12.0 mmol) was added to a solution of bis(hydroxymethyl)[2.2]paracyclophane (1.0 g, 4.0 mmol) in anhydrous $CH_2Cl_2$ (100 mL). The reaction mixture was stirred for 24 h. $Et_2O$ (50 mL) was added to the reaction mixture and the solution was flushed through a plug of silica gel, which was then rinsed with $CH_2Cl_2$ (200 mL). The solvent was removed under reduced pressure to yield the title compound as brown powder (0.9 g, 91%). m.p. = 163-164 °C. $^1$H NMR (300 MHz, $CDCl_3$): δ 9.80 (s, 2H, aldehyde), 6.98 (d, *J* = 2.0 Hz, 2H, Ar-H), 6.75 (dd, *J* = 7.9, 1.8 Hz, 2H, Ar-H), 6.65 (d, *J* = 7.9 Hz, 2H, Ar-H), 4.08-4.18 (m, 2H, bridge-$CH_2$), 3.04-3.22 (m, 6H, bridge-$CH_2$). $^{13}$C NMR (75 MHz, $CDCl_3$): δ 191.4 (carbonyl), 142.7, 140.4, 137.9, 136.9, 136.1, 134.6 (Ar-C), 34.7, 31.8 (bridge-C). IR (ATR): 2927, 2860, 2734, 1675, 1588, 1226, 1143, 718 $cm^{-1}$. MS (EI), m/z (%) = 264.1 ($M^+$, 60), 104.1 (100). HRMS calculated for $C_{18}H_{16}O_2$, 264.1150; found 264.1150, Δ = 0.0 ppm.

## 5.2.9. 4,15-Diethenyl[2.2]paracyclophane[2]

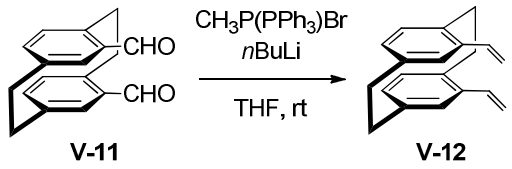


V-11 V-12

*n*BuLi (4.3 mL of a 1.6 M solution in hexane, 6.8 mmol) was added to a mixture of methyltriphenylphosphonium bromide (3.6 g, 10 mmol) in THF (100 mL). The reaction mixture was stirred for 2 h at room temperature. A solution of 4,15-diformyl[2.2]paracyclophane (900 mg, 3.00 mmol) in THF (20 mL) was added to the reaction mixture. The mixture was stirred for 16 h, the mixture was cooled to 0 °C and water (20 mL) was added. The organic layer was separated. The aqueous layer was extracted with $CH_2Cl_2$ (100 mL) and the organic layers were combined and washed with water (100 mL) and brine (100 mL) sequentially and dried over $MgSO_4$. The solvent was removed under reduced pressure and the residue was subjected to a flash chromatography ($CH_2Cl_2$, silica gel) followed by recrystallization from hexane to obtain the title compound as a white powder (400 mg, 45%). m.p. 163-164°C (Lit:[2] 165 °C). $^1$H NMR (300 MHz, $CDCl_3$) δ 6.82 (dd, *J* = 17.6, 11.4 Hz, 2 H, vinylic), 6.59 (d, *J* = 1.2 Hz, 2 H, Ar–H), 6.49 (d, *J* = 7.9 Hz, 2 H, Ar–H), 6.45 (dd, *J* = 7.9, 1.8 Hz, 2 H, Ar–H), 5.36 (dd, *J* = 17.3, 1.4 Hz, 2 H, vinylic), 5.08 (dd, *J* = 10.8, 1.4 Hz, 2 H, vinylic), 3.48–3.60 (m, 2 H, $CH_2$), 2.90–3.10 (m, 6 H, $CH_2$). $^{13}$C NMR (75 MHz, $CDCl_3$) δ 139.4, 138.1, 137.3, 135.5, 134.6, 132.4, 129.8, 114.7 ($sp^2$ C), 83.4, 81.2 (C=C), 35.1, 32.5 ($CH_2$). IR (ATR): 3080, 3000, 2921, 2853, 1629, 1461, 905, 714 cm$^{-1}$. MS (EI): *m*/*z* (%) 260.1 ($M^+$, 54), 129.1 (100). HRMS calculated for $C_{20}H_{20}$, 260.1565; found 260.1575, Δ = 3.8 ppm.

**5.2.10. (*E*)-1-Butyl-4-(4-iodostyryl)benzene**

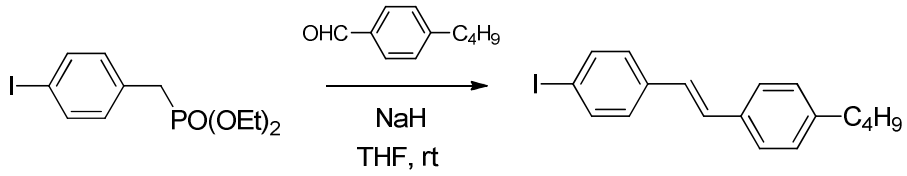


**V-13**

NaH (850 mg, 35.3 mmol) was added to a solution of diethyl 4-iodobenzylphosphonate (2.5 g, 7.1 mmol) in THF (100 mL) at 0 °C. A solution of 4-butylbenzaldehyde (950 mg, 5.90 mmol) was added dropwise to the reaction mixture. A mixture was stirred at room temperature for 36 h and water (50 mL) was added to the reaction mixture followed by addition of $Et_2O$ (50 mL). The organic layer was separated and dried over $MgSO_4$. The solvent was removed under reduced pressure and the residue was subjected to a flash column chromatography (hexane, silica gel) to afford the title compound as white powder (1.5 g, 71%). m.p. = 163-164°C. $^1$H NMR (300 MHz, $CDCl_3$): δ 7.65 (d, *J* = 8.5 Hz, 2 H, Ar-H), 7.41 (d, *J* = 8.2 Hz, 2 H, Ar-H), 7.23 (d, *J* = 8.5 Hz, 2 H, Ar-H), 7.17 (d, *J* = 8.2 Hz, 2 H, Ar-H), 2.61 (t, *J* = 7.9 Hz, 2 H, $CH_2$), 1.60 (pentet, *J* = 7.1 Hz, 2 H, $CH_2$), 1.35 (sextet, *J* = 7.9 Hz, 2 H, $CH_2$), 0.92 (t, *J* = 7.3 Hz, 2 H, $CH_3$). $^{13}$C NMR (75 MHz, $CDCl_3$): δ 142.9, 137.7, 137.1, 134.3, 129.5, 128.8, 128.1, 126.5, 126.4, 92.5 (Ar-C and C=C), 35.4, 33.6, 22.4 ($CH_2$), 14.0 ($CH_3$). IR (ATR): 3020, 2960, 2850, 1482, 1007, 971, 821 $cm^{-1}$. MS (EI): *m*/*z* (%) 362.0 ($M^+$, 100), 318.9 (70). HRMS calculated for $C_{18}H_{19}I$, 362.0532; found 362.0544, Δ = 3.3 ppm.

**5.2.11. (*E*)-2,5-Dimethylstilbene, $Me_2PV_2$[8]**

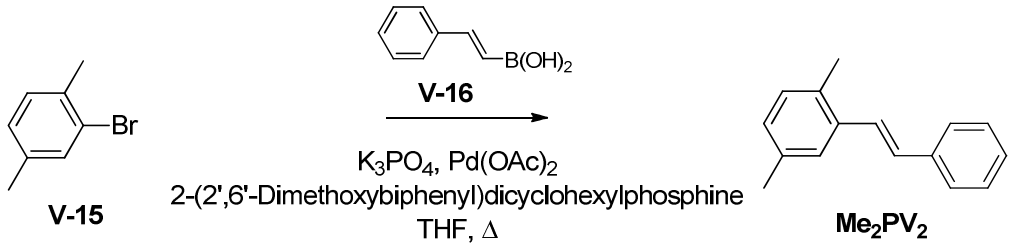


A mixture of 2-bromo-*p*-xylene (370 mg, 2.00 mmol), (*E*)-β-styrene boronic acid (450 mg, 3.00 mmol), $K_3PO_4$ (850 mg, 4.00 mmol), $Pd(OAc)_2$ (5.0 mg, 0.01 mmol), and 2-(2',6'-dimethoxybiphenyl)dicyclohexylphosphine (16 mg, 20 μmol) in THF (4 mL) was stirred at 40 °C for 24 h. Ethyl acetate (20 mL) was added and the reaction mixture was flushed through a short plug of silica gel with additional ethyl acetate. The solvent was removed under reduced pressure and the residue was subjected to a flash column chromatography (95% hexanes/5% ethyl acetate, silica gel) to afford the title compound as a white solid (420 mg, 97%), m.p. = 40-41 °C (Lit:[8] 42-43 °C). $^1$H NMR (300 MHz, $CDCl_3$): δ 7.50 (d, *J* = 8 Hz, 2 H, Ar-H), 7.28-7.40 (m, 3 H, Ar-H), 7.23 (d, *J* = 8 Hz, 2 H, Ar-H), 6.96-7.06 (m, 3 H, Ar-H and vinyl), 2.36 (s, 3 H, $CH_3$), 2.33 (s, 3 H, $CH_3$). $^{13}$C NMR (75 MHz, $CDCl_3$): δ 137.7, 136.0, 135.4, 132.7, 130.3, 130.0, 128.6, 128.3, 127.4, 126.5, 126.4, 125.9, 21.0, 19.4. IR (ATR): 3026, 2922, 1599, 1499, 1448, 1266, 961 $cm^{-1}$.

## 5.2.12. Stacked dimer, *pg*-Cp[$PV_2$]$_2$

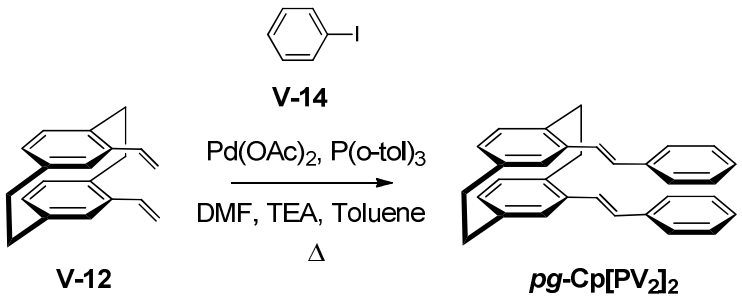


A solution of 1-iodobenzene (500 mg, 2.70 mmol), $Pd(OAc)_2$ (31 mg, 0.14 mmol), $P(o\text{-}tol)_3$ (85 mg, 0.28 mmol) and 4,15-diethenyl[2.2]paracyclophane (100 mg, 400 μmol) in a 2:1:1 v/v mixture of DMF, triethylamine and toluene (8 mL) was stirred at 90 °C for 48 h under Ar. The reaction mixture was cooled to room temperature and poured into MeOH (150 mL). The precipitated solid was removed by filtration and recrystallized from ethanol to afford the desired product as a white solid (120 mg, 76% yield). m.p. = 164-165 ºC. $^1$H NMR (300 MHz, $CDCl_3$): δ 7.23–7.28 (m, 2H, Ar-H), 7.18 (d, *J* = 16.1 Hz, 2H, vinyl), 7.08–7.14 (m, 8H, Ar-H), 6.71 (d, *J* = 1.8 Hz, 2H, Ar-H), 6.69 (d, *J* = 16.1 Hz, 2H, vinyl), 6.55 (d, *J* = 7.9 Hz, 2H, Ar-H), 6.50 (dd, *J* = 7.9, 1.8 Hz, 2H, Ar-H), 3.62-3.73 (m, 2H, bridge-$CH_2$), 2.99-3.12 (m, 6H, bridge-$CH_2$). $^{13}$C NMR (75 MHz, $CDCl_3$): δ 139.4, 137.8, 137.6, 134.8, 132.2, 130.3, 129.6, 128.4, 127.5, 127.1 (Ar-C), 126.4 (C=C), 35.0, 32.9 ($CH_2$). IR (ATR): 3020, 2930, 2850, 1595, 1495, 1446, 951, 755 cm$^{-1}$. MS (EI): m/z (%) 412.2 ($M^+$, 50), 205.1 (100). HRMS calculated for $C_{32}H_{28}$, 412.2191; found 412.2189, Δ = 0.5 ppm.

**5.2.13. 2-((*E*)-4-((*E*)-4-butylstyryl)styryl)-1,4-dimethylbenzene, $Me_2PV_3$**

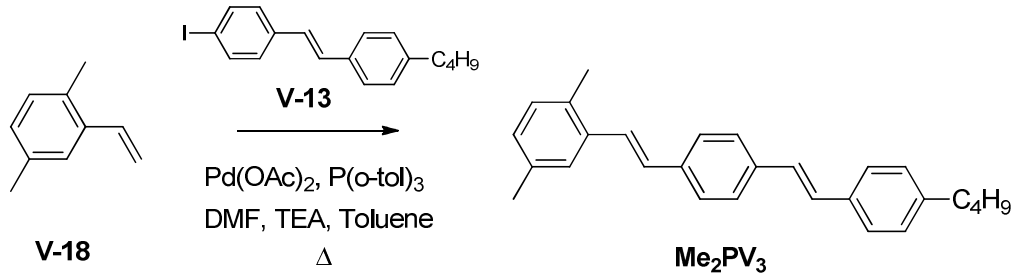


A solution of (*E*)-1-butyl-4-(4-iodostyryl)benzene (100 mg, 280 μmol), $Pd(OAc)_2$ (6.0 mg, 28 μmol), $P(o\text{-}tol)_3$ (17 mg, 56 μmol) and 2,5-dimethylstyrene (74.0 mg, 560 μmol) in a 2:1:1 v/v mixture of DMF, triethylamine and toluene (8 mL) was stirred at 90 °C for 48 h under Ar. The reaction mixture was cooled to room temperature and poured into MeOH (150 mL). The precipitated solid was removed by filtration and recrystallized from ethanol to afford a yellow solid (230 mg, 83% yield). m.p. = 120-122 ºC. $^1$H NMR (300 MHz, $CDCl_3$): δ 7.51 (s, 4H, Ar-H), 7.43 (m, 3H, Ar-H and vinyl), 7.33 (d, *J* = 15Hz, 1H, vinyl), 7.15-7.20 (m, 2H, Ar-H), 7.04-7.10 (m, 3H, Ar-H and vinyl), 6.93-7.03 (m, 2H, Ar-H and vinyl), 2.62 (t, *J* = 6Hz, 2H, Ar-$CH_2$), 2.40 (s, 3H, Ar-$CH_3$), 2.35 (s, 3H, Ar-$CH_3$), 1.61 (pentet, *J* = 9Hz, 2H, $CH_2$), 1.35 (sextet, *J* = 9Hz, 2H, $CH_2$), 0.93 (t, *J* = 6Hz, 3H, $CH_3$). $^{13}$C NMR (75 MHz, $CDCl_3$): δ 142.7, 136.9, 136.8, 136.1, 135.5, 134.7, 132.8, 130.3, 129.3, 128.7, 128.4, 128.3, 127.3, 126.5, 126.3, 125.8 (Ar-C and vinyl-C), 35.4, 33.6 (Ar-$CH_3$), 22.4, 21.1, 19.5 ($CH_2$), 13.9 ($CH_3$). IR (ATR): 3020, 2963, 2847, 1520, 1260, 1097, 1014, 957, 801 cm$^{-1}$. MS (EI): m/z (%) 366.2 ($M^+$, 100), 323.2 (30). HRMS calculated for $C_{28}H_{30}$, 366.2348; found 366.2355, Δ = 1.9 ppm.

## 5.2.14. Stacked trimer, *pg*-Cp[$PV_3$]$_2$

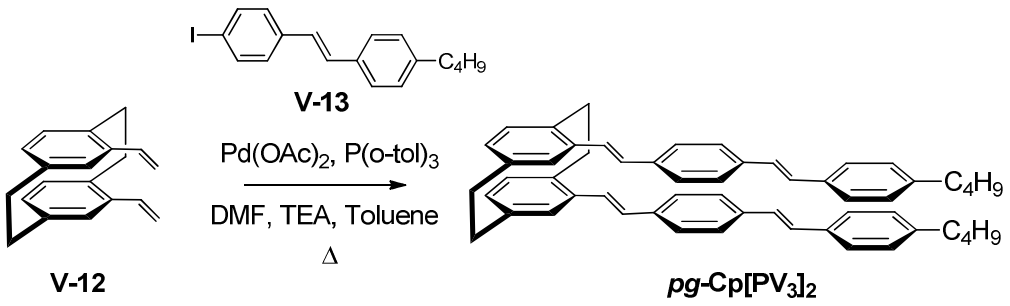


A solution of (*E*)-1-butyl-4-(4-iodostyryl)benzene (235 mg, 650 μmol), $Pd(OAc)_2$ (7 mg, 27 μmol), $P(o\text{-tol})_3$ (16 mg, 54 μmol) and 4,15-diethenyl[2.2]paracyclophane (70 mg, 0.27 mmol) in a 2:1:1 v/v mixture of DMF, triethylamine and toluene (8 mL) was stirred at 90 °C for 48 h under Ar. The reaction mixture was cooled to room temperature and poured into MeOH (150 mL). The precipitated solid was removed by filtration and recrystallized from ethanol to afford the desired product as a white solid (150 mg, 76% yield). m.p. = 244-246 ºC. $^1$H NMR (300 MHz, $CD_2Cl_2$): δ 7.30 (m, 8H, Ar-H), 7.26 (d, *J* = 12Hz, 2H, vinyl), 7.23 (d, *J* = 12Hz, 2H, vinyl), 7.20 (d, *J* = 15Hz, 2H, vinyl), 7.02-7.07 (m, 8H, Ar-H), 6.77 (d. *J* = 3Hz, 2Hz, Ar-H), 6.73 (d, *J* = 15Hz, 2H, vinyl), 6.58 (d, *J* = 6Hz, 2H, Ar-H), 6.53 (dd, *J* = 6, 3Hz, 2H, Ar-H), 3.66-3.72 (m, 2H, bridge-$CH_2$), 3.05-3.12 (m, 6H, bridge-$CH_2$), 2.62 (t, *J* = 3Hz, 4H, Ar-$CH_2$), 1.55-1.75 (m, 4H, $CH_2$), 1.35-1.45 (m, 4H, $CH_2$), 0.97 (t, *J* = 6Hz, 6H, $CH_3$). The low solubility of the product precluded analysis by $^{13}$C NMR spectroscopy. IR (ATR): 3020, 2930, 2850, 1595, 1495, 1446, 951, 755 cm$^{-1}$. MS (EI): m/z (%) 728.4 ($M^+$, 100), 363.2 (60). HRMS calculated for $C_{56}H_{56}$, 728.4382; found 728.4380, Δ = 0.3 ppm.

## 5.3. Results and Discussion

### 5.3.1. Synthesis of the 4,15-Diethenyl[2.2]paracyclophane Scaffold

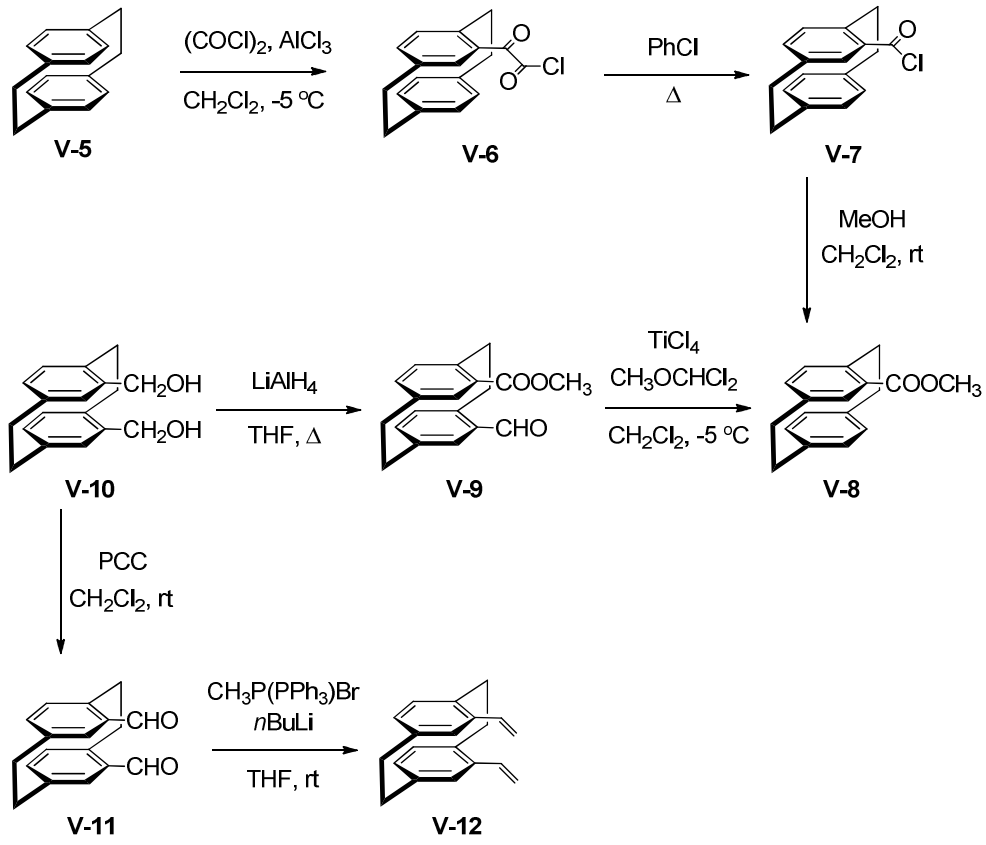


**Figure 5.2.** Synthesis of 4,15-diethenyl[2.2]paracyclophane, **V-12**.

Our synthetic approach to prepare 4,15-diethenyl[2.2]paracyclophane in seven steps from commercially available [2.2]paracyclophane is illustrated in Figure 5.2.[2, 5, 6, 7] This followed the route developed by Hopf et al. with small modifications. [2.2]Paracyclophane was monofunctionlized by treating it with oxalyl chloride in the presence of aluminum trichloride to give [2.2]paracyclophane-4-glyoxyl chloride, **V-6** in near quantitative yield (~ 99%). It is an important to control the temperature of the reaction since there is a strong exotherm. The intermediate glyoxyl chloride was used immediately in the next step. Upon heating in a solution

of 1-chlorobenzene at reflux, the glyoxylic chloride **V-6** underwent decarbonylation to afford corresponding the acid chloride, **V-7.** The solvent was removed using vacuum distillation but the acid chloride remained contaminated with a trace amount of left over 1-chlorobenzene. The acid chloride **V-7** was treated with methanol to obtain methyl [2.2]paracyclophane-4-carboxylate, **V-8**, in very high yields (> 95%). The ester **V-8** was subjected to a Rieche formylation using α,α'-dichloromethylmethyl ether and titanium tetrachloride in anhydrous dichloromethane to give methyl-15-formyl[2.2]paracyclophane-4-carboxylate,**V-9**. This is the most important step in this synthesis because the reaction takes place in a regioselective manner on the carbon atom below the ester-substituted position by virtue of the coordination of $TiCl_4$ to the carbonyl in the reaction pathway to provide the pseudo-germinal substitution pattern in **V-9**. Precautions were taken to maintain the temperature of reaction mixture at -5 °C to avoid possible side reactions. Careful work-up is required when quenching the reaction mixture with ice-cold water. Analytically pure product was obtained by recrystallization from cyclohexane. Reduction of **V-9** to give 4,15-bis(hydroxymethyl)[2.2]paracyclophane (**V-10**), followed by oxidation with pyridinium chlorochromate (PCC), afforded dialdehyde **V-11**, from which the divinyl monomer (**V-12**) was prepared. In our hands, the use of PCC as oxidant gave significantly higher yields of **V-11** than the use of DDQ reported by Hopf.[7] A Wittig reaction of **V-11** with methyltriphenylphosphonium bromide gave 4,15-diethenyl[2.2]paracyclophane, **V-12** The use of an excess of methyltriphenylphosphonium bromide provided improved yields compared to the literature procedure.

### 5.3.2. Synthesis of Phenylene Vinylene Arms

We decided to synthesize (*E*)-1-butyl-4-(4-iodostyryl)benzene **V-13** which could be installed on 4,15-diethenyl[2.2]paracyclophane (**V-12**) to prepare the π-stacked trimer, ***pg*-Cp[PV$_3$]$_2$**. The linear side chain (butyl group) was chosen to impart the solubility and avoid the steric hindrance in the resulting stacked product. Commercially available phosphonate and aldehyde were used. Treatment of phosphonate with NaH, followed by addition of the aldehyde in dry THF gave **V-13** in good yields (60%), Figure 5.3. The pure trans analog was obtained by column chromatography followed by recrystallization from EtOH.

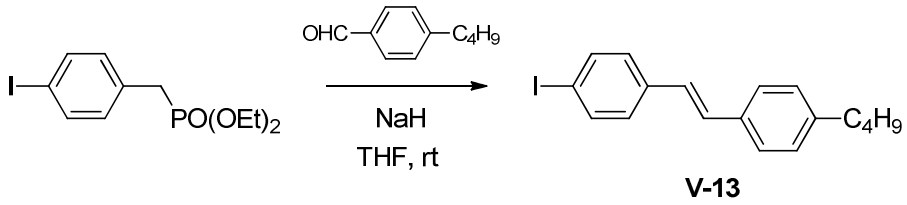


**Figure 5.3.** Synthesis of (*E*)-1-butyl-4-(4-iodostyryl)benzene, **V-13**.

### 5.3.3. Synthesis of π-stacked Oligo(phenylene vinylene)s

The Heck reaction was used to install 1-iodobenzene on the 4,15-diethenyl[2.2]paracyclophane core. Treatment of the diethenyl compound **V-12** with a large excess (3-4 eq.) of commercially available 1-iodobenzene in the presence of $Pd(OAc)_2$ and $P(o\text{-}tol)_3$ in dry DMF/triethylamine/toluene at 90 °C for 2 d gave the corresponding stacked stilbene, ***pg*-Cp[$PV_2$]$_2$**, in good yield (76%). The stacked stilbene was sensitive to light because unidentified NMR signal appeared upon expore to a light. Hence, column chromatography was avoided due to light sensitive nature of the stacked stilbene. Recrystallization from EtOH provided stacked dimer ***pg*-Cp[$PV_2$]$_2$** as white solid. Precautions were taken not to expose the stacked dimer to light and chlorinated solvents for a long period of time.

Similarly, synthesis of the stacked trimer ***pg*-Cp[$PV_3$]$_2$** was accomplished by the Heck coupling of **V-12** and (*E*)-1-butyl-4-(4-iodostyryl)benzene, **V-13**. Precipitation in MeOH followed by repeated recrystallization from EtOH provided the required stacked trimer as a yellow solid in satisfactory yield (70%), Figure 5.4. Similar precautions as described above were taken to avoid decomposition of product.

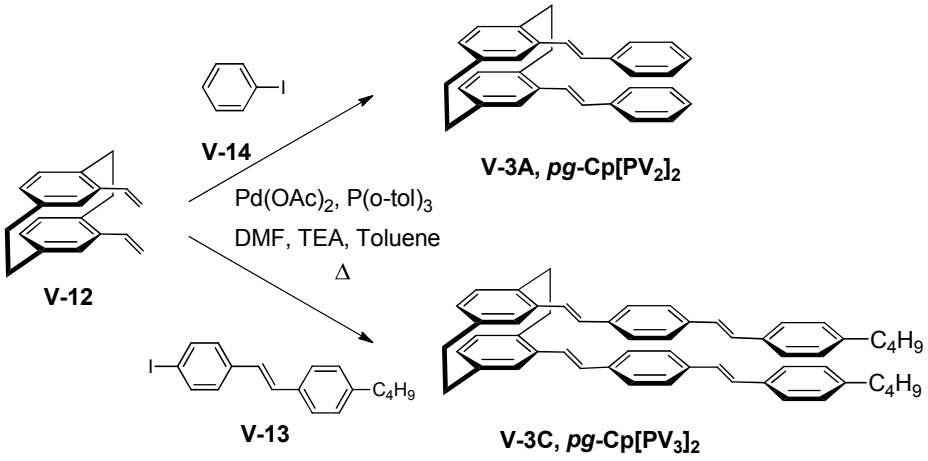


**Figure 5.4.** Synthesis of ***pg*-Cp[PV$_2$]$_2$** and ***pg*-Cp[PV$_2$]$_2$**.

### 5.3.4. Synthesis of Unstacked Models

The Suzuki-Miyaura coupling was used to couple (*E*)-β-styrene boronic acid and 2-bromo-*p*-xylene.[8] Treatment of **V-15** with an excess (1.5 eq.) of commercially available (*E*)-β-styrene boronic acid in the presence of $Pd(OAc)_2$, $K_3PO_4$ and 2-(2',6'-dimethoxybiphenyl)dicyclohexylphosphine in dry THF at 40 °C gave corresponding unstacked dimethylstilbene, **Me$_2$PV$_2$**, in good yield (97%). Surprisingly, attempts to prepare **V-17** by coupling dimethylstyrene and 1-iodobenzene using Heck reaction did not provide the required compound in our hands.

In contrast to the synthesis of unstacked dimer **Me$_2$PV$_3$**, synthesis of the unstacked trimer **Me$_2$PV$_3$** was accomplished by the Heck coupling of dimethylstyrene **V-18** to (*E*)-1-butyl-4-(4-iodostyryl)benzene, **V-13**. Precipitation in MeOH followed by recrystallization from EtOH provided required unstacked trimer **Me$_2$PV$_3$** as yellow solid in good yield (83%), Figure 5.5.

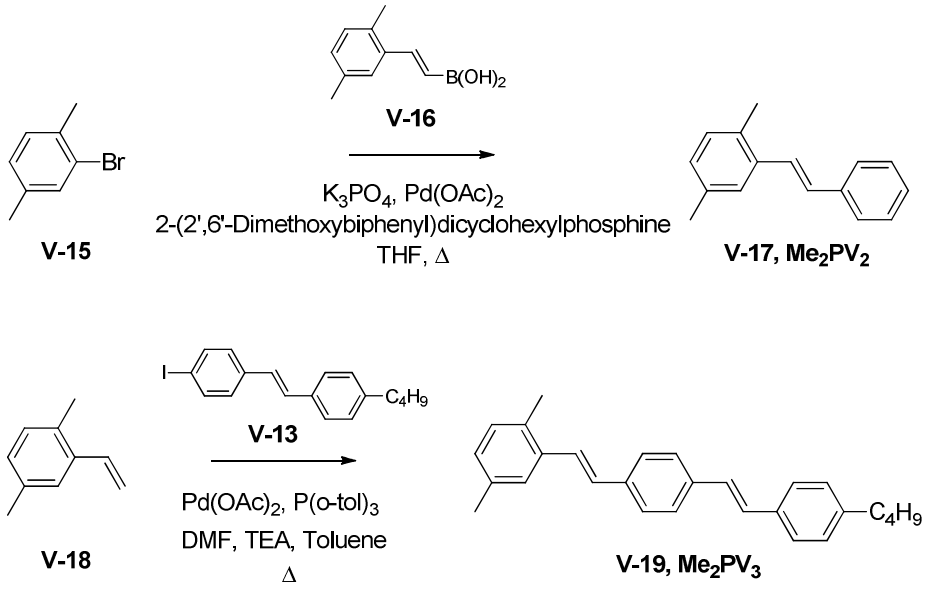


**Figure 5.5.** Synthesis of **$Me_2PV_2$** and **$Me_2PV_3$**.

### 5.3.5. Structural Characterization. $^{1}$H NMR and $^{13}$C NMR Spectroscopy

The simple $^{1}$H NMR spectrum of 4,15-diethenyl[2.2]paracyclophane is consistent with the notion that the compound exists in a preferred confirmation in which the two vinyl groups are oriented away from the neighboring ethano bridge to minimize the steric interactions between them, Figure 5.6. The symmetry of *pg* diethenyl compound is apparent from the AMX pattern for the identical 1,2,4-trisubstituted arenes. In addition, the 1H NMR signal for the hydrogen atoms on the ethano bridges that are facing the vinyl substituents are shifted downfield relative to the other hydrogen atoms on the bridge.

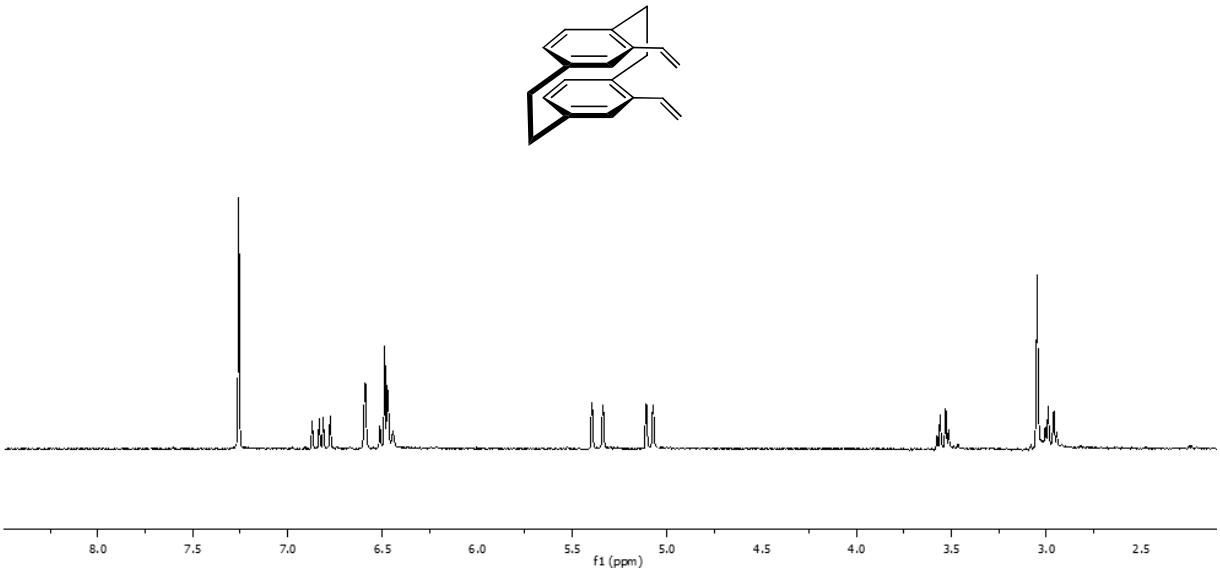


**Figure 5.6.** $^{1}$H NMR ($CDCl_3$, 23 °C): 4,15-diethenyl[2.2]paracyclophane, **V-12**.

The $^{1}$H NMR of the distyryl compound ***pg*-Cp[PV$_2$]$_2$** confirms the trans configuration of double bond in each stilbene chromophore which if the steric repulsion between the ethano bridge and conjugated substituents results in a similar conformation, gives the two stilbene units stacked atop one another, Figure 5.7. The AMX pattern was observed in the NMR of the stacked

stilbene: doublet at 6.71 ppm ($J$ = 1.8 Hz), doublet at 6.55 ppm ($J$ = 7.9 Hz), and doublet of doublet at 6.50 ppm ($J$ = 7.9, 1.8 Hz). Such a simple pattern indicates that ***pg*-Cp[PV$_2$]$_2$** has a plane of symmetry and stilbene chromophores atop one another. Also, the two distinct doublets at 7.18 ppm and 6.69 ppm ($J$ = 16.1 Hz) confirmed the trans configuration of the stilbene chromophores.

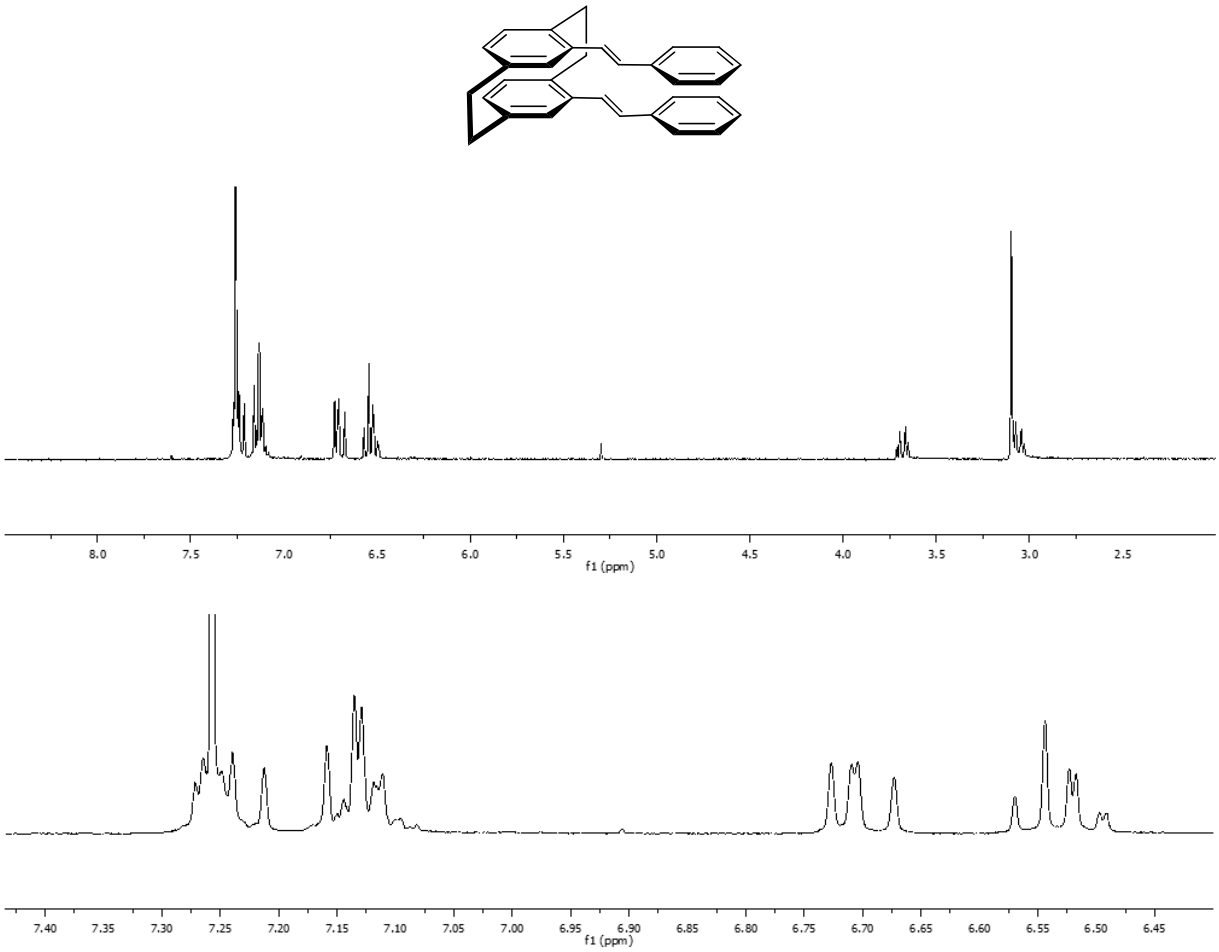


**Figure 5.7.** $^1$H NMR spectra ($CDCl_3$, 23 °C): Stacked dimer, ***pg*-Cp[PV$_2$]$_2$** (top) and magnified view of region (6.40-7.45ppm) (bottom).

Similar sets of peaks were observed for the *pseudo-germinal* [2.2]paracyclophane core of ***pg*-Cp[PV$_3$]$_2$**, Figure 5.8. The AMX pattern was observed in the 1H NMR of stacked trimer ***pg*-Cp[PV$_3$]$_2$**: doublet at 6.77 ppm ($J$ = 1.8 Hz), doublet at 6.58 ppm ($J$ = 7.9 Hz), and doublet of doublet at 6.53 ppm ($J$ = 7.9, 1.8 Hz). Also, the α-methylene proton of butyl chain appear as a triplet ($J$ = 3.0 Hz). While such a simple pattern shows that the compound is symmetrical, it does not allow for the assignment of the conformations as specifically cisoid and transoid, Figure 5.9.

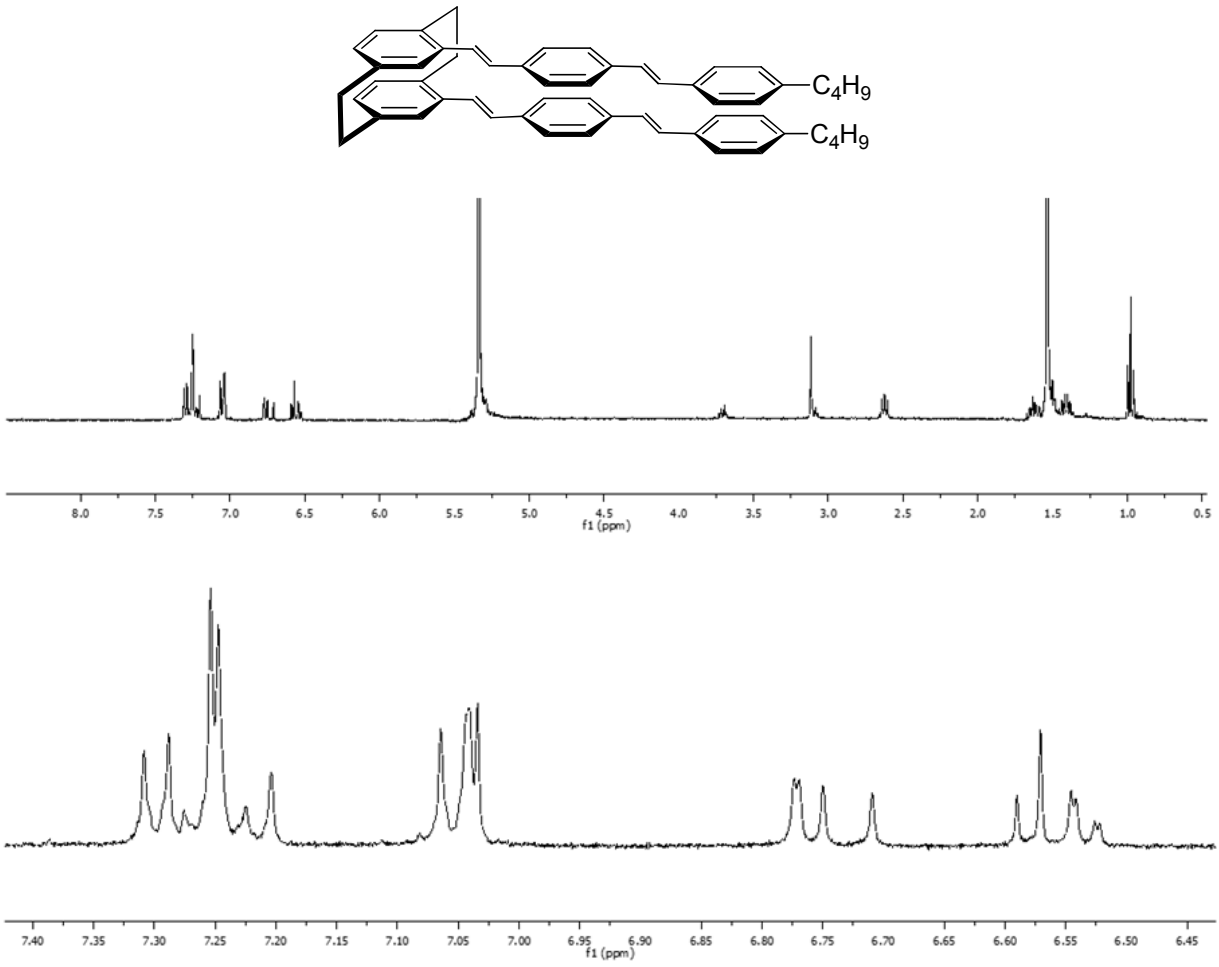


**Figure 5.8.** $^1$H NMR spectra ($CD_2Cl_2$, 23 °C): Stacked trimer, ***pg*-Cp[PV$_3$]$_2$** (top) and magnified view of region (6.45-7.40 ppm) (bottom).

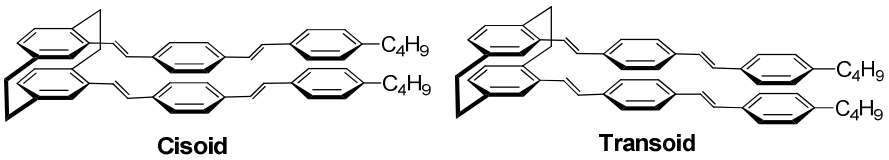


**Figure 5.9.** Cisoid and transoid conformations of chromophore, $\mathbf{PV_3}$.

### 5.3.6. UV-Vis and Fluorescence spectroscopy

The stacked oligomers and unstacked linear analogues were characterized by UV-Vis and fluorescence spectroscopy to explore the effect of stacking on the electronic structure of the conjugated tiers. The stacked dimer ***pg*-Cp[$PV_2$]$_2$** ($\lambda_{max}$ = 295 nm) shows a small hypsochromic shift (1 nm) in absorbance relative to its unstacked model **$Me_2PV_2$** ($\lambda_{max}$ = 297 nm), Figure 5.10. The stacked stilbene ***pg*-Cp[$PV_2$]$_2$** exhibits the red shifted absorption edge in contrast to that of model **$Me_2PV_2$** which suggests that a weakly allowed optical transition is present in the case of the stacked compound. The emission spectrum shows much larger differences between the stacked and unstacked compounds. The stacked dimer shows an emission peak at 432 nm, which is significantly red shifted from that of the unstacked counterpart (365 nm), Figure 5.11. Such a red shifted peak for ***pg*-Cp[$PV_2$]$_2$** is characteristic of excimer-like emission.

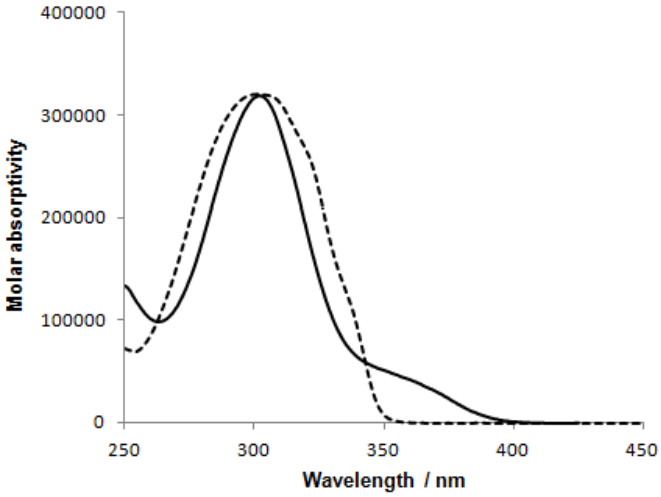


**Figure 5.10.** UV-vis spectra: ***pg*-Cp[PV$_2$]$_2$** (solid) and **Me$_2$PV$_2$** (dotted), $c$ = 2.4 × 10$^{-6}$ M in $CHCl_3$, T = 23 °C.

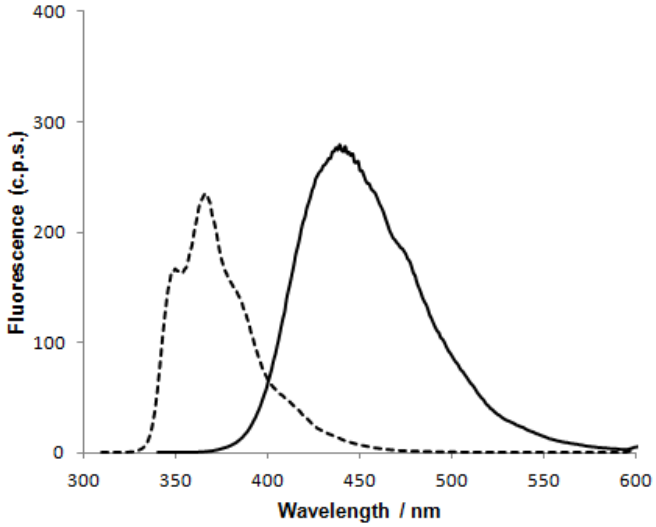


**Figure 5.11.** Fluorescence spectra: Top, ***pg*-Cp[PV$_2$]$_2$** (solid) and **Me$_2$PV$_2$** (dotted), $c$ = 2.4 × 10$^{-6}$ M in $CHCl_3$, T = 23 °C.

The well resolved peaks were obtained by plotting emission profile on the energy scale and after their deconvolution of spectra into distinct contributions, Figure 5.12. The emission spectrum of **$Me_2PV_2$** possesses three distinct peaks at 3.56 eV, 3.39 eV and 3.22 eV and, in addition, has a broad tail, which is centered on 3.14 eV. On the other hand, the emission spectrum of the stacked stilbene ***pg*-Cp[$PV_2$]$_2$** possesses a broad peak (2.87 eV) with a distinct tail (~ 2.66 eV) and does not possess any well-resolved vibrational features as seen in the unstacked analogue. So, this suggests that the emission ***pg*-Cp[$PV_2$]$_2$** is due to the excimer-like state which arises due to interaction between closely packed stilbene chromophores in the stacked compound.

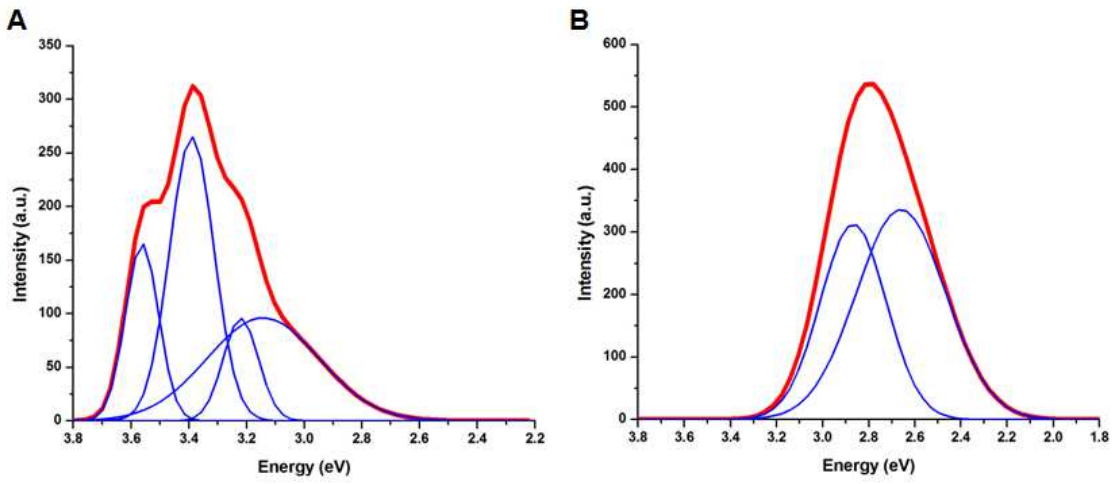


**Figure 5.12.** Fluorescence spectra on an energy scale and their deconvolution into distinct contributions: A, **$Me_2PV_2$** and B, ***pg*-Cp[$PV_2$]$_2$**, $c = 2.4 \times 10^{-6}$ M in $CHCl_3$, T = 23 °C.

For "trimer" **$Me_2PV_3$**, the absorption maximum is at 352 nm, whereas that of the stacked "trimer" (***pg*-Cp[$PV_3$]$_2$**) is at 350 nm. Thus, similar to the stilbene analogue, the absorption maximum of the stacked compound is blue shifted only slightly relative to the unstacked linear

analog. Again, there is a tail at the absorption edge at ~ 3.07 eV, which can be rationalized as an effect of stacking. The emission spectrum of **$Me_2PV_3$** possesses three distinct peaks at 401, 424 and 450 along with a tail ~ 462 nm. On the other hand, in contrast to the smaller analogue, the emission spectrum of the stacked "trimer" resembles well with that of the unstacked analogue; the emission spectrum possesses three well-resolved peaks at 405, 427 and 454 and a broad tail ~ 484 nm. Thus by comparing the absorption and emission spectra of the stacked and unstacked molecules, we can conclude that the stacked dimer emission is entirely from an excimeric state. On the other hand, the stacking of **$Me_2PV_3$** does not lead to significant change of the emission spectrum, which is mainly dominated by the local-state contribution.

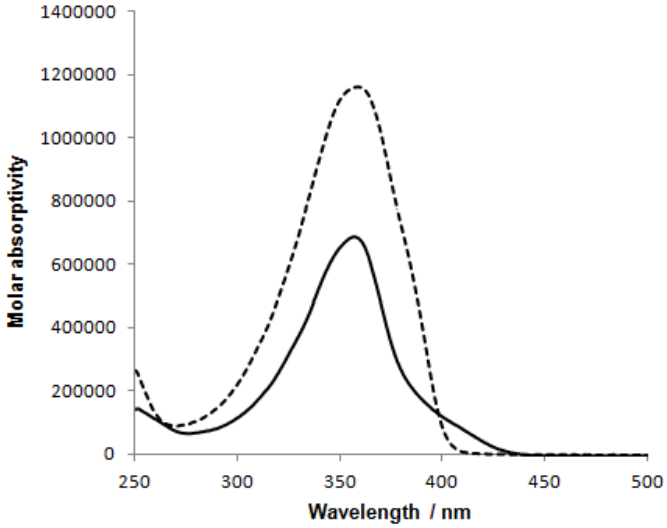


**Figure 5.13.** UV-vis spectra: ***pg*-Cp[$PV_3$]$_2$** (solid) and **$Me_2PV_3$** (dotted), $c = 3 \times 10^{-6}$ M in $CHCl_3$, T = 23 °C.

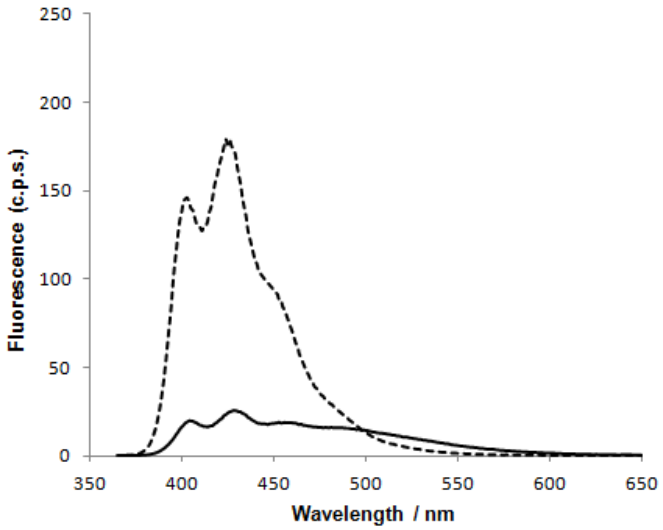


**Figure 5.14.** Fluorescence spectra: Top, ***pg*-Cp[PV$_3$]$_2$** (solid) and **Me$_2$PV$_3$** (dotted), $c = 3 \times 10^{-6}$ M in $CHCl_3$, T = 23 °C.

The deconvoluted emission profiles on an energy scale provided better comparison between the stacked trimer ***pg*-Cp[PV$_3$]$_2$** and its unstacked counterpart **Me$_2$PV$_3$**. The emission spectrum of **Me$_2$PV$_3$** possesses three distinct peaks at 3.09 eV, 2.92 eV and 2.75 eV and a tail ~ 2.68 eV. On the other hand, in contrast to the stcked dimer ***pg*-Cp[PV$_2$]$_2$**, the emission spectrum of ***pg*-Cp[PV$_3$]$_2$** resembles to that of the unstacked analogue **Me$_2$PV$_3$**; the emission spectrum possesses three well-resolved peaks at 3.06 eV, 2.90 eV and 2.73 eV and a broad tail at 2.56 eV. So, the emission of stacked trimer is dominated by contribution from a local-state over the excimer-like state.

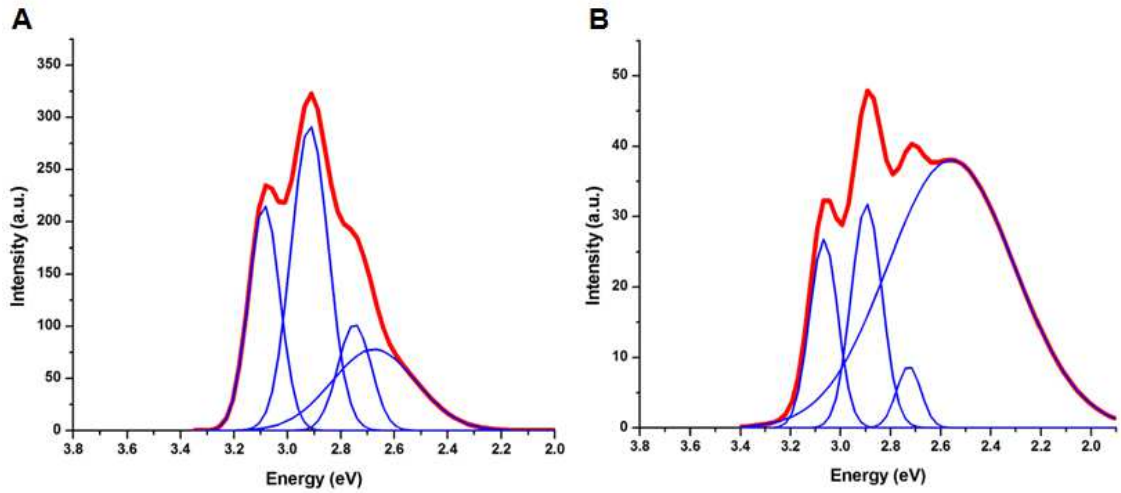


**Figure 5.15.** Fluorescence spectra on an energy scale and their deconvolution into distinct contributions: A, **Me$_2$PV$_3$** and B, ***pg*-Cp[PV$_3$]$_2$**, $c = 3 \times 10^{-6}$ M in $CHCl_3$, T = 23 °C.

**Table 5.1**: Absorption and emission maxima (in nm) of stacked (***pg*-Cp[PV$_2$]$_2$** and ***pg*-Cp[PV$_3$]$_2$**) and unstacked (**Me$_2$PV$_2$** and **Me$_2$PV$_3$**) molecules.

| | Absorption nm | Emission nm |
|---|---|---|
| **Me$_2$PV$_2$** | 297 | 348, 365, 385, 394 |
| ***pg*-Cp[PV$_2$]$_2$** | 295, 366[s] | 432, 466 |
| **Me$_2$PV$_3$** | 352 | 401, 424, 450, 462 |
| ***pg*-Cp[PV$_3$]$_2$** | 350, 403[s] | 405, 427, 454, 484 |

[s]Shoulder peak

Analysis of the emission spectra indicates that at least two electronic states contribute to the fluorescence of both stacked systems. The similarity between absorption spectra of the stacked and unstacked analogs, and the tails seen in the spectra of stacked systems also support this model. Based on this analysis we conclude that the single-tier (local, $S_2$) state that is responsible for absorption and emission of the unstacked systems is also responsible for the high-energy emission bands. The additional low-energy emission band and the absorption edge tail seen in both ***pg*-Cp[PV$_2$]$_2$** and ***pg*-Cp[PV$_3$]$_2$** is attributed to an inter-oligomer excimer-like state ($S_1$). This conclusion is supported by the results of the excited-state calculations (provided in Appendix A.2) obtained by Dr. Sukrit.

As described above, the emission of the stacked dimer is due to the "excimer" state in contrast to that of stacked trimer. This is due to a small energy of activation ($E_a$) for stacked dimer ***pg*-Cp[PV$_2$]$_2$** compared to that of stacked trimer ***pg*-Cp[PV$_3$]$_2$**, Figure 5.16. The relative contributions of $S_1$ and $S_2$ states to the overall emission spectra depends on the interplay of several molecular parameters; (i) the energy of activation ($E_a$), (ii) energy difference between the relaxed $S_1$ and $S_2$ states ($\Delta E^0$) and (iii) the reorganization energy ($\lambda$).

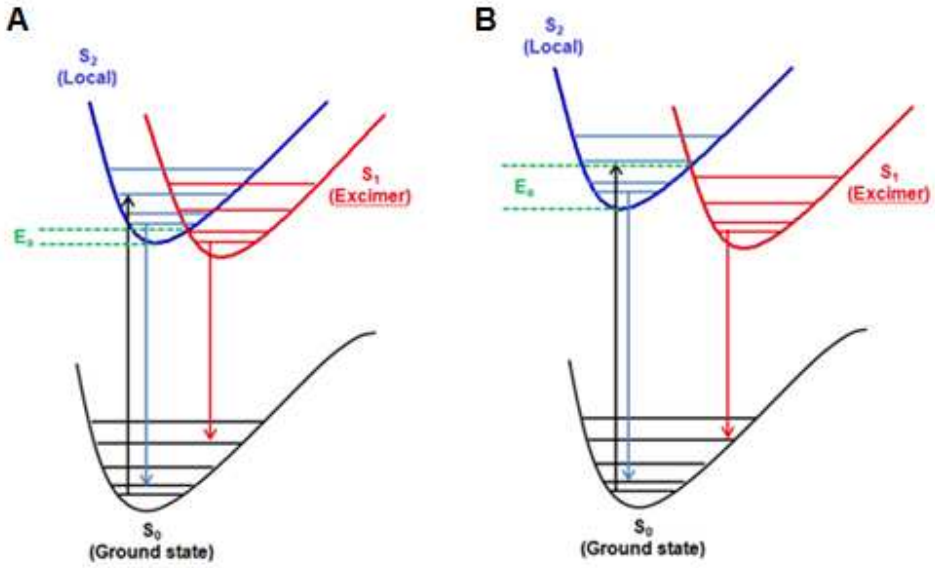


**Figure 5.16.** Local-excited state ($S_2$, blue), excimer-like state ($S_1$, red), and ground state ($S_0$, black); $E_a$, energy required to cross barrier from local state to the excimer-like state; A, ***pg*-Cp[PV$_2$]$_2$** and B, ***pg*-Cp[PV$_3$]$_2$**.

## 5.4. Conclusions

In conclusion, we prepared stacked oligo(phenylene vinylene)s using 4,15-diethenyl[2.2]paracyclophane as a scaffold. The conjugated arms were installed to such scaffold using Heck coupling reaction. The identity of the desired compounds was confirmed using NMR spectroscopy. The emission spectrum of stacked stilbene showed low energy emission due to the "excimer-like" state formation. The significantly large Stokes shifts associated with our stacked dimer is due to possible formation of an extended "excimer-like" state arising from stacking of entire conjugated chains. The synthetic strategy would be useful to build multidecker stacked oligo(phenylene vinylene)s and study their optoelectronic properties.

## 5.5. References


1. Bartholomew, G. P.; Bazan, G. C., *Accounts of Chemical Research* **2001,** *34,* 30. Bazan, G. C.; Oldham, W. J.; Lachicotte, R. J.; Tretiak, S.; Chernyak, V.; Mukamel, S., *Journal of the American Chemical Society* **1998,** *120*, 9188.

2. Bondarenko, L.; Hentschel, S.; Greiving, H.; Grunenberg, J.; Hopf, H.; Dix, I.; Jones, P. G.; Ernst, L., *Chemistry A European Journal* **2007,** *13*, 3950.

3. Chai, J. D.; Head-Gordon, M., *Journal of Chemical Physics* **2008,** *128*.

4. Chai, J. D.; Head-Gordon, M., *Physical Chemistry Chemical Physics* **2008,** *10*, 6615.

5. Psiorz, M.; Schmid, R., *Chemische Berichte-Recueil* **1987,** *120*, 1825.

6. Zitt, H.; Dix, I.; Hopf, H.; Jones, P. G., *European Journal of Organic Chemistry* **2002**, 2298.

7. Sergeeva, E. V.; Rozenberg, V. I.; Antonov, D. Y.; Vorontsov, E. V.; Starikova, Z. A.; Fedyanin, I. V.; Hopf, H., *Chemistry A European Journal* **2005,** *11*, 6944.

8. Barder, T. E.; Walker, S. D.; Martinelli, J. R.; Buchwald, S. L., *Journal of the American Chemical Society* **2005,** *127*, 4685.

# CHAPTER 6

# SYNTHESIS OF MONOMERS TO PREPARE MULTILAYERED π-STACKED CONJUGATED POLYMERS

## 6.1. Introduction

In the previous chapter, we showed that (pseudo-geminal, *pg*) 4,15-diethenyl[2.2]paracyclophane[1] undergoes Heck cross-coupling[2] to provide the π-stacked "dimers" of oligo(phenylene vinylene)s. In this chapter, we report the syntheses of analogous pseudo-geminal 4,15-diethynyl[3] and dihalo-substituted [2.2]paracyclophanes[4] using the procedures described by Hopf, and report their use as monomers in cross-coupling reactions with difunctional arenes. Such difuctional arenes include dihalo-substituted benzo-fused dithiophene[5] and dialkoxy benzene.

## 6.2. Synthesis

General procedures and methods are described in Chapter 2.

### 6.2.1. 4,15-Diethynyl[2.2]paracyclophane[1]

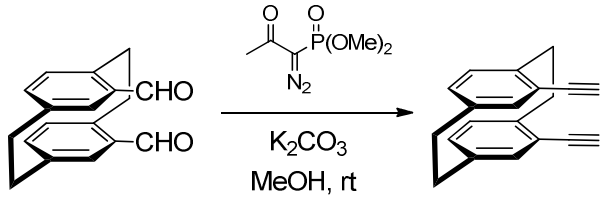


V-11 VI-1

A suspension of 4,15-diformyl[2.2]paracyclophane (1.32 g, 5.00 mmol) and potassium carbonate (3.10 g, 22.5 mmol) in MeOH (100 mL) was stirred for 30 min. Bestmann reagent (2.50 g, 13.0 mmol) was added dropwise and the reaction mixture was stirred for 60 h. $Et_2O$ (50 mL) was added and the solution was washed with saturated aqueous $NaHCO_3$. The aqueous layer was extracted with $CH_2Cl_2$ (2 x 100 mL) and combined organic layers were dried over $MgSO_4$. The solvent was removed under reduced pressure and the residue was subjected to flash column chromatography ($CH_2Cl_2$) to afford the title compound as a white crystalline solid (475 mg, 36%). m.p. 145-146 °C (Lit:[1] 145 °C). $^1$H NMR (300 MHz, $CDCl_3$) δ 6.67 (d, *J* = 1.8 Hz, 2 H, Ar–H), 6.47 (d, *J* = 7.8 Hz, 2 H, Ar–H), 6.41 (dd, *J* = 7.8, 1.8 Hz, 2 H, Ar–H), 3.77–3.82 (m, 2 H, $CH_2$), 3.04 (s, 2 H, ≡C–H), 2.91–2.99 (m, 6 H, $CH_2$). $^{13}$C NMR (75 MHz, $CDCl_3$) δ 142.4, 139.2, 136.2, 133.9, 133.5, 122.6 (Ar), 83.4, 81.2 (C≡C), 34.8, 33.4 ($CH_2$). IR (ATR): 3301, 3013, 2947, 1588, 1495 cm$^{-1}$. MS (EI): *m*/*z* (%) 256.0 ($M^+$, 54), 127.9 (100). HRMS calculated for $C_{20}H_{16}$, 256.1248; found 256.1252, Δ = 1.5 ppm.

## 6.2.2. [2.2]Paracyclophane-4,15-dicarboxylic acid[6]

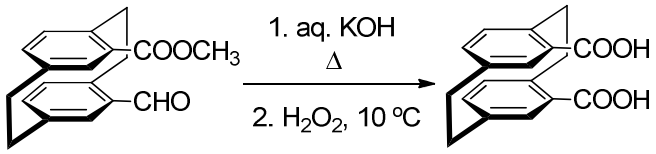


V-9 VI-2

A mixture of methyl 15-formyl[2.2]paracyclophane-4-carboxylate (15 g, 51 mmol) and KOH (10.0 g, 178 mmol) in water/ethanol (180/20 mL) was heated at reflux for 24 h. The reaction mixture was cooled to 10 °C and $H_2O_2$ (35%, 200 mL, 2.05 mmol) was added dropwise. The mixture was stirred at room temperature for 24 h. The solution was cooled to 0 °C and acidified with concentrated hydrochloric acid. The precipitate was collected by filtration, washed with water, and air dried to give [2.2]paracyclophane-4,15-dicarboxylic acid as colorless solid (14 g, 94%). MP = 336-337 °C (Lit:[6] 340-342 °C). $^1$H NMR (300 MHz, $d_6$-DMSO): δ 7.01 (d, 2H, $J$ = 1.8 Hz Ar-H), 6.69 (dd, 2H, $J$ = 7.6, 1.8 Hz, Ar-H), 6.63 (d, 2H, $J$ = 7.6 Hz, Ar-H), 4.04-4.08 (m, 2H, bridge-$CH_2$), 3.02-3.05 (m, 4H, bridge-$CH_2$), 2.92-2.96 (m, 2H, bridge-$CH_2$). $^{13}$C NMR (75 MHz, $d_6$-DMSO): δ 167.5 (carbonyl), 142.2, 139.3, 136.3, 135.9, 133.8, 131.0 (Ar-C), 34.2, 34.0 (bridge-C). IR (ATR): 3435, 3429, 3148, 3037, 2967, 2870, 1688, 1489, 1297, 931 cm$^{-1}$.

### 6.2.3. [2.2]Paracyclophane-4,15-diacid chloride[6]

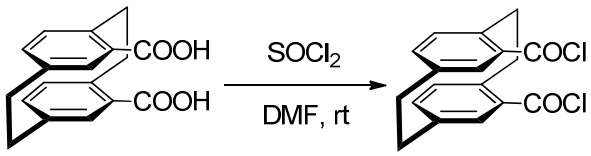


VI-2 VI-3

A solution of [2.2]paracyclophane-4,15-dicarboxylic acid (10.0 g, 33.8 mmol) and $SOCl_2$ (12.0 g, 101 mmol) in DMF (100 mL) was heated at 60 °C for 12 h. The solvent was removed by vacuum distillation to yield the title compound as a yellow solid. $^1$H NMR (300 MHz, $CDCl_3$): δ 7.38 (d, 2H, *J* = 1.8 Hz Ar-H), 6.79 (dd, 2H, *J* = 7.6, 1.8 Hz, Ar-H), 6.68 (d, 2H, *J* = 7.6 Hz, Ar-H), 3.85-4.10 (m, 2H, bridge-$CH_2$), 2.95-3.10 (m, 6H, bridge-$CH_2$). MS (EI), m/z (%) = 294.1 ($M^+$, 100), 266.1 (65), 162.1 (95), 104.1 (75). (Further characterization was not performed since a small amount of DMF remained in the product).

## 6.2.4. [2.2]Paracyclophane-4,15-dicarbonyl diazide[6]

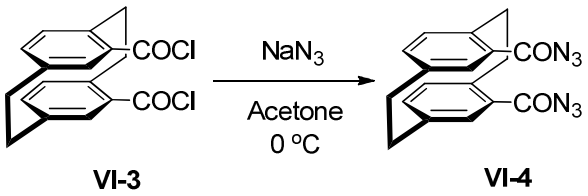


VI-3 VI-4

A solution of sodium azide (22.2 g, 342 mmol) in water (170 mL) was added dropwise over 1 h to a solution of [2.2]paracyclophane-4,15-diacylchloride (11 g, 34 mmol) in acetone (150 mL). The mixture was stirred for 6 h and ice-cold water (500 mL) was added. The precipitate was collected by filtration through a glass frit funnel. The solid was washed with water, air dried and further dried in a desiccator over phosphorus pentoxide to yield [2.2]paracyclophane-4,15-dicarbonyl diazide as a pale yellow solid (11.4 g, 96%). (Melting point was not determined due to the explosive nature of diazides). $^{1}$H NMR (300 MHz, $d_6$-DMSO): δ 7.07 (d, 2H, $J$ = 1.8 Hz Ar-H), 6.84 (dd, 2H, $J$ = 7.6, 1.8 Hz, Ar-H), 6.76 (d, 2H, $J$ = 7.6 Hz, Ar-H), 3.99-4.10 (m, 2H, bridge-$CH_2$), 3.08-3.12 (m, 4H, bridge-$CH_2$), 2.92-2.96 (m, 2H, bridge-$CH_2$). $^{13}$C NMR (75 MHz, $d_6$-DMSO): δ 172.6 (carbonyl), 143.1, 140.6, 138.7, 137.1, 134.1, 130.3 (Ar-C), 34.3, 33.8 (bridge-C). IR (ATR): 3285, 2927, 2864, 2136, 1711, 1642, 1436, 1230, 997, 715 cm$^{-1}$.

## 6.2.5. 4,15-Diisocyanato[2.2]paracyclophane[6]

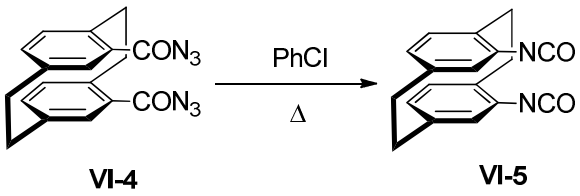


VI-4 VI-5

A solution of [2.2]paracyclophane-4,15-dicarbonyl diazide (8.4 g, 24 mmol) in anhydrous toluene (150 mL) was heated at reflux for 2 h. The solvent was removed under reduced pressure to give title compound as a brown solid (6.6 g, 94 %). MP = 150-151 °C (Lit:[6] 153 °C). $^{1}$H NMR (300 MHz, $CDCl_3$): δ 6.47 (d, 2H, *J* = 1.8 Hz Ar-H), 6.43 (dd, 2H, *J* = 7.6, 1.8 Hz, Ar-H), 6.25 (d, 2H, *J* = 7.6 Hz, Ar-H), 3.47-3.57 (m, 2H, bridge-$CH_2$), 2.89-3.15 (m, 6H, bridge-$CH_2$). $^{13}$C NMR (75 MHz, $CDCl_3$): δ 141.2, 135.1, 133.6, 132.4, 130.8, 130.2 (Ar-C), 34.7, 31.0 (bridge-C). IR (ATR): 3452, 3086, 2980, 2931, 2877, 1618, 1429, 1280, 1097, 838, 735 $cm^{-1}$.

## 6.2.6. 4,15-Diamino[2.2]paracyclophane[6]

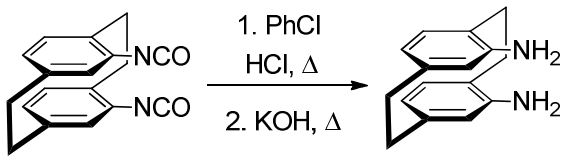


VI-5 VI-6

A mixture of 4,15-diisocyanato[2.2]paracyclophane (7.1 g, 25 mmol) in ethanol (250 mL) was heated at reflux for 24 h. A solution of KOH (10.0 g, 178 mmol) in water (40 mL) was added to the mixture at room temperature and the resulting suspension was heated at reflux for 48 h. The mixture was added to an ice-cold aqueous 20% solution of KOH (400 mL), and the precipitate was collected by filtration through a glass frit funnel. The precipitate was washed with water and dried in a desiccator over phosphorus pentoxide to yield 4,15-diamino[2.2]paracyclophane as a light brown solid (4.7 g, 81%). MP = 205-206 °C (Lit:[6] 203 °C). $^{1}$H NMR (300 MHz, $d_6$-DMSO): δ 6.12 (d, 2H, $J$ = 1.8 Hz Ar-H), 5.80 (dd, 2H, $J$ = 7.6, 1.8 Hz, Ar-H), 5.77 (d, 2H, $J$ = 7.6 Hz, Ar-H), 3.26-3.36 (m, 2H, bridge-$CH_2$), 2.60-2.84 (m, 6H, bridge-$CH_2$). $^{13}$C NMR (75 MHz, $d_6$-DMSO): δ 147.8, 139.7, 134.9, 123.6, 123.2, 121.9 (Ar-C), 35.2, 30.1 (bridge-C). IR (ATR): 3475, 3372, 3329, 3040, 2933, 2857, 1625, 1419, 1290, 881, 718 cm$^{-1}$.

## 6.2.7. 4,15-Diazo[2.2]paracyclophane[4]

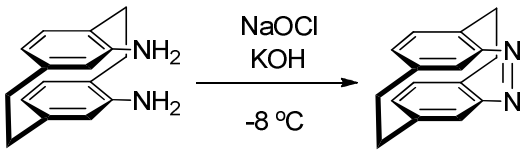


VI-6 VI-7

A mixture of 4,15-diamino[2.2]paracyclophane (2.4 g, 10 mmol) and KOH (10.0 g, 178 mmol) in ethanol/water (140/10 mL) was stirred for 30 min. The reaction mixture was cooled to -10 °C, and an aqueous solution (15%) of sodium hypochlorite (200 mL) was added dropwise. The mixture was stirred for 1 h at -10 °C and the mixture was added to the ice-cold water (400 mL). The aqueous layer was extracted with $CH_2Cl_2$ (100 mL) and the combined organic extracts were dried over $MgSO_4$. Removal of the solvent under reduced pressure followed by flash chromatography (100% $CH_2Cl_2$) yielded 4,15-diazo[2.2]paracyclophane as a yellow solid (2.2 g, 96%). MP = 231-232 °C (Lit:[4] 235 °C). $^1$H NMR (300 MHz, $CDCl_3$): δ 6.37 (dd, 2H, *J* = 7.9, 1.8 Hz Ar-H), 6.30 (d, 2H, *J* = 7.9 Hz, Ar-H), 5.63 (d, 2H, *J* = 1.8 Hz, Ar-H), 2.94-3.17 (m, 4H, bridge-$CH_2$), 2.81-2.91 (m, 4H, bridge-$CH_2$), 2.43-2.54 (m, 2H, bridge-$CH_2$). $^{13}$C NMR (75 MHz, $CDCl_3$): δ 141.2, 134.1, 130.8, 129.7, 127.3 (Ar-C), 35.9, 31.1 (bridge-C). IR (ATR): 3041, 3029, 2964, 2891, 2851, 1584 $cm^{-1}$.

## 6.2.8. 4,15-Dibromo[2.2]paracyclophane[4]

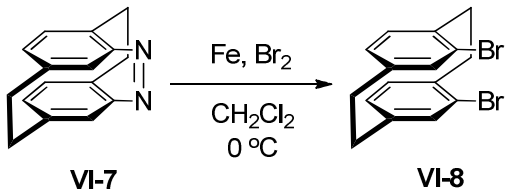


VI-7 VI-8

A mixture of 4,15-diazo[2.2]paracyclophane (150 mg, 640 μmol) and iron powder (150 mg, 2.77 mmol) in anhydrous $CH_2Cl_2$ was stirred at -10°C for 15 min. A solution of bromine (103 mg, 1.28 mmol) in anhydrous $CH_2Cl_2$ (15 mL) was added dropwise and the mixture was stirred at the same temperature for 1 h. The iron powder was separated by filtration and the solvent was removed under reduced pressure. The black residue was subjected to flash column chromatography (5% $CH_2Cl_2$ / 95% hexane) to give the title compound as a colorless solid (140 mg, 60%). MP = 182-183 °C (Lit:[4] 180 °C). $^1$H NMR (300 MHz, $CDCl_3$) δ 6.78 (d, *J* = 1.4 Hz, 2 H, Ar–H), 6.53 (m, 4 H, Ar–H), 3.64–3.80 (m, 2 H, $CH_2$), 2.90–3.15 (m, 6 H, $CH_2$). $^{13}$C NMR (75 MHz, $CDCl_3$): δ 140.9, 138.5, 135.7, 135.1, 132.3, 125.1 (Ar-C), 34.7, 34.6 ($CH_2$). IR (ATR): 3068, 3018, 2938, 1896, 1584, 1462, 1031, 867 cm$^{-1}$. MS (EI): *m*/*z* (%) 363.9 ($M^+$, 20), 182.0 (100). HRMS calculated for $C_{16}H_{14}Br_2$, 363.9462; found 363.9467, Δ = 1.4 ppm.

## 6.2.9. 4,15-Diiodo[2.2]paracyclophane[4]

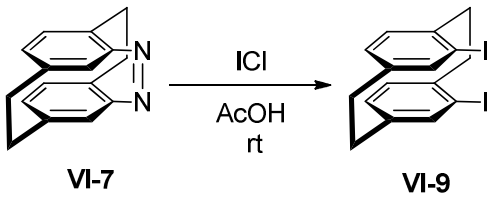


VI-7 VI-9

A solution of 4,15-diazo[2.2]paracyclophane (600 mg, 2.55 mmol) in glacial acetic acid (60 mL) was stirred at 0°C for 10 min. Iodine monochloride (460 mg, 2.82 mmol) was added dropwise and the mixture was stirred at room temperature for 1 h. $Et_2O$ (50 mL) was added and the organic layer was washed with water (50 mL), saturated aq. $NaHCO_3$ (50 mL), and brine (50 mL) sequentially. The organic layer was dried over $MgSO_4$ and the solvent was removed under reduced pressure. The brown residue was subjected to flash column chromatography (20% $CH_2Cl_2$/80% hexane) to give the title compound as a colorless solid (260 mg, 61%). MP = 237-238 °C (Lit:[4] 239 °C). $^1$H NMR (300 MHz, $CDCl_3$) δ 7.06 (d, *J* = 1.5 Hz, 2 H, Ar–H), 6.51 (m, 4 H, Ar–H), 3.51–3.75 (m, 2 H, $CH_2$), 2.88–3.22 (m, 6 H, $CH_2$). $^{13}$C NMR (75 MHz, $CDCl_3$) δ 142.4, 141.8, 140.7, 133.8, 133.3, 99.8 (Ar), 38.9, 34.6 ($CH_2$). IR (ATR, neat): 3024, 2955, 1579, 1462, 1026, 866 $cm^{-1}$. MS (EI): *m*/*z* (%) 459.9 ($M^+$, 70). HRMS calculated for $C_{16}H_{14}I_2$, 459.9185; found 459.9187, Δ = 0.4 ppm.

**6.2.10. 1,4-Diiodo-2,5-bis(nonyloxy)benzene[3]**

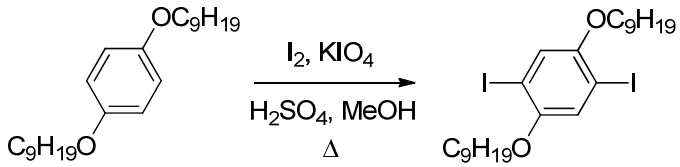


**VI-10**

A solution of bis(nonyloxy)benzene (18 g, 50 mmol), $I_2$ (12.8 g, 100 mmol), $KIO_4$ (11.5 g, 100 mmol) and conc. $H_2SO_4$ (1 mL) in methanol (250 mL) was heated at reflux for 12 h. Sat. sodium sulfite (250 mL) was added and the mixture was extracted with $CH_2Cl_2$ (250 mL). The organic extract was washed with sat. sodium sulfite (250 mL) followed by $H_2O$ (250 mL). The solvent was removed under reduced pressure and the residue was recrystallized from MeOH to afford 1,4-diiodo-2,5-bis(nonyloxy)benzene as a colorless crystalline solid (26.0 g, 87% yield). MP = 85-87°C. $^1$H NMR (300 MHz, $CDCl_3$): δ 7.16 (s, 2 H, Ar-H), 3.92 (t, *J* = 6.5 Hz, 4 H, $OCH_2$), 1.79 (pentet, *J* = 6.7 Hz, 4 H, $CH_2$), 1.18-1.62 (m, 28 H, $CH_2$) 0.88 (t, *J* = 6.5 Hz, 6 H, $CH_3$). $^{13}$C NMR (75 MHz, $CDCl_3$): δ 152.7, 122.6, 86.2 (Ar-C), 70.3 ($OCH_2$), 31.8, 29.5, 29.3, 29.2, 29.1, 26.0, 22.7 ($CH_2$), 14.1 ($CH_3$). IR (ATR): 2847, 2359, 1485, 1456, 1387, 1348, 1264, 1209, 1053, 1013, 1004, 993, 936, 850, 794 $cm^{-1}$. MS (EI): *m*/*z* (%) 614.2 ($M^+$, 75), 361 (100); HRMS calculated for $C_{24}H_{40}O_2I_2$, 614.1107; found 614.1118, Δ = 1.7 ppm.

**6.2.11. 1,4-Diiodo-2,5-bis(dodecyloxy)benzene[7]**

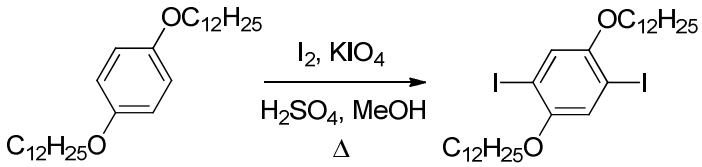


**VI-11**

A solution of bis(dodecyloxy)benzene (10.0 g, 22.4 mmol), $I_2$ (5.70 g, 44.8 mmol), $KIO_4$ (5.15 g, 44.8 mmol) and conc. $H_2SO_4$ (1 mL) in methanol (250 mL) was heated at reflux for 12 h. Sat. sodium sulfite (250 mL) was added and the mixture was extracted with $CH_2Cl_2$ (250 mL). The organic extract was washed with sat. sodium sulfite (250 mL) followed by $H_2O$ (250 mL). The solvent was removed under reduced pressure and the residue was recrystallized from MeOH to afford 1,4-diiodo-2,5-bis(dodecyloxy)benzene as a colorless crystalline solid (14 g, 89% yield). MP = ##-##°C. $^1$H NMR (300 MHz, $CDCl_3$): δ 7.16 (s, 2 H, Ar–H), 3.91 (t, *J* = 6.3 Hz, 4 H, $OCH_2$), 1.79 (pentet, *J* = 6.4 Hz, 4 H, $CH_2$), 1.19-1.58 (m 40 H, $CH_2$) 0.87 (t, *J* = 6.4 Hz, 6 H, $CH_3$). $^{13}$C NMR (75 MHz, $CDCl_3$): δ 152.6, 122.3, 86.6 (Ar-C), 70.2 ($OCH_2$), 31.8, 29.6, 29.5, 29.4 (2C), 29.3, 29.2, 29.1, 26.0, 22.7 ($CH_2$), 14.1 ($CH_3$). IR (ATR): 2853, 2351, 1459, 1386, 1344, 1262, 1057, 1009, 994, 932, 852, 797 cm$^{-1}$. MS (EI): *m*/*z* (%) 698.2 ($M^+$, 75), 445.2 (100); HRMS calculated for $C_{30}H_{52}O_2I_2$, 698.1217; found 698.1223, Δ = 0.8 ppm.

## 6.2.12. 3-Thiophenecarboxylic acid chloride[5]

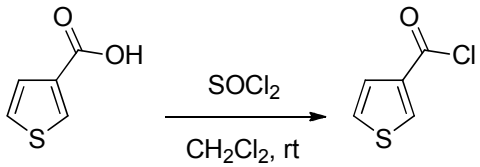


**VI-12** **VI-13**

Thionyl chloride (6.0 mL, 78 mmol) was added to a solution of 3-thiophenecarboxylic acid (5.0 g, 39 mmol) in dry $CH_2Cl_2$ (100 mL) and the mixture was stirred at room temperature for 6 h. The solvent was removed under reduced pressure to afford 3-thiophenecarboxylic acid chloride as a colorless solid (5.65 g, 99% yield). $^1$H NMR (300 MHz, $CDCl_3$): δ 8.38 (dd, *J* = 3.0, 1.1 Hz, 1 H, Th-$H_2$), 7.58 (dd, *J* = 5.0, 1.1 Hz, 1 H, Th-$H_5$), 7.38 (dd, *J* = 5.2, 3.0 Hz, 1 H, Th-$H_4$). $^{13}$C NMR (75 MHz, $CDCl_3$): δ 161.1 (carbonyl), 138.4, 137.0, 128.1, 127.2 (Th). IR (ATR): 3085, 2987, 2765, 1751, 1574, 1387, 1263, 1144, 932, 723, 639 $cm^{-1}$.

**6.2.13. *N,N*-Diethylthiophene-3-carboxamide[8]**

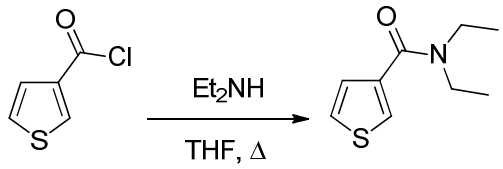


**VI-13** **VI-14**

Diethylamine (8.5 mL, 82 mmol) was added dropwise to a solution of 3-thiophenecarboxylic acid chloride (6.0 g, 41 mmol) in a dry THF (100 mL). The solution was heated to reflux for 12 h, cooled, diluted with $CH_2Cl_2$ (100 mL) and washed with water (3 x 100 mL). The organic layer was dried over $MgSO_4$ and the solvent was removed under reduced pressure to give *N,N*-diethylthiophene-3-carboxamide as a pale yellow oil (7.4 g, 98%). $^1$H NMR (300 MHz, $CDCl_3$) δ 7.45 (dd, *J* = 3.0, 1.1 Hz, 1 H, Th-$H_2$), 7.30 (dd, *J* = 5.0, 3.0 Hz, 1 H, Th-$H_5$), 7.16 (dd, *J* = 5.0, 1.1 Hz, 1 H, Th-$H_4$), 3.41 (br s, 4 H, $CH_2$), 1.21 (t, *J* = 6.7 Hz, 6 H, $CH_3$). $^{13}$C NMR (75 MHz, $CDCl_3$) δ 166.6 (carbonyl), 137.5, 126.8, 125.7, 125.0 (Th), 68.0 ($CH_2$), 19.3 ($CH_3$). IR (ATR): 3146, 3045, 2951, 1742, 1685, 1546, 1370, 1299, 1188, 1075, 961, 835 cm$^{-1}$. MS (EI): *m*/*z* (%) 183.1 ($M^+$, 85).

**6.2.14. Benzo[1,2-*b*:4,5-*b'*]dithiophene-4,8-dione[5]**

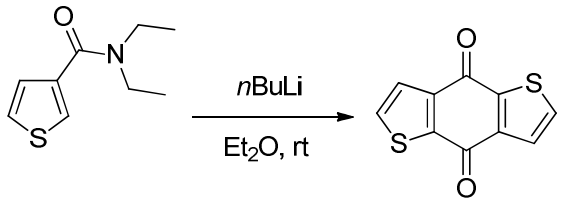


**VI-14** **VI-15**

*n*-Butyllithium (15 mL, 2.5 M in hexane, 37 mmol) was added dropwise into the solution of N, N-diethylthiophene-3-carboxamide (5.9 g, 32 mmol) in dry $Et_2O$ (100 ml) with vigorous stirring under dry nitrogen. After 10 min, a light yellow precipitate began to form. The reaction mixture was stirred for 12 h. Ice water was added and the precipitate was collected by filtration. Recrystallization of the filtrate from glacial acetic acid afforded benzo[1,2-*b*:4,5-*b'*]dithiophene-4,8-dione as a green powder (1.84 g, 52%). m.p. 260-261 °C (lit:[5] 262–263 °C). $^1$H NMR (300 MHz, $CDCl_3$): δ 7.68 (d, $J$ = 6.0 Hz, 2 H, Th-$H_\alpha$), 7.63 (d, $J$ = 6.0 Hz, 2 H, Th-$H_\beta$). $^{13}$C NMR (75 MHz, $CDCl_3$): δ 174.5 (carbonyl), 144.9, 142.8, 133.6, 126.6 (Th–C). IR (ATR): 3088, 2997, 2948, 1775, 1632, 1500, 1404, 1269, 1217, 796 cm$^{-1}$. MS (EI): *m*/*z* (%) 219.9 ($M^+$, 70).

**6.2.15. 4,8-Dihydroxy-4,8-di(1-octynyl)-benzo[1,2-*b*:4,5-*b'*]dithiophene**

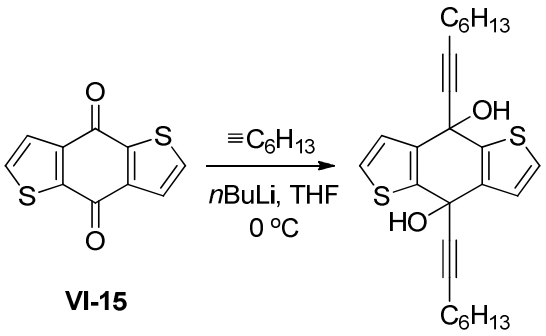


**VI-15** **VI-16**

A solution of *n*-butyllithium (28 mL of a 1.6 M solution in hexanes, 44 mmol) was added dropwise to a solution of 1-octyne (5.5 g, 50 mmol) in dry THF (50 mL) at 0 °C. The reaction mixture was stirred at room temperature for 2 h and then cooled to 0 °C. Benzo[1,2-*b*:4,5-*b'*]dithiophene-4,8-dione (2.5 g, 11 mmol) was added to the solution, and the mixture was heated to reflux for 8 h. The mixture was allowed to cool to room temperature and ice-water (100 mL) was added. The mixture was extracted with $CH_2Cl_2$ (100 mL), the organic layer was dried over $MgSO_4$ and the solvent was removed under reduced pressure. The residue was subjected to column chromatography (20% ethyl acetate/80% hexane) to afford the title compound as a colorless solid (4.8 g, 96%). m.p. 74-75 °C. $^1$H NMR (300 MHz, $CDCl_3$): δ 7.38 (d, *J* = 5.9 Hz, 2 H, Th-$H_\alpha$), 7.28 (d, *J* = 5.9 Hz, 2 H, Th-$H_\beta$), 2.74 (s, 2 H, hydroxy), 2.21 (t, *J* = 7.0 Hz, 4 H, α-$CH_2$), 1.49 (pentet, *J* = 6 Hz, 4 H, β-$CH_2$), 1.21-1.41 (m, 12 H, $CH_2$), 0.87 (t, *J* = 6.6 Hz, 6 H, $CH_3$). $^{13}$C NMR (75 MHz, $CDCl_3$): δ 142.4, 139.2, 127.0, 125.3 (Th), 87.0 (–C≡), 81.5 (C-OH), 63.4 (≡C–), 31.2, 28.5, 28.2, 22.5, 18.8 ($CH_2$), 14.0 ($CH_3$). IR (ATR): 3320, 2944, 2884, 1478, 1400, 1275, 1138, 916 cm$^{-1}$. MS (EI): *m*/*z* (%) 440.2 ($M^+$, 20), 423.2 (100). HRMS calculated for $C_{26}H_{32}O_2S_2$, 440.1844; found 440.1848, Δ = 0.9 ppm.

**6.2.16. 4,8-Di(1-octynyl)benzo[1,2-*b*:4,5-*b'*]dithiophene**

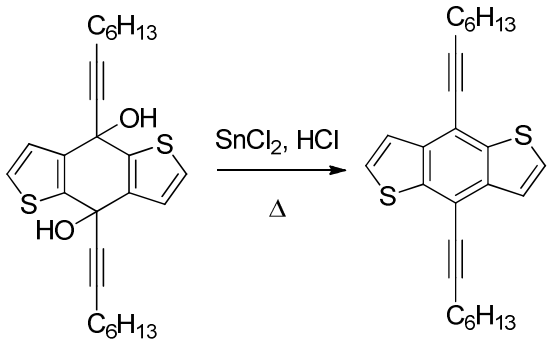


**VI-16** **VI-17**

A solution of $SnCl_2$ (25 g) in 10% aq. HCl (50 mL) was added dropwise to a solution of 4,8-dihydroxy-4,8-di(1-octynyl)benzo[1,2-*b*:4,5-*b'*]dithiophene (4.2 g, 9.6 mmol) in THF (60 mL). The reaction mixture was heated at 60 °C for 12 h. The organic layer was washed with water (100 mL), followed by saturated aq. $NaHCO_3$ (100 mL), and brine (100 mL). The organic layer was dried over $MgSO_4$ and the solvent was removed under reduced pressure. The residue was purified by flash chromatography on silica-gel (100% hexane) to afford 4,8-di(1-octynyl)benzo[1,2-*b*:4,5-*b'*]dithiophene as colorless solid (3.5 g, 90%). m.p. 60-61 °C. $^1$H NMR (300 MHz, $CDCl_3$): δ 7.56 (d, *J* = 5.5 Hz, 2 H, Th-$H_\alpha$), 7.47 (d, *J* = 5.5 Hz, 2 H, Th-$H_\beta$), 2.62 (t, *J* = 7 Hz, 4 H, α-$CH_2$), 1.73 (pentet, *J* = 6 Hz, 4 H, β-$CH_2$), 1.60 (m, 4 H, $CH_2$), 1.38 (m, 8 H, $CH_2$), 0.92 (t, *J* = 7 Hz, 6 H, $CH_3$). $^{13}$C NMR (75 MHz, $CDCl_3$): δ 140.1, 138.2, 127.5, 123.2, 112.1 (Ar), 100.4 (–C≡), 84.1 (≡C–), 31.4, 28.7, 28.6, 22.6, 20.0 ($CH_2$), 14.1 ($CH_3$). IR (ATR): 2988, 2930, 2834, 2207, 1449, 1365, 1275, 1139, 989 cm$^{-1}$. MS (EI): *m*/*z* (%) 406.2 ($M^+$, 100), 335.1 (30). HRMS calculated for $C_{26}H_{30}S_2$, 406.1789; found 406.1788, Δ = 0.2 ppm.

**6.2.17. 4,8-Dioctylbenzo[1,2-*b*:4,5-*b'*]dithiophene**

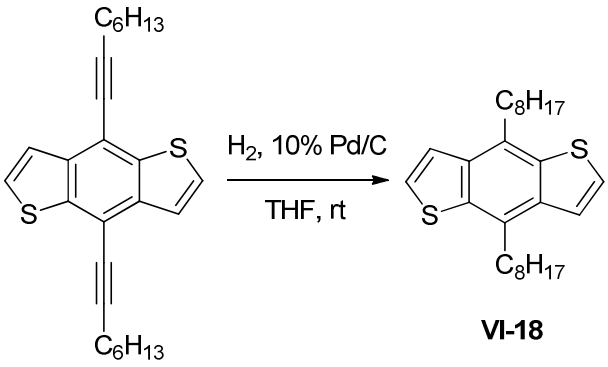


**VI-17** **VI-18**

A mixture of 4,8-di(1-octynyl)benzo[1,2-*b*:4,5-*b'*]dithiophene (3.2 g, 7.9 mmol) and 5% Pd/C (1.6 g, 1.6 mmol) in dry THF (100 mL) was stirred under an atmosphere of $H_2$ in a round bottom flask at room temperature for 36 h. The solvent was removed under reduced pressure and the crude residue was subjected to column chromatography on silica gel (100% hexane) to afford 4,8-dioctylbenzo[1,2-*b*:4,5-*b'*]dithiophene as white needles (1.8 g, 55%). m.p. 51-52 °C. $^1$H NMR (300 MHz, $CDCl_3$) δ 7.48 (d, *J* = 5.8 Hz, 2 H, Th-$H_\alpha$), 7.43 (d, *J* = 5.8 Hz, 2 H, Th-$H_\beta$), 3.17 (t, *J* = 7.9 Hz, 4 H, Ph-$CH_2$), 1.79 (m, 4 H, $CH_2$), 1.20-1.54 (m, 20 H, $CH_2$), 0.87 (t, *J* = 6.4 Hz, 6 H, $CH_3$). $^{13}$C NMR (75 MHz, $CDCl_3$): δ 139.0, 135.9, 127.9, 125.1, 115.3 (Ar), 33.5, 31.9, 30.0, 29.6, 29.4, 29.2, 22.7 ($CH_2$), 14.1 ($CH_3$). IR (ATR): 3118, 3068, 2944, 2865, 1644, 1591, 1449, 1358, 1182, 825 cm$^{-1}$. MS (EI): *m/z* (%) 414.2 ($M^+$, 100), 315.1 (55). HRMS calculated for $C_{26}H_{38}S_2$, 414.2415; found 414.2417, Δ = 0.5 ppm.

**6.2.18. 2,6-Diiodo-4,8-dioctylbenzo[1,2-*b*:4,5-*b'*]dithiophene**

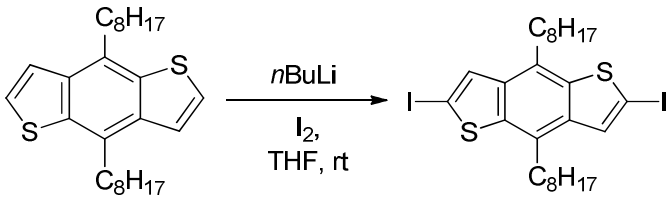


**VI-18** **VI-19**

A solution of *n*-butyllithium (1.9 mL of a 1.6 M solution in hexanes, 3.0 mmol,) was added dropwise to a solution of 4,8-dioctylbenzo[1,2-b:4,5-b']dithiophene (0.4 g, 0.9 mmol) in dry THF (20 mL) at -20 °C. The reaction mixture was stirred at room temperature for 2 h, and iodine (0.90 g, 3.9 mmol) was added. The mixture was stirred for 12 h, washed with saturated aq. sodium sulfite (50 mL) and water (50 mL), and dried over $MgSO_4$. The solvent was removed under reduced pressure and the residue was purified by recrystallization from MeOH to give 2,6-diiodo-4,8-dioctylbenzo[1,2-*b*:4,5-*b'*]dithiophene as yellow powder (640 mg, 99%). m.p. 146-147 °C. $^1$H NMR (300 MHz, $CDCl_3$) δ 7.61 (s, 2 H, Th-H), 3.0 (t, *J* = 7.6 Hz, 4 H, Ph-$CH_2$), 1.74 (p, *J* = 6.0 Hz, 4 H, $CH_2$), 1.20-1.50 (m, 20 H, $CH_2$), 0.88 (t, *J* = 6.1 Hz, 6 H, $CH_3$). $^{13}$C NMR (75 MHz, $CDCl_3$) δ 141.7, 136.6, 131.8, 126.7, 78.3 (Ar), 33.4, 31.9, 29.8, 29.6, 29.4, 29.2, 22.7 ($CH_2$), 14.1 ($CH_3$). IR (ATR): 3010, 2940, 2900, 1446, 1385, 1260, 861 cm$^{-1}$. MS (EI): *m*/*z* (%) 666.1 ($M^+$, 100), 566.9 (35). HRMS calculated for $C_{26}H_{36}S_2I_2$, 666.0348; found 666.0350, Δ = 0.3 ppm.

## 6.3. Results and Discussion

### 6.3.1. Synthesis of 4,15-Diethynyl[2.2]paracyclophane

The synthesis of 4,15-diformyl[2.2]paracyclophane **V-11** is reported in chapter 5. The dialdehyde **V-11** was treated with dimethyl 1-diazo-2-oxo-propylphosphonate (Bestmann-Ohira reagent)[9] in the presence of potassium carbonate in methanol at room temperature to afford the required 4,15-diethynyl[2.2]paracyclophane, **VI-1**, Figure 6.1.[1] We obtained better yields (50%) for this reaction compared to the procedure described by Hopf by using a large excess of Bestmann-Ohira reagent (4-5 eq). The synthesis of dialkyne **VI-1** was accompanied by an intramolecular Cannizzaro process yielding 4-methoxycarbonyl-15-hydroxymethyl[2.2]paracyclophane which is a second major product of this reaction. The isolation of dialkyne from the byproducts was accomplished using flash chromatography ($CH_2Cl_2$). Precautions were taken to not to expose the dialkyne to a light for long period of time because of the possible cyclization reaction between closely spaced triple bonds observed by Hopf.[10]

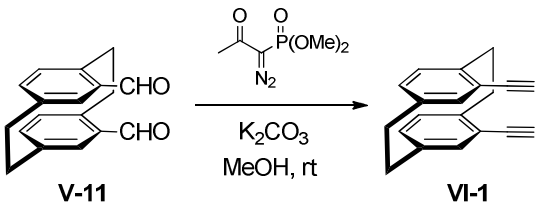


**Figure 6.1.** Synthesis of dialkyne, **VI-1**.

### 6.3.2. Synthesis of 4,15-Dihalo[2.2]paracyclophane

Once the *pg* regiochemistry is obtained through the Rieche formylation to afford methyl 15-formyl[2.2]paracyclophane-4-carboxylate (**V-9**),[11] the syntheses of 4,15-dibromo[2.2]paracyclophane (***pg*-CpBr$_2$**)[4] and 4,15-diiodo[2.2]paracyclophane (***pg*-CpI$_2$**)[4] are completed in seven steps based on literature procedures.[6] This followed the synthetic methodology developed by Hopf. Oxidation of **V-9** upon sequential treatment with potassium hydroxide and a large excess of hydrogen peroxide afforded [2.2]paracyclophane-4,15-dicarboxylic acid, **VI-2**. The addition of hydrogen peroxide should be very slow and at a low temperature to control the exothermicity of reaction. The diacid **VI-2** was converted to a corresponding diacid chloride using thionyl chloride in DMF. The diacid chloride **VI-3** was subsequently converted to [2.2]paracyclophane-4,15-dicarbonyl diazide **VI-4** by treatment of sodium azide in acetone. The diazide **VI-4** was not stored for a long time and used immediately in the next step to obtain 4.15-diisocyanato[2.2]paracyclophane **VI-5** by a double Curtius arrangement. Hydrolysis of diisocyanate **VI-5** gave diamine **VI-6** in good yields (70%). The diamine was dried over phosphorous pentoxide in a dessicator rather than in the open air to avoid its oxidation. The diamine **VI-6** is a useful starting material for the preparation of 4,15-dihalo[2.2]paracyclophanes. Oxidation of **VI-6** using sodium hypochlorite in ethanol in the presence of potassium hydroxide provided the azo-bridged paracyclophane, **VI-7**. Exposure of the azo-paracyclophane **VI-7** to bromine in the presence of iron catalyst gave required 4,15-dibromo[2.2]paracyclophane ***pg*-CpBr$_2$** in satisfactory yield. Similarly, the diiodide ***pg*-CpI$_2$** was obtained when azo-paracyclophane was treated with iodine monochloride in glacial acetic acid. These dihalo compounds were explored as potential monomers to prepare stacked polymers by metal catalyzed cross coupling reactions, Chapter 7.

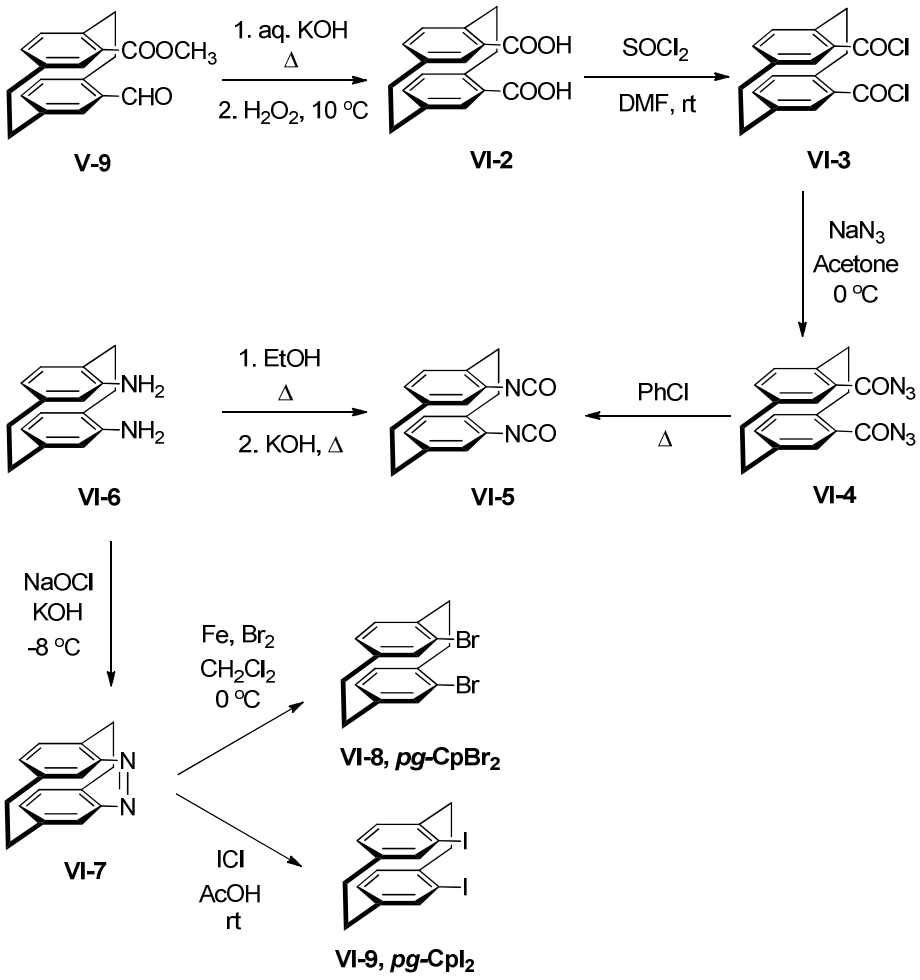


**Figure 6.2.** Synthesis of dibromide **VI-8** and diiodide **VI-9**.

### 6.3.3. Synthesis of 1,4-Diiodo-2,5-bis(alkoxy)benzene

1,4-Diiodo-2,5-bis(alkoxy)benzene was prepared according to procedures reported in the literature.[7] Treatment of 1,4-dinonyloxybenzene with iodine in the presence of potassium periodate in methanol provided 1,4-diiodo-2,5-bis(nonyloxy)benzene, **VI-10**, Figure 6.3. Pure diiodide was obtained by recrystallization from methanol. The use of an excess of iodine (2.5 eq.) was favorable to ensure complete diiodination. Similarly, 1,4-diiodo-2,5-bis(dodecyloxy)benzene **VI-11** was also prepared in a hope that the longer alkoxy chains would improve the solubility of the resulting polymers.

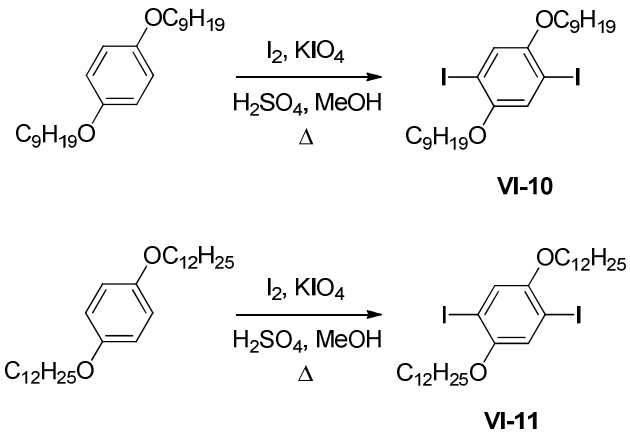


**Figure 6.3.** Synthesis of diiodide **VI-10** and **VI-11**.

### 6.3.4. Synthesis of 2,6-Diiodo-4,8-dioctylbenzo[1,2-*b*:4,5-*b'*]dithiophene

We prepared 2,6-diiodo-4,8-dioctylbenzo[1,2-*b*:4,5-*b'*]dithiophene according to published procedures for the synthesis of other 4,8-dialkyl homologs, Figure 6.4.[5] We started with 3-thiophenecarboxylic acid **VI-12** which was converted to corresponding acid chloride using thionyl chloride. Although the acid **VI-12** is not soluble in dichloromethane, a homogeneous reaction mixture was obtained upon addition of thionyl chloride. Treatment of **VI-13** with diethylamine in THF provided *N*,*N*-diethylthiophene-3-carboxamide in excellent yield (95%).[8] The slow addition of *n*-butyllithium to a solution of amide **VI-14** in diethyl ether resulted in a double cyclization to give benzo[1,2-*b*:4,5-*b'*]dithiophene-4,8-dione, **VI-15**. 1-Octyne was lithiated upon treatment with *n*-butyllithium and exposed to the dione to give 4,8-dihydroxy-4,8-di(1-octynyl)-benzo[1,2-*b*:4,5-*b'*]dithiophene, **VI-16**. After work-up, the diol was carried to a next step without any further purification. 4,8-Dioctylbenzo[1,2-*b*:4,5-*b'*]dithiophene **VI-18** was obtained by treatment of **VI-17** with a catalytic amount of Pd/C catalyst in a hydrogen atmosphere. While preparing **VI-17** we found that isolation of diol **VI-16**, followed by reduction, provided better yields than attempts to conduct this conversion in a single step. Lithiation of **VI-18** (*n*-BuLi) followed by addition of iodine afforded the diiodo analog 2,6-diiodo-4,8-dioctyllbenzo[1,2-*b*:4,5-*b'*]dithiophene **VI-19** in a quantitative yield. We prepared the 2,6-diiodo analog of **VI-18** rather than the previously reported dibromide to make use of the greater reactivity of aryl iodides in Sonogashira coupling reactions.

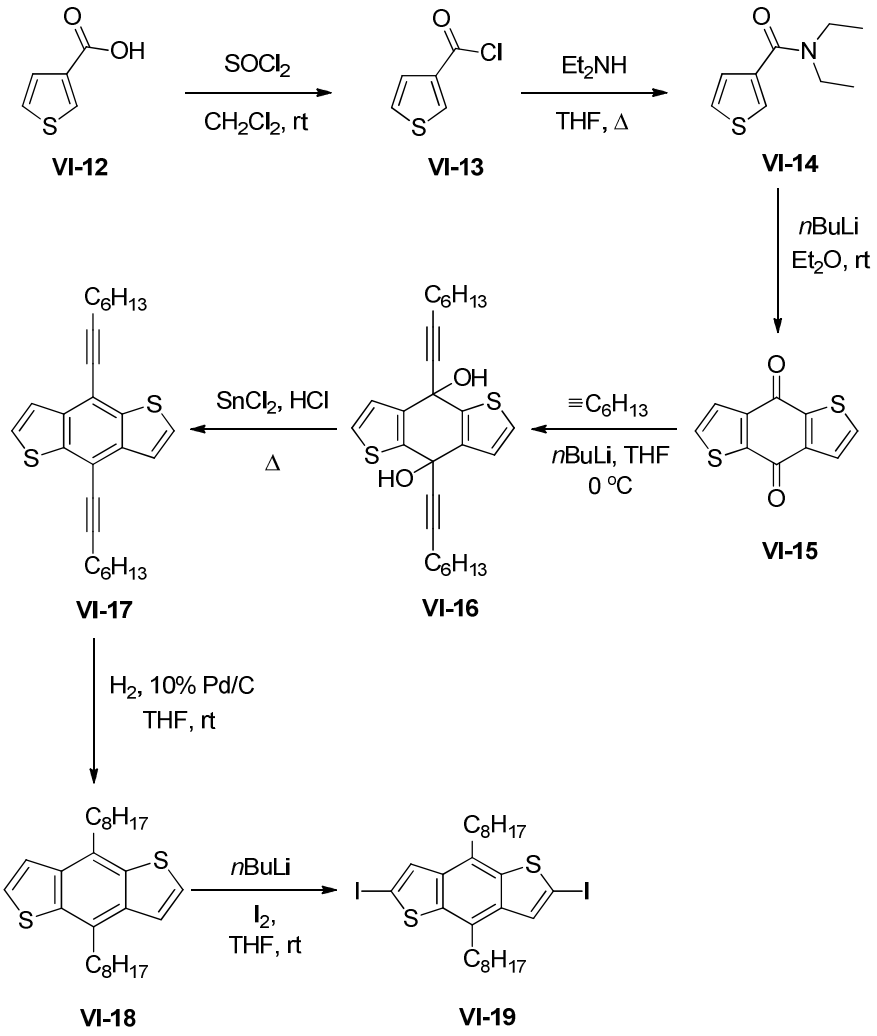


**Figure 6.4.** Synthesis of diiodide, **VI-19**.

## 6.4. Conclusions

The compounds reported in this chapter were prepared on multigram scale in satisfactory yield via multistem syntheses. These *pg* paracyclophane compounds could be useful as monomers to prepare π-stacked conjugated oligomers and polymers.

## 6.5. References


1. Bondarenko, L.; Hentschel, S.; Greiving, H.; Grunenberg, J.; Hopf, H.; Dix, I.; Jones, P. G.; Ernst, L., *Chemistry A European Journal* **2007,** *13*, 3950.

2. Heck, R. F.; Nolley, J. P., *Journal of Organic Chemistry* **1972,** *37*, 2320.

3. Jagtap, S. P.; Collard, D. M., *Journal of the American Chemical Society* **2010,** *132*, 12208.

4. El Shaieb, K.; Narayanan, V.; Hopf, H.; Dix, I.; Fischer, A.; Jones, P. G.; Ernst, L.; Ibrom, K., *European Journal of Organic Chemistry* **2003**, 567.

5. Liang, Y. Y.; Feng, D. Q.; Wu, Y.; Tsai, S. T.; Li, G.; Ray, C.; Yu, L. P., *Journal of the American Chemical Society* **2009,** *131*, 7792.

6. Zitt, H.; Dix, I.; Hopf, H.; Jones, P. G., *European Journal of Organic Chemistry* **2002**, 2298.

7. Evenson, S. J.; Mumm, M. J.; Pokhodnya, K. I.; Rasmussen, S. C., *Macromolecules* **2011,** *44*, 835.

8. Hou, J. H.; Park, M. H.; Zhang, S. Q.; Yao, Y.; Chen, L. M.; Li, J. H.; Yang, Y., *Macromolecules* **2008,** *41*, 6012.

9. Roth, G. J.; Leipold, B.; Muller, S. G.; Bestmann, H. J., *Synthesis-Stuttgart* **2004**, 640.

10. Kubitschke, J.; Hopf, H.; Jones, P. G.; Dix, I.; Ernst, L., *European Journal of Organic Chemistry* **2008**, 548.

11. Psiorz, M.; Schmid, R., *Chemische Berichte-Recueil* **1987,** *120*, 1825.

# CHAPTER 7

# SYNTHESIS AND CHARACTERIZATION OF π-STACKED MULTILAYERED CONJUGATED POLYMERS

## 7.1. Introduction

To extend the utility of pseudo-geminal (pg) cyclophane as a scaffold, we chose to synthesize and explore the use of (*pg*) cyclophanes bearing alkyne, alkene and halogen substituent as monomers in the preparation of π-stacked conjugated polymers. Previous chapter deals with synthesis of various potential monomers while in this chapter we subjected them in combination to common metal-catalyzed cross coupling reactions to prepare π-stacked polymer, Figure 7.1.

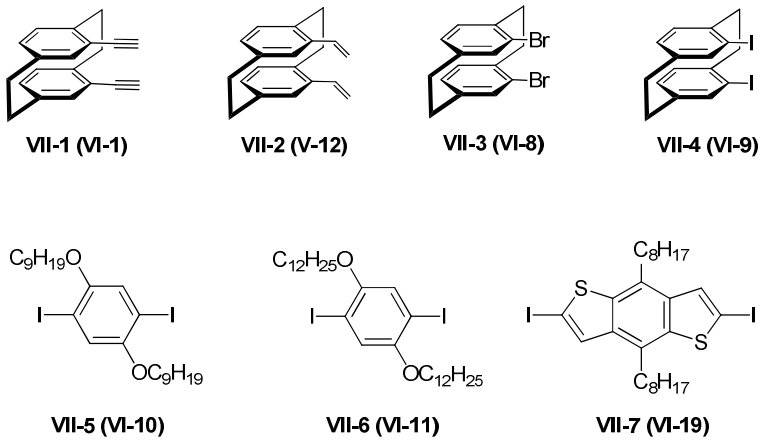


**Figure 7.1.** Monomers to prepare π-stacked polymers

A number of polymeric pseudo-para [2.2]paracyclophanes have been prepared by metal-catalyzed cross-coupling of *pp* dibromo[2.2]paracyclophane[1] with bismetalloarenes, 7.2A. These approaches provide polymers in which relatively short conjugated oligomeric tiers are arranged in a stair case fashion in which the terminal phenyl rings are held in a stacked manner.[2] There is a single example of an analogous pseudo-ortho [2.2]paracyclophane polymer.[3] In these polymers only the terminal phenyl rings of each conjugated unit are subject to cofacial overlap within the [2.2]paracyclophane scaffold. However, these studies demonstrate that even this limited amount of π-stacking has a large influence on the electronic and optical properties of the assembly of conjugated systems relative to the behavior of analogous unstacked oligomers consisting of the same conjugated unit.

Here we report a synthetic strategy to prepare a polymeric system consisting of a pseudo-geminal (*pg*) [2.2]paracyclophane scaffold that contains a more extensive overlap of conjugated chromophores, Figure 7.2B. We also prepared a linear unstacked model compound which resembles the single tier of the polymeric structure, Figure 7.2C. We studied the optical and electrochemical properties of these π-stacked polymers in comparison to their model compounds in order to study the effect of multilayered stacking.

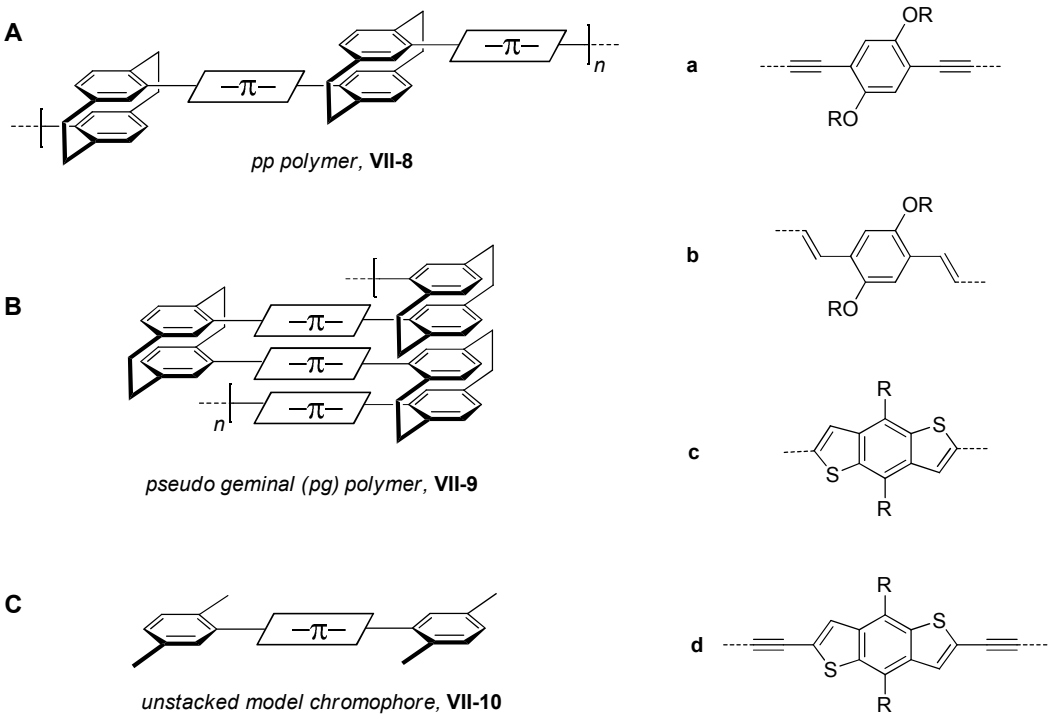


**Figure 7.2.** A, Pseudo-para (*pp*) polymers, **VII-8**, consisting of π-conjugated tiers a-b; B, Pseudo-geminal (*pg*) polymers **VII-9**; and C, linear models **VII-10** which resemble a single unstacked tier of the polymers.

## 7.2. Synthesis

General procedures and methods are described in Chapter 2.

### 7.2.1. Pseudo-geminal phenylene ethynylene polymer, *pg*-poly($PE_3$)[4]

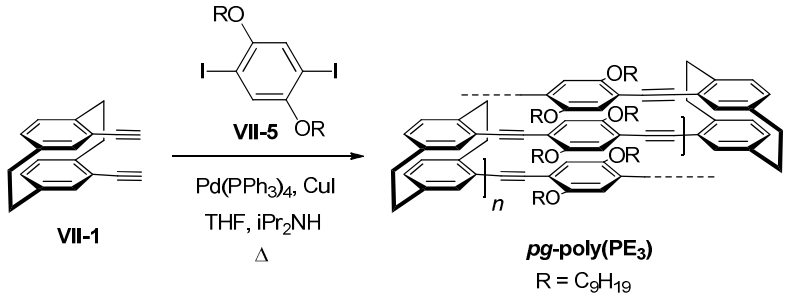


A solution of 4,15-diethynyl[2.2]paracyclophane (70 mg, 0.27 mmol), 1,4-diiodo-2,5-bis(nonyloxy)benzene (170 mg, 270 μmol), $Pd(PPh_3)_4$ (15 mg, 12 μmol), and CuI (3 mg, 1 μmol) in a mixture of THF (5 mL) and diisopropylamine (5 mL) was heated at 70 °C for 2 d. The mixture was poured into methanol (100 mL) and the precipitated solid was removed by filtration. The solid was sequentially extracted in a Soxhlet extractor with methanol, hexane, and chloroform. The solvent was removed from the chloroform fraction under reduced pressure to afford ***pg*-poly($PE_3$)** as an orange solid (100 mg, 60% yield). $^1$H NMR: see Results and Discussion. IR (ATR): 2923, 2847, 1588, 1502, 1260, 1210, 1031, 798 $cm^{-1}$. GPC (THF, UV–vis detector, PS standards): 5 kDa (DP = 8), PDI = 1.7; Elemental analysis: found C, 79.61%; H, 8.30%; I, 3.37% (see Results and Discussion).

## 7.2.2. 1,4-Bis(2,5-dimethylphenylethynyl)-2,5-bis(nonyloxy)benzene, $Me_4PE_3$[4]

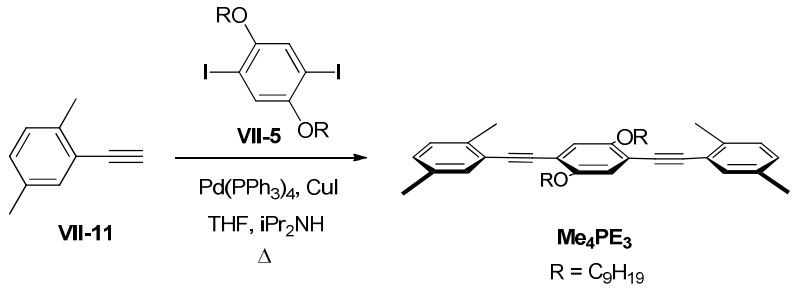


A solution of 1,4-diiodo-2,5-bis(nonyloxy)benzene (250 mg, 0.407 mmol), (2,5-dimethylphenyl)acetylene (150 mg, 1.15 mmol), $Pd(PPh_3)_2Cl_2$ (28 mg, 41 μmol) and CuI (8 mg, 0.04 mmol) in a mixture of THF (2 mL) and diisopropylamine (2 mL) was heated at 70 °C for 2 d. $CH_2Cl_2$ was added (50 mL) and the mixture was washed with sat. aq. $NH_4Cl$ (50 mL) and water (50 mL). The solvent was removed under reduced pressure and the residue was triturated with MeOH and hexane to afford **$Me_4PE_3$** as a pale yellow solid (226 mg, 90% yield). m.p. 117-118 °C. $^1$H NMR (300 MHz, $CDCl_3$) δ 7.33 (d, 2H, *J* = 1.4 Hz, 2H, Ar–H), 7.16 (d, *J* = 7.6 Hz, 2H, Ar–H), 7.03 (dd, *J* = 7.6, 1.4 Hz, 2H, Ar–H), 7.00 (s, 2H, Ar–H, central ring), 4.02 (t, 4H, *J* = 6.4 Hz, $OCH_2$), 2.51(s, 6H, Ar–$CH_3$), 2.31 (s, 6H, Ar–$CH_3$), 1.84 (pentet, 4H, *J* = 6 Hz, $CH_2$), 1.51 (m, 4H, $CH_2$), 1.21-1.39 (m, 24H, $CH_2$), 0.88 (t, *J* = 7.6 Hz, 6H, $CH_3$). $^{13}$C NMR (75 MHz, $CDCl_3$): δ 153.5, 137.2, 134.9, 132.3, 129.5, 129.1, 123.0, 116.5, 114.0 (Ar), 94.2, 89.6 (C≡C), 69.5 ($OCH_2$), 31.8, 29.6, 29.5, 29.4, 29.3, 26.2, 22.7, 20.8, 20.3, 14.1 ($sp^3$ C). IR (ATR): 2962, 2934, 2875 (C–H stretch), 2106 (C≡C), 1495, 1221, 977 cm$^{-1}$; EI MS: *m*/*z* (%) 618.1 ($M^+$, 100); HRMS calculated for $C_{44}H_{58}O_2$, 618.4438; found 618.4437, Δ = 0.1 ppm.

## 7.2.3. Pseudo-geminal phenylene vinylene polymer, *pg*-poly($PV_3$)

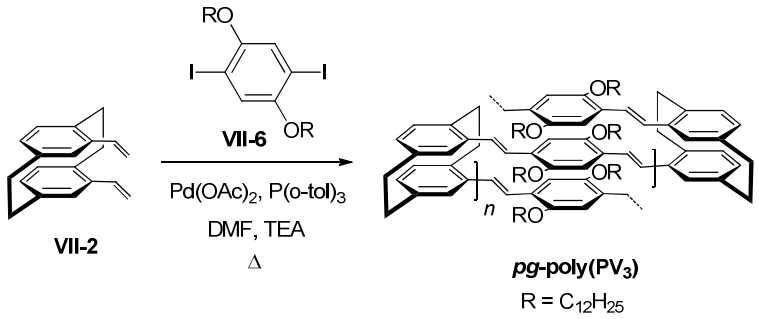


A solution of 4,15-diethenyl[2.2]paracyclophane (100 mg, 380 μmol), 1,4-diiodo-2,5-bis(dodecyloxy)benzene (268 mg, 380μmol), $Pd(OAc)_2$ (9 mg, 0.04 μmol), and $P(o\text{-}tol)_3$ (24 mg, 78 μmol) in a mixture of DMF (8 mL), toluene (1 mL) and triethylamine (3 mL) was heated at 90 °C for 2 d. The mixture was poured into methanol (150 mL) and the precipitated solid was removed by filtration. The solid was dissolved in a minimum volume of $CH_2Cl_2$ and the solution was reprecipitated into acetone (100 mL) to afford ***pg*-poly($PV_3$)** as a yellow solid (120 mg, 45% yield). $^1H$ NMR: see Results and Discussion. IR (ATR): 2917, 2850, 1492, 1389, 1216, 1024, 854 $cm^{-1}$. GPC (THF, UV–vis detector, PS standards): 4.6 kDa (DP = 6), PDI = 1.3. Elemental analysis: found C, 80.25%; H, 9.73%, I, 0.49% (See results and Discussion).

## 7.2.4. 1,4-Bis(2,5-dimethylphenylvinyl)-2,5-bis(dodecyloxy)benzene, $Me_4PV_3$[5]

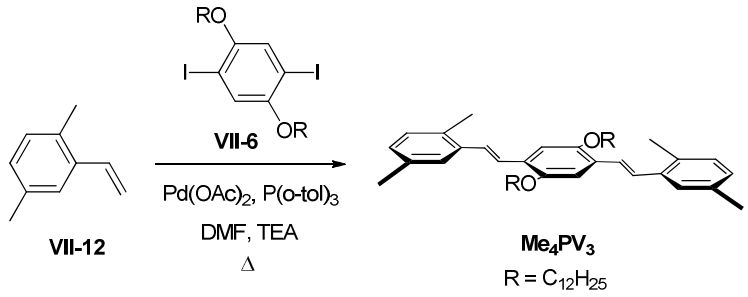


A solution of 1,4-diiodo-2,5-bis(dodecyloxy)benzene (500 mg, 720 μmol), (2,5-dimethylphenyl)vinylene (285 mg, 2.16 mmol), $Pd(OAc)_2$ (16.0 mg, 72.0 μmol) and $P(o\text{-}tol)_3$ (44 mg, 1.4 mmol) in a mixture of DMF (9 mL) and triethylamine (3 mL) was heated at 70 °C for 2 d. The mixture was poured into methanol (150 mL) and the precipitated solid was removed by filtration. The residue was purified by recrystallization from ethanol to afford **$Me_4PV_3$** as a bright yellow solid (420 mg, 81% yield). m.p. 89-90 °C. $^1$H NMR (300 MHz, $CDCl_3$) δ 7.43 (br s, 2H, Ar–H), 7.38 (d, *J* = 15 Hz, 2H, vinylic), 7.28 (d, *J* = 15 Hz, 2H, vinylic), 7.09 (s, 2H, Ar–H, central ring), 7.07 (d, *J* = 8.2 Hz, 2H, Ar–H), 7.00 (d, *J* = 8.2 Hz, 2H, Ar–H), 4.05 (t, *J* = 6 Hz, 4H, $OCH_2$), 2.40 (s, 6H, Ar–$CH_3$), 2.36 (s, 6H, Ar–$CH_3$), 1.86 (p, *J* = 6 Hz, 4H, $CH_2$), 1.22-1.57 (m, 36H, $CH_2$), 0.85 (t, *J* = 6 Hz, 6H, $CH_3$). $^{13}$C NMR (75 MHz, $CDCl_3$): δ 151.2, 136.8, 135.5, 132.7, 130.2, 128.1, 127.1, 126.0, 129.4 (Ar–C), 111.4 (two vinylic), 69.6 ($OCH_2$), 31.9, 29.7 (two), 29.6, 29.5, 29.4, 29.3, 26.3, 22.7, 21.1, 19.6, 14.1 ($sp^3$ C). IR (AT-IR, neat): 2917, 2851, 1513, 1493, 1224, 1038, 967 $cm^{-1}$; MS (MALDI), *m*/*z* (%) 706.5 ($M^+$, 100); HRMS calculated for $C_{50}H_{74}O_2$, 706.5689; found 706.5718, Δ = 4.7 ppm.

## 7.2.5. Pseudo-geminal fused-thiophene polymer, *pg*-poly(CP-E-BDT)

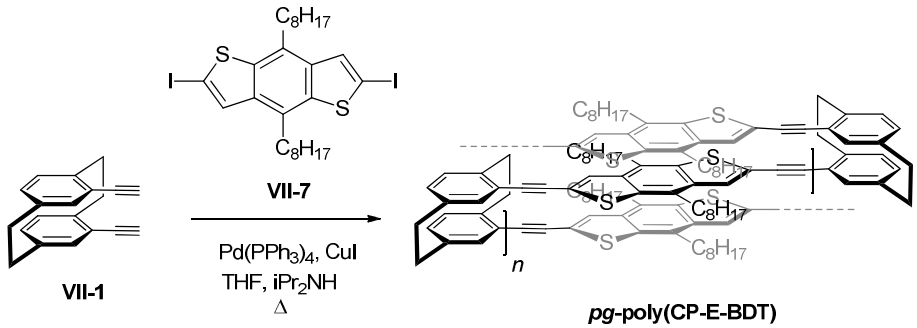


A solution of monomers 4,15-diethynyl[2.2]paracyclophane (100 mg, 400 μmol) and 2,6-diiodo-4,8-dioctylbenzo[1,2-*b*:4,5-*b'*]dithiophene (260 mg, 400 μmol), $Pd(PPh_3)_4$ (23 mg, 20 μmol), and CuI (0.004 g, 0.020 mmol) in a mixture of THF (5 mL) and diisopropylamine (5 mL) was heated at 70 °C for 3 d. The mixture was poured into methanol (100 mL) and the precipitated solid was removed by filtration. The solid was dissolved in a minimum volume of $CH_2Cl_2$ and the solution was reprecipitated into acetone (100 mL) to afford ***pg*-poly(CP-E-BDT)** as an orange solid (175 mg, 66% yield). $^1$H NMR: see Results and Discussion. IR (ATR): 2927, 2854, 1588, 1449, 1260, 1173, 1060, 884, 818 $cm^{-1}$. GPC (THF, UV–vis detector, PS standards): 9.5 kDa (DP = 14), PDI = 1.7. Elemental analysis: found C, 80.06%; H, 7.49%, I, 0.91% (see Results and Discussion).

**7.2.6. 2,6-Bis(2,5-dimethylphenyl)-4,8-dioctylbenzo[1,2-b:4,5-b']dithiophene, E-BDT-Xy$_2$**

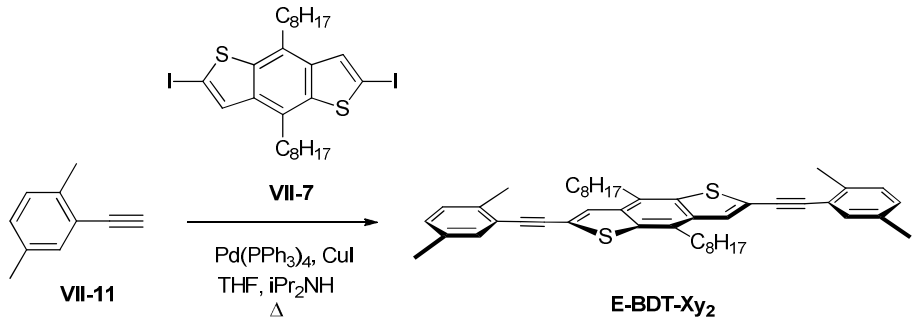


A solution of 2,6-diiodo-4,8-dioctylbenzo[1,2-*b*:4,5-*b'*]dithiophene (100 mg, 0.150 mmol), (2,5-dimethylphenyl)acetylene (0.078 mg, 600 μmol), $Pd(PPh_3)_2Cl_2$ (10 mg, 15 μmol), $PPh_3$ (4.0 mg, 15 μmol) and CuI (0.003 g, 0.015 mmol) in a mixture of THF (2 mL) and diisopropylamine (2 mL) was heated at 70 °C for 2 d. $CH_2Cl_2$ (50 mL) was added and the mixture was washed with sat. aq. $NH_4Cl$ (50 mL) and water (50 mL). The solvent was removed under reduced pressure and the residue was triturated with MeOH and hexane to afford **E-BDT-Xy$_2$** as a pale yellow solid (90 mg, 90% yield). m.p. 147-148 °C. $^1$H NMR (300 MHz, $CDCl_3$): δ 7.53 (s, 2 H, β Th–H), 7.29 (br s, 2 H, Ph–H), 7.07 (d, *J* = 8 Hz, 2 H, Ph–H), 7.02 (d, *J* = 8 Hz, 2 H, Ph–H), 3.03 (t, 4 H, *J* = 6.4 Hz, Ar–$CH_2$), 2.44 (s, 6 H, Ph–$CH_3$), 2.30 (s, 6 H, Ph–$CH_3$), 1.74 (p, 4H, *J* = 6 Hz, $CH_2$), 1.10-1.48 (m, 20 H, $CH_2$), 0.81 (t, *J* = 7.6 Hz, 6H, $CH_3$). $^{13}$C NMR (75 MHz, $CDCl_3$): δ 138.1, 137.3, 136.3, 135.2, 132.3, 129.8, 129.5, 128.9, 126.4, 123.1, 122.1 (Ar–C), 94.6, 87.0 (C≡C), 32.0, 30.0, 29.7, 29.6, 29.5, 29.2, 22.7, 20.8, 20.3, 14.1 ($sp^3$ C). IR (ATR): 2988, 2942, 2834, 1620, 1510, 1477, 1275, 1072, 874, 749 cm$^{-1}$; EI MS: *m*/*z* (%) 670.3 ($M^+$, 100), 571.2 (45). HRMS calculated for $C_{46}H_{54}S_2$, 670.3677; found 670.3665, Δ = 0.1 ppm.

## 7.3. Results and Discussion

### 7.3.1. Synthesis of π-Stacked PE Polymer and Linear Unstacked Model

A Sonogashira cross-coupling condensation polymerization[6] of *pg* diethynyl monomer (**VII-1**)[7] and 1,4-diiodo-2,5-bis(nonyloxy)benzene (**VII-5**)[4] in the presence of a catalytic amount of $Pd(PPh_3)_4$ and CuI in a mixture of diisopropylamine and THF afforded the stacked phenylene ethynylene polymer ***pg*-poly($PE_3$)**, Figure 7.3. The crude polymer was precipitated by addition of the reaction mixture to a large volume of methanol. Fractionation by Soxhlet extraction of the precipitate with methanol, hexane and chloroform gave ***pg*-poly($PE_3$)** as an orange solid (60% isolated yield). The linear unstacked phenylene ethynylene model compound, **$Me_4PE_3$**, was prepared by coupling of diiodide **VII-5** and 2,4-dimethylphenylacetylene, **VII-11**.[4]

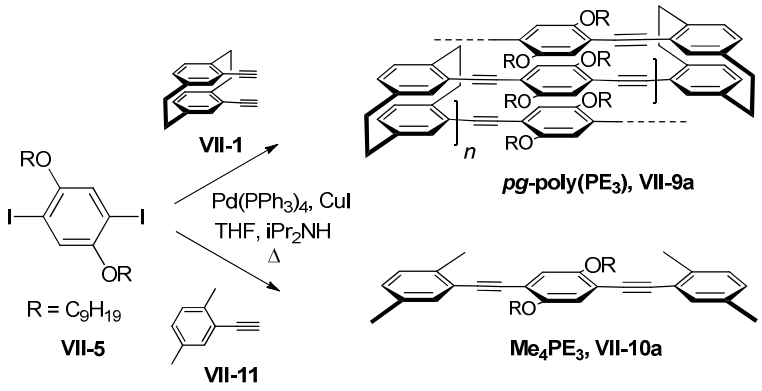


**Figure 7.3**. Phenylene ethynylene stacked polymer and unstacked model: Sonogashira cross-coupling polymerization of monomers **VII-5** and **VII-1** to afford π-stacked polymer ***pg*-poly($PE_3$)**; and synthesis of unstacked linear model **$Me_4PE_3$** (R = *n*-$C_9H_{19}$).

### 7.3.2. Synthesis of π-Stacked PV Polymer and Linear Unstacked Model

The corresponding stacked phenylene vinylene polymer was prepared by a Heck coupling polymerization[8] of 4,15-diethenyl[2.2]paracyclophane (**VII-2**) and 1,4-diiodo-2,5-bis(dodecyloxy)benzene (**VII-6**) in the presence of a catalytic amount of $Pd(OAc)_2$ and CuI in a mixture of DMF and triethylamine, Figure 7.4. The polymer was purified by precipitation of reaction mixture into a large volume of methanol, followed by reprecipitation of a dichloromethane solution of the crude product into acetone to give ***pg*-poly($PV_3$)** as an orange solid (45% isolated yield). The linear unstacked analog, **$Me_4PV_3$**, was obtained by an analogous Heck coupling of diiodide **VII-6** and 2,4-dimethylstyrene, **VII-12**.

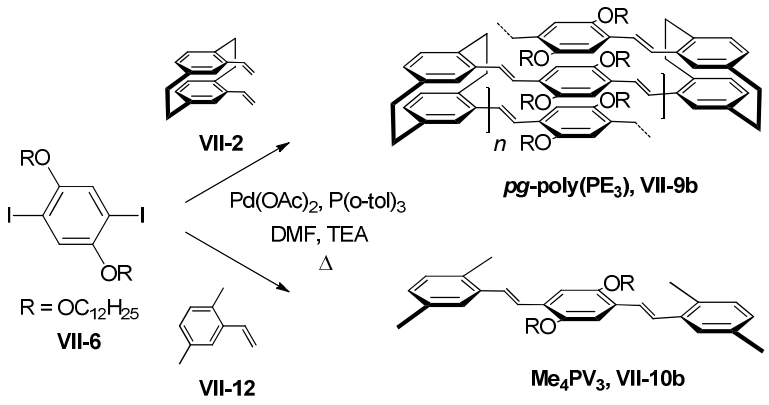


**Figure 7.4**. Phenylene vinylene stacked polymer and unstacked model: Heck cross-coupling polymerization of monomers **VII-6** and **VII-2** to afford π-stacked polymer ***pg*-poly($PV_3$)**; and synthesis of unstacked linear model, **$Me_4PV_3$** (R = *n*-$C_{12}H_{25}$).

### 7.3.3. Attempted metal-catalyzed reactions of 4,15-Dihalo[2.2]paracyclophane

Our initial attempts to polymerize the *pg* dihalides **VII-3**[9] and **VII-4**[9] with 2,6-bis(trimethylstannyl)-4,8-dioctylbenzo[1,2-*b*:4,5-*b*']dithiophene[10] using Stille coupling conditions ($Pd(PPh_3)_4$, toluene/DMF) were unsuccessful. We were also unable to couple the *pg* -dihalo[2.2]paracyclophanes with 2-trimethylstannyl-4-octylthiophene using Stille coupling conditions[11] ($Pd_2(dba)_3$, toluene/THF), or with 4-octyl-2-thienylmagnesium bromide using Kumada coupling conditions[12] ($Ni(dppp)Cl_2$, $Et_2O$). To further explore the reactivity of *pg* dihalo[2.2]paracyclophanes as monomers, we attempted a Sonogashira cross-coupling reaction of iodide **VII-4** with 1,4-diethynyl-2,5-bis(nonyloxy)benzene in the presence of $Pd(PPh_3)_4$ to give **VII-9a**. This was also unsuccessful, which was somewhat surprising given that 4,15-diethynyl[2.2]paracyclophane successfully undergoes Sonogashira coupling with 2,5-dialkoxy-1,4-diiodobenezenes to give the same desired product.[4] Other regioisomers (e.g., the *pp* analog) of dihalo[2.2]paracyclophane do undergo cross-couplings with organometallic reagents.[13]

This lack of reactivity of *pg* dihalo[2.2]paracyclophanes could be due to short distance between the two halogen atoms which may hinder the oxidative insertion of palladium required for the reaction to proceed (the bromine-bromine interatomic distance in ***pg*CP-Br$_2$** is 3.7 Å).[9] This unforeseen obstacle to cross-coupling led us to modify our approach to prepare DBT-based ladder polymers.

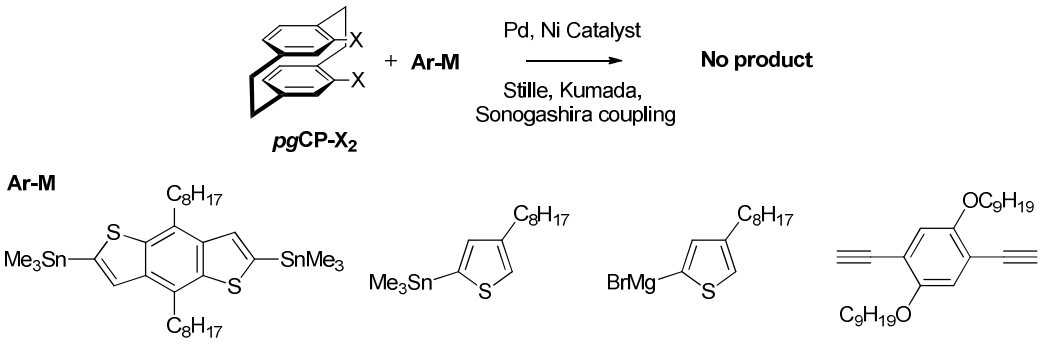


**Figure 7.5.** Attempts to perform cross-couplings with *pg* dihalo[2.2]paracyclophane failed: Stille coupling (treatment with 2,6-bis(trimethylstannyl-4,8-dialkylbenzo[1,2-*b*:4,5-*b*']dithiophene or 2-trimethylstannyl-4-octylthiophene), Kumada coupling (exposure to 4-octyl-2-thienylmagnesium bromide), and Sonogashira coupling (attempted reaction with 1,4-diethynyl-2,5-bis(nonyloxy)benzene).

### 7.3.4. Synthesis of π-Stacked BDT Polymer and Linear Unstacked Model

We returned to the use of *pg*-diethynyl[2.2]paracyclophane (**VII-1**) as a monomer and conducted a polymerization with a suitable dihalo derivative of **VII-7** to afford a stacked BDT-ethynylene polymer. We prepared the 2,6-diiodo analog (**VII-7**) rather than the previously reported dibromide to make use of the greater reactivity of aryl iodides in Sonogashira coupling reactions. Sonogashira cross-coupling condensation polymerization of di(ethyne) **VII-1** and diiodide **VII-7** proceeded smoothly to afford ***pg*-poly(CP-E-BDT)** (**VII-9d**), Figure 7.6. The crude product was purified by precipitation to give the polymer as an orange solid (70% isolated yield). **E-BDT-Xy$_2$** (**VII-10d**) was prepared as a model for the unstacked tier of the polymer by coupling of **VII-7** with 2,4-dimethylphenylacetylene, **VII-11**.

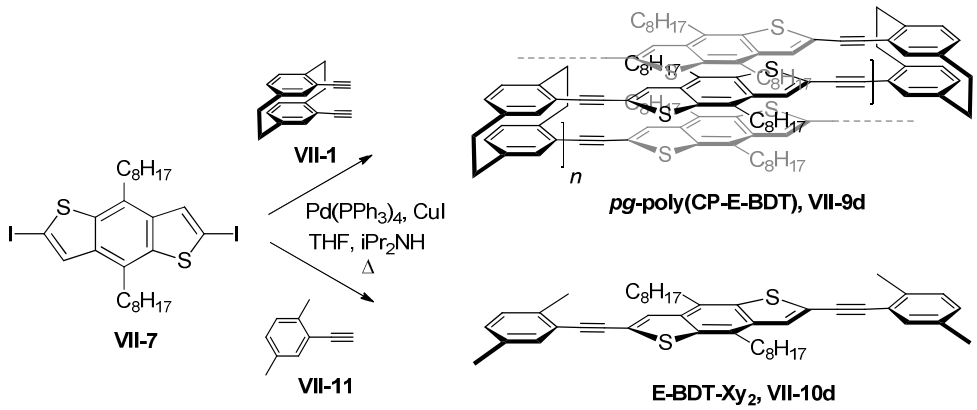


**Figure 7.6.** Fused-thiophene stacked polymer and unstacked model: Sonogashira cross-coupling polymerization of **VII-7** and **VII-1** to afford the multitiered polymer ***pg*-poly(CP-E-BDT)**; and synthesis of unstacked linear model, **E-BDT-$Xy_2$**.

### 7.3.5. Structural Characterization

Although all of the π-stacked polymers ***pg*-poly($PE_3$)**, ***pg*-poly($PV_3$)**, and ***pg*-poly(CP-E-BDT)** are soluble in deuterated chloroform, the $^1$H NMR spectra of these solutions consist of sets of very broad peaks. The chemical shifts of the peaks are consistent with the expected polymeric structures, and the spectra indicated the absence of unreacted monomer, catalyst and solvent. However, the spectra provide no additional details regarding the polymer structure. The broadening of these peaks arises from the rigid nature of the polymers since the rotation of each of the oligomeric tiers is severely hindered by the close-packed multi-layer architecture.

The relative molecular weight of the polymers (relative to polystyrene standards) was determined by gel permeation chromatography with THF as the eluent. The number average molecular weight ($M_n$) and polydispersity index (PDI) of polymers are recorded in the Table 1, together with the mass percentage of iodine in the polymer determined from combustion analysis. Any iodine arises from any iodoarene end groups remaining in the polymer. We note that while the mass percentage of iodine in ***pg*-poly($PE_3$)** is significantly higher (3.37%) than in either ***pg*-poly($PV_3$)** and ***pg*-poly(CP-E-BDT)**, these values depend on both the molecular weight of the polymer and the ratio of end groups (i.e., the two types of end group dervived from either the iodoarene or the cyclophane monomers). The amount of iodine in the ***pg*-poly($PE_3$)**, assuming a 1:1 ratio of chain ends (consistent with the monomer feed ratio used in this step-growth polymerization), corresponds to a degree of polymerization of 6. The far lower content of iodine in the other materials might indicate either a higher molecular weight (which is inconsitant with data from GPC), or a lower proportion of iodoarene chain ends.

Further evidence for the polymeric nature of the isolated product comes from infrared spectroscopy. The infrared spectra of ***pg*-poly($PE_3$)** and ***pg*-poly(CP-E-BDT)** (Figure 7.7,

spectra B and C, respectively) show the absence of an alkyne C–H stretching mode (~3300 $cm^{-1}$) that is present in the spectrum of the diethynyl monomer (spectrum A). The spectra of the polymers also include signatures of the long alkyl chains of the dialkyl(oxy)arene units derived from the diodo monomer. Similarly, the infrared spectrum of ***pg*-poly($PV_3$)** (Figure 9, spectrum E) lacks a vinylic C-H stretching peak at 3080 $cm^{-1}$ which is a signature of the alkene present in diethenyl monomer (spectrum D).

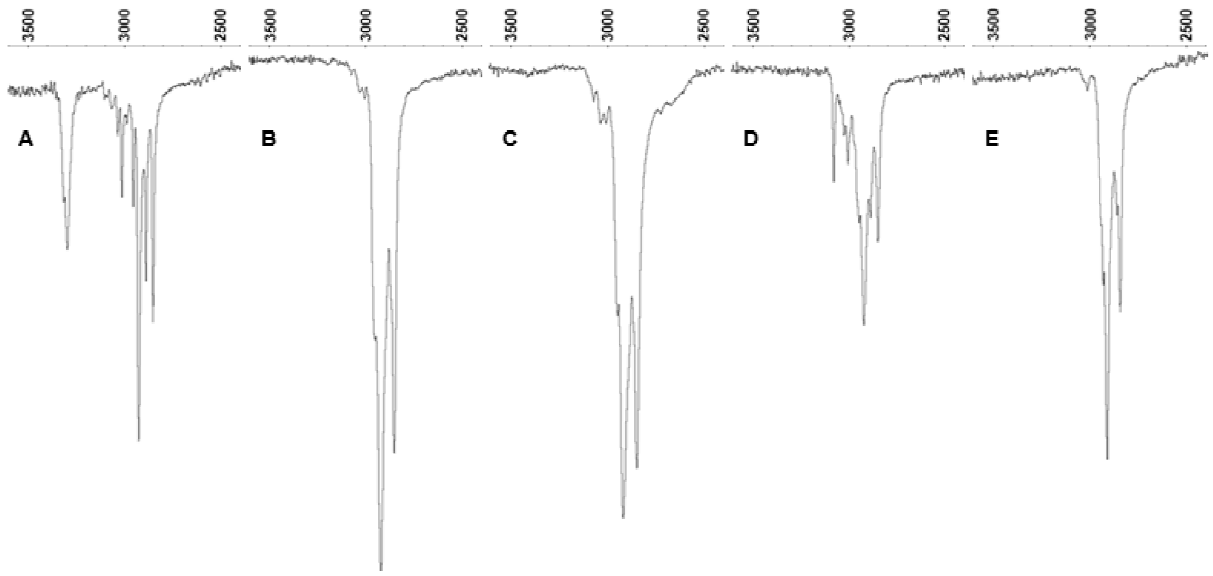


**Figure 7.7.** C-H stretching region (3600-2400 $cm^{-1}$) of the infrared spectra of monomers and polymers: A, 4,15-diethynyl[2.2]paracyclophane monomer, **VII-1**; B, phenylene ethynylene polymer, ***pg*-poly($PE_3$)**; C, fused-thiophene polymer, ***pg*-poly(CP-E-BDT)**; D, 4,15-diethenyl[2.2]paracyclophane monomer, **VII-2**; E, phenylene vinylene polymer, ***pg*-poly($PV_3$)**.

**Table 7.1.** Molecular Weight and PDI of Polymers

| | Gel permeation chromatography[a] | | | | Mass %[b] |
|---|---|---|---|---|---|
| | $M_n$ $10^3$ kD | $M_w$ $10^3$ kD | PDI | DP | Iodine |
| ***pg*-poly($PE_3$)** | 5.0 | 8.5 | 1.7 | 8 | 3.37 |
| ***pg*-poly($PV_3$)** | 4.6 | 5.8 | 1.3 | 6 | 0.49 |
| ***pg*-poly(CP-E-BDT)** | 9.5 | 16.5 | 1.7 | 14 | 0.91 |

[a] Calibrated with polystyrene standards, THF eluent; [b] From combustion analysis

### 7.3.6. UV-Vis and Fluorescence Spectroscopy

The UV-visible and fluorescence spectra of the stacked polymers were recorded and compared to those of the corresponding linear unstacked model compounds. Absorption and emission maxima for all of polymers and model compounds are presented in Table 2. In each case, the polymers have similar absorption maxima to those of the corresponding unstacked model compounds. However, the absorption edge of all of the polymers are red-shifted by ca. 50 nm compared to their models,indicating that the stacked architecture of the polymers does have some influence on the electronic ground state. There are more significant differences between the emission spectra of the multitier stacked polymers and their corresponding linear models. Whereas the emission spectra of the linear unstacked model compounds consists of a relatively sharp peak, or set of vibronic peaks, the emissions from the polymers are significantly broadened and red shifted. The lower intensity of the emission of the polymer may be ascribed to fluorescence quenching resulting from stacking of the conjugated tiers. Such quenching is commonly observed for thin films of conjugated polymers, in which the chains are in close contact (i.e. in a close packed stacked arrangement), and in solutions containing aggregates of polymer chains, relative to the emission from solutions of the same polymers.[9]

The Stokes shift of ***pg*-poly($PE_3$)** (171 nm) is significantly larger than that of the linear unstacked model **$Me_4PE_3$** (28 nm), Figure 7.8. The similarity of the absorption maxima of the stacked polymer an unstacked linear model suggests that a chromophore with an electronic structure that resembles that of a single conjugated tier is responsible for absorption in the polymer. As with the *pp* polymer the excited state can undergo rapid energy transfer to form a lower-energy “phane” electronic state. Emission from this lower energy state is red-shifted relative to that from the unstacked single tier model compound. The magnitude of the Stokes

shift of ***pg*-poly(PE$_3$)** is significantly larger that of the pseudo-para analog (***pp*-poly(PE$_3$)**, 28 nm)[3], and pseudo-ortho analog (***po*-poly(PE$_3$)**, 34 nm).[3] Thus the magnitude of the relaxation in the excited state of the pseudo-geminal analog may be ascribed to the multi-layer arrangement of the conjugated chromophoric tiers which are stacked their entire length. This is in contrast to the limited overlap between chromophores in the pseudo-para and pseudo-ortho analogs, which is restricted to stacking of the terminal rings of the conjugated chromophores (i.e., the rings of the cyclophane). The delocalization of exciton over the specific number of tiers is very difficult to interpret. To achieve that understanding, we will have to separate the polymeric chains with specific number of tiers (n = 1, 2, 3, etc.)

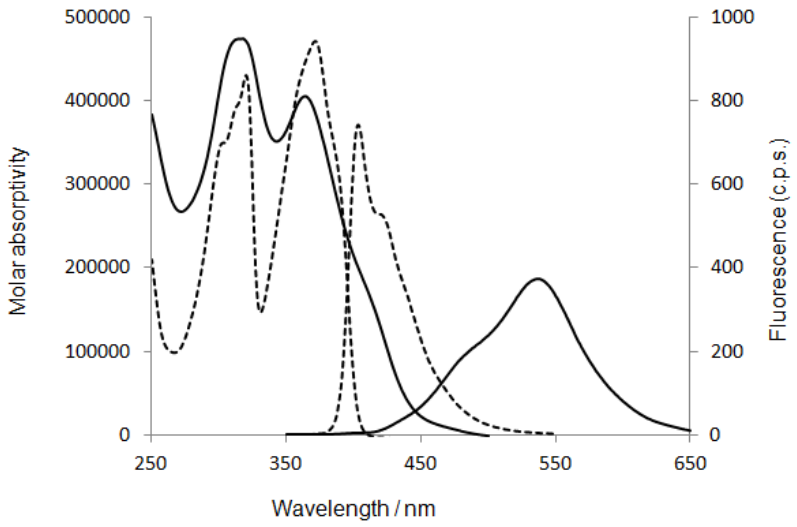


**Figure 7.8**. UV-visible and fluorescence spectra: A, ***pg*-poly(PE$_3$)** (solid) and unstacked model, **Me$_4$(PE$_3$)** (dotted); B, ***pg*-poly(PV$_3$)** (solid) and unstacked model, **Me$_4$(PV$_3$)** (dotted); C, ***pg*-poly(CP-E-BDT)** (solid) and unstacked model, **E-BDT-Xy$_2$** (dotted). *c* = 1 mg/100 mL.

Similarly, the phenylene vinylene stacked polymer ***pg*-poly($PV_3$)**, when excited at the absorption maxima 390 nm, displays a larger Stokes shift (97 nm) compared to the unstacked model **$Me_4PV_3$** (54 nm) and pseudo-para analog ***pp*-poly($PV_3$)** (64 nm)[5], Figure 7.9. While significantly larger than that of these regioisomeric polymers, the magnitude of this shift is smaller than that of the PE analog. This may be explained by the incomplete overlap of the phenylene vinylene tiers that arises from the presence of a mixture of conformers of the diethenylbenzene unit in the middle of each chromophore. Hopf observed that the two vinyl groups of 4,15-divinyl[2.2]paracyclophane, **VII-2**, orient away from the neighboring ethano bridge to minimize steric interactions.[7] However, rotation about the other vinyl-aryl bonds in each chromophore can still lead to multiple combinations of cisoid and transoid divinylbenzene conformations throughout the polymeric architecture, Figure 7.10. While transoid-transoid (and cisoid-cisoid) diads remain fully stacked along the entire length of the conjugated tiers, a transoid-cisoid diad provides a break in stacking which limits the extent of overlap between π-systems. Accordingly, the relaxation of the excited state may be smaller, thereby leading to a smaller Stokes shift.

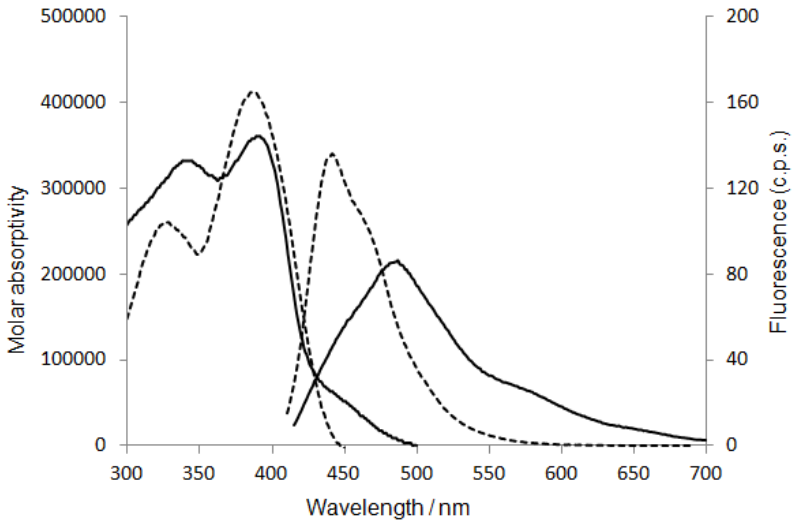


**Figure 7.9**. UV-visible and fluorescence spectra: A, ***pg*-poly(PE$_3$)** (solid) and unstacked model, **Me$_4$(PE$_3$)** (dotted); B, ***pg*-poly(PV$_3$)** (solid) and unstacked model, **Me$_4$(PV$_3$)** (dotted); C, ***pg*-poly(CP-E-BDT)** (solid) and unstacked model, **E-BDT-Xy$_2$** (dotted). *c* = 1 mg/100 mL.

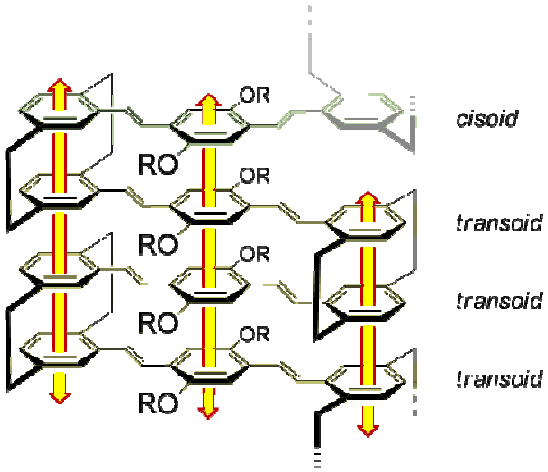


**Figure 7.10.** Cisoid and transoid conformations of chromophoric tier in the stacked polymer, ***pg*-poly(PV$_3$)**.

The emission of the ***pg*-poly(CP-E-BDT)**, when excited at 365 nm, consists of a broad peak which is considerably red shifted ($\lambda_{max}$ = 490, 520 nm) compared to the unstacked model that has three sharp emission peaks at 420, 445 and 476 nm, Figure 7.11. The large Stokes shift of the polymer (127 nm) is consistent with the linear combination of 2,6-disubstituted BDT and ethynylene units which keeps the tiers in a fully-stacked arrangement.

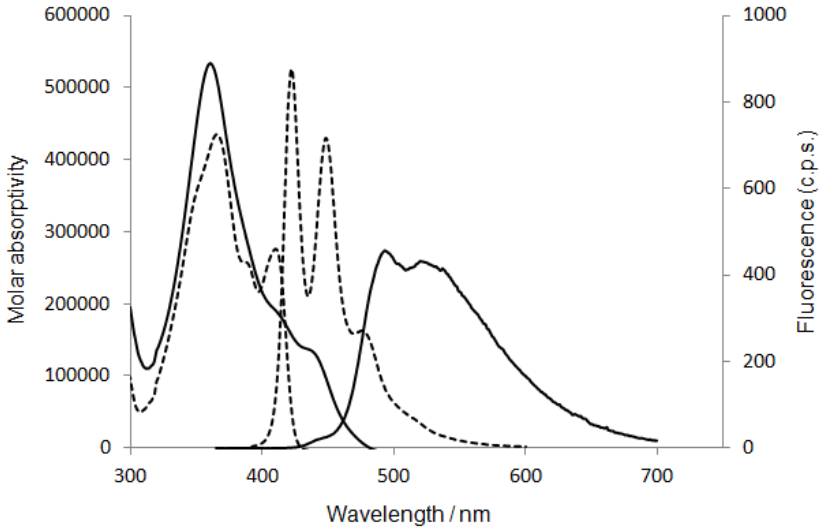


**Figure 7.11**. UV-visible and fluorescence spectra: A, ***pg*-poly($PE_3$)** (solid) and unstacked model, **$Me_4$($PE_3$)** (dotted); B, ***pg*-poly($PV_3$)** (solid) and unstacked model, **$Me_4$($PV_3$)** (dotted); C, ***pg*-poly(CP-E-BDT)** (solid) and unstacked model, **E-BDT-$Xy_2$** (dotted). *c* = 1 mg/100 mL.

**Table 7.2.** Absorption and emission spectra.

| | Absorption maxima $\lambda_{max}$/nm | Absorption edge shift[e] nm | Emission maxima $\lambda_{max}$/nm | Stokes shift nm |
|---|---|---|---|---|
| ***pg*-poly($PE_3$)** [a] | 320, 359 | 77 | 530 | 171 |
| **$Me_4(PE_3)$** [a] | 321, 374 | - | 402, 413 | 28 |
| ***pp*-poly($PE_3$)** [b] | 319, 386 | - | 414, 438 | 28 |
| ***po*-poly($PE_3$)** [c] | 319, 377 | - | 411, 434 | 34 |
| ***pg*-poly($PV_3$)** [a] | 340, 390 | 50 | 487 | 97 |
| **$Me_4(PV_3)$** [a] | 327, 387 | - | 441 | 54 |
| ***pp*-poly($PV_3$)** [d] | 398 | - | 462 | 64 |
| ***pg*-poly(CP-E-BDT)**[a] | 364 | 56 | 491, 515 | 127 |
| **E-BDT-$Xy_2$**[a] | 370, 415 | - | 421, 447, 476 | 51 |

[a] [analyte] = 1 mg in 100 mL of $CHCl_3$. [b] spectra shown in Ref. 3. [c] spectra shown in Ref. 3. [d] spectra shown in Ref. 5. [e] end of absorption edge the compared to model compound.

### 7.3.7. Differential Pulse Voltammetry (DPV)

The electrochemical properties of the stacked polymer ***pg*-poly(CP-E-BDT)** and the linear unstacked model **E-BDT-$Xy_2$** were studied by cyclic voltammetry (CV), 7.12. A film was prepared by drop casting a $CHCl_3$ solution of the polymer in on a gold electrode and the cyclic voltammogram was recorded in a 0.1 M solution of *n*-$Bu_4NPF_6$ in acetonitrile. The voltammogram of the unstacked model was determined in a 1 mM solution in dichloromethane containing 0.1 M *n*-$Bu_4NPF_6$. The polymer film exhibits an irreversible oxidation wave at +1.12 V versus Ag wire quasi-reference electrode, whereas the voltammogram of the unstacked linear model compound has one reversible oxidation peak at +1.14 V, Figure 8. The similarity of the oxidation potentials of the polymer and model unstacked oligomer again suggests a similarity in the electronic structure of the ground states, in contrast to the electronic structures of their excited states.

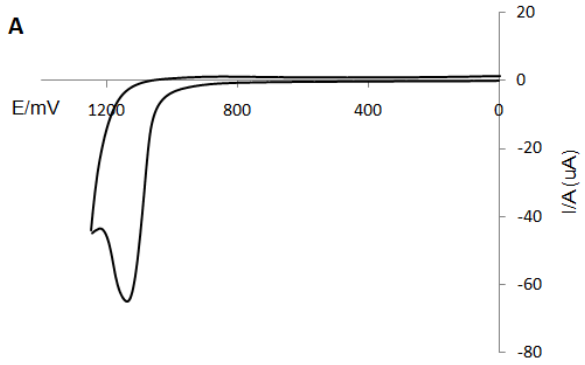

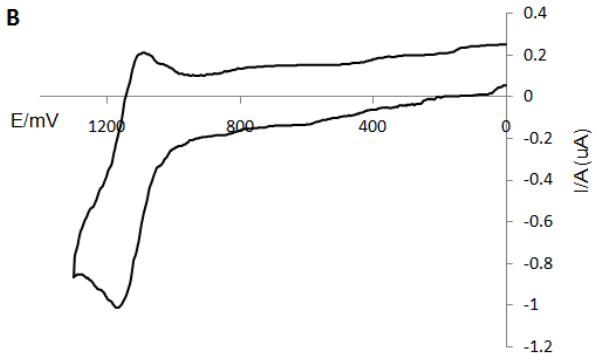


**Figure 7.12**. Differential pulse voltammetry. A, pseudo-geminal cyclophane polymer, ***pg*-poly(CP-E-BDT)** (thin film deposited on gold electrode in acetonitrile containing 0.1M *n*-$Bu_4NPF_6$). B, unstacked xylyl analog, **E-BDT-$Xy_2$** (1 mM in $CH_2Cl_2$ containing 0.1M *n*-$Bu_4NPF_6$) (Potential measured against a Ag quasi-reference electrode; scanning potential = 100 mV/s.

## 7.4. Conclusions

The pseudo-geminal (*pg*) [2.2]paracyclophane(CP) core is a useful scaffold to build polymers consisting of conjugated units that are stacked over their entire length. The stacking of the conjugated tiers in these soluble materials ressembles the close-packed cofacial assembly of segments of conjugated polymer chains in semiconducting thin films. The *pg* dihalo[2.2]paracyclophanes are unreactive towards common coupling reactions (Stille, Kumada, Sonogashira), which severely limits their use as monomers. However, the diethynyl *pg* [2.2]paracyclophane and diethenyl *pg* [2.2]paracyclophane analogs successfully undergo polymerizations with dihaloarenes by Sonogashia and Heck coupling reactions, respectively, to afford multi-tiered stacked conjugated polymers. The multilayered polymers exhibit the effect of extensive π-π interactions between the stacked conjugated tiers. This is most pronounced in the excited state with the formation of a phane state by virtue of the extended overlap along the entire length of the stacked chromophores.

## 7.5. References


1. Reich, H. J.; Cram, D. J., *Journal of the American Chemical Society* **1969**, *91*, 3527.

2. Salhi, F.; Collard, D. M., *Advanced Materials* **2003**, *15*, 81. Morisaki, Y.; Chujo, Y., *Bulletin of the Chemical Society of Japan* **2009**, *82*, 1070. Guyard, L.; An, M. N. D.; Audebert, P., *Advanced Materials* **2001**, *13*, 133.

3. Morisaki, Y.; Wada, N.; Arita, M.; Chujo, Y., *Polymer Bulletin* **2009**, *62*, 305.

4. Jagtap, S. P.; Collard, D. M., *Journal of the American Chemical Society* **2010**, *132*, 12208.

5. Morisaki, Y.; Ishida, T.; Chujo, Y., *Macromolecules* **2002**, *35*, 7872.

6. Sonogashira, K.; Tohda, Y.; Hagihara, N., *Tetrahedron Letters* **1975**, 4467.

7. Bondarenko, L.; Hentschel, S.; Greiving, H.; Grunenberg, J.; Hopf, H.; Dix, I.; Jones, P. G.; Ernst, L., *Chemistry A European Journal* **2007**, *13*, 3950.

8. Heck, R. F.; Nolley, J. P., *Journal of Organic Chemistry* **1972**, *37*, 2320.

9. Chen, L.; McBranch, D.; Wang, H.; Helgeson, R.; Wudl, F.; Whitten, D., *Proceedings of the National Academy of Sciences* **1999**, *96*, 12287.

# CHAPTER 8

# EXTENDING THE CONJUGATED TIER OF π-STACKED POLYMERS

## 8.1. Introduction

The previous chapter deals with the use of pseudo-geminal substituted [2.2]paracyclophane core to prepare the multitiered π-stacked conjugated polymers. These polymers contain relatively short conjugated oligomers, consisting of only three arene rings, arranged in a multilayered fashion. To further extend the amount of π-π interactions between stacked conjugated units, we chose to increase the length of the conjugated tiers of the polymer.

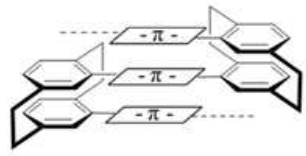


VIII-1

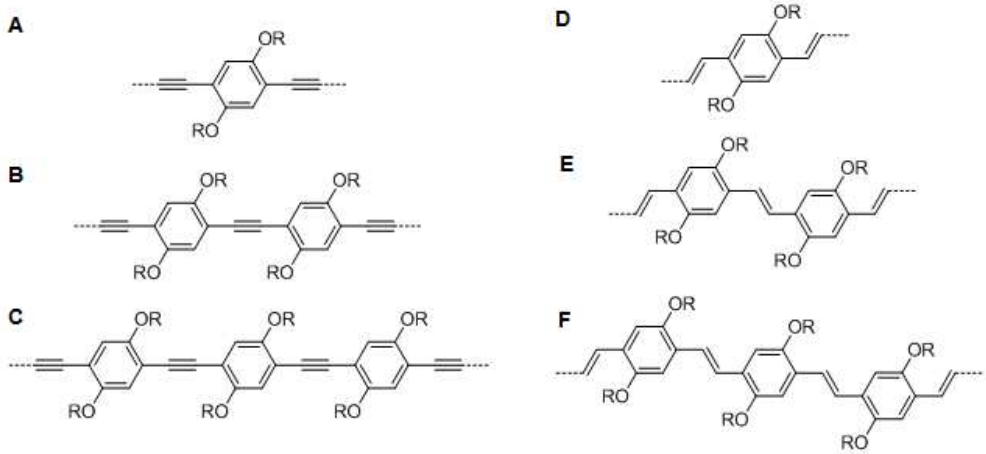


**Figure 8.1.** Molecular structures of multilayered π-stacked conjugated polymers: polymers containing oligo(phenylene ethynylene) units, **VIII-1A**, **B**, and **C**; and polymers containing oligo(phenylene vinylene) units, **VIII-1D**, **E**, and **F**.

In this chapter, we report the synthesis of diiodo-terminated conjugated oligomers as monomers (Figure 8.2) and their use to prepare the π-stacked polymers containing extended conjugated tiers. We also report the effect of length of conjugation on the optical properties of the polymers compared to the corresponding unstacked model compounds.

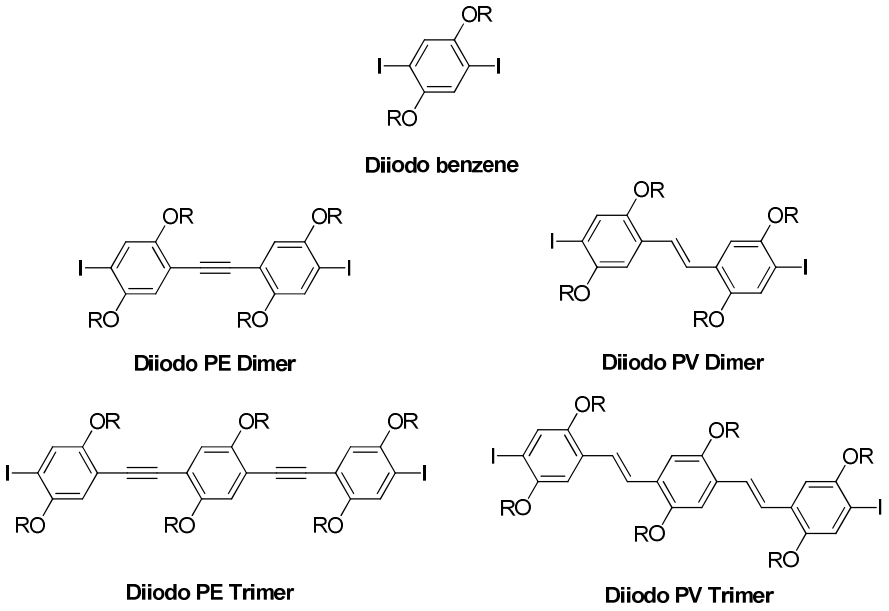


**Figure 8.2.** Diiodo conjugated oligomers which serve as monomers to extend tiers of the multilayered π-stacked conjugated polymers.

## 8.2. Synthesis

General procedures and methods are described in Chapter 2.

### 8.2.1. 2-Nitro-1,4-bis(1-octyn-1-yl)benzene[1]

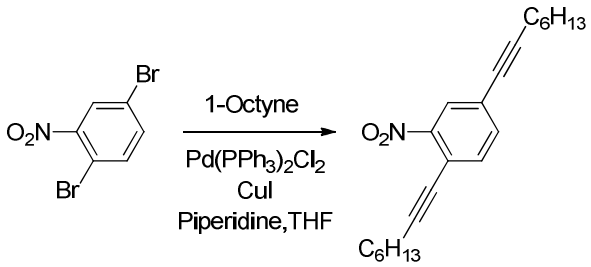


**VIII-18** **VIII-19**

A solution of 1,4-dibromo-2-nitrobenzene (10.0 g, 35.6 mmol), $Pd(PPh_3)_2Cl_2$ (2.50 g, 3.57 mmol), $PPh_3$ (470 mg, 1.80 mmol), CuI (340 mg, 1.80 mmol) and 1-octyne (16.8 g, 160 mmol) in a 1:1 v/v mixture of THF and triethylamine (100 mL) was stirred for 12 h under Ar. $CH_2Cl_2$ (50 mL) was added and the solution was washed with sat. $NH_4Cl$ (100 mL) and water (100 mL). The organic layer was dried over $MgSO_4$ and the solvent was removed under reduced pressure. The crude residue was subjected to column chromatography (5% ethyl acetate / 95% hexanes; silica gel) to afford the title compound as yellow oil (9.7 g, 80%). $^1$H NMR (300 MHz, $CDCl_3$): δ 7.95 (d, *J* = 1.4 Hz, 1H, Ar-H), 7.48 (dd, *J* = 8.1, 1.4 Hz, 1H, Ar-H), 7.45 (dd, *J* = 8.1, 1.4 Hz, 1H, Ar-H), 2.47 (t, *J* = 7.0 Hz, 2H, ≡C-$CH_2$), 2.41 (t, *J* = 7.1 Hz, 2H, ≡C-$CH_2$), 1.53-1.68 (br m, 4H, $CH_2$), 1.22-1.53 (br m, 12H, $CH_2$), 0.94 (t, *J* = 7.0 Hz, 6H, $CH_3$). $^{13}$C NMR (75 MHz, $CDCl_3$): δ 149.7, 134.9, 134.3, 127.1, 124.1, 117.9 (Ar-C), 100.5, 94.7, 78.4, 75.8 (alkyne-C), 31.2 (2 C), 28.5, 28.4, 28.3, 28.2, 22.4 (2 C), 19.8, 19.4, 13.9 (2 C) ($CH_3$). IR (ATR): 2914, 2840, 1602, 1512, 1210, 1040, 828 cm$^{-1}$; MS (EI): m/z (%) 339.1 ($M^+$, 100).

## 8.2.2. 2-Amino-1,4-dioctylbenzene[1]

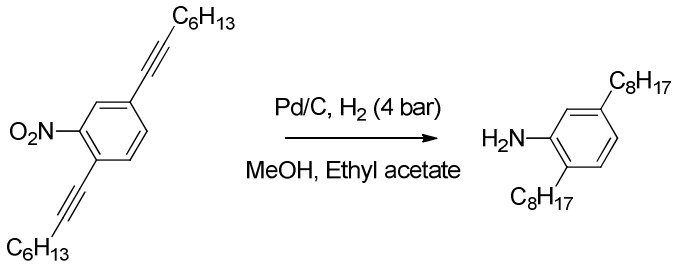


**VIII-19** **VIII-20**

A solution of 2-nitro-1,4-bis(1-octyn-1-yl)benzene (5.5 g, 16 mmol) and 10% Pd/C (70 mg) in a 1:1 v/v mixture of MeOH and ethyl acetate (200 mL) was stirred for 24 h under $H_2$ (55 psi). Ethyl acetate (100 mL) was added and the solution was flushed through a short plug of silica gel. The solvent was removed under reduced pressure to afford the title compound as an orange oil (4.9 g, 95%). $^1$H NMR (300 MHz, $CDCl_3$): δ 6.95 (d, *J* = 7.6 Hz, 1H, Ar-H), 6.58 (dd, *J* = 7.6, 1.7 Hz, 1H, Ar-H), 6.52 (d, *J* = 1.7 Hz, 1H, Ar-H), 3.56 (br s, 2H, $NH_2$), 2.41-2.54 (m, 4H, Ar-$CH_2$), 1.49-1.69 (m, 4H, $CH_2$), 1.17-1.47 (m, 20H, $CH_2$), 0.89 (t, *J* = 6.1 Hz, 6H, $CH_3$). $^{13}$C NMR (75 MHz, $CDCl_3$): δ 143.8, 141.7, 129.3, 124.4, 118.9, 115.7 (Ar-C), 35.6, 31.8 (2 C), 31.3, 30.9, 29.8, 29.4 (2 C), 29.3, 29.2 (2 C), 28.9, 22.6 (2 C) ($CH_2$), 13.9 (2 C) ($CH_3$). IR (ATR): 3465, 3369, 2923, 2847, 1625, 1509, 1462, 1290, 868 $cm^{-1}$; MS (EI): m/z (%) 317.2 ($M^+$, 100), 218.1 (70); HRMS calculated for $C_{22}H_{39}N$, 317.3083; found 317.3078, Δ = 1.6 ppm.

## 8.2.3. 4-Iodo-2,5-dioctylaniline[1]

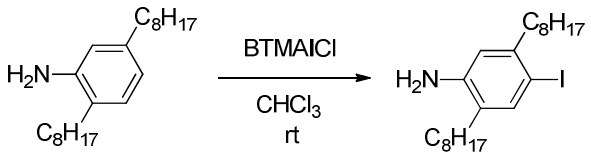


**VIII-20** **VIII-21**

A solution of benzyltrimethylammonium dichloroiodate (4.8 g, 14 mmol) in $CH_2Cl_2$ (10 mL) was added dropwise to a mixture of 2-amino-1,4-dioctylbenzene (4.0 g, 13 mmol) and $NaHCO_3$ (2.1 g, 24 mmol) in a 1:1 v/v mixture of $CH_2Cl_2$ and MeOH (20 mL) at 0 °C. The reaction mixture was stirred for 30 min and water (50 mL) was added. The organic layer was separated and dried over $MgSO_4$. The solvent was removed under reduced pressure and the residue was subjected to column chromatography (5% ethyl acetate / 95% hexanes; silica gel) to afford the title compound as a brown oil (4.2 g, 80%). $^1$H NMR (300 MHz, $CDCl_3$): δ 7.40 (s, 1H, Ar-H), 6.55 (s, 1H, Ar-H), 3.57 (br s, 2H, $NH_2$), 2.55 (t, *J* = 8.1 Hz, 2H, Ar-$CH_2$), 2.38 (t, *J* = 7.8 Hz, 2H, Ar-$CH_2$), 1.48-1.62 (m, 4H, Ar-$CH_2$), 1.20-1.41 (m, 20H, $CH_2$), 0.88 (t, *J* = 6.3 Hz, 6H, $CH_3$). $^{13}$C NMR (75 MHz, $CDCl_3$): δ 144.5, 143.6, 139.5, 127.3, 116.5, 86.7 (Ar-C), 40.3, 31.8 (2 C), 30.5, 30.4, 29.6, 29.4 (2 C), 29.2 (2 C), 28.7, 22.7 (2 C), 14.1 (2 C) ($sp^3$ C); IR (ATR): 3478, 3378, 2917, 2850, 1615, 1485, 1396, 1260, 884 $cm^{-1}$; MS (EI): m/z (%) 443.3 ($M^+$, 100); HRMS calculated for $C_{22}H_{38}NI$, 443.2049; found 443.2060, Δ = 2.5 ppm.

## 8.2.4. 1-(2,5-Dioctyl-4-iodophenyl)-3,3-diethyl-triazene

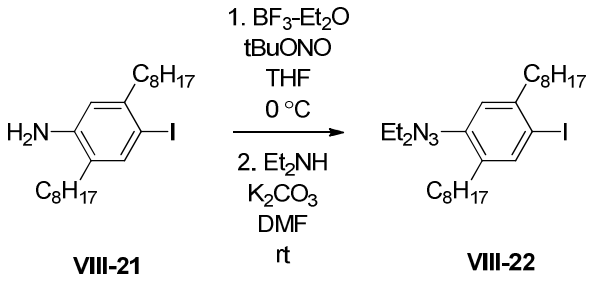


**VIII-21** **VIII-22**

*t*-BuONO (3.8 g, 37 mmol) was added to a mixture of 4-iodo-2,5-dioctylaniline (5.50 g, 12.4 mmol) and $BF_3Et_2O$ (7.0 g, 50 mmol) in anhydrous THF (100 mL) at -10 °C. The reaction mixture was stirred for 30 min. The solvent was removed under reduced pressure and the residue was dissolved in DMF (50 mL) followed by addition of $K_2CO_3$ (3.5 g, 25 mmol) and anhydrous diethylamine (4.0 g, 55 mmol) at -10 °C. The reaction mixture was stirred at room temperature for 2 h. Ethyl acetate (200 mL) was added. The resulting solution was washed with water (200 mL) and the organic layer was dried over $MgSO_4$. The solvent was removed under reduced pressure and the residue was subjected to column chromatography (1% ethyl acetate / 99% hexanes) on a basic alumina to afford the title compound as a yellow oil (5.0 g, 77%). $^1$H NMR (300 MHz, $CDCl_3$): δ 7.59 (s, 1H, Ar-H), 7.19 (s, 1H, Ar-H), 3.75 (q, 4H, N-$CH_2$), 2.62-2.73 (m, 4H, Ar-$CH_2$), 1.52-1.63 (m, 4H, $CH_2$), 1.25-1.42 (m, 30H, $CH_2$), 0.86-0.93 (m, 6H, $CH_3$). $^{13}$C NMR (75 MHz, $CDCl_3$): δ 148.7, 142.9, 140.0, 137.0, 117.1, 95.7 (Ar-C), 40.6, 31.7 (2 C), 31.1, 31.0 (2 C), 30.5, 30.4, 29.6, 29.4 (2 C), 29.3, 29.1 (2 C), 28.6, 28.1, 22.6 (2 C), 14.1 (2 C) ($sp^3$ C); IR (ATR): 3325, 2923, 2854, 1652, 1386, 1094, 947 $cm^{-1}$; MS (EI): m/z (%) 527.2 ($M^+$, 70), 229.1 (100); HRMS calculated for $C_{26}H_{46}N_3I$, 527.2737; found 527.2753, Δ = 3.0 ppm.

## 8.2.5. 1-(2,5-Dioctyl-4-trimethylsilylethynylphenyl)-3,3-diethyl-triazene

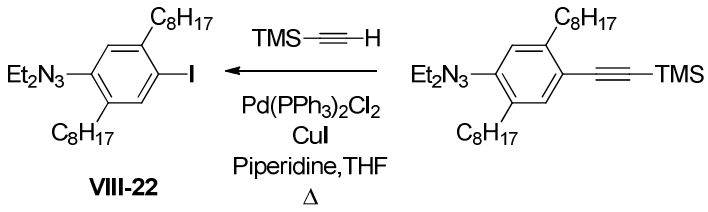


A solution of 1-(2,5-dioctyl-4-iodophenyl)-3,3-diethyl-triazene (2.0 g, 3.8 mmol), $Pd(PPh_3)_2Cl_2$ (133 mg, 190 µmol), $PPh_3$ (50 mg, 0.19 mmol), CuI (36 mg, 0.19 mmol) and TMS-acetylene (750 g, 7.60 mmol) in a 1:1 v/v mixture of THF and triethylamine (30 mL) was stirred for 24 h under Ar. $CH_2Cl_2$ (50 mL) was added and the solution was washed with sat. $NH_4Cl$ (100 mL) and water (100 mL). The organic layer was dried over $MgSO_4$ and the solvent was removed under reduced pressure. The crude residue was subjected to column chromatography (2% ethyl acetate / 98% hexanes) on basic alumina to afford the title compound as a yellow oil (1.8 g, 96%). $^1$H NMR (300 MHz, $CDCl_3$): δ 7.25 (s, 1H, Ar-H), 7.17 (s, 1H, Ar-H), 3.75 (q, *J* = 6.0 Hz, 4H, N-$CH_2$), 2.64-2.76 (m, 4H, Ar-$CH_2$), 1.55-1.66 (m, 4H, $CH_2$), 1.19-1.41 (m, 26H, $CH_2$ and $CH_3$), 0.82-0.93 (m, 6H, $CH_3$), 0.24 (s, 9H, Si-$CH_3$).

## 8.2.6. 1-(2,5-Dioctyl-4-ethynylphenyl)-3,3-diethyl-triazene

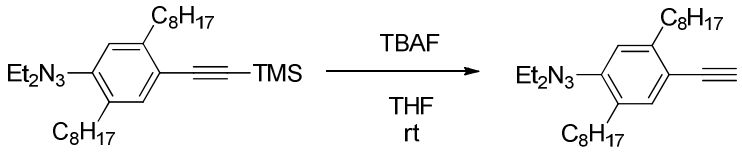


**VIII-23**

Tetrabutylammonium fluoride (1.3 g, 5.2 mmol, 1.0 M in THF) was added dropwise to a solution of 1-(2,5-dioctyl-4-trimethylsilylethynylphenyl)-3,3-diethyl-triazene (2.0 g, 4.0 mmol) in anhydrous THF (30 mL) at room temperature and the reaction mixture was stirred for 12 h. The solvent was removed under reduced pressure and the residue was flushed through a short plug of neutral alumina with hexanes (100 mL) to afford the title compound as a yellow oil (1.7 g, 98%). $^1$H NMR (300 MHz, $CDCl_3$): δ 7.22 (s, 1H, Ar-H), 7.18 (s, 1H, Ar-H), 3.75 (q, *J* = 6.0 Hz, 4H, N-$CH_2$), 3.25(s, 3H, alkyne-$CH_3$), 2.64-2.76 (m, 4H, Ar-$CH_2$), 1.55-1.66 (m, 4H, $CH_2$), 1.19-1.41 (m, 26H, $CH_2$ and $CH_3$), 0.82-0.93 (m, 6H, $CH_3$), 0.24 (s, 9H, Si-$CH_3$).

## 8.2.7. Ditriazene-PE-trimer

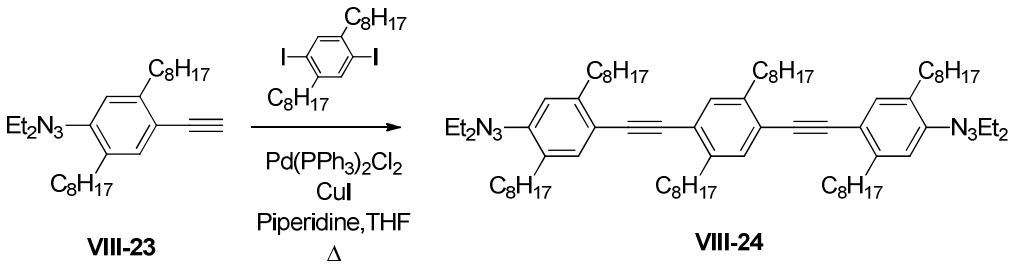


A solution of 1,4-diiodo-2,5-dioctylbenzene (830 mg, 1.50 mmol), $Pd(PPh_3)_2Cl_2$ (52 mg, 75 µmol), $PPh_3$ (39.0 mg, 150 µmol), CuI (14 mg, 75 µmol) and 1-(2,5-dioctyl-4-ethynylphenyl)-3,3-diethyl-triazene (1.6 g, 3.8 mmol) in a 1:1 v/v mixture of THF and triethylamine (40 mL) was stirred at 50 °C for 48 h under Ar. $CH_2Cl_2$ (50 mL) was added and the solution was washed with sat. $NH_4Cl$ (100 mL) and water (100 mL). The organic layer was dried over $MgSO_4$ and the solvent was removed under reduced pressure. The crude residue was subjected to a column chromatography (hexanes) in basic alumina followed by recrystallization from hexanes to afford the title compound as orange solids (400 mg, 24%). m.p. = 62-64 °C. $^1$H NMR (300 MHz, $CDCl_3$): δ 7.33 (s, 2H, Ar-H), 7.32 (s, 1H, Ar-H), 7.23 (s, 1H, Ar-H), 3.77 (q, *J* = 7.2 Hz, 8H, N-$CH_2$), 2.70-2.88 (m, 12H, Ar-$CH_2$), 1.10-1.80 (br m, 84H, $CH_3$ and $CH_2$), 0.80-0.89 (m, 18H, $CH_3$). $^{13}$C NMR (75 MHz, $CDCl_3$): δ 152.8, 148.7, 142.8, 141.6, 134.8, 133.7, 132.2, 122.8, 119.1, 116.4, 105.0 (Ar-C), 93.7, 91.4 (≡C), 34.7, 34.2, 31.9, 31.4, 31.3, 31.0, 30.7, 29.7, 29.6, 29.5 (3C), 29.4, 29.3 (3C), 22.7, 14.1 (6C) ($sp^3$ C). IR (ATR): 2953, 2923, 2854, 1466, 1376, 1233, 1100, 891 cm$^{-1}$; MS (MALDI): m/z (%) 1149.1 ($M^+$, 85); HRMS calculated for $C_{78}H_{128}N_6$, 1149.0200; found 1149.0310, Δ = 9.6 ppm.

## 8.2.8. Diiodo-PE-trimer

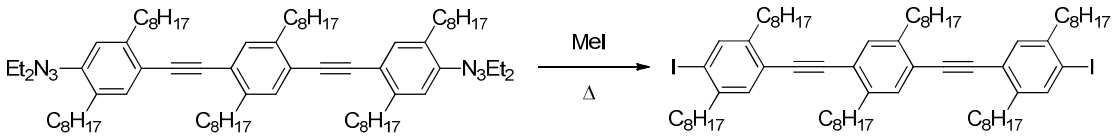


VIII-24 VIII-25

A solution of ditriazene-PE-trimer (350 mg, 305 µmol) and MeI (2 mL) was stirred at 120 °C for 12 h in a sealed pressure tube. The reaction mixture was cooled down to room temperature and flushed through a short plug of silica gel with hexanes to afford the title compound as a yellow solid (355 mg, 97%). m.p. = 60-62 °C. $^{1}$H NMR (300 MHz, $CDCl_3$): δ 7.67 (s, 2H, Ar-H), 7.34 (s, 2H, Ar-H), 7.30 (s, 2H, Ar-H), 2.58-2.88 (m, 12H, Ar-$CH_2$), 1.10-1.80 (br m, 72H, $CH_2$), 0.80-0.89 (m, 18H, $CH_3$). $^{13}$C NMR (75 MHz, $CDCl_3$): δ 143.7, 142.7, 141.9, 139.4, 132.3, 122.9, 122.7 (Ar-C), 100.5, 92.3 (≡C), 40.2, 34.2, 33.8, 31.8, 30.7, 30.6, 30.2, 29.6, 29.5 (3C), 29.4, 29.3 (3C), 29.2, 22.6, 14.1 (6 C) ($sp^3$ C); IR (ATR): 2927, 2847, 1492, 1466, 1376, 1120, 884, 715 $cm^{-1}$; MS (MALDI): m/z (%) 1202.6 ($M^+$, 65); HRMS calculated for $C_{70}H_{108}I_2$, 1202.6541; found 1202.6511, Δ = 2.5 ppm.

## 8.2.9. Model trimer, $Me_4PE_3$

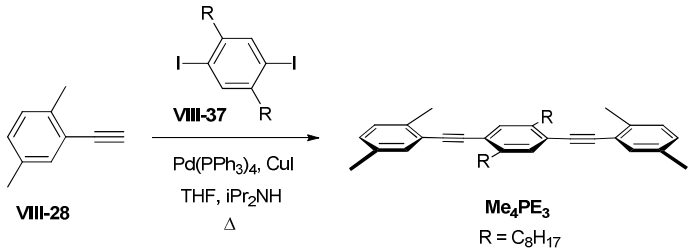


A solution of 1,4-diiodo-2,5-dioctylbenzene (200 mg, 360 µmol), (2,5-dimethylphenyl)acetylene (190 mg, 1.44 mmol), $Pd(PPh_3)_2Cl_2$ (25 mg, 36 µmol), $PPh_3$ (9.0 mg, 36 µmol) and CuI (7.0 mg, 36 µmol) in a mixture of THF (3 mL) and diisopropylamine (4 mL) was heated at 70 °C for 2 d. The reaction mixture was cooled to room temperature and poured into MeOH (200 mL). The precipitated solid was removed by filtration and triturated with EtOH to afford **$Me_4PE_3$** as a pale yellow solid (170 mg, 85% yield). m.p. 58-60 °C. $^1$H NMR (300 MHz, $CDCl_3$) δ 7.35 (s, 2H, Ar-H, central ring), 7.33 (d, 2H, *J* = 1.4 Hz, 2H, Ar–H), 7.12 (d, *J* = 7.5 Hz, 2H, Ar–H), 7.04 (dd, *J* = 7.5, 1.4 Hz, 2H, Ar–H), 2.81 (t, 4H, *J* = 7.4 Hz, Ar-$CH_2$), 2.48 (s, 6H, Ar–$CH_3$), 2.31 (s, 6H, Ar–$CH_3$), 1.69 (pentet, 4H, *J* = 7.4 Hz, $CH_2$), 1.18-1.47 (m, 24H, $CH_2$), 0.85 (t, *J* = 7.6 Hz, 6H, $CH_3$). $^{13}$C NMR (75 MHz, $CDCl_3$): δ 141.9, 135.1, 132.3 (2 C), 129.4, 129.1, 123.0, 122.7 (Ar-C), 92.9, 91.9 (C≡C), 34.3, 31.8, 30.7, 29.6, 29.5, 29.3, 22.7, 20.7, 20.4, 14.1 ($sp^3$ C). IR (ATR): 2960, 2923, 2850, 1495, 1263, 1087, 1014, 888, 808 cm$^{-1}$; EI MS: *m*/*z* (%) 558.3 ($M^+$, 100); HRMS calculated for $C_{42}H_{54}$, 558.4226; found 558.4221, Δ = 0.9 ppm.

## 8.2.10. Model pentamer, $Me_4PE_5$

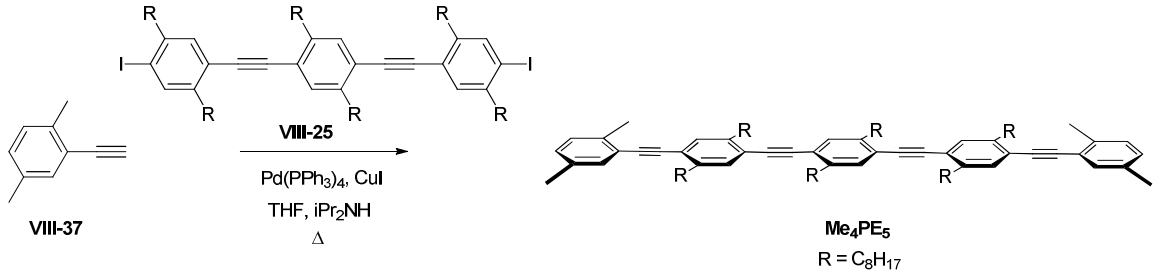


A solution of diodide **VIII-25** (50 mg, 40 µmol), (2,5-dimethylphenyl)acetylene (21 mg, 0.16 mmol), $Pd(PPh_3)_2Cl_2$ (3 mg, 4 µmol), PPh3 (2 mg, 4 µmol), and CuI (1 mg, 4 µmol) in a mixture of THF (2 mL) and diisopropylamine (3 mL) was heated at 70 °C for 2 d. The reaction mixture was cooled to room temperature and poured into MeOH (200 mL). The precipitated solid was removed by filtration and triturated with EtOH to afford **$Me_4PE_5$** as a pale yellow solid (45 mg, 90% yield). m.p. 84-86 °C. $^1$H NMR (300 MHz, $CDCl_3$) δ 7.38 (s, 6H, Ar-H), 7.34 (d, 2H, *J* = 1.4 Hz, 2H, Ar–H), 7.14 (d, *J* = 7.6 Hz, 2H, Ar–H), 7.06 (dd, *J* = 7.6, 1.4 Hz, 2H, Ar–H), 2.84 (t, 12H, *J* = 7.8 Hz, Ar-$CH_2$), 2.50 (s, 6H, Ar–$CH_3$), 2.33 (s, 6H, Ar–$CH_3$), 1.61-1.79 (m, 12H, $CH_2$), 1.15-1.46 (m, 60H, $CH_2$), 0.88 (m, 18H, $CH_3$). $^{13}$C NMR (75 MHz, $CDCl_3$): δ 141.9, 141.8, 136.8, 135.1, 132.4, 129.4, 129.2, 123.0, 122.9, 122.8, 122.6 (Ar), 93.2, 93.1, 92.9, 91.9 (C≡C), 34.3, 34.2, 32.0, 31.9, 30.7, 29.7, 29.6, 29.5, 29.4, 29.2, 22.7, 22.6, 20.8, 20.4, 14.1 ($sp^3$ C). IR (ATR): 2923, 2847, 1608, 1499, 1452, 1260, 1094, 1017, 891, 788 cm$^{-1}$; MALDI MS: *m*/*z* (%) 1207.3 ($M^+$, 100); HRMS calculated for $C_{90}H_{126}$, 1206.9860; found 1206.9862, Δ = 0.2 ppm.

## 8.2.11. Pseudo-geminal phenylene ethynylene polymer, *pg*-poly($PE_3$)

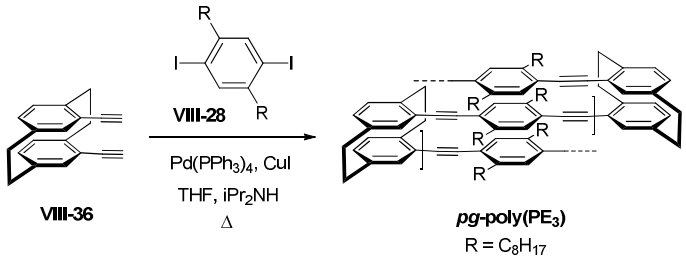


A solution of 4,15-diethynyl[2.2]paracyclophane **VIII-36** (64 mg, 0.25 mmol), 1,4-diiodo-2,5-dioctylbenzene **VIII-28** (140 mg, 0.250 mmol), $Pd(PPh_3)_4$ (15 mg, 13 μmol), and CuI (3.0 mg, 13 μmol) in a mixture of toluene (3 mL) and diisopropylamine (3 mL) was heated at 70 °C for 2 d. The mixture was poured into methanol (200 mL) and the precipitated solid was removed by filtration. The solid was dissolved in a minimum volume of $CH_2Cl_2$ and the solution was reprecipitated into acetone (100 mL) to afford ***pg*-poly($PE_3$)** as a orange solid (80 mg, 57% yield). $^1H$ NMR: see Results and Discussion. IR (ATR): 2920, 2857, 1588, 1492, 1250, 1094, 1024, 888, 811 $cm^{-1}$. GPC (THF, UV–vis detector, PS standards): 3.5 kDa (DP = 7 and PDI = 1.4).

## 8.2.12. Pseudo-geminal phenylene ethynylene polymer, *pg*-poly($PE_5$)

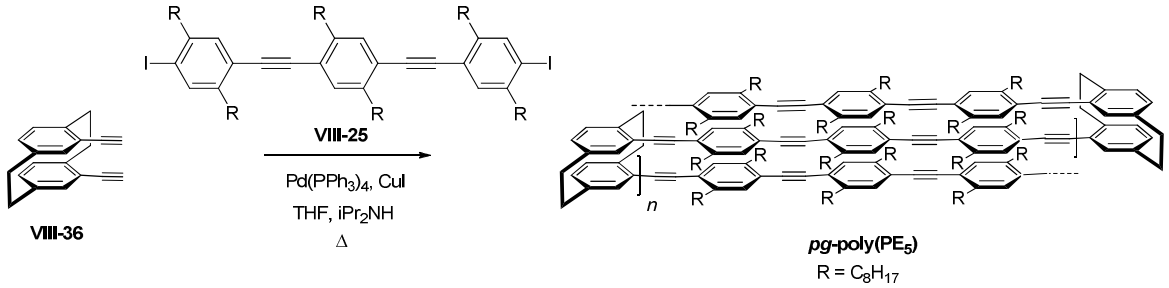


A solution of 4,15-diethynyl[2.2]paracyclophane **VIII-36** (64 mg, 0.25 mmol), diiodide **VIII-25** (300 mg, 250 μmol), $Pd(PPh_3)_4$ (15 mg, 13 μmol), and CuI (3.0 mg, 13 μmol) in a mixture of toluene (3 mL) and diisopropylamine (3 mL) was heated at 70 °C for 2 d. The mixture was poured into methanol (200 mL) and the precipitated solid was removed by filtration. The solid was dissolved in a minimum volume of $CH_2Cl_2$ and the solution was reprecipitated into acetone (100 mL) to afford ***pg*-poly($PE_5$)** as a orange solid (125 mg, 41% yield). $^1$H NMR: see Results and Discussion. IR (ATR): 2920, 2847, 1588, 1495, 1452, 1260, 1097, 1017, 884, 801 $cm^{-1}$. GPC (THF, UV–vis detector, PS standards): 6.1 kDa (DP = 5 and PDI = 1.7).

## 8.2.13. 1,4-Diiodo-2,5-dioctylbenzene

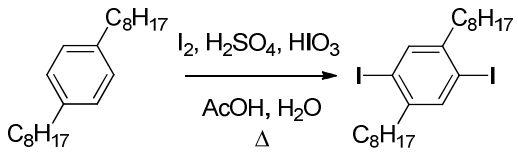


**VIII-28**

A solution of 1,4-dioctylbenzene (23 g, 76 mmol), iodine (19 g, 76 mmol), $HIO_3$ (6.7 g, 38 mmol), $H_2SO_4$ (10 mL), water (2 mL) in a 4:1 v/v mixture of acetic acid and $CCl_4$ (100 mL) was heated at reflux for 24 h. The reaction mixture was cooled down to room temperature and poured on crushed ice (300 g). $CHCl_3$ (100 mL) was added and the organic layer was separated and washed with NaOH (10%) until a yellow organic solution was obtained. The organic layer was dried over $MgSO_4$, the solvent was removed under reduced pressure, and the residue was recrystallized from MeOH to afford the title compound as a white powder (35 g, 83%). MP = 50-51 °C. $^1$H NMR (300 MHz, $CDCl_3$): δ 7.61 (s, 2H, Ar-H), 2.60 (t, *J* = 7.5 Hz, 4H, Ar-$CH_2$), 1.48-1.63 (br m, 4H, $CH_2$), 1.21-1.45 (br m, 12H, $CH_2$), 0.91 (t, *J* = 7.5 Hz, 6H, $CH_3$). $^{13}$C NMR (75 MHz, $CDCl_3$): δ 144.8, 139.2, 100.3 (Ar-C), 39.8, 31.8, 30.2, 29.3 (3C), 22.7, 14.1 ($sp^3$ C). IR (ATR): 2953, 2917, 2847, 1466, 1356, 1050, 881 $cm^{-1}$; MS (EI): m/z (%) 554.1 ($M^+$, 100); HRMS calculated for $C_{22}H_{36}I_2$, 554.00907; found 554.0897, Δ = 1.8 ppm.

**8.2.14. 2,5-Dioctyl-4-iodobenzaldehyde**

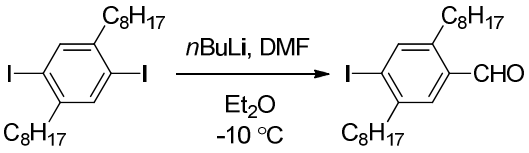


**VIII-28** **VIII-29**

*n*BuLi (11.3 mL of a 1.6M solution in hexane, 0.018 mol) was added dropwise to a solution of 1,4-diiodo-2,5-dioctylbenzene (10.0 g, 18.0 mmol) in anhydrous diethyl ether (200 mL) at -10 °C. The reaction mixture was stirred at this temperature for 2 h. DMF (2.1 mL, 27 mmol) was added and the mixture was stirred at room temperature for 24 h. Water (100 mL) was added, and the organic layer was separated and dried over $MgSO_4$. The solvent was removed under reduced pressure and the residue was subjected to column chromatography (5% ethyl acetate / 95% hexanes) to afford the title compound as a white powder (6.0 g, 73%). $^1$H NMR (300 MHz, $CDCl_3$): δ 10.2 (s, 1H, aldehyde), 7.75 (s, 1H, Ar-H), 7.58 (s, 1H, Ar-H), 2.89 (t, *J* = 7.5 Hz, 2H, Ar-$CH_2$), 2.71 (t, *J* = 7.5 Hz, 2H, Ar-$CH_2$), 1.49-1.69 (br m, 4H, $CH_2$), 1.17-1.46 (br m, 12H, $CH_2$), 0.94 (m, 6H, $CH_3$). MS (EI): m/z (%) 456.2 ($M^+$, 100); HRMS calculated for $C_{23}H_{37}IO$, 456.1889; found 456.1884, Δ = 1.1 ppm. The sample contained a small amount of deiodinated-aldehyde and was used without further purification.

**8.2.15. (2,5-Dioctyl-4-iodophenyl)methanol**

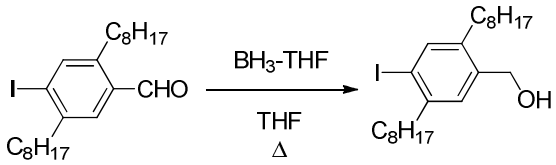


**VIII-29** **VIII-30**

$BH_3$-THF (16.5 mL, 16.5 mmol, 1.0 M in THF) was added dropwise to a solution of impure 2,5-dioctyl-4-iodobenzaldehyde (5.0 g, 11 mmol) in anhydrous THF (100 mL) at room temperature. The reaction mixture was heated at reflux for 6 h. After cooling to room temperature, the solvent was removed under reduced pressure and the residue was flushed through the a short plug of silica gel with 50% ethyl acetate / 50% hexanes, and the solvent was removed to afford the title compound as a white powder (4.7 g, 94%). $^1$H NMR (300 MHz, $CDCl_3$): δ 7.61 (s, 1H, Ar-H), 7.19 (s, 1H, Ar-H), 4.64 (s, 2H, $OCH_2$), 2.65 (t, *J* = 7.5 Hz, 2H, Ar-$CH_2$), 2.54 (t, *J* = 7.5 Hz, 2H, Ar-$CH_2$), 1.46-1.63 (br m, 4H, $CH_2$), 1.17-1.46 (br m, 12H, $CH_2$), 0.87 (m, 6H, $CH_3$). MS (EI): m/z (%) 458.2 ($M^+$, 100); HRMS calculated for $C_{23}H_{39}IO$, 458.2046; found 458.2058, Δ = 2.6 ppm. The sample contained a small amount of deiodinated-alcohol and was used without further purification.

**8.2.16. 1-(Bromomethyl)-2,5-dioctyl-4-iodobenzene**

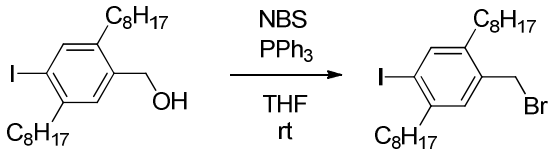


**VIII-30** **VIII-31**

NBS (2.0 g, 11 mmol) was added in portions to a solution of (2,5-dioctyl-4-iodophenyl)methanol (4.2 g, 9.2 mmol), and $PPh_3$ (2.9 g, 11 mmol) in anhydrous THF (100 mL) at 0 °C. The reaction mixture was stirred at room temperature for 1 h. Ethyl acetate (50 mL) was added and the organic layer was washed with water (100 mL) and brine (100 mL). The organic layer was separated and dried over $MgSO_4$. The residue was flushed through a short plug of silica gel with 1% ethyl acetate / 99% hexanes. The solvent was removed and the residue was recrystallized from a 9:1 v/v mixture of ethanol and hexanes to afford the title compound as a white powder (4.5 g, 96%). m.p. = 40-42 °C. $^1$H NMR (300 MHz, $CDCl_3$): δ 7.62 (s, 1H, Ar-H), 7.12 (s, 1H, Ar-H), 4.44 (s, 2H, $BrCH_2$), 2.48-2.71 (m, 4H, Ar-$CH_2$), 1.49-1.67 (br m, 4H, $CH_2$), 1.19-1.45 (br m, 12H, $CH_2$), 0.88 (m, 6H, $CH_3$). $^{13}$C NMR (75 MHz, $CDCl_3$): δ 143.4, 141.1, 140.3, 135.5, 130.8, 101.3 (Ar-C), 40.2, 31.8, 31.4, 31.1, 30.8, 30.1, 29.6, 29.4 (3C), 29.2 (2C), 22.7 (2C), 14.1 (2C) ($sp^3$ C). IR (ATR): 2923, 2854, 1466, 1203, 967, 891 $cm^{-1}$; MS (EI): m/z (%) 520.1 ($M^+$, 100); HRMS calculated for $C_{23}H_{38}IBr$, 520.1202; found 520.1233, Δ = 6.0 ppm.

**8.2.17. Diethyl (2,5-dioctyl-4-iodophenyl)methylphophonate**

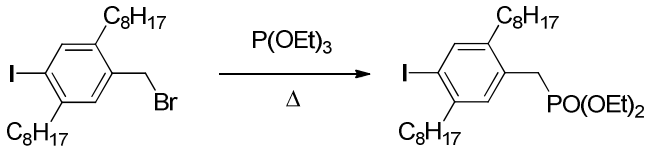


**VIII-31** **VIII-32**

A solution of 1-(bromomethyl)-2,5-dioctyl-4-iodobenzene (4.0 g, 8.0 mmol) and $P(OEt)_3$ (5 mL, mmol) was heated in a sealed pressure tube at 140 °C for 12 h. The reaction mixture was cooled to room temperature and subjected to a column chromatography (10% ethyl acetate / 90% hexanes) to afford the title compound as a yellow oil (4.3 g, 97%). $^1$H NMR (300 MHz, $CDCl_3$): δ 7.59 (s, 1H, Ar-H), 7.11 (d, $^4J_{P\text{-}H}$ = 3.0 Hz, 1H, Ar-H), 3.92-4.06 (m, 4H, O-$CH_2$), 3.08 (d, $^2J_{P\text{-}H}$ = 21.0 Hz, 2H, P-$CH_2$), 2.54-2.68 (m, 4H, Ar-$CH_2$), 1.45-1.59 (m, 4H, $CH_2$), 1.22-1.41 (m, 16H, $CH_3$ and $CH_2$), 0.88 (t, $J$ = 6.0 Hz, 6H, $CH_3$). $^{13}$C NMR (75 MHz, $CDCl_3$): δ 143.9, 142.4, 139.2, 130.9, 130.0, 99.0 (Ar-C), 62.2 (2C), 41.0, 31.6, 31.2, 31.0, 30.6, 30.3, 29.4, 29.2 (3C), 29.0 (2C), 22.5 (2C), 14.8 (2C) ($sp^3$ C). IR (ATR): 2958, 1472, 1211, 1028, 934 cm$^{-1}$; MS (EI): m/z (%) 578.2 ($M^+$, 100); HRMS calculated for $C_{27}H_{48}IPO_3$, 578.2386; found 578.2385, Δ = 0.2 ppm.

**8.2.18. (*E*)-1,2-bis(4-iodo-2,5-dioctylphenyl)ethylene**

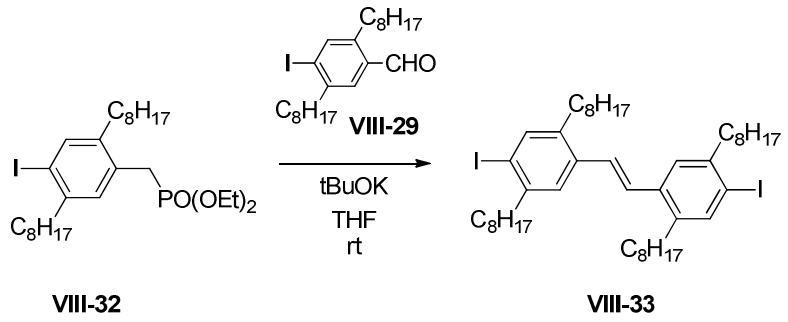


**VIII-32** **VIII-33**

A reaction mixture of diethyl (2,5-dioctyl-4-iodophenyl)methylphophonate (800 mg, 1.75 mmol), 2,5-dioctyl-4-iodobenzaldehyde (1.2 g, 2.1 mmol) and potassium tert-butoxide (510 g, 4.55 mmol) in anhydrous THF (60 mL) was stirred at room temperature for 36 h. Water (50 mL) was added and stirred for 30 min. $CHCl_3$ (50 mL) was added and the solution was washed with water (100 mL) and brine (100 mL). The organic layer was dried over $MgSO_4$ and the solvent was removed under reduced pressure. The residue was subjected to column chromatography (hexanes) to afford the title compound as yellow solids (1.2 g, 80%). m.p. = 58-60 °C. $^1$H NMR (300 MHz, $CDCl_3$): δ 7.62 (s, 1H, Ar-H), 7.32 (s, 1H, Ar-H), 7.08 (s, 1H, vinyl-H), 2.69 (t, *J* = 6.0 Hz, 4H, Ar-$CH_2$), 2.62 (t, *J* = 6.0 Hz, 4H, Ar-$CH_2$), 1.46-1.67 (m, 8H, $CH_2$), 1.15-1.44 (m, 40H, $CH_2$), 0.82-0.94 (m, 12H, $CH_3$). $^{13}$C NMR (75 MHz, $CDCl_3$): δ 143.0, 140.2, 140.1, 136.3, 127.6, 126.4, 99.6 (Ar-C and vinyl-C), 40.4, 32.6 (2 C), 31.8, 31.1, 30.4, 29.5, 29.4 (3C), 29.3, 29.2, 22.7, 22.6, 14.2, 14.1 ($sp^3$ C); IR (ATR): 2917, 2854, 1469, 1373, 1140, 891, 725 $cm^{-1}$; MS (EI): m/z (%) 880.0 ($M^+$, 100); HRMS calculated for $C_{46}H_{74}I_2$, 880.3880; found 880.3893, Δ = 1.5 ppm.

## 8.2.19. Model trimer, $Me_4PV_3$

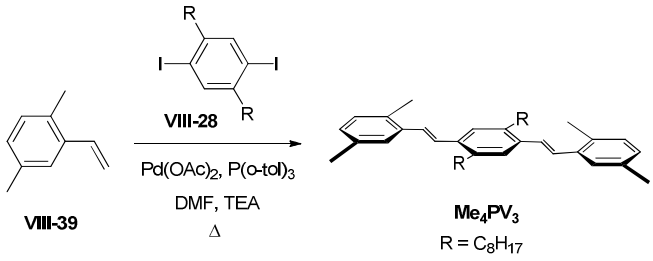


A solution of 1,4-diiodo-2,5-dioctylbenzene (200 mg, 0.36 μmol), (2,5-dimethylphenyl)vinylene (190 mg, 1.45 mmol), $Pd(OAc)_2$ (8.0 mg, 36 μmol) and $P(o\text{-}tol)_3$ (22 mg, 72 μmol) in a mixture of DMF (2 mL), toluene (1 mL) and triethylamine (1 mL) was heated at 70 °C for 2 d. The mixture was poured into methanol (200 mL) and the precipitated solid was removed by filtration. The residue was purified by recrystallization from ethanol to afford **$Me_4PV_3$** as a bright yellow solid (150 mg, 75%). m.p. = 100-102 °C. $^1$H NMR (300 MHz, $CDCl_3$) δ 7.43 (br s, 2H, Ar–H), 7.38 (d, *J* = 1.4 Hz, 2H, Ar-H), 7.20 (s, 4H, vinylic), 7.09 (d, *J* = 7.6 Hz, 2H, Ar–H), 7.01 (dd, *J* = 7.6, 1.4 Hz, 2H, Ar–H), 2.75 (t, *J* = 6 Hz, 4H, Ar-$CH_2$), 2.40 (s, 6H, Ar–$CH_3$), 2.37 (s, 6H, Ar–$CH_3$), 1.64 (pentet, *J* = 6 Hz, 4H, $CH_2$), 1.15-1.45 (m, 20H, $CH_2$), 0.81-0.90 (m, 6H, $CH_3$). $^{13}$C NMR (75 MHz, $CDCl_3$): δ 138.5, 136.7, 135.5, 135.4, 132.8, 130.3, 128.2, 127.6, 127.4, 126.9, 126.1 (Ar-C and vinyl-C), 33.3, 31.8, 31.4, 29.7, 29.5, 29.3, 22.6, 21.1, 19.6, 14.1 ($sp^3$ C). IR (ATR): 2920, 2847, 1456, 1273, 1087, 1024, 964, 791 cm$^{-1}$; MS (EI), *m*/*z* (%) 562.4 ($M^+$, 100); HRMS calculated for $C_{50}H_{74}$, 562.4539; found 562.4545, Δ = 1.1 ppm.

## 8.2.20. Model tetramer, $Me_4PV_4$

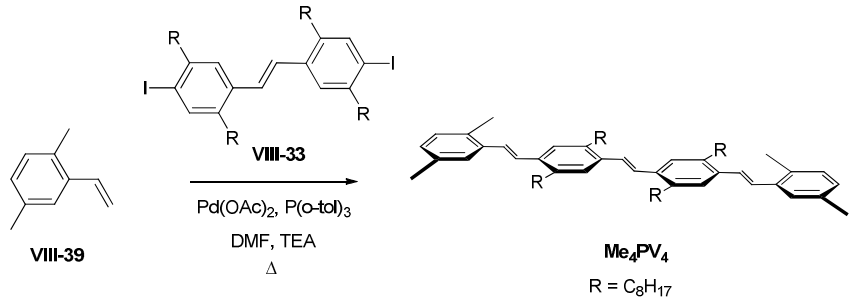


A solution of 1,4-diiodo-2,5-dioctylbenzene (150 mg, 170 μmol), (2,5-dimethylphenyl)vinylene (90 mg, 0.68 mmol), $Pd(OAc)_2$ (4.0 mg, 17 μmol) and $P(o\text{-tol})_3$ (10 mg, 34 μmol) in a mixture of DMF (2 mL), toluene (1 mL) and triethylamine (1 mL) was heated at 70 °C for 2 d. The mixture was poured into methanol (200 mL) and the precipitated solid was removed by filtration. The residue was purified by recrystallization from ethanol to afford **$Me_4PV_4$** as a bright yellow solid (125 mg, 83%). m.p. = 118-120 °C. $^1$H NMR (300 MHz, $CDCl_3$) δ 7.37-7.45 (br m, 6H, Ar–H and vinylic), 7.19-7.25 (m, 2H, Ar-H and vinylic), 7.09 (d, *J* = 7.5 Hz, 2H, Ar-H), 7.01 (dd, 2H, *J* = 7.5, 1.4 Hz, 2H, Ar–H), 2.76 (t, *J* = 7.8 Hz, 8H, Ar-$CH_2$), 2.41 (s, 6H, Ar–$CH_3$), 2.37 (s, 6H, Ar–$CH_3$), 1.58-1.72 (m, 8H, $CH_2$), 1.12-1.51 (m, 40H, $CH_2$), 0.81-0.89 (m, 12H, $CH_3$). $^{13}$C NMR (75 MHz, $CDCl_3$): δ 138.5, 136.8, 135.7, 135.4, 135.2, 132.7, 130.2, 128.1, 127.5, 127.3, 126.9 (2 C), 126.2 (Ar–C and vinylic), 33.3, 33.2, 31.8, 31.3, 31.2, 29.6 (2 C), 29.4 (2 C), 29.2 (2 C), 22.5, 21.0, 19.4 ($CH_2$), 14.0 ($CH_3$). IR (ATR, neat): 2923, 2847, 1499, 1256, 1094, 1024, 961, 795 cm$^{-1}$; MS (EI), *m*/*z* (%) 888.5 ($M^+$, 100); HRMS calculated for $C_{66}H_{96}$, 888.7512; found 888.7515, Δ = 0.3 ppm.

## 8.2.21. Pseudo-geminal phenylene vinylene polymer, *pg*-poly($PV_3$)

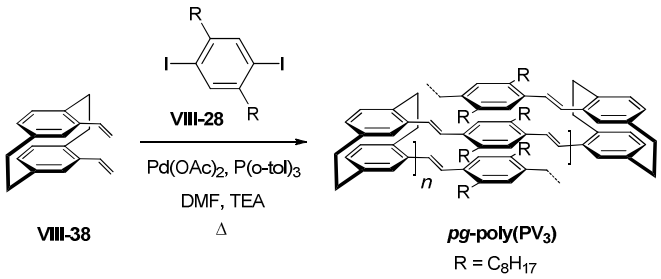


A solution of 4,15-diethenyl[2.2]paracyclophane (100 mg, 380 μmol), 1,4-diiodo-2,5-dioctylbenzene (210 mg, 380 μmol), $Pd(OAc)_2$ (9.0 mg, 38 μmol), and $P(o\text{-}tol)_3$ (23 mg, 76 μmol) in a mixture of DMF (3 mL), toluene (1.5 mL) and triethylamine (1.5 mL) was heated at 90 °C for 2 d. The mixture was poured into methanol (200 mL) and the precipitated solid was removed by filtration. The solid was dissolved in a minimum volume of $CH_2Cl_2$ and the solution was reprecipitated into acetone (100 mL) to afford ***pg*-poly($PV_3$)** as a yellow solid (45 mg, 46% yield). $^1H$ NMR: see Results and Discussion. IR (ATR): 2914, 2854, 1665, 1452, 1260, 1087, 798 $cm^{-1}$. GPC (THF, UV–vis detector, PS standards): 3.0 kDa (DP = 6 and PDI = 1.2).

## 8.2.22. Pseudo-geminal phenylene vinylene polymer, *pg*-poly($PV_3$)

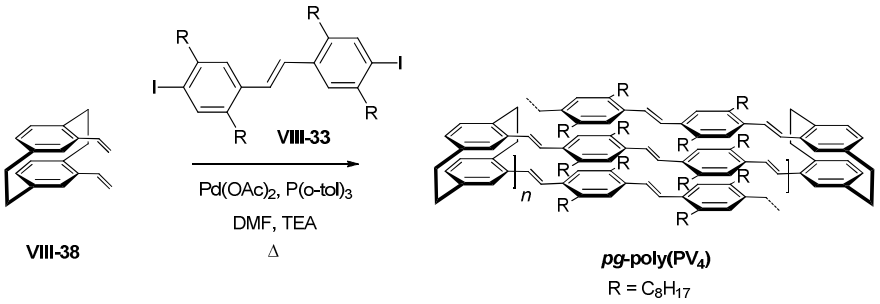


A solution of 4,15-diethenyl[2.2]paracyclophane (100 mg, 380 μmol), 1,4-diiodo-2,5-dioctylbenzene (335 mg, 380 μmol), $Pd(OAc)_2$ (9.0 mg, 38 μmol), and $P(o\text{-}tol)_3$ (23 mg, 76 μmol) in a mixture of DMF (3 mL), toluene (2 mL) and triethylamine (2 mL) was heated at 90 °C for 2 d. The mixture was poured into methanol (200 mL) and the precipitated solid was removed by filtration. The solid was dissolved in a minimum volume of $CH_2Cl_2$ and the solution was reprecipitated into acetone (100 mL) to afford ***pg*-poly($PV_4$)** as a yellow solid (56 mg, 59% yield). $^1H$ NMR: see Results and Discussion. IR (ATR): 2920, 2854, 1462, 1260, 1094, 1017, 732 $cm^{-1}$. GPC (THF, UV–vis detector, PS standards): 4.4 kDa (DP = 5 and PDI = 1.3).

## 8.3. Results and Discussion

### 8.3.1. Synthesis of Diiodo-PE Trimer

In our first attempted synthesis strategy to prepare alkoxy substituted PE trimer diiodide **VIII-8**, we decided to couple two equivalents of ethynyl-bromide **VIII-5** to diiodo-dialkoxybenzene **VIII-6** using a Sonogashira reaction. The synthetic route to obtain the key intermediate **VIII-5** from commercially available hydroquinone is described below, Figure 8.3. The starting material hydroquinone was alkylated to install the alkoxy chains in the benzene ring using a Williamson ether synthesis. The monobromination followed by iodination provided the monoiodo-monobromide, **VIII-3**.[2] Sonogashira coupling with propargyl alcohol selectively replaced the iodide.[3] The oxidative deprotection[4] gave the key intermediate acetylene, **VIII-5**. The ethynyl-monobromide **VIII-5** was coupled to diiodo-dialkoxybenene **VIII-6** to obtain the dibromo-PE-trimer, **VIII-7**. We wanted to have the diiodo analog **VIII-8** instead of **VIII-7** given the fact that iodo-arenes are more reactive compared to the corresponding bromo-counterpart in a Sonogashira reaction. Unfortunately, the *n*-butyllithium mediated bromine-iodine exchange did not provide a pure diiodo-PE-trimer, **VIII-8**.[4] The separation of diodide **VIII-8** from dibromide **VIII-1** and monoiodo-monobromo compound using any of the purification methods (column chromatography, recrystallization and trituration) was unsuccessful.

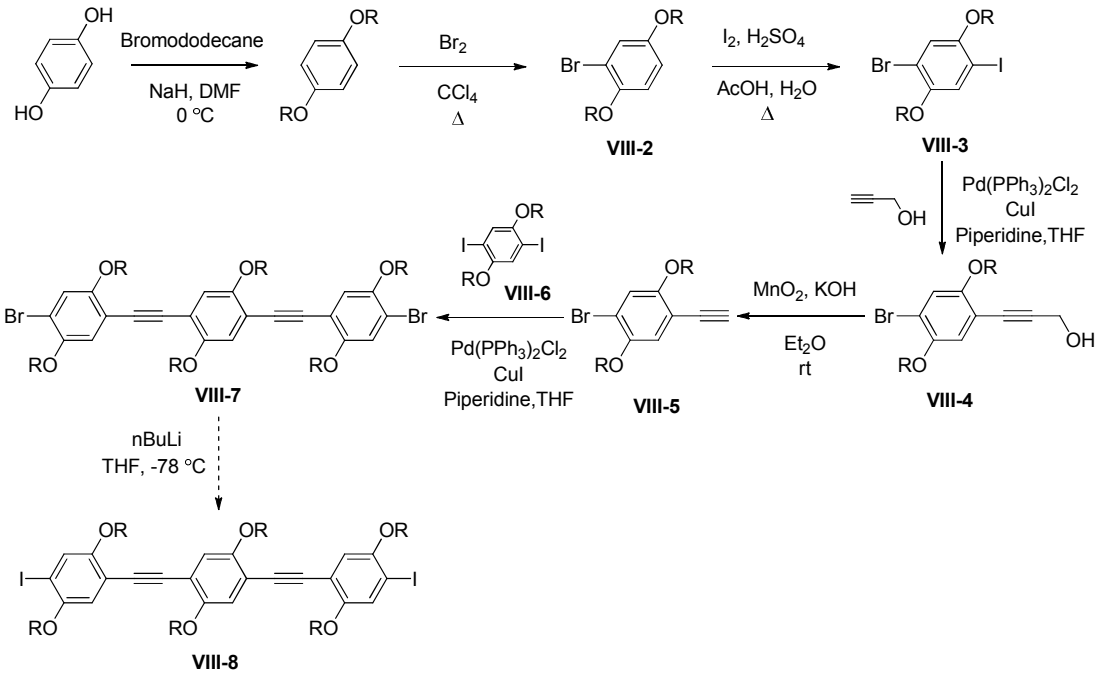


**Figure 8.3.** Attempted synthesis of alkoxy substituted diiodo-PE-trimer, **VIII-8** (OR = -$OC_9H_{19}$).

To avoid the bromine-iodine exchange, we decided to modify the synthetic route and explore the utility of triazene substituted arenes as precursors to iodo-terminated trimer, **VIII-8**, Figure 8.4.[5] The triazene-trimer, **VIII-14**, could be synthesized from a key intermediate monotriazene-ethynylbenzene, **VIII-13**. The nitration of bromobenzene **VIII-2** provided the mononitro-monobromide **VIII-9** in high yield. The reduction of the nitro group by treatment with tin metal and concentrated HCl at low temperature gave the corresponding amine **VIII-10** in a quantitative yield. However, higher temperatures in this reduction led to the acid promoted dealkylation of the side chains. The diazotization of **VIII-10** with $BF_3$-$Et_2O$ and *t*-BuONO followed by treatment with diethylamine yielded the monotriazene-monobromide, **VIII-11**. Unfortunately, a Sonogashira coupling of TMS-acetylene to monotriazene-monobromide did not provide a pure TMS-protected alkyne, **VIII-12**. This could be due to low reactivity of electron

rich bromoarenes substrate towards Sonogashira coupling. The desired product is inseparable from the unreacted starting material by any of the purification methods. This problem can be tackled in two ways: use of iodine instead of bromine, and replacement of strongly electron donating alkoxy groups with alkyl chains.

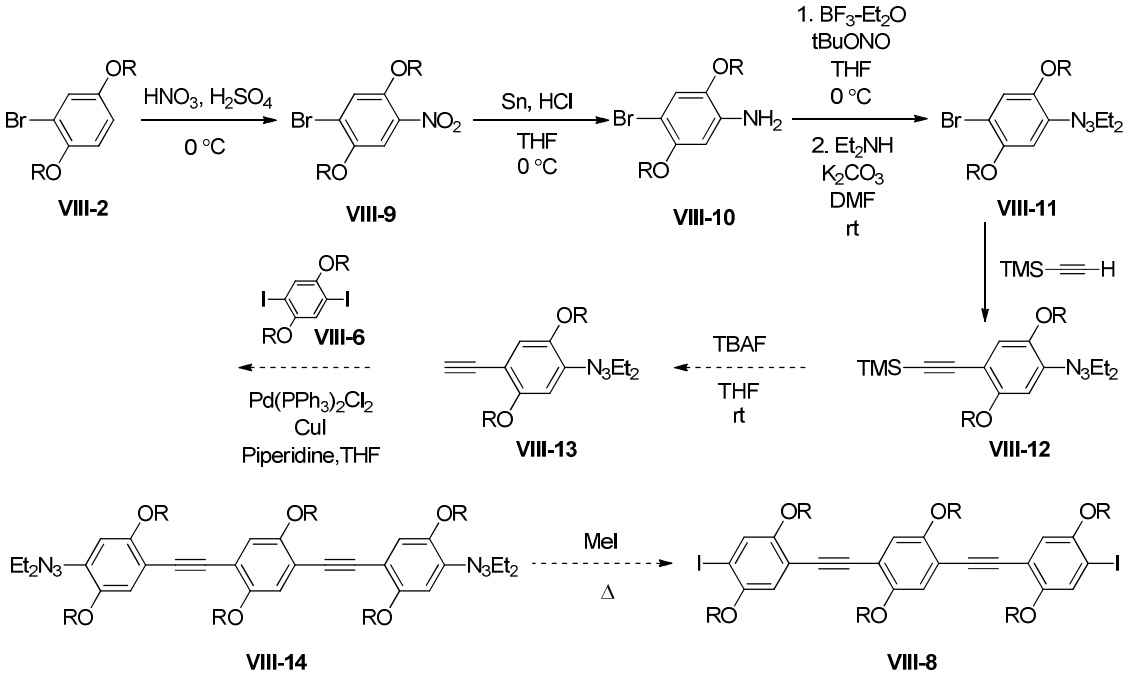


**Figure 8.4.** Attempted synthesis of alkoxy substituted diiodo-PE-trimer, **VIII-8** (OR = -$OC_9H_{19}$).

We chose to replace the bromine with iodine in this synthetic strategy, as iodo-arenes often undergo Sonogashira reactions in a quantitative yield, and iodine is tolerant to the diazotization chemistry according to the literature, Figure 8.5. However, the reduction of mononitro-monoiodide **VIII-16** to obtain the corresponding amine led to the deiodination of the substrate. So, the iodine is not favorable in this synthetic route.

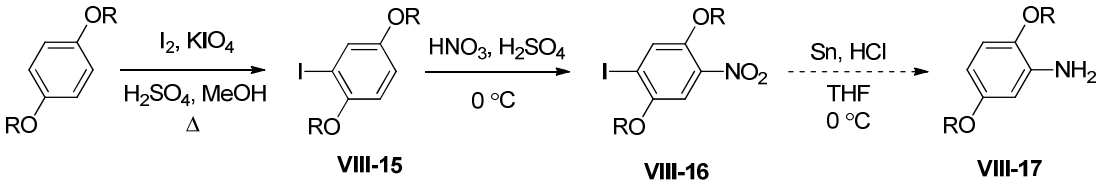


**Figure 8.5.** Attempted synthesis of alkoxy substituted monoamino-iodide which provided deiodinated analog, **VIII-17** (OR = $-OC_9H_{19}$).

We did not attempt the analogous synthesis with alkyl chains in place of alkoxy chains and focused on the preparation of the required monoamino-monoiodide analog having alkyl side chains using a different route, **VIII-21**, Figure 8.6.[1]

The synthesis of monoiodo-aniline **VIII-21** was carried according to a literature procedure, Figure 8.6.[1] The commercially available dibromide **VIII-18** was subjected to a Sonogashira coupling with 1-octyne to obtain the dialkynylated nitrobenzene **VIII-19**. A use of small amount of DMF facilitates the coupling of alkyne and reduces the reaction time to provide required product in high yield (~80%). The alkyne and nitro groups of **VIII-19** were reduced in a single step in the presence of a catalytic amount of Pd/C and hydrogen atmosphere to furnish the aniline, **VIII-20**. The reduction was performed under 3 atm of hydrogen using a hydrogenator to improve the yield of the reaction. The aniline **VIII-20** was iodinated by using benzyltrimethylammonium dichloroiodate ($BTMAICl_2$) to afford the monoiodo-aniline, **VIII-21**. The conversion of aniline **VIII-21** to the triazene-iodide **VIII-22** requires the formation of diazonium salt by treatment with $BF_3$-$Et_2O$ and *t*-BuONO followed by removal of the solvent. The salt was used in a subsequent step without purification. Careful handling is required due to explosive nature of diazonium salts. The salt was dissolved in a mixture of DMF and

diethylamine at low temperature and the mixture was stirred to obtain triazene-iodide, **VIII-22**. Neutral alumina was used to column chromatograph **VIII-22** because triazene groups are sensitive towards acidic silica gel. The triazene-iodide **VIII-22** was subjected to a Sonogashira coupling with TMS-acetylene followed by desilylation with tetrabutylammonium fluoride to furnish the required triazene-phenylacetylene, **VIII-23**. In the next step, two equivalents of **VIII-23** and diiodide **VIII-6** underwent a Sonogashira reaction to obtain the triazene-trimer, **VIII-24**. The attempts to purify **VIII-24** using column chromatography were unsuccessful. However, a pure triazene-trimer was obtained by recrystallization from hexanes. The nucleophilic substitution reaction in the presence of 1-iodomethane provided the required diiodo-PE-trimer, **VIII-25** in high yield. The use of pressure tube is required for this step and careful work-up is necessary due to the toxicity of iodomethane.

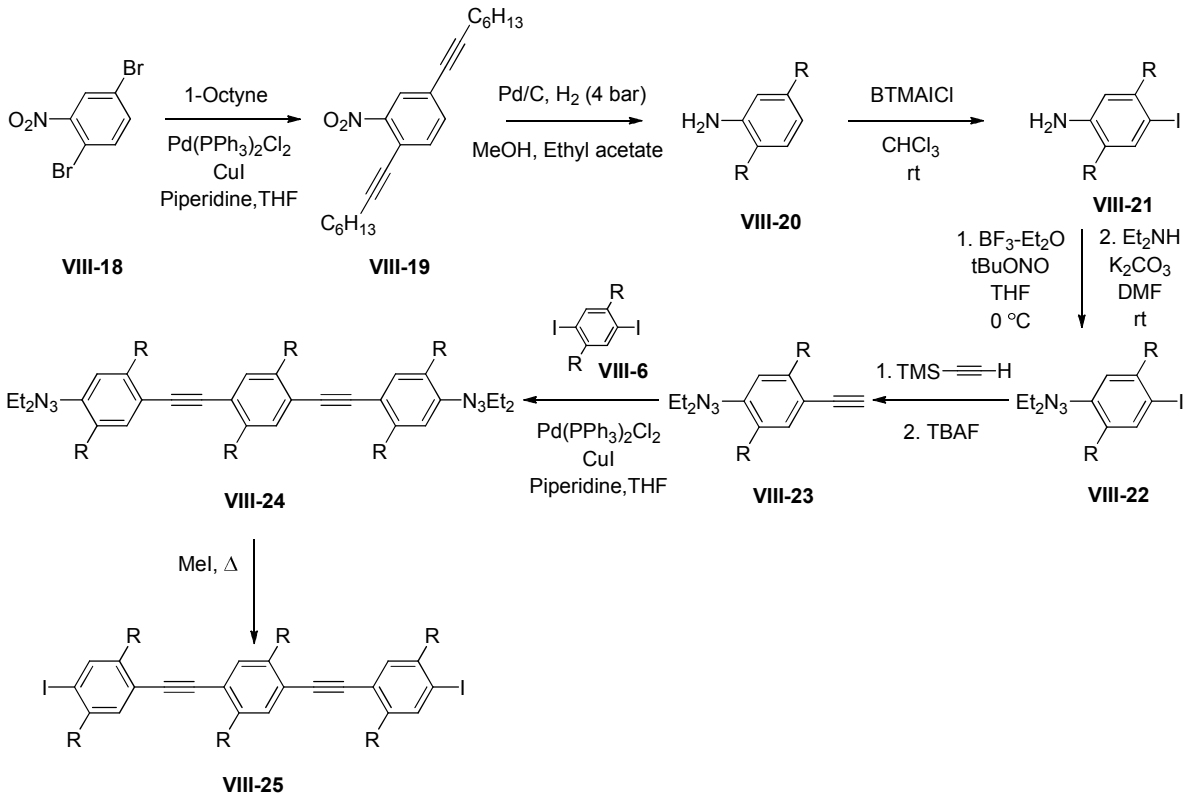


**Figure 8.6.** Successful synthesis of alkyl substituted diiodo-PE-trimer, **VIII-25** (R = *n*-$C_8H_{17}$).

## 8.3.2. Attempted Synthesis of alkyl-substituted Diiodo-PE Dimer

The diiodo-PE-dimer **VIII-27** could be synthesized as described below, Figure 8.7. The triazene-phenylacetylene **VIII-23** and triazene-iodide **VIII-22** were subjected to a Sonogashira reaction conditions to obtain the corresponding triazene-PE-dimer, **VIII-12**. Unfortunately, the required PE-dimer **VIII-12** is inseparable from the diyne byproduct of the Sonogashira coupling formed by oxidative homocoupling. Attempts to purify **VIII-26** by chromatography, recrystallization from hexanes, or trituration from methanol, were all unsuccessful. Unfortunately, synthesis of diiodo-PE-dimer **VIII-27** is not possible using the other synthetic routes for synthesizing the diiodo-PE-trimer.

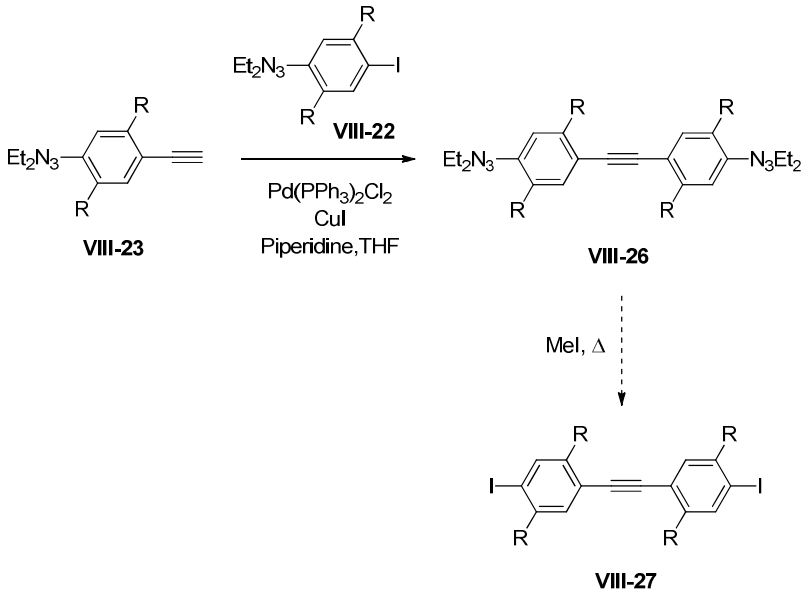


**Figure 8.7.** Attempted synthesis of diiodo-PE-dimer, **VIII-27** (R = *n*-$C_8H_{17}$).

### 8.3.3. Synthesis of Alkyl-substituted Diiodo-PV Dimer

The synthesis of diiodo-PV-dimer **VIII-33** was carried out according to the literature procedure, Figure 8.8.[6] The diiodide **VIII-28** was obtained in high yield (>95%) by treatment of 1,4-dioctyloxybenzene with iodine in the presence of $KIO_4$. Lithiation of the diiodide **VIII-28** with one equivalent of *n*-butyllithium followed by quenching with anhydrous DMF provided the monoaldehyde, **VIII-29**. The product isolated from column chromatography contained ca. 10% of the deiodinated-aldehyde, which is inseparable from the required iodo-aldehyde, **VIII-29**. Attempts to purify **VIII-29** by recrystallization were also unsuccessful. We decided to continue with the crude product in a subsequent reduction to obtain the monoalcohol **VIII-30**. A bromination of crude **VIII-30** using NBS in the presence of triphenylphosphine provided the bromomethyl-iodide **VIII-31** which could be purified by recrystallization from a mixture of solvents (10% hexane/90% ethanol). Precautions need to be taken because of a light sensitive behavior of **VIII-31**. The corresponding phosphonate **VIII-32** was obtained by treatment of bromide **VIII-31** with triethylphosphite in a quantitative yield (>95%). The phosphonate **VIII-32** and monoaldehyde **VIII-29** were subjected to a Wittig reaction conditions to afford the diiodo-PV-dimer, **VIII-33**. Column chromatography followed by recrystallization was required to obtain the pure diodo dimer, which was kept in the dark.

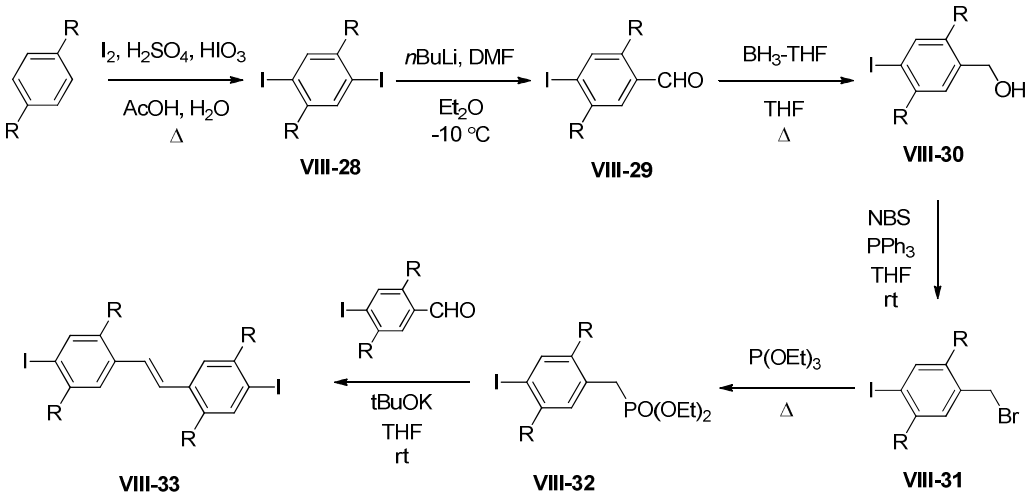


**Figure 8.8.** Successful synthesis of alkyl-substituted diiodo-PV-dimer, **VIII-33** (R = *n*-$C_8H_{17}$).

### 8.3.4. Synthesis of Diiodo-PV Trimer

The diiodo-PV-trimer **VIII-35** could be synthesized according to the route shown in Figure 8.9. Treatment of the diiodide **VIII-28** with two equivalents of *n*-butyllithium followed by quenching with anhydrous DMF provided dialdehyde **VIII-34** in good yield (>85%).[6] The dialdehyde **VIII-34** and phosphonate **VIII-32** were subjected to a Wittig reaction conditions to afford the required diiodo-PV-trimer, **VIII-35**. Unfortunately, we were not able to separate the pure PV-trimer from the byproducts of the reaction by any of the purification methods (column chromatography, recrystallization, and trituration). $^1$H NMR analysis showed that the majority of the crude material was the monoaldehyde analog formed by coupling of the phosphonate on only one of the sides of **VIII-34**.

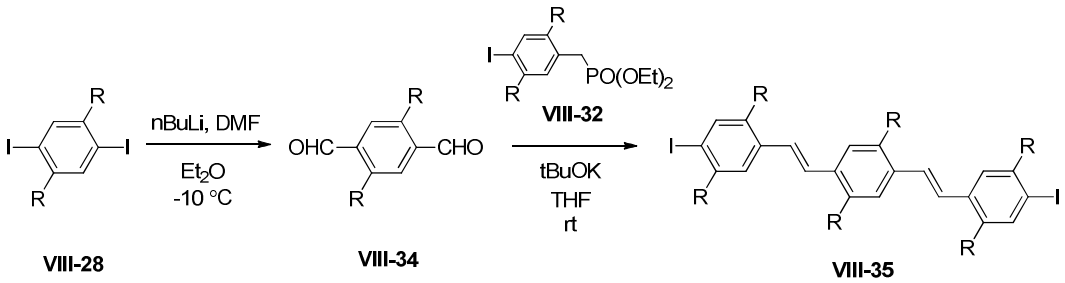


**Figure 8.9.** Attempted synthesis of alkyl-substituted diiodo-PV-trimer, **VIII-35** (R = *n*-$C_8H_{17}$).

### 8.3.5. Summary of Synthesis of Diiodo Oligomers

The syntheses of diiodo oligomers are relatively difficult compared to the corresponding bromo analogs. The synthetic strategy described in figure 8.6 is useful to prepare the diiodo PE oligomers with odd number of arenes. However, the synthesis of diiodo PE dimer is not possible with any of the synthetic strategies we tried. For PV oligomers, synthesis of diiodo dimer is relatively easy. However, the same synthetic route is not useful to prepare the diiodo PV trimer.

### 8.3.6. Synthesis of π-Stacked PE Polymers and Linear Unstacked Models

A Sonogashira cross-coupling[3] condensation polymerization of *pg* diethynyl monomer **VIII-36** and 1,4-diiodo-2,5-bis(octyl)benzene **VIII-28** in the presence of a catalytic amount of $Pd(PPh_3)_4$ and CuI in a mixture of diisopropylamine and THF afforded the stacked phenylene ethynylene polymer ***pg*-poly($PE_3$)**, Figure 8.10.[7] The crude polymer was precipitated by addition of the reaction mixture to a large volume of methanol. Reprecipitation of a dichloromethane solution of the crude product into acetone gave ***pg*-poly($PE_3$)** as an orange solid (65% isolated yield). The linear unstacked phenylene ethynylene model compound, **$Me_4PE_3$**, was prepared by coupling of diiodide **VIII-28** and 2,4-dimethylphenylacetylene, **VIII-37**.

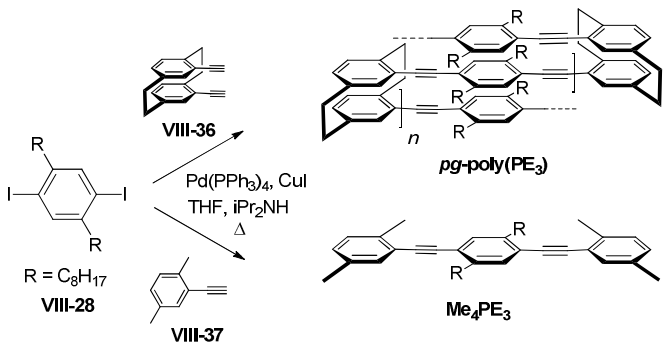


**Figure 8.10.** Phenylene ethynylene stacked polymer and unstacked model: Sonogashira cross-coupling polymerization of monomers **VIII-28** and **VIII-36** to afford π-stacked polymer ***pg*-poly($PE_3$)**; and synthesis of unstacked linear model **$Me_4PE_3$** (R = *n*-$C_8H_{17}$).

The π-stacked polymer ***pg*-poly(PE$_5$)** was obtained by a Sonogashira cross-coupling condensation polymerization of *pg* diethynyl monomer **VIII-36** and diiodide **VIII-25** in the presence of a catalytic amount of $Pd(PPh_3)_4$ and CuI in a mixture of diisopropylamine and THF as described for ***pg*-poly(PE$_3$)**, Figure 8.11. Similarly, the unstacked analog, **Me$_4$PE$_5$**, was prepared by coupling of diiodide **VIII-25** and 2,4-dimethylphenylacetylene, **VIII-37**.

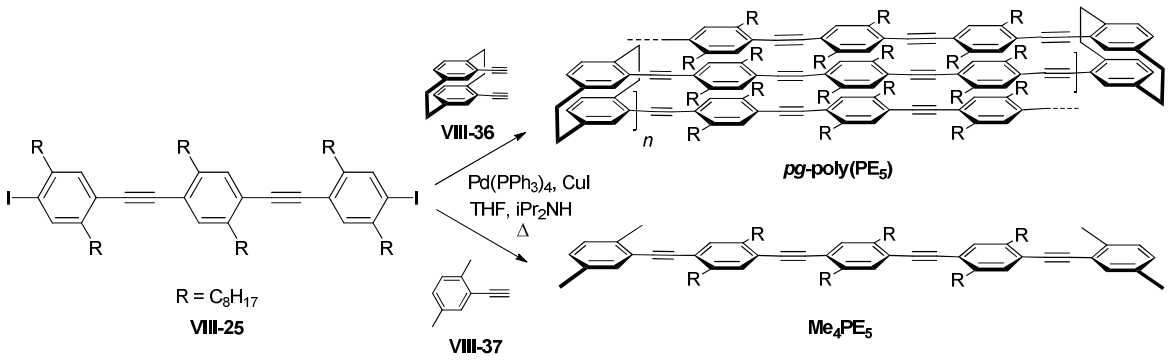


**Figure 8.11.** Phenylene ethynylene stacked polymer and unstacked model: Sonogashira cross-coupling polymerization of monomers **VIII-25** and **VIII-36** to afford π-stacked polymer ***pg*-poly(PE$_5$)**; and synthesis of unstacked linear model **Me$_4$PE$_5$** (R = *n*-$C_8H_{17}$).

### 8.3.7. Synthesis of π-Stacked PV Polymers and Linear Unstacked Models

The π-stacked phenylene vinylene polymer was prepared by a Heck coupling[8] polymerization of 4,15-diethenyl[2.2]paracyclophane **VIII-38** and 1,4-diiodo-2,5-bis(octyl)benzene **VIII-28** in the presence of a catalytic amount of $Pd(OAc)_2$ and CuI in a mixture of DMF and triethylamine, Figure 8.12. The polymer was purified by precipitation of reaction mixture into a large volume of methanol, followed by reprecipitation of a dichloromethane solution of the crude product into acetone to give ***pg*-poly($PV_3$)** as an orange solid (46% isolated yield). The linear unstacked analog, **$Me_4PV_3$** , was obtained by an analogous Heck coupling of diiodide **VIII-28** and 2,4-dimethylstyrene, **VIII-39**.

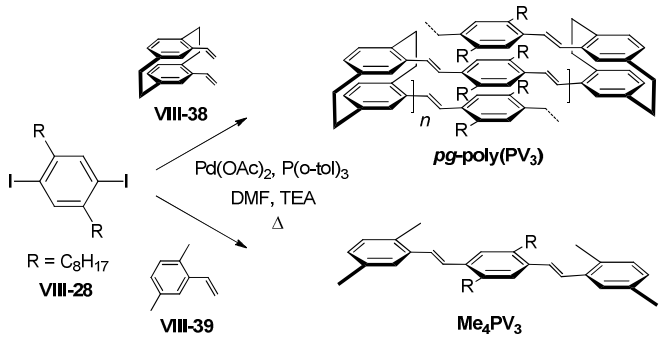


**Figure 8.12.** Phenylene vinylene stacked polymer and unstacked model: Heck cross-coupling polymerization of monomers **VIII-28** and **VIII-39** to afford π-stacked polymer ***pg*-poly($PV_3$)**; and synthesis of unstacked linear model, **$Me_4PV_3$** (R = *n*-$C_8H_{17}$).

Heck cross-coupling condensation polymerization of divinyl cyclophane **VIII-38** and diiodide **VIII-33** afforded ***pg*-poly($PV_4$)**, Figure 8.13. The crude product was purified by precipitation to give the polymer as an orange solid (59% isolated yield). **$Me_4PV_4$** was prepared as a model for the unstacked tier of the polymer by coupling of **VIII-33** with 2,4-dimethylstyrene, **VIII-39**.

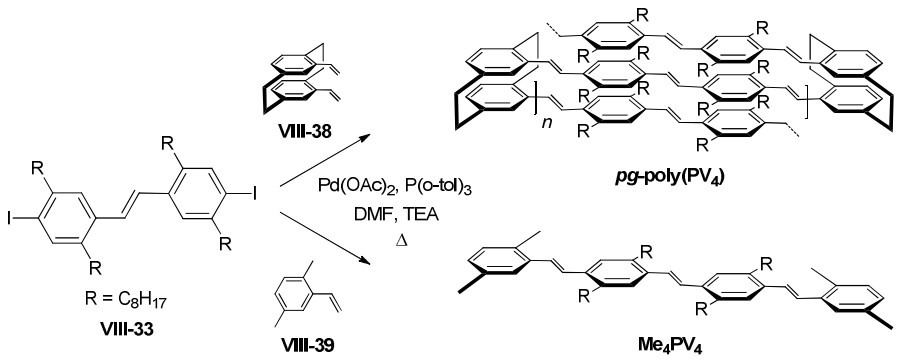


**Figure 8.13.** Phenylene vinylene stacked polymer and unstacked model: Heck cross-coupling polymerization of monomers **VIII-33** and **VIII-38** to afford π-stacked polymer ***pg*-poly($PV_4$)**; and synthesis of unstacked linear model, **$Me_4PV_4$** (R = *n*-$C_8H_{17}$).

### 8.3.8. Structural Characterization

Although all of the π-stacked polymers ***pg*-poly($PE_3$)**, ***pg*-poly($PE_5$)**, ***pg*-poly($PV_3$)** and ***pg*-poly($PV_4$)** are soluble in deuterated chloroform, the $^1$H NMR spectra of these solutions consist of sets of very broad peaks. The broadening of these peaks arises from the rigid nature of the polymers since the rotation of each of the oligomeric tiers is severely hindered by the close-packed multi-layer architecture. The chemical shifts of the peaks are consistent with the expected polymeric structures, and the spectra indicated the absence of unreacted monomer, catalyst and solvent. However, the spectra provide no additional details regarding the polymer structure.

The relative molecular weight of the polymers (relative to polystyrene standards) was determined by gel permeation chromatography with THF as the eluent. The number average molecular weight ($M_n$) and polydispersity index (PDI) of polymers are recorded in the Table 1.

**Table 8.1.** Molecular Weight and PDI of Polymers

| | Gel permeation chromatography[a] | | | |
|---|---|---|---|---|
| | $M_n$ $10^3$ kD | $M_w$ $10^3$ kD | PDI | DP |
| ***pg*-poly($PE_3$)** | 3.5 | 5.1 | 1.4 | 7 |
| ***pg*-poly($PE_5$)** | 6.1 | 10.9 | 1.7 | 5 |
| ***pg*-poly($PV_3$)** | 3.0 | 3.5 | 1.2 | 6 |
| ***pg*-poly($PV_4$)** | 4.4 | 5.6 | 1.3 | 5 |

[a] Calibrated with polystyrene standards, THF eluent

Further evidence for the polymeric nature of the isolated product comes from infrared spectroscopy. The infrared spectra of ***pg*-poly(PE$_3$)** and ***pg*-poly(PE$_5$)** (Figure 8.14, spectra B and C, respectively) show the absence of an alkyne C–H stretching mode (~3300 cm$^{-1}$) that is present in the spectrum of the diethynyl monomer **VII-1** (spectrum A). The spectra of the polymers also include signatures of the long alkyl chains of the dialkyl(oxy)arene units derived from the diodo monomer.

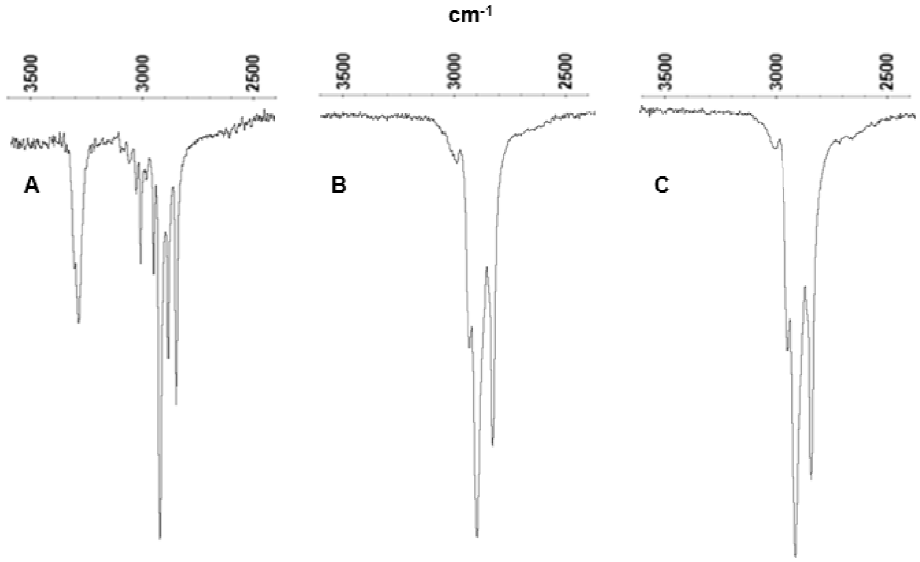


**Figure 8.14.** C-H stretching region (3600-2400 cm$^{-1}$) of the infrared spectra of monomers and polymers: A, 4,15-diethynyl[2.2]paracyclophane monomer, **VII-1**; B, ***pg*-poly(PE$_3$)**; C, ***pg*-poly(PE$_5$)**.

Similarly, the infrared spectra of ***pg*-poly($PV_3$)** and ***pg*-poly($PV_4$)** (Figure 8.15, spectra B and C, respectively) lack a vinylic C-H stretching peak at 3080 $cm^{-1}$ which is a signature of the alkene present in diethenyl monomer **VII-2** (spectrum A).

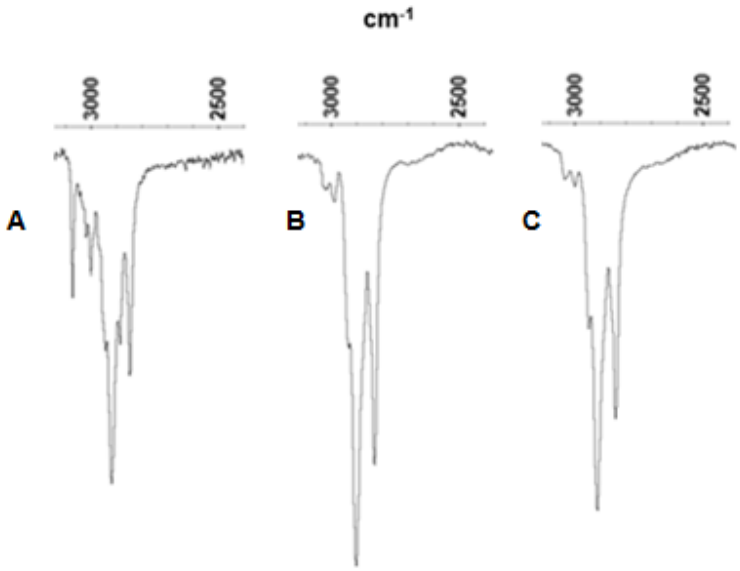


**Figure 8.15.** C-H stretching region (3600-2400 $cm^{-1}$) of the infrared spectra of monomers and polymers: A, 4,15-diethenyl[2.2]paracyclophane monomer, **VII-2**; B, ***pg*-poly($PV_3$)**; C, ***pg*-poly($PV_4$)**.

### 8.3.9. UV-Vis and Fluorescence spectroscopy

The UV-visible and fluorescence spectra of the stacked polymers were recorded and compared to those of the corresponding linear unstacked model compounds. The absorption and emission maxima for all polymers and their unstacked linear counterparts are shown in Table 2. The absorption profiles of the π-stacked polymers and the corresponding unstacked models resemble to one another. For each pair, the polymer and the unstacked model compound have similar absorption maxima. However, the polymers have the red shifted (ca. 50 nm) absorption edge compared to their models which indicates some π-π interactions in the electronic ground state. The striking differences were observed in the emission profiles stacked polymers compared to their unstacked linear models. The emission spectra of the linear unstacked model compounds consist of a relatively sharp peak, or set of vibronic peaks. However the emissions from the polymers are significantly broadened and red shifted. The lower intensity of the emission of the polymer may be ascribed to fluorescence quenching resulting from stacking of the conjugated tiers.

The emission of the ***pg*-poly($PE_3$)**, when excited at 326 nm, consists of a broad peak which is considerably red shifted ($\lambda_{max}$ = 502 nm) compared to the unstacked model that has three sharp emission peaks at 363, 380 and 418 nm, Figure 8.16. Thus, the multi-layer arrangement of the conjugated chromophoric tiers which are stacked their entire length is responsible for the delocalization of exciton over the number of tiers. Such relaxation over multiple layers leads a low energy red shifted emission relative to that from the unstacked single tier model compound. Similar behavior was noticed in the pair of stacked polymer ***pg*-poly($PE_5$)** ($\lambda_{max}$ = 490 nm) and model compound **$Me_4PE_5$** ($\lambda_{max}$ = 406, 428 nm), Figure 8.17.

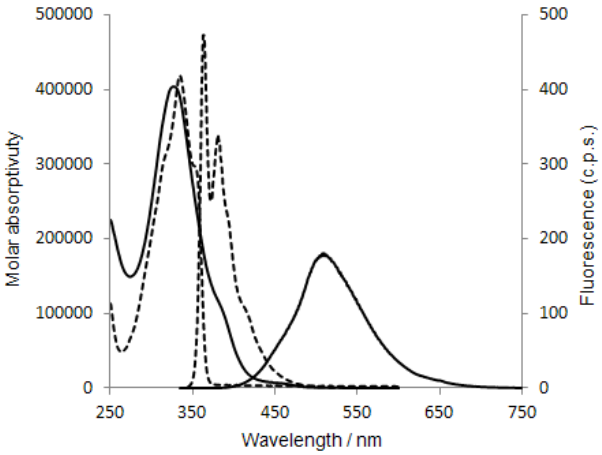


**Figure 8.16**. UV-visible and fluorescence spectra: A, ***pg*-poly(PE$_3$)** (solid) and unstacked model, **Me$_4$(PE$_3$)** (dotted). *c* = 1 mg/100 mL.

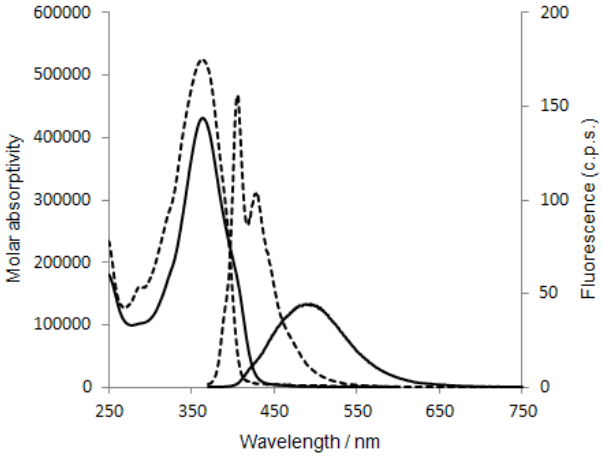


**Figure 8.17**. UV-visible and fluorescence spectra: A, ***pg*-poly(PE$_5$)** (solid) and unstacked model, **Me$_4$(PE$_5$)** (dotted). *c* = 1 mg/100 mL.

Surprisingly, the emission maximum of the polymer ***pg*-poly(PE$_3$)**, with shorter conjugated chromophoric tiers, is more red shifted ($\lambda_{max}$ = 502 nm) than ***pg*-poly(PE$_5$)** ($\lambda_{max}$ = 490 nm). This could be due to the number of tiers present in the multilayered arrangements of these polymers. The GPC data indicates that degree of polymerization for ***pg*-poly(PE$_5$)** is lower than that of ***pg*-poly(PE$_3$)** (Section 8.3.23, Table 1).

The phenylene vinylene stacked polymer ***pg*-poly(PV$_3$)**, when excited at the absorption maxima (349 nm), displays a larger Stokes shift (115 nm) compared to the unstacked model **Me$_4$PV$_3$** (68 nm). Similar trend in a Stokes shift was observed for the pair of the stacked polymer ***pg*-poly(PV$_4$)** (133 nm) and model **Me$_4$PV$_4$** (81 nm). The comparison between emission profiles of ***pg*-poly(PV$_3$)** and ***pg*-poly(PV$_3$)** suggests that the longer the conjugation length of chromophoric tier, larger the Stokes shift for the system given the equal number of tiers in multilayered arrangement.

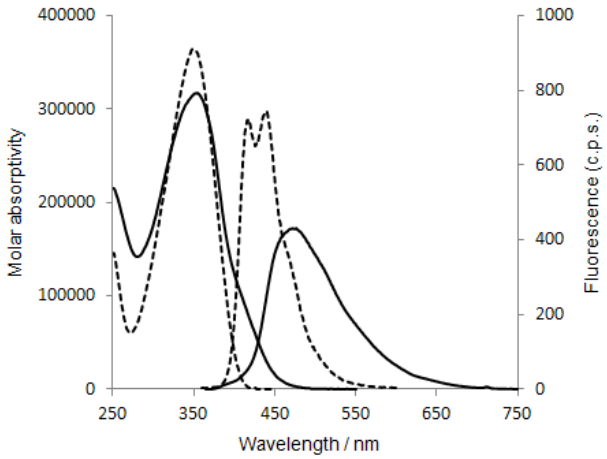


**Figure 8.18**. UV-visible and fluorescence spectra: A, ***pg*-poly(PV$_3$)** (solid) and unstacked model, **Me$_4$(PV$_3$)** (dotted). *c* = 1 mg/100 mL.

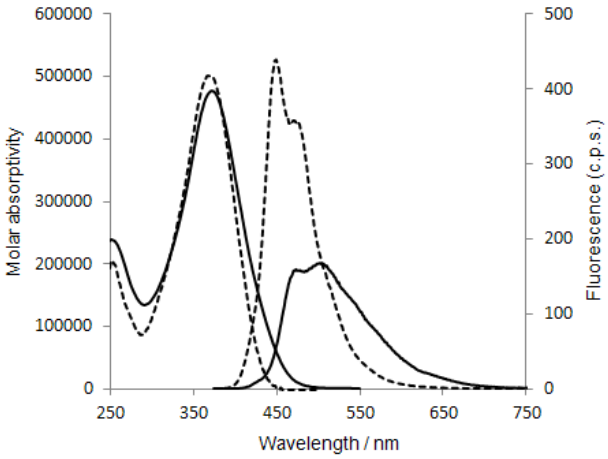


**Figure 8.19**. UV-visible and fluorescence spectra: A, ***pg*-poly($PV_4$)** (solid) and unstacked model, **$Me_4(PV_4)$** (dotted). *c* = 1 mg/100 mL.

**Table 8.2.** Absorption and emission spectra.

| | Absorption maxima $\lambda_{max}$/nm | Absorption edge shift[b] nm | Emission maxima $\lambda_{max}$/nm | Stokes shift nm |
|---|---|---|---|---|
| **$Me_4PE_3$**[a] | 333 | - | 363, 380 | 30 |
| ***pg*-poly($PE_3$)**[a] | 326 | 56 | 502 | 176 |
| **$Me_4PE_5$**[a] | 364 | - | 406, 428 | 42 |
| ***pg*-poly($PE_5$)**[a] | 360 | 24 | 490 | 130 |
| **$Me_4PV_3$**[a] | 350 | - | 418, 440 | 68 |
| ***pg*-poly($PV_3$)**[a] | 349 | 58 | 464 | 115 |
| **$Me_4PV_4$**[a] | 369 | - | 450, 471 | 81 |
| ***pg*-poly($PV_4$)**[a] | 367 | 36 | 474, 500 | 133 |

[a] [analyte] = 1 mg in 100 mL of $CHCl_3$. [b] end of absorption edge the compared to model compound.

## 8.4. Conclusions

The pseudo-geminal (*pg*) [2.2]paracyclophane (CP) core is a useful scaffold to build polymers consisting of conjugated units that are stacked over their entire length. For phenylene ethynylene series, the lower Stokes shift for the polymer ***pg*-poly($PE_5$)** with longer conjugated tier was unexpected. It could be due to less number of tiers in the multilayered arrangement of the polymer which leads to lower π-π interactions between the conjugated units. This may arise from a steric crowding around the diethynyl monomer which restricts the molecular weight. For phenylene vinylene series, Stokes shift is a function of conjugation length of tier of the polymer structure. The multilayered polymers exhibit the effect of ground state π-π interactions between the stacked conjugated tiers. This interaction is even larger when such stacked polymeric architecture is in excited state which facilitates delocalization of excitons over multiple tiers. The stacking of the conjugated tiers in these soluble materials resembles the close-packed cofacial assembly of segments of conjugated polymer chains in semiconducting thin films.

## 8.5. References


1. Sorensen, J. K.; Fock, J.; Pedersen, A. H.; Petersen, A. B.; Jennum, K.; Bechgaard, K.; Kilsa, K.; Geskin, V.; Cornil, J.; Bjornholm, T.; Nielsen, M. B., *Journal of Organic Chemistry* **2011**, *76*, 245.

2. Meier, H.; Ickenroth, D.; Stalmach, U.; Koynov, K.; Bahtiar, A.; Bubeck, C., *European Journal of Organic Chemistry* **2001**, 4431.

3. Sonogashira, K.; Tohda, Y.; Hagihara, N., *Tetrahedron Letters* **1975**, 4467.

4. Ziener, U.; Godt, A., *Journal of Organic Chemistry* **1997**, *62*, 6137.

5. Gonzalez-Rojano, N.; Arias-Marin, E.; Navarro-Rodriguez, D.; Weidner, S., *Synlett* **2005**, 1259.

6. Jian, H. H.; Tour, J. M., *Journal of Organic Chemistry* **2005**, *70*, 3396.

7. Jagtap, S. P.; Collard, D. M., *Journal of the American Chemical Society* **2010**, *132*, 12208.

8. Heck, R. F.; Nolley, J. P., *Journal of Organic Chemistry* **1972**, *37*, 2320.

# CHAPTER 9

# FUTURE OUTLOOK

## 9.1. Future Directions in Research

This thesis has demonstrated the design and use of the new molecular architectures that can be used as scaffolds to prepare π-stacked conjugated oligomers and polymers. The detailed experiments and characterization performed on these compounds shows that such stacking imparts extensive π-π interactions between the conjugated units. However, the study deals with only p-dopable conjugated oligomers and polymers.

A large body of work focuses on the study of the alternating donor-acceptor copolymers for their applications in organic photovoltaic cells.[1] Spontaneous phase separation leads to the formation of a nanoscale bulk heterojunction material in which there is an interpenetrating donor and acceptor conjugated units.[2] To attain a higher efficiency with these devices, a greater fundamental understanding of the optoelectronic properties of these donor-acceptor polymers is required.

Model compounds have been prepared to probe the charge transfer between the donor and acceptor conjugated units held on top of each other.[3] The design and characterization of π-stacked polymers having donor and acceptor units stacked atop one another would be useful in developing an understanding of the nature of the interactions between the subunits. The 4,15-diethynyl[2.2]paracyclophane (**VI-1**)[4] could be an interesting scaffold to prepare such polymers, Figure 9.1. The study and characterization of π-stacked donor-acceptor polymers could be

extrapolated to predict the optical and electrochemical properties of such copolymers in the solid state.

Electron accepting conjugated polymers generally contain electron withdrawing substituents such as fluorine[5] or cyano[6] groups, or have nitrogen-containing heteroaromatic units in the conjugated backbone (e.g., quinoline,[7] pyramidine,[8] pyridine,[9] thienopyrazine,[10] and quinoxaline[11]). Several quinoxaline-containing donor-acceptor alternating copolymers have been explored in efforts to prepare low band gap and electroluminescent materials, including those with thiophene[12], fluorene[13] and phenylene units[14]. Based on these studies, quinoxaline would be a good choice as an electron acceptor unit.

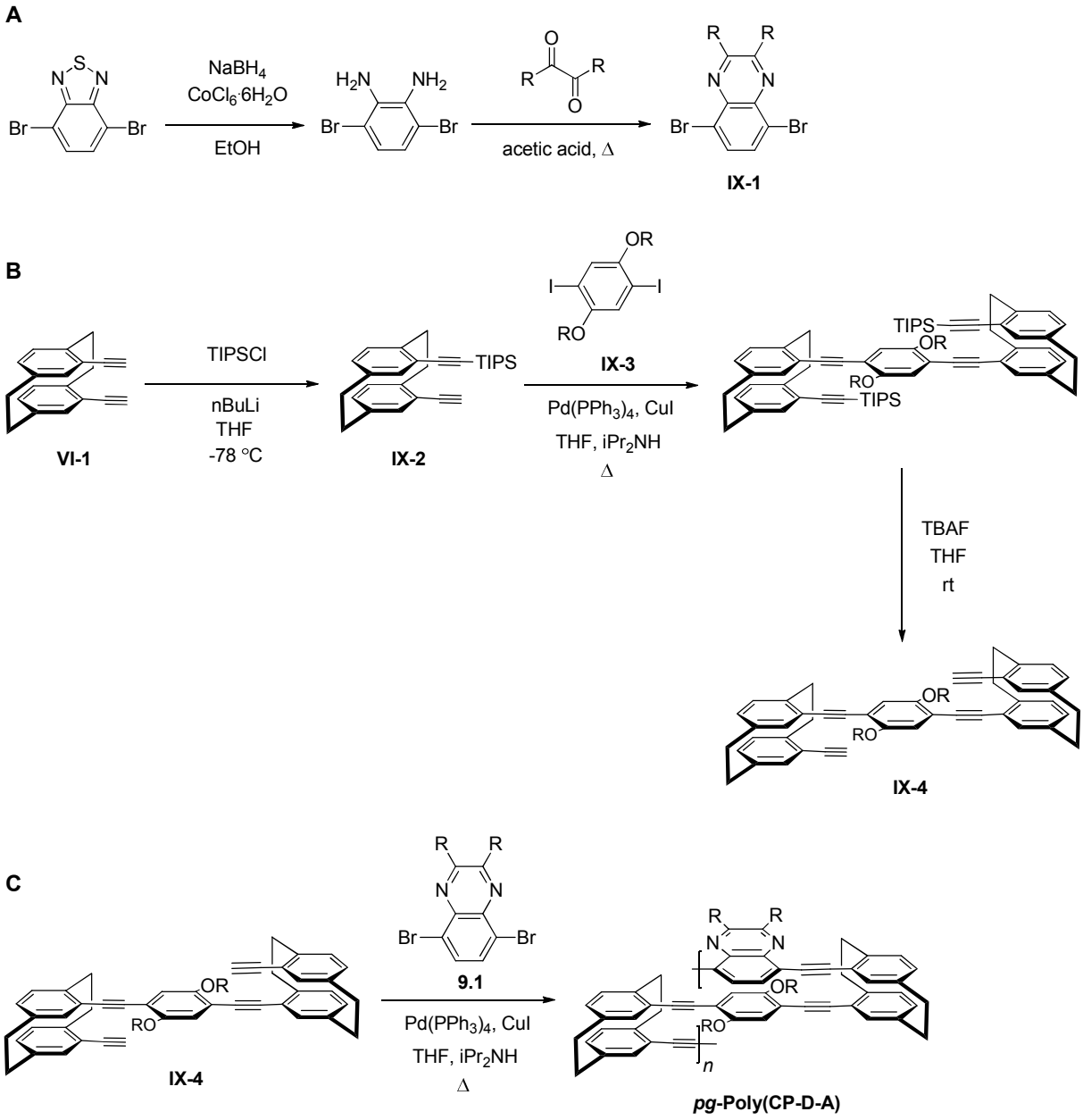


**Figure 9.** A, Synthesis of dibromoquinoxaline monomer, **IX-1**; B, Synthesis of diethynyl monomer, **IX-4**; and preparation of stacked donor-acceptor polymer, ***pg*-Poly(CP-D-A)**.

The dibromoquinoxaline **IX-1** could be prepared according to literature procedures to provide the electron acceptor unit in the polymer, Figure 9A.[15] A proposed synthesis of diethynyl monomer **IX-4** is depicted in the Figure 9B. Lithiation of 4,15-diethynyl[2.2]paracyclophane using a stoichiometric amount of *n*-butyllithium at low temperature would provide monosilyl paracyclophane, **IX-2**. Coupling of diiodide **IX-3** and monoethynyl paracyclophane **IX-2** using a Sonogashira cross-coupling reaction followed by deprotection in the presence of tetrabutylammonium fluoride would give the required diethynyl monomer, **IX-4**. The π-stacked conjugated polymer ***pg*-Poly(CP-D-A)** can be prepared by subjecting dibromoquinoxaline **IX-1** and diethynyl **IX-4** to a Sonogashira reaction in the presence of catalytic amount of $Pd(PPh_3)_4$ and CuI in diisopropylamine and THF.[16] The resultant polymer will have donor and acceptor unit stacked atop one another throughout the multilayered polymeric structure.

The synthesis, structural characterization, optical, and electrochemical investigations will provide insight to study the effect of charge transfer between electron donor and acceptor conjugated units. Various donor and acceptor units could be explored to prepare such π-stacked donor-acceptor conjugated polymer and study the nature of interaction between them.

## 9.2. References


1. Colladet, K.; Fourier, S.; Cleij, T. J.; Lutsen, L.; Gelan, J.; Vanderzande, D.; Nguyen, L. H.; Neugebauer, H.; Sariciftci, S.; Aguirre, A.; Janssen, G.; Goovaerts, E., *Macromolecules* **2007,** *40,* 65.
2. Granstrom, M.; Petritsch, K.; Arias, A. C.; Lux, A.; Andersson, M. R.; Friend, R. H., *Nature* **1998,** *395,* 257.
3. Griffiths, K. E.; Stoddart, J. F., *Pure and Applied Chemistry* **2008,** *80,* 485.
4. Bondarenko, L.; Hentschel, S.; Greiving, H.; Grunenberg, J.; Hopf, H.; Dix, I.; Jones, P. G.; Ernst, L., *Chemistry A European Journal* **2007,** *13,* 3950.
5. Jin, Y.; Kim, K.; Park, S. H.; Song, S.; Kim, J.; Jung, J.; Lee, K.; Suh, H., *Macromolecules* **2007,** *40,* 6799.
6. Greenham, N. C.; Moratti, S. C.; Bradley, D. D. C.; Friend, R. H.; Holmes, A. B., *Nature* **1993,** *365,* 628.
7. Saito, N.; Kanbara, T.; Nakamura, Y.; Yamamoto, T.; Kubota, K., *Macromolecules* **1994,** *27,* 756.
8. Kanbara, T.; Kushida, T.; Saito, N.; Kuwajima, I.; Kubota, K.; Yamamoto, T., *Chemistry Letters* **1992**, 583.
9. Yamamoto, T.; Maruyama, T.; Zhou, Z. H.; Ito, T.; Fukuda, T.; Yoneda, Y.; Begum, F.; Ikeda, T.; Sasaki, S.; Takezoe, H.; Fukuda, A.; Kubota, K., *Journal of the American Chemical Society* **1994,** *116,* 4832.
10. Wen, L.; Duck, B. C.; Dastoor, P. C.; Rasmussen, S. C., *Macromolecules* **2008,** *41,* 4576.
11. Jonforsen, M.; Johansson, T.; Inganas, O.; Andersson, M. R., *Macromolecules* **2002,** *35,* 1638.

12. Zhang, G. B.; Fu, Y. Y.; Zhang, Q.; Xie, Z. Y., *Polymer* **2010,** *51*, 2313. Lee, B. L.; Yamamoto, T., *Macromolecules* **1999,** *32*, 1375.

13. Kulkarni, A. P.; Zhu, Y.; Jenekhe, S. A., *Macromolecules* **2005,** *38*, 1553.

14. Liu, C. L.; Tsai, J. H.; Lee, W. Y.; Chen, W. C.; Jenekhe, S. A., *Macromolecules* **2008,** *41*, 6952.

15. Tsami, A.; Bunnagel, T. W.; Farrell, T.; Scharber, M.; Choulis, S. A.; Brabec, C. J.; Scherf, U., *Journal of Materials Chemistry* **2007,** *17*, 1353.

16. Sonogashira, K.; Tohda, Y.; Hagihara, N., *Tetrahedron Letters* **1975**, 4467.

# APPENDICES

## A. Computational Work (by Dr. Sukrit Mukhopadhyay)

## A.1. Chapter 4

### *a) Synthesis of stacked and unstacked model compounds.*

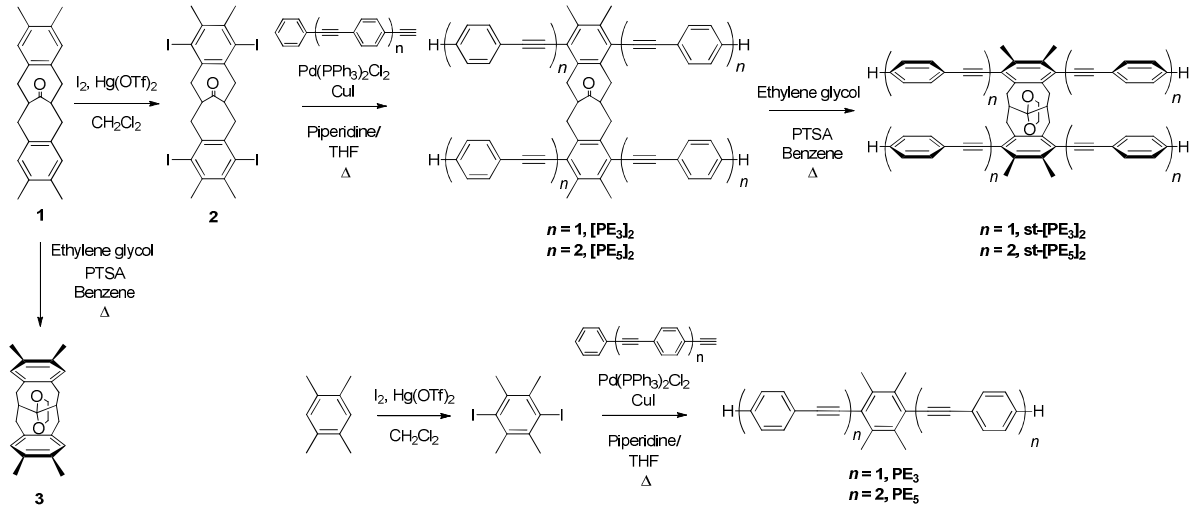


**Figure 1.** Synthesis of stacked compounds **3** (***st*-[PE$_1$]$_2$**), ***st*-[PE$_3$]$_2$** and ***st*-[PE$_5$]$_2$**; and unstacked linear analogs **PE$_3$**, and **PE$_5$**.

### *b) X-ray crystal structures.*

The X-ray crystal structure of ketal ***st*-[PE$_1$]$_2$** confirms that bicycloundecanone core adopts a pseudo chair-pseudo chair conformation with a cofacially stacked arrangement of the fused benzene rings. The distance between the centers of the stacked benzene rings ($d_1$) is 3.42 Å, Figure 3A and Table 1. The benzene rings are titled at an angle ($\theta_1$) of 16.8° with respect to one another: The inner pairs of aromatic carbon atoms (i.e., those fused to the bicyclic structure) are 3.03 Å apart, whereas the outer pair (methyl substituted) are held at a distance of 3.74 Å. Thus, this conformation is similar to that reported by Mataka for the compound lacking the methyl substituents ($d_1$ = 3.56 Å; $\theta_1$ = 25°).

Similarly, the X-ray crystal structure of ***st*-[PE$_3$]$_2$** confirms the pseudo chair-pseudo chair conformation of the bicyclic scaffold in the presence of the phenylene ethynylene arms, Figure 3B. The central rings of the stacked conjugated trimer moieties are separated by an intercentroid distance ($d_1$) of 3.42 Å, with an angle ($\theta_1$) of 17.9° between them. The dihedral angles between bridgehead and benzylic protons determined from the crystallographic data are consistent with the coupling constants obtained from $^1$H NMR analysis of solutions of the ketals: The 6 Hz coupling constant between the bridgehead and equatorial benzylic hydrogens is consistent with dihedral angle of 52°, and the 47° dihedral angle the bridgehead and axial positions results in a 2 Hz coupling (using Karplus equation[16]). Thus, comparison of the conformation of the cores of ***st*-[PE$_1$]$_2$** and ***st*-[PE$_3$]$_2$** indicates that the incorporation of the four conjugated arms does not cause repulsion between the moieties and that the stacked chair-chair conformation observed in the solid state is preserved in solution.

The X-ray crystal structure of ***st*-[PE$_3$]$_2$** also indicates that the peripheral rings are in a stacked arrangement, albeit that there are slight distortions from planarity and linearity in the stacked trimeric segments. The intercentroid distances between pairs of rings on the periphery of the molecule are 3.84 Å ($d_2$) and 4.01 Å ($d_3$), Figure 3B. The larger intercentroid distance between these pairs (referred to hereafter as "stack 2" and "stack 3") compared to the central pair ("stack 1", separated by $d_1$) results from a small in-plane bending of one segment towards, and the other away from, the bicyclic scaffold, Figure 3B. This results in an offset between the rings that we characterize by a slip distance ($d_s$), Figure 3B. The peripheral rings in ***st*-[PE$_3$]$_2$** are titled by an average of 5° out of the plane of the central aromatic rings, thereby retaining conjugation along their entire length. Being unconstrained by fusion to the scaffold itself, the pairs of peripheral rings adopt a more co-planar arrangement ($\theta_2$ = 1.7°; $\theta_3$ = 11.9°) than the central rings ($\theta_1$ = 17.9°). The small differences in the bending and torsion in the phenylene ethynylenes on one side of the scaffold and in one of the segments of the stacked structure may be ascribed to crystal packing forces since those are absent in our calculations. We note that the optimized geometries lead to $\theta_1$ and $\theta_2$ values between 1°-2°. The stacked pentamer, ***st*-[PE$_5$]$_2$**, does not provide diffraction-quality crystals to allow a similar crystallographic analysis.

***c) DFT-Optimized Ground-State Geometries.***

The optimized geometries of the ground state of ***st*-[PE$_3$]$_2$** and of ***st*-[PE$_5$]$_2$** were obtained using the ωB97XD functional with the 6-31g* basis set. We considered both the isolated molecules and the molecules embedded in a dielectric continuum taking implicit account of the solvent (here, $CHCl_3$ corresponds to ε = 4.7). The calculations reveal that the solvent has only a marginal effect on the optimized ground-state geometry in both systems (Table 1). The DFT-derived geometry of ***st*-[PE$_3$]$_2$** compares well with that obtained from the crystal structure, Table 1. In particular, the calculations reproduce well the slight non-linearity and twisting of the two conjugated tiers; the slip displacement of the peripheral benzene rings apparent in the top view of the calculated geometry (Figure 4) closely matches that observed in the X-ray crystal structure, Figure 3C. In the ground-state optimized geometry, the slip distance within both stacks 2 and 3 is 1.65 Å; in the X-ray crystal structure, the slip distance between the benzene rings in stack 2 of ***st*-[PE$_3$]$_2$** is 1.33 Å.

The inter centroid distances and torsional angles of ***st*-[PE$_5$]$_2$**, along with the slip distances between the inner pairs of stacked rings (stacks 2 and 3, $d_s$ = 1.60 Å) are comparable to those in the stacked trimer, ***st*-[PE$_3$]$_2$**. The slip distances between the pairs of external rings in the ***st*-[PE$_5$]$_2$** units (stacks 4 and 5) are only slightly larger (1.7 Å) than for the inner pairs. Thus, this result underlines that *the conjugated pentamer units are held in close proximity over their entire length*.

**Table 1**. Comparison of selected structural parameters (distances, $d_i$, and angles, $\theta_i$) of stacked compounds from X-ray diffraction and DFT optimization of ground-state (gs) and excited-state (ex) geometries.

| Geometry | Inter-centroid distance (Å) | | | | | Inter-plane angle (°) | | | | |
|---|---|---|---|---|---|---|---|---|---|---|
| | $d_1$ | $d_2$ | $d_3$ | $d_4$ | $d_5$ | $\theta_1$ | $\theta_2$ | $\theta_3$ | $\theta_4$ | $\theta_5$ |
| *Experimental* | | | | | | | | | | |
| X-ray crystallography | | | | | | | | | | |
| ***st*-[PE$_1$]$_2$** | 3.42 | - | - | - | - | 16.8 | - | - | - | - |
| ***st*-[PE$_3$]$_2$** | 3.42 | 3.81 | 4.00 | - | - | 17.9 | 1.7 | 11.9 | - | - |
| *ωB97X-D/6-31g** | | | | | | | | | | |
| Gs | 3.39 | 3.76 | 3.76 | - | - | 15.5 | 1.4 | 1.5 | - | - |
| Gs ($CHCl_3$) | 3.39 | 3.78 | 3.78 | - | - | 12.8 | 1.6 | 1.7 | - | - |
| Ex | 3.15 | 3.54 | 3.54 | - | - | 10.8 | 4.9 | 4.6 | - | - |
| ***st*-[PE$_5$]$_2$** | | | | | | | | | | |
| *ωB97X-D/6-31g** | | | | | | | | | | |
| Gs | 3.39 | 3.69 | 3.69 | 3.79 | 3.80 | 13.6 | 0.6 | 1.4 | 2.00 | 2.2 |
| Gs ($CHCl_3$) | 3.40 | 3.68 | 3.68 | 3.82 | 3.81 | 12.8 | 0.7 | 1.6 | 1.2 | 1.8 |
| Ex | 3.17 | 3.47 | 3.47 | 3.71 | 3.71 | 11.0 | 0.2 | 1.4 | 1.3 | 1.8 |

***d) UV-visible and fluorescence spectroscopies.***

The stacked oligomers and unstacked linear analogues were characterized by UV-Vis and fluorescence spectroscopies to explore the effect of stacking on the electronic structure of the conjugated moieties. The absorption maximum of the stacked trimer, ***st*-[PE$_3$]$_2$**, (330 nm) is slightly blue shifted by 60 meV relative to that of the unstacked linear analog **PE$_3$** (325 nm). As seen from Figure 5, the absorption edge of ***st*-[PE$_3$]$_2$** contains a low-energy tail, which is absent in the unstacked analog. A priori, such an absorption could be due either to a weak optically allowed electronic state contributing to the absorption in the stacked trimer or to broadening of the monomeric state due to coupling between two moieties. The stacked compound shows emission maxima at 382 nm and 397 nm, which are red shifted from the maxima displayed by the unstacked analog (360 and 375 nm), Figure 5. In addition, the stacked system shows a weak emission that appears as a broad shoulder in the low-energy part of the spectrum at approximately 490 nm (~ 2.5 eV, see inset of Figure 5A).

More pronounced differences are observed between the spectra of the pentameric homologs, ***st*-[PE$_5$]$_2$** and **PE$_5$**. The absorption and emission maxima of both stacked and unstacked pentamers are red shifted from those of the corresponding trimers, as expected from the greater extent of conjugation. The absorption maximum of the stacked system is again slightly blue shifted (~ 90 meV) relative to the unstacked oligomer (355 nm versus 365 nm, Table 1); as in the stacked trimer, a tail at the low-energy edge is present. The most interesting feature, however, is that the emission spectrum of the stacked pentamer, Figure 5B, is significantly different from that of the stacked trimer. It is in fact dominated by a broad transition at low-energy with a maximum at ca. 495 nm. A low-intensity high-energy band at 398 nm (~ 3.1 eV) that matches well the emission maximum of the unstacked linear analog **PE$_5$** is also observed.

Analysis of the emission spectra points to the fact that at least two electronic states appear to contribute to the fluorescence of both stacked systems. In order to obtain a firm assessment of the nature of these excited states, we turn next to a discussion of the excited states of the unstacked and stacked systems, based on the results of TD-DFT calculations.

**Table 2.** Absorption and emission maxima.

| | Absorption (nm) [17] | Emission (nm) [17] |
|---|---|---|
| **[PE$_3$]**[a] | 330 | 360, 375[c] |
| | [3.76][e] | [3.44, 3.31][e] |
| ***st*-[PE$_3$]$_2$**[a] | 325 | 382, 397[c], 490[d] |
| | [3.81][e] | [3.30, 3.13, 2.52][e] |
| **[PE$_5$]**[b] | 365 | 399, 418[c] |
| | [3.40][e] | [3.11, 2.97][e] |
| ***st*-[PE$_5$]$_2$**[b] | 355 | 398 (weak), 495 (br) |
| | [3.49][e] | [3.09, 2.40][e] |

[a] [analyte] = 3 x $10^{-5}$ M in $CHCl_3$. [b] [analyte] = 1.8 x $10^{-5}$ M in $CHCl_3$. [c] Vibronic band. [d] Shoulder. [e] Energies for transitions are computed from de-convoluted spectra.

***e) TDDFT Characterization of the Excited-State Properties.***

To gain further insight into the effect of π-stacking on the photo-physical properties of conjugated oligomers, we have optimized the geometries of the lowest excited states of the stacked systems and the unstacked model oligomers by means of TD-DFT calculations. The calculated excited-state energies are listed in Table 3. The TD-DFT $S_0 \rightarrow S_1$ transition energies of the unstacked oligomers are somewhat overestimated (~ 0.2 eV) compared to the experimental absorption maxima; in agreement with experiment, a ~ 0.4-0.3 eV decrease in $S_1$ energy is calculated in **PE$_5$** compared to **PE$_3$**. In both unstacked oligomers, the $S_1$ state can be described essentially by a single one-electron excitation from the highest occupied molecular orbital (HOMO) to the lowest unoccupied molecular orbital (LUMO). The implicit inclusion of the solvent (geometry optimizations followed by the excited-state calculations using TD-DFT) predicts a ca. 0.1 eV decrease in optical gaps, but the trends remain the same as for the calculations from the isolated molecules (see SI). The relaxation energy (λ) of the $S_1$ state of **PE$_5$** is estimated to be substantially smaller than that of **PE$_3$** (0.06 vs. 0.15 eV), which is consistent

with a more delocalized nature of the excited state in the more extended system. This result is in good agreement with the observed emission spectra; with the increase in oligomer length (Figure 5), there occurs a decrease in the ratio of the 0-1 and 0-0 vibration peaks that are well-resolved in the emission bands of both oligomers.

**Table 3.** DFT estimates of the energy, oscillator strength (in parentheses) and relaxation energy λ of the local (*L*) and excimer (*E*) states. All energies are in eV.

| Molecule | State | Ground state | Excited state | λ |
|---|---|---|---|---|
| **$PE_3$** | $S_1$ | 4.02 (1.72) | 3.53 | 0.15 |
| ***st*-$[PE_3]_2$** | $S_1$(E)<br>$S_2$(L) | 3.70 (0.01)<br>4.06 (2.61) | 2.61 | 0.56 |
| **$PE_5$** | $S_1$ | 3.61 (3.76) | 3.21 | 0.06 |
| ***st*-$[PE_5]_2$** | $S_1$(E)<br>$S_2$(L) | 3.41 (0.01)<br>3.66 (6.71) | 2.52 | 0.42 |

The TD-DFT calculations reveal that the first-excited state of both ***st*-$[PE_3]_2$** and ***st*-$[PE_5]_2$** is dominated by HOMO→LUMO and HOMO-1→LUMO+1 excitations, *i.e.*, $\psi(S_1) = a\left|H \rightarrow L\right\rangle + b\left|H-1 \rightarrow L+1\right\rangle$. Furthermore, by performing a transformation to the oligomer MO basis set, it can be shown (see SI for details) that $\psi(S_1)$ can be represented as a linear combination of two oligomer-localized $\left|AB^*\right\rangle$ and $\left|A^*B\right\rangle$ excitations and two inter-oligomer charge-transfer (CT) $\left|A^+B^-\right\rangle$ and $\left|A^-B^+\right\rangle$ excitations:[18]

$$\psi(S_1) = a\left|H \rightarrow L\right\rangle + b\left|H-1 \rightarrow L+1\right\rangle$$
$$= \left(\frac{a+b}{2}\right)\left(\left|A^{*}B\right\rangle - \left|AB^{*}\right\rangle\right) + \left(\frac{a-b}{2}\right)\left(\left|A^{-}B^{+}\right\rangle - \left|A^{+}B^{-}\right\rangle\right) \quad (1)$$

TD-DFT calculations carried out at the ground-state geometry indicate that the $S_1$ state of both systems possesses a significant CT character, *ca*. 15% and 10% for ***st*-[PE$_3$]$_2$** and ***st*-[PE$_5$]$_2$**, respectively. Importantly, the CT contribution increases as the stacked systems relax to the equilibrium geometry of the $S_1$ state. In this case, we find that the intra-chain and CT excitations contribute approximately equally to $\psi(S_1)$ (we note that similar results are obtained at the semi-empirical intermediate neglect of differential overlap (INDO) level of theory, see SI). Based on these findings, we ascribe the $S_1$ states of the stacked systems to excimer-like states (*E*). As a result of their CT character, the $S_1$ states undergo large structural relaxations upon excitation. Thus, in the fully relaxed $S_1$ geometry of the stacked systems, the inter-centroid distance (***d$_i$***) between the individual oligomer arms is reduced by *ca*. 0.20 Å compared to the ground-state geometry; furthermore, the angle between the inner-most benzene rings (***θ$_1$***) decreases by 3-5° (Table 1). Such significant changes in geometry lead to large relaxation energies that reach some 0.5 eV. These results are consistent with the fact that low-energy emission bands are broad and structureless.

In addition, the TD-DFT calculations reveal that the $S_2$ states in both ***st*-[PE$_3$]$_2$** and ***st*-[PE$_5$]$_2$** can be described as a linear combination of $S_1$ states of the individual arms. The $S_2$ states are thus excitonic in nature and can be assigned as local (*L*) states (a detailed description of the $S_2$ state is provided in the SI). The similarity between the energies of the $S_2$ states in the stacked systems and the energies of the $S_1$ states in the unstacked oligomers suggests that upon stacking the single-arm states are only weakly affected by inter-oligomer interactions.

The calculations also show that the difference between the energies of the excimer-like state of ***st*-[PE$_3$]$_2$** and ***st*-[PE$_5$]$_2$** in their relaxed geometries is very small, *ca*. 0.09 eV. These theoretical results agree well with the fact that the low-energy emission peaks of ***st*-[PE$_3$]$_2$** and ***st*-[PE$_5$]$_2$** appear at nearly the same energy (~ 2.4 eV, 490 nm). Inspection of the frontier orbitals contributing to the excimer states indicates that in the case of the stacked trimer, ***st*-[PE$_3$]$_2$**, the molecular orbitals are delocalized over the entire length of the oligomer segment; in contrast, for the stacked pentamer ***st*-[PE$_5$]$_2$**, the frontier molecular orbitals are restricted to the central three-

ring section of the pentamer segments (Figure 6). This explains the similarity between the *E* states of ***st*-[PE$_3$]$_2$** and ***st*-[PE$_5$]$_2$**.

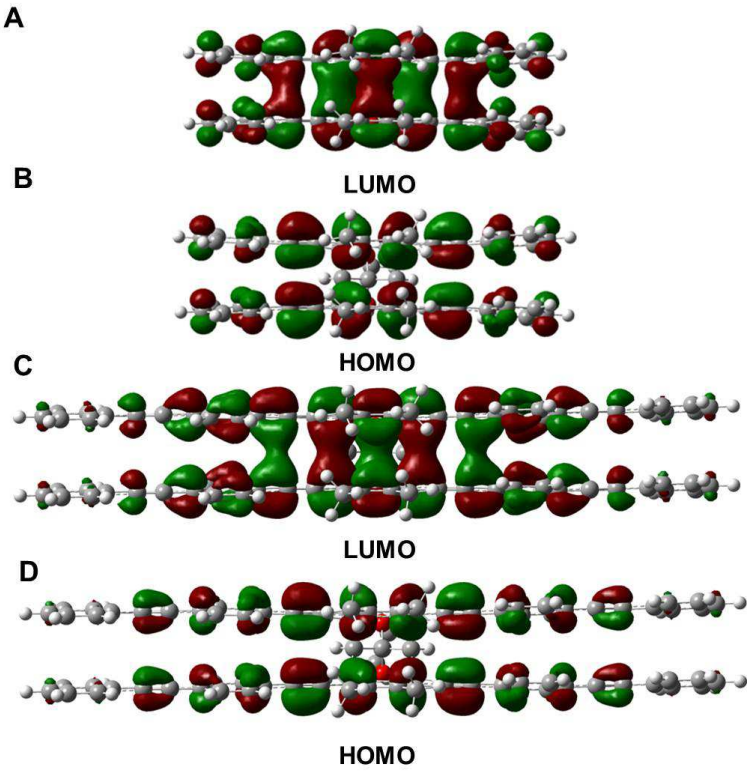


**Figure 6.** Frontier molecular orbitals of ***st*-[PE$_3$]$_2$** (A and B) and ***st*-[PE$_5$]$_2$** (C and D) of the $S_1$ state (in optimized geometries).

To summarize at this stage, the electronic-structure calculations indicate that:

(i) the absorption band and high-energy emission band in both ***st*-[PE$_3$]$_2$** and ***st*-[PE$_5$]$_2$** are related to the second excited state, which corresponds to the lowest excited state (*L*-state) of the unstacked oligomers; and

(ii) the low-energy broad emission band arises from the lowest excited state, which is an excimer-like state; as a result of the large geometry relaxation, this band is significantly red-shifted in comparison to the lowest energy emission in the unstacked oligomers.

The next point is to rationalize the differences in the overall shapes of the emission spectra of ***st*-[PE$_3$]$_2$** and ***st*-[PE$_5$]$_2$**. In general, the emission features are expected to depend on the

relative populations and emission characteristics of the *L* and *E* states. Here, in the absence of temperature- and time-resolved measurements, we use a simple three-state model such as the one sketched in Figure 7. In this framework, the emission intensities from the relevant excited states can be analyzed following Zachariasse and co-workers by using the rate equation described by Eq. 2.[19] The ratio of emission intensities from the *E* and *L* states (*i.e.*, $I(E)/I(L)$) can then be written as:

$$\frac{I(E)}{I(L)} = \frac{k_r(E)}{k_r(L)} \times \frac{k_r(L \rightarrow E)\tau_0(E)}{k_r(E \rightarrow L)\tau_0(E)+1} \qquad (2)$$

where $k_r(E)$ and $k_r(L)$ are the radiative rate constants of the *E* and *L* states, $k_r(L \rightarrow E)$ and $k_r(E \rightarrow L)$ are the forward and backward reaction rates between the local and excimer states, and $\tau_0(E)$ is the fluorescence lifetime of the *E* state. While a detailed investigation of these kinetic processes is beyond the scope of this work, the main differences between the emission patterns in ***st*-[PE$_3$]$_2$** and ***st*-[PE$_5$]$_2$** can be analyzed on the basis of the spectroscopic and theoretical data presented above. The TD-DFT calculations indicate that $k_r(E)/k_r(L)$ is of the order of $10^{-2}$ for both stacked systems. This suggests that the difference between the emission intensities of ***st*-[PE$_3$]$_2$** and ***st*-[PE$_5$]$_2$** is related to the second factor in Eq. 2:

$$\frac{k_r(L \rightarrow E)\tau_0(E)}{k_r(E \rightarrow L)\tau_0(E)+1} = B(L \rightarrow E) \qquad (3)$$

When $k_r(E \rightarrow L)\tau_0(E) >> 1$, one obtains $B(L \rightarrow E) = k_r(L \rightarrow E)/k_r(E \rightarrow L)$ and parameter *B* is then proportional to the free energy difference (driving force), $\Delta G_0$, related to the $L \rightarrow E$ transition. This approximation turns out to work well for ***st*-[PE$_5$]$_2$**. Indeed, using the experimental energies and the calculated relaxation energies, we estimate for this system that $\Delta G_0 \approx 0.40$ eV and $k_r(L \rightarrow E)/k_r(E \rightarrow L) \approx 10^4$. The ratio of the forward and backward rates, along with the value of $10^{-2}$ derived for $k_r(E)/k_r(L)$, is consistent with the much stronger emission from the excimer state than from the local state by approximately two orders of magnitude. The lower bound for $k_r(L \rightarrow E)$ in this case is given by the condition $k_r(L \rightarrow E)\tau_0(E) > 10^4$. We note that in related cofacially-stacked perylene-diimide dimers, $\tau_0$ was found to be about $10^{-7}$ s.[20] Assuming a similar value for $\tau_0$ in the present systems would lead to $k_r(L \rightarrow E) > 10^{11}$ s$^{-1}$ for ***st*-**

**[PE$_5$]$_2$**. In the case of ***st*-[PE$_3$]$_2$**, we estimate $\Delta G_0 \approx 0.24$ eV and $k_r(L \rightarrow E)/k_r(E \rightarrow L) \approx 10^7$. These results suggest that, for ***st*-[PE$_3$]$_2$**, $k_r(E \rightarrow L)\tau_0(E)$ is less than one and parameter $B$ is determined by $k_r(L \rightarrow E)\tau_0(E)$. According to Eq. 1 and recalling that $k_r(E)/k_r(L) \approx 10^{-2}$, the product $k_r(L \rightarrow E)\tau_0(E)$ should then be smaller than 100 in order to reproduce a stronger emission from the local state than from the excimer state, as is experimentally observed. This result sets an upper bound for the forward reaction rate in ***st*-[PE$_3$]$_2$** with $k_r(L \rightarrow E) < 10^9$ s$^{-1}$ . Based on the constraints that this analysis places on the forward rate constant $k_r(L \rightarrow E)$, the activation barrier for the transition from the local excited state to the excimer state in ***st*-[PE$_3$]$_2$** is at least 0.1 eV larger than in ***st*-[PE$_5$]$_2$**.

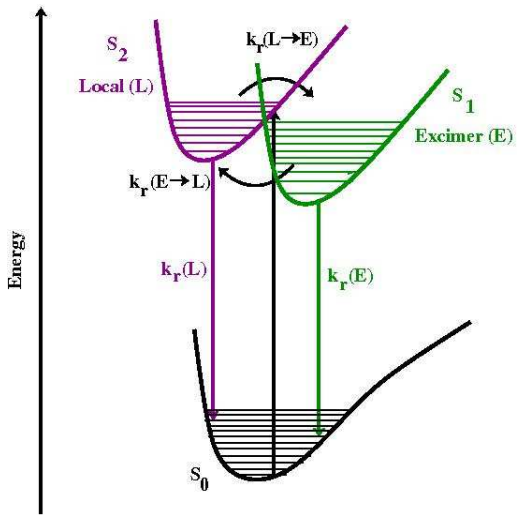


**Figure 7**: Schematic diagram showing the lowest local-excited state ($L$) (marked in purple) and the excimer-like state ($E$) (marked in green). The ground state is marked in black. The photo-induced absorption is marked by a black arrow pointing upwards. The radiative rate constants from the $L$ ($k_r(L)$) and $E$ states ($k_r(E)$) and the forward ($k_r(L \rightarrow E)$) and backward ($k_r(E \rightarrow L)$) rate constants between the $L$ and the $E$ states are also depicted.

Thus, this simple three-level model provides a reasonable description of the difference in the emission spectra of ***st*-[PE$_3$]$_2$** and ***st*-[PE$_5$]$_2$** by correlating the relative populations in the local and excimeric states. In the case of both stacked molecules, absorption leads to population of the

*L*-state. This is followed by a substantial geometric relaxation; by comparing the experimental absorption and emission spectra of the stacked and unstacked molecules, such a relaxation is found to be on the order of 0.4 eV with the TDDFT results comparing well with the experimental observations. In ***st*-[PE$_3$]$_2$**, the emission spectra is dominated by a radiative transition from the *L*-state, as sketched in Figure 8A. In addition to this process, a small fraction of the locally-excited population decays into the low-lying excimeric state. Such a transition, however, is associated to an activation barrier, which restricts the excited-state population predominately into the higher-lying *L*-state. Therefore, the presence of the low-lying *E*-state results only in a broad tail in the emission spectra that is absent in the corresponding unstacked analogue, **PE$_3$**. In contrast, in the case of ***st*-[PE$_5$]$_2$,** the activation barrier appears to be lower than in ***st*-[PE$_3$]$_2$**. As a consequence, there occurs a significant transfer of population from the *L*-state to the *E*-state, leading to a significant red-shift in emission, see Figure 8B.

Interestingly, cyclophane-type stacked compounds, which provide for spatially limited interchain interactions, do not present contributions from excimeric states in their photo-physics. Thus, it is important to note that the design of the stacked molecules achieved in the present work, significantly modifies the low-energy photo-physics compared to that in the pseudo-para substituted stacked cyclophane of Figure 1A. In the latter case, the excimeric state ("phane-state") remains higher in energy compared to *L*-state, particularly for longer oligomers. As a result, the emission of **CP[PE$_3$]$_2$** is due to the local *L*-state only, with no contribution from the *E*-state, as sketched in Figure 8C.

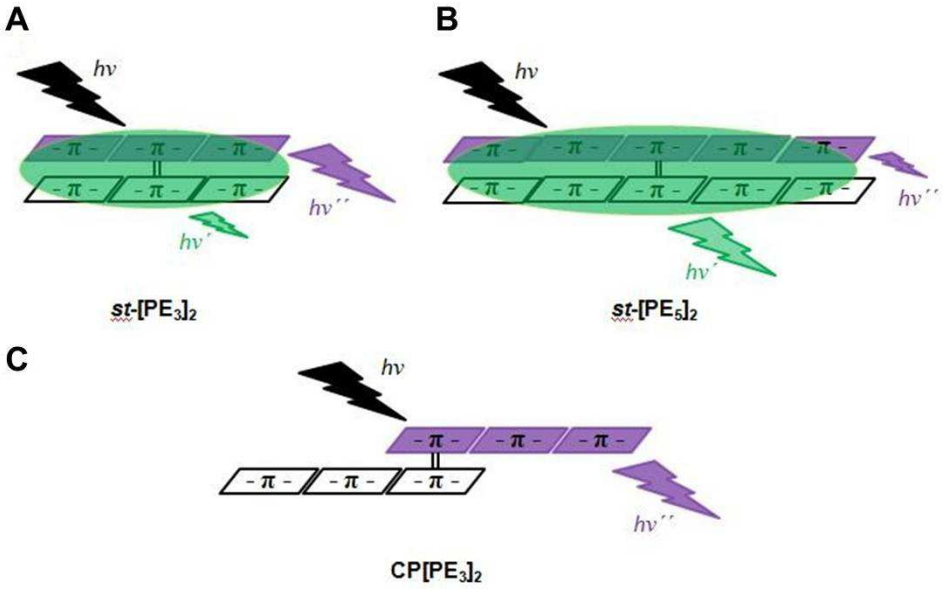


**Figure 8.** Schematic representation of the photophysical behavior of stacked oligo(phenylene ethynylene)s: A, benzo-fused bicyclo[4.4.1]undecane based stacked compounds, ***st*-[PE$_3$]$_2$ (A)** and ***st*-[PE$_5$]$_2$ (B)**; and pseudo-para [2.2]paracyclophane based stacked compound, **CP[PE$_3$]$_2$ (C)**.

***f) Conclusions***

A combined experimental and theoretical study of well-defined stacked oligo(phenylene ethynylene)s provides very useful insights into the effect of π-π interactions on the electronic structure of closely packed conjugated chains. Our synthetic strategy results in molecular architectures where oligomer units are stacked atop one another in such a way that strong electronic interactions occur over the entire length of the chromophoric moieties.

The absorption and emission spectra of the stacked compounds were compared to those of the individual unstacked oligomers. These optical studies, when analyzed together with the results of TDDFT calculations, clearly demonstrate the effect of inter-chain interactions on the low-energy photo-physics of stacked compounds. The consideration of a simple three-state model provides an explanation for the large red shift observed in ***st*-[PE$_5$]$_2$** compared to its shorter analogue ***st*-[PE$_3$]$_2$**; the reason lies in the competition between emission from a local excited state and from an excimer state.

Interestingly, cyclophane-type stacked compounds, which provide for spatially limited interchain interactions, do not present contributions from excimer states in their photophysics. Thus, stacked molecules such as ***st*-[PE$_3$]$_2$** and ***st*-[PE$_5$]$_2$** serve as better-suited platforms to develop an understanding of the interactions between cofacially stacked conjugated chains, since they more closely resemble the arrangement of the π-systems of semiconducting organic oligomers and polymers in thin-film organic electronic devices.

***References***


1. (a) Bredas, J. L.; Beljonne, D.; Coropceanu, V.; Cornil, J., *Chemical Reviews* **2004,** *104* (11), 4971-5003; (b) Bredas, J. L.; Cornil, J.; Beljonne, D.; dos Santos, D.; Shuai, Z. G., *Accounts of Chemical Research* **1999,** *32* (3), 267-276; (c) Cornil, J.; dos Santos, D. A.; Crispin, X.; Silbey, R.; Bredas, J. L., *Journal of the American Chemical Society* **1998,** *120* (6), 1289-1299; (d) Bredas, J. L.; Street, G. B., *Accounts of Chemical Research* **1985,** *18* (10), 309-315; (e) Warshel, A.; Karplus, M., *Journal of the American Chemical Society* **1972,** *94* (16), 5612-&; (f) Yang, S. C.; Graupner, W.; Guha, S.; Puschnig, P.; Martin, C.; Chandrasekhar, H. R.; Chandrasekhar, M.; Leising, G.; Ambrosch-Draxl, C.; Scherf, U., *Physical Review Letters* **2000,** *85* (11), 2388-2391.
2. Moliton, A.; Hiorns, R. C., *Polymer International* **2004,** *53* (10), 1397-1412.
3. (a) Jenekhe, S. A.; Osaheni, J. A., *Science* **1994,** *265* (5173), 765-768; (b) Sluch, M. I.; Godt, A.; Bunz, U. H. F.; Berg, M. A., *Journal of the American Chemical Society* **2001,** *123* (26), 6447-6448.
4. (a) Garnier, F.; Hajlaoui, R.; Yassar, A.; Srivastava, P., *Science* **1994,** *265* (5179), 1684-1686; (b) Sirringhaus, H.; Tessler, N.; Friend, R. H., *Science* **1998,** *280* (5370), 1741-1744; (c) Katz, H. E.; Lovinger, A. J.; Johnson, J.; Kloc, C.; Siegrist, T.; Li, W.; Lin, Y. Y.; Dodabalapur, A., *Nature* **2000,** *404* (6777), 478-481.
5. (a) Burroughes, J. H.; Bradley, D. D. C.; Brown, A. R.; Marks, R. N.; Mackay, K.; Friend, R. H.; Burns, P. L.; Holmes, A. B., *Nature* **1990,** *347* (6293), 539-541; (b) Sheats, J. R.; Antoniadis, H.; Hueschen, M.; Leonard, W.; Miller, J.; Moon, R.; Roitman, D.; Stocking, A., *Science* **1996,** *273* (5277), 884-888; (c) Friend, R. H.; Gymer, R. W.; Holmes, A. B.; Burroughes, J. H.; Marks, R. N.; Taliani, C.; Bradley, D. D. C.; Dos

Santos, D. A.; Bredas, J. L.; Logdlund, M.; Salaneck, W. R., *Nature* **1999,** *397* (6715), 121-128.

6. (a) Sariciftci, N. S.; Smilowitz, L.; Heeger, A. J.; Wudl, F., *Science* **1992,** *258* (5087), 1474-1476; (b) Halls, J. J. M.; Walsh, C. A.; Greenham, N. C.; Marseglia, E. A.; Friend, R. H.; Moratti, S. C.; Holmes, A. B., *Nature* **1995,** *376* (6540), 498-500; (c) Yu, G.; Gao, J.; Hummelen, J. C.; Wudl, F.; Heeger, A. J., *Science* **1995,** *270* (5243), 1789-1791.
7. (a) Bartholomew, G. P.; Bazan, G. C., *Accounts of Chemical Research* **2001,** *34* (1), 30-39; (b) Morisaki, Y.; Chujo, Y., *Progress in Polymer Science* **2008,** *33* (3), 346-364; (c) Salhi, F.; Lee, B.; Metz, C.; Bottomley, L. A.; Collard, D. M., *Organic Letters* **2002,** *4* (19), 3195-3198; (d) Guyard, L.; Audebert, P., *Electrochemistry Communications* **2001,** *3* (4), 164-167.
8. Song, C.; Swager, T. M., *Organic Letters* **2008,** *10* (16), 3575-3578.
9. (a) Mataka, S.; Takahashi, K.; Mimura, T.; Hirota, T.; Takuma, K.; Kobayashi, H.; Tashiro, M.; Imada, K.; Kuniyoshi, M., *Journal of Organic Chemistry* **1987,** *52* (13), 2653-2656; (b) Mataka, S.; Shigaki, K.; Sawada, T.; Mitoma, Y.; Taniguchi, M.; Thiemann, T.; Ohga, K.; Egashira, N., *Angewandte Chemie-International Edition* **1998,** *37* (18), 2532-2534; (c) Knoblock, K. M.; Silvestri, C. J.; Collard, D. M., *Journal of the American Chemical Society* **2006,** *128* (42), 13680-13681.
10. Morisaki, Y.; Sawamura, T.; Murakami, T.; Chujo, Y., *Organic Letters* **2010,** *12* (14), 3188-3191.
11. Giaimo, J. M.; Lockard, J. V.; Sinks, L. E.; Scott, A. M.; Wilson, T. M.; Wasielewski, M. R., *Journal of Physical Chemistry A* **2008,** *112* (11), 2322-2330.
12. Mangalum, A.; Morgan, B. P.; Hanley, J. M.; Jecen, K. M.; McGill, C. J.; Robertson, G. A.; Smith, R. C., *Chemical Communications* **2010,** *46* (28), 5136-5138.
13. Kaikawa, T.; Takimiya, K.; Aso, Y.; Otsubo, T., *Organic Letters* **2000,** *2* (26), 4197-4199.
14. Bazan, G. C.; Oldham, W. J.; Lachicotte, R. J.; Tretiak, S.; Chernyak, V.; Mukamel, S., *Journal of the American Chemical Society* **1998,** *120* (36), 9188-9204.
15. *Handbook of conducting polymers*. 3rd ed / ed.; CRC: Boca Raton, Fla. ;, 2007.
16. Karplus, M., *Journal of the American Chemical Society* **1963,** *85* (18), 2870-+.

17. Veldman, D.; Chopin, S. M. A.; Meskers, S. C. J.; Groeneveld, M. M.; Williams, R. M.; Janssen, R. A. J., *Journal of Physical Chemistry A* **2008,** *112* (26), 5846-5857.
18. Shirai, S.; Iwata, S.; Tani, T.; Inagaki, S., *Journal of Physical Chemistry A* **2011,** *115* (26), 7687-7699.
19. Druzhinin, S. I.; Ernsting, N. P.; Kovalenko, S. A.; Lustres, L. W.; Senyushkina, T. A.; Zachariasse, K. A., *Journal of Physical Chemistry A* **2006,** *110* (9), 2955-2969.
20. Veldman, D.; Chopin, S. M. A.; Meskers, S. C. J.; Janssen, R. A. J., *Journal of Physical Chemistry A* **2008,** *112* (37), 8617-8632.
21. Chai, J. D.; Head-Gordon, M., *Journal of Chemical Physics* **2008,** *128* (8).
22. Chai, J. D.; Head-Gordon, M., *Physical Chemistry Chemical Physics* **2008,** *10* (44), 6615-6620.
23. Frisch, M. J. T. *et al*., *Gaussian 09*, A.02; Gaussian Inc.: Wallingford CT, 2009.

## A.2. Chapter 5

### *a) Theoretical Methodology*

The geometry optimization of the individual oligomers (**$Me_2PV_2$** and **$Me_2PV_3$**) are performed using B3LYP hybrid functional[3] and 6-31g** basis set. In addition to the gas phase optimized geometries, optimizations are also performed in the solvent phase using polarizable continuum model[4] (PCM); the dielectric constant is chosen to be that of the chloroform ($\varepsilon = 4.7$). Using these ground state optimized geometries, time-dependent density functional theory (TDDFT) calculations are performed to obtain the low-lying excited states of the oligomers, using both B3LYP and ωB97X[5] (long-range corrected) functionals and 6-31g** basis set. The range separated functional predicts correct energies for states with large CT contributions, whose energies are usually underestimated using B3LYP functional. The long-range corrected functional is primarily chosen in order to compare the energies of the ground and low-lying excited states of the unstacked oligomers with the corresponding stacked analogue. For the sake of comparison with the ground state, the geometries of the first excited ($S_1$) states of **$Me_2PV_2$** and **$Me_2PV_3$** are obtained using both TD-B3LYP functional and 6-31g** basis set. On these geometries, the TDDFT energies are computed using B3LYP and ωB97XD functional, which are used to compare with the experimental fluorescence spectra.

For stacked molecules (***pg*-$Cp[PV_2]_2$** and ***pg*-$Cp[PV_3]_2$**), the geometry optimizations are performed using B3LYP-D/6-31g**[6] methods. For the sake of simplicity, the butyl-groups attached to the terminal phenyl rings of ***pg*-$Cp[PV_3]_2$** are replaced by hydrogen atoms. In these molecules, the dispersion interaction is essential in predicting the relative orientation of the individual stacks (**$Me_2PV_2$** and **$Me_2PV_3$**). In addition, similar to unstacked analogues, the geometry optimizations are also performed in presence of solvent dielectric ($\varepsilon = 4.7$). Using these geometries, the excited state energies are obtained using TD- ωB97X-D/6-31g** method.[7] In this case, the long-range corrected functional (ωB97X-D) is preferred over B3LYP-D functional because it correctly predicts the nature of the charge transfer (CT) state, which is important for predicting the energies of low-lying excited states for the stacked compounds. The geometry of the first excited state ($S_1$) is obtained using TD-B3LYP-D/6-31g** method. As done in case of ground state geometries, the energies of low-lying excited states in $S_1$ state geometry are obtained using TD-ωB97X-D/6-31g** method, which are compared to experimental

fluorescence spectra. The geometry optimization of ground and excited states using B3LYP-D functional is performed using Turbomole 6.1 package,[8] whereas the geometry optimizations and TDDFT calculations using ωB97X/ωB97X-D functional are performed using Gaussian 09 package.[9]

***b) Structure of stacked and un-stacked molecules***

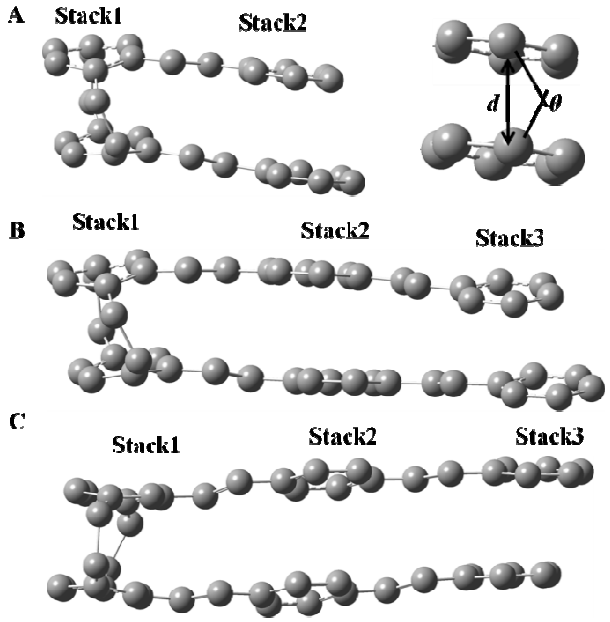


**Figure 4.** Optimized ground state geometries of **(A)** ***pg*-Cp[$PV_2$]$_2$**, **(B)** ***pg*-Cp[$PV_3$]$_2$** (cisoid conformer) and **(C)** ***pg*-Cp[$PV_3$]$_2$** (transoid conformer), obtained using B3LYP-D/6-31g** method. For clarity, the hydrogen atoms are not shown in the figure. d and θ denote the distance and torsional angles between the pair of phenyl rings, belonging to the same stack.

**Table 1:** Comparison of selected structural parameters (distance ($d_i$) and angle ($a_i$) between the stack) of the paracyclophane bridge and the stacked compounds (***pg*-Cp[PV$_2$]$_2$** and ***pg*-Cp[PV$_3$]$_2$**) in ground and excited-state optimized geometries, obtained using B3LYP-D/6-31g** method in gas-phase. Structural parameters of two different conformations of ***pg*-Cp[PV$_3$]$_2$** (cisoid and transoid) are tabulated. The distances and the angles are marked in Figure 4.

| Molecule | Conformation | Geometry | Distance (Å) | | | Angle (degree) | | |
|---|---|---|---|---|---|---|---|---|
| | | | $d_1$ | $d_2$ | $d_3$ | $\theta_1$ | $\theta_2$ | $\theta_3$ |
| ***Cp*** | - | GS | 3.08 | - | - | 3.9 | - | - |
| | - | EX | 2.89 | - | - | 3.7 | - | - |
| ***pg*-Cp[PV$_2$]$_2$** | - | GS | 3.11 | 3.79 | - | 6.5 | 7.8 | - |
| | - | EX | 2.99 | 3.33 | - | 4.3 | 5.3 | - |
| ***pg*-Cp[PV$_3$]$_2$** | cisoid | GS | 3.11 | 3.67 | 3.79 | 6.2 | 6.9 | 6.9 |
| | | EX | 3.02 | 3.33 | 3.50 | 3.6 | 5.2 | 4.2 |
| | transoid | GS | 3.11 | 3.70 | 3.75 | 6.4 | 7.8 | 7.9 |
| | | EX | 3.02 | 3.31 | 3.51 | 3.8 | 5.3 | 4.6 |

In this section the focus is mainly on the structural properties of the stacked molecules (***pg*-Cp[PV$_2$]$_2$** and ***pg*-Cp[PV$_3$]$_2$**) in the ground and $S_1$ optimized geometries. A few of the structural parameters are tabulated in Table 1. For the sake of comparison, the structural parameters of the Cyclophane (**Cp**) bridge are also tabulated in the same table. The structural parameters include (i) distance between the centers and (ii) the torsional angles between the phenyl rings, corresponding to individual stacks. The side-view of gas-phase optimized geometries, distances, angles and the nomenclature of the stacks are indicated in Figure 4. The top view is depicted in Figure S1 in SI.

The X-ray crystal structure of **Cp** indicates that the distance and the torsional angle between the stacks are 3.10 Å and 4.3º respectively. These structural parameters compare well with those of the ground state optimized geometry. In the excited state, the stacking distance reduces by 0.19 Å. Such a reduction in stacking distances is even more prominent with the stacked molecules (***pg*-Cp[PV$_2$]$_2$** and ***pg*-Cp[PV$_3$]$_2$**). In ground state of ***pg*-Cp[PV$_2$]$_2$**, the stacking distance at the bridge position (Stack1) is comparable to that in **Cp**, whereas that in the

peripheral stack increases to 3.79 Å. Such an increase in the stacking distance at the peripheral rings is due to the increase in the slip distance (1.87 Å) between the two phenyl rings. In the excited state, the stacking distances at the bridge position is slightly smaller as compared to the ground state (0.12 Å), whereas the same at the peripheral position reduces by 0.46 Å. The reduction in the stacking distance is attributed to the formation of inter-stack excimer-like state (E), whose energies and geometries are discussed in the next section. In the ground state optimized geometries the dihedral angle ($\theta_i$) between the phenyl rings are within 6-8°, whereas the same in excited state reduces by ~ 2°. Furthermore, the geometry of ***pg*-Cp[PV$_2$]$_2$** is optimized in presence of solvent dielectric. The optimized geometry thus obtained is comparable to the gas-phase optimized geometry.

Similar trends in structural parameters are observed in case of both the conformers of ***pg*-Cp[PV$_3$]$_2$** in ground state**.** The stacking distances and torsional angles between the bridged phenyl pair are comparable to those of the stacked "dimer". On the other hand, the stacking distances of the neighboring phenyl rings are smaller than the stack2 of ***pg*-Cp[PV$_2$]$_2$** by 0.13 Å. For the peripheral phenyl rings (stack3), the stacking distances are larger than that of the stack2 by ~ 0.1 Å. All the dihedral angles are comparable to that of ***pg*-Cp[PV$_2$]$_2$**. In excited state, similar to ***pg*-Cp[PV$_2$]$_2$**, the stacking distance of bridged phenyl reduces 0.09 Å, whereas the same for stack2 and stack3 reduces by ~ 0.35 Å and 0.25 Å respectively. Thus the change in geometry of the peripheral rings due to excitation is less significant as compared to the phenyl rings neighboring the **Cp** bridge. Similar to ***pg*-Cp[PV$_2$]$_2$,** the solvent phase optimized geometries are close to the gas-phase optimized structure.

**Table 2**: Absorption and emission maxima (in nm and eV) of stacked (***pg*-Cp[PV$_2$]$_2$** and ***pg*-Cp[PV$_3$]$_2$**) and unstacked (**Me$_2$PV$_2$** and **Me$_2$PV$_3$**) molecules.

| Molecule | Absorption Maxima nm (eV) | Emission Maxima nm (eV) |
|---|---|---|
| **Me$_2$PV$_2$** | 297 (4.17)[a] | 345, 359, 381, 396 (3.59, 3.45, 3.25, 3.13[s])[a] |
| ***pg*-Cp[PV$_2$]$_2$** | 296, 358[s] (4.19, 3.38[s])[a] | 429, 463 (2.89, 2.68)[a] |
| **Me$_2$PV$_3$** | 352 (3.52)[a] | 396, 416, 440, 475 (3.13, 2.97, 2.82, 2.61[s])[a] |
| ***pg*-Cp[PV$_3$]$_2$** | 350, 404[s] (3.54, 3.07[s])[a] | 404, 427, 446, 481 (3.07, 2.90, 2.78, 2.58[s])[a] |

[s] Shoulder peak. [a] Energies for transitions are computed from de-convoluted spectra.

The stacked oligomers and unstacked linear analogues were characterized by UV-Vis and fluorescence spectroscopy to explore the effect of stacking on the electronic structure of the conjugated tiers. The absorption and fluorescence spectra of stacked and unstacked molecules are depicted in Figure 5. The absorption maximum of the stacked "dimer" (***pg*-Cp[PV$_2$]$_2$**) (4.19 eV) is blue shifted by 20 meV relative to the unstacked linear analog, **Me$_2$PV$_2$** (4.17 eV). In addition, the absorption spectra of the stacked molecule, in contrast to that of **Me$_2$PV$_2$**, contains a low energy tail (mentioned as shoulder peak in Table 2), which is the signature of the cofacial stacking. The emission spectrum of **Me$_2$PV$_2$** possesses three distinct peaks at 3.59 eV, 3.45 eV and 3.25 eV and, in addition, has a broad tail, which is centered on 3.13 eV. The 0-0 emission band is significantly red-shifted compared to the absorption maxima (~ 0.6 eV). The additional peaks are associated to the vibrational progression of 0-0 emission band (3.59 eV). On the other hand, the emission spectrum of the stacked "dimer" possesses a broad peak (2.89 eV) with a distinct tail at ~ 2.68 eV and does not possess any well-resolved vibrational features as seen in the unstacked analogue. In addition, the emission spectrum of the stacked "dimer" is significantly red-shifted compared to its unstacked analogue. For **Me$_2$PV$_3$**, the absorption maximum is at 3.52 eV, whereas that of the stacked "trimer" (***pg*-Cp[PV$_3$]$_2$**) is at 3.54 eV.

Similar to the stilbene analogue, the absorption maximum of the stacked "trimer" is blue shifted by 20 meV relative to the unstacked linear analog. In addition, similar to its smaller analogue, the stacked molecule possesses an absorption edge at ~ 3.07 eV, which can be rationalized as the effect of stacking. Similar to **$Me_2PV_2$**, the emission spectrum of **$Me_2PV_3$** possesses three distinct peaks at 3.13 eV, 2.97 eV and 2.82 eV and a tail ~ 2.61 eV. The 0-0 emission band (3.13 eV) is red-shifted from the absorption maxima by 0.4 eV. The additional peaks are associated to the vibrational progression of 0-0 emission band. On the other hand, in contrast to the smaller analogue, the emission spectrum of the stacked "trimer" resembles well with that of the unstacked analogue; the emission spectrum possesses three well-resolved peaks at 3.07 eV, 2.90 eV and 2.78 eV and a broad tail at 2.58 eV. Thus by comparing the absorption and emission spectra of the stacked and unstacked molecules, we can conclude that the stacked dimer emission is mostly from an excimeric state, as observed in ***st*-$[PE_5]_2$**. On the other hand, the stacking of **$Me_2PV_3$** does not lead to significant change of the emission spectrum, which is mainly dominated by the local-state contribution. This issue is discussed in further details in the next section.

***c) Computational Results***

To gain further insight into the photo-physical properties of the stacked and un-stacked molecules, the energy and the oscillator strengths of a few low-lying excited states are computed using TDDFT method. The computed gaps, oscillator strengths and ground state relaxation energies are listed in Table 3. For individual oligomers, the TDDFT $S_0 \rightarrow S_1$ transition energies are overestimated by ~ 0.3 eV compared to the experimental absorption maxima, but in agreement with experiment, show ~0.6 eV decrease in $S_1$ energy in **$Me_2PV_3$** compared to **$Me_2PV_2$**. In addition, the inclusion of the solvent (geometry optimizations followed by excited state calculations using TDDFT) predicts ~0.2 eV decrease in optical gap for **$Me_2PV_2$** and ~0.15 eV for **$Me_2PV_3$**. Thus combining the above two schemes, the experimentally observed absorption maxima are well reproduced by the TD-DFT procedure. On the other hand, gas-phase TD-B3LYP predicts the first excited state of **$Me_2PV_2$** at 3.98 eV, whereas that of the **$Me_2PV_3$** is at 3.25 eV (both cisoid and transoid molecules possess the same gaps). Thus B3LYP underestimates the energy gap by ~0.2-0.3 eV, which is expected to increase with the inclusion of solvent effects. The computed energy gaps using ωB97X functional is higher compared to that

obtained using B3LYP functional, which is mainly due to larger contribution of the HF exchange functional, which tend to localize the excited states. The relaxed $S_1$ energy of **$Me_2PV_2$** and **$Me_2PV_3$** are at 3.6 eV and 3.2 eV (The difference in the relaxed $S_1$ state for the cisoid and transoid conformations is 0.07 eV). The TDDFT energies compare well with the experimentally observes 0-0 emission band of **$Me_2PV_2$** and **$Me_2PV_3$**. The TD-B3LYP underestimates the relaxed $S_1$ states of **$Me_2PV_2$** and **$Me_2PV_3$** by ~0.3-0.4 eV. The ground state relaxation energies for **$Me_2PV_2$** is 0.4 eV, whereas that of **$Me_2PV_3$** varies between 0.36-0.29 eV (the transoid conformation has smaller relaxation energy). Such a large relaxation is primarily due to the planarization of the phenyl rings in the excited states, where the dihedral angles varies between 0-15º, in comparison to ~ 30° torsion between the phenyl rings in ground state. The computed relaxation energies are comparable to the vibrational progression (~ 0.5 eV) of **$Me_2PV_2$** and **$Me_2PV_3$**.

Now we focus on the computed spectra of ***pg*-$Cp[PV_2]_2$** and ***pg*-$Cp[PV_3]_2$**. In ***pg*-$Cp[PV_2]_2$**, the $S_1$ state is dominated by HOMO→LUMO transition with small contributions from the HOMO-1→LUMO+1 transition. Such a linear combination indicates that the $S_1$ state in the stacked systems has significant inter-oligomer CT contributions.[10] The computed $S_1$ state is overestimated compared to the absorption shoulder by ~ 0.2 eV. In presence of solvent, the $S_1$ state is stabilized by 0.05 eV. Such a small stabilization in presence of solvent dielectric is because of the presence of two symmetric CT contributions, which results in negligible dipole moment of this state. On the other hand, the computed $S_2$ state is at 4.19 eV, which is comparable to experimental absorption maxima and is also comparable to the $S_1$ state of the unstacked oligomer. In presence of solvent, the $S_2$ state is stabilized by 0.09 eV, which is roughly half of that of the corresponding oligomer (0.2 eV). However, as a result of CT contributions, the $S_1$ state experience very large structural relaxations upon excitation (2.27 eV). In this relaxed geometry, the stacking distances between the phenyl rings (stack2) reduces by 0.46 Å compared to the ground state geometry. In this geometry the first excited state is dominated only by HOMO→LUMO transition, which indicates to the increase of CT character in the first excited state. Such significant change in geometry also leads to large ground state relaxation energies of ~0.7 eV. By adding the relaxed $S_1$ state energy (2.27 eV) with the ground state relaxation (0.71 eV), we predict the 0-0 transition from the $S_1$ state at 2.98 eV, which correspond well with

experimentally observed 2.89 eV emission peak. The broad tail is a consequence of large vibrational relaxation.

Similar to ***pg*-Cp[PV$_2$]$_2$**, the $S_1$ state of ***pg*-Cp[PV$_3$]$_2$** is ~ 0.1 eV higher than the absorption shoulder and is dominated by HOMO→LUMO transition with small contributions from the HOMO-1→LUMO+1 transition. The solvent phase calculations reduce the $S_1$ energy by 0.02 eV. Furthermore, the energy of $S_2$ state is at ~ 3.60 eV, which is close in energy as compared to the $S_1$ state (3.52 eV) of the corresponding oligomer. The $S_2$ state is stabilized by 0.1 eV in presence of solvent dielectric. Thus the computed $S_1$ and $S_2$ states compare well with the experimental absorption spectra. Similar to ***pg*-Cp[PV$_2$]$_2$**, the $S_1$ state of ***pg*-Cp[PV$_3$]$_2$** experience large structural relaxations upon excitation (2.12 eV). In this relaxed geometry, the stacking distances between the phenyl rings (stack2) reduce by ~ 0.35 Å compared to the ground state geometry. Such significant changes in geometry lead to large ground state relaxation energies of ~ 0.65 eV. The difference in energy between the first excited states of stacked "dimer" and "trimer" is much smaller in the excited state relaxed geometry as compared to that in the ground state geometry (0.15 eV w.r.t 0.38 eV). The inspection of the frontier orbitals contributing to relaxed $S_1$ states of ***pg*-Cp[PV$_2$]$_2$** and ***pg*-Cp[PV$_3$]$_2$** indicate that for ***pg*-Cp[PV$_2$]$_2$** the molecular orbitals are delocalized over the entire length of the molecule, whereas for ***pg*-Cp[PV$_3$]$_2$** the orbitals are mainly localized over the dimer segment (Figure 6). The TDDFT results also indicate that the relaxed 0-0 band of $S_1$ state (2.77 eV) is significantly lower in energy than the 0-0 emission peak (3.07 eV). This clearly indicates that the fluorescence is primarily observed form the relaxed oligomeric state ($S_2$; *L*-state), as opposed from the low-lying $S_1$ state. A slightly broader tail of the stacked "trimer" as compared to its unstacked oligomer is plausibly due to some amount of population in the low-energy $S_1$ state (*E*-state). From these results, we conclude that the emission of the stacked "dimer" is primarily due to the low-lying $S_1$ state, whereas the same for the stacked "trimer" is primarily dominated by the higher lying local state ($S_2$).

**Table 3**: Vertical excitation energies ($E_{ge}$ in eV) and oscillator strengths ($f_{ge}$) of un-stacked and stacked molecules computed at ground and excited-state optimized geometries in gas-phase. The relaxation energies ($\lambda_{gs}$) of the ground states in the gas-phase are mentioned here.

| Molecule | Conformation | State | $E_{ge}$ ($f_{ge}$) | | $\lambda_{gs}$ |
|---|---|---|---|---|---|
| | | | Ground State | Excited State | |
| **$Me_2PV_2$** | - | $S_1$ | 4.46 (0.91) | 3.58 (0.92) | 0.44 |
| ***pg*-$Cp[PV_2]_2$** | - | $S_1$<br>$S_2$ | 3.58 (0.01)<br>4.19 (0.66) | 2.27 (0.01) | 0.71 |
| **$Me_2PV_3$** | cisoid | $S_1$ | 3.85 (1.92) | 3.28 (1.97) | 0.36 |
| | transoid | $S_1$ | 3.83 (1.94) | 3.21 (1.95) | 0.29 |
| ***pg*-$Cp[PV_3]_2$** | cisoid | $S_1$<br>$S_2$ | 3.17 (0.02)<br>3.64 (2.24) | 2.12 (0.01) | 0.65 |
| | transoid | $S_1$<br>$S_2$ | 3.21 (0.02)<br>3.60 (2.26) | 2.11 (0.01) | 0.66 |

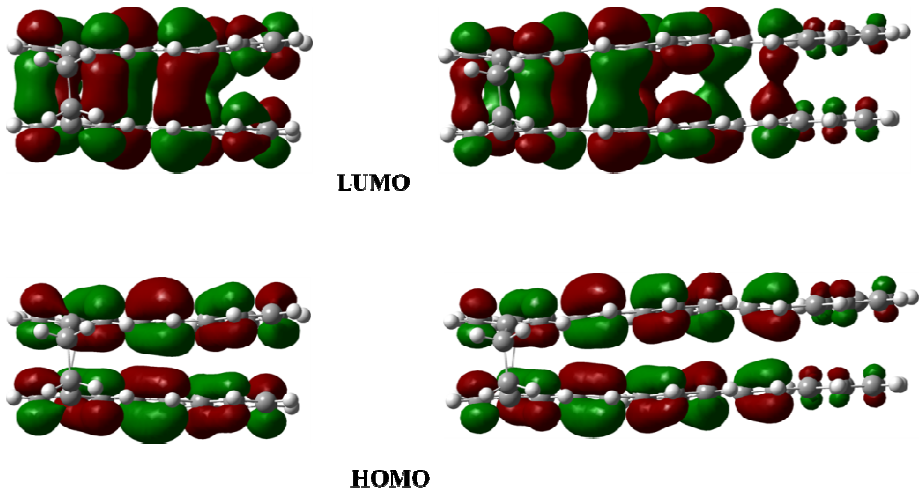


**Figure 6.** Frontier molecular orbitals of ***pg*-$Cp[PV_2]_2$** (left panel) and transoid-***pg*-$Cp[PV_3]_2$** (right panel) in the $S_1$ optimized geometry.

The relative contributions of *L*- and *E*-states (Figure 7) to the overall emission spectra depends on the interplay of several molecular parameters; (i) the energy of activation ($E_{ac}$), (ii) energy difference between the relaxed $S_1$ and $S_2$ states ($\Delta E^0$) and (iii) the reorganization energy ($\lambda$). In this case the $\Delta E^0$ is negative and $E_{ac}$ can be computed using the following equation;[11]

$$E_{ac} = \frac{\lambda}{4}\left(1 - \frac{\Delta E^0}{\lambda}\right)^2 \quad (1)$$

where, the symbols have their usual meanings. By comparing the emission spectra of ***pg*-Cp[PV$_2$]$_2$** and **Me$_2$PV$_2$** the relaxed local-state is expected at 3.59 eV. The theoretically computed local-state at the relaxed $S_1$ geometry is at 4.64 eV. This state is identified as local-state because it is primarily dominated by the HOMO-1→LUMO and HOMO→LUMO+1 transitions. Considering these energies, the computed $\Delta E^0$ and the $\lambda$ are 0.61 eV and 1.05 eV respectively. Using $\Delta E^0$ and the $\lambda$, the computed $E_{ac}$ is 0.03 (of the order of $k_BT$ at room temperature). Such a low activation barrier results is shifting of the population from the local-state to the $S_1$ state, which has contribution from both excitonic and CT contributions. Similar calculations on ***pg*-Cp[PV$_3$]$_2$** predicts the activation barrier of 0.10 eV, which from an Arrhenius type of argument indicates that the population of the local-state ($S_2$) will be ~ $10^2$ times higher than the $S_1$ state.

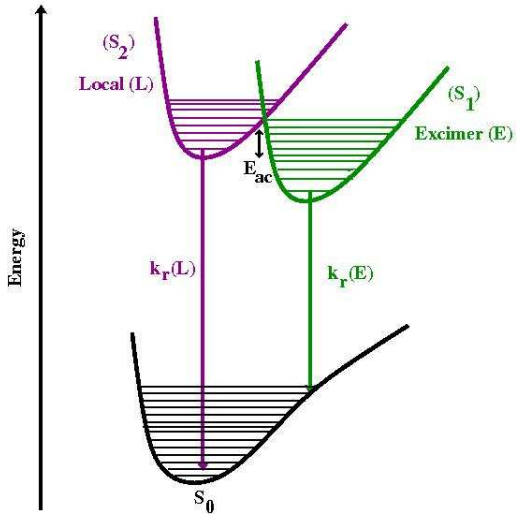


**Figure 7**: Schematic diagram showing the lowest local-excited state (*L*) (marked in purple) and the excimer-like state (*E*) (marked in green). The ground state is marked in black. The

radiative rate-constants from the *L* ($k_r(L)$) and the *E* states ($k_r(E)$). The activation barrier ($E_{ac}$) between the *L*- and *E*-state is depicted in the figure.

The above description clearly explains the difference in emission spectra of ***pg*-Cp[PV$_2$]$_2$** and ***pg*-Cp[PV$_3$]$_2$**, which depend on the relative population of the *L*- and *E*-state (Figure 7). In both the stacked compounds, absorption of incident photon results in population of the *L*-state. This is followed by a non-radiative geometric relaxation of the *L*-state, which primarily involves planarization of the phenyl-vinylene (PV) oligomers. Such a relaxation results in lowering of energy by 0.6-0.5 eV, depending on the length of the oligomer. This relaxed *L*-state in these stacked systems is higher in energy compared to *E*-state, irrespective of chain length. This is in sharp contrast to the pseudo-para and pseudo-ortho substituted cyclophane derivatives, as synthesized by Bazan.[2a, 2c] In these molecules the relative energy of the *L*-state and the *E*-state (referred to as "phane-state") is dependent on the length of the oligomers in each tier. For shorter oligomers, the first excited state is mainly and "excimer-state" delocalized over the two phenyl units of the cyclophane molecule. This is evident from the excited state ($S_1$) optimization followed by the natural-transition orbital (NTO) analysis (Figure 8), which clearly shows that the para-analogue has significant "phane-state" contribution as opposed to the excimer contribution to the $S_1$ state of ***pg*-Cp[PV$_2$]$_2$**. The *E*-state of ***pg*-Cp[PV$_2$]$_2$** is delocalized over the entire molecule because of the cofacial stacking of the **PV$_2$** oligomers. Thus the broad emission spectra of ***pg*-Cp[PV$_2$]$_2$** is due to the shift of excited state population from the *L*-state to *E*-state due to the low activation barrier between these two states. On the contrary, this activation barrier for ***pg*-Cp[PV$_3$]$_2$** increases by ~ 0.1 eV, which hinders such population transfer, resulting in oligomer-type ($PV_3$) emission with broad low-energy tail. This is also in contrast to its ortho- and para-analogues, as synthesized by Bazan et al.[2a, 2c] The NTO analysis (The NTOs of ortho-analogue are shown in Figure 9) of the relaxed first excited states of ortho- and para-analogues are primarily localized on one chain and thus characterized as "oligomer-like" emission by Bazan et al.

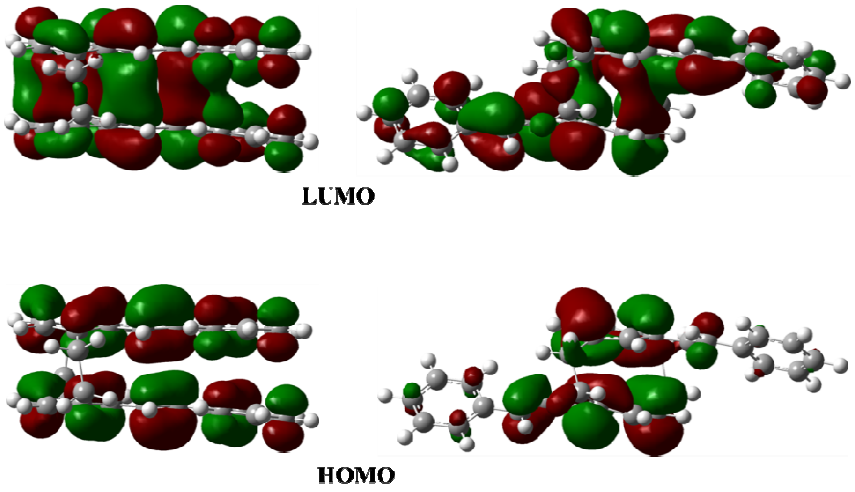


**Figure 8**: NTO orbitals of ***pg*-Cp[PV$_2$]$_2$** (left panel) and ***pp*-Cp[PV$_2$]$_2$** (right panel) in the relaxed $S_1$ geometry.

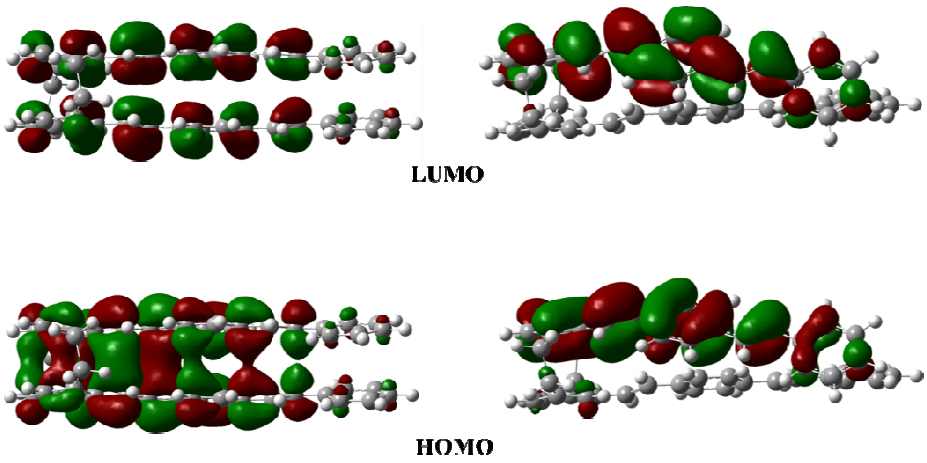


**Figure 9**: NTO orbitals of trans-***pg*-Cp[PV$_3$]$_2$** (left panel) and trans-***po*-Cp[PV$_3$]$_2$** (right-panel) in the relaxed $S_1$ geometry.

A combined experimental and theoretical study of well-defined stacked oligo(phenylene vinnylene)s provides insights into the electronic structure arising from interaction of π-systems in closely packed conjugated oligomers (or segments of analogous polymers). Our synthetic strategy results in stacking the oligomers on top of one another, which results in strong

electronic interaction throughout the entire length of the tier. Furthermore, we studied the effect of inter-chain interactions by varying the length of the oligomer. In order to have further insight into the effect of electronic interactions between the two tiers, the absorption and emission spectra of the stacked compounds are compared with those of the individual oligomers. Such a study along with the TDDFT calculations, clearly demonstrates the effect of inter-chain interaction on the low-energy photo-physics of stacked compounds. Furthermore, the TDDFT calculations combined with experimental absorption and emission spectra, demonstrates the effect of conjugation length on the relative energies of the local and excimeric states. The three-state model, described in previous section, enumerates the reason behind larger stokes shift of ***pg*-Cp[PV$_2$]$_2$** compared to its longer analogue (***pg*-Cp[PV$_3$]$_2$**), which is primarily due to low activation barrier between the *L*- and *E*-state. Thus the study of these stacked molecules (***pg*-Cp[PV$_2$]$_2$** and ***pg*-Cp[PV$_3$]$_2$**) clearly indicate to the effect of structural modification on the energy of the *E*-state relative to *L*-state. At this juncture, it is also important to note that the design of our molecules significantly restricts the fluctuation of one tier with respect to the other and thus provides a better resemblance with the arrangement of the π-systems in thin film electrooptic devices with high packing density.

***d) References***


1. (a) Bredas, J. L.; Beljonne, D.; Coropceanu, V.; Cornil, J., Charge-transfer and energy-transfer processes in pi-conjugated oligomers and polymers: A molecular picture. *Chemical Reviews* **2004,** *104* (11), 4971-5003; (b) Mishra, A.; Behera, R. K.; Behera, P. K.; Mishra, B. K.; Behera, G. B., Cyanines during the 1990s: A review. *Chemical Reviews* **2000,** *100* (6), 1973-2011.
2. (a) Bazan, G. C.; Oldham, W. J.; Lachicotte, R. J.; Tretiak, S.; Chernyak, V.; Mukamel, S., Stilbenoid dimers: Dissection of a paracyclophane chromophore. *Journal of the American Chemical Society* **1998,** *120* (36), 9188-9204; (b) Bartholomew, G. P.; Bazan, G. C., Bichromophoric paracyclophanes: Models for interchromophore delocalization. *Accounts of Chemical Research* **2001,** *34* (1), 30-39; (c) Oldham, W. J.; Miao, Y. J.; Lachicotte, R. J.; Bazan, G. C., Stilbenoid dimers: Effect of conjugation length and relative chromophore orientation. *Journal of the American Chemical Society* **1998,** *120* (2), 419-420.
3. Becke, A. D., DENSITY-FUNCTIONAL THERMOCHEMISTRY .3. THE ROLE OF EXACT EXCHANGE. *Journal of Chemical Physics* **1993,** *98* (7), 5648-5652.
4. Tomasi, J.; Mennucci, B.; Cammi, R., Quantum mechanical continuum solvation models. *Chemical Reviews* **2005,** *105* (8), 2999-3093.
5. Chai, J. D.; Head-Gordon, M., Systematic optimization of long-range corrected hybrid density functionals. *Journal of Chemical Physics* **2008,** *128* (8).
6. (a) Grimme, S., Accurate description of van der Waals complexes by density functional theory including empirical corrections. *Journal of Computational Chemistry* **2004,** *25* (12), 1463-1473; (b) Grimme, S., Semiempirical GGA-type density functional constructed with a long-range dispersion correction. *Journal of Computational Chemistry* **2006,** *27* (15), 1787-1799.
7. Chai, J. D.; Head-Gordon, M., Long-range corrected hybrid density functionals with damped atom-atom dispersion corrections. *Physical Chemistry Chemical Physics* **2008,** *10* (44), 6615-6620.

8. Ahlrichs, R.; Bar, M.; Haser, M.; Horn, H.; Kolmel, C., ELECTRONIC-STRUCTURE CALCULATIONS ON WORKSTATION COMPUTERS - THE PROGRAM SYSTEM TURBOMOLE. *Chemical Physics Letters* **1989,** *162* (3), 165-169.
9. Frisch, M. J. T., G. W.; Schlegel, H. B.; Scuseria, G. E.; Robb, M. A.; Cheeseman, J. R.; Montgomery, Jr., J. A.; Vreven, T.; Kudin, K. N.; Burant, J. C.; Millam, J. M.; Iyengar, S. S.; Tomasi, J.; Barone, V.; Mennucci, B.; Cossi, M.; Scalmani, G.; Rega, N.; Petersson, G. A.; Nakatsuji, H.; Hada, M.; Ehara, M.; Toyota, K.; Fukuda, R.; Hasegawa, J.; Ishida, M.; Nakajima, T.; Honda, Y.; Kitao, O.; Nakai, H.; Klene, M.; Li, X.; Knox, J. E.; Hratchian, H. P.; Cross, J. B.; Bakken, V.; Adamo, C.; Jaramillo, J.; Gomperts, R.; Stratmann, R. E.; Yazyev, O.; Austin, A. J.; Cammi, R.; Pomelli, C.; Ochterski, J. W.; Ayala, P. Y.; Morokuma, K.; Voth, G. A.; Salvador, P.; Dannenberg, J. J.; Zakrzewski, V. G.; Dapprich, S.; Daniels, A. D.; Strain, M. C.; Farkas, O.; Malick, D. K.; Rabuck, A. D.; Raghavachari, K.; Foresman, J. B.; Ortiz, J. V.; Cui, Q.; Baboul, A. G.; Clifford, S.; Cioslowski, J.; Stefanov, B. B.; Liu, G.; Liashenko, A.; Piskorz, P.; Komaromi, I.; Martin, R. L.; Fox, D. J.; Keith, T.; Al-Laham, M. A.; Peng, C. Y.; Nanayakkara, A.; Challacombe, M.; Gill, P. M. W.; Johnson, B.; Chen, W.; Wong, M. W.; Gonzalez, C.; and Pople, J. A *Gaussian 09*, A.02; Gaussian Inc.: Wallingford CT, 2009.
10. Shirai, S.; Iwata, S.; Tani, T.; Inagaki, S., Ab Initio Studies of Aromatic Excimers Using Multiconfiguration Quasi-Degenerate Perturbation Theory. *Journal of Physical Chemistry A* **2011,** *115* (26), 7687-7699.
11. (a) Barbara, P. F.; Meyer, T. J.; Ratner, M. A., Contemporary issues in electron transfer research. *Journal of Physical Chemistry* **1996,** *100* (31), 13148-13168; (b) Marcus, R. A.; Sutin, N., ELECTRON TRANSFERS IN CHEMISTRY AND BIOLOGY. *Biochimica Et Biophysica Acta* **1985,** *811* (3), 265-322.

**B. NMRs**

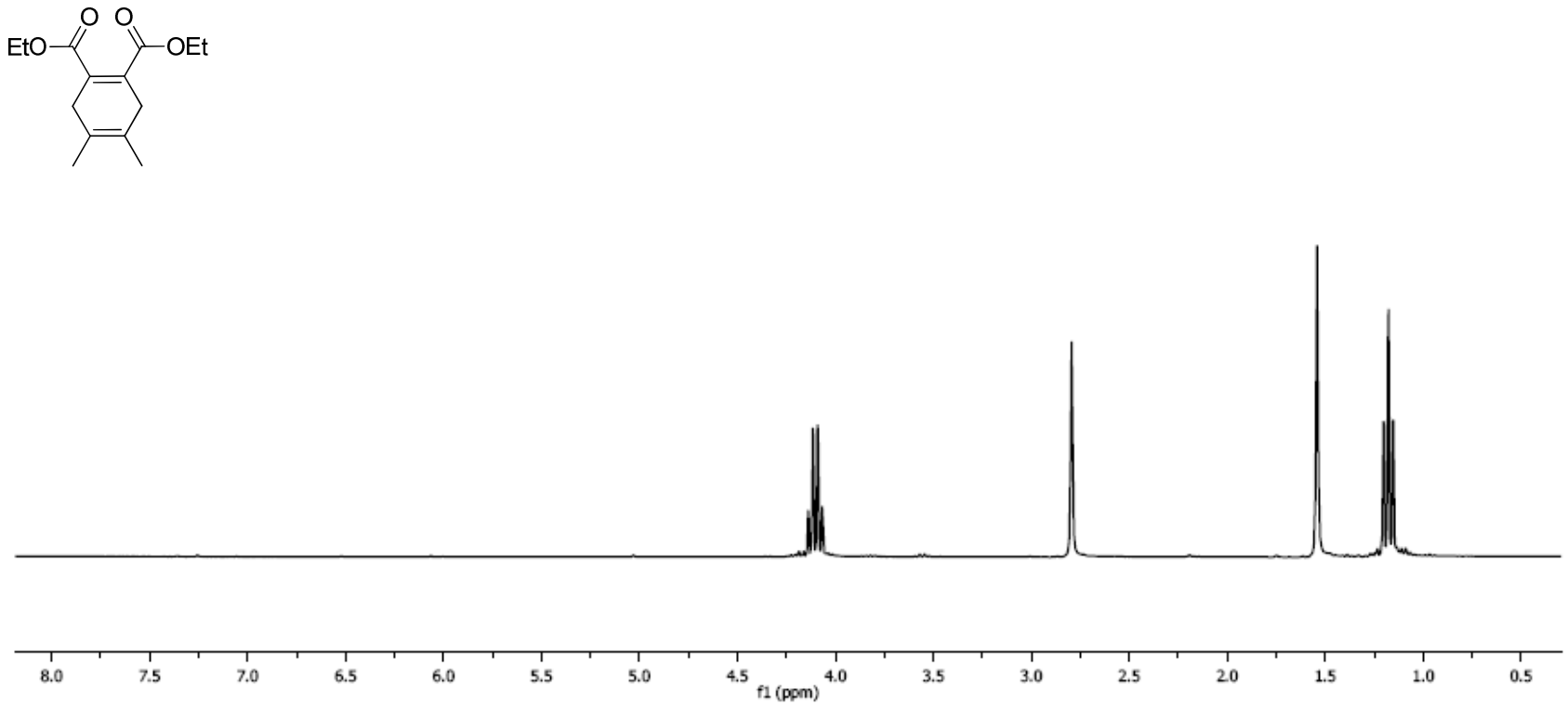


**Figure 1A.** $^{1}$H NMR spectrum of **III-1** (300 MHz, $CDCl_3$, 23 °C).

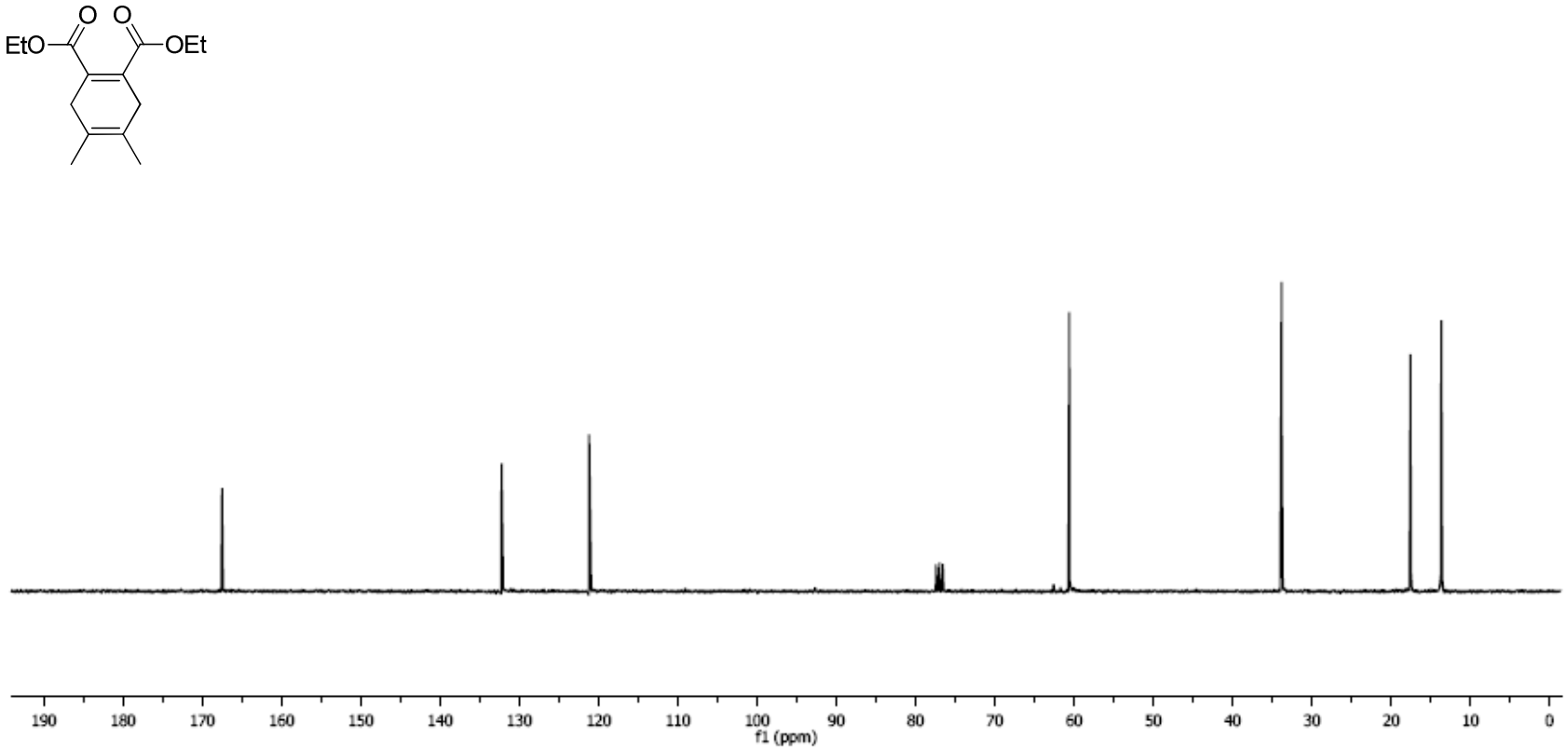


**Figure 1B.** $^{13}C$ NMR spectrum of **III-1** (75 MHz, $CDCl_3$, 23 °C).

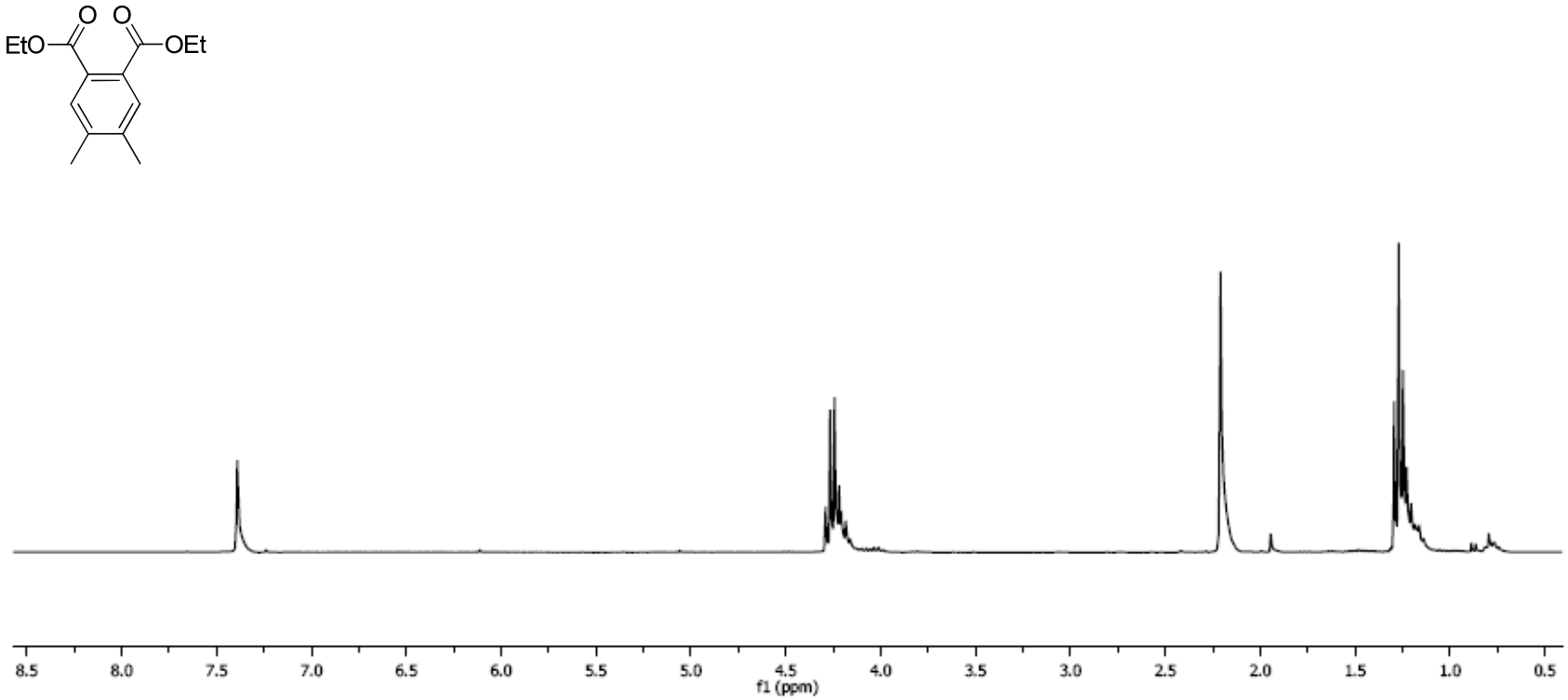


**Figure 2A.** $^{1}$H NMR spectrum of **III-2** (300 MHz, $CDCl_3$, 23 °C).

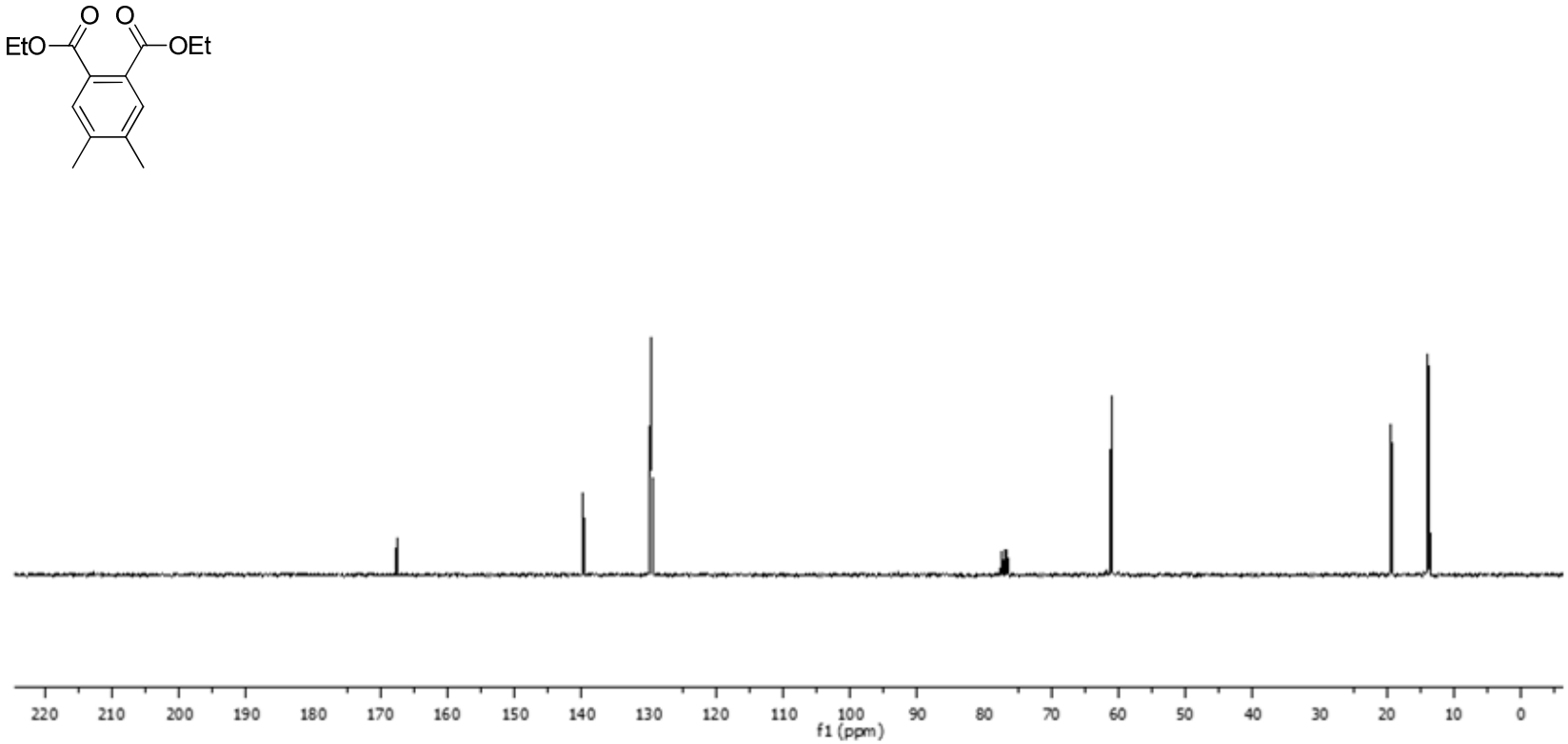


**Figure 2B.** $^{13}C$ NMR spectrum of **III-2** (75 MHz, $CDCl_3$, 23 °C).

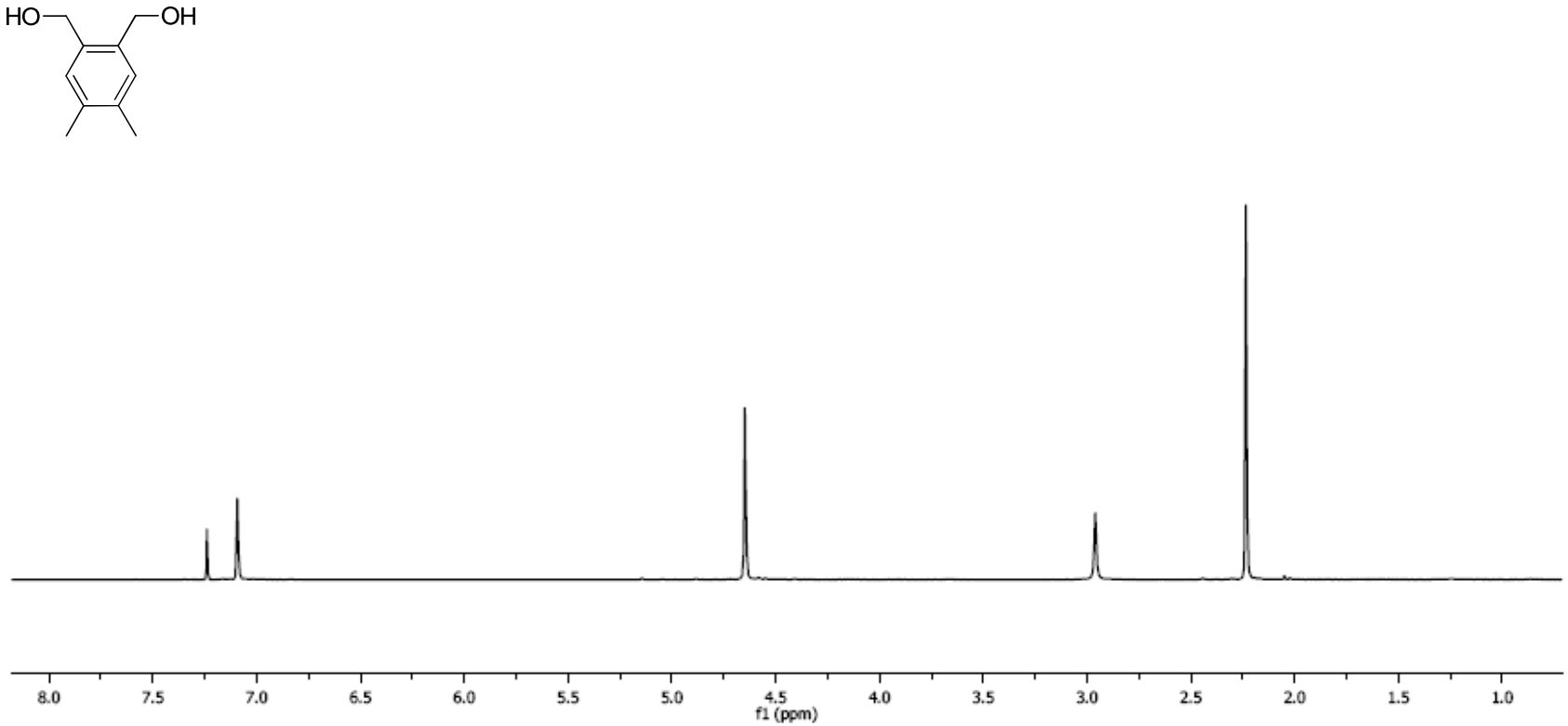


**Figure 3A.** $^{1}$H NMR spectrum of **III-3** (300 MHz, $CDCl_3$, 23 °C).

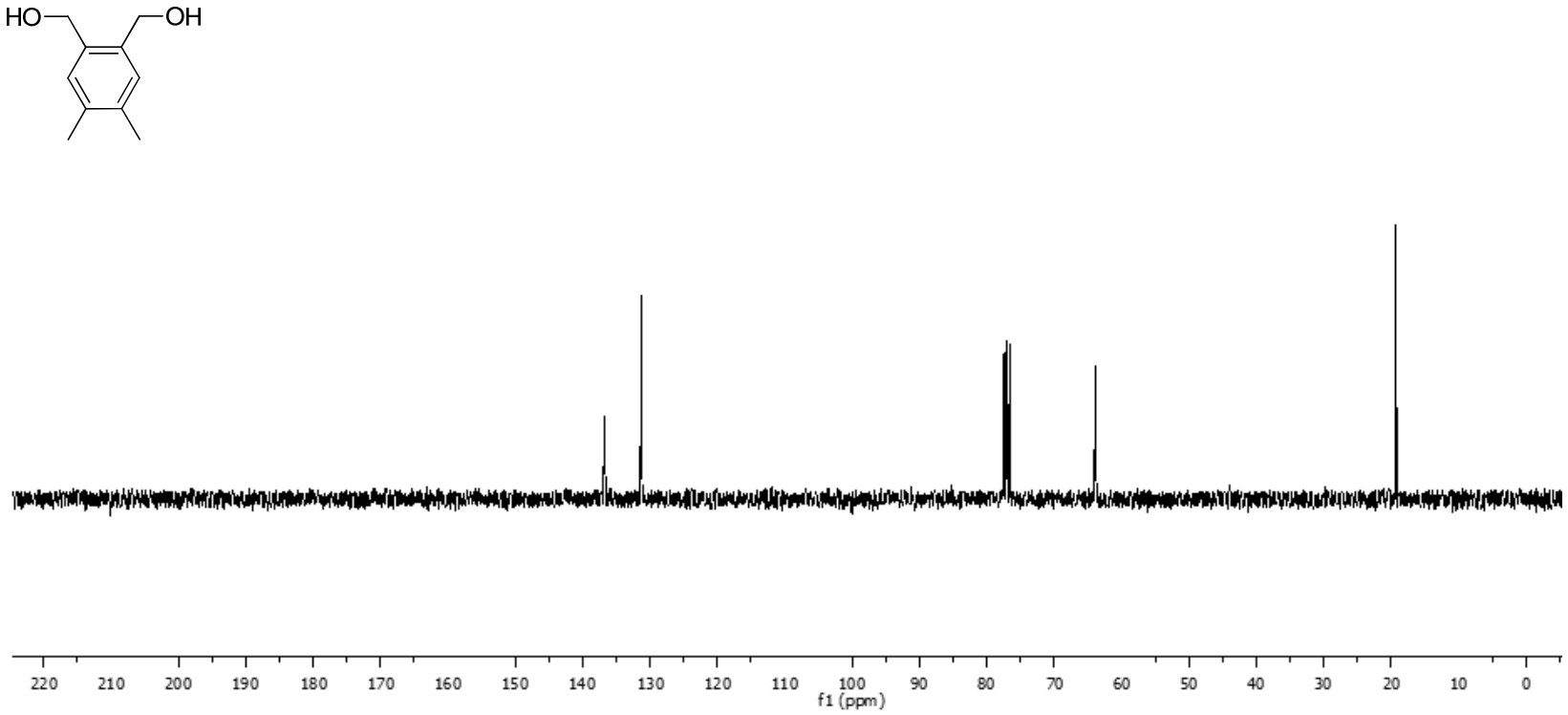


**Figure 3B.** $^{13}C$ NMR spectrum of **III-3** (75 MHz, $CDCl_3$, 23 °C).

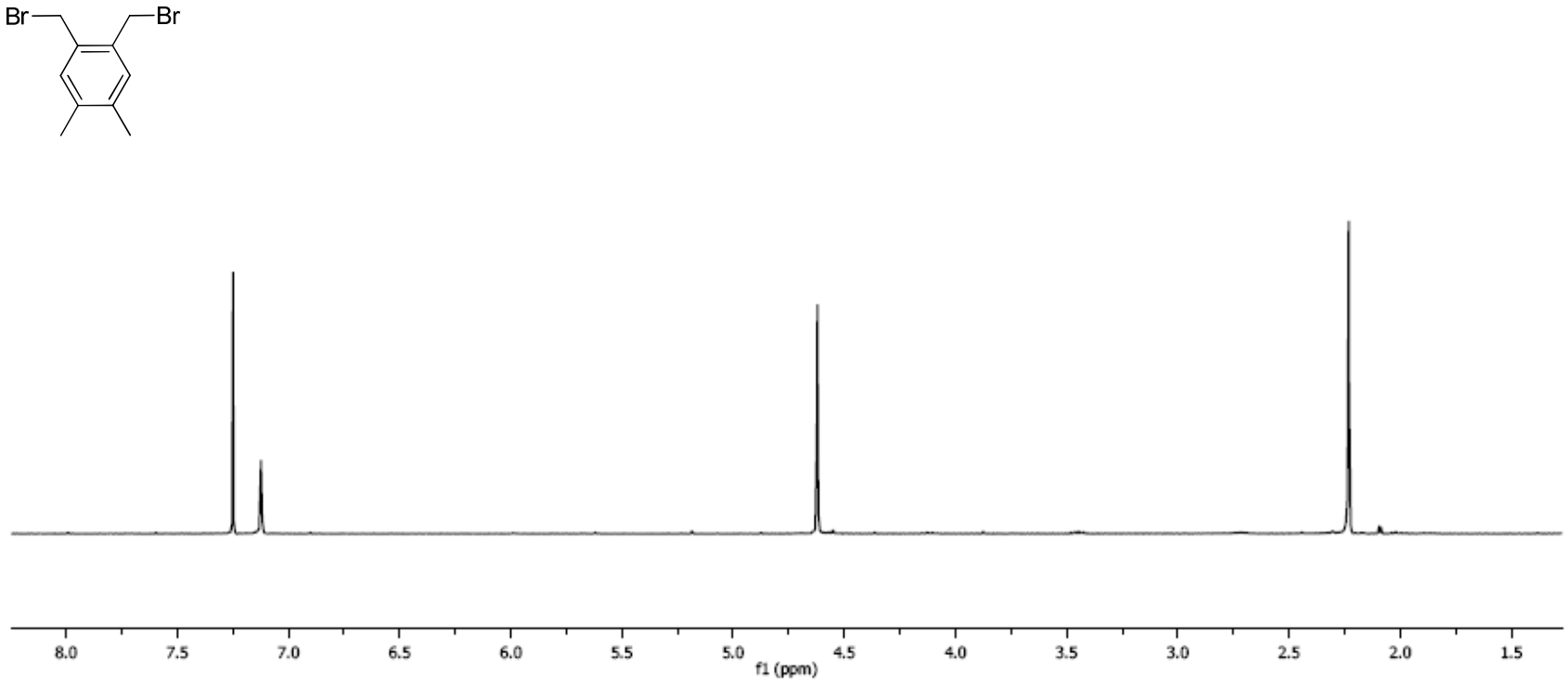


**Figure 4A.** $^{1}$H NMR spectrum of **III-4** (300 MHz, $CDCl_3$, 23 °C).

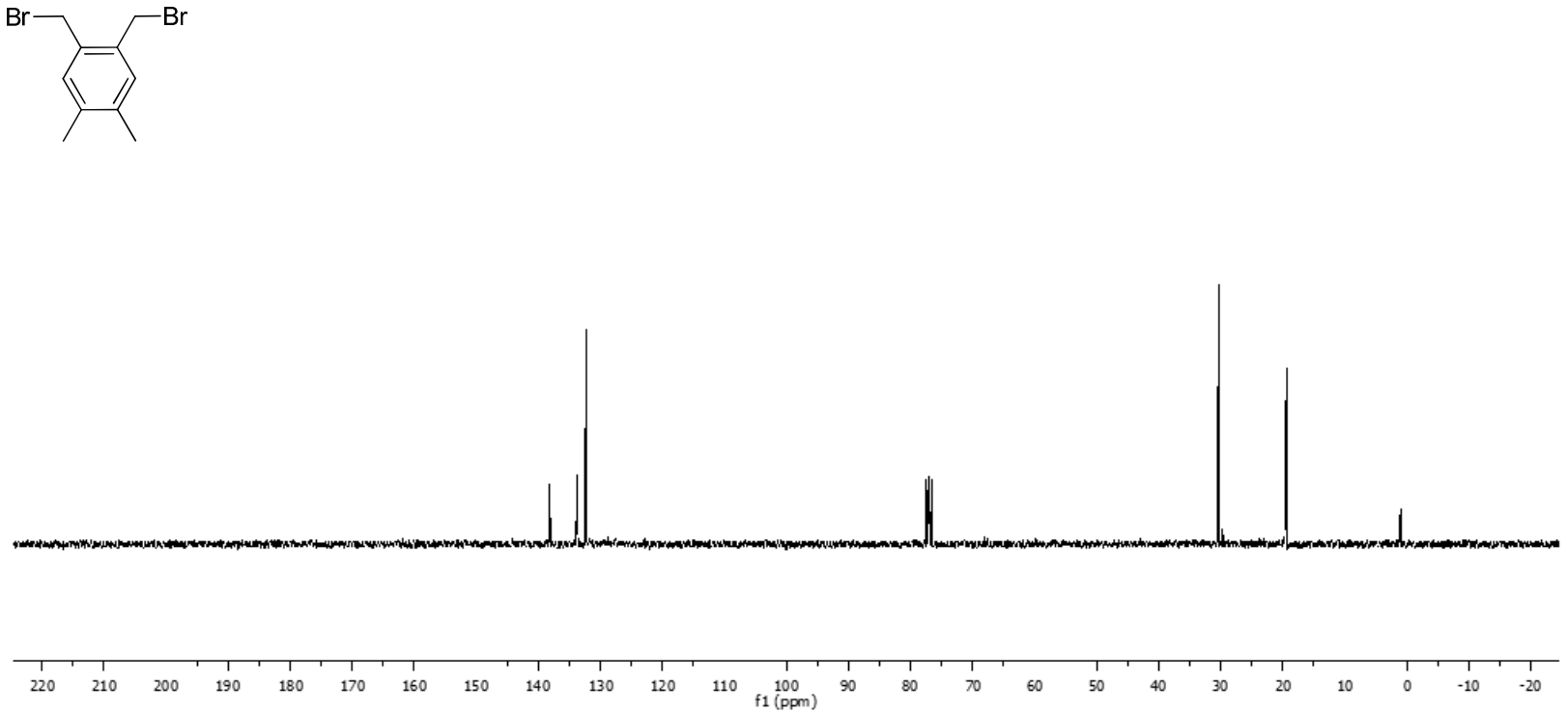


**Figure 4B.** $^{13}C$ NMR spectrum of **III-4** (75 MHz, $CDCl_3$, 23 °C).

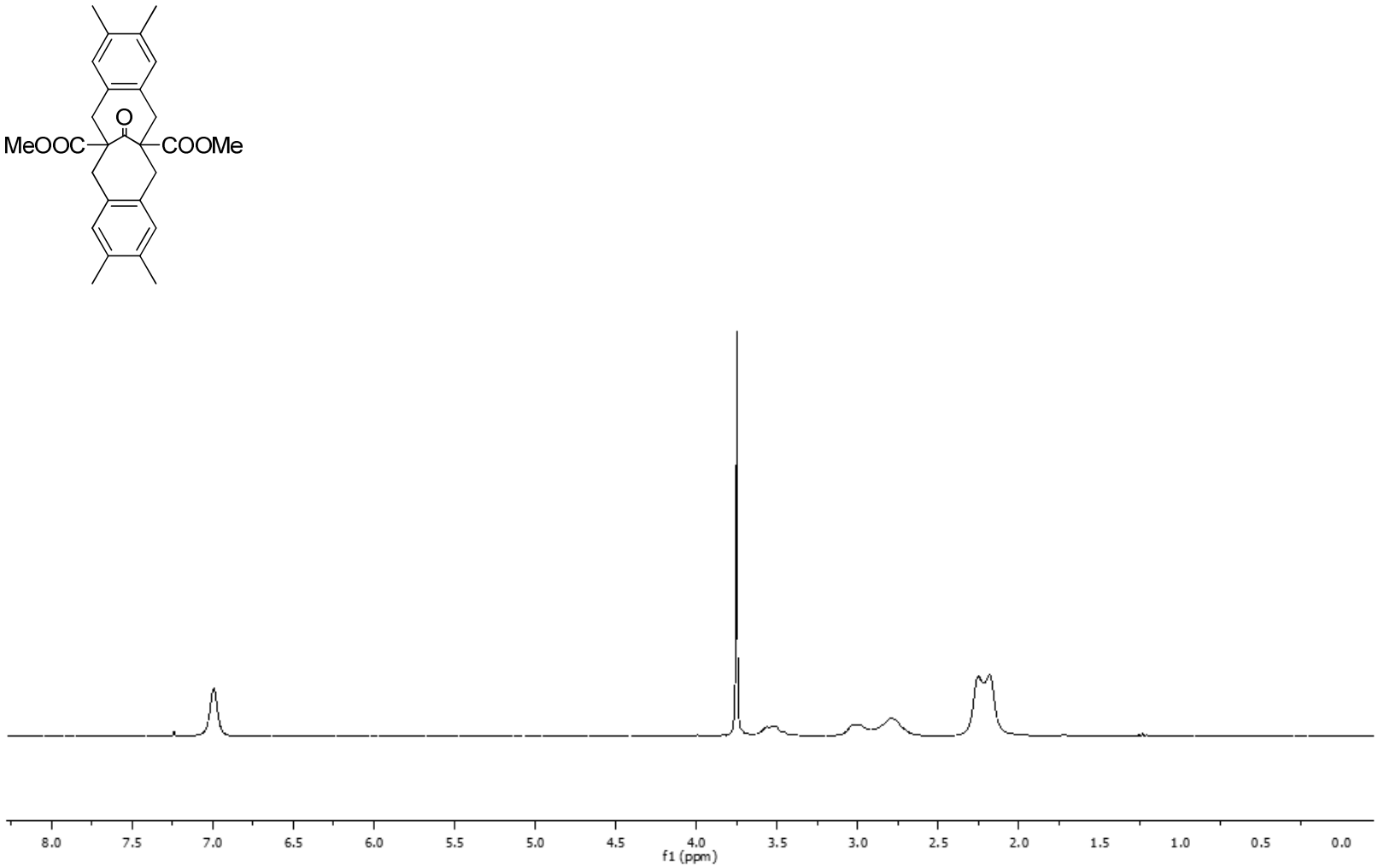


**Figure 5A.** $^{1}$H NMR spectrum of **III-5** (300 MHz, $CDCl_3$, 23 °C).

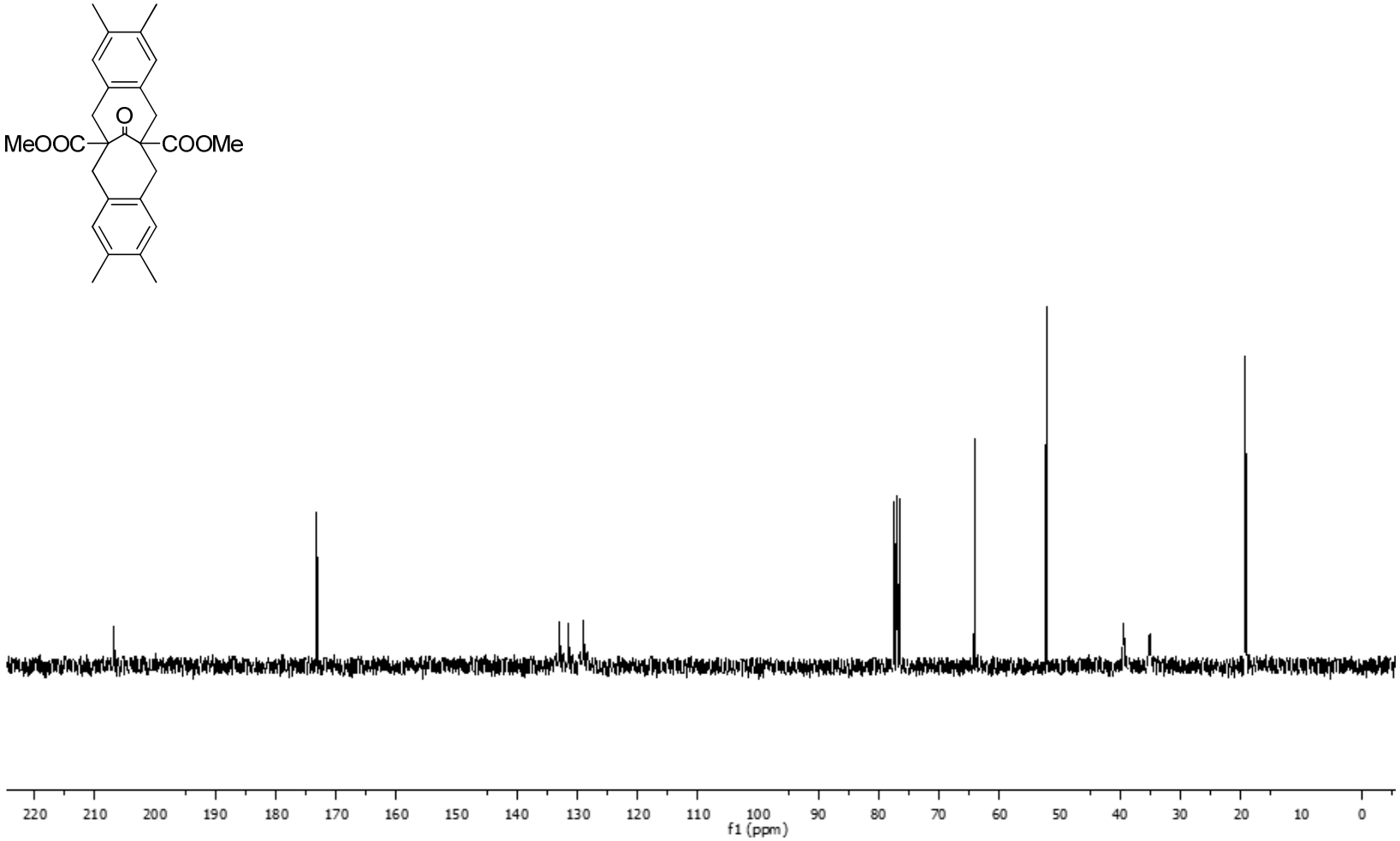


**Figure 5B.** $^{13}C$ NMR spectrum of **III-5** (75 MHz, $CDCl_3$, 23 °C).

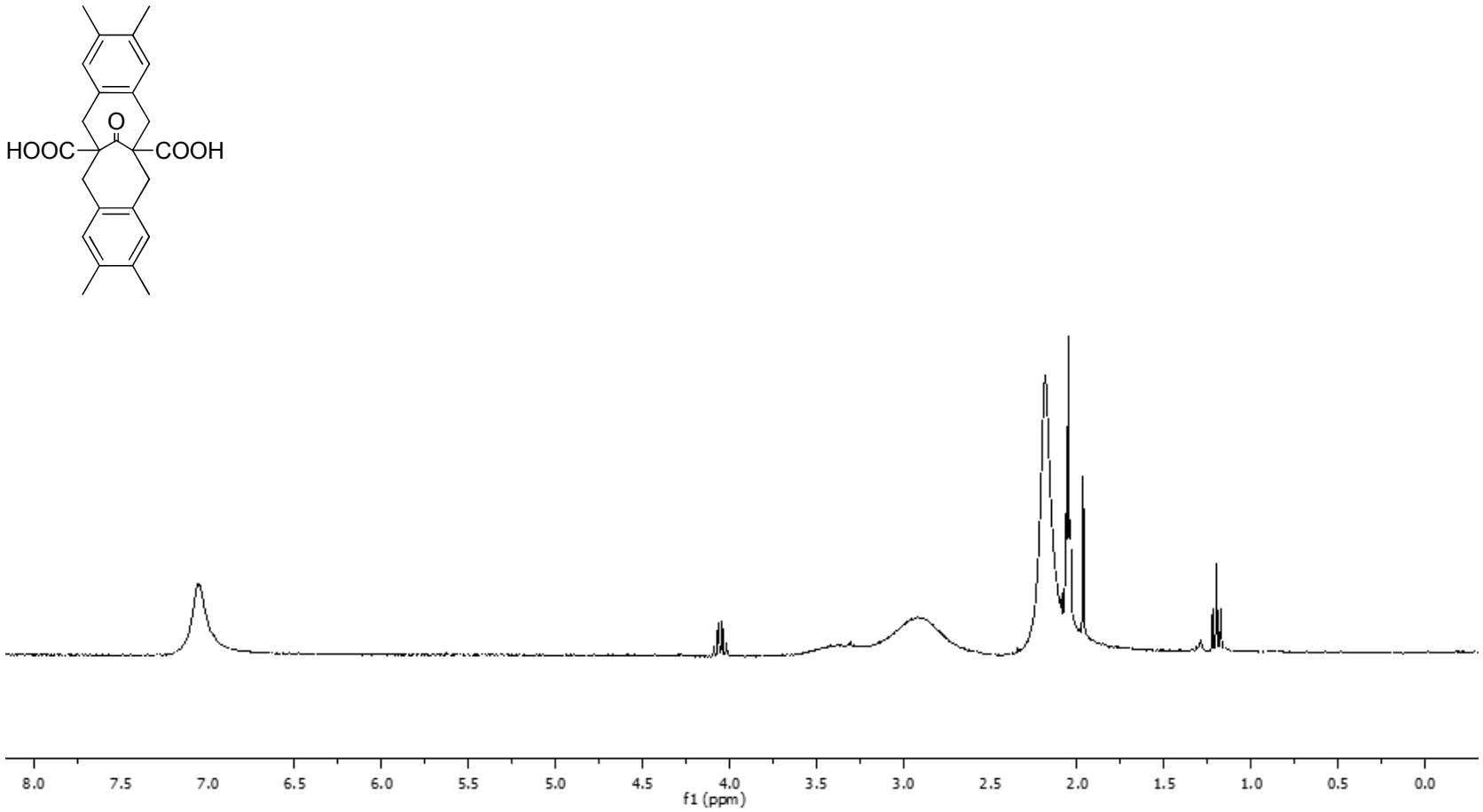


**Figure 6A.** $^{1}$H NMR spectrum of **III-6** (300 MHz, acetone-$d_6$, 23 °C).

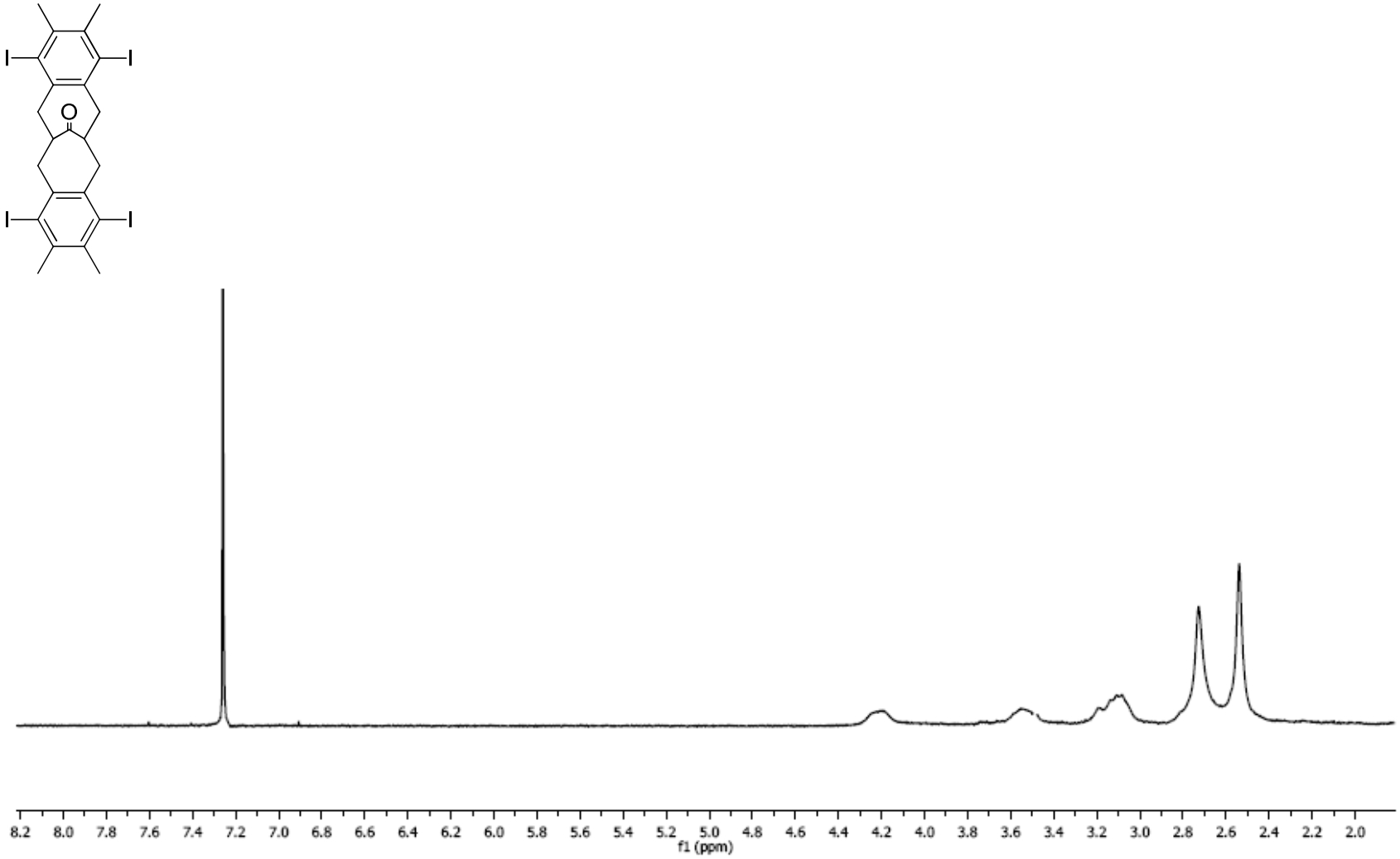


**Figure 7A.** $^{1}$H NMR spectrum of **IV-1** (300 MHz, $CDCl_3$, 23 °C).

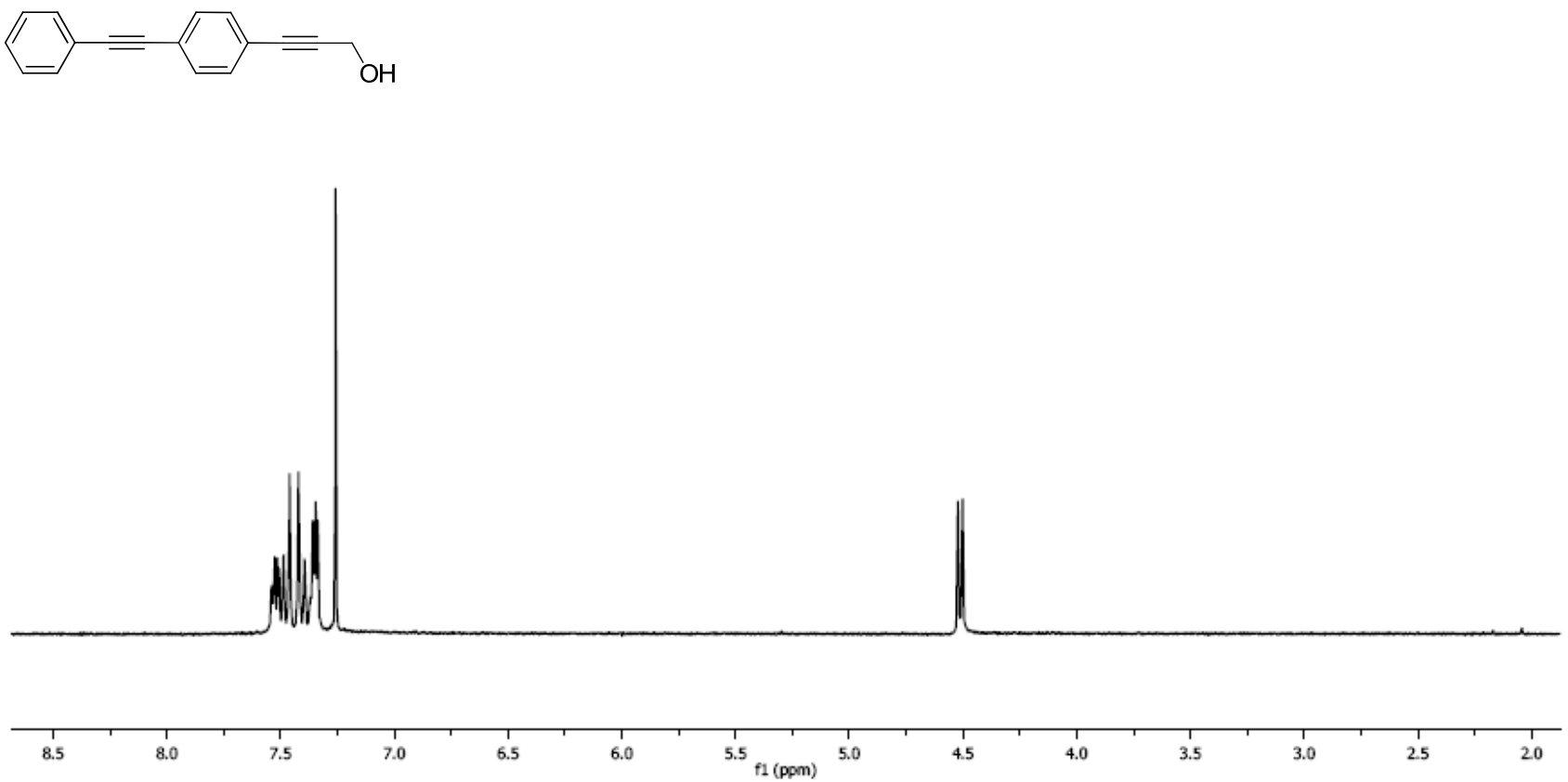


**Figure 8A.** $^{1}$H NMR spectrum of **IV-3** (300 MHz, $CDCl_3$, 23 °C).

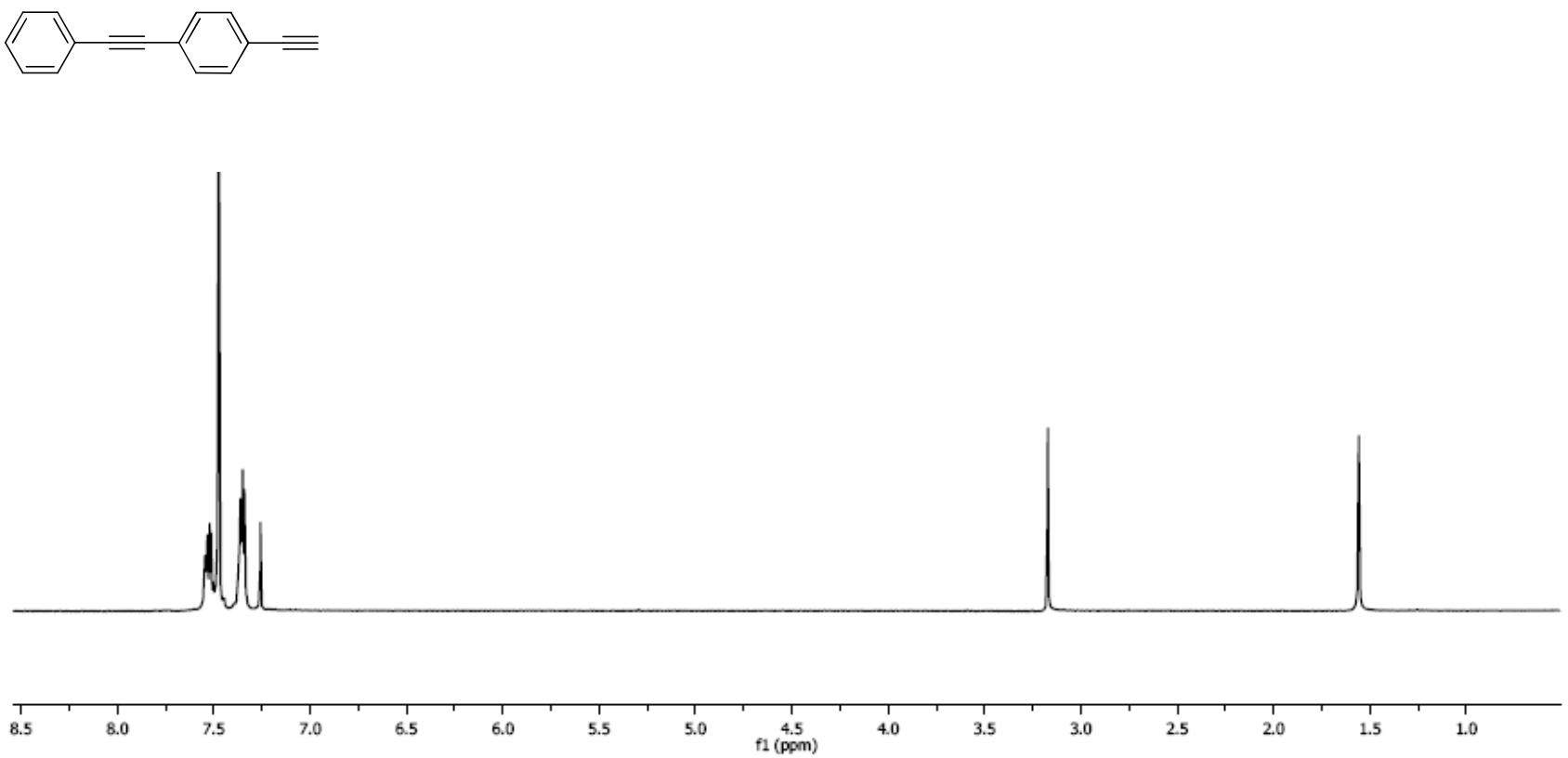


**Figure 9A.** $^{1}$H NMR spectrum of **IV-4** (300 MHz, $CDCl_3$, 23 °C).

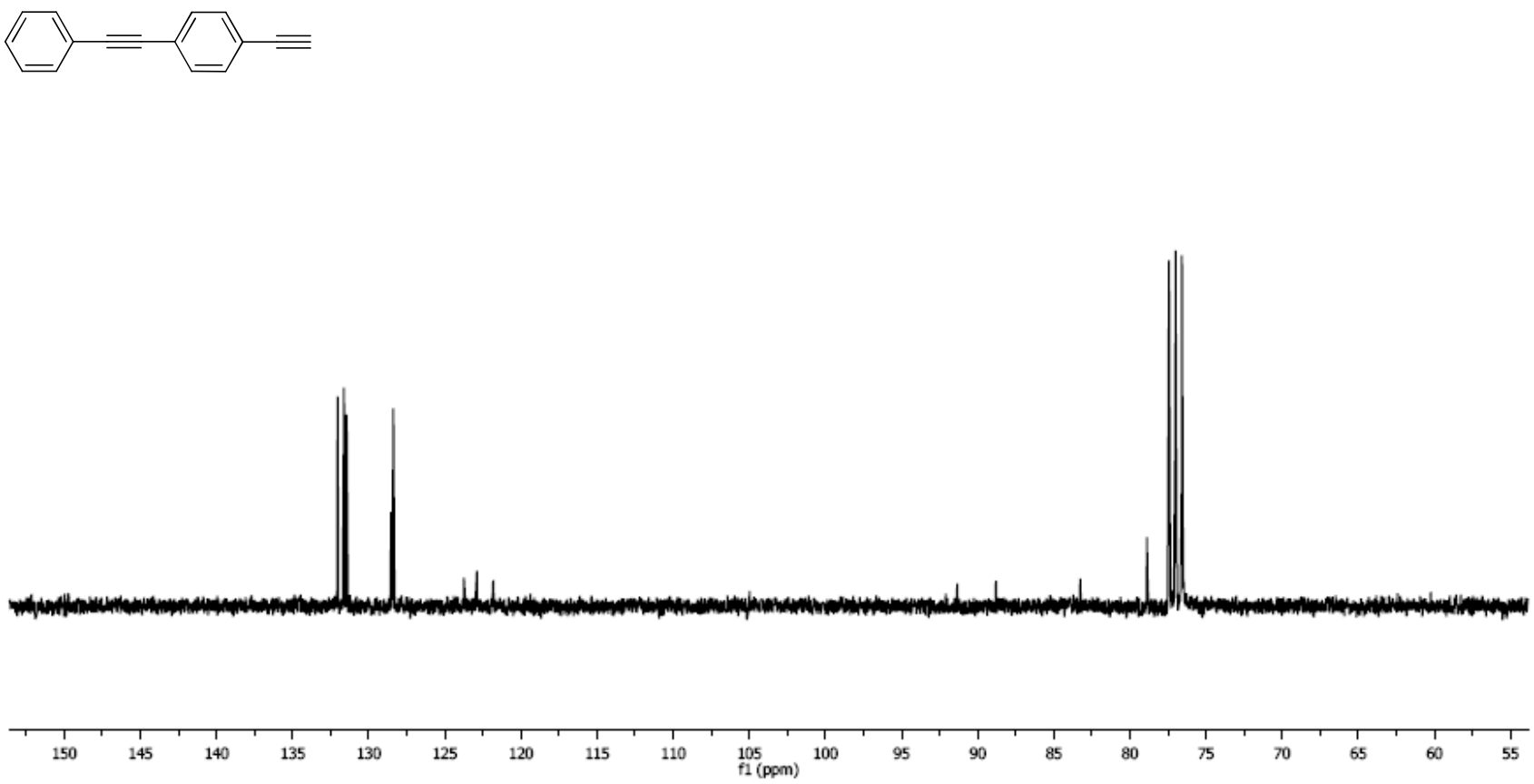


**Figure 9B.** $^{13}C$ NMR spectrum of **IV-4** (75 MHz, $CDCl_3$, 23 °C).

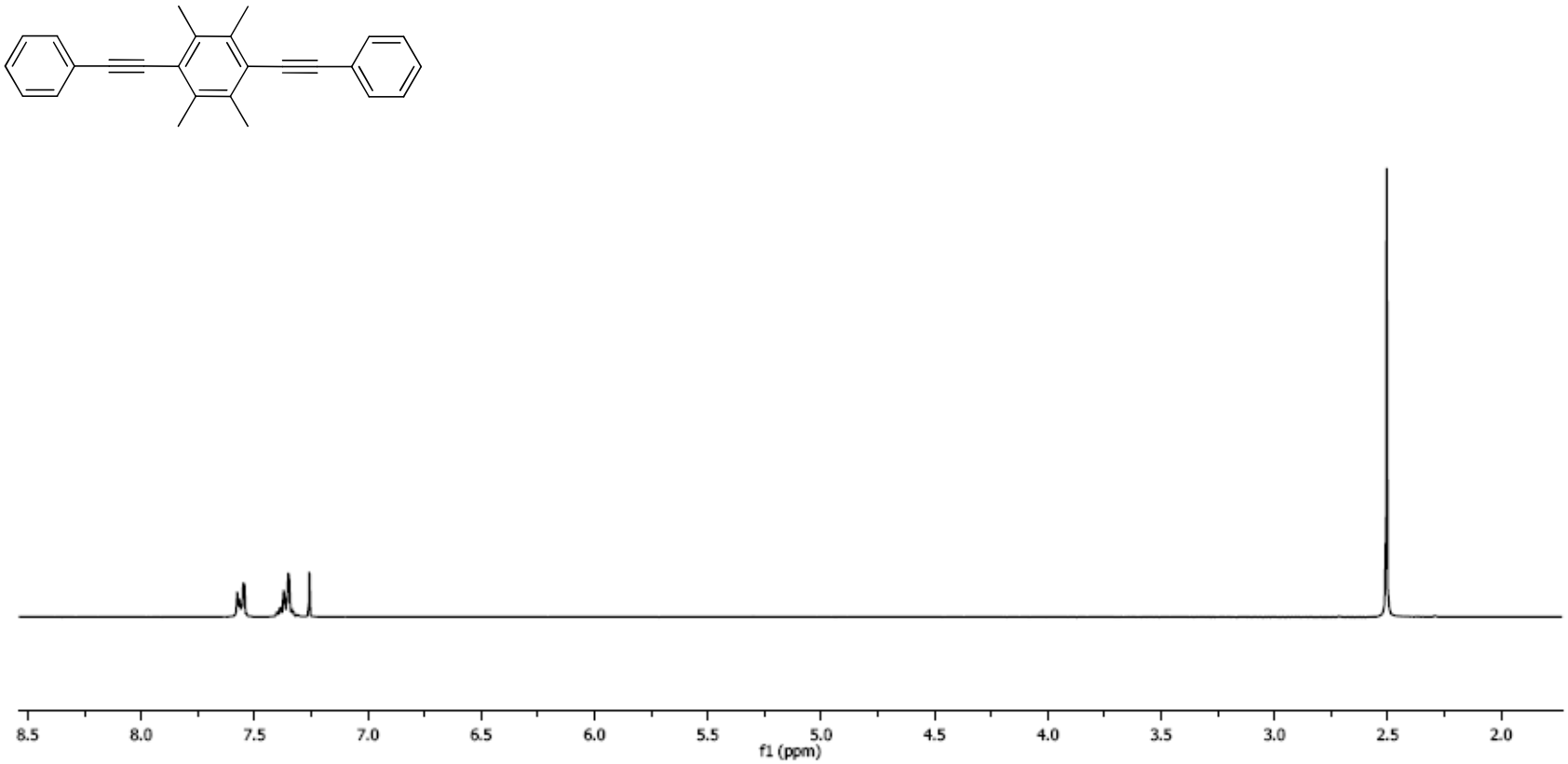


**Figure 10A.** $^{1}$H NMR spectrum of **PE$_3$** (300 MHz, $CDCl_3$, 23 °C).

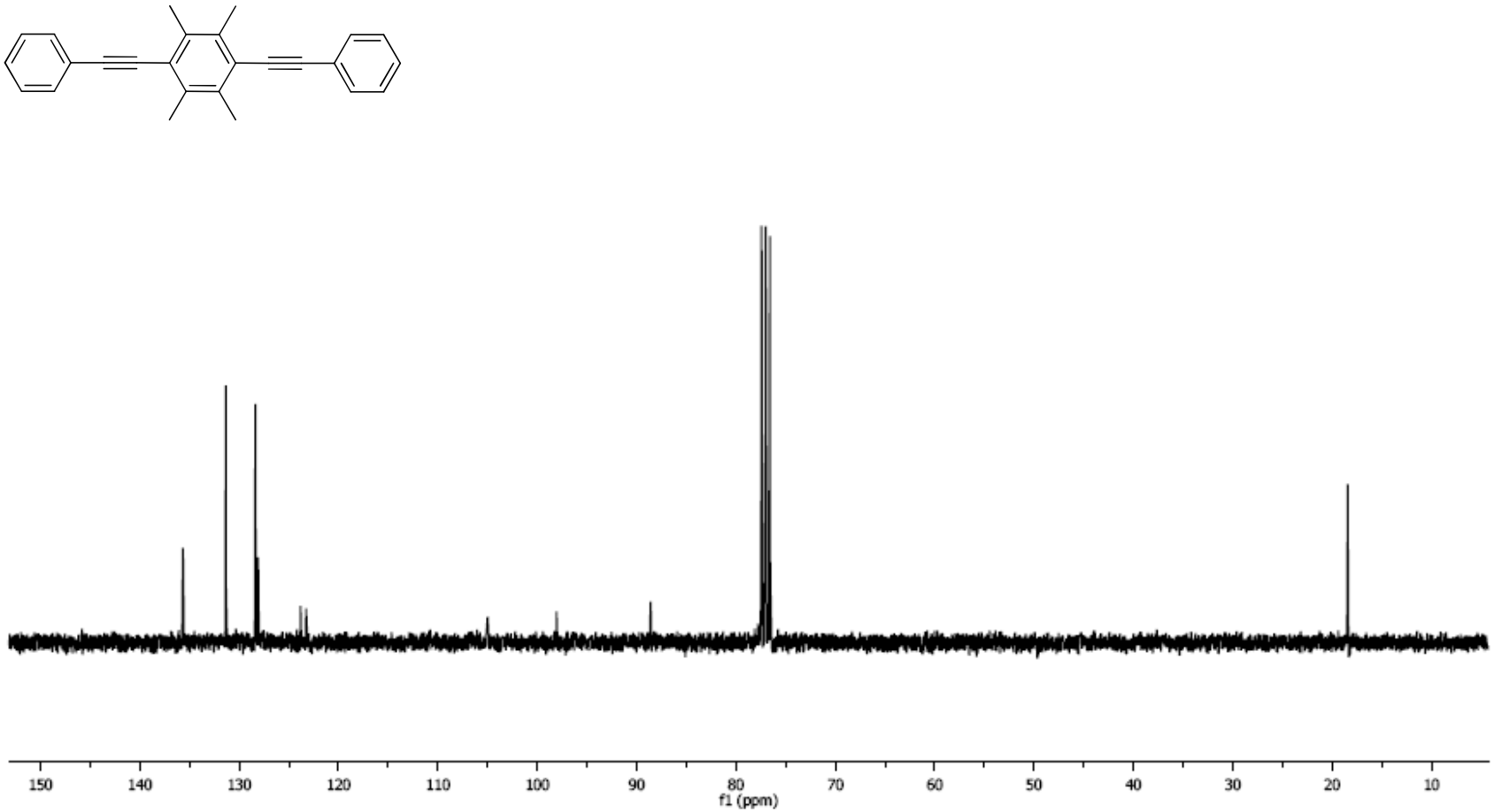


**Figure 10B.** $^{13}C$ NMR spectrum of **$PE_3$** (75 MHz, $CDCl_3$, 23 °C).

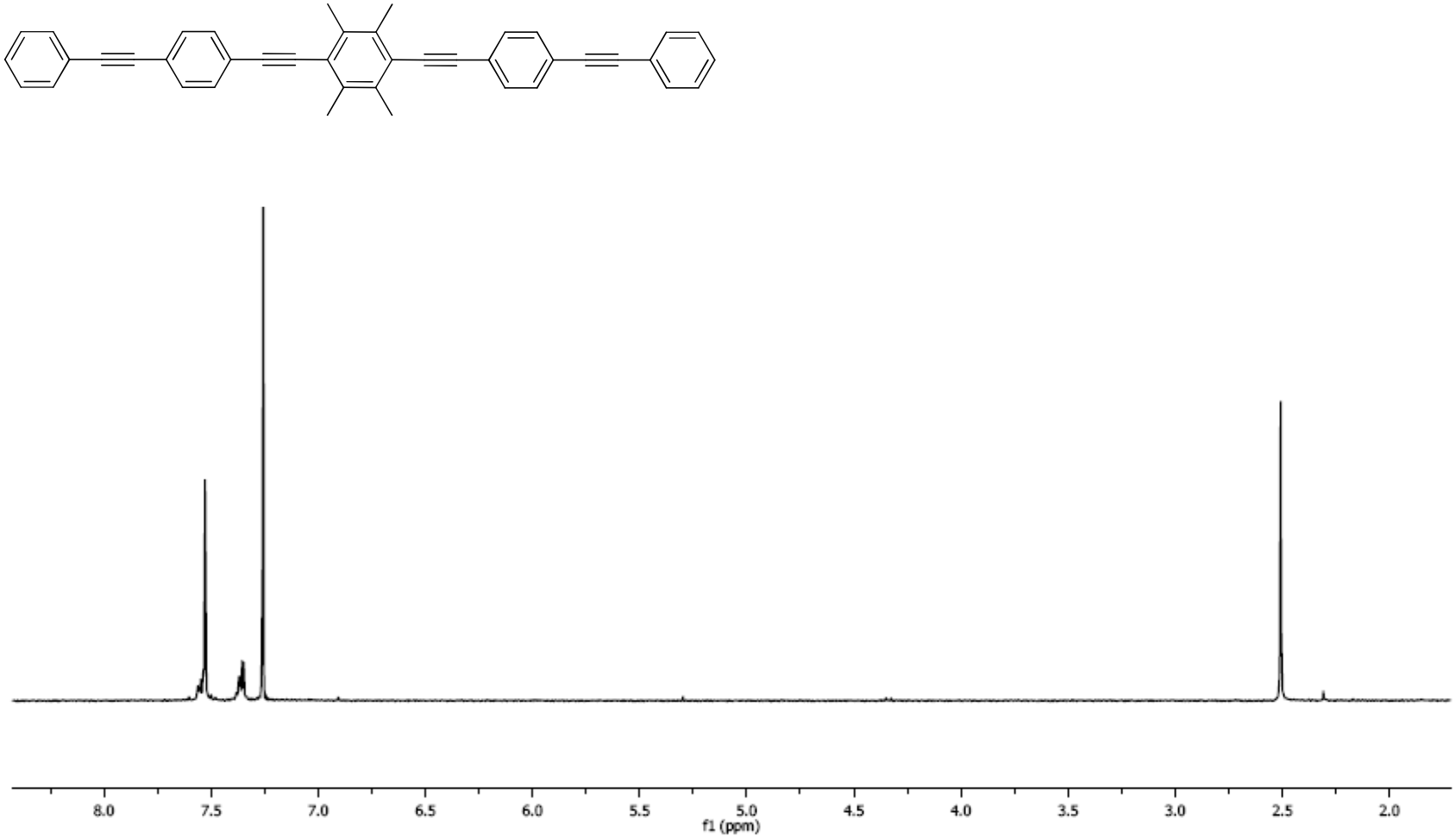


**Figure 11A.** $^{1}$H NMR spectrum of **PE$_5$** (300 MHz, $CDCl_3$, 23 °C).

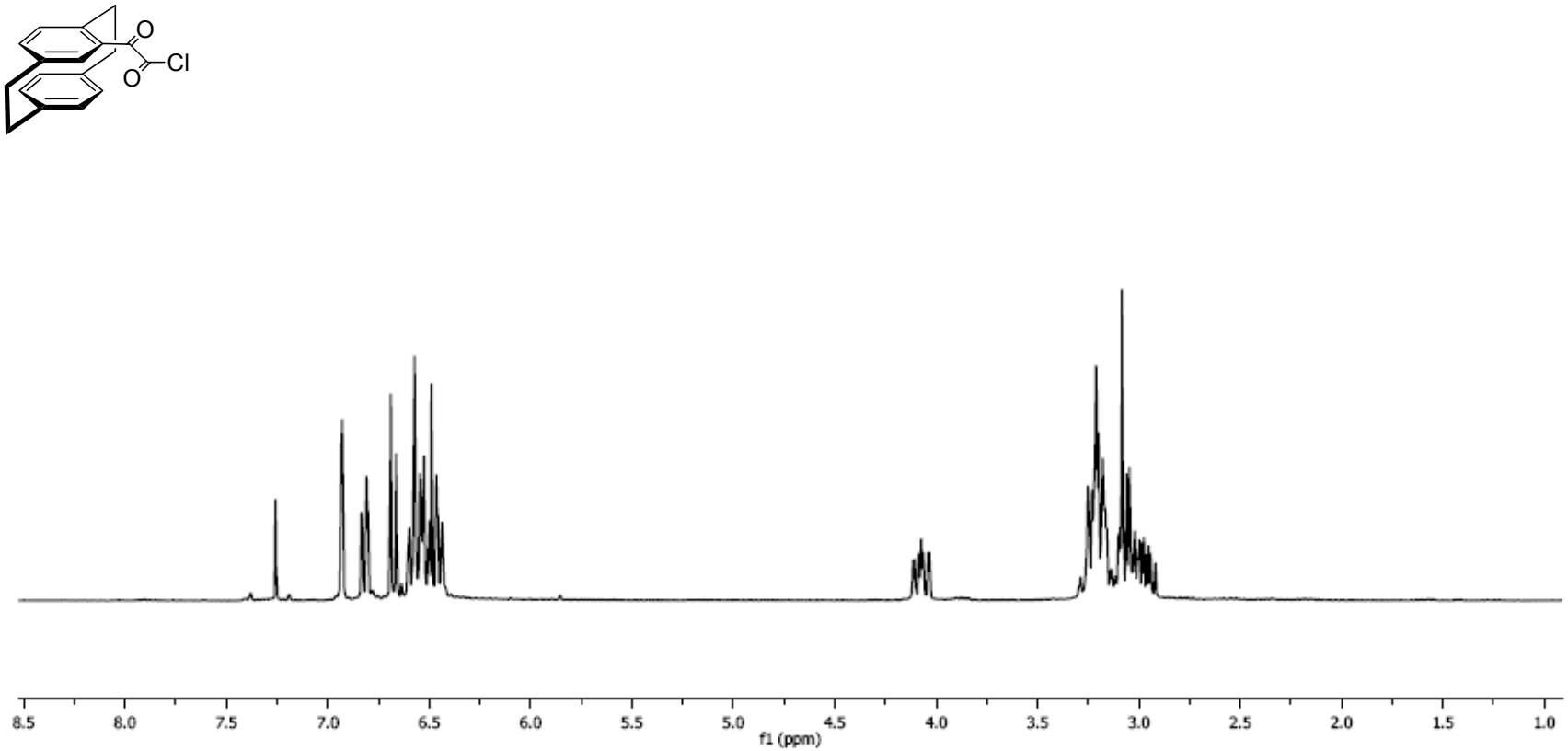


**Figure 12A.** $^{1}$H NMR spectrum of **V-6** (300 MHz, $CDCl_3$, 23 °C).

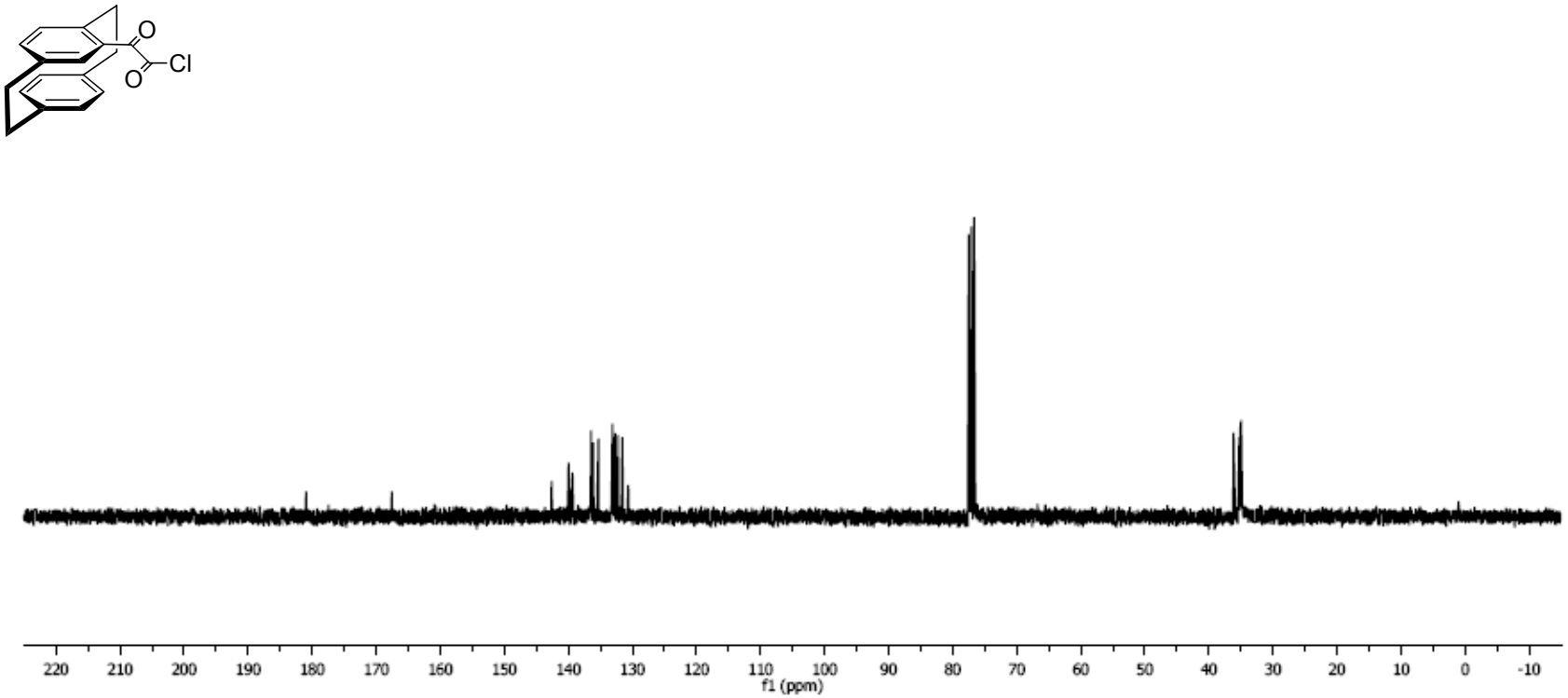


**Figure 12B.** $^{13}C$ NMR spectrum of **V-6** (75 MHz, $CDCl_3$, 23 °C).

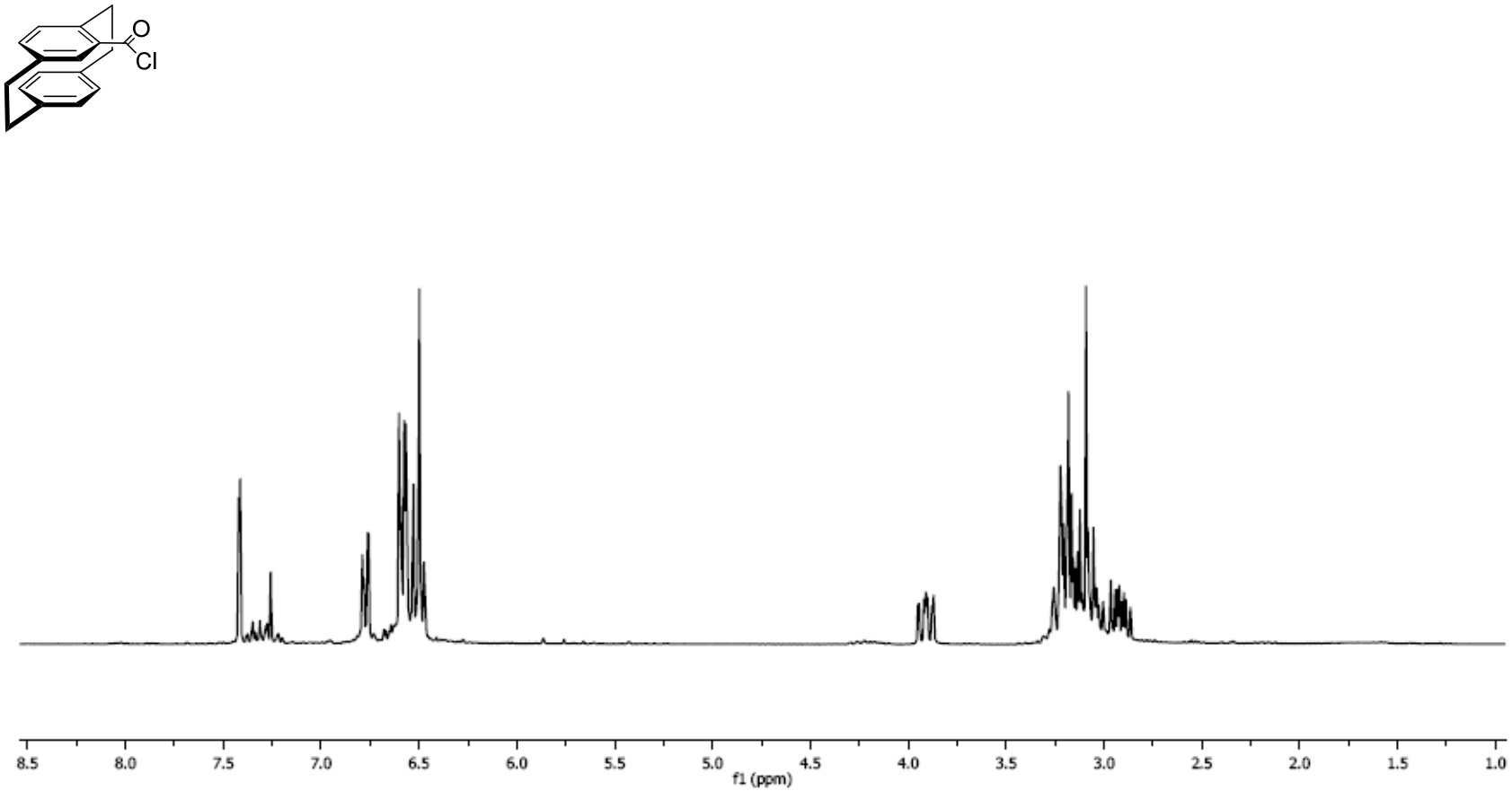


**Figure 13A.** $^{1}$H NMR spectrum of **V-7** (300 MHz, $CDCl_3$, 23 °C).

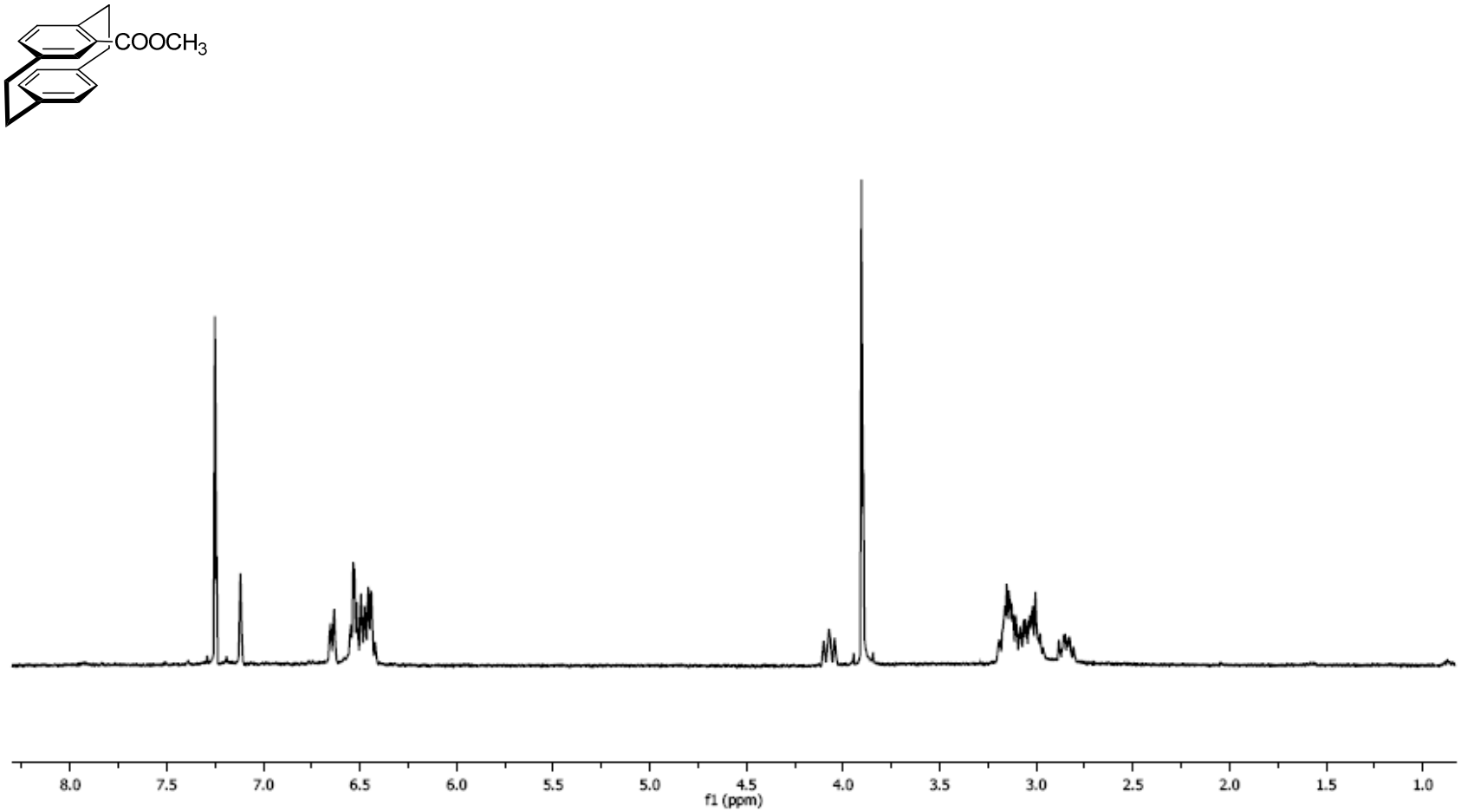


**Figure 14A.** $^{1}$H NMR spectrum of **V-8** (300 MHz, $CDCl_3$, 23 °C).

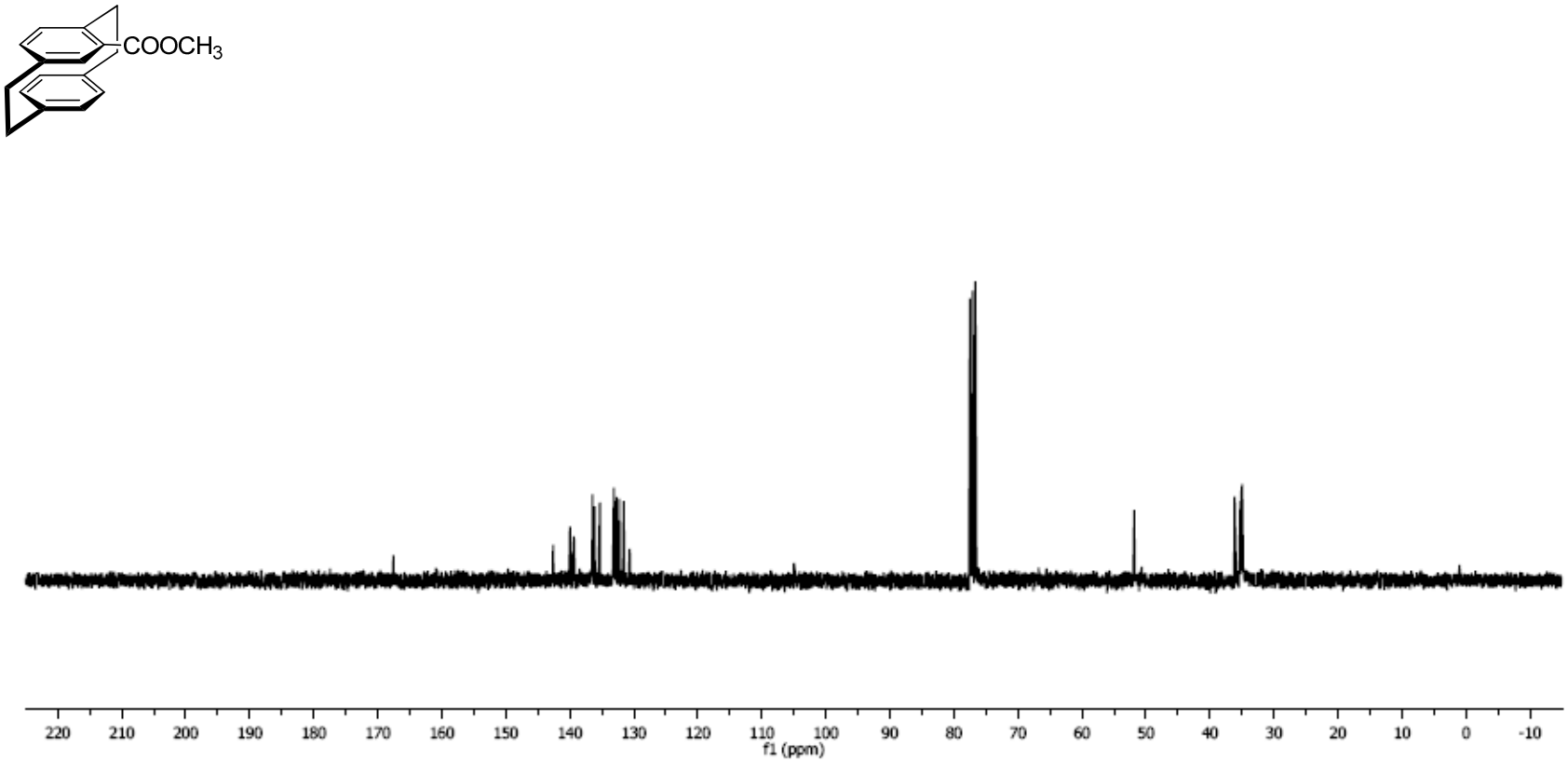


**Figure 14B.** $^{1}$H NMR spectrum of **V-8** (300 MHz, $CDCl_3$, 23 °C).

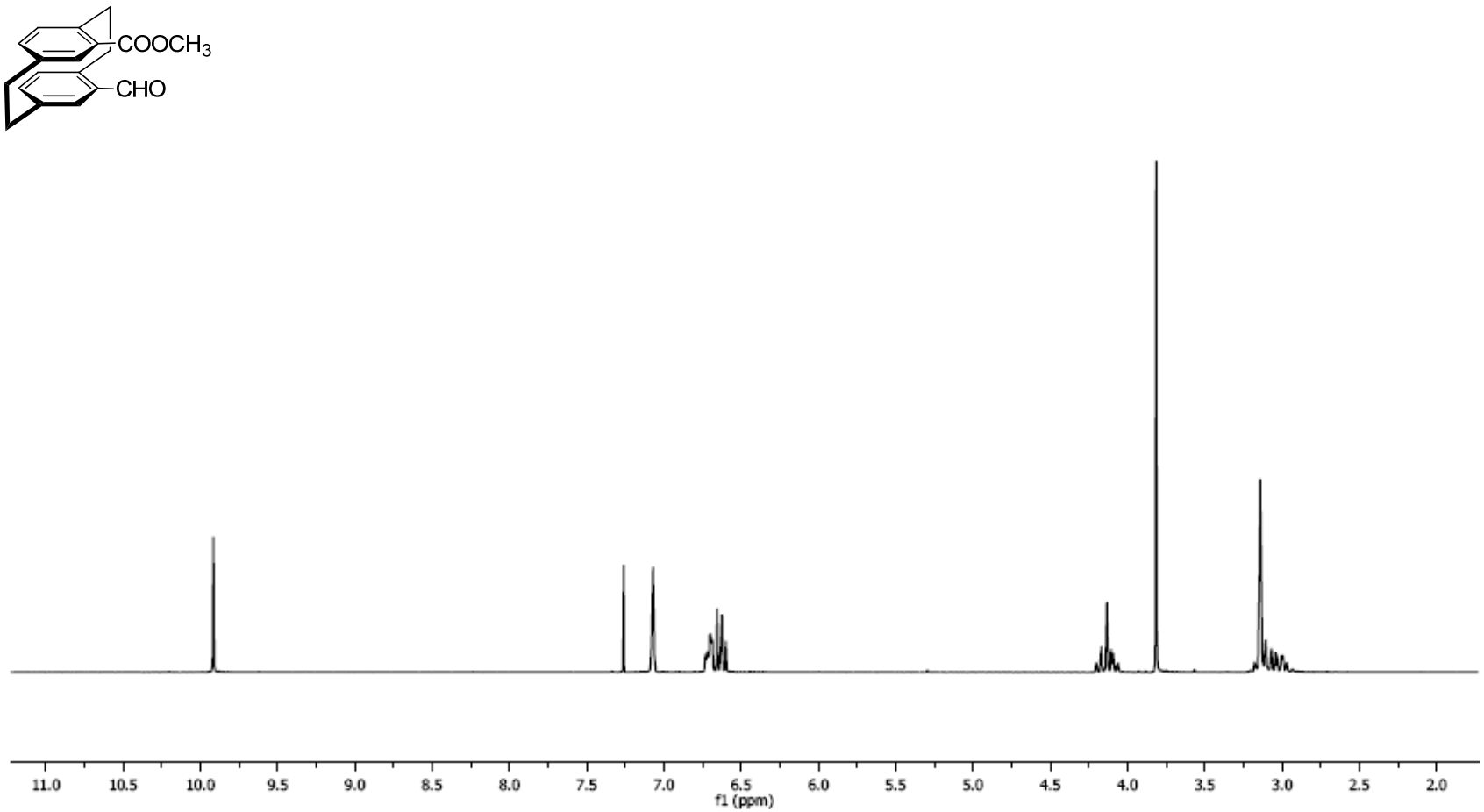


**Figure 15A.** $^{1}$H NMR spectrum of **V-9** (300 MHz, $CDCl_3$, 23 °C).

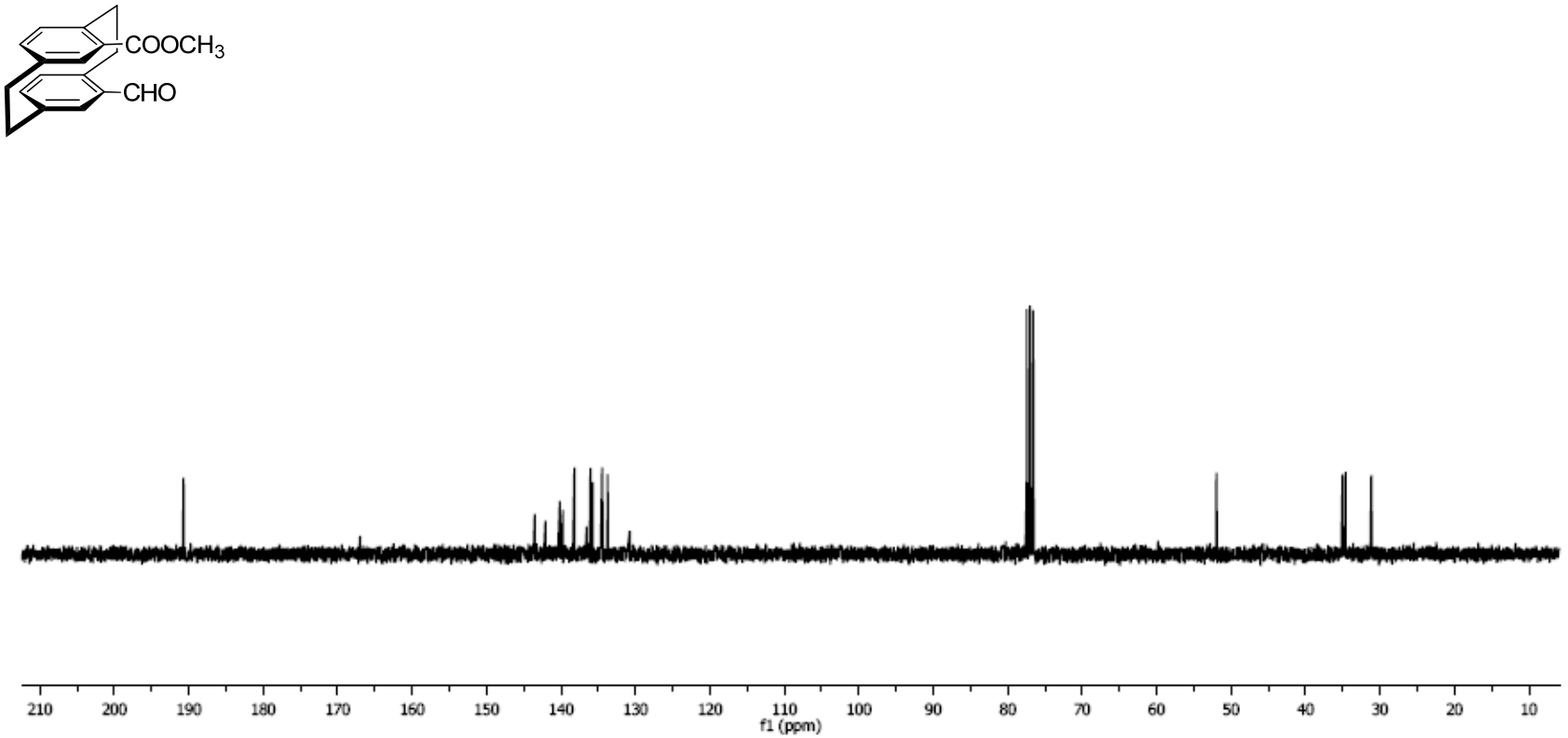


**Figure 15B.** $^{13}C$ NMR spectrum of **V-9** (75 MHz, $CDCl_3$, 23 °C).

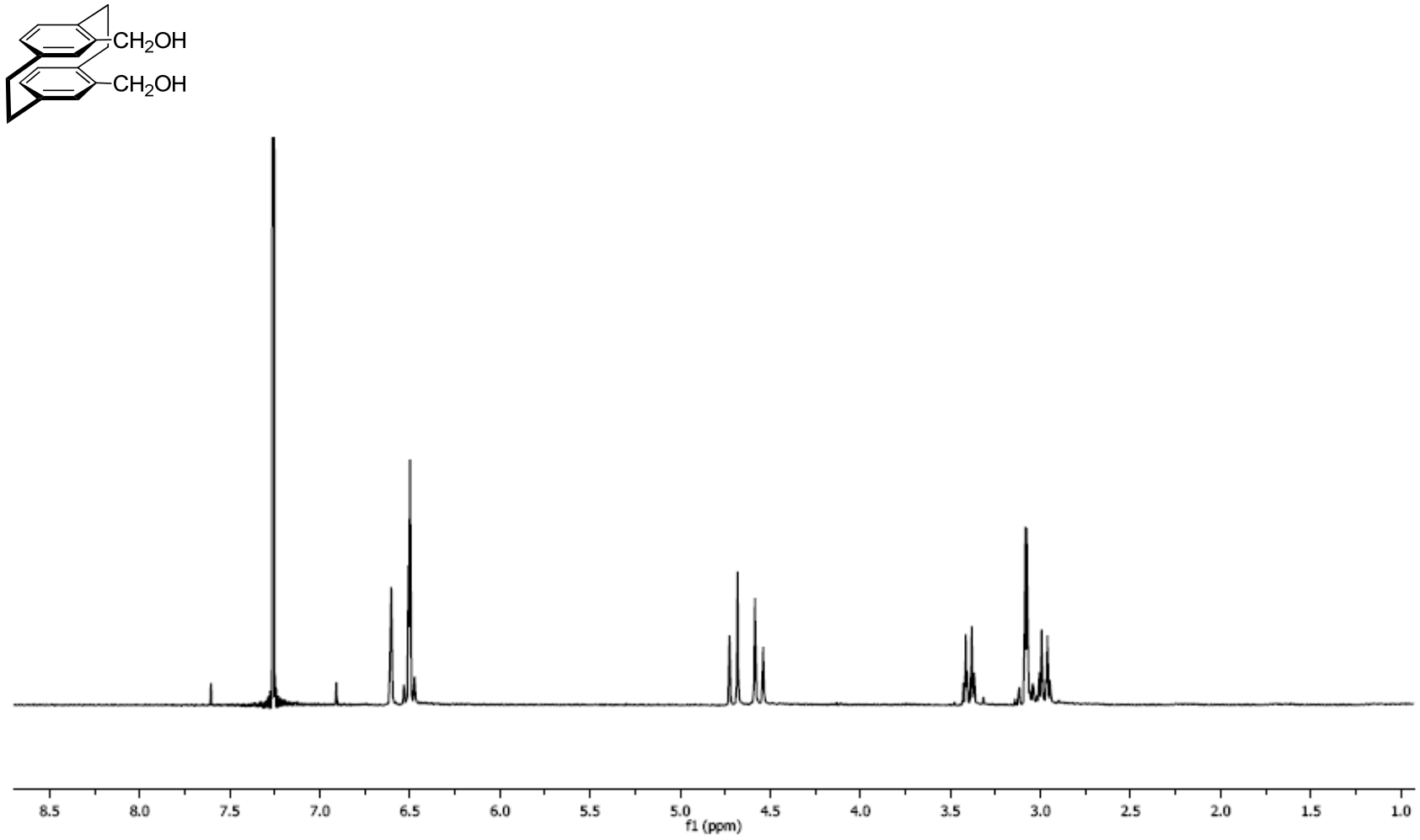


**Figure 16A.** $^{1}$H NMR spectrum of **V-10** (300 MHz, $CDCl_3$, 23 °C).

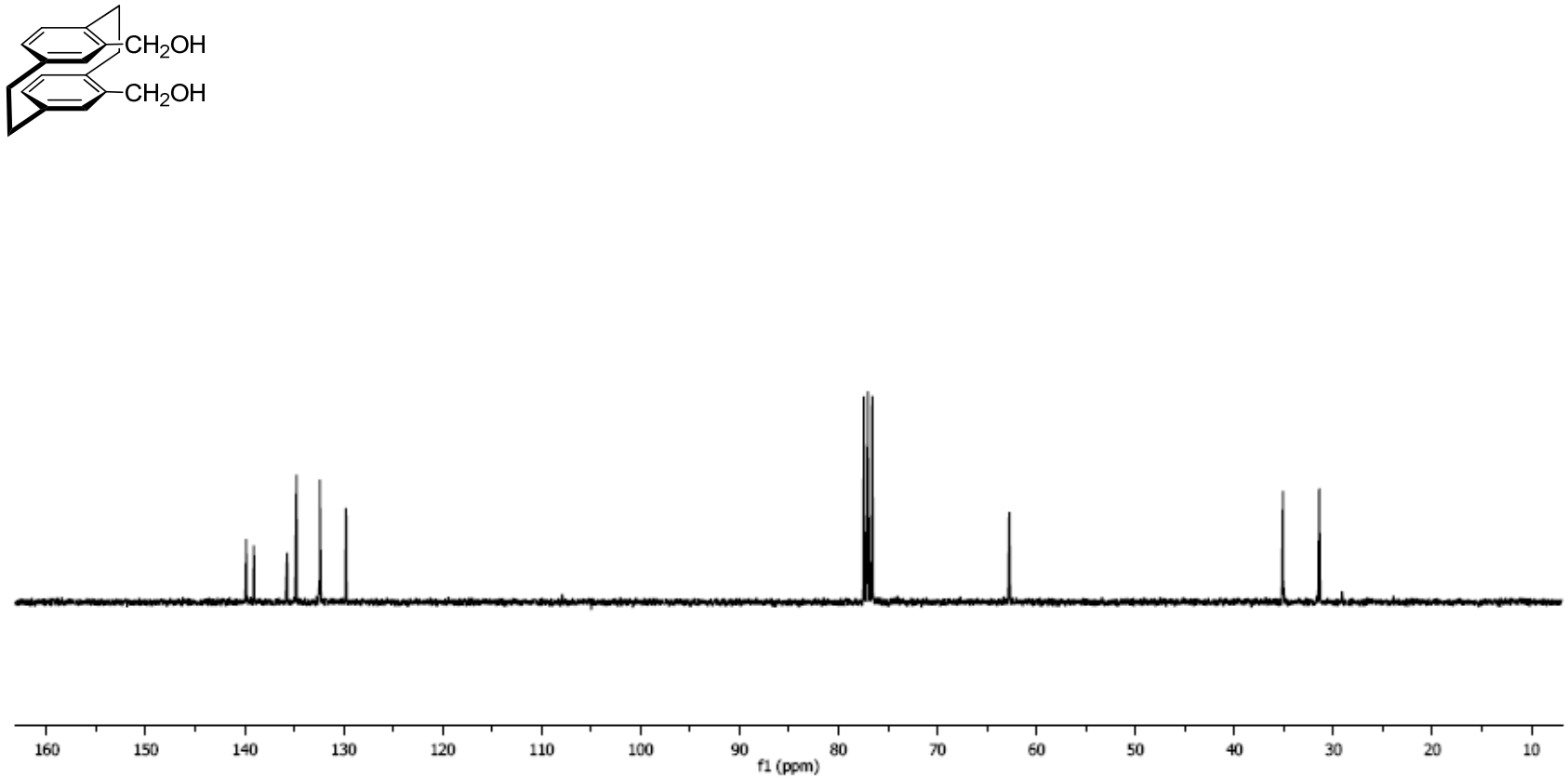


**Figure 16B.** $^{13}C$ NMR spectrum of **V-10** (75 MHz, $CDCl_3$, 23 °C).

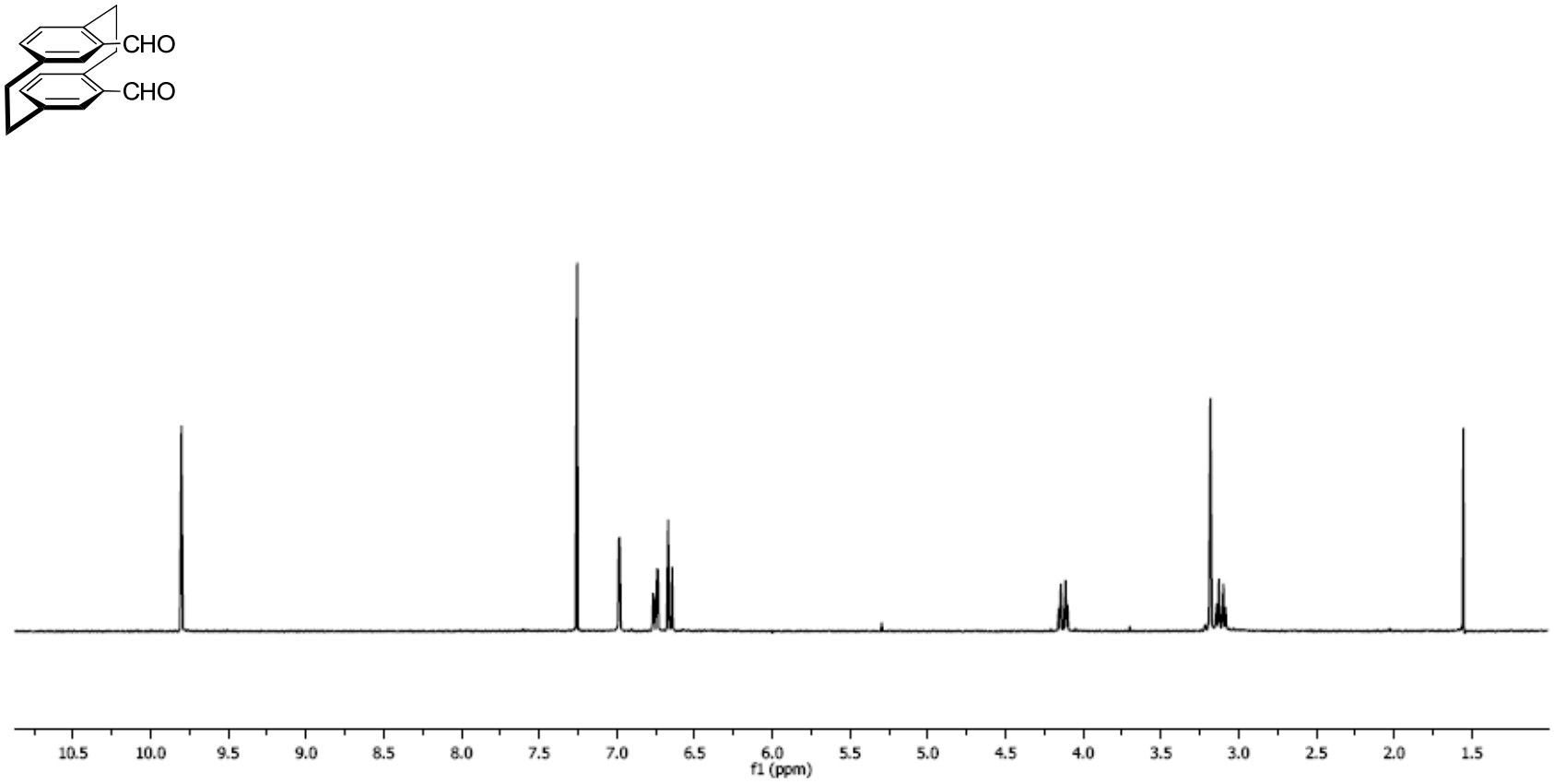


**Figure 17A.** $^{1}$H NMR spectrum of **V-11** (300 MHz, $CDCl_3$, 23 °C).

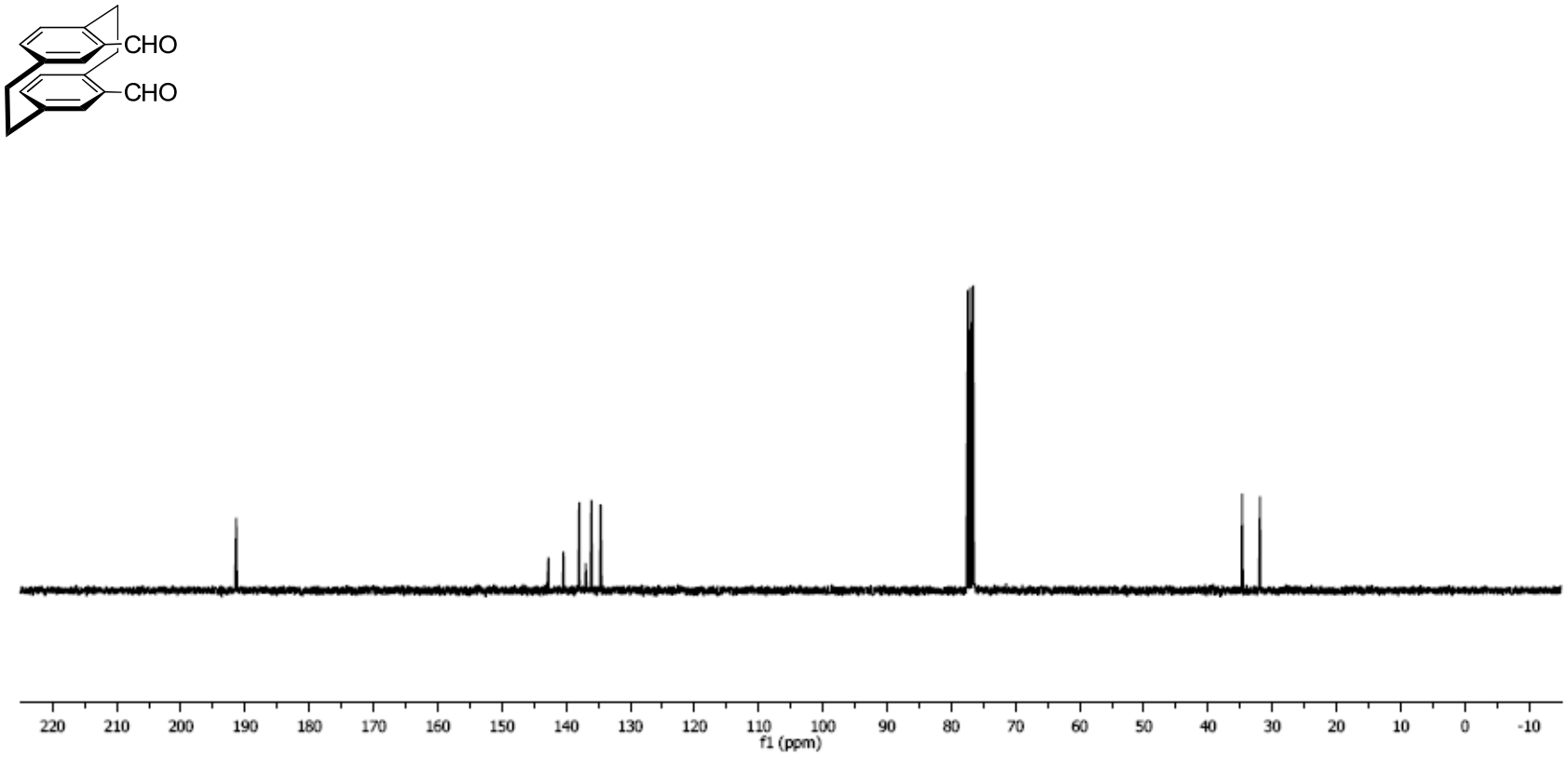


**Figure 17B.** $^{13}C$ NMR spectrum of **V-11** (75 MHz, $CDCl_3$, 23 °C).

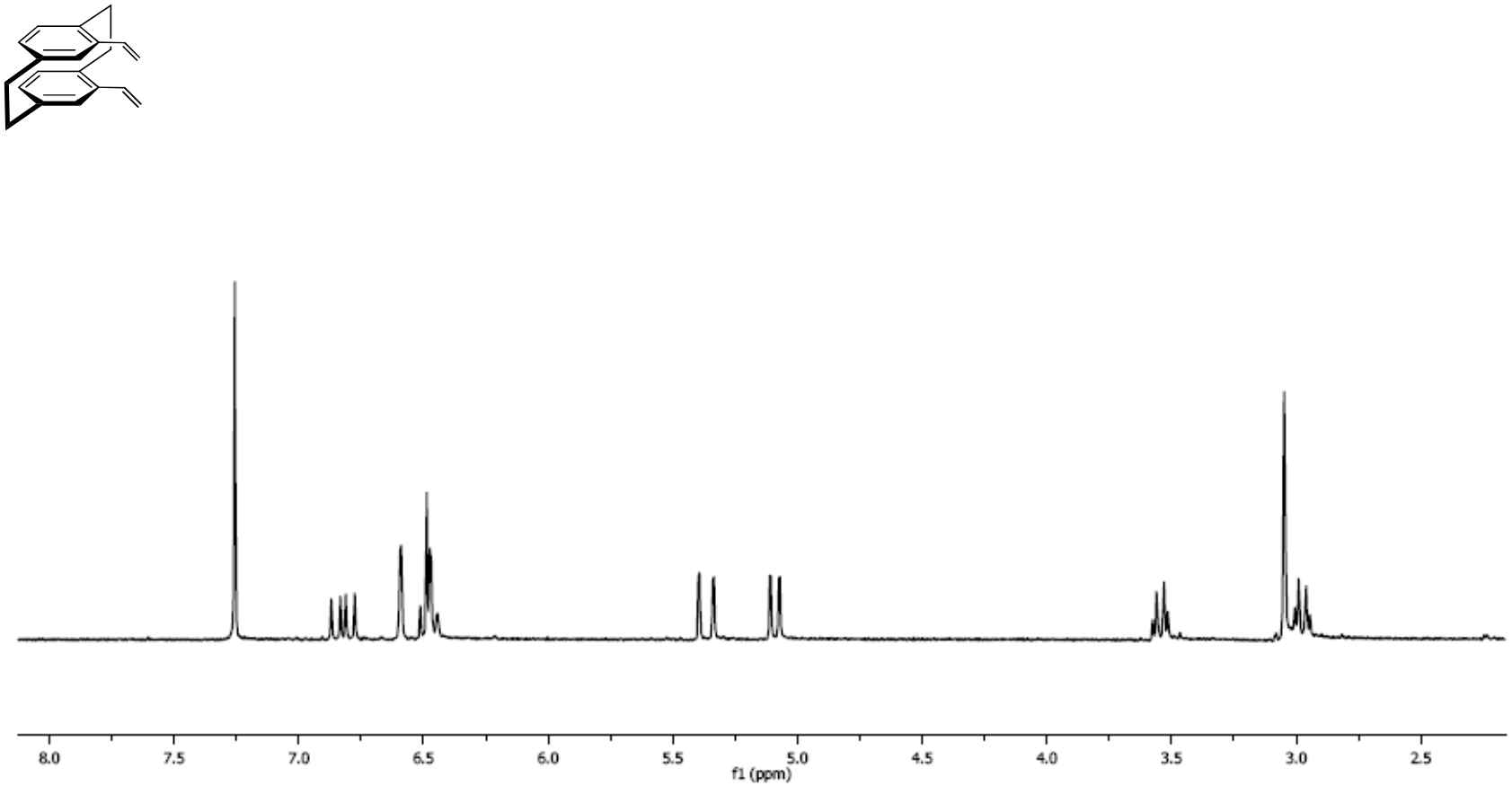


**Figure 18A.** $^{1}$H NMR spectrum of **V-12** (300 MHz, $CDCl_3$, 23 °C).

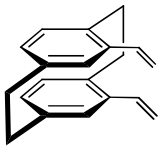

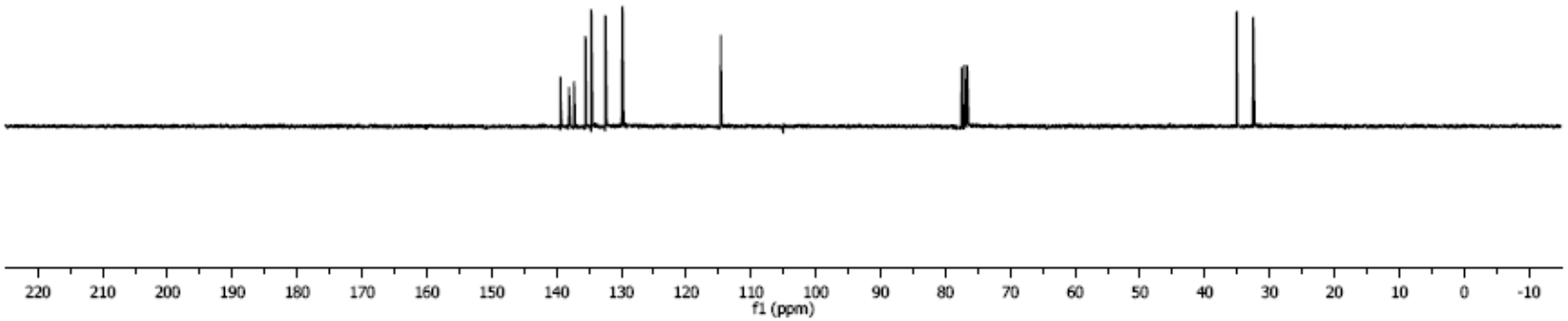


**Figure 18B.** $^{13}C$ NMR spectrum of **V-12** (75 MHz, $CDCl_3$, 23 °C).

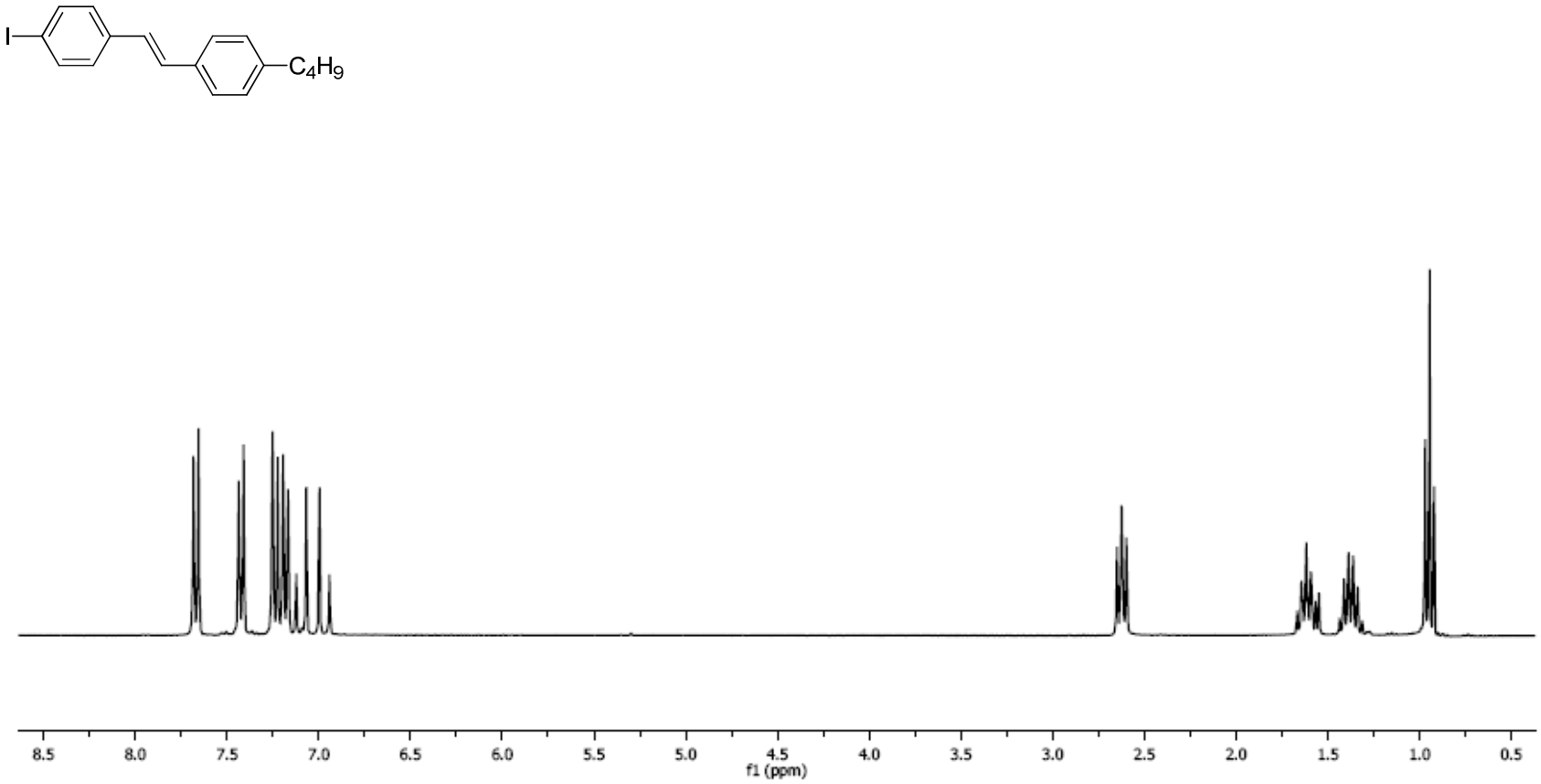


**Figure 19A.** $^{1}$H NMR spectrum of **V-13** (300 MHz, $CDCl_3$, 23 °C).

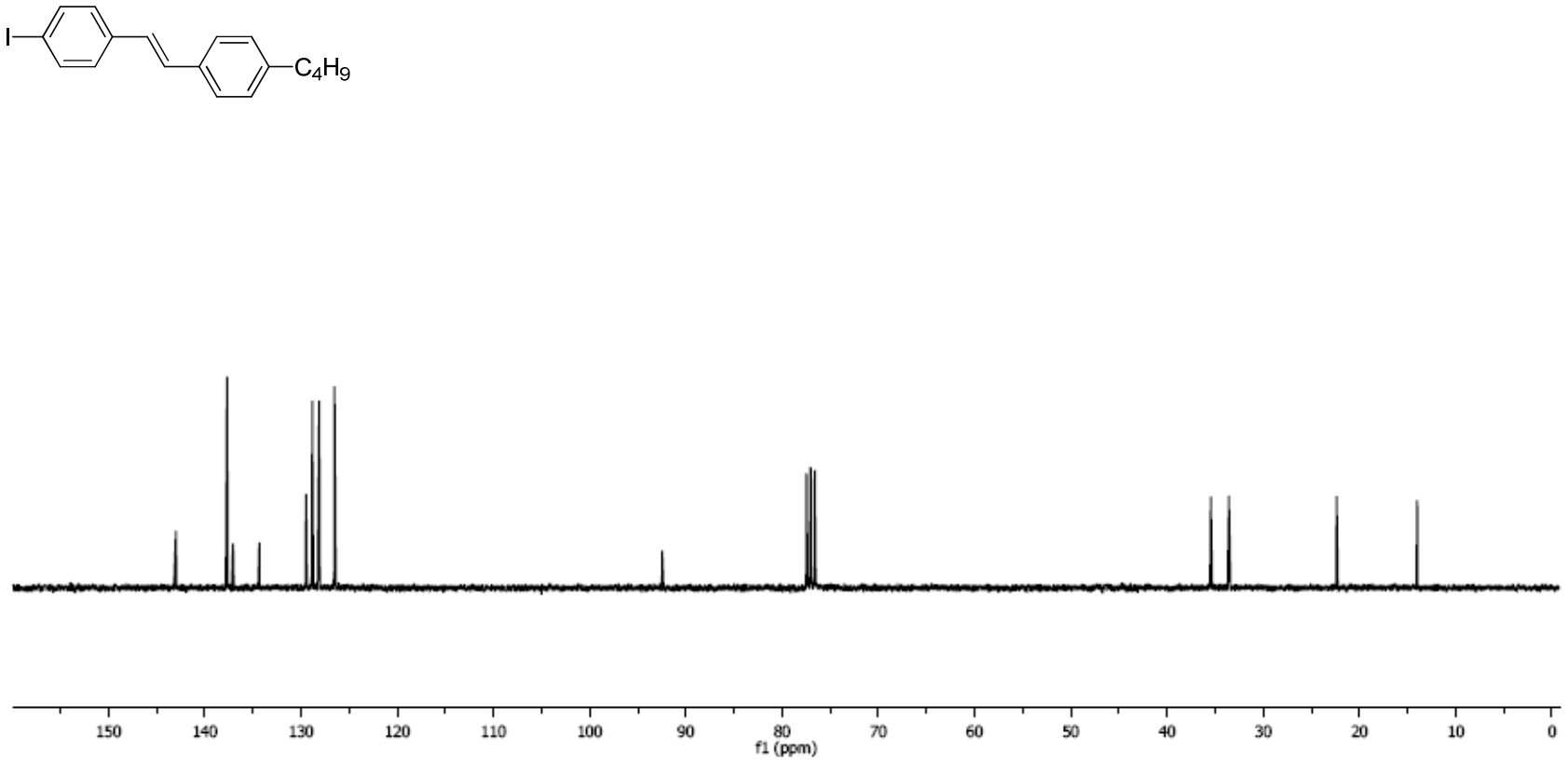


**Figure 19B.** $^{13}C$ NMR spectrum of **V-13** (75 MHz, $CDCl_3$, 23 °C).

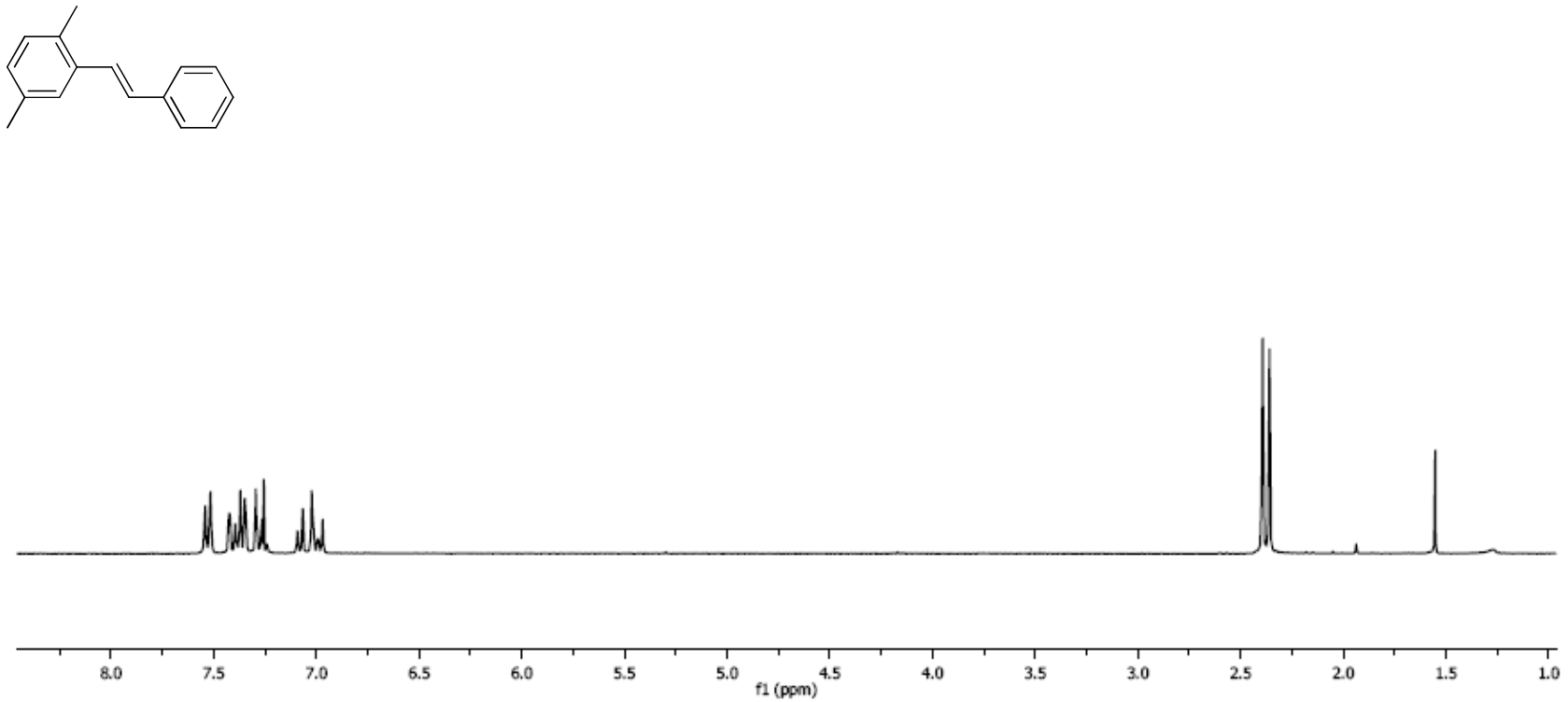


**Figure 20A.** $^{1}$H NMR spectrum of **$Me_2PV_2$** (300 MHz, $CDCl_3$, 23 °C).

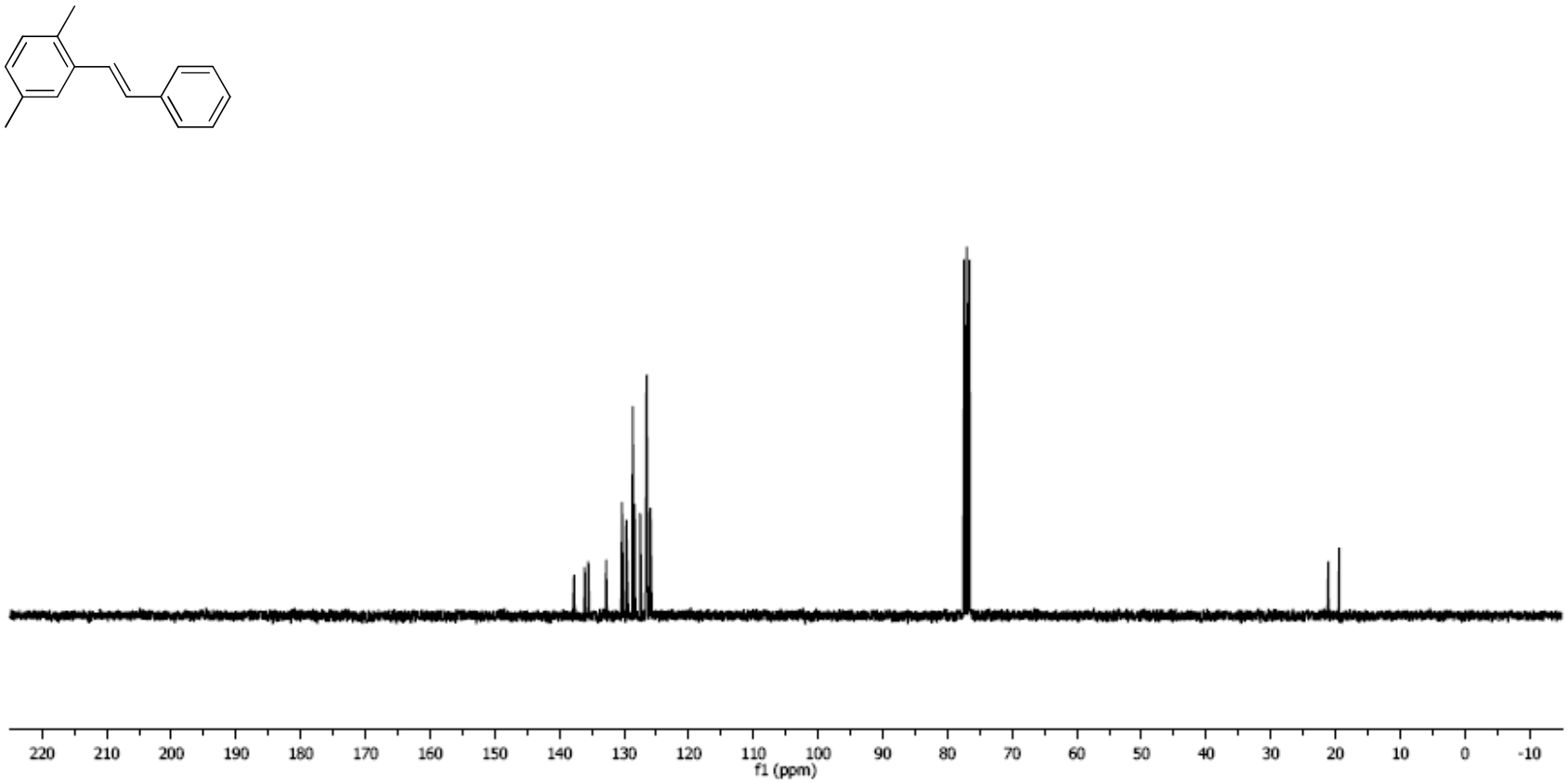


**Figure 20B.** $^{13}$C NMR spectrum of **$Me_2PV_2$** (75 MHz, $CDCl_3$, 23 °C).

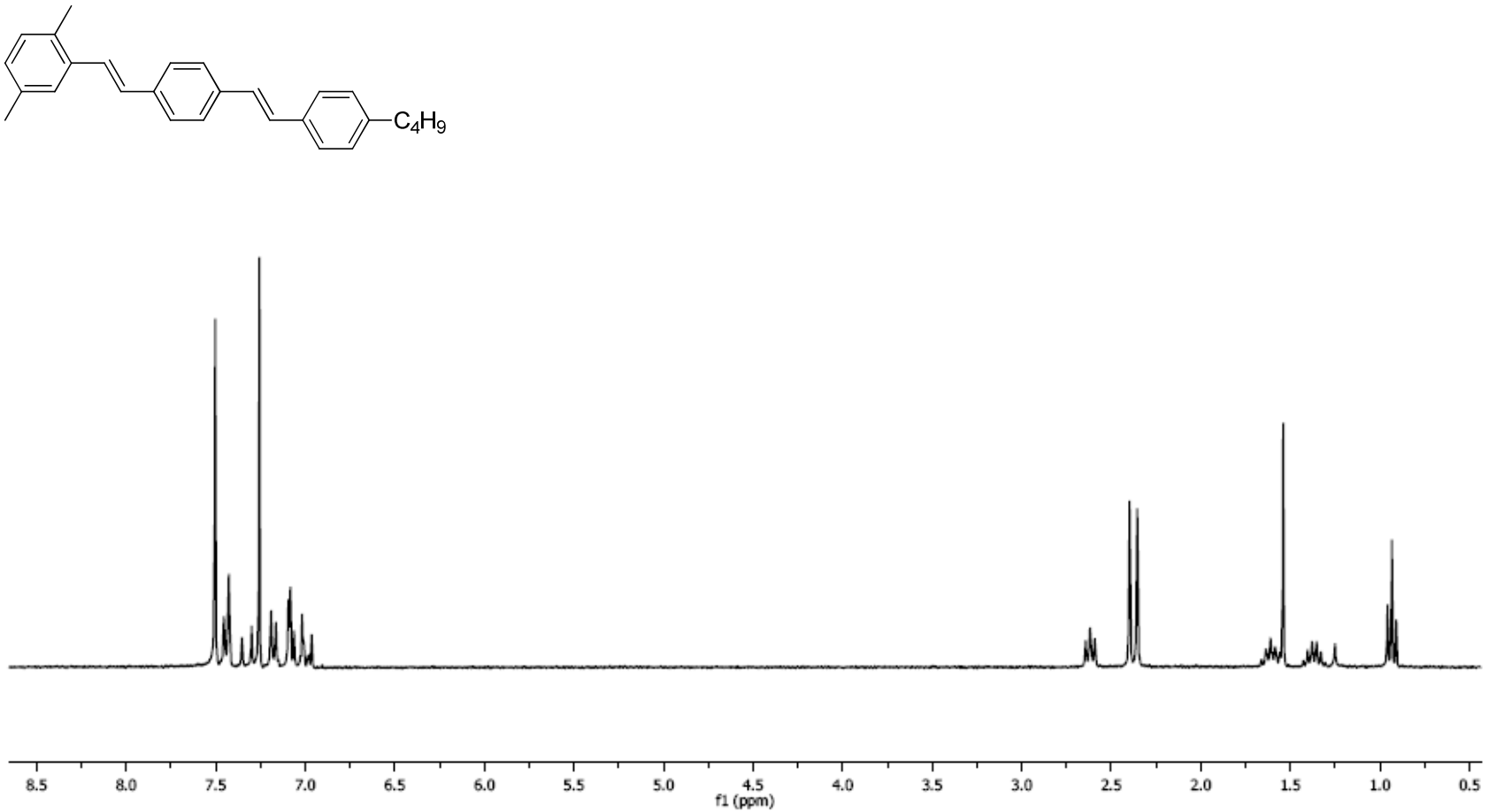


**Figure 21A.** $^{1}$H NMR spectrum of **$Me_2PV_3$** (300 MHz, $CDCl_3$, 23 °C).

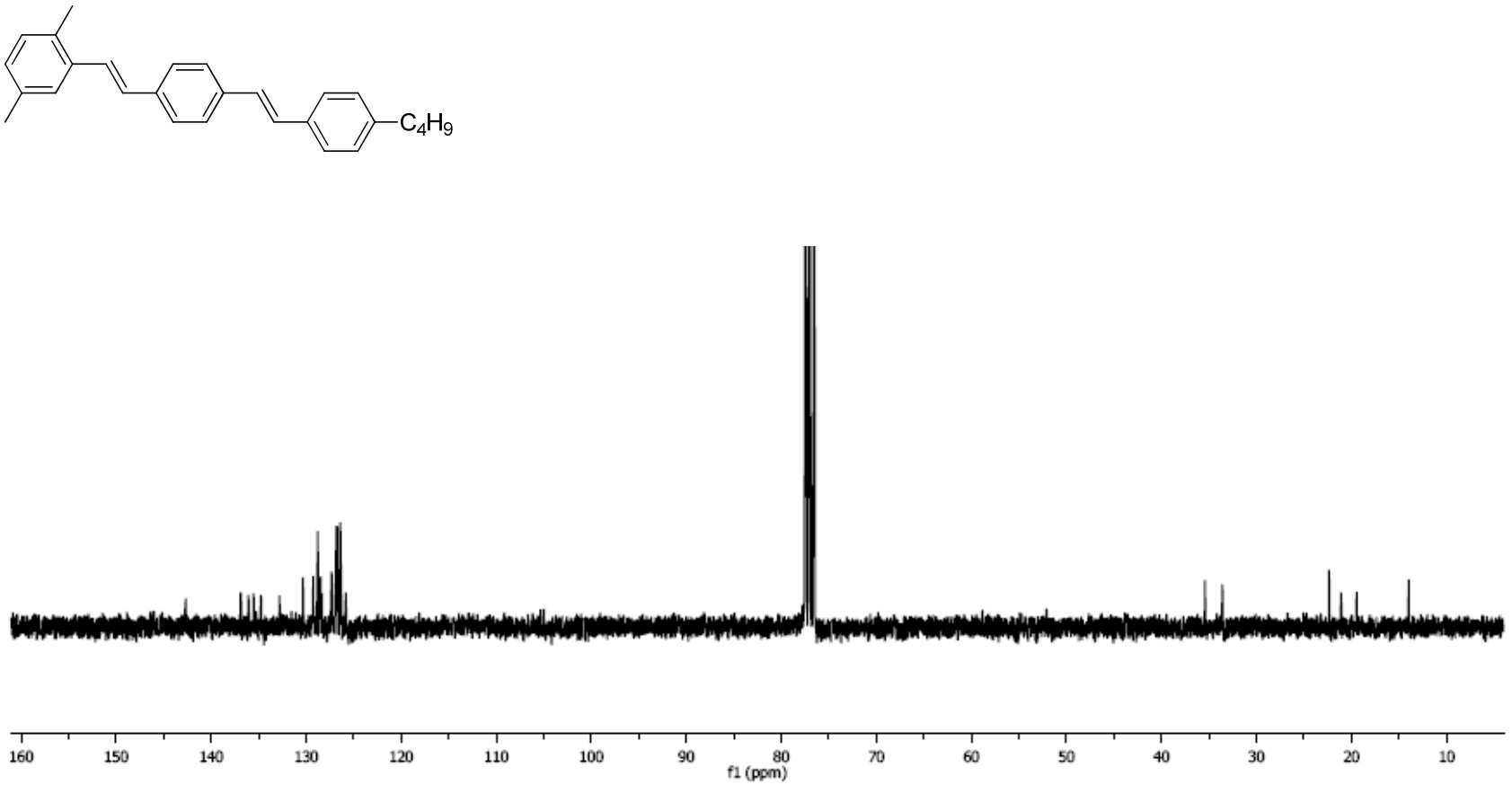


**Figure 21B.** $^{13}$C NMR spectrum of **$Me_2PV_3$** (75 MHz, $CDCl_3$, 23 °C).

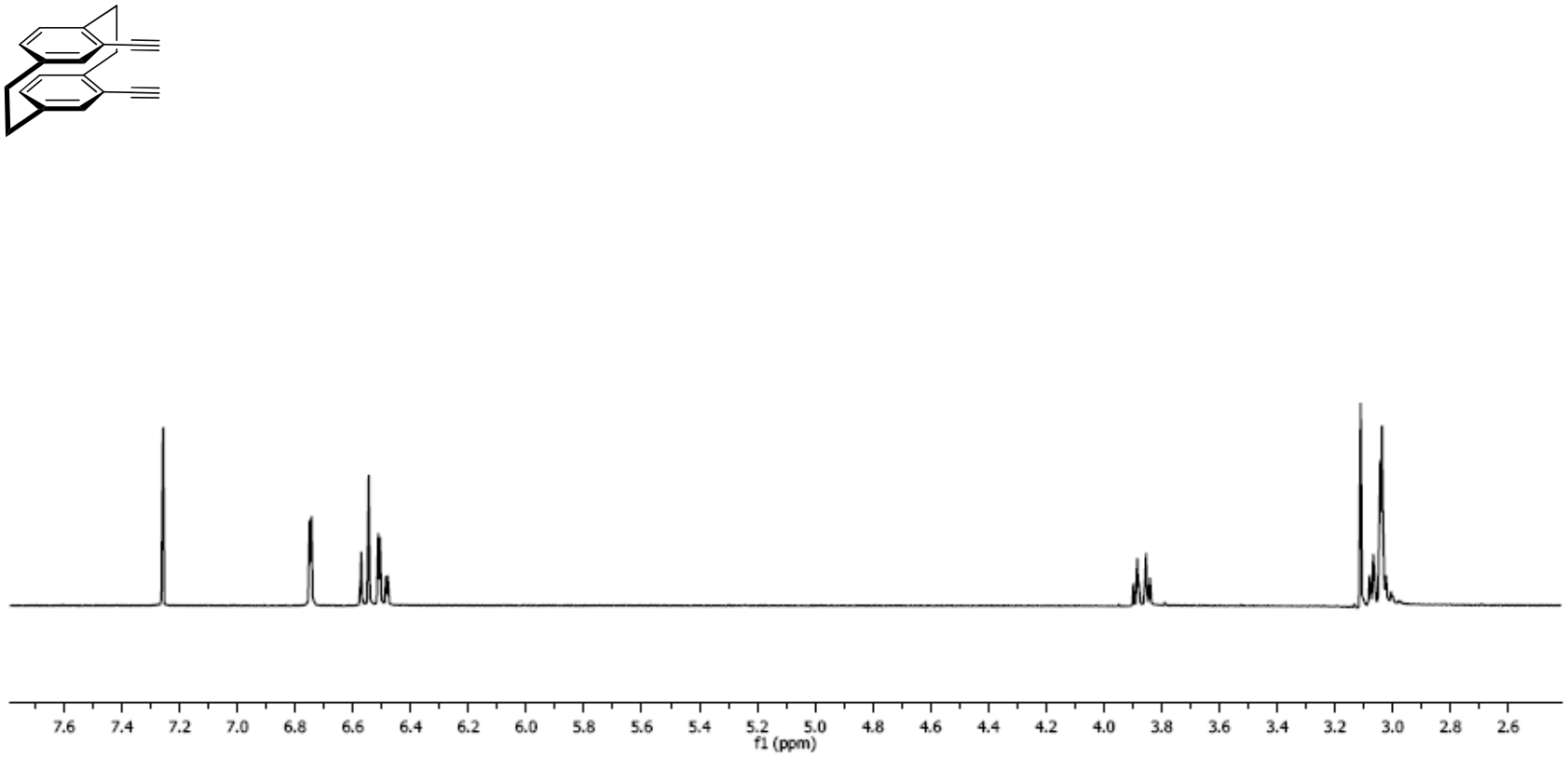


**Figure 22A.** $^{1}$H NMR spectrum of **VI-1** (300 MHz, $CDCl_3$, 23 °C).

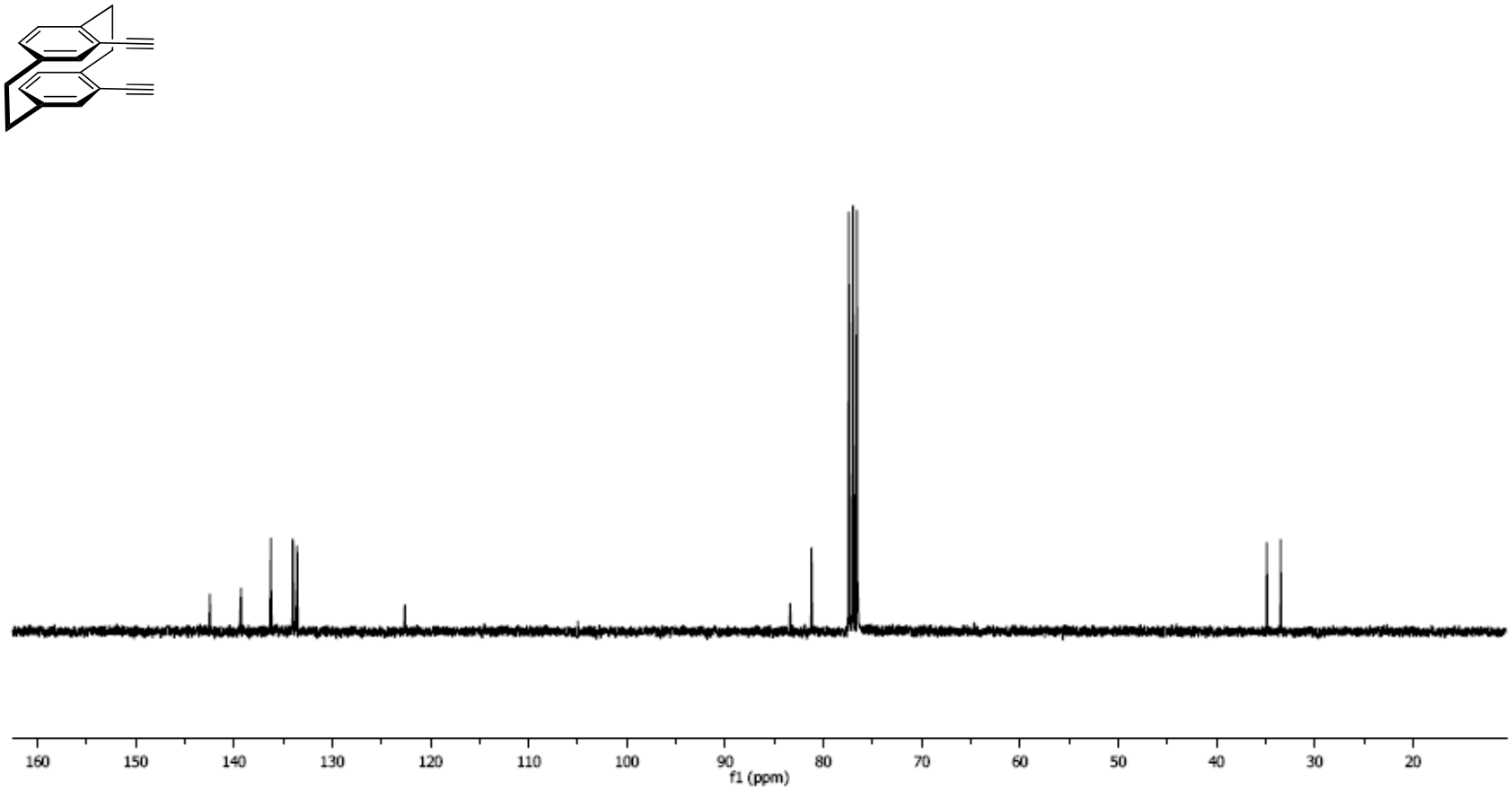


**Figure 22B.** $^{13}C$ NMR spectrum of **VI-1** (75 MHz, $CDCl_3$, 23 °C).

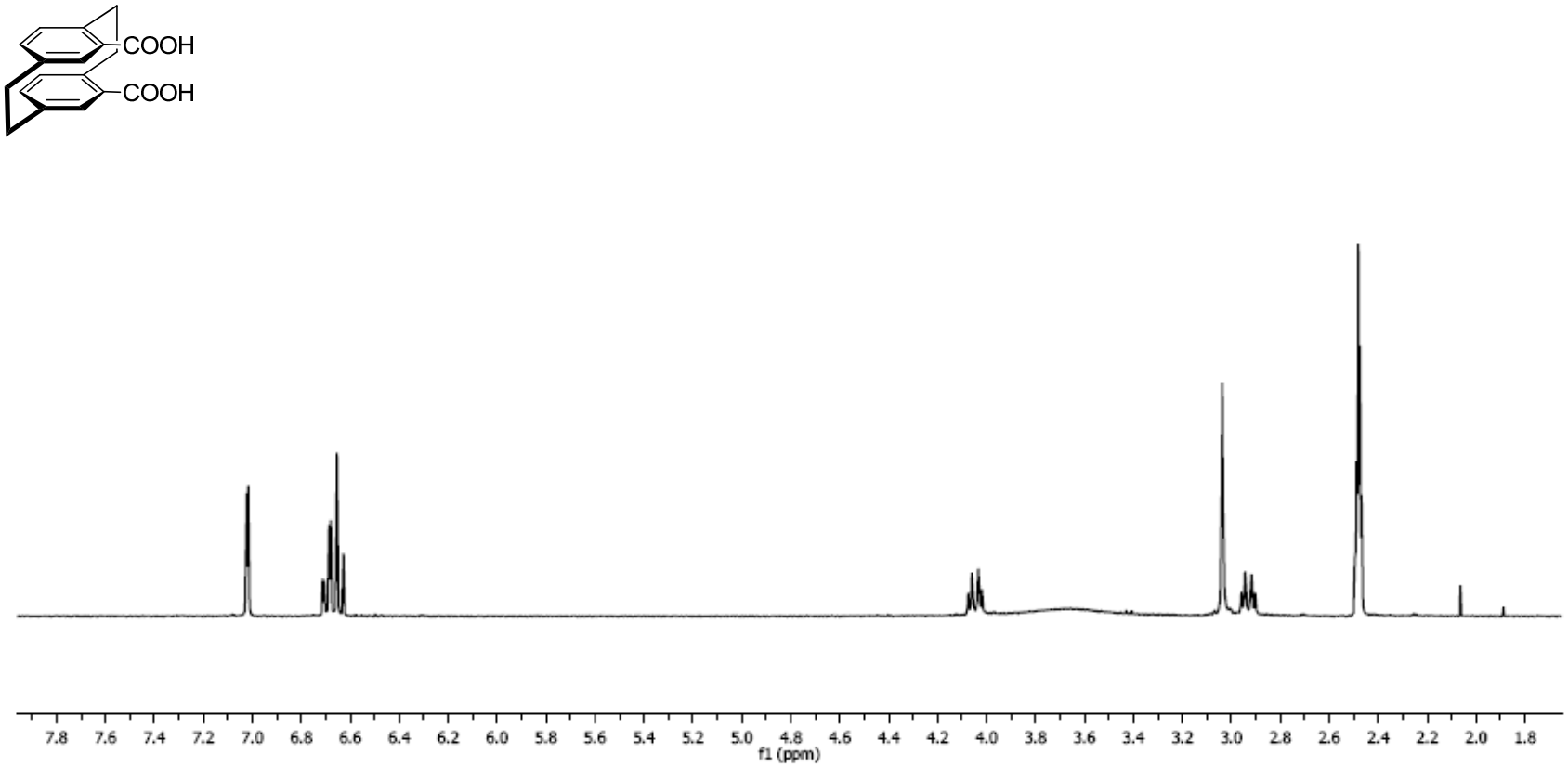


**Figure 23A.** $^{1}$H NMR spectrum of **VI-2** (300 MHz, acetone-$d_6$, 23 °C).

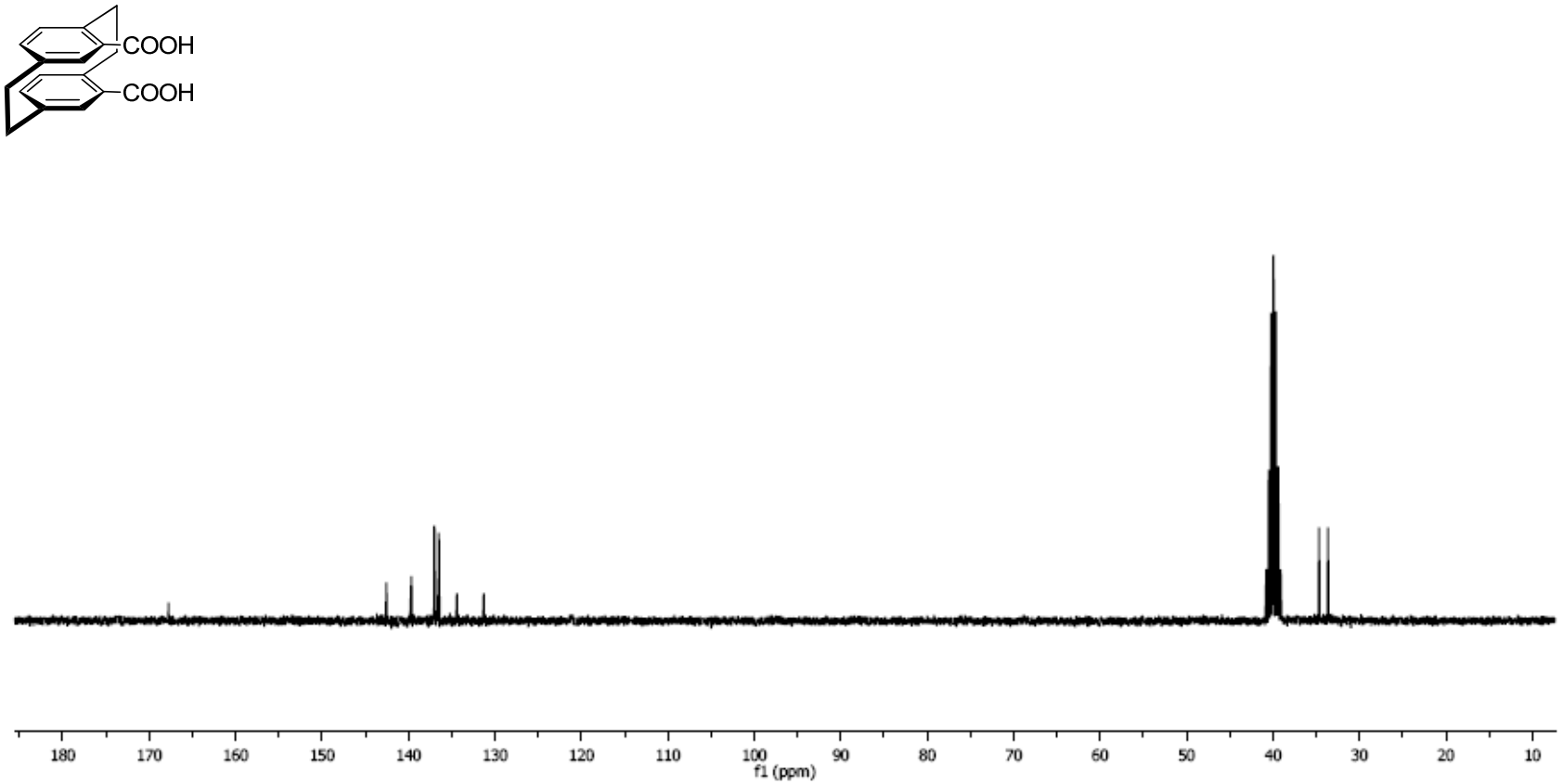


**Figure 23B.** $^{13}$C NMR spectrum of **VI-2** (75 MHz, acetone-$d_6$, 23 °C).

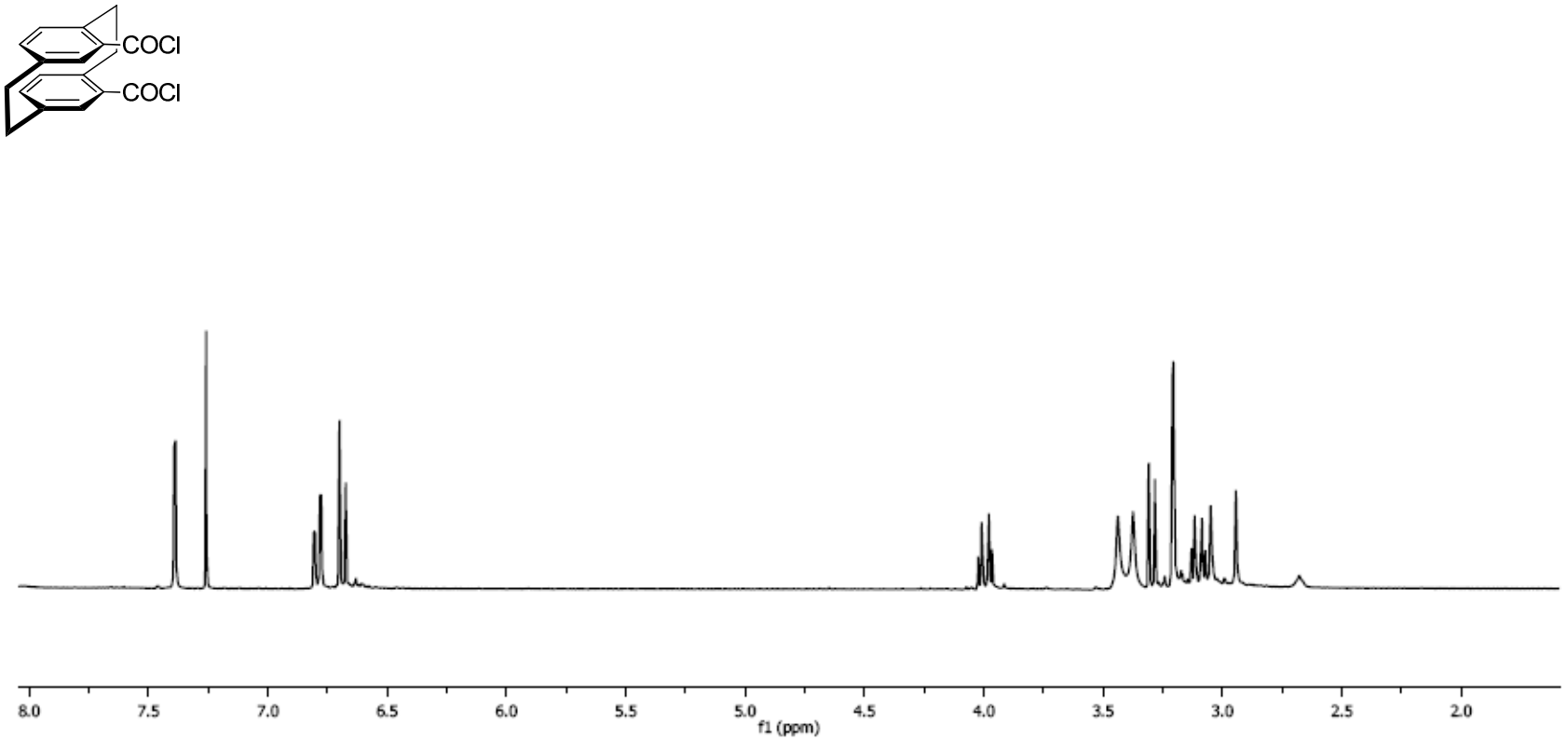


**Figure 24A.** $^{1}$H NMR spectrum of **VI-3** (300 MHz, $CDCl_3$, 23 °C).

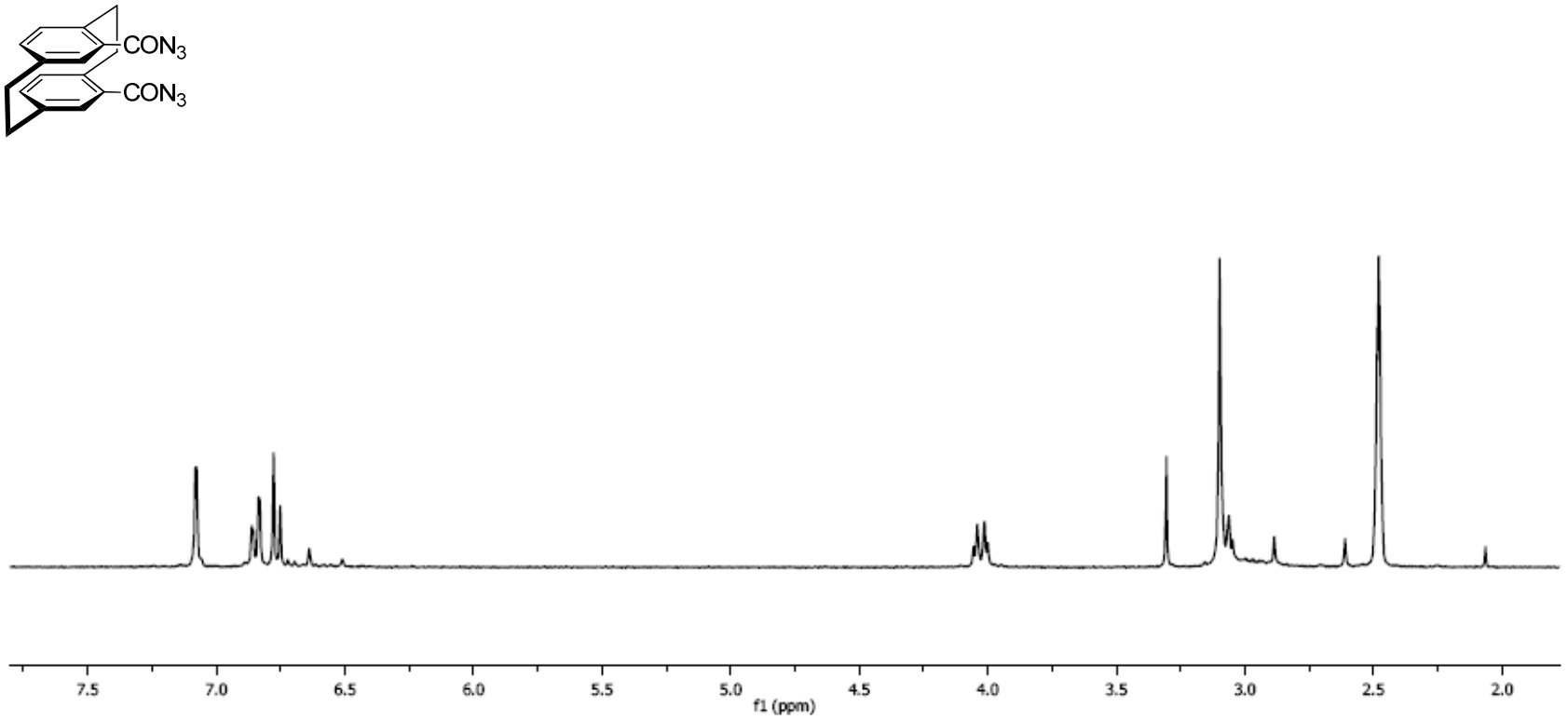


**Figure 25A.** $^{1}$H NMR spectrum of **VI-4** (300 MHz, DMSO-$d_6$, 23 °C).

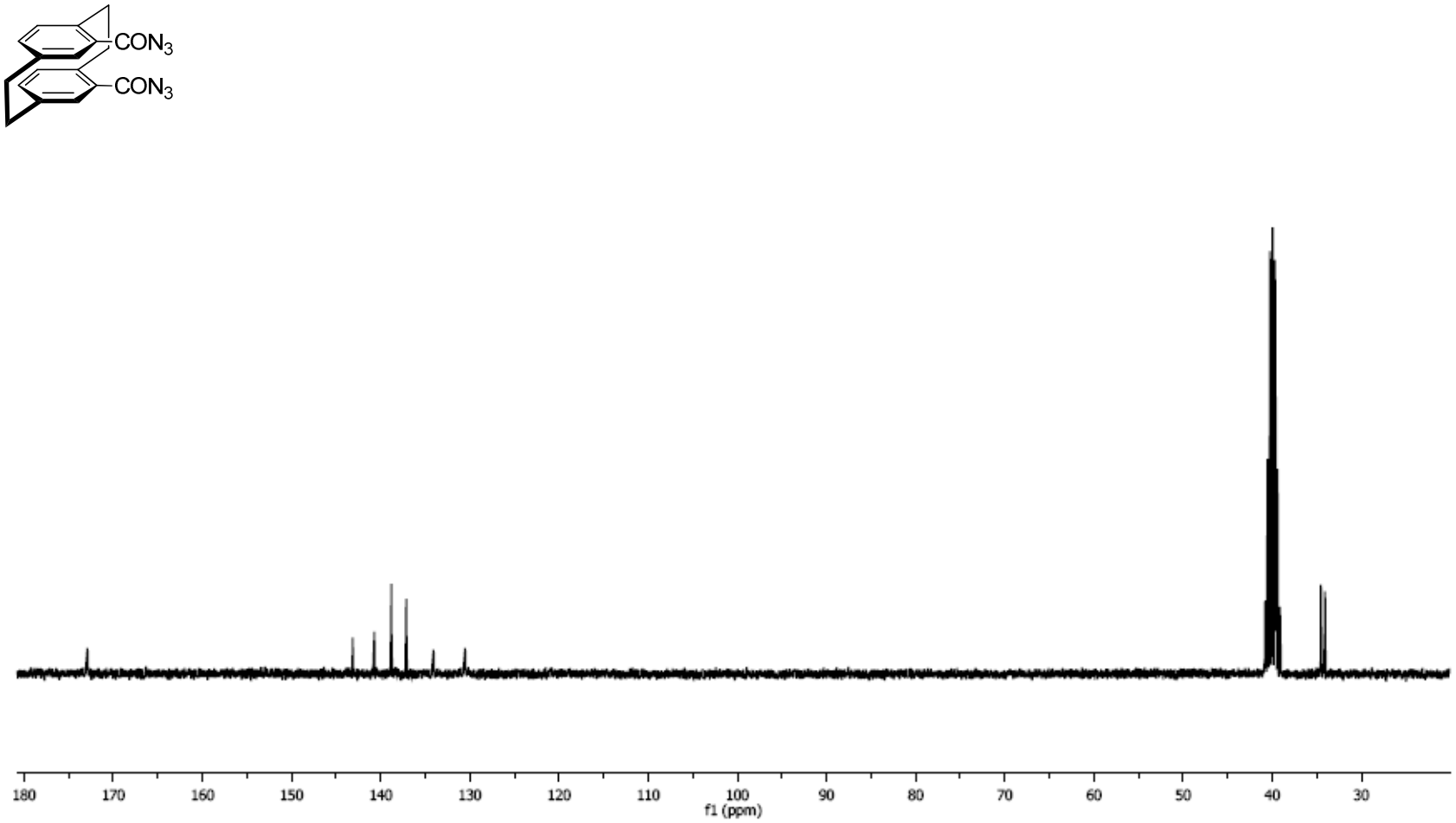


**Figure 25B.** $^{13}$C NMR spectrum of **VI-4** (75 MHz, DMSO-$d_6$, 23 °C).

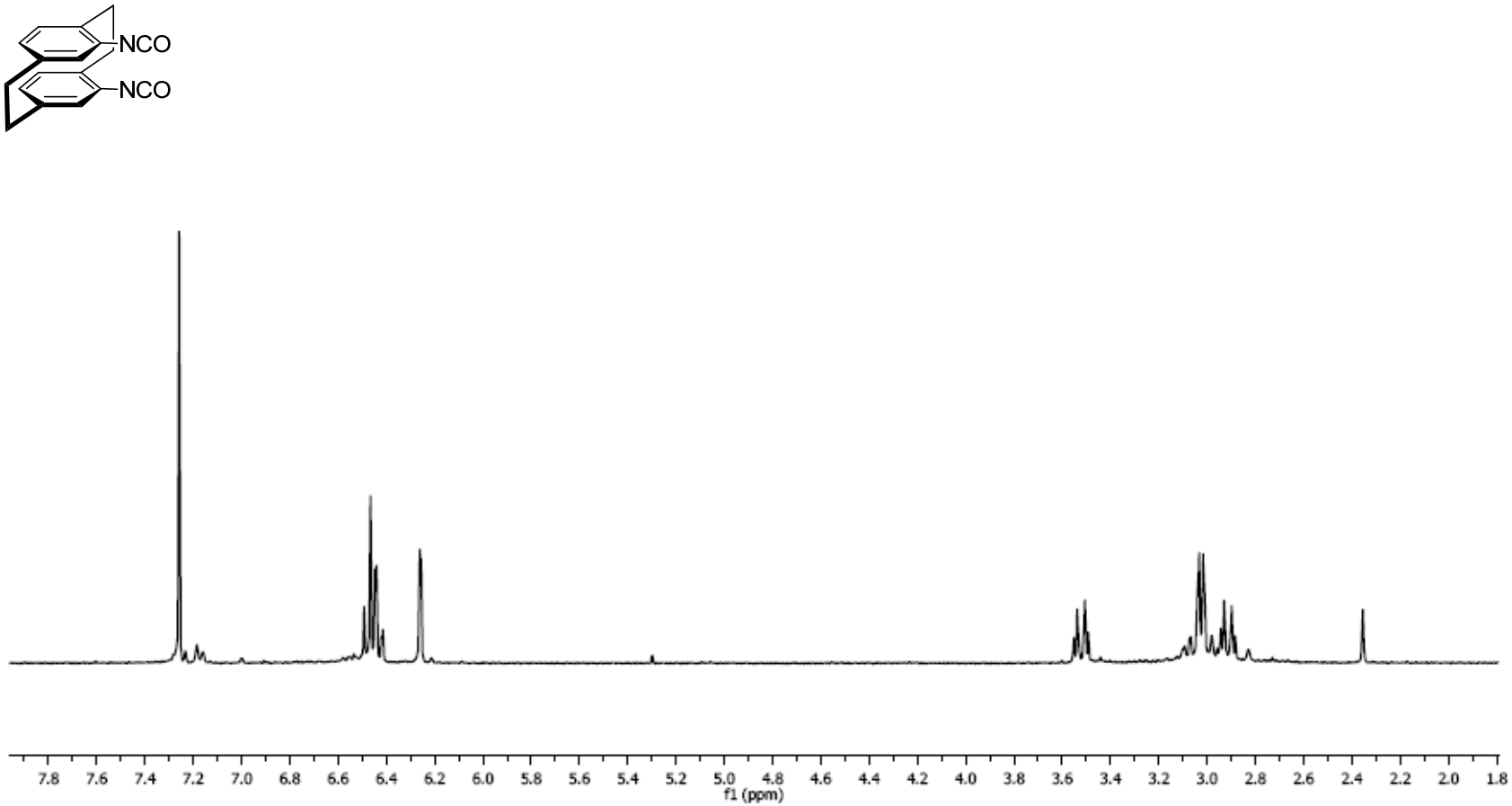


**Figure 26A.** $^{1}$H NMR spectrum of **VI-5** (300 MHz, $CDCl_3$, 23 °C).

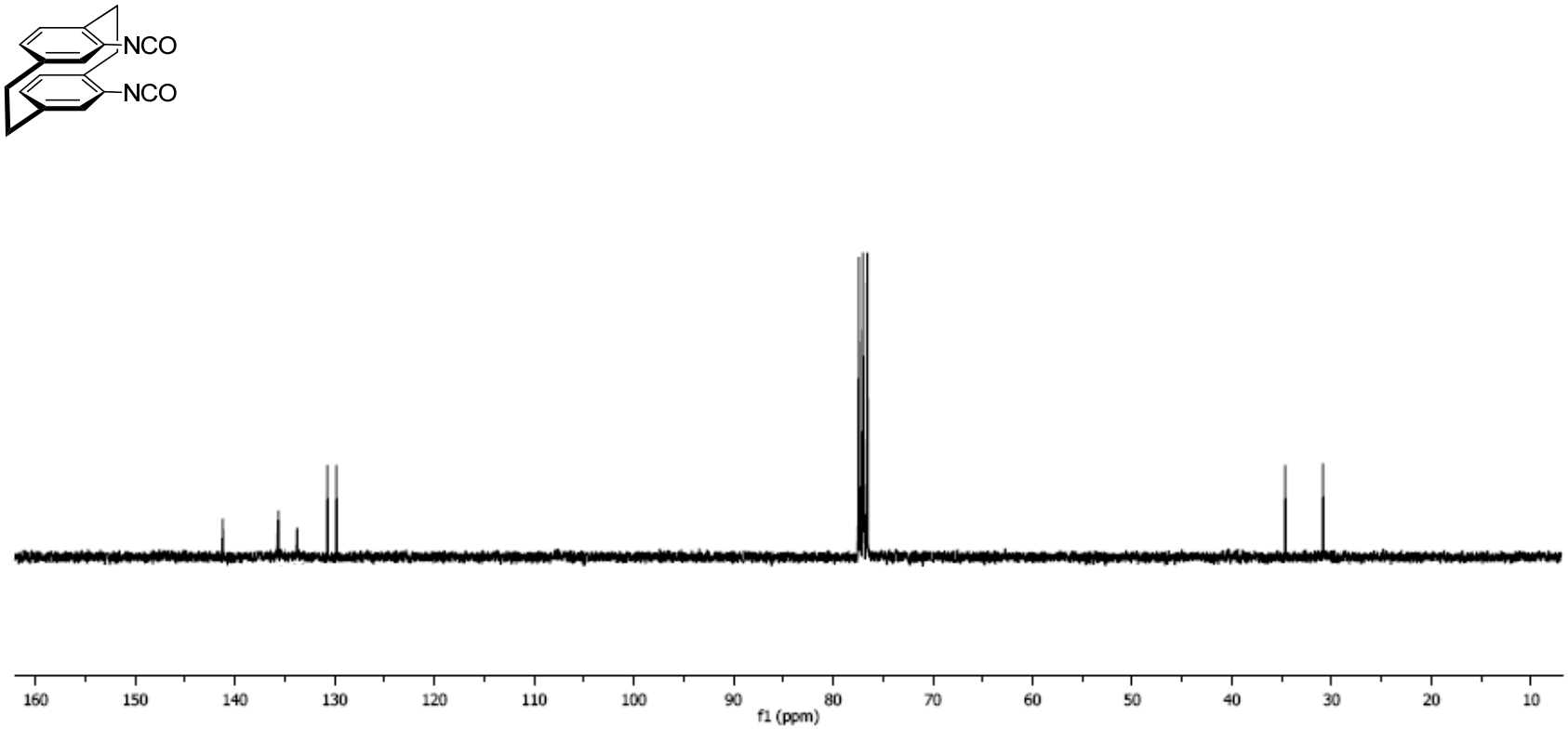


**Figure 26B.** $^{13}C$ NMR spectrum of **VI-5** (75 MHz, $CDCl_3$, 23 °C).

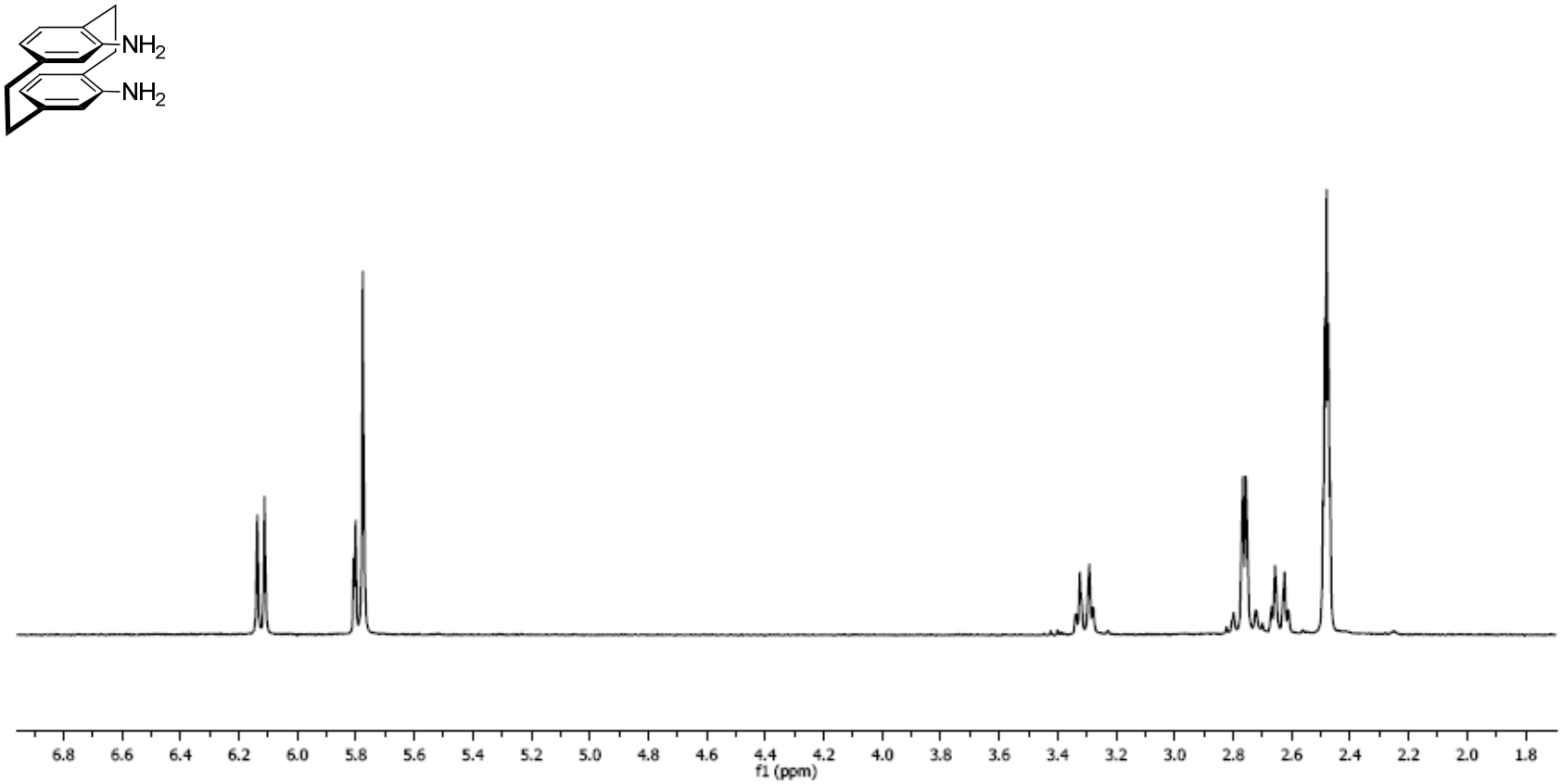


**Figure 27A.** $^{1}$H NMR spectrum of **VI-6** (300 MHz, DMSO-$d_6$, 23 °C).

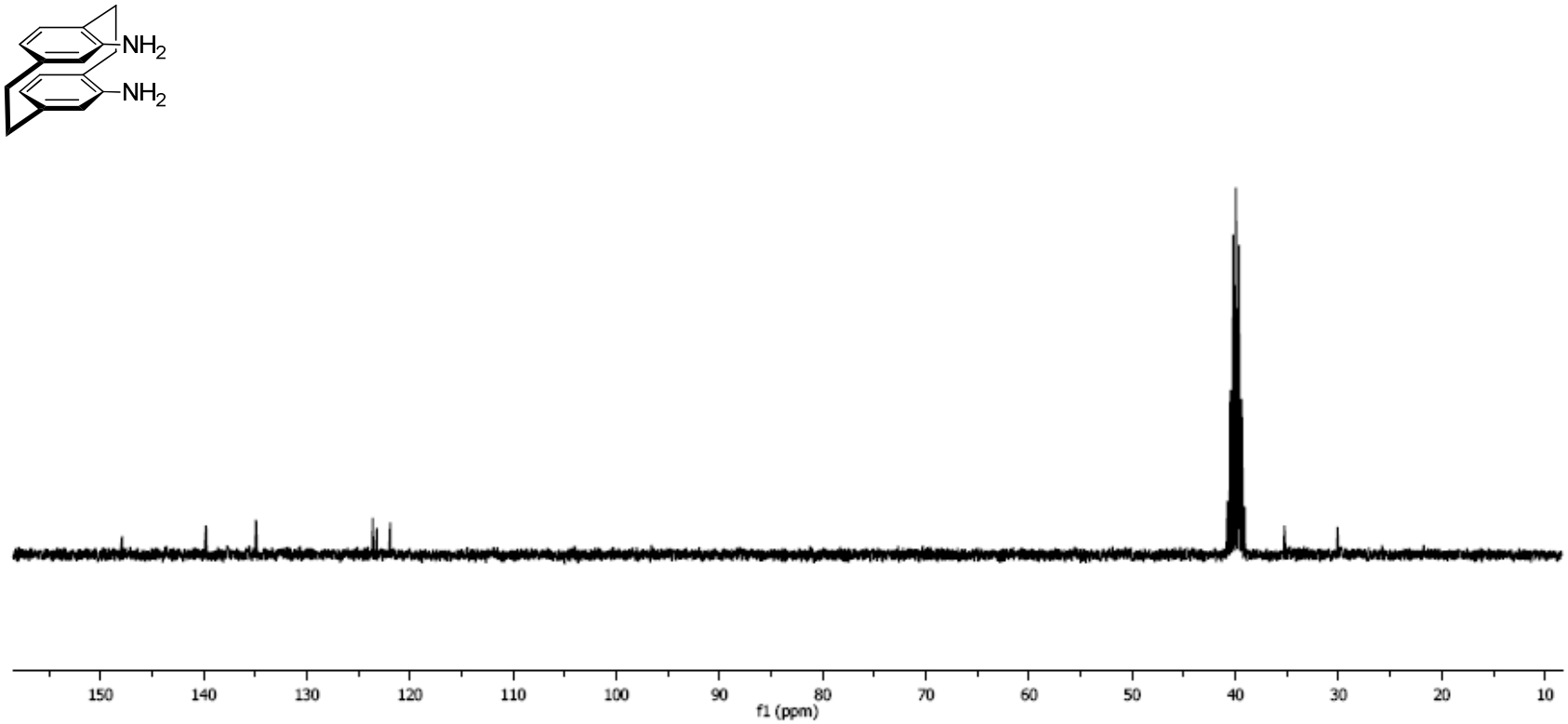


**Figure 27B.** $^{13}$C NMR spectrum of **VI-6** (75 MHz, DMSO-$d_6$, 23 °C).

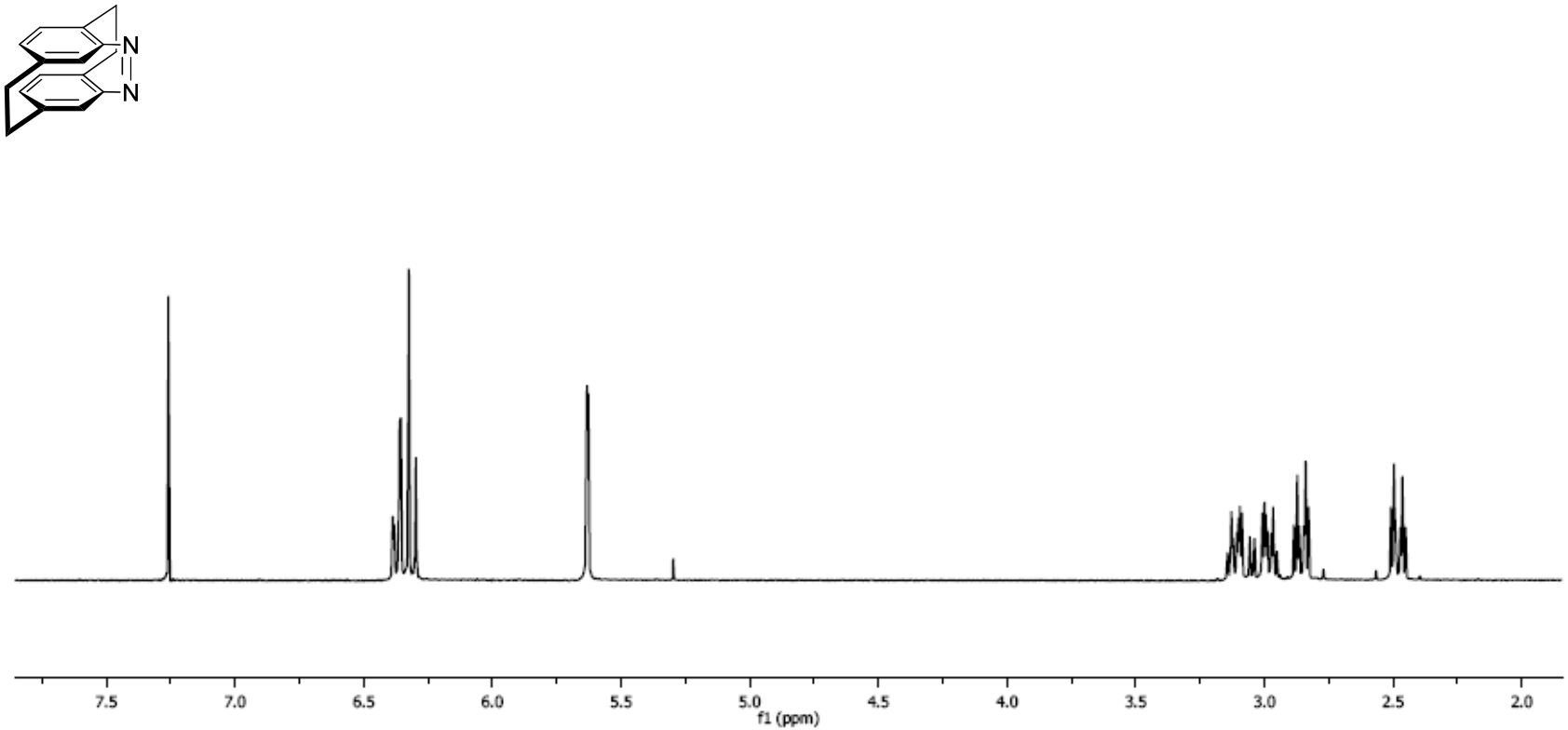


**Figure 28A.** $^{1}$H NMR spectrum of **VI-7** (300 MHz, $CDCl_3$, 23 °C).

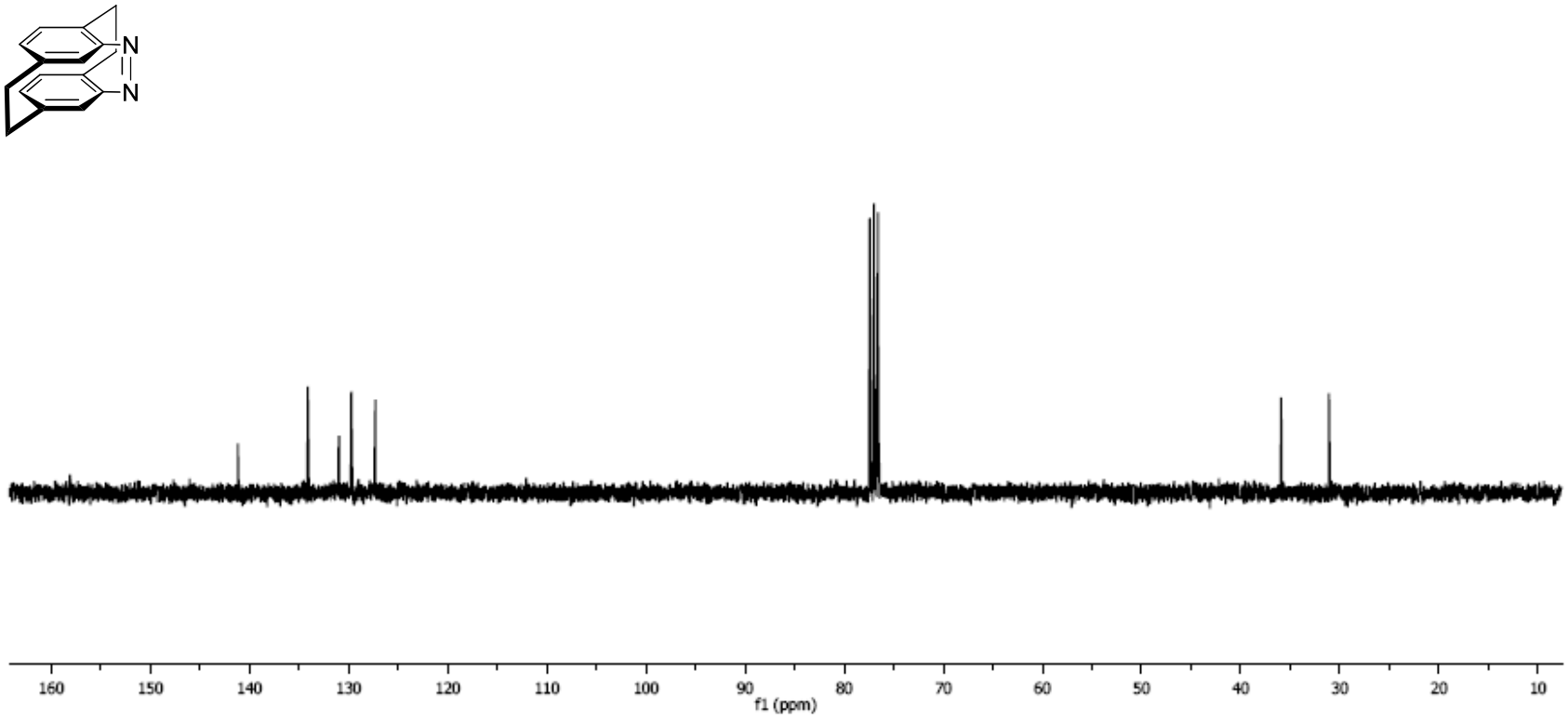


**Figure 28B.** $^{13}C$ NMR spectrum of **VI-7** (75 MHz, $CDCl_3$, 23 °C).

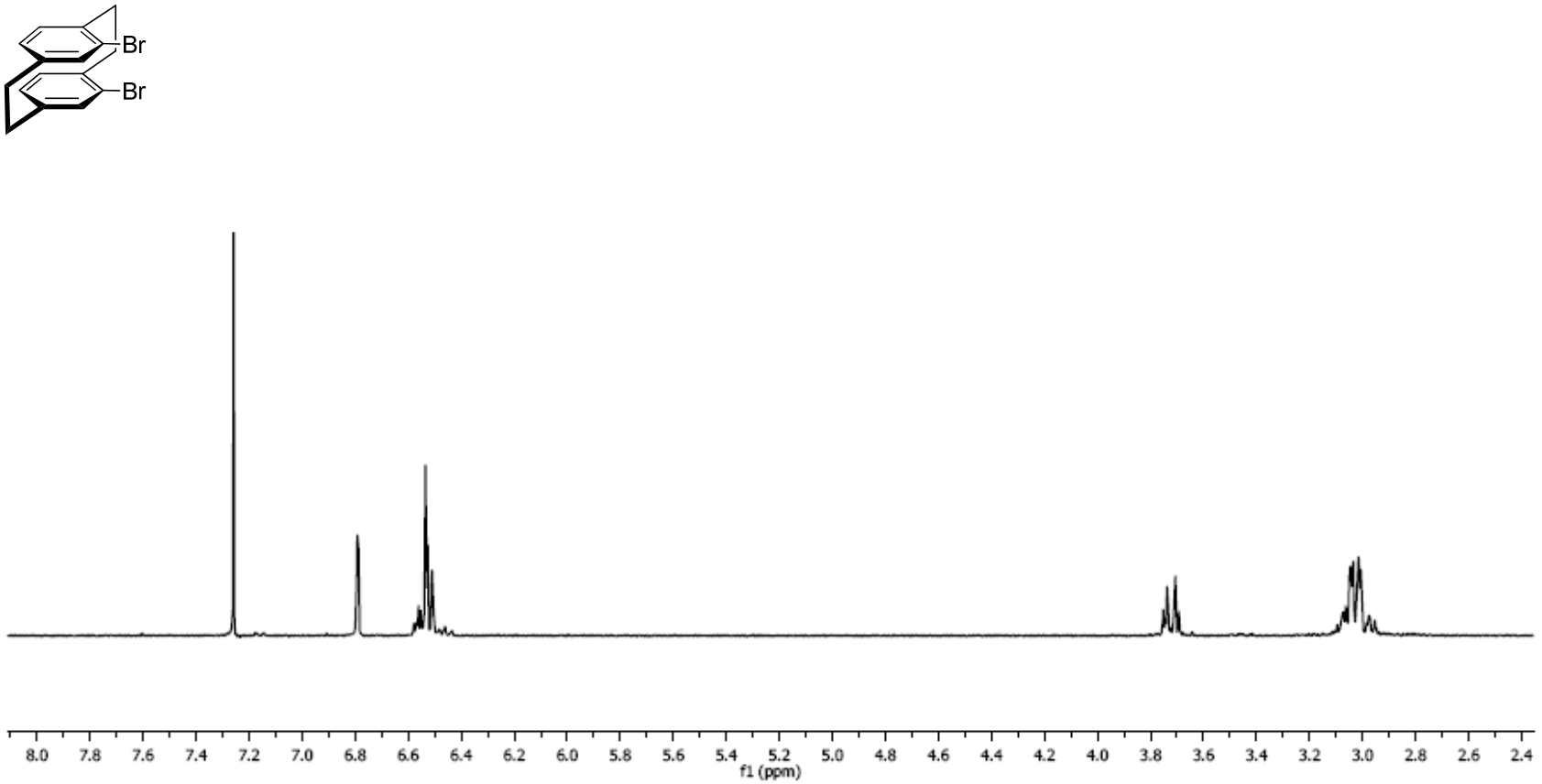


**Figure 29A.** $^{1}$H NMR spectrum of ***pg*-CpBr$_2$** (300 MHz, $CDCl_3$, 23 °C).

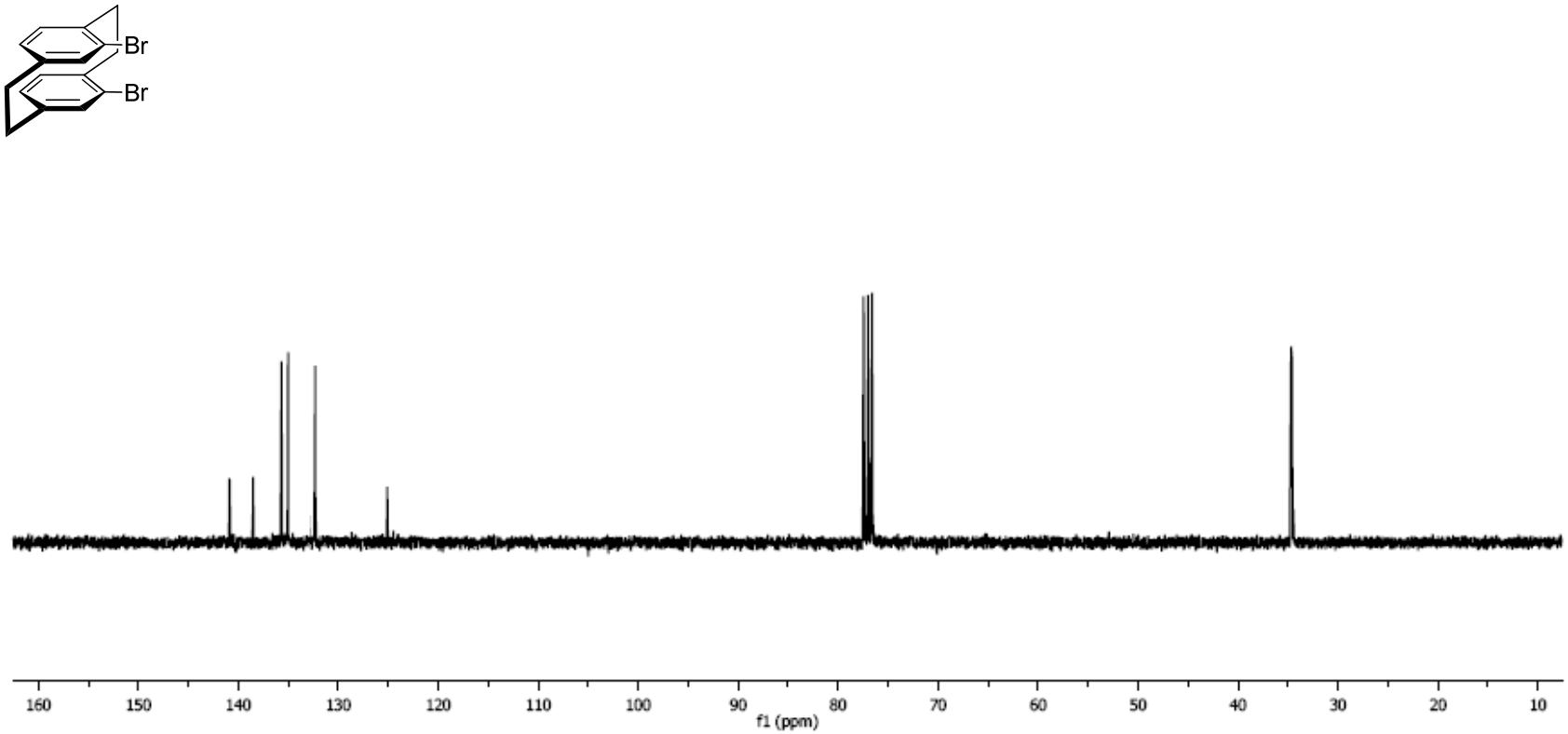


**Figure 29B.** $^{13}$C NMR spectrum of ***pg*-CpBr$_2$** (75 MHz, $CDCl_3$, 23 °C).

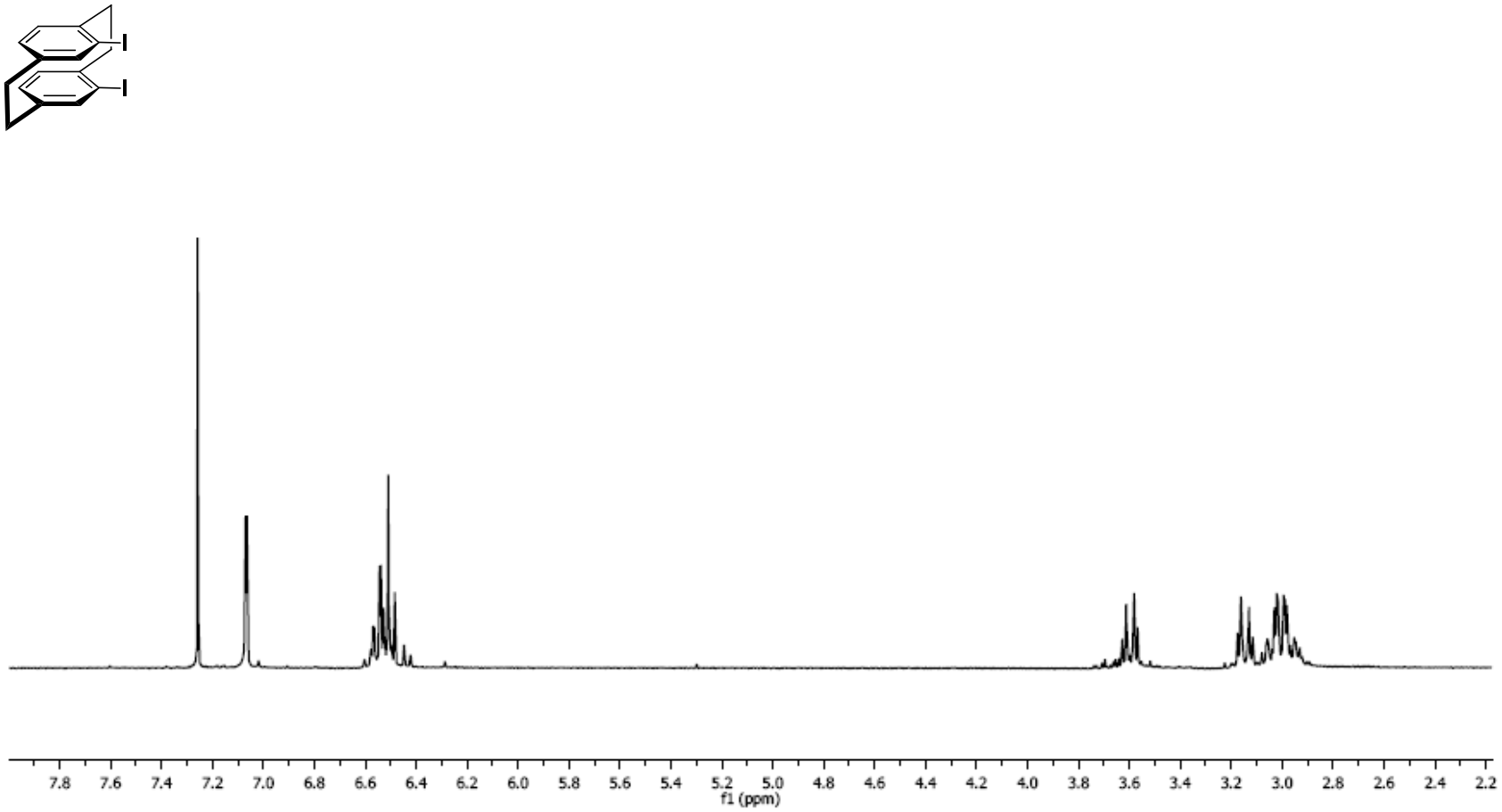


**Figure 30A.** $^{1}$H NMR spectrum of ***pg*-$CpI_2$** (300 MHz, $CDCl_3$, 23 °C).

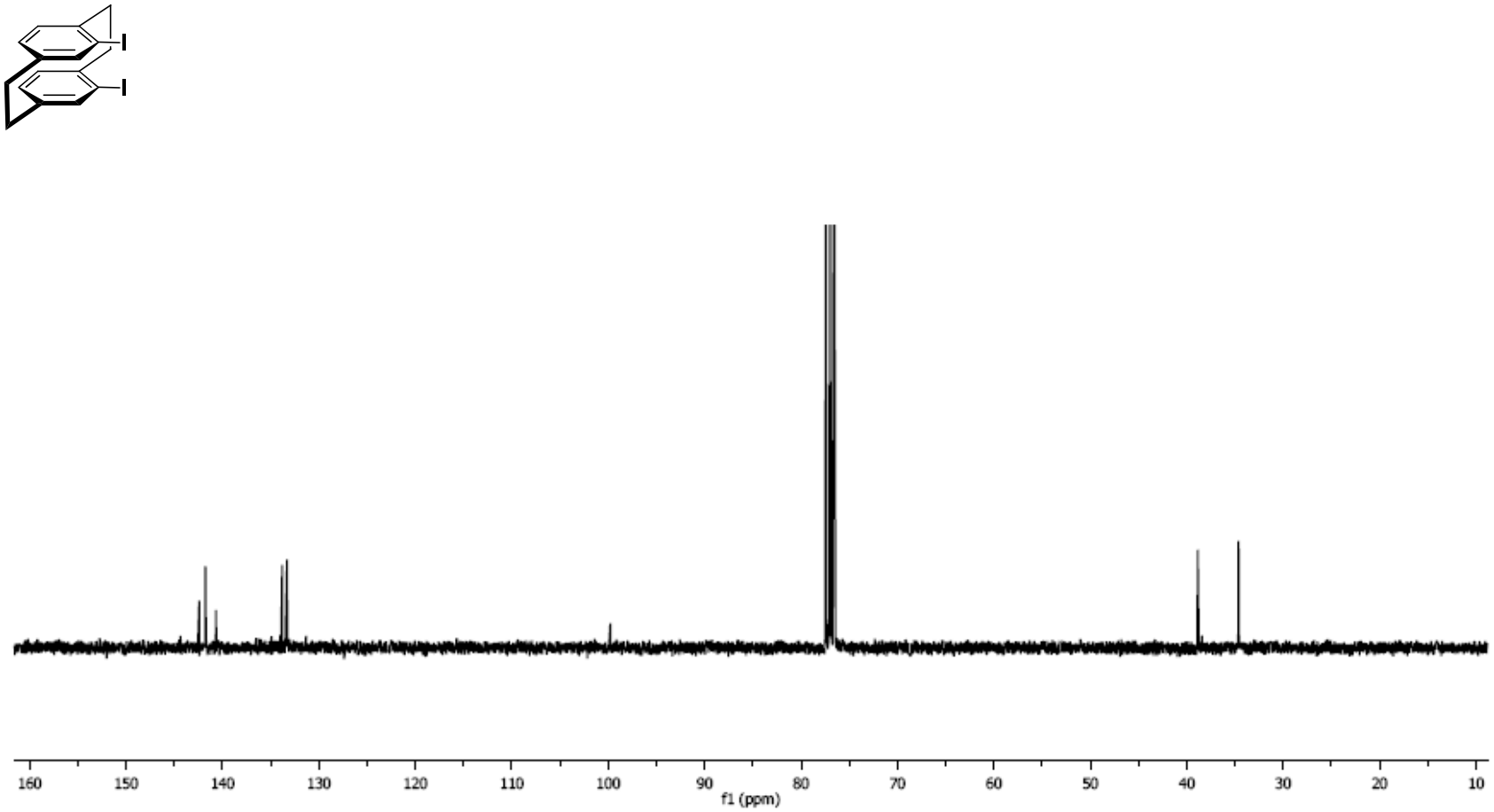


**Figure 30B.** $^{13}$C NMR spectrum of ***pg*-CpI$_2$** (75 MHz, $CDCl_3$, 23 °C).

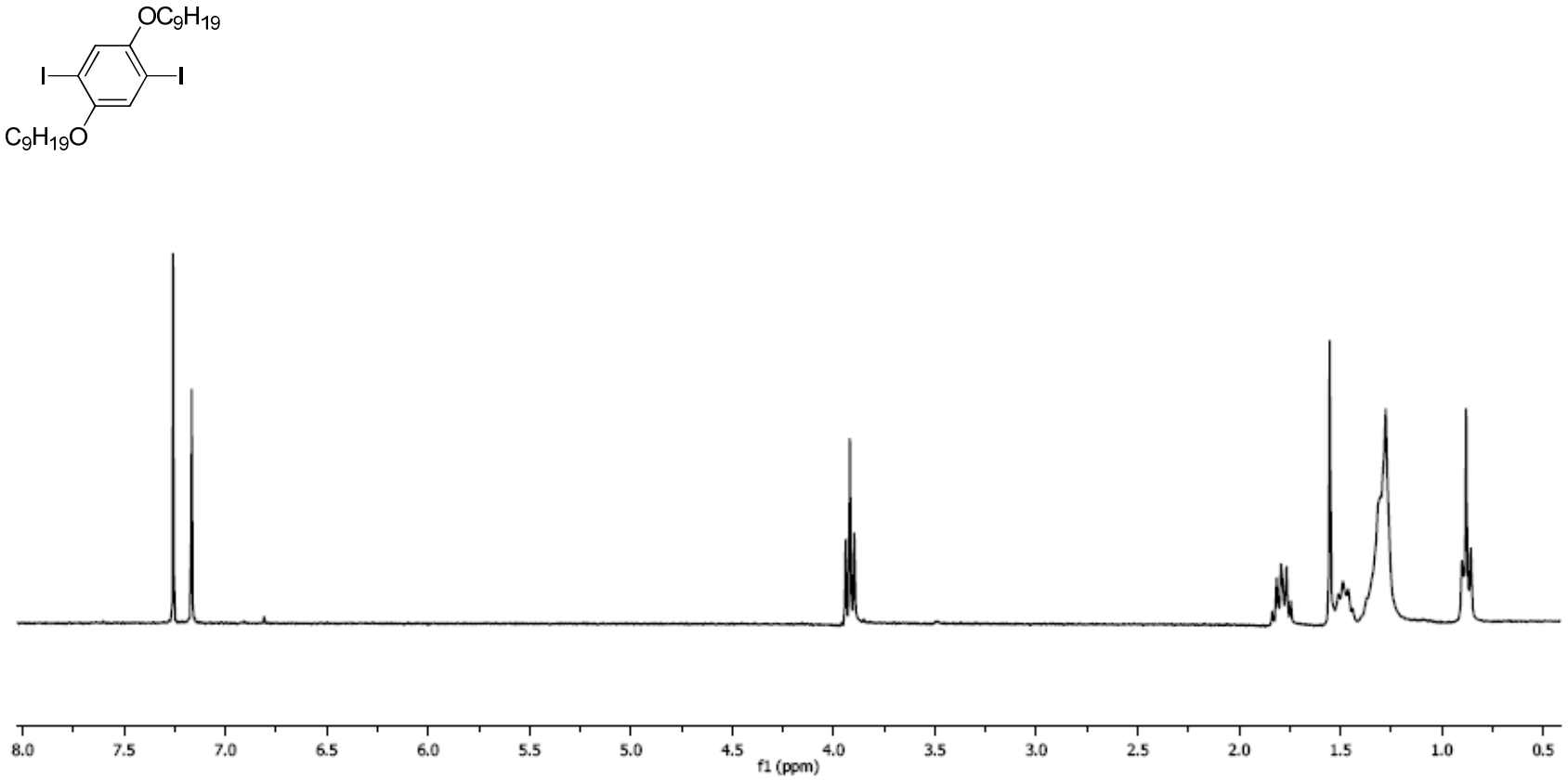


**Figure 31A.** $^{1}$H NMR spectrum of **VI-10** (300 MHz, $CDCl_3$, 23 °C).

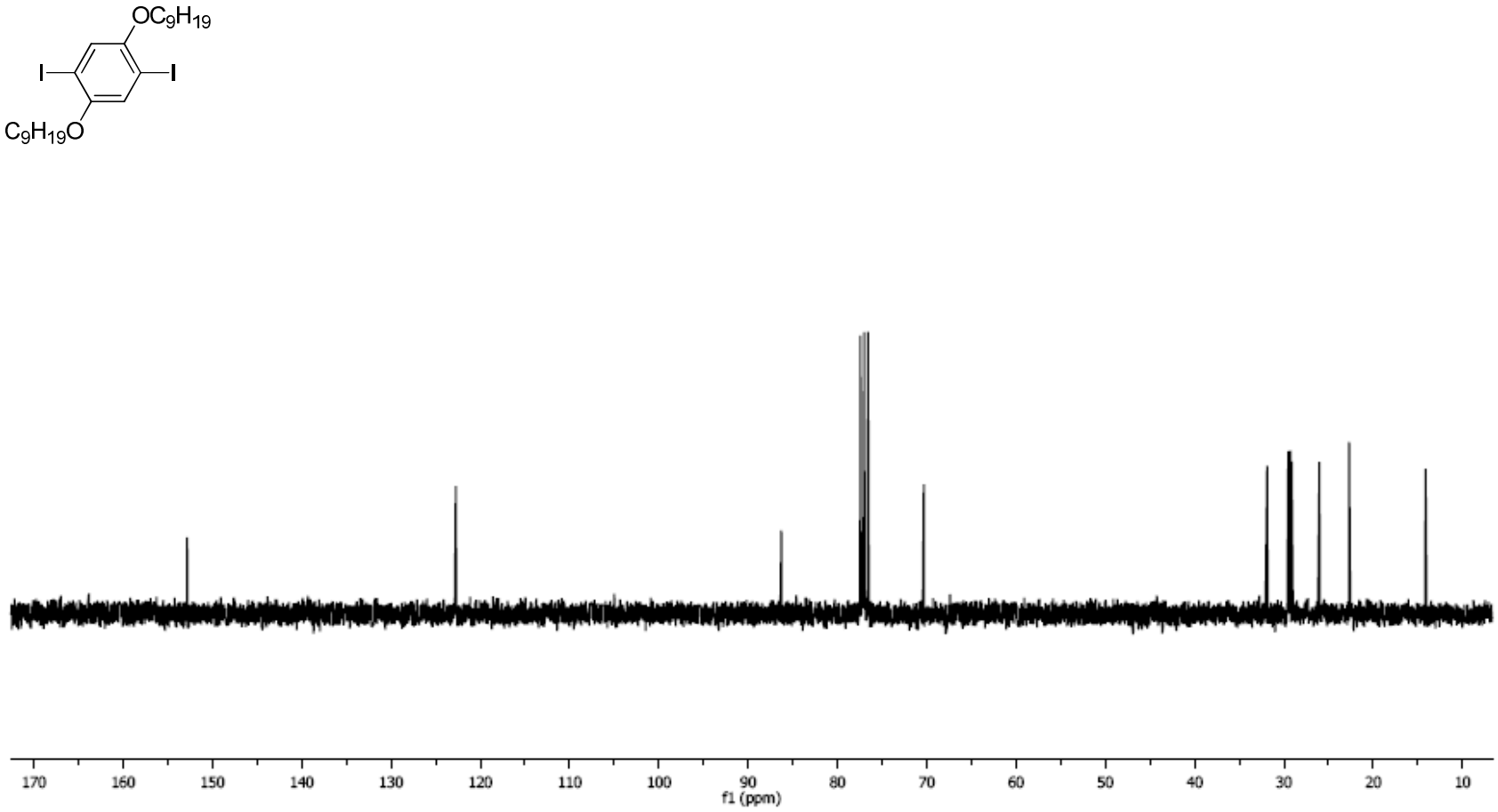


**Figure 31B.** $^{13}C$ NMR spectrum of **VI-10** (75 MHz, $CDCl_3$, 23 °C).

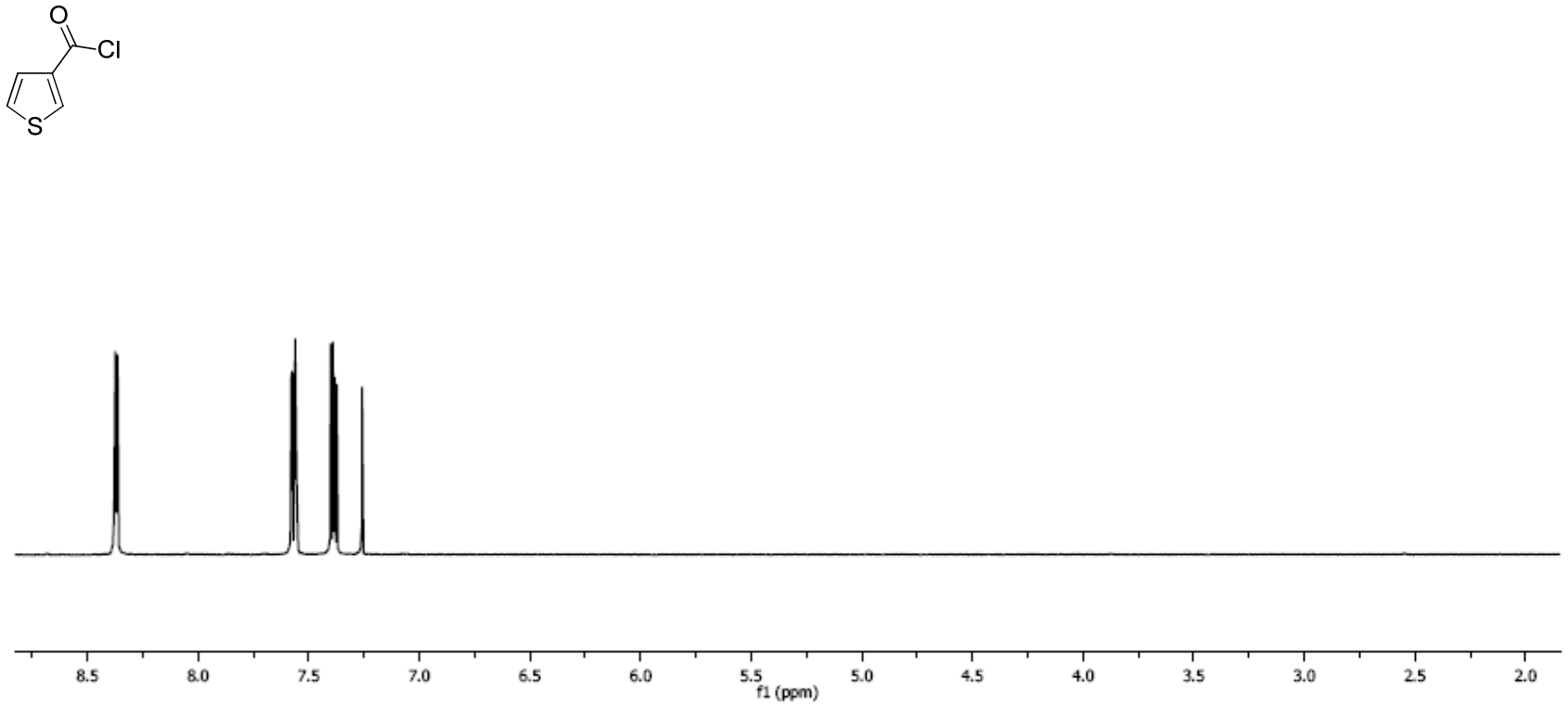


**Figure 32A.** $^{1}$H NMR spectrum of **VI-13** (300 MHz, $CDCl_3$, 23 °C).

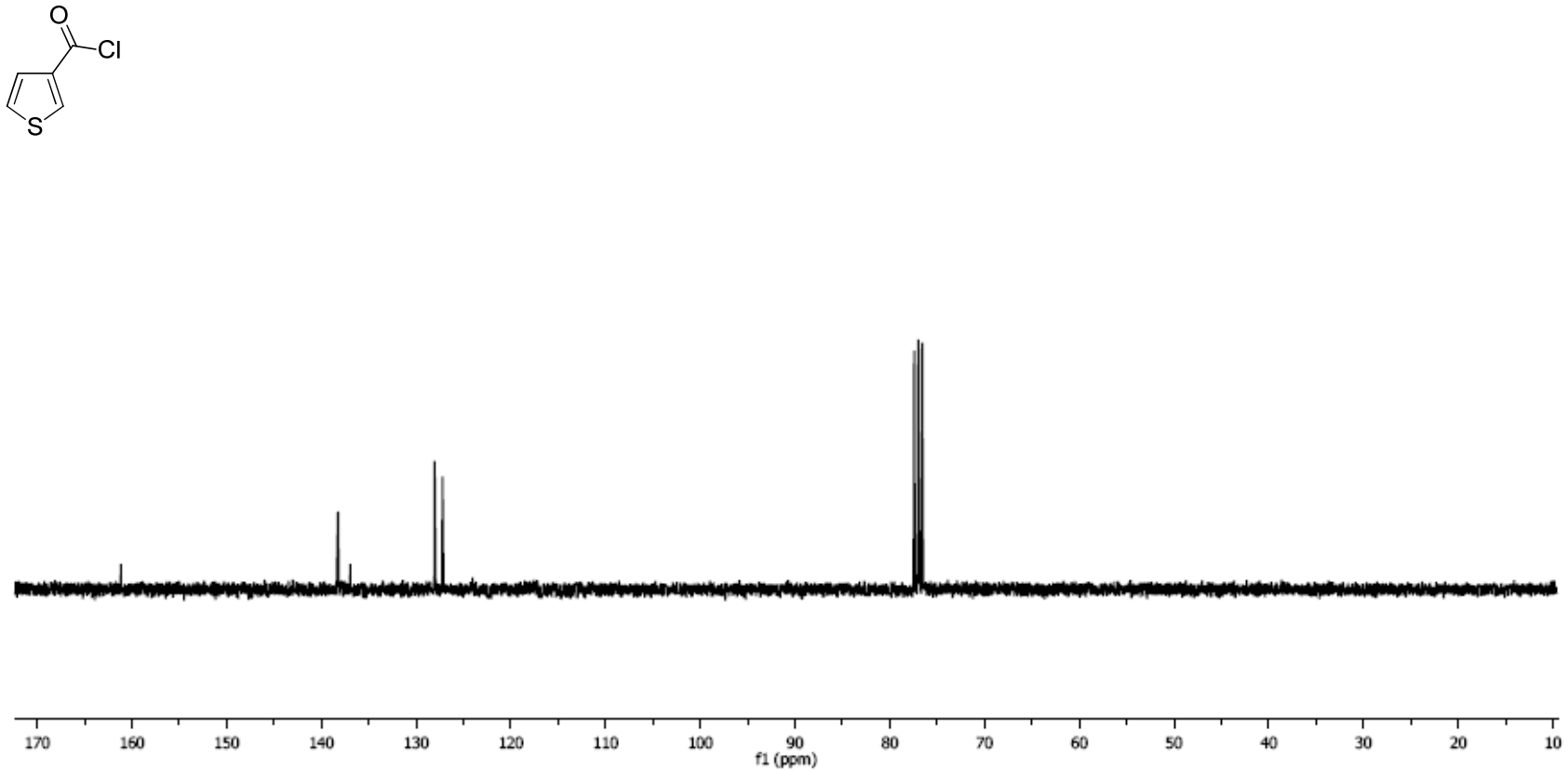


**Figure 32A.** $^{13}C$ NMR spectrum of **VI-13** (75 MHz, $CDCl_3$, 23 °C).

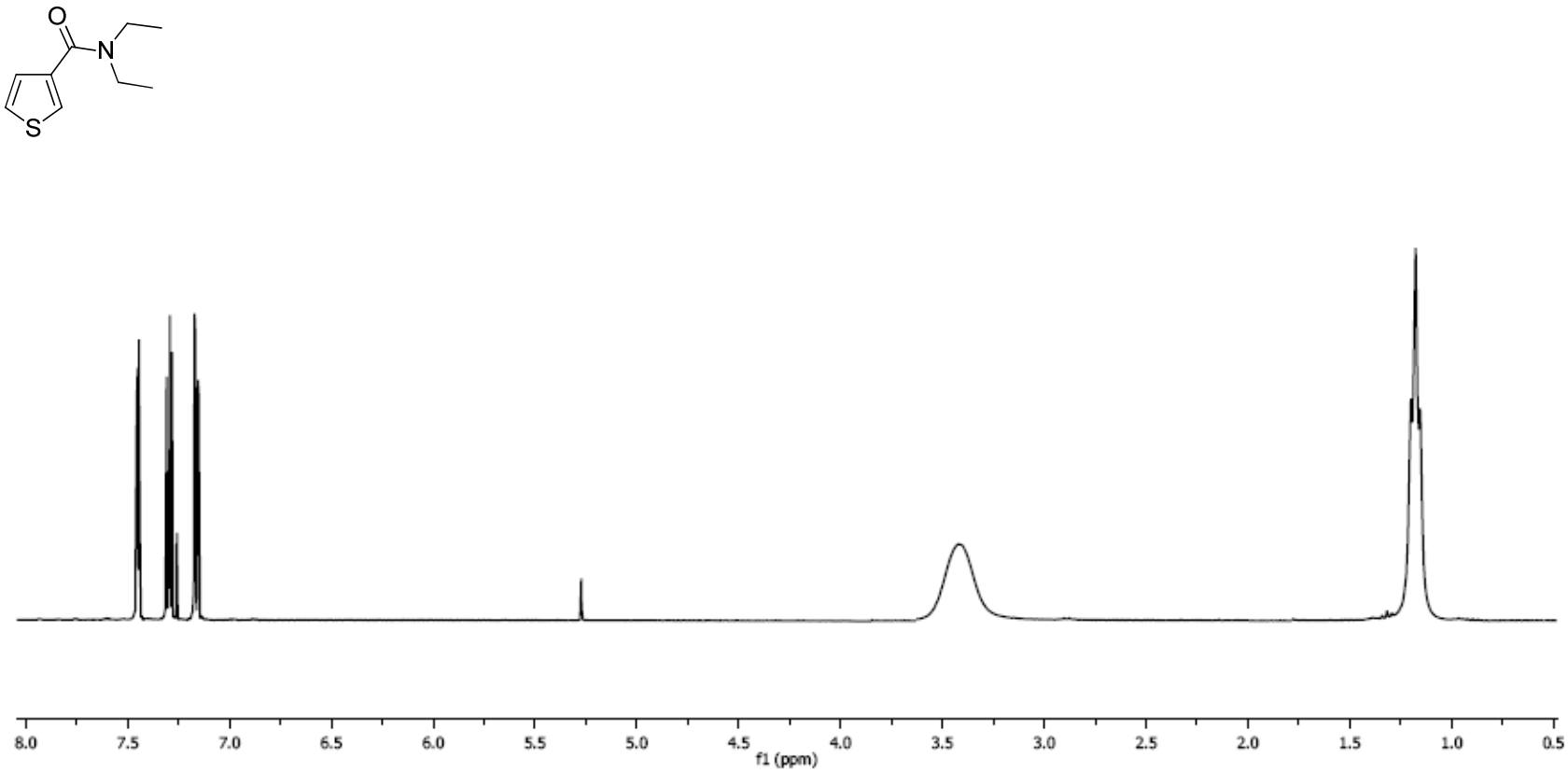


**Figure 33A.** $^{1}$H NMR spectrum of **VI-14** (300 MHz, $CDCl_3$, 23 °C).

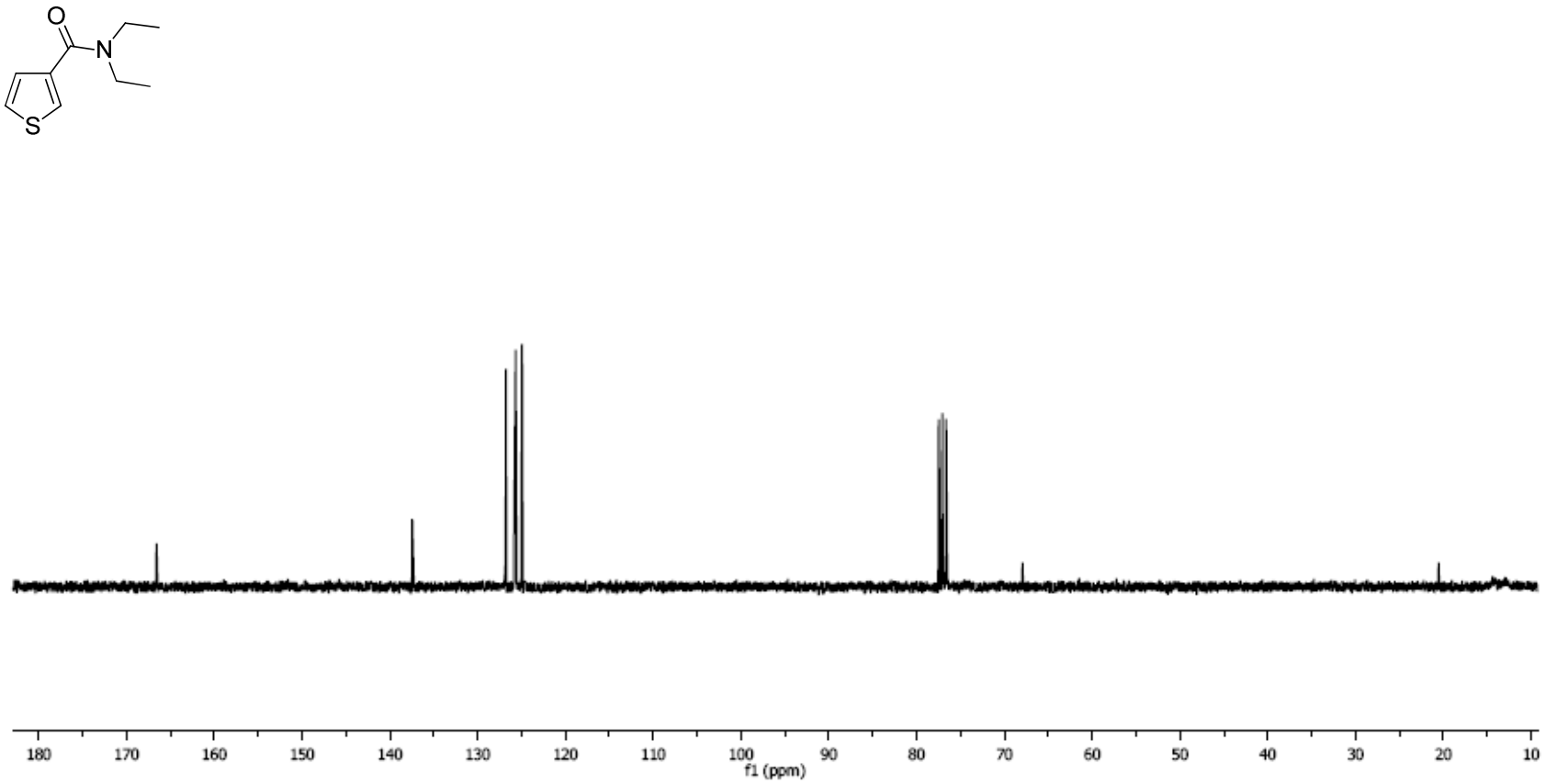


**Figure 33B.** $^{13}C$ NMR spectrum of **VI-14** (75 MHz, $CDCl_3$, 23 °C).

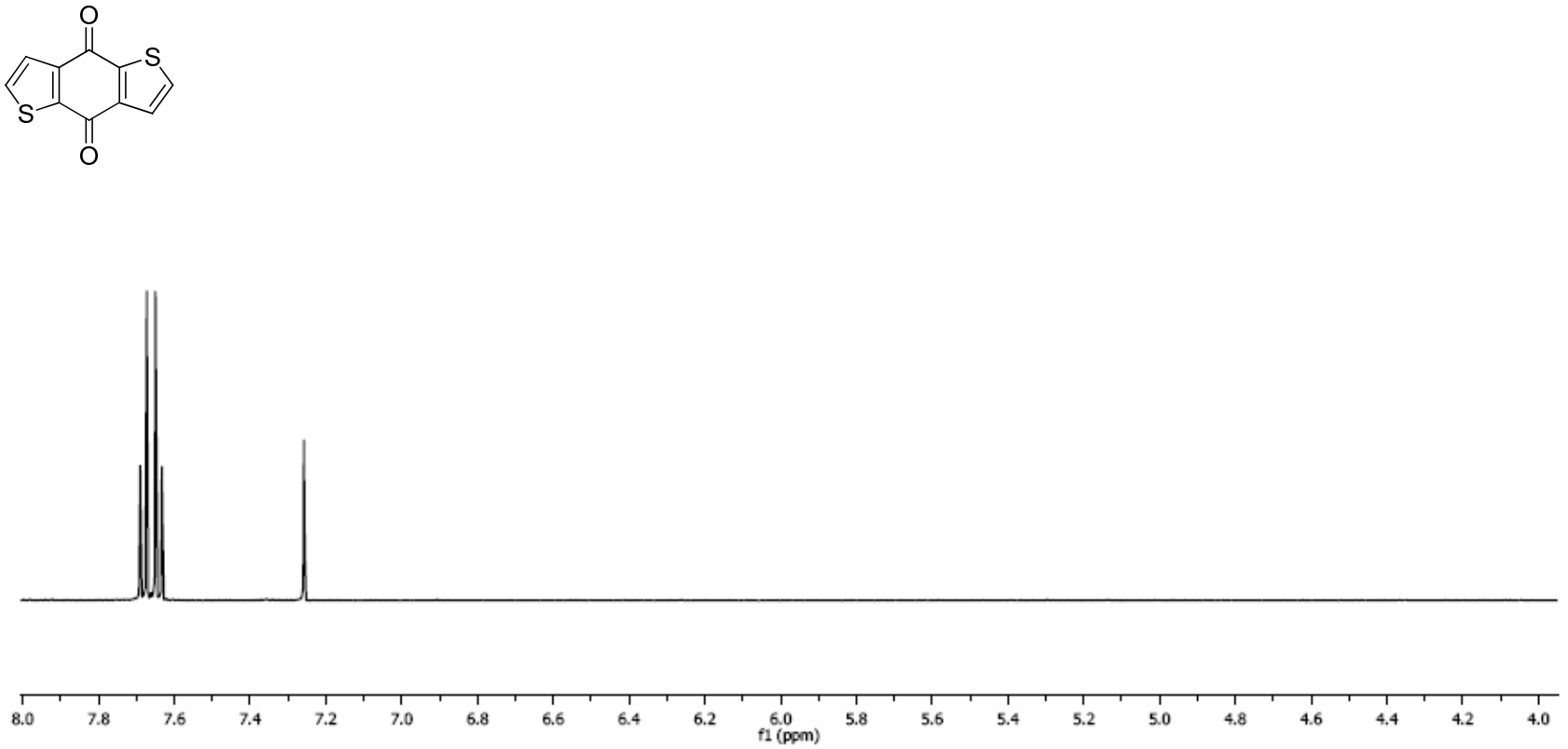


**Figure 34A.** $^{1}$H NMR spectrum of **VI-15** (300 MHz, $CDCl_3$, 23 °C).

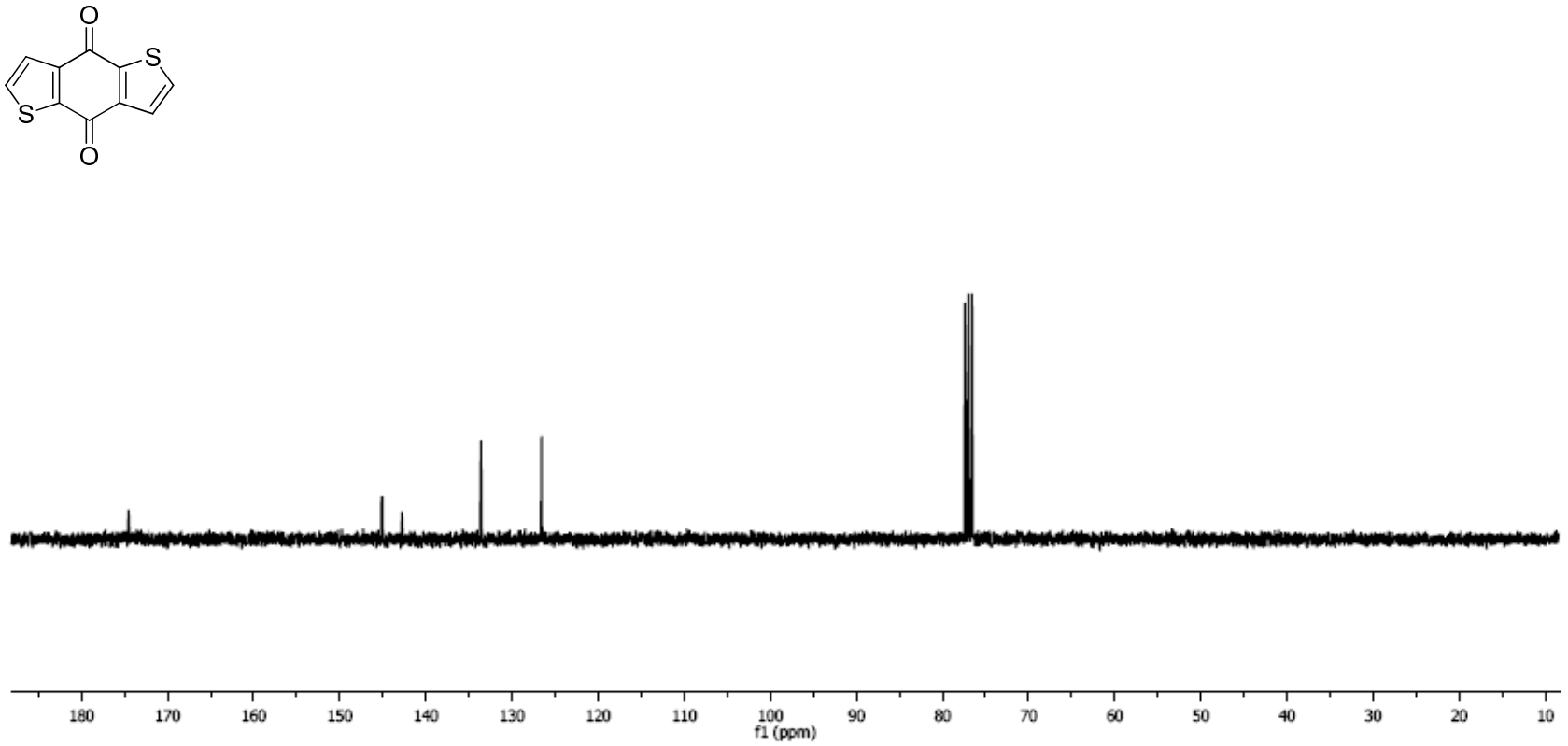


**Figure 34B.** $^{13}C$ NMR spectrum of **VI-15** (75 MHz, $CDCl_3$, 23 °C).

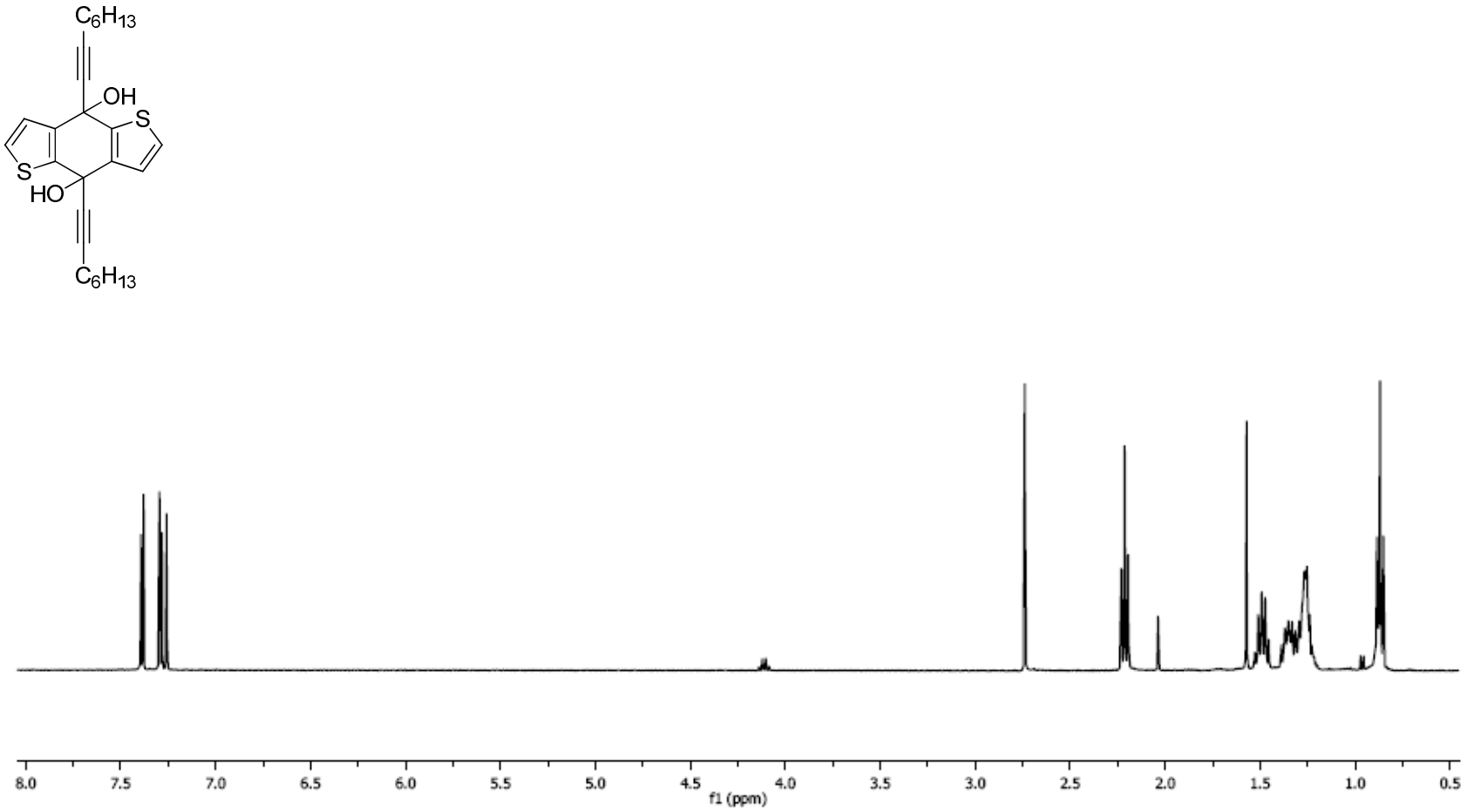


**Figure 35A.** $^{1}$H NMR spectrum of **VI-16** (300 MHz, $CDCl_3$, 23 °C).

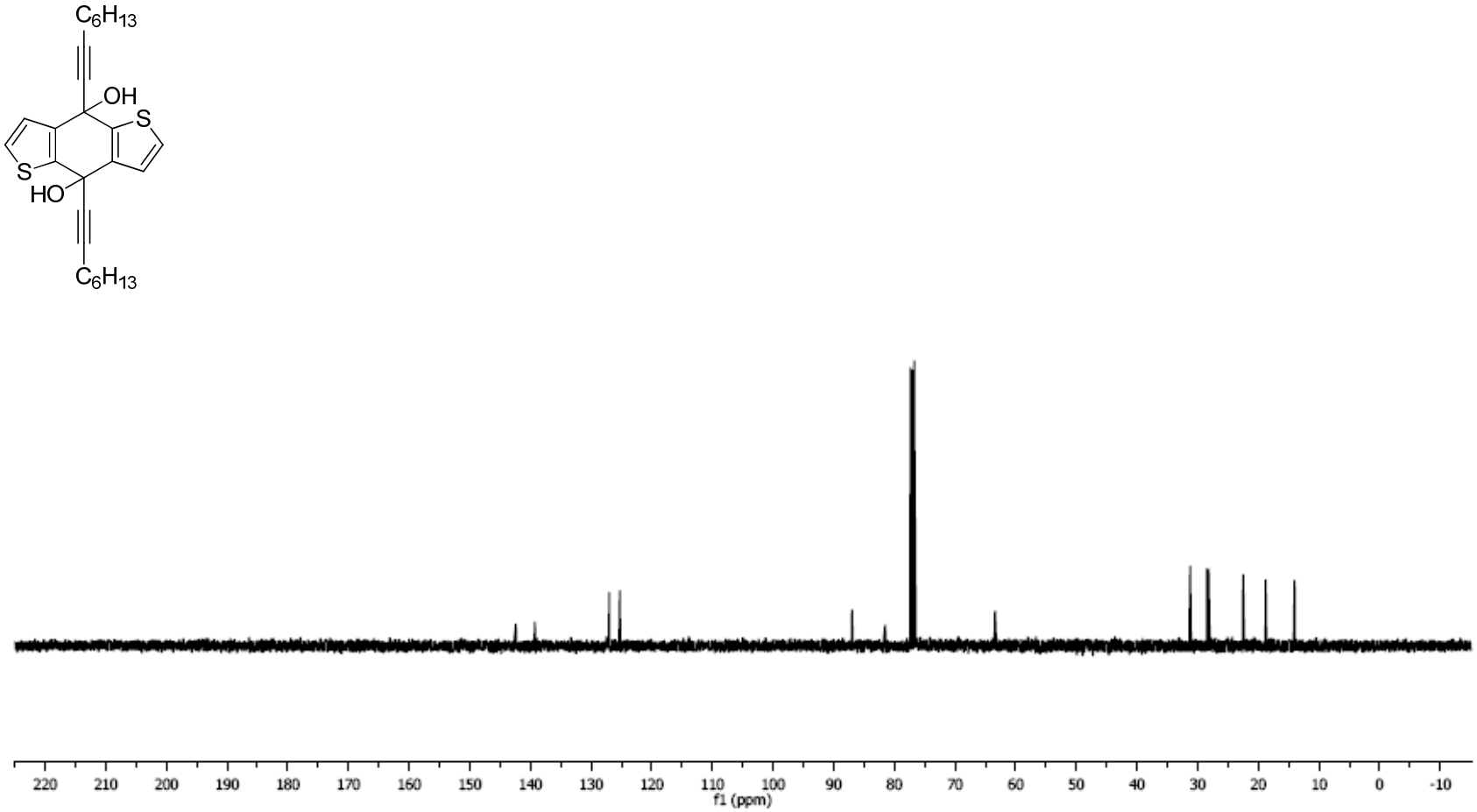


**Figure 35B.** $^{13}C$ NMR spectrum of **VI-16** (75 MHz, $CDCl_3$, 23 °C).

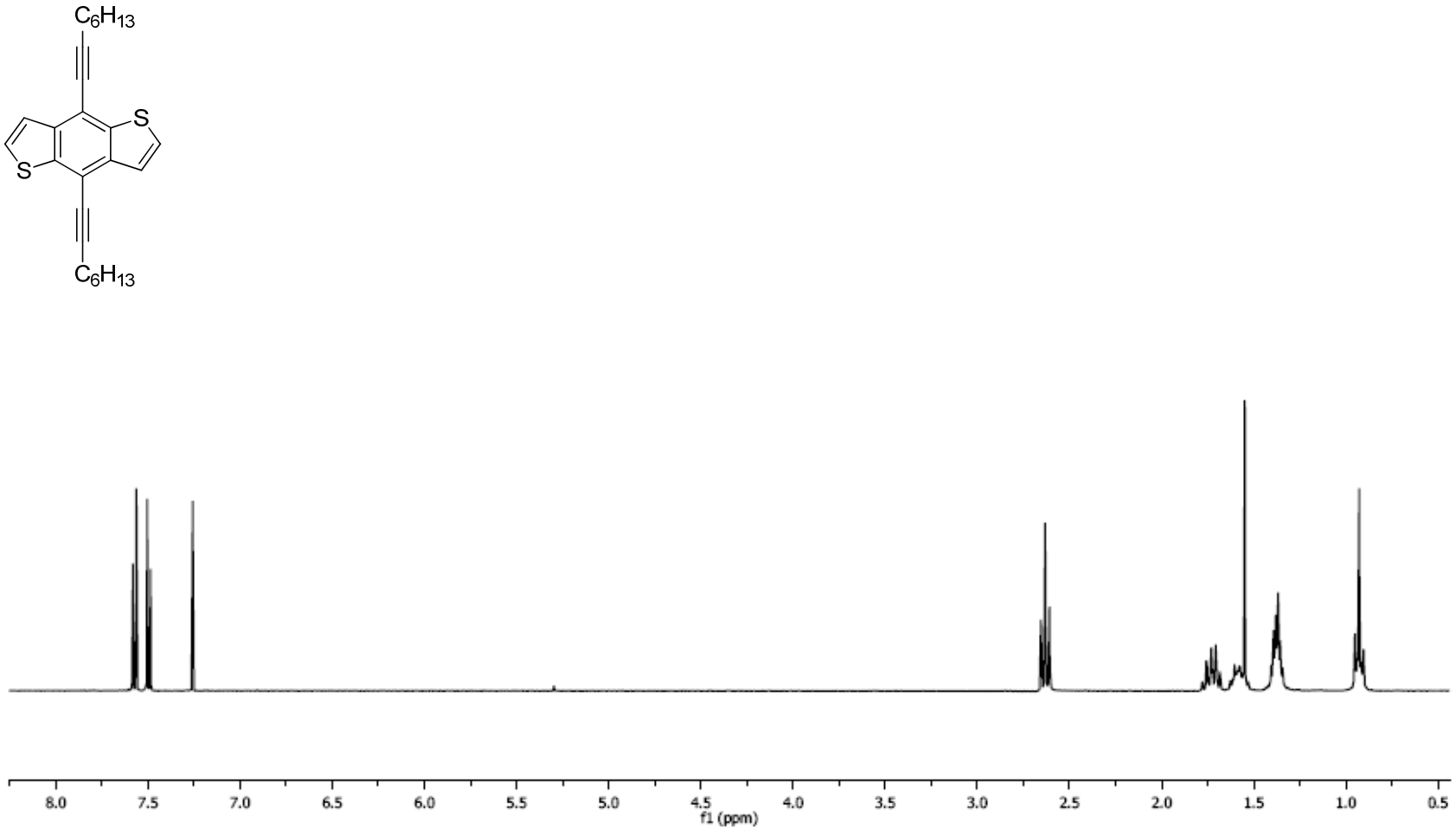


**Figure 36A.** $^{1}$H NMR spectrum of **VI-17** (300 MHz, $CDCl_3$, 23 °C).

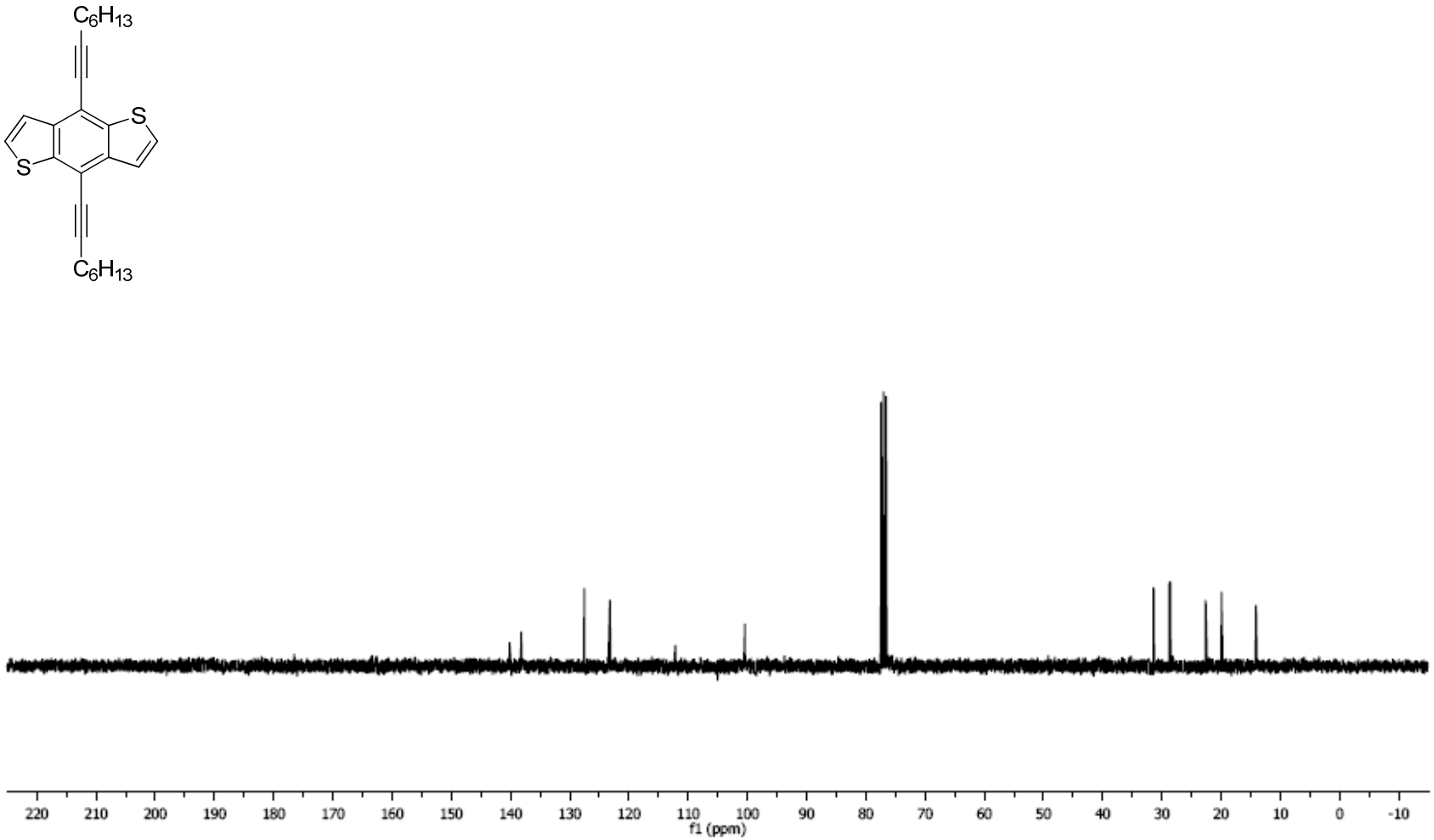


**Figure 36B.** $^{13}C$ NMR spectrum of **VI-17** (75 MHz, $CDCl_3$, 23 °C).

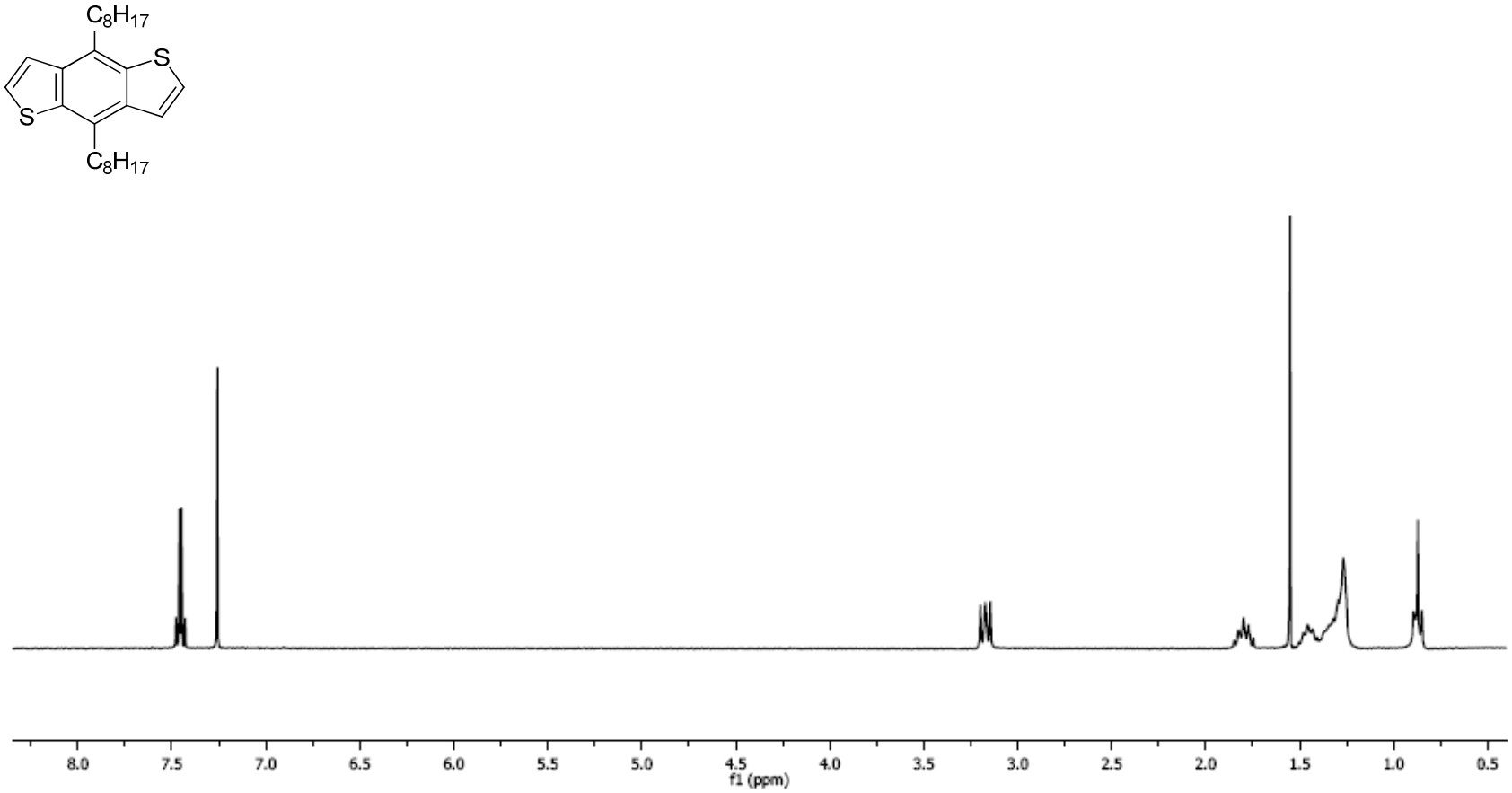


**Figure 37A.** $^{1}$H NMR spectrum of **VI-18** (300 MHz, $CDCl_3$, 23 °C).

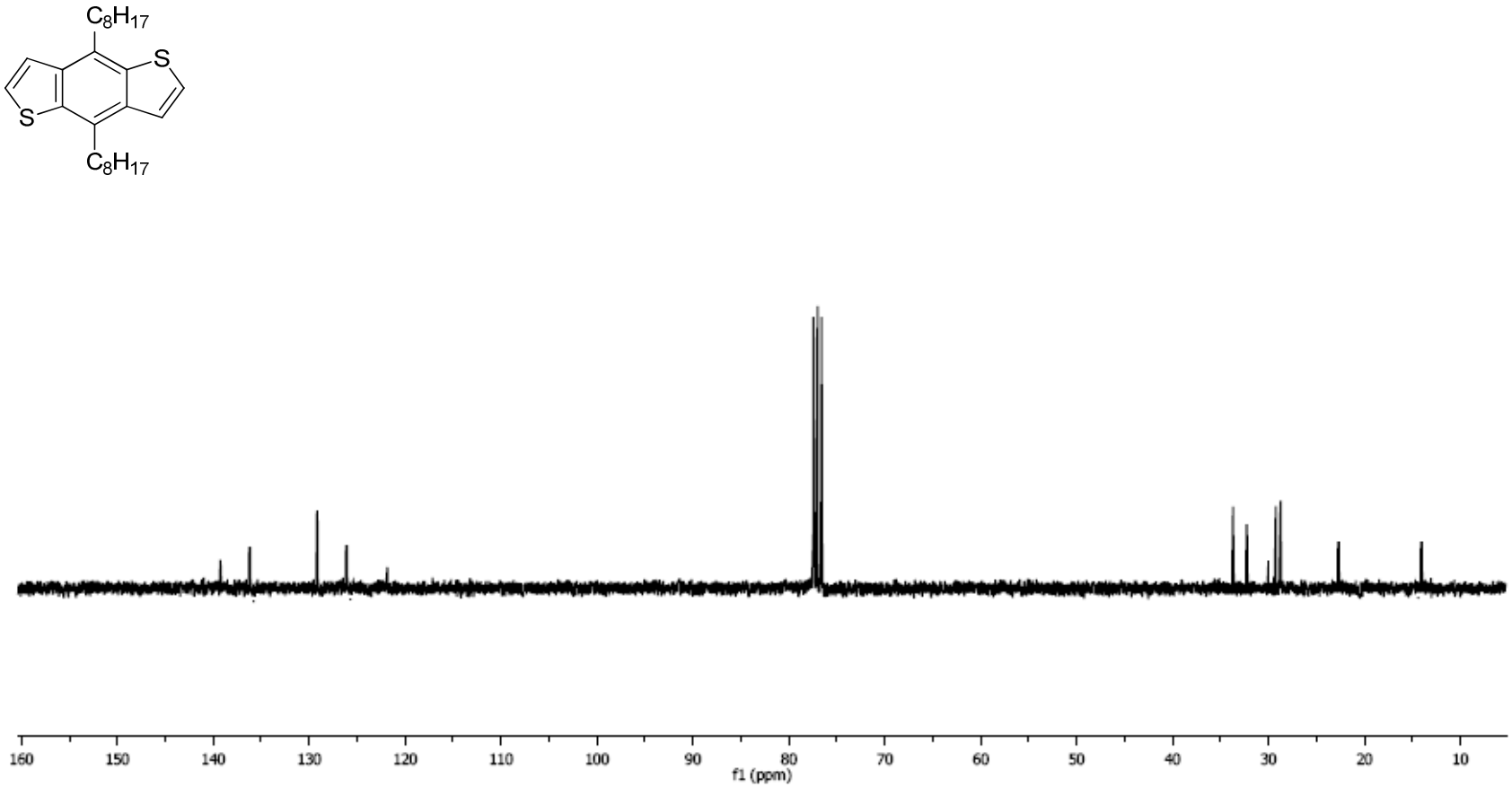


**Figure 37B.** $^{13}C$ NMR spectrum of **VI-18** (75 MHz, $CDCl_3$, 23 °C).

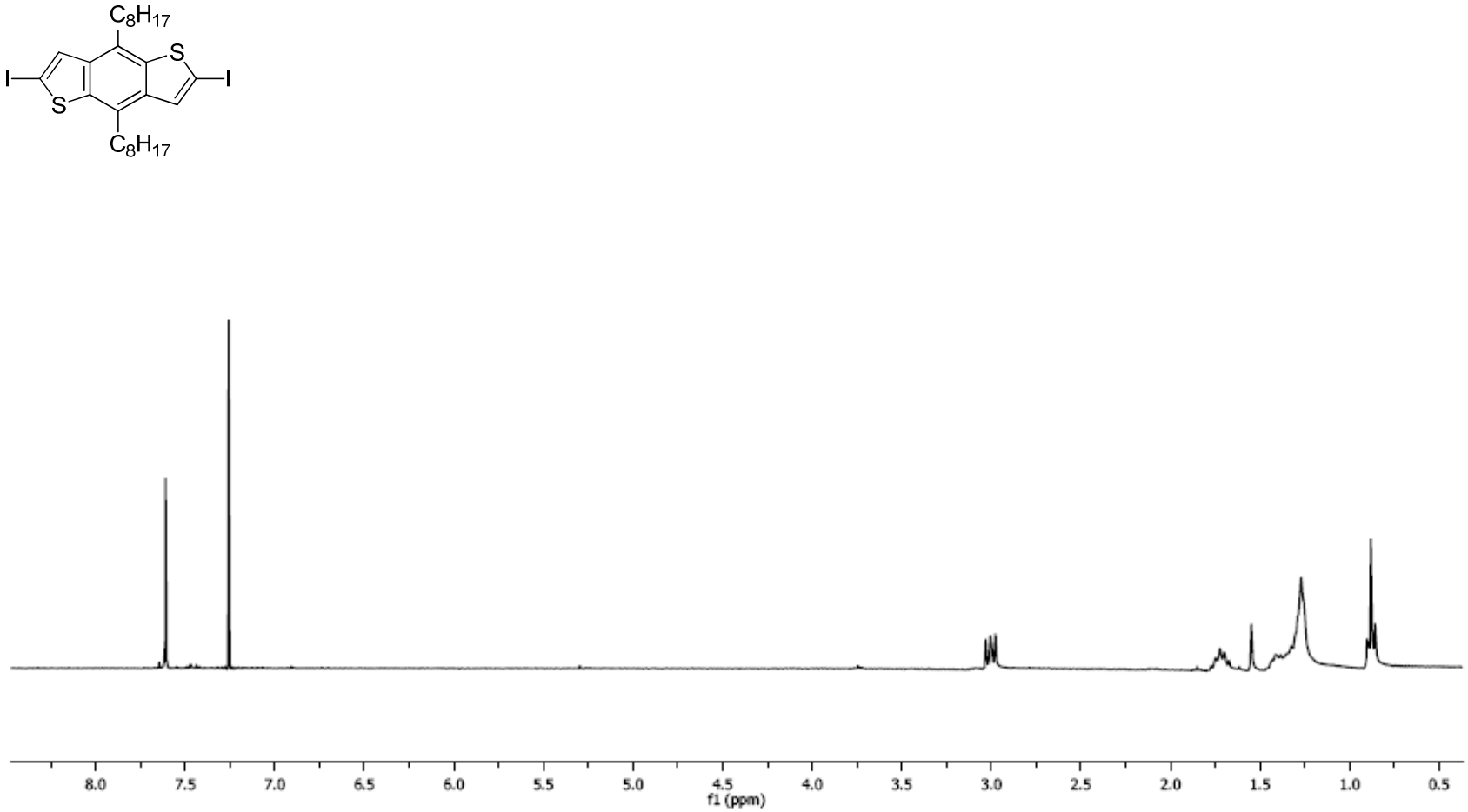


**Figure 38A.** $^{1}$H NMR spectrum of **VI-19** (300 MHz, $CDCl_3$, 23 °C).

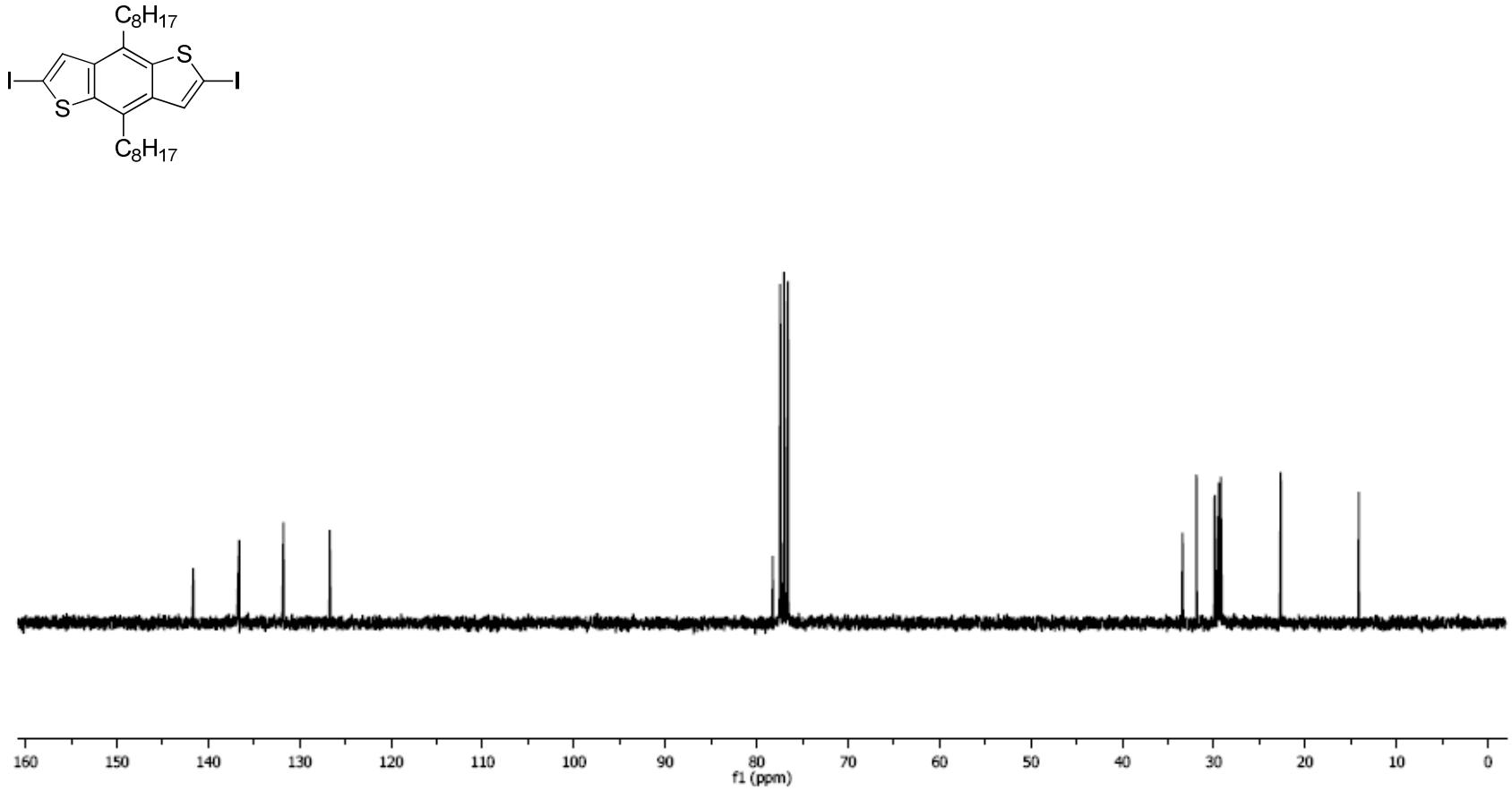


**Figure 38B.** $^{13}C$ NMR spectrum of **VI-19** (75 MHz, $CDCl_3$, 23 °C).

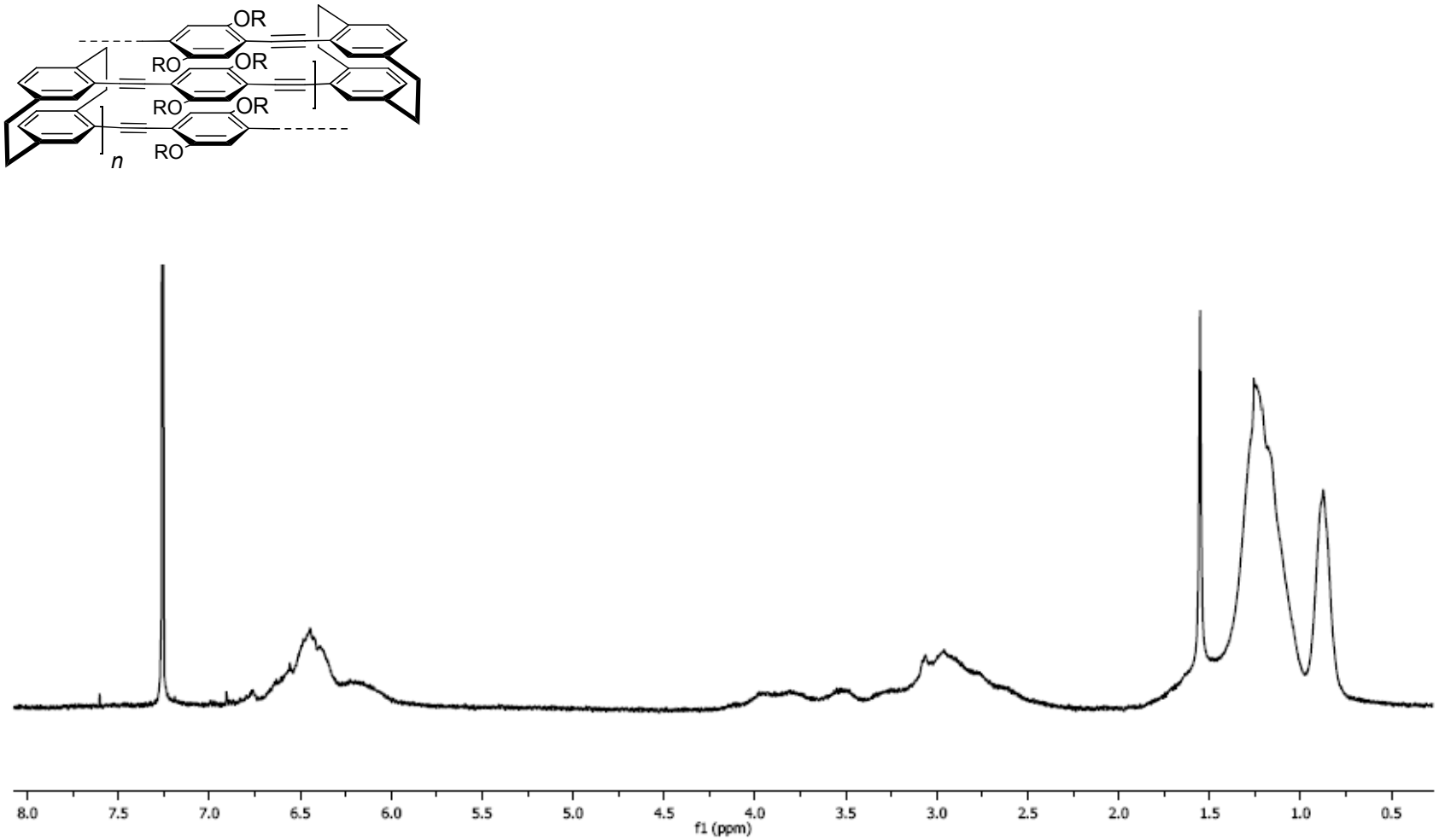


**Figure 39A.** $^{1}$H NMR spectrum of ***pg*-poly($PE_3$)** (300 MHz, $CDCl_3$, 23 °C).

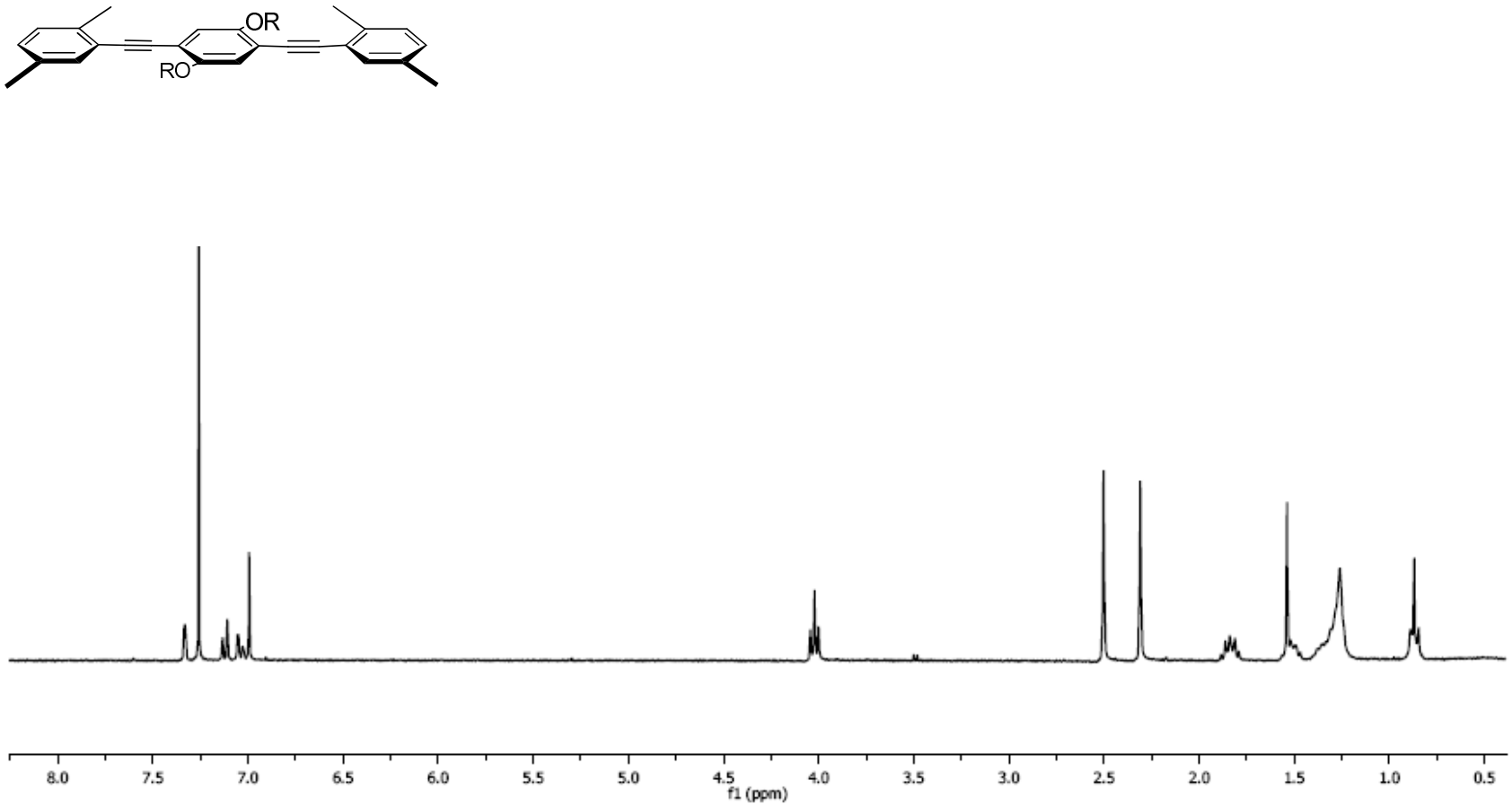


**Figure 40A.** $^{1}$H NMR spectrum of **$Me_4PE_3$** (300 MHz, $CDCl_3$, 23 °C).

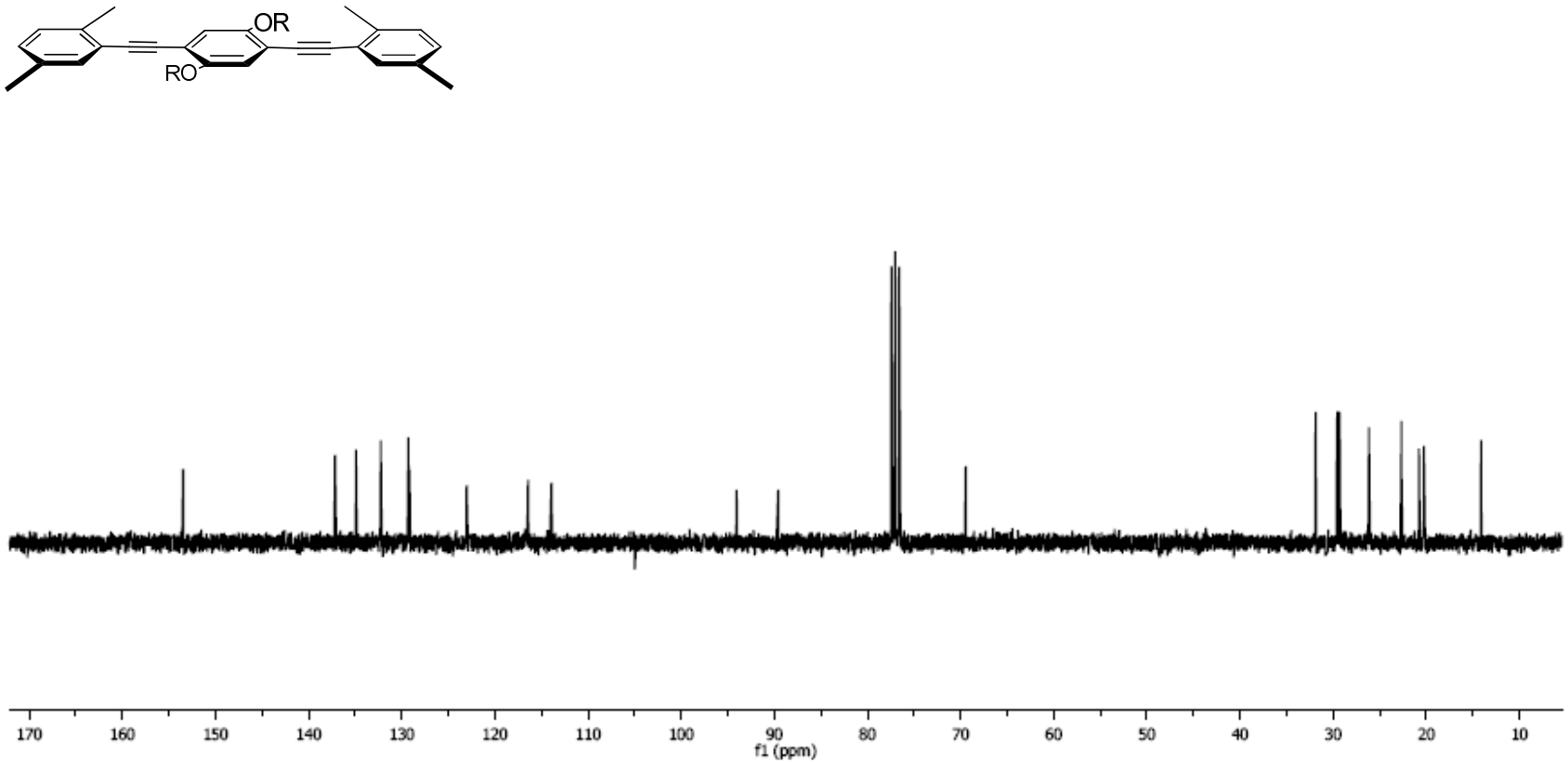


**Figure 40B.** $^{13}C$ NMR spectrum of **$Me_4PE_3$** (75 MHz, $CDCl_3$, 23 °C).

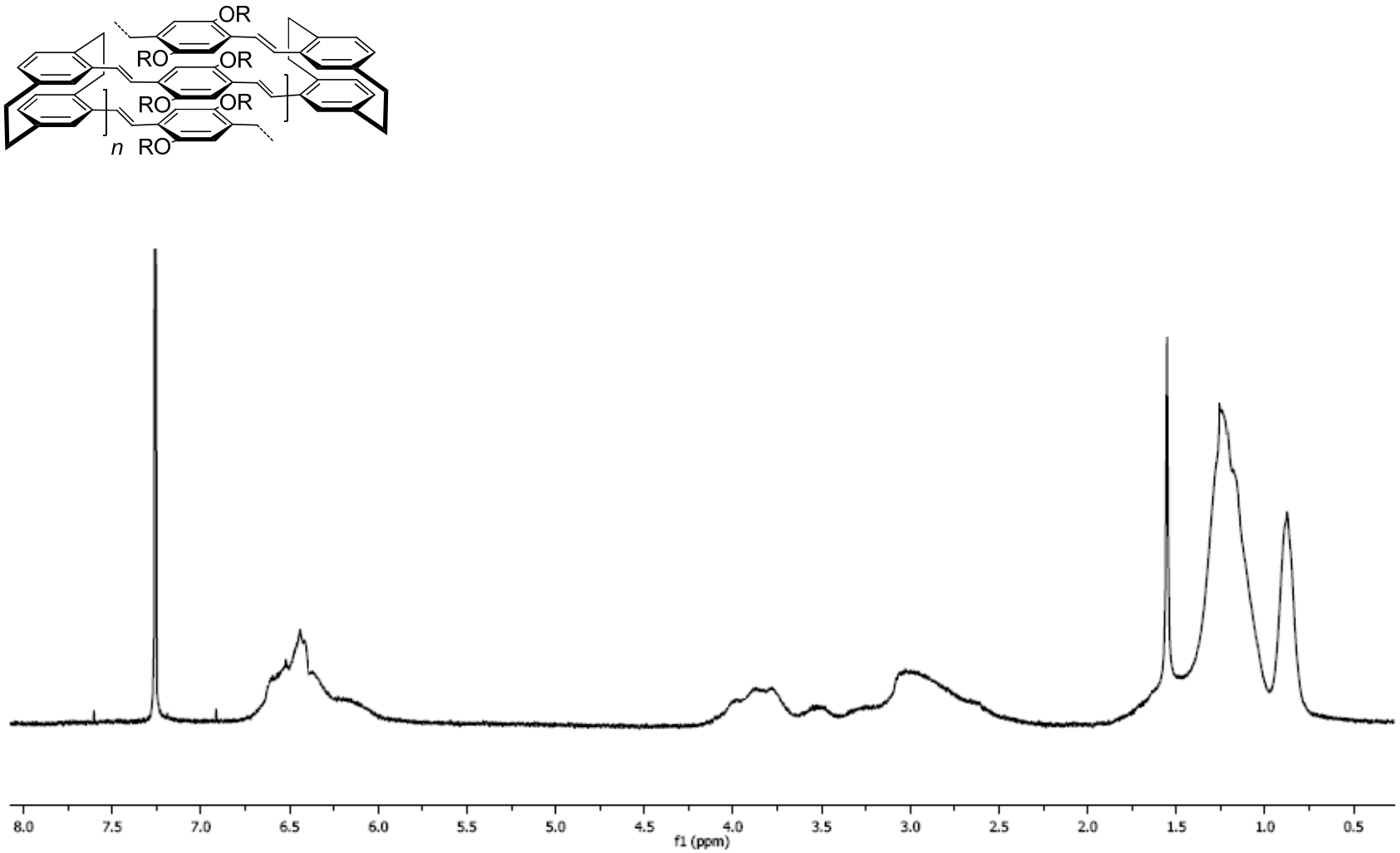


**Figure 41A.** $^{1}$H NMR spectrum of ***pg*-poly($PV_3$)** (300 MHz, $CDCl_3$, 23 °C).

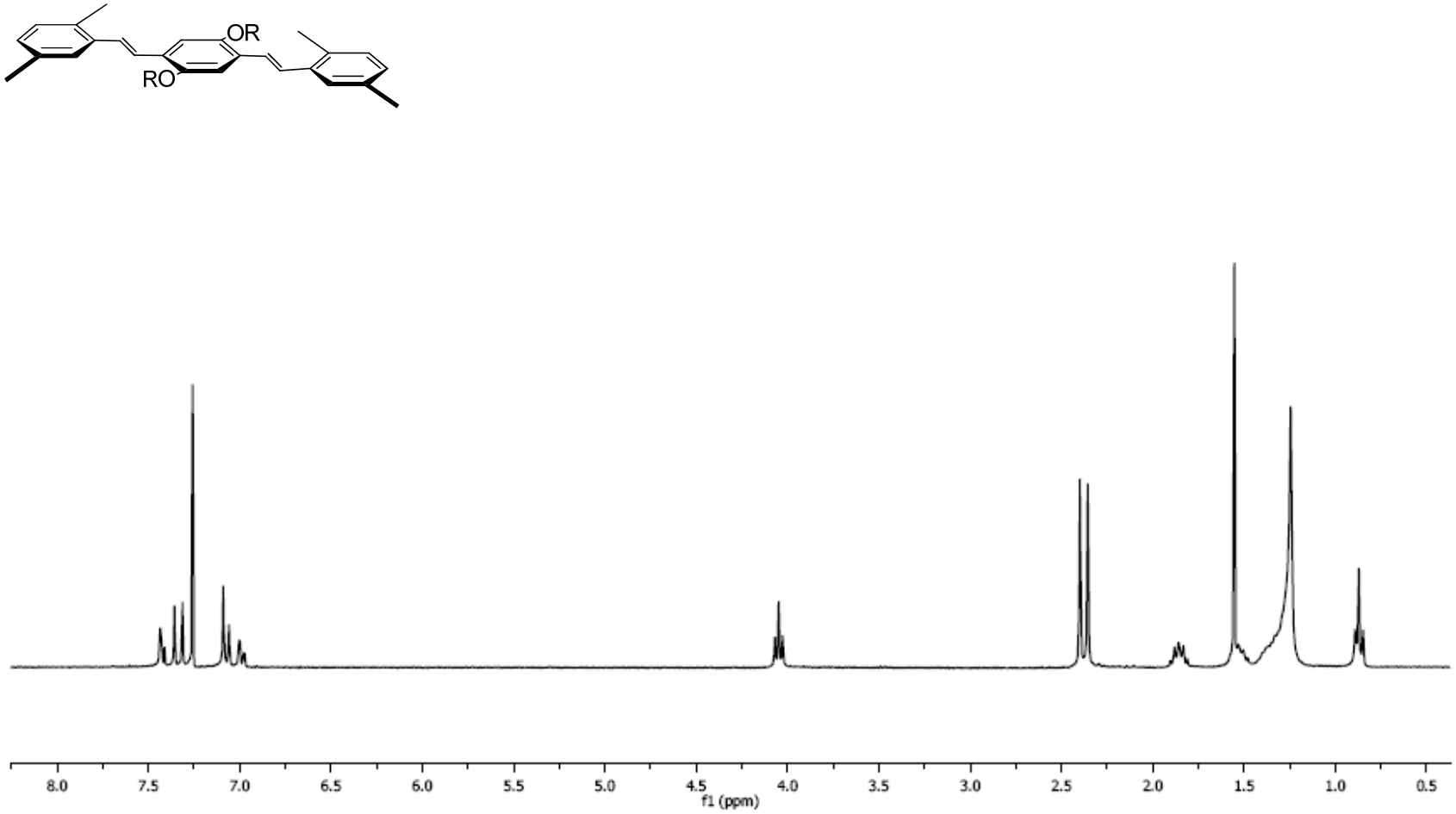


**Figure 42A.** $^{1}$H NMR spectrum of **$Me_4PV_3$** (300 MHz, $CDCl_3$, 23 °C).

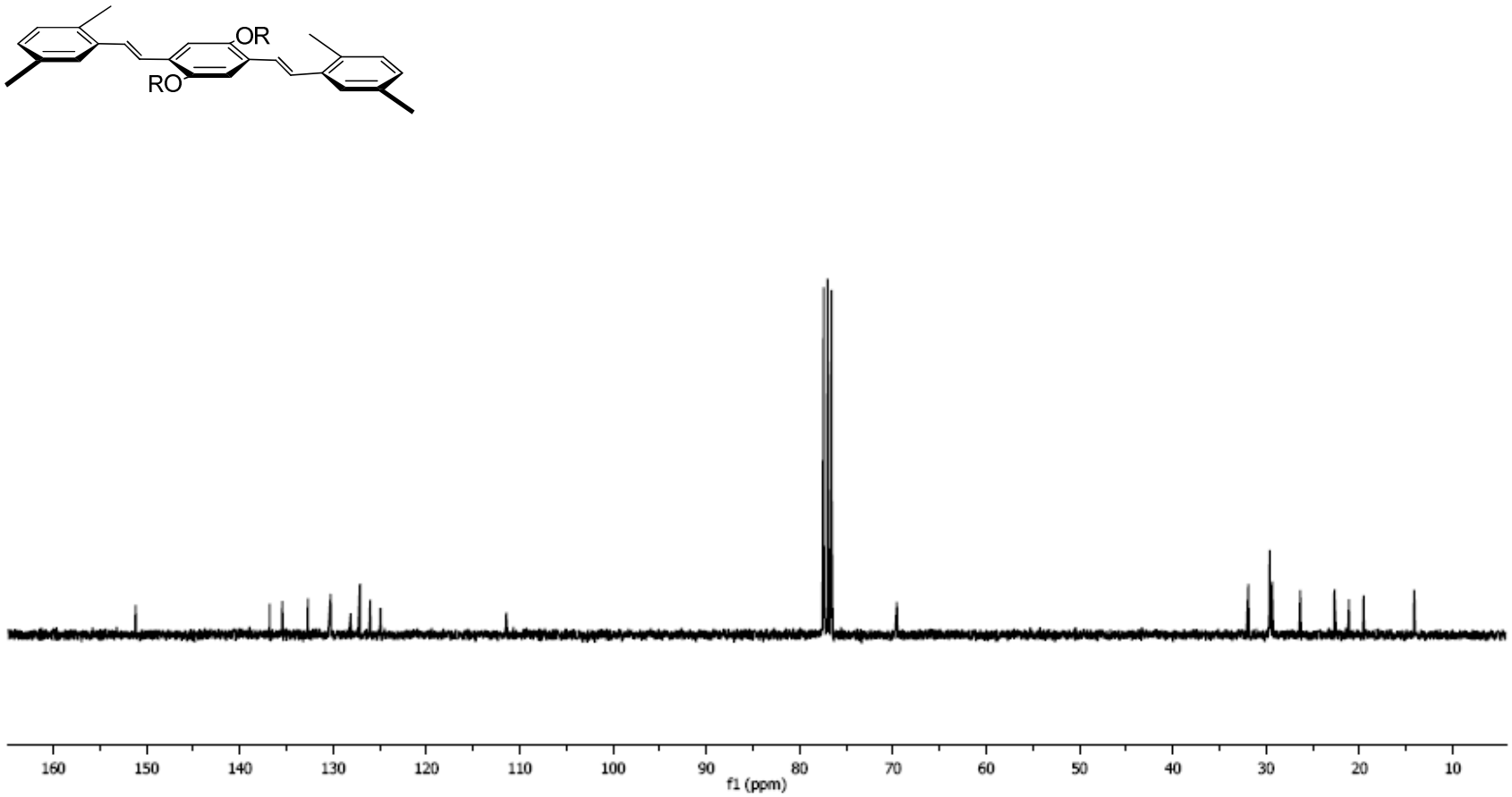


**Figure 42B.** $^{13}C$ NMR spectrum of **$Me_4PV_3$** (75 MHz, $CDCl_3$, 23 °C).

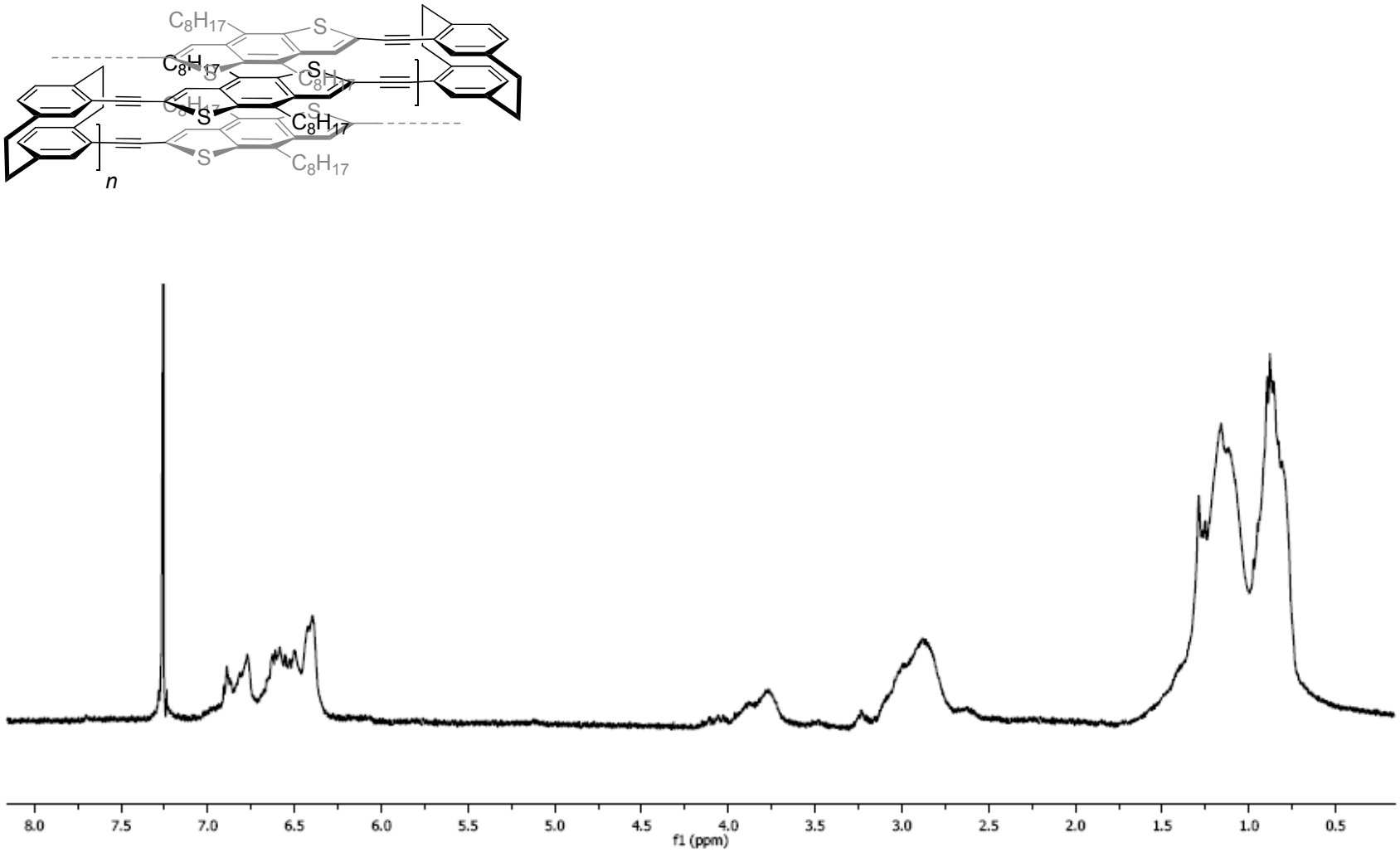


**Figure 43A.** $^{1}$H NMR spectrum of ***pg*-poly(CP-E-BDT)** (300 MHz, $CDCl_3$, 23 °C).

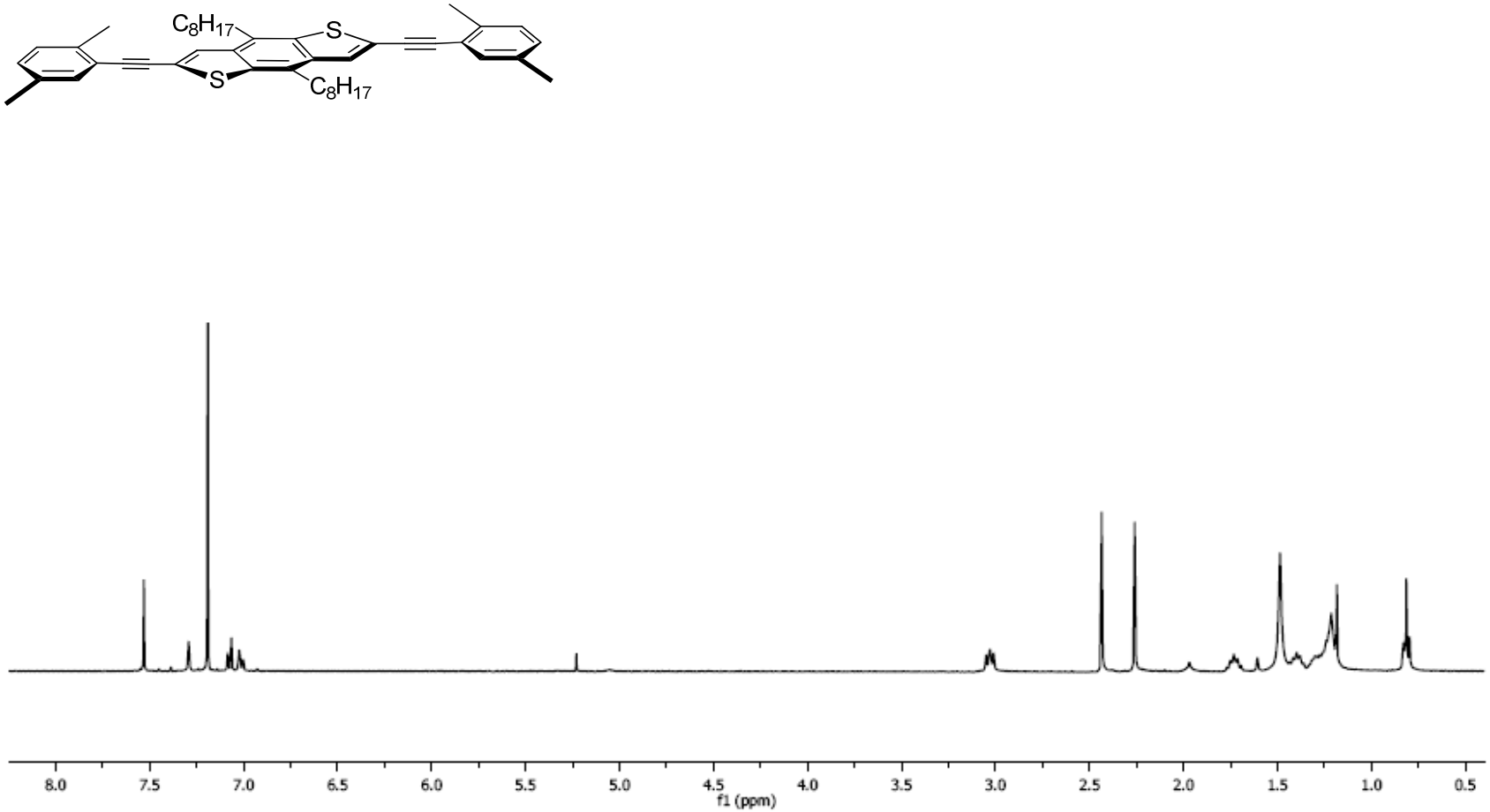


**Figure 44A.** $^{1}$H NMR spectrum of **E-BDT-Xy$_2$** (300 MHz, $CDCl_3$, 23 °C).

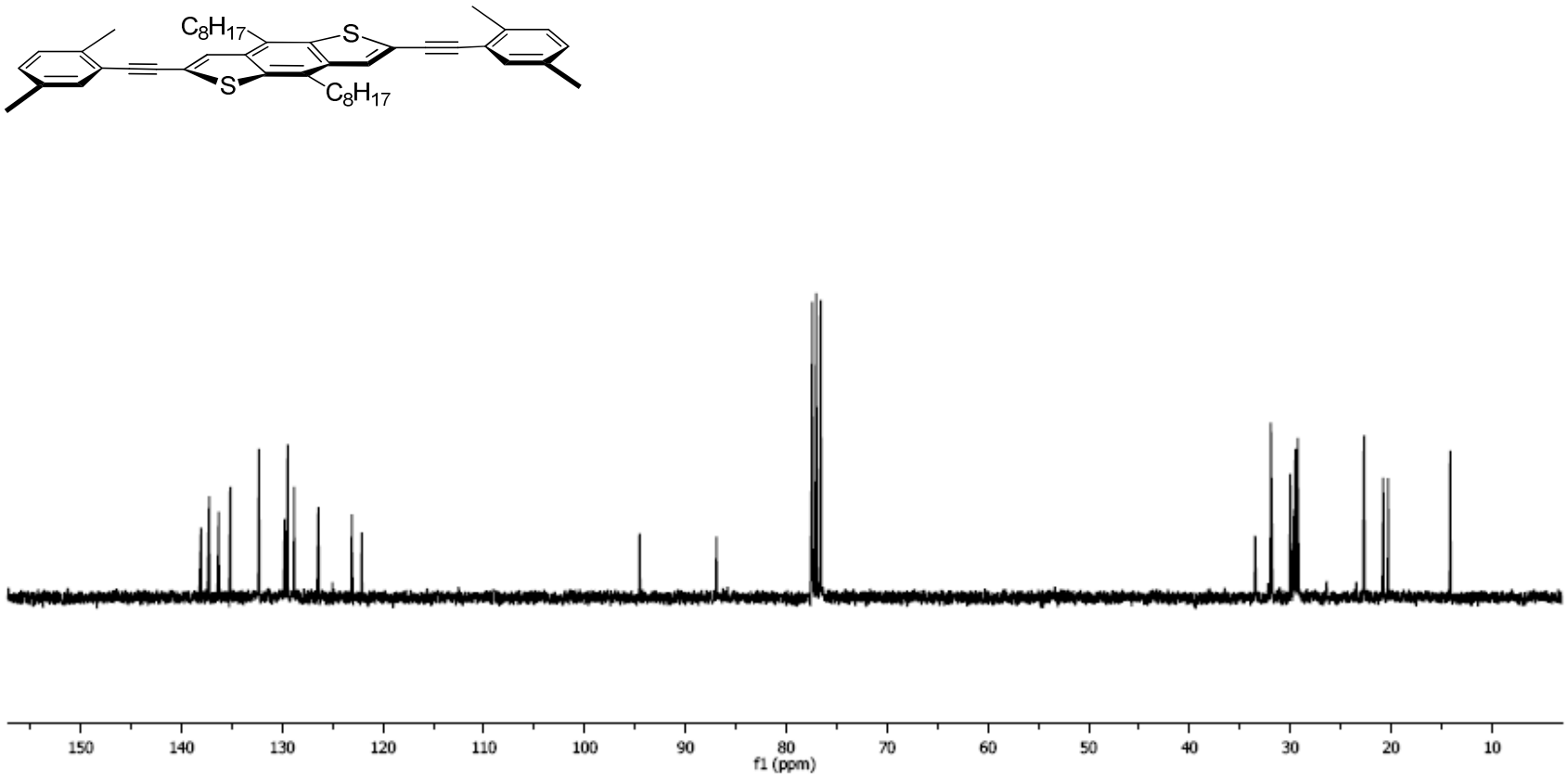


**Figure 44B.** $^{13}C$ NMR spectrum of **E-BDT-Xy$_2$** (75 MHz, $CDCl_3$, 23 °C).

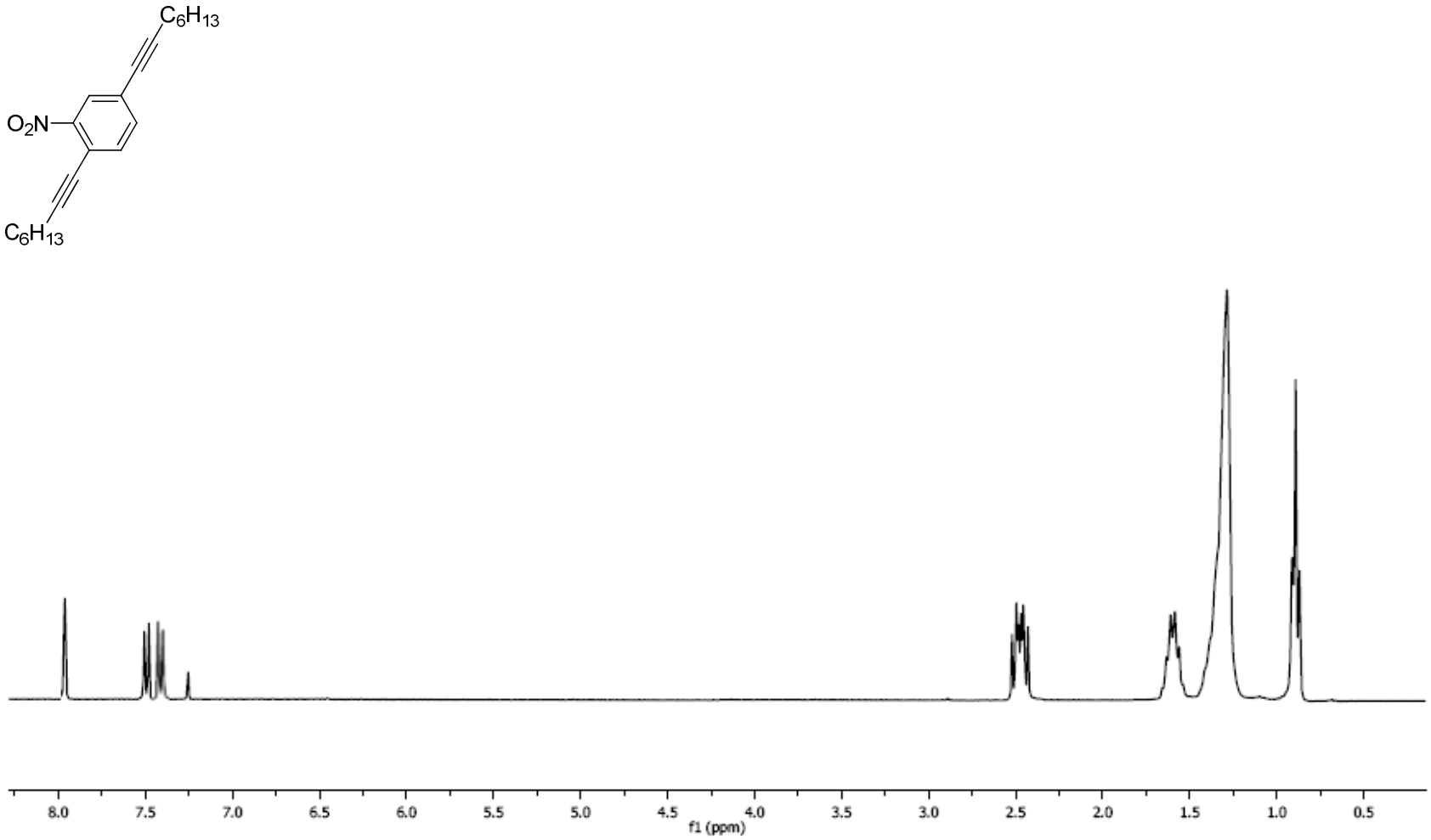


**Figure 45A.** $^{1}$H NMR spectrum of **VIII-6** (300 MHz, $CDCl_3$, 23 °C).

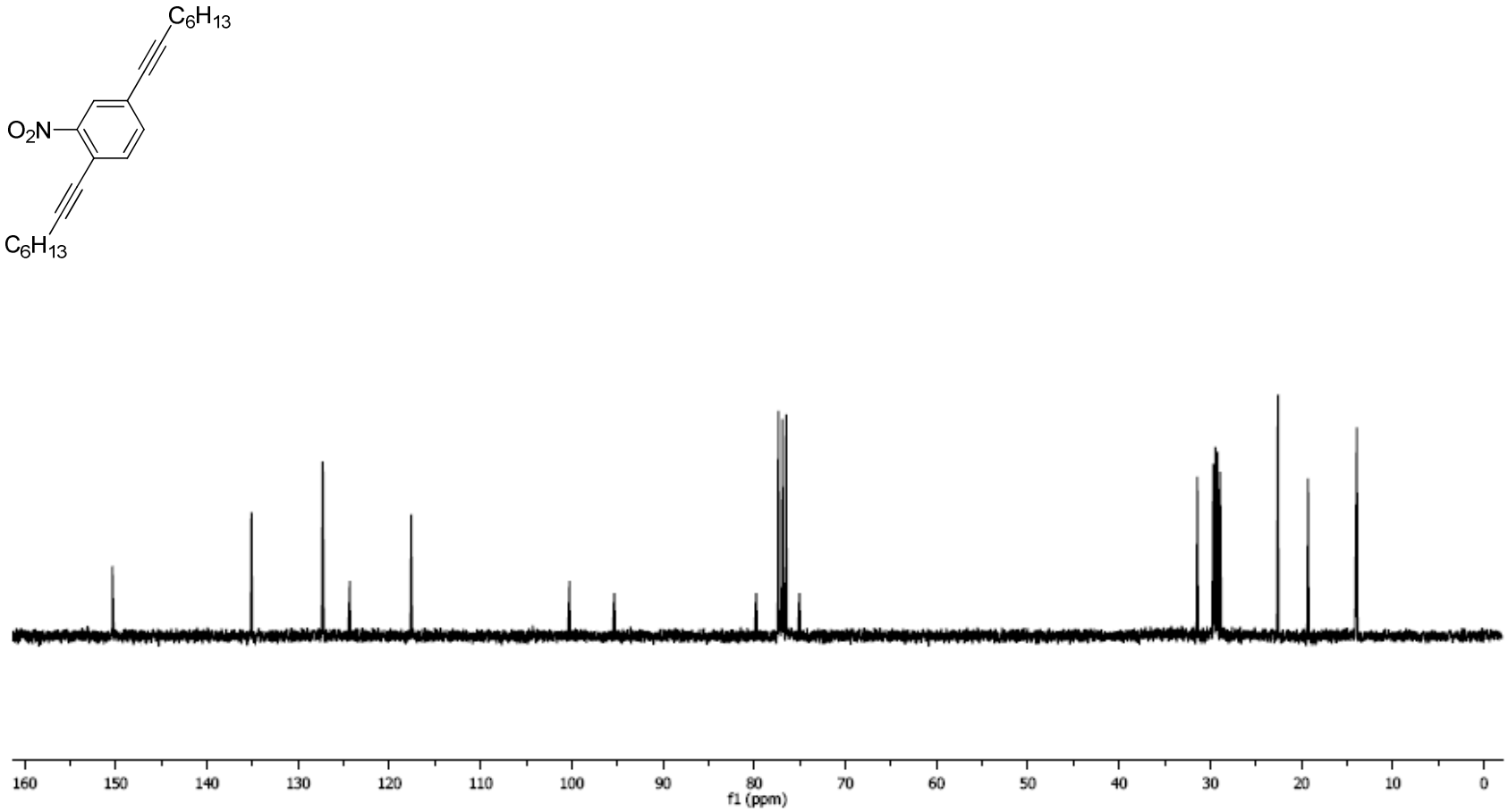


**Figure 45B.** $^{13}$C NMR spectrum of **VIII-6** (75 MHz, $CDCl_3$, 23 °C).

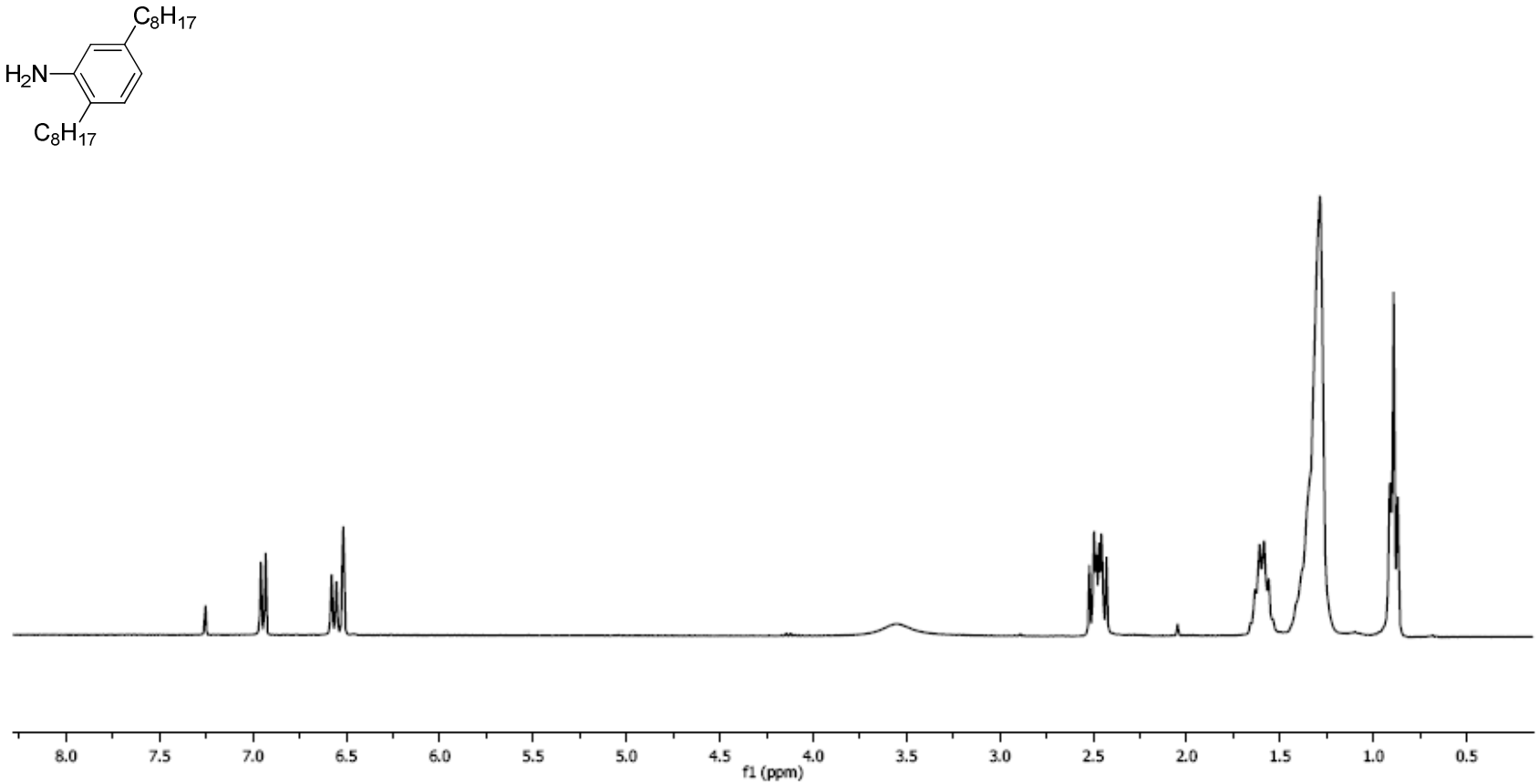


**Figure 46A.** $^{1}$H NMR spectrum of **VIII-7** (300 MHz, $CDCl_3$, 23 °C).

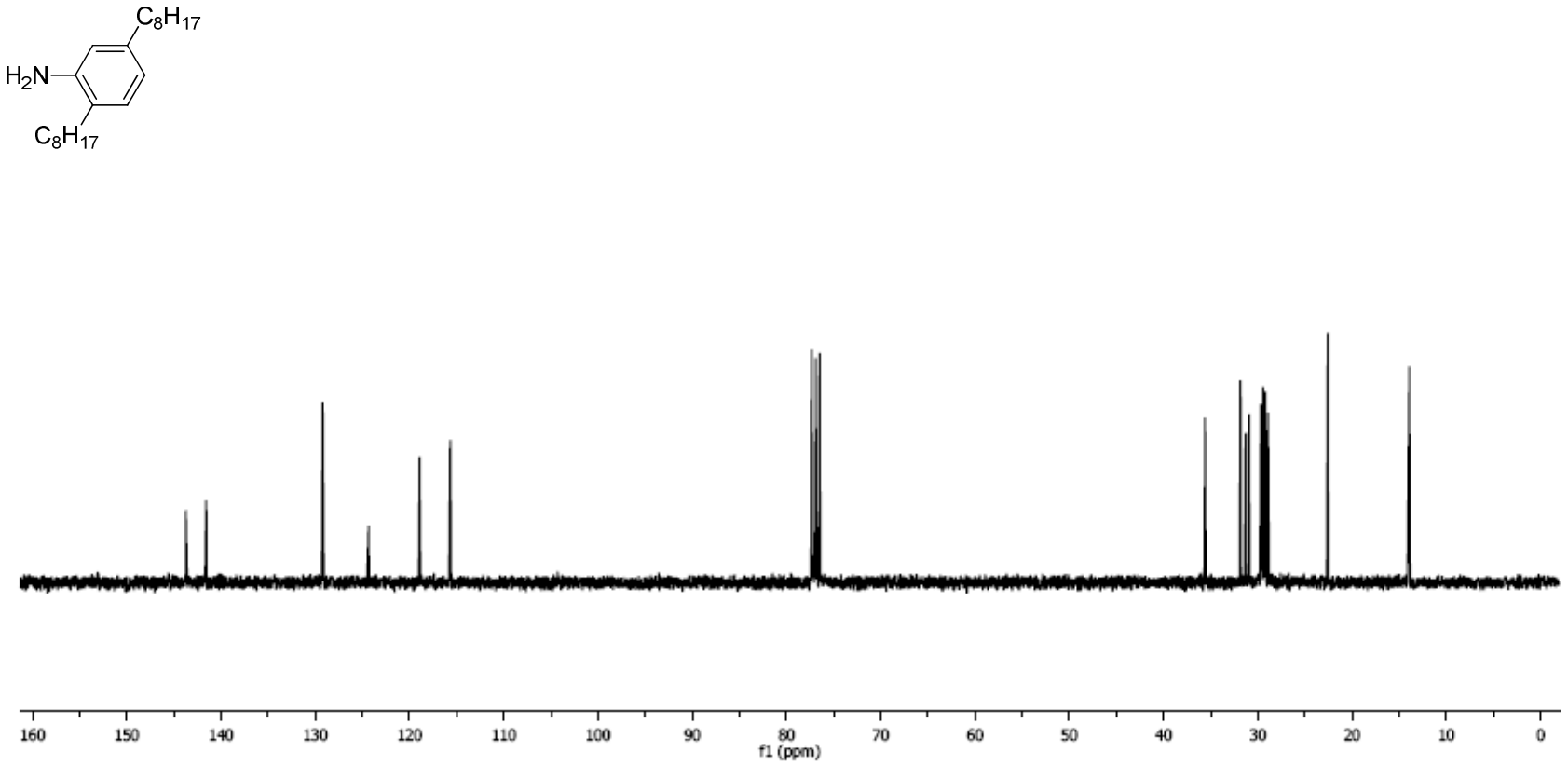


**Figure 46B.** $^{13}$C NMR spectrum of **VIII-7** (75 MHz, $CDCl_3$, 23 °C).

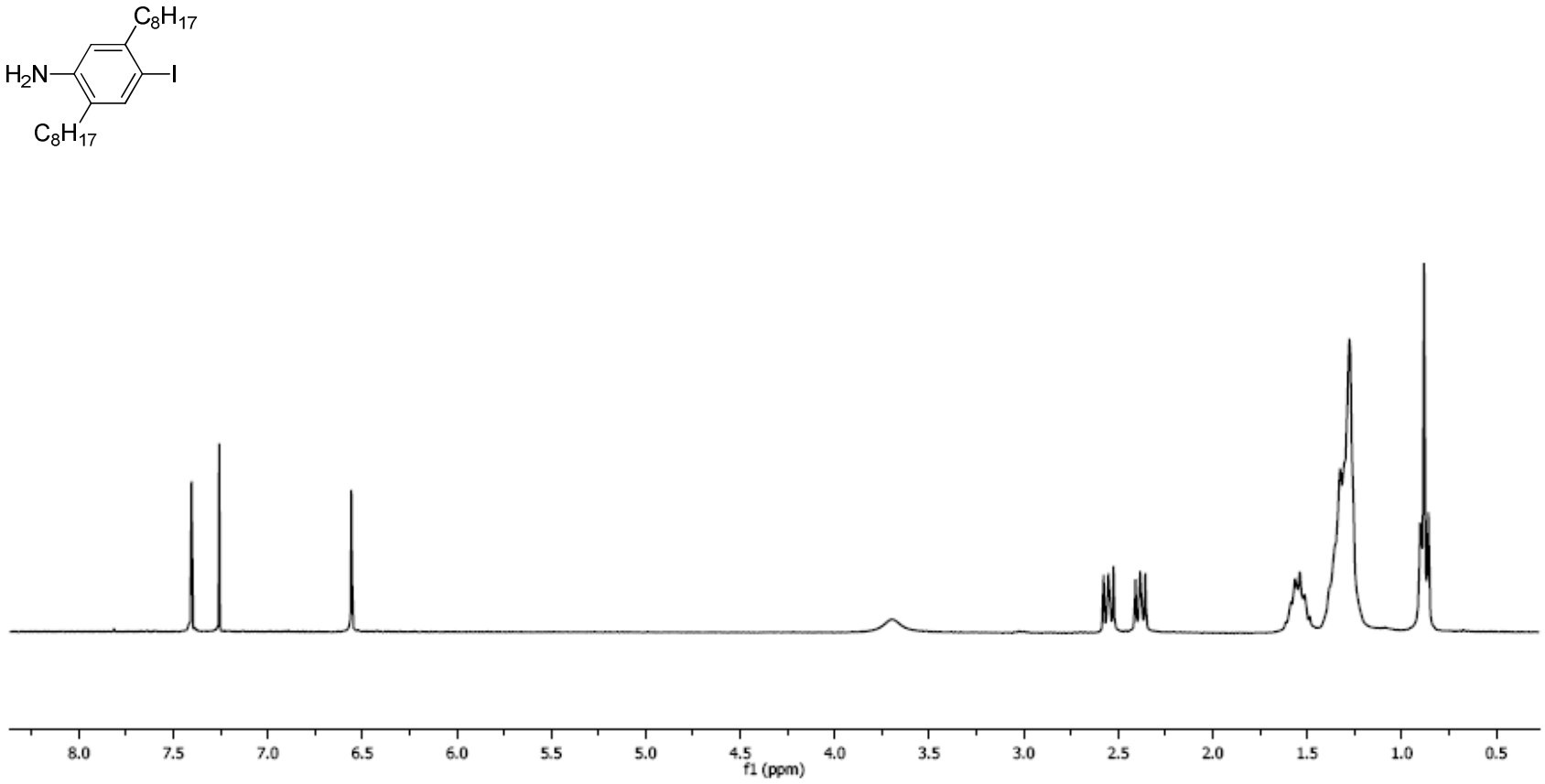


**Figure 47A.** $^{1}$H NMR spectrum of **VIII-8** (300 MHz, $CDCl_3$, 23 °C).

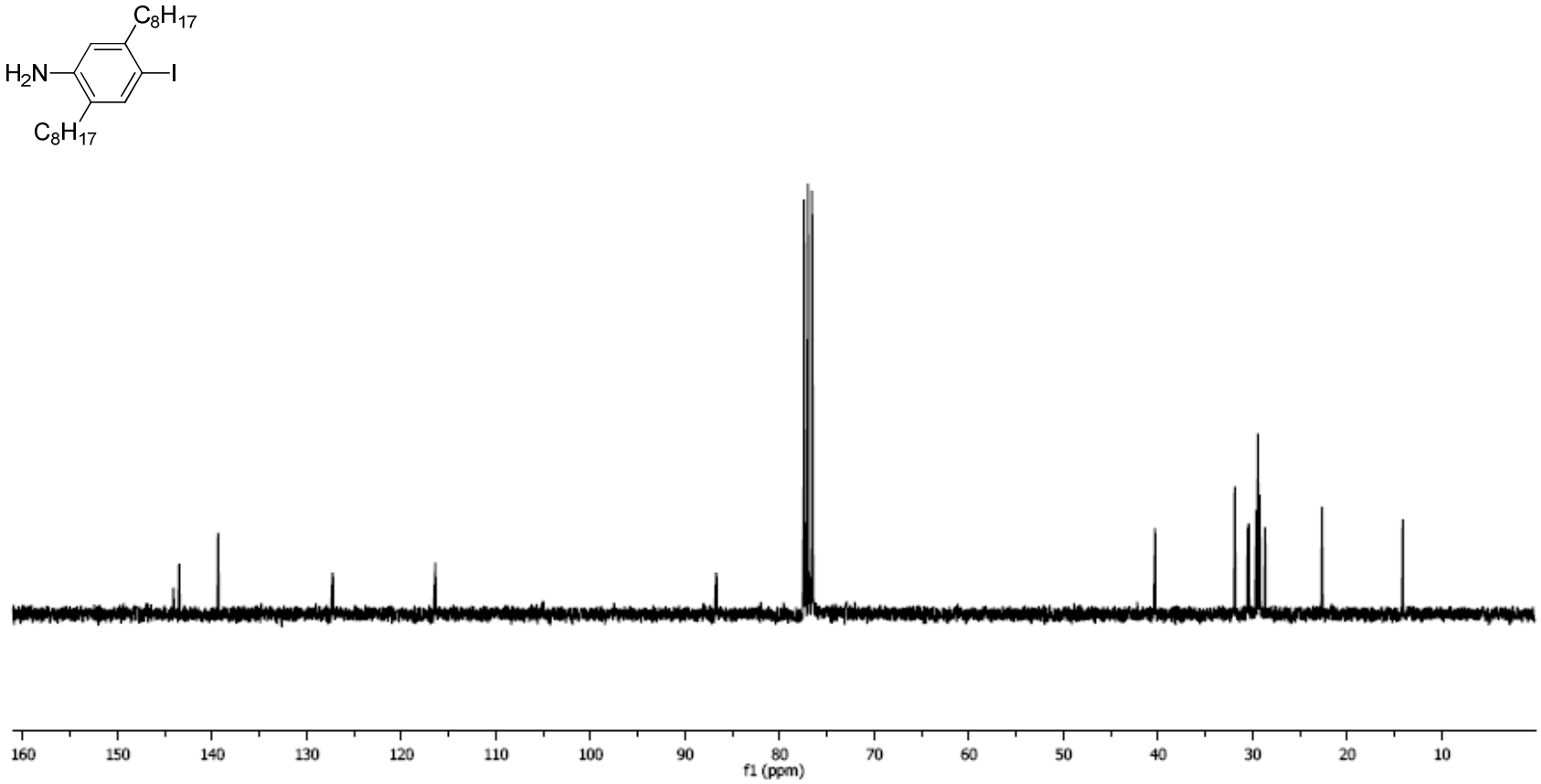


**Figure 47B.** $^{13}$C NMR spectrum of **VIII-8** (75 MHz, $CDCl_3$, 23 °C).

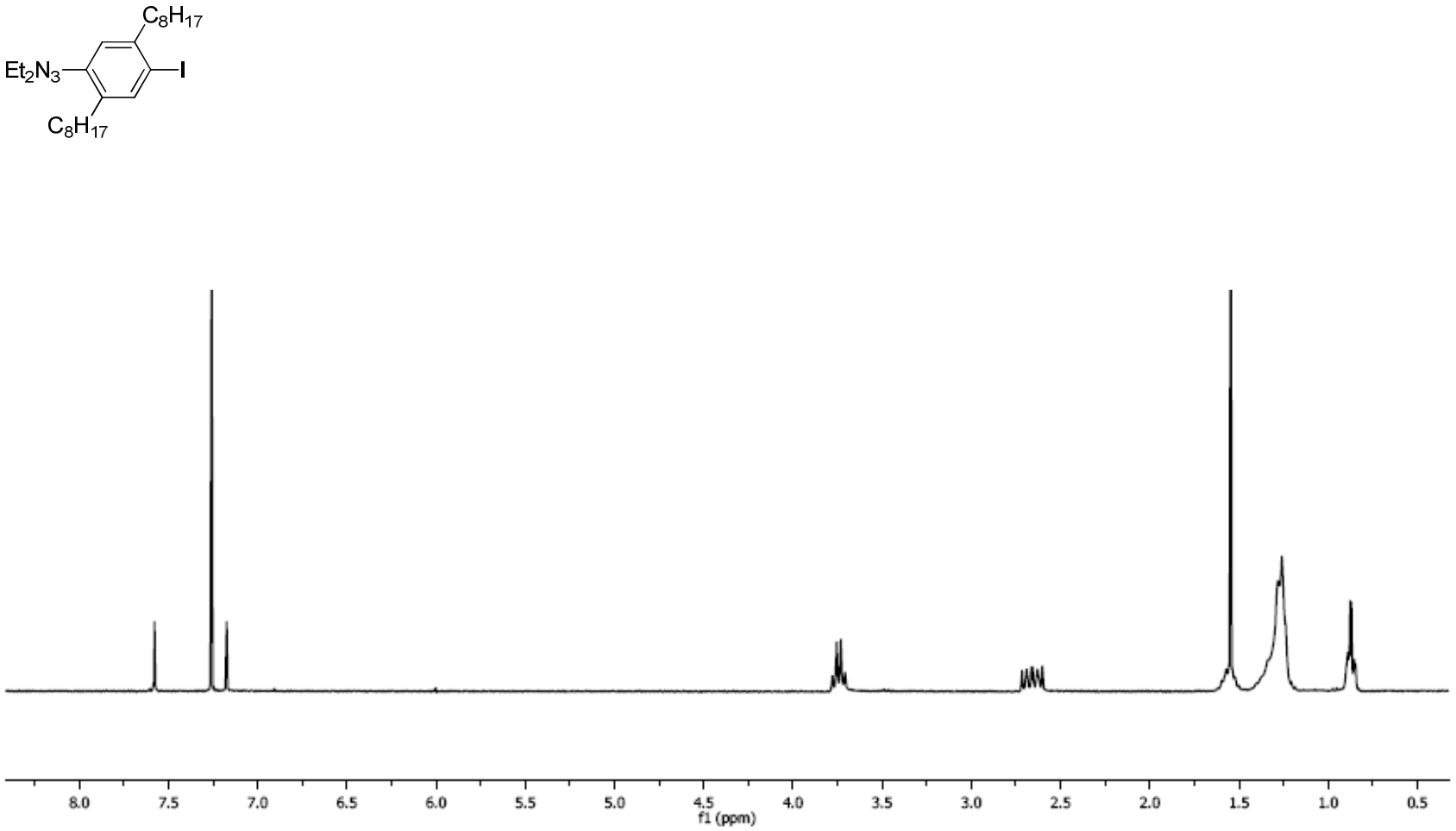


**Figure 48A.** $^{1}$H NMR spectrum of **VIII-9** (300 MHz, $CDCl_3$, 23 °C).

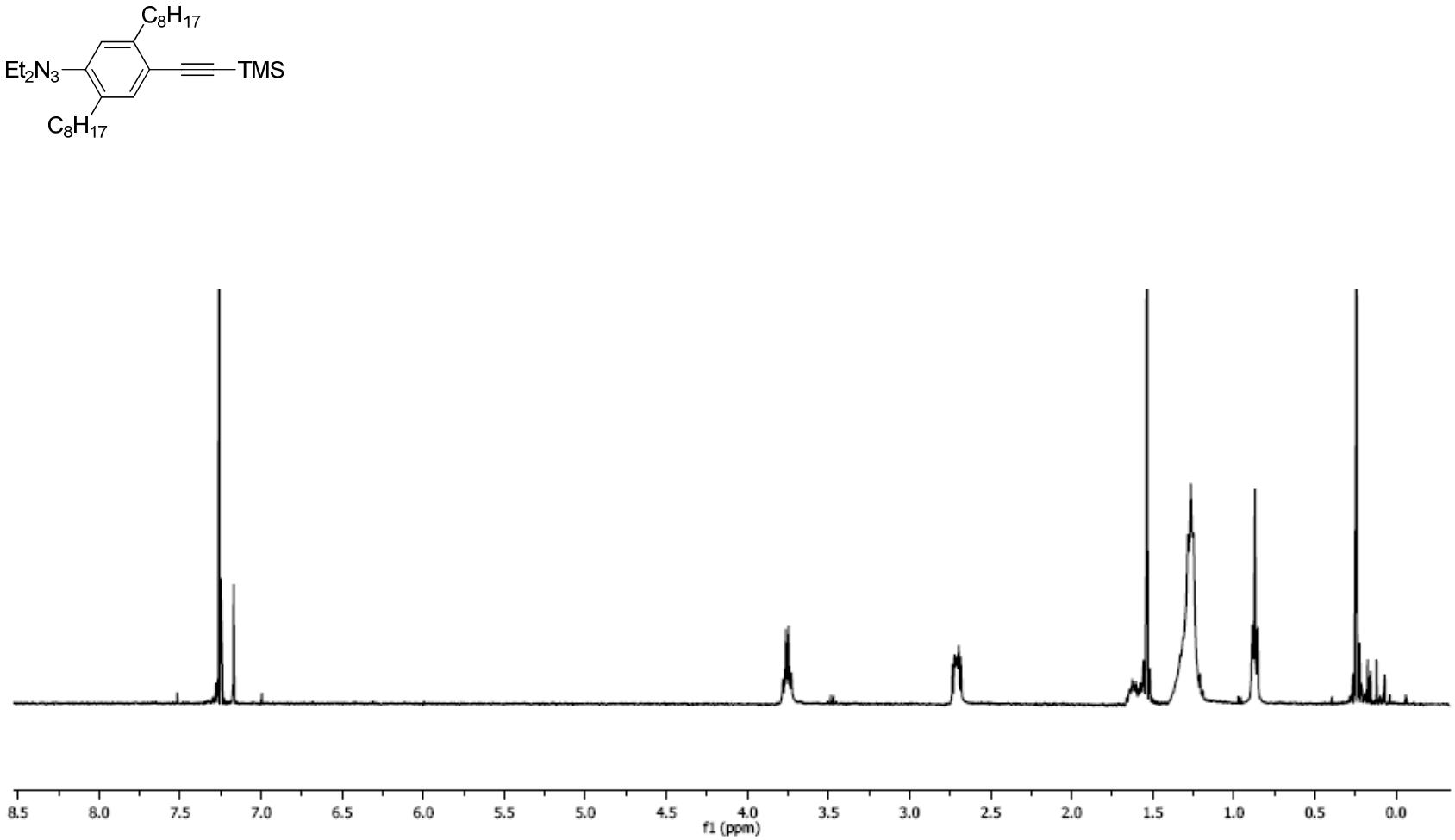


**Figure 49A.** $^{1}$H NMR spectrum of **VIII-10** (300 MHz, $CDCl_3$, 23 °C).

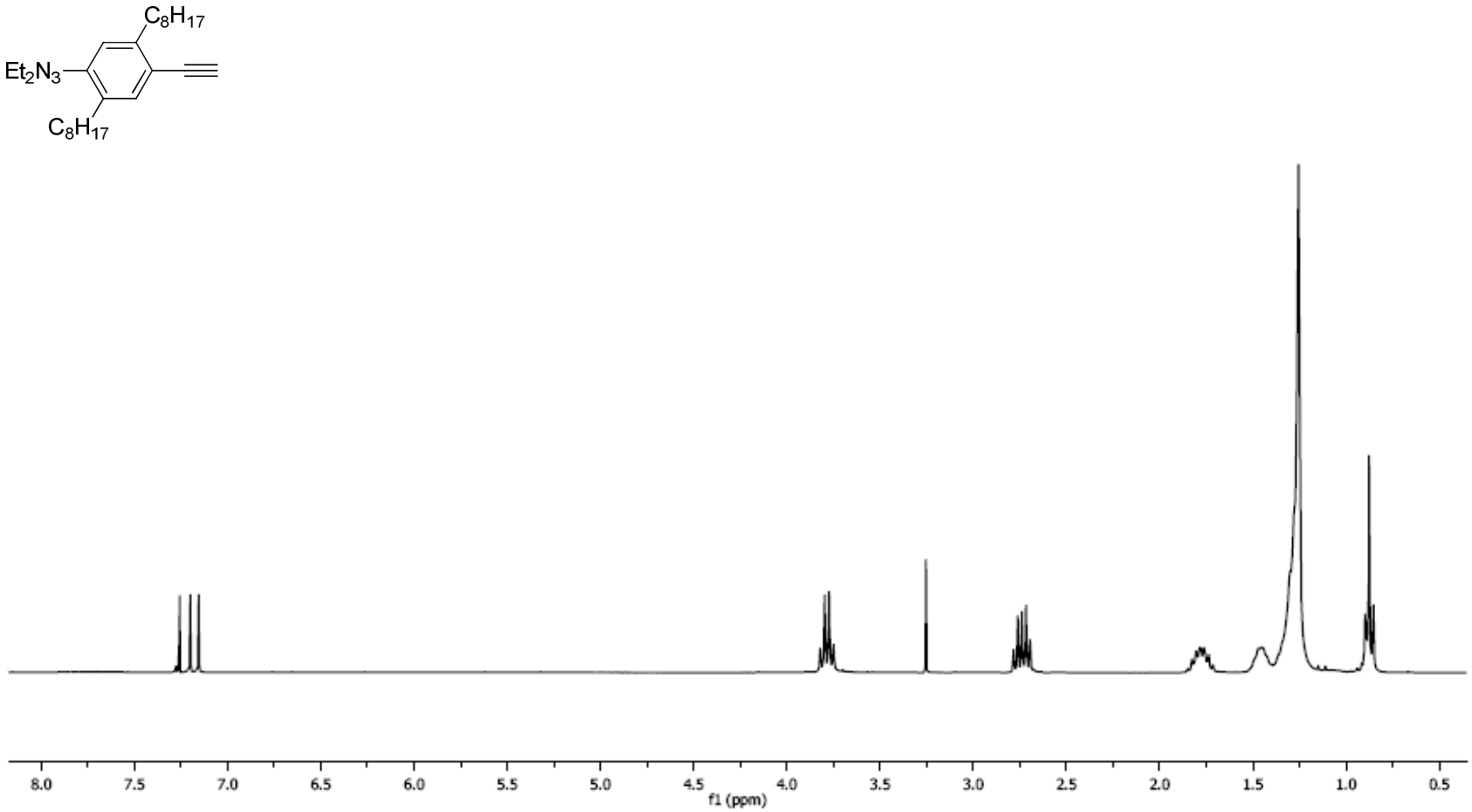


**Figure 50A.** $^{1}$H NMR spectrum of **VIII-11** (300 MHz, $CDCl_3$, 23 °C).

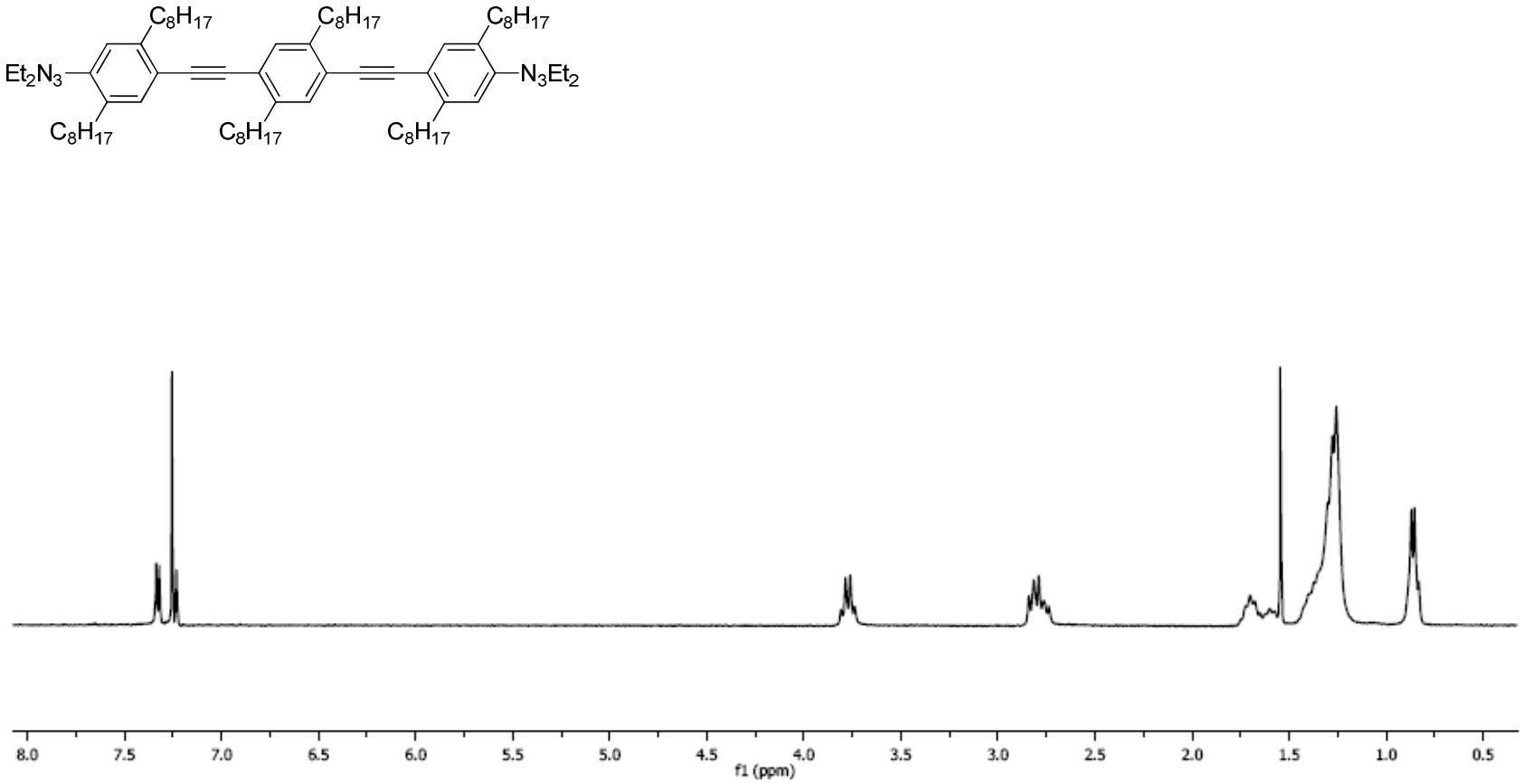


**Figure 51A.** $^{1}$H NMR spectrum of **VIII-4** (300 MHz, $CDCl_3$, 23 °C).

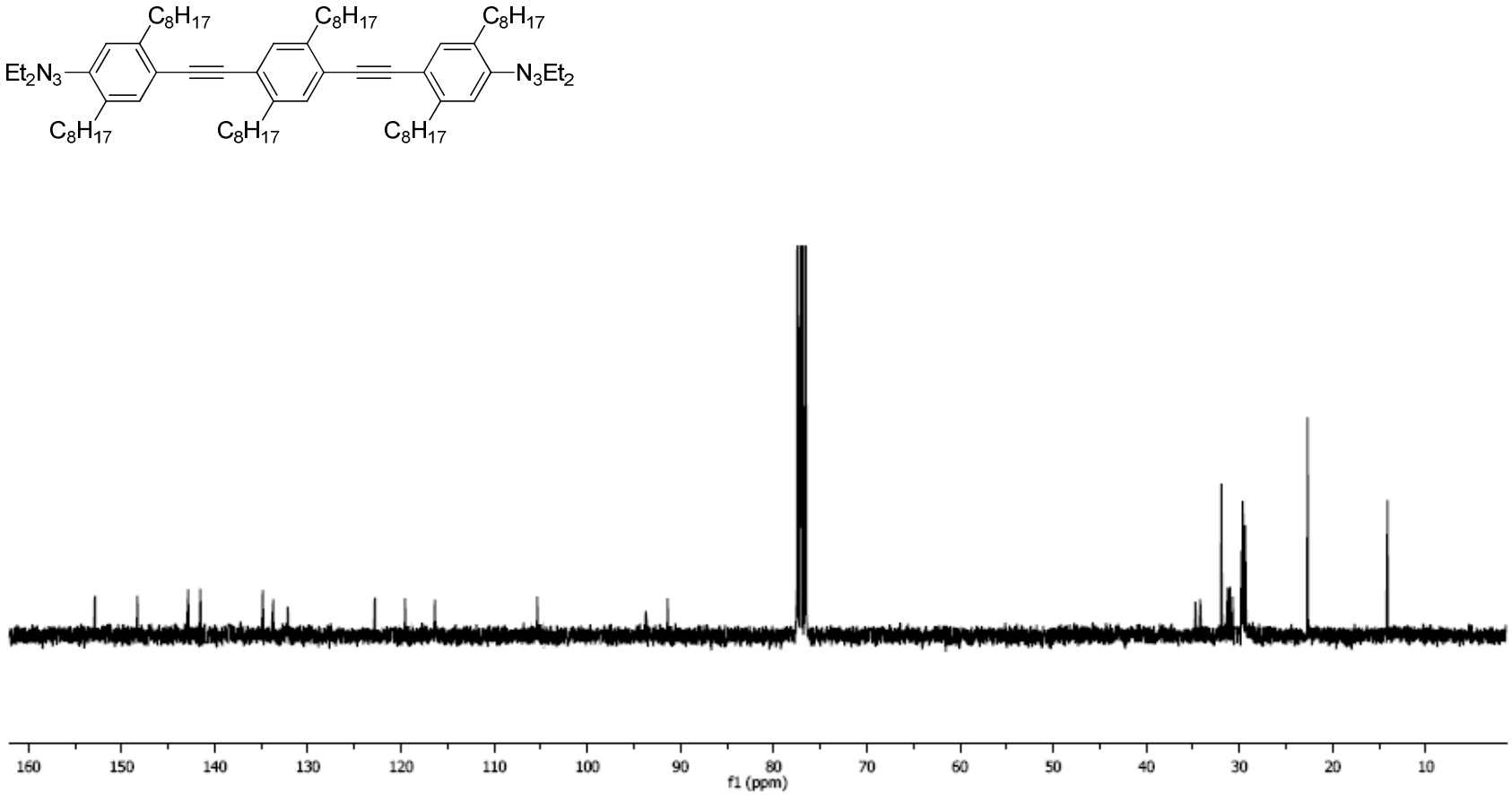


**Figure 51B.** $^{13}C$ NMR spectrum of **VIII-4** (75 MHz, $CDCl_3$, 23 °C).

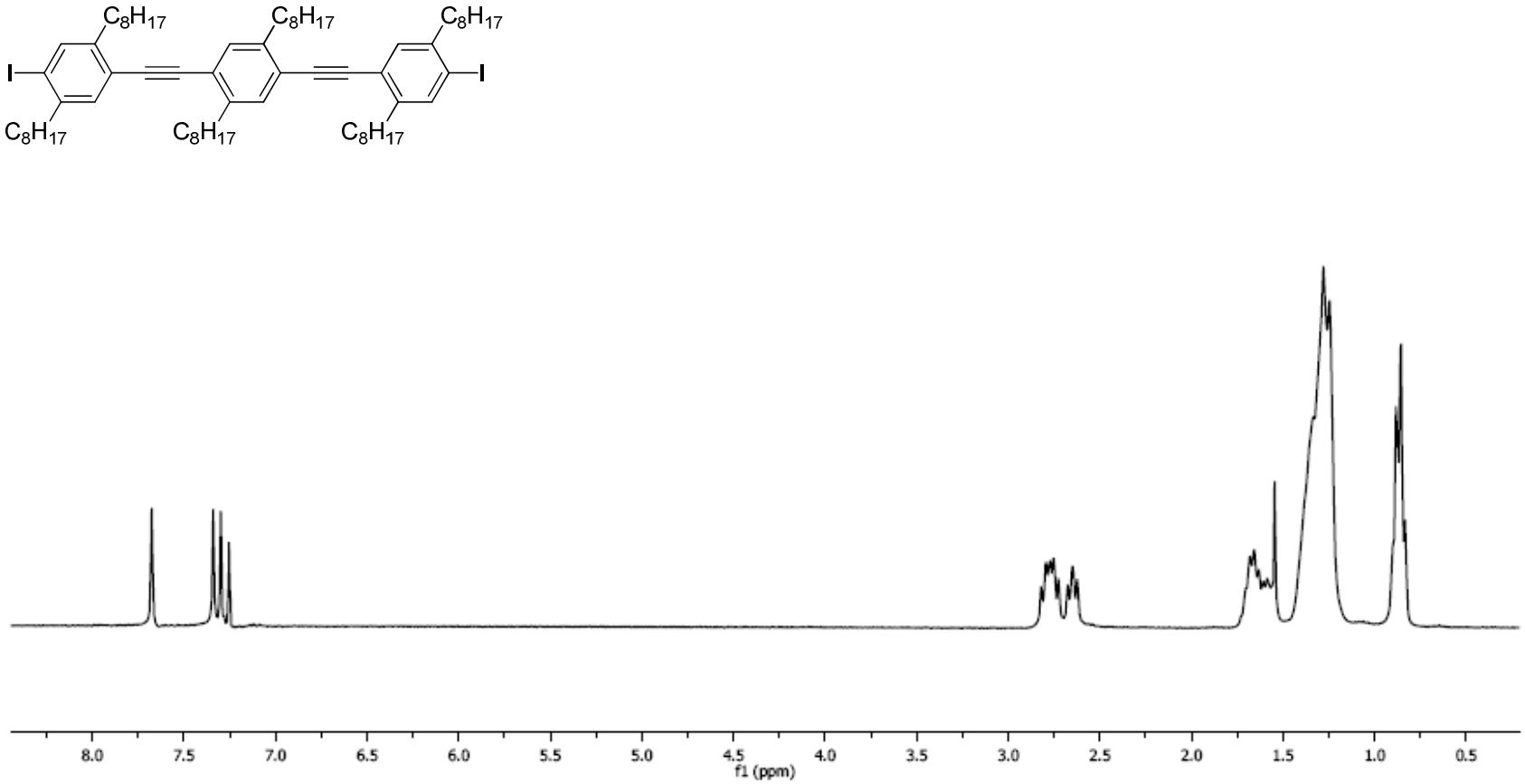


**Figure 52A.** $^{1}$H NMR spectrum of **VIII-2** (300 MHz, $CDCl_3$, 23 °C).

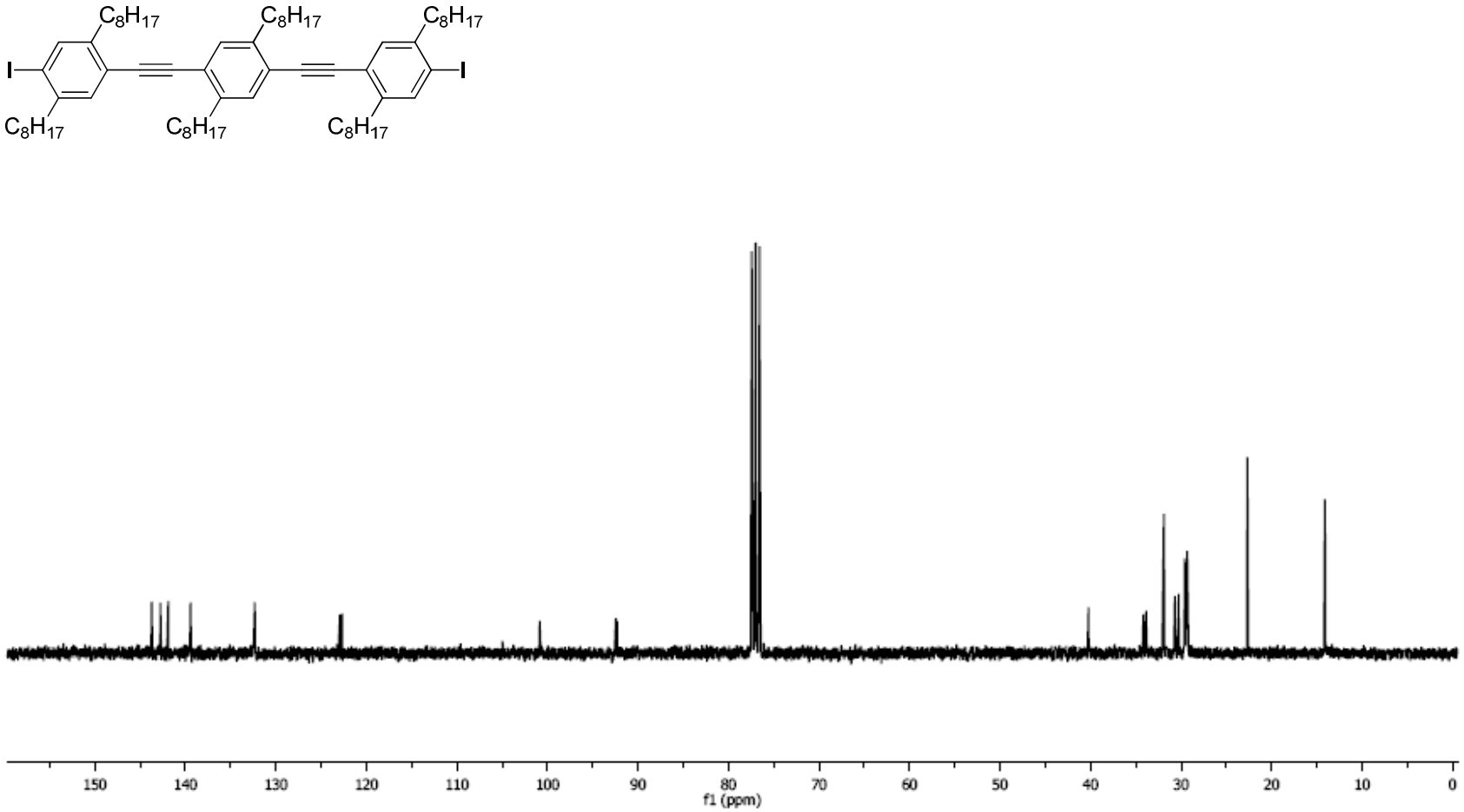


**Figure 52B.** $^{13}C$ NMR spectrum of **VIII-2** (75 MHz, $CDCl_3$, 23 °C).

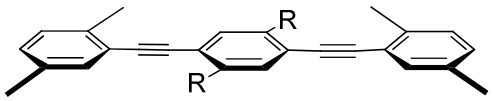


**$Me_4PE_3$**

R = $C_8H_{17}$

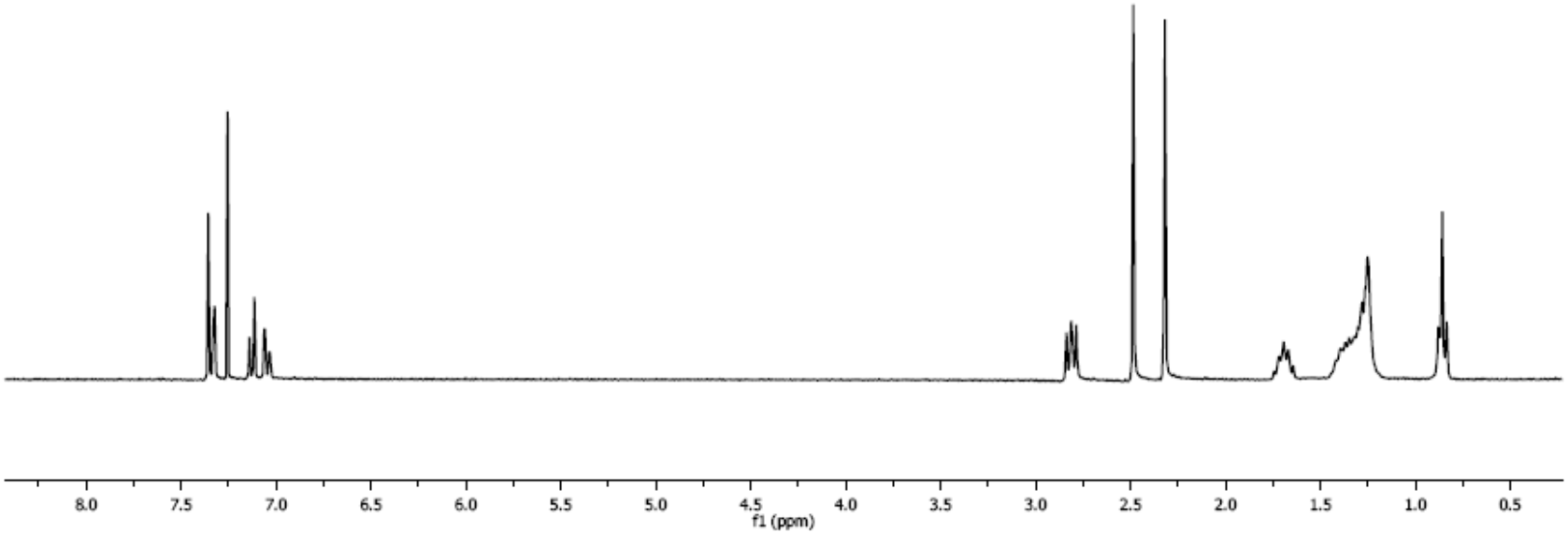


**Figure 53A.** $^1$H NMR spectrum of **$Me_4PE_3$** (300 MHz, $CDCl_3$, 23 °C).

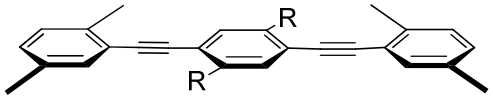


**$Me_4PE_3$**

R = $C_8H_{17}$

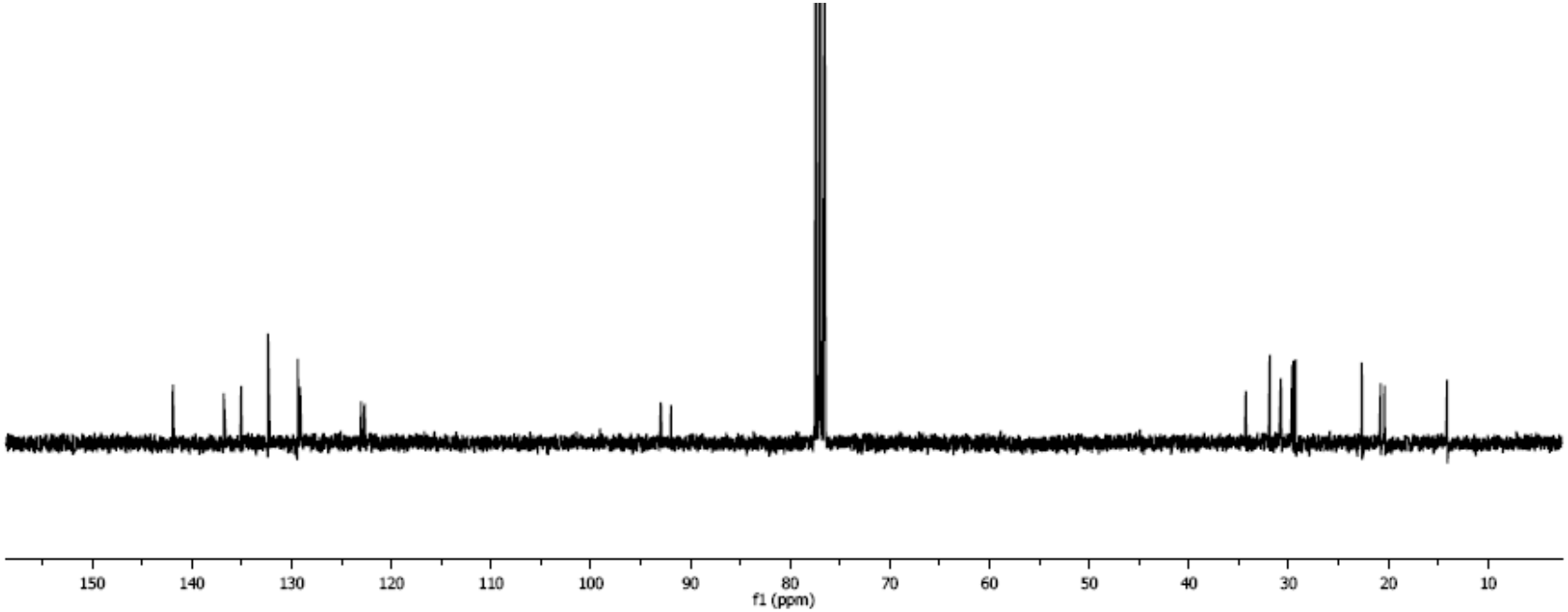


**Figure 53B.** $^{13}C$ NMR spectrum of **$Me_4PE_3$** (75 MHz, $CDCl_3$, 23 °C).

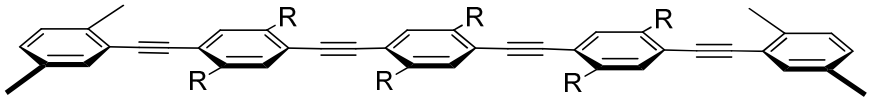


**$Me_4PE_5$**

R = $C_8H_{17}$

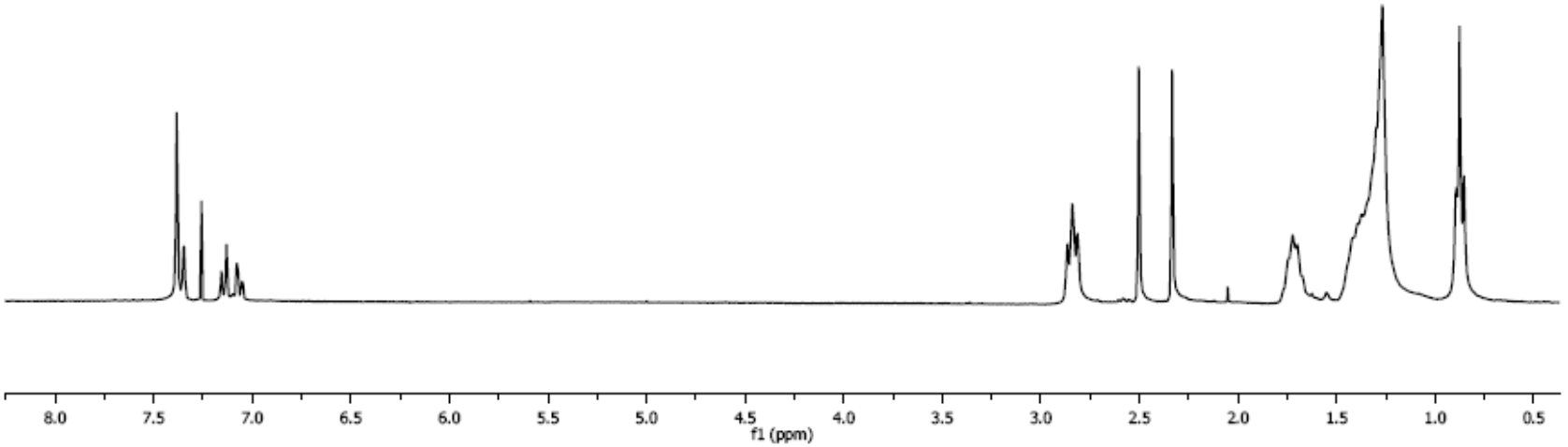


**Figure 54A.** $^1$H NMR spectrum of **$Me_4PE_5$** (300 MHz, $CDCl_3$, 23 °C).

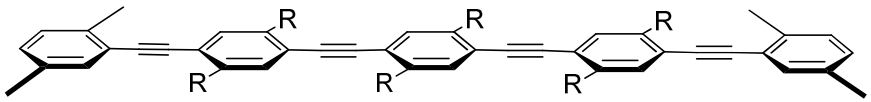


**$Me_4PE_5$**

R = $C_8H_{17}$

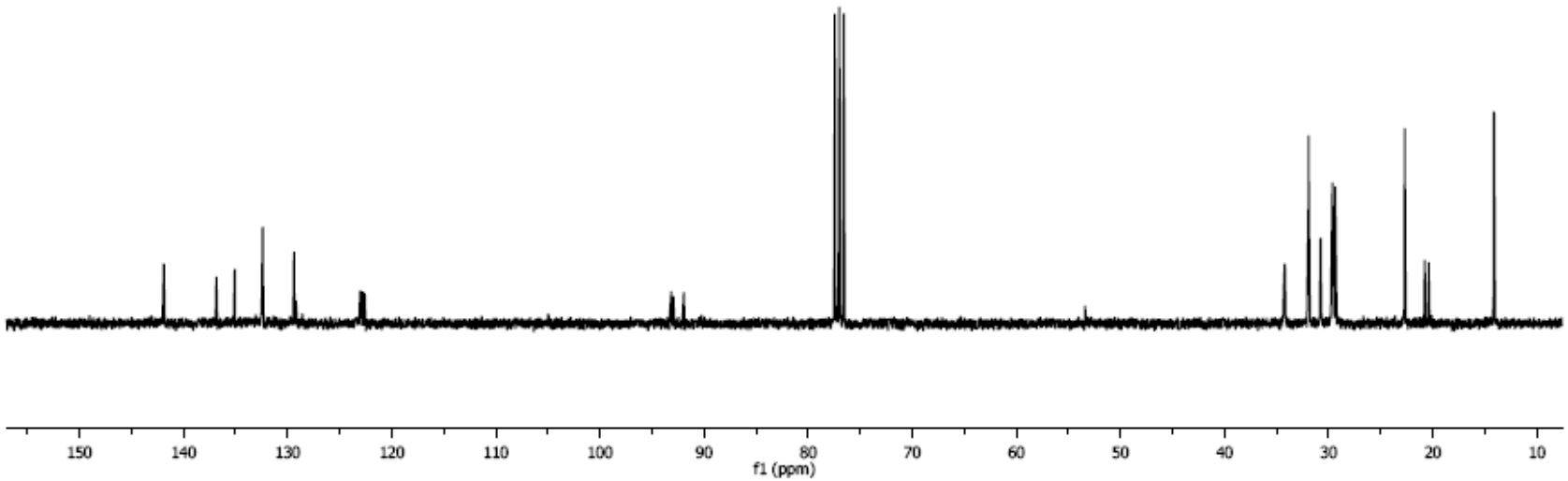


**Figure 54B.** $^{13}C$ NMR spectrum of **$Me_4PE_5$** (75 MHz, $CDCl_3$, 23 °C).

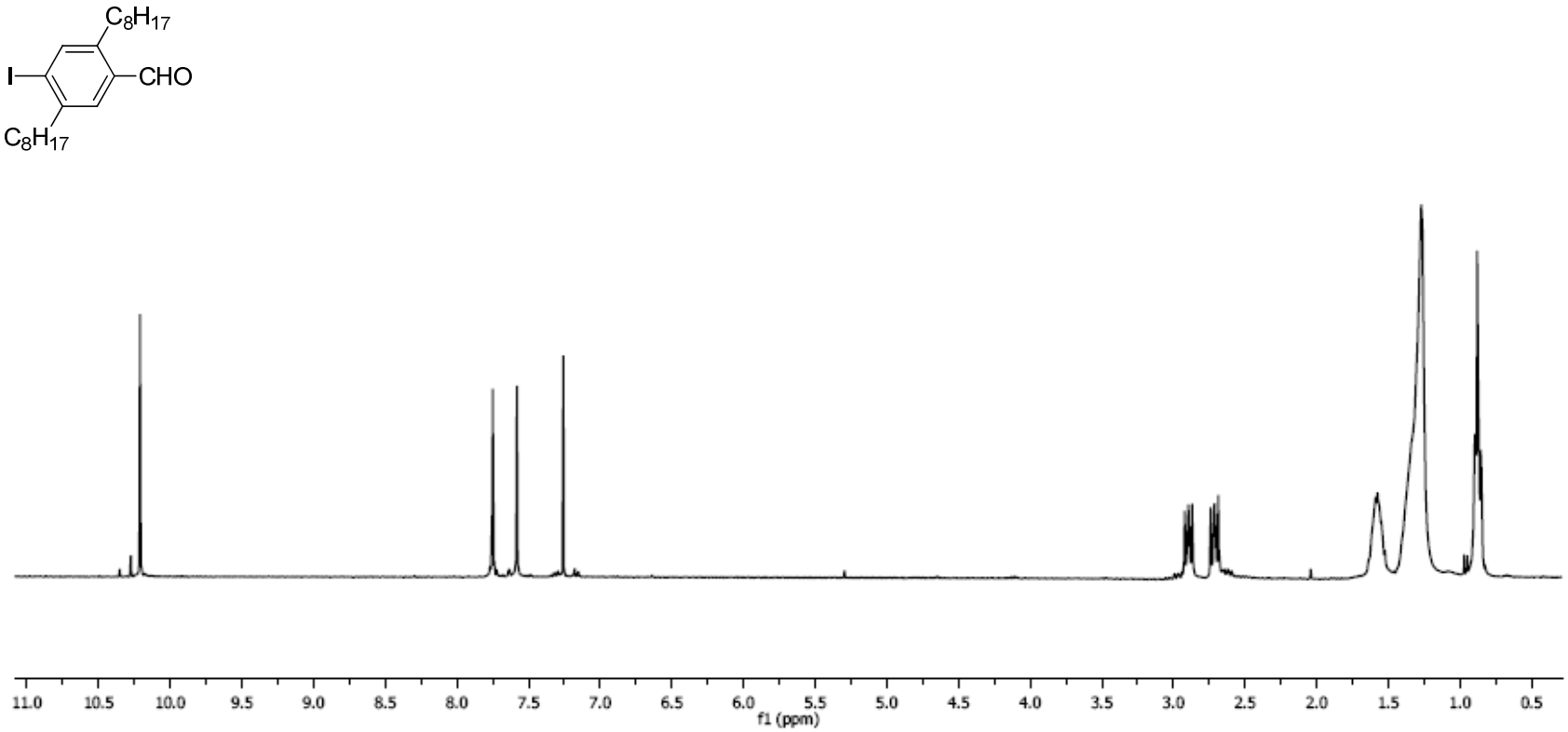


**Figure 55A.** $^{1}$H NMR spectrum of **VIII-14** (300 MHz, $CDCl_3$, 23 °C).

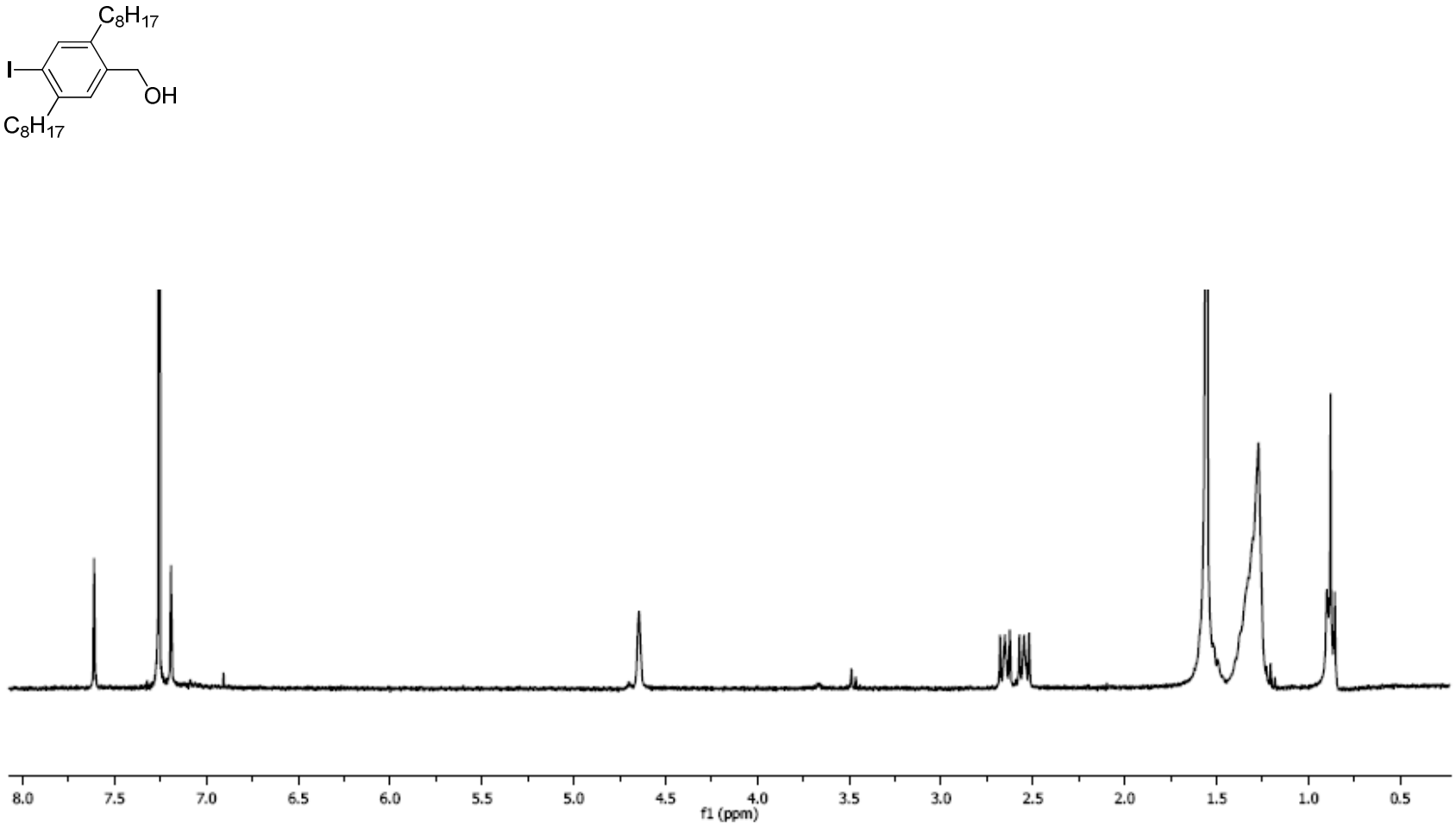


**Figure 56A.** $^{1}$H NMR spectrum of **VIII-15** (300 MHz, $CDCl_3$, 23 °C).

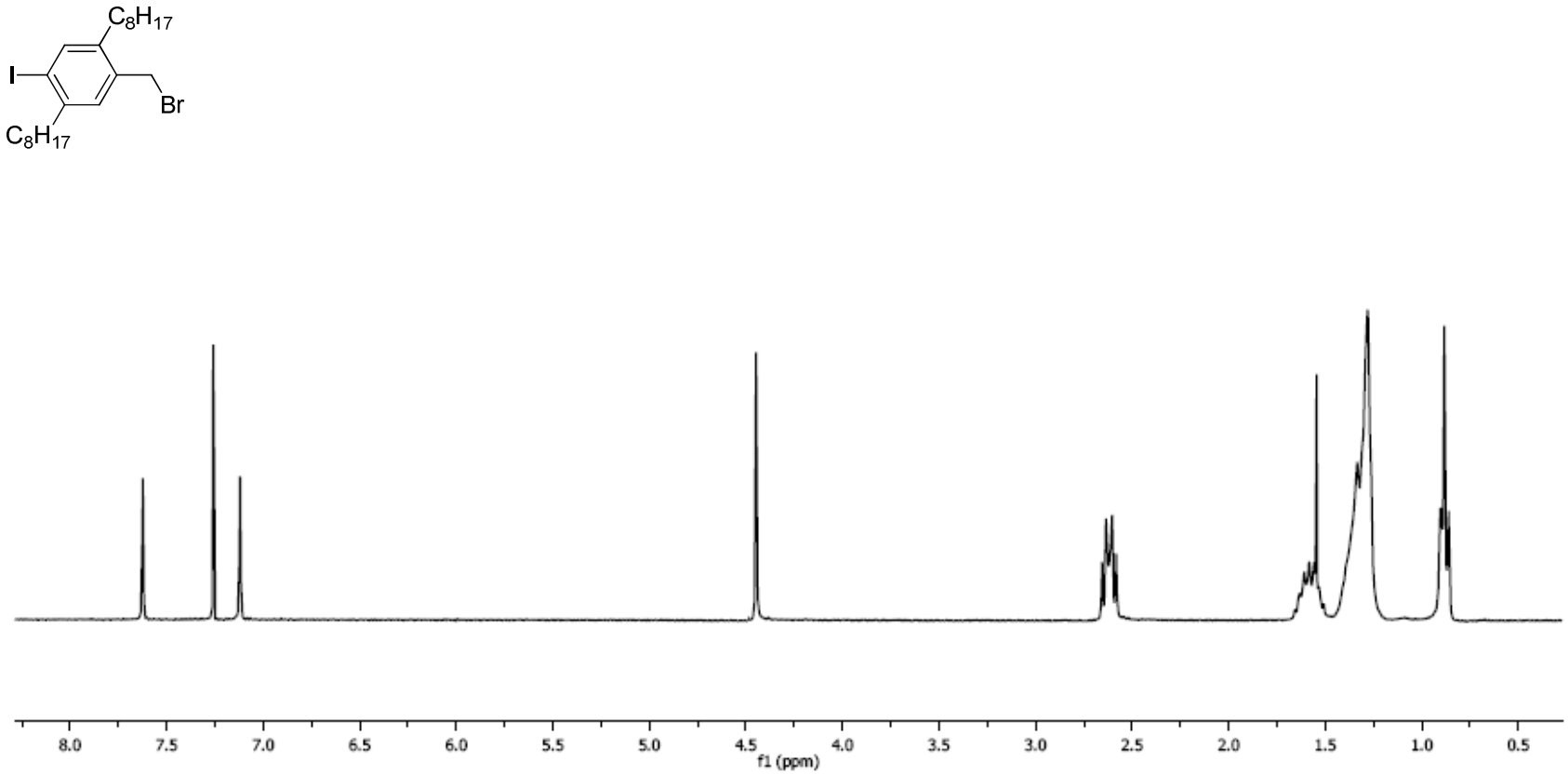


**Figure 57A.** $^{1}$H NMR spectrum of **VIII-16** (300 MHz, $CDCl_3$, 23 °C).

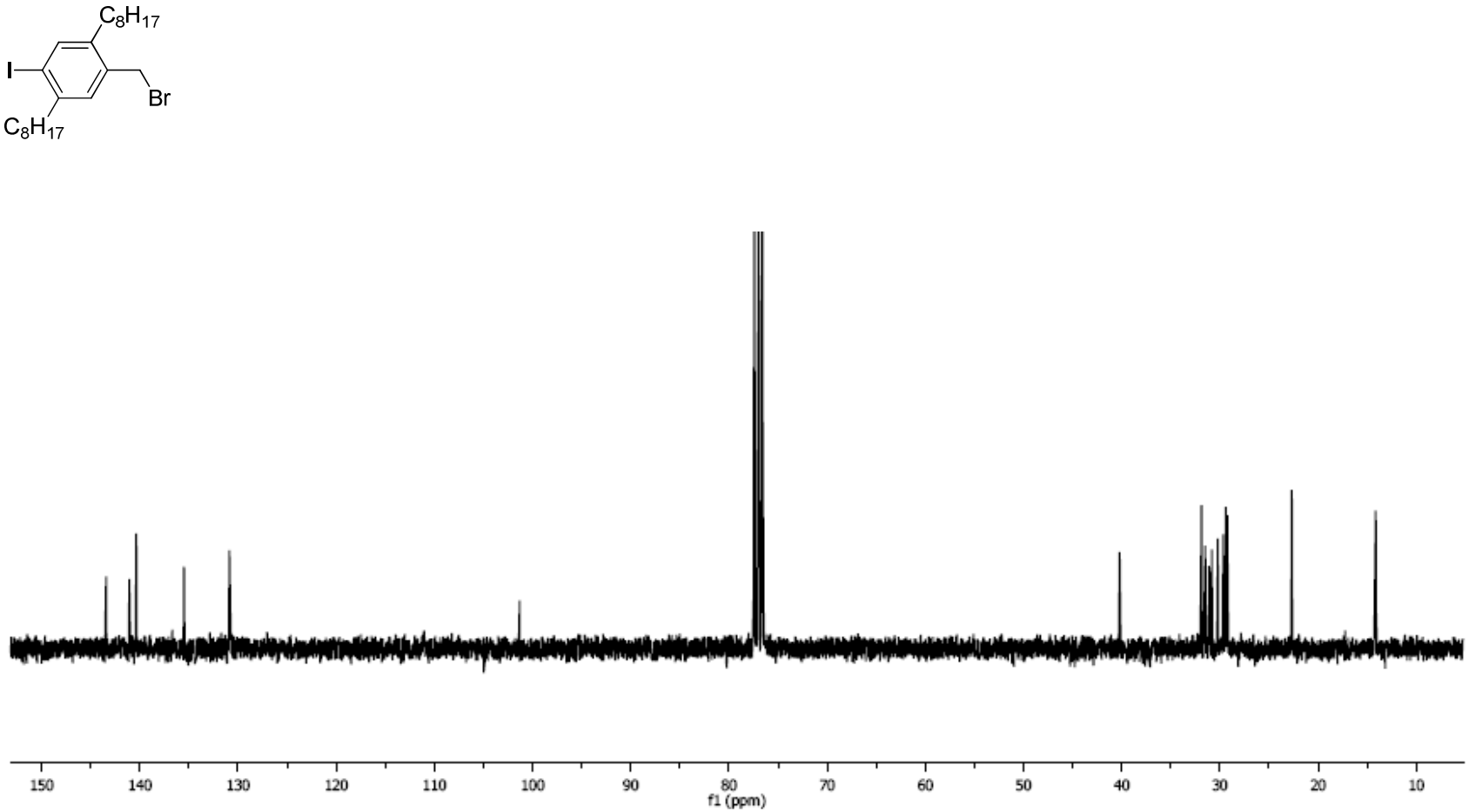


**Figure 57B.** $^{13}C$ NMR spectrum of **VIII-16** (75 MHz, $CDCl_3$, 23 °C).

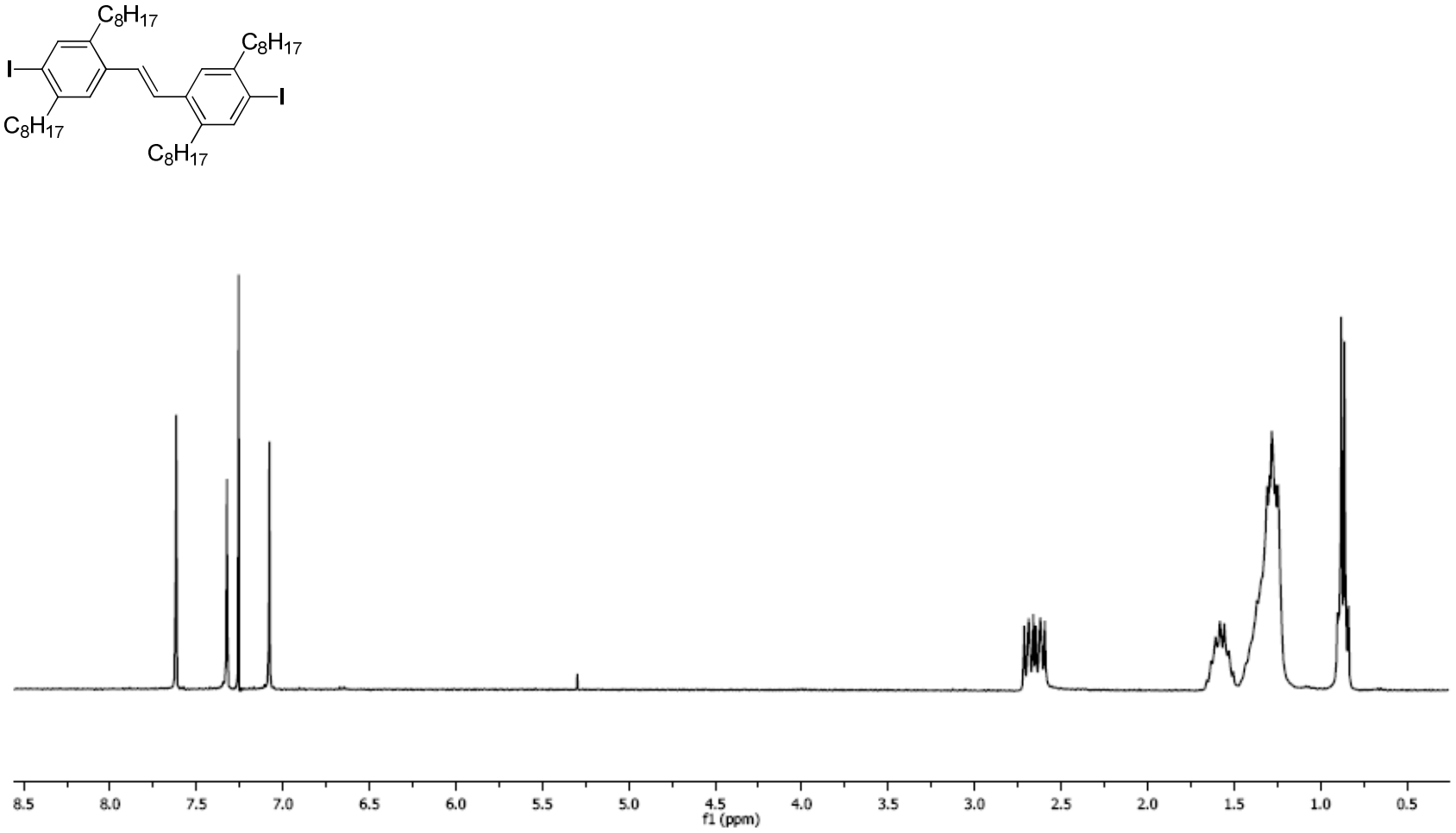


**Figure 58A.** $^{1}$H NMR spectrum of **VIII-18** (300 MHz, $CDCl_3$, 23 °C).

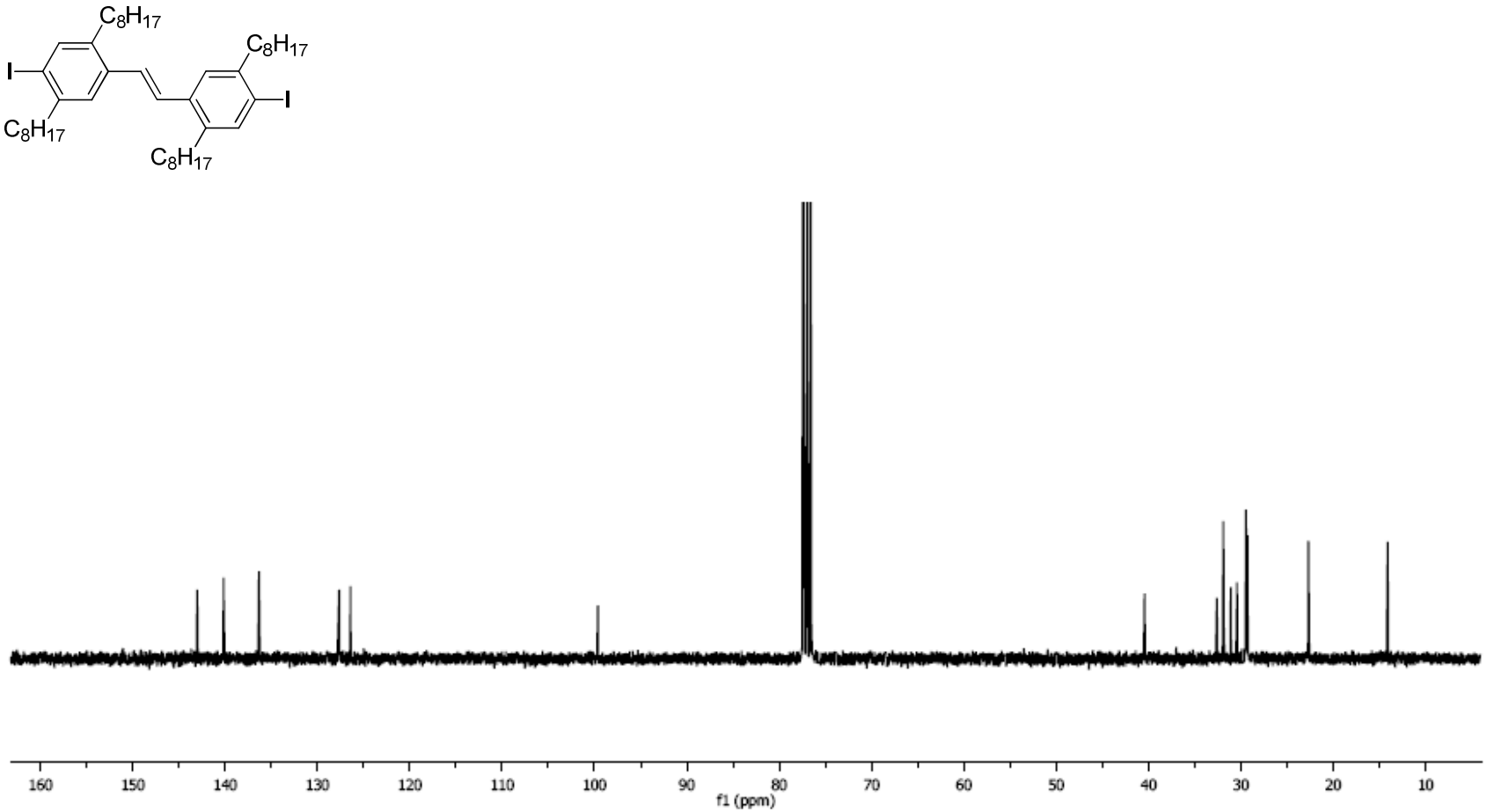


**Figure 58B.** $^{13}C$ NMR spectrum of **VIII-18** (75 MHz, $CDCl_3$, 23 °C).

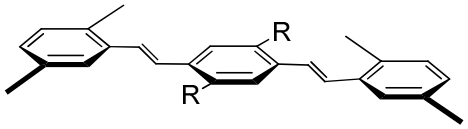


**$Me_4PV_3$**

R = $C_8H_{17}$

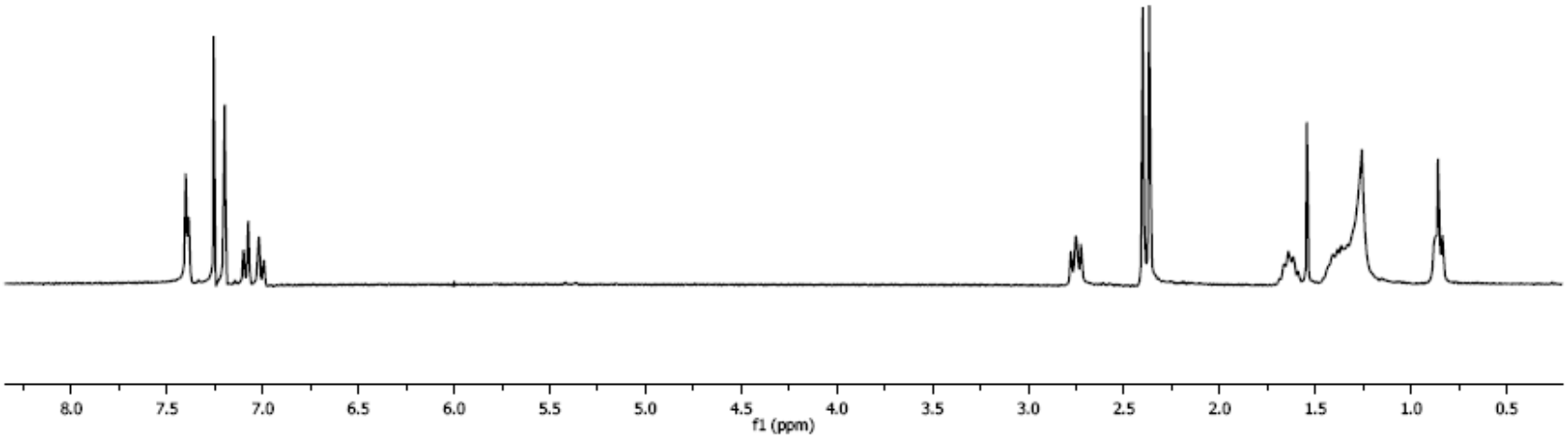


**Figure 59A.** $^1$H NMR spectrum of **$Me_4PV_3$** (300 MHz, $CDCl_3$, 23 °C).

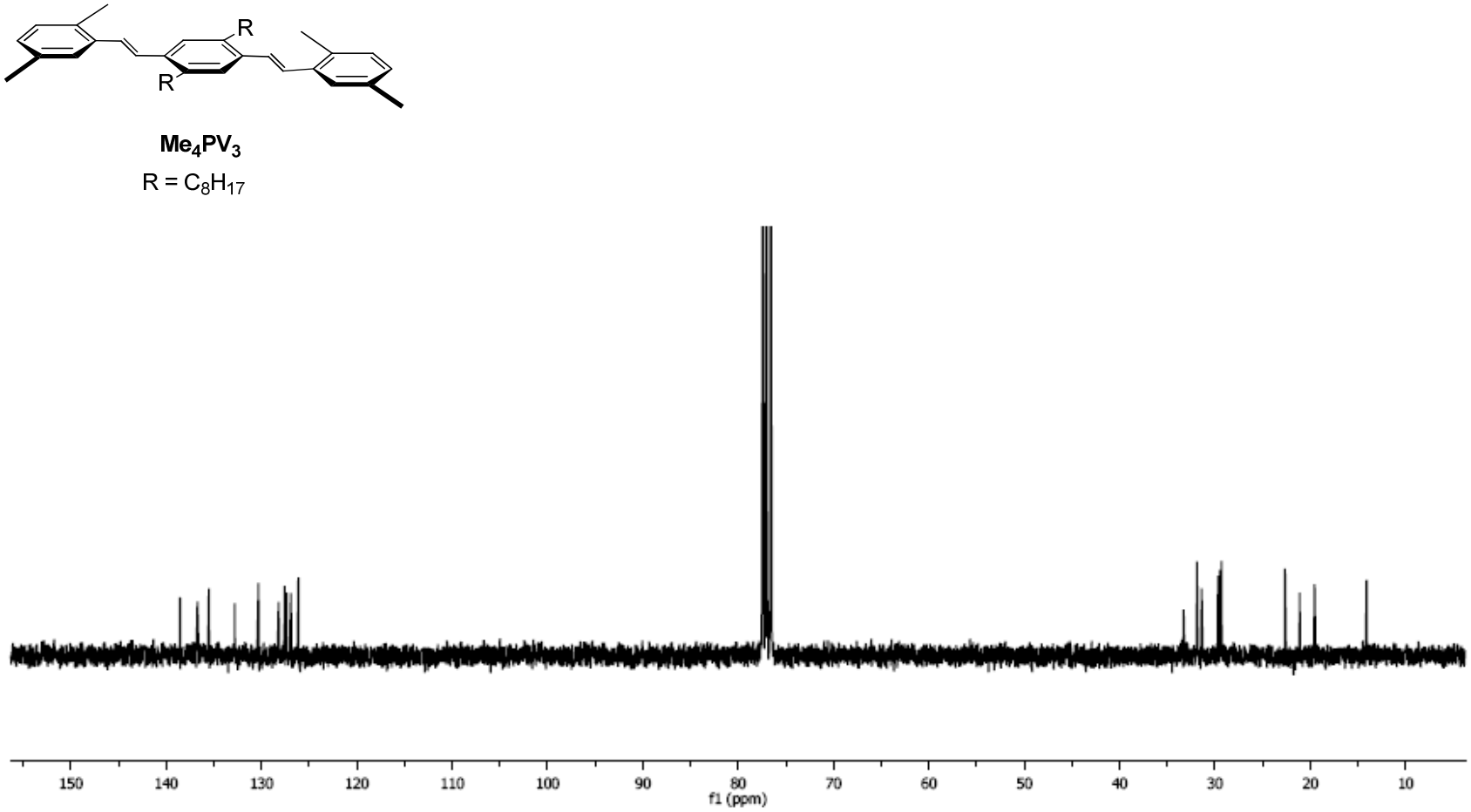


**Figure 59B.** $^{13}C$ NMR spectrum of **$Me_4PV_3$** (75 MHz, $CDCl_3$, 23 °C).

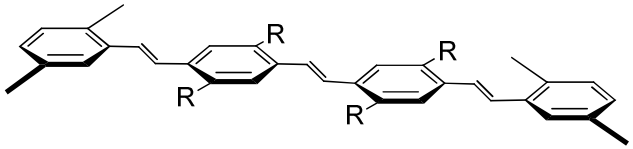


**$Me_4PV_4$**

R = $C_8H_{17}$

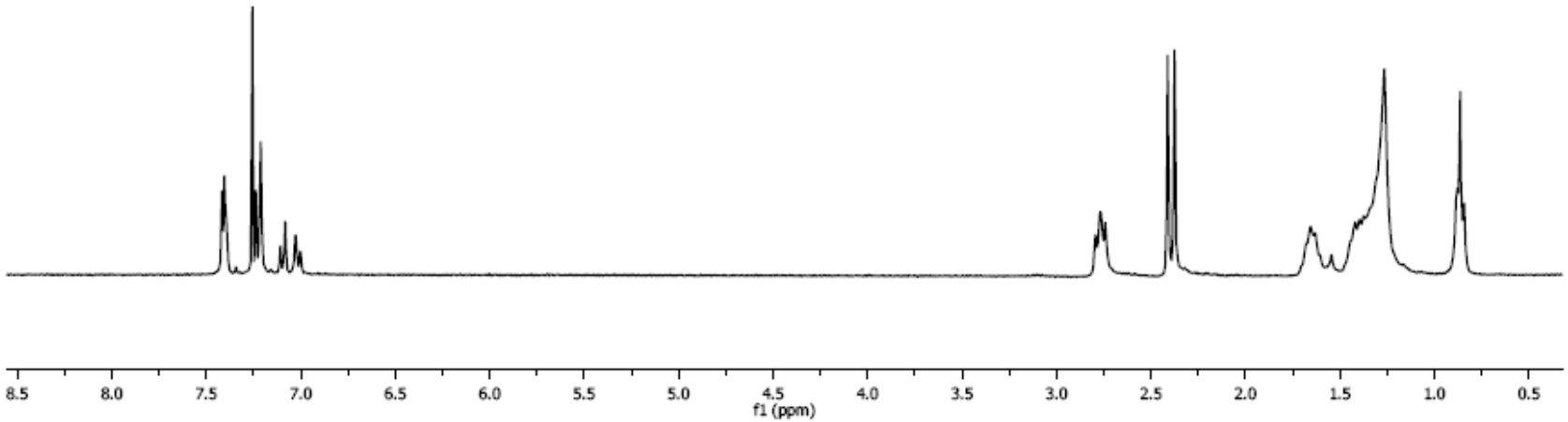


**Figure 60A.** $^1$H NMR spectrum of **$Me_4PV_4$** (300 MHz, $CDCl_3$, 23 °C).

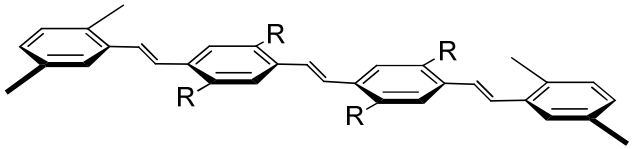


**$Me_4PV_4$**

R = $C_8H_{17}$

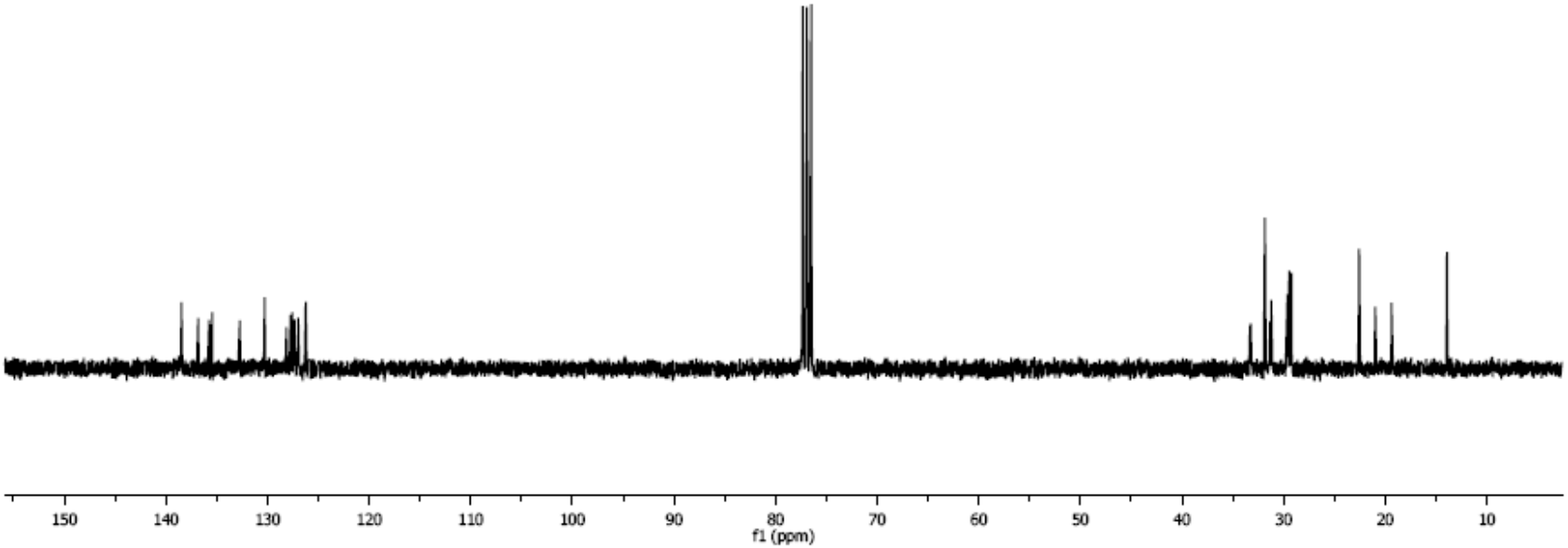


**Figure 60B.** $^{13}C$ NMR spectrum of **$Me_4PV_4$** (75 MHz, $CDCl_3$, 23 °C).

## C. X-ray Crystal Structure data

### C.1. Ethylene-ketal III-8

A suitable crystal of **ethylene-ketal III-8** was coated with Paratone N oil, suspended in a small fiber loop and placed in a cooled nitrogen gas stream at 173 K on a Bruker D8 SMART APEX CCD sealed tube diffractometer with graphite monochromated MoKα (0.71073Å) radiation. Data was measured using a series of combinations of phi and omega scans with 10 s frame exposures and 0.3º frame widths. Data collection, indexing and initial cell refinements were all carried out using

SMART[3] software. Frame integration and final cell refinements were done using SAINT[4] software. The final cell parameters were determined from least-squares refinement on 3398 reflections. The SADABS[5] program was used to carry out absorption corrections. The structure was solved using Direct methods and difference Fourier techniques (SHELXTL, V6.12).[6] Hydrogen atoms were placed in their expected chemical positions using the HIX command and were included in the final cycles of least-squares with isotropic Uij's related to the riding atom. The C-H distances were fixed at 0.93 Å (aromatic), 0.98 (methane), 0.97 Å ($CH_2$), or 0.96 Å ($CH_3$). All non-hydrogen atoms were refined anisotropically. Scattering factors and anomalous dispersion corrections are taken from the *International Tables for x-ray Crystallography*.[7] Structure solution, refinement, graphics and generation of publication materials were performed using SHELXTL, V6.12 software. Additional details of data collection and structure refinement are given in Tables T1-T6. The crystals were all intimately twinned to some degree so data was collected on one clean sample that contained approximately equal contributions of the two components. The unit cells for each component were determined by using a beta test program written by George Sheldrick called Cell_Now. The reflection data was processed with SAINT, taking into account the overlapping of reflections from the two components and were corrected for absorption effects S9 by using TWINABS, a version of SADABS. The structure was solved using only the data that was generated by component 1, however the final refinements used all the data and included the contributions from both components.

**Table 1.** Crystal data and structure refinement for **ethylene-ketal III-8**.

| | | |
|---|---|---|
| Identification code | sj_ks | |
| Empirical formula | C25 H30 O2 | |
| Formula weight | 362.49 | |
| Temperature | 173(2) K | |
| Wavelength | 1.54178 Å | |
| Crystal system | Monoclinic | |
| Space group | P2(1)/c | |
| Unit cell dimensions | a = 12.5978(8) Å | α = 90°. |
| | b = 8.2640(6) Å | β = 101.106(3)°. |
| | c = 18.7438(12) Å | γ = 90°. |
| Volume | 1914.8(2) $Å^3$ | |
| Z | 4 | |
| Density (calculated) | 1.257 $Mg/m^3$ | |
| Absorption coefficient | 0.601 $mm^{-1}$ | |
| F(000) | 784 | |
| Crystal size | 0.37 x 0.25 x 0.18 $mm^3$ | |
| Theta range for data collection | 3.58 to 69.27°. | |
| Index ranges | -14<=h<=14, -9<=k<=9, -22<=l<=22 | |
| Reflections collected | 16494 | |
| Independent reflections | 3428 [R(int) = 0.0420] | |
| Completeness to theta = 69.27° | 96.1 % | |
| Absorption correction | Semi-empirical from equivalents | |
| Max. and min. transmission | 0.8996 and 0.8083 | |
| Refinement method | Full-matrix least-squares on $F^2$ | |
| Data / restraints / parameters | 3428 / 0 / 244 | |
| Goodness-of-fit on $F^2$ | 1.040 | |
| Final R indices [I>2sigma(I)] | R1 = 0.0479, wR2 = 0.1303 | |
| R indices (all data) | R1 = 0.0510, wR2 = 0.1334 | |
| Largest diff. peak and hole | 0.424 and -0.354 $e.Å^{-3}$ | |

**Table 2.** Atomic coordinates ( x $10^4$) and equivalent isotropic displacement parameters ($Å^2$x $10^3$) for **ethylene-ketal III-8**. U(eq) is defined as one third of the trace of the orthogonalized $U^{ij}$ tensor.

| | x | y | z | U(eq) |
|---|---|---|---|---|
| C(1) | 8572(1) | 9372(2) | 1679(1) | 33(1) |
| C(2) | 8909(1) | 8328(2) | 2356(1) | 31(1) |
| C(3) | 8032(1) | 7091(2) | 2460(1) | 34(1) |
| C(4) | 7075(1) | 7736(2) | 2755(1) | 31(1) |
| C(5) | 6366(1) | 8877(2) | 2370(1) | 33(1) |
| C(6) | 5516(1) | 9448(2) | 2678(1) | 36(1) |
| C(7) | 5373(1) | 8985(2) | 3366(1) | 35(1) |
| C(8) | 6096(1) | 7877(2) | 3759(1) | 34(1) |
| C(9) | 6915(1) | 7256(2) | 3435(1) | 33(1) |
| C(10) | 4486(2) | 9743(2) | 3691(1) | 48(1) |
| C(11) | 6025(2) | 7435(2) | 4530(1) | 45(1) |
| C(12) | 7605(1) | 10488(2) | 1664(1) | 35(1) |
| C(13) | 6536(1) | 9563(2) | 1654(1) | 39(1) |
| C(14) | 9396(1) | 9302(2) | 3042(1) | 32(1) |
| C(15) | 8664(1) | 10357(2) | 3402(1) | 30(1) |
| C(16) | 7945(1) | 11501(2) | 3029(1) | 32(1) |
| C(17) | 7305(1) | 12375(2) | 3420(1) | 37(1) |
| C(18) | 7350(1) | 12184(2) | 4159(1) | 36(1) |
| C(19) | 8088(1) | 11079(2) | 4539(1) | 34(1) |
| C(20) | 8721(1) | 10195(2) | 4149(1) | 33(1) |
| C(21) | 6580(2) | 13112(3) | 4533(1) | 54(1) |
| C(22) | 8174(2) | 10805(2) | 5346(1) | 47(1) |
| C(23) | 7839(1) | 11867(2) | 2224(1) | 37(1) |
| C(24) | 9897(2) | 9732(3) | 999(1) | 66(1) |
| C(25) | 9091(2) | 8675(3) | 613(1) | 66(1) |
| O(1) | 9478(1) | 10358(1) | 1583(1) | 38(1) |
| O(2) | 8351(1) | 8333(2) | 1054(1) | 42(1) |

**Table 3.** Bond lengths [Å] and angles [°] for **ethylene-ketal III-8**.

| | | | |
|---|---|---|---|
| C(1)-O(2) | 1.4358(18) | C(19)-C(22) | 1.511(2) |
| C(1)-O(1) | 1.4413(18) | C(20)-H(20A) | 0.9500 |
| C(1)-C(12) | 1.523(2) | C(21)-H(21A) | 0.9800 |
| C(1)-C(2) | 1.525(2) | C(21)-H(21B) | 0.9800 |
| C(2)-C(14) | 1.541(2) | C(21)-H(21C) | 0.9800 |
| C(2)-C(3) | 1.545(2) | C(22)-H(22A) | 0.9800 |
| C(2)-H(2A) | 1.0000 | C(22)-H(22B) | 0.9800 |
| C(3)-C(4) | 1.516(2) | C(22)-H(22C) | 0.9800 |
| C(3)-H(3A) | 0.9900 | C(23)-H(23A) | 0.9900 |
| C(3)-H(3B) | 0.9900 | C(23)-H(23B) | 0.9900 |
| C(4)-C(9) | 1.387(2) | C(24)-O(1) | 1.402(2) |
| C(4)-C(5) | 1.400(2) | C(24)-C(25) | 1.427(3) |
| C(5)-C(6) | 1.392(2) | C(24)-H(24A) | 0.9900 |
| C(5)-C(13) | 1.511(2) | C(24)-H(24B) | 0.9900 |
| C(6)-C(7) | 1.390(2) | C(25)-O(2) | 1.389(2) |
| C(6)-H(6A) | 0.9500 | C(25)-H(25A) | 0.9900 |
| C(7)-C(8) | 1.397(2) | C(25)-H(25B) | 0.9900 |
| C(7)-C(10) | 1.508(2) | | |
| C(8)-C(9) | 1.392(2) | O(2)-C(1)-O(1) | 105.65(11) |
| C(8)-C(11) | 1.510(2) | O(2)-C(1)-C(12) | 108.59(12) |
| C(9)-H(9A) | 0.9500 | O(1)-C(1)-C(12) | 107.76(13) |
| C(10)-H(10A) | 0.9800 | O(2)-C(1)-C(2) | 108.60(13) |
| C(10)-H(10B) | 0.9800 | O(1)-C(1)-C(2) | 108.84(12) |
| C(10)-H(10C) | 0.9800 | C(12)-C(1)-C(2) | 116.84(12) |
| C(11)-H(11A) | 0.9800 | C(1)-C(2)-C(14) | 113.60(13) |
| C(11)-H(11B) | 0.9800 | C(1)-C(2)-C(3) | 112.84(12) |
| C(11)-H(11C) | 0.9800 | C(14)-C(2)-C(3) | 114.81(12) |
| C(12)-C(23) | 1.539(2) | C(1)-C(2)-H(2A) | 104.7 |
| C(12)-C(13) | 1.546(2) | C(14)-C(2)-H(2A) | 104.7 |
| C(12)-H(12A) | 1.0000 | C(3)-C(2)-H(2A) | 104.7 |
| C(13)-H(13A) | 0.9900 | C(4)-C(3)-C(2) | 116.85(13) |
| C(13)-H(13B) | 0.9900 | C(4)-C(3)-H(3A) | 108.1 |
| C(14)-C(15) | 1.519(2) | C(2)-C(3)-H(3A) | 108.1 |
| C(14)-H(14A) | 0.9900 | C(4)-C(3)-H(3B) | 108.1 |
| C(14)-H(14B) | 0.9900 | C(2)-C(3)-H(3B) | 108.1 |
| C(15)-C(20) | 1.395(2) | H(3A)-C(3)-H(3B) | 107.3 |
| C(15)-C(16) | 1.400(2) | C(9)-C(4)-C(5) | 118.34(14) |
| C(16)-C(17) | 1.391(2) | C(9)-C(4)-C(3) | 120.06(14) |
| C(16)-C(23) | 1.519(2) | C(5)-C(4)-C(3) | 121.54(14) |
| C(17)-C(18) | 1.384(2) | C(6)-C(5)-C(4) | 118.73(14) |
| C(17)-H(17A) | 0.9500 | C(6)-C(5)-C(13) | 119.55(14) |
| C(18)-C(19) | 1.397(2) | C(4)-C(5)-C(13) | 121.63(14) |
| C(18)-C(21) | 1.511(2) | C(7)-C(6)-C(5) | 122.58(15) |
| C(19)-C(20) | 1.390(2) | C(7)-C(6)-H(6A) | 118.7 |

| | | | |
|---|---|---|---|
| C(5)-C(6)-H(6A) | 118.7 | C(18)-C(17)-C(16) | 123.47(15) |
| C(6)-C(7)-C(8) | 118.80(14) | C(18)-C(17)-H(17A) | 118.3 |
| C(6)-C(7)-C(10) | 119.95(15) | C(16)-C(17)-H(17A) | 118.3 |
| C(8)-C(7)-C(10) | 121.17(15) | C(17)-C(18)-C(19) | 118.72(14) |
| C(9)-C(8)-C(7) | 118.33(14) | C(17)-C(18)-C(21) | 120.06(16) |
| C(9)-C(8)-C(11) | 120.86(15) | C(19)-C(18)-C(21) | 121.18(15) |
| C(7)-C(8)-C(11) | 120.72(14) | C(20)-C(19)-C(18) | 117.91(14) |
| C(4)-C(9)-C(8) | 123.12(15) | C(20)-C(19)-C(22) | 120.60(15) |
| C(4)-C(9)-H(9A) | 118.4 | C(18)-C(19)-C(22) | 121.46(14) |
| C(8)-C(9)-H(9A) | 118.4 | C(19)-C(20)-C(15) | 123.63(15) |
| C(7)-C(10)-H(10A) | 109.5 | C(19)-C(20)-H(20A) | 118.2 |
| C(7)-C(10)-H(10B) | 109.5 | C(15)-C(20)-H(20A) | 118.2 |
| H(10A)-C(10)-H(10B) | 109.5 | C(18)-C(21)-H(21A) | 109.5 |
| C(7)-C(10)-H(10C) | 109.5 | C(18)-C(21)-H(21B) | 109.5 |
| H(10A)-C(10)-H(10C) | 109.5 | H(21A)-C(21)-H(21B) | 109.5 |
| H(10B)-C(10)-H(10C) | 109.5 | C(18)-C(21)-H(21C) | 109.5 |
| C(8)-C(11)-H(11A) | 109.5 | H(21A)-C(21)-H(21C) | 109.5 |
| C(8)-C(11)-H(11B) | 109.5 | H(21B)-C(21)-H(21C) | 109.5 |
| H(11A)-C(11)-H(11B) | 109.5 | C(19)-C(22)-H(22A) | 109.5 |
| C(8)-C(11)-H(11C) | 109.5 | C(19)-C(22)-H(22B) | 109.5 |
| H(11A)-C(11)-H(11C) | 109.5 | H(22A)-C(22)-H(22B) | 109.5 |
| H(11B)-C(11)-H(11C) | 109.5 | C(19)-C(22)-H(22C) | 109.5 |
| C(1)-C(12)-C(23) | 112.87(13) | H(22A)-C(22)-H(22C) | 109.5 |
| C(1)-C(12)-C(13) | 113.10(13) | H(22B)-C(22)-H(22C) | 109.5 |
| C(23)-C(12)-C(13) | 115.27(13) | C(16)-C(23)-C(12) | 119.93(13) |
| C(1)-C(12)-H(12A) | 104.8 | C(16)-C(23)-H(23A) | 107.3 |
| C(23)-C(12)-H(12A) | 104.8 | C(12)-C(23)-H(23A) | 107.3 |
| C(13)-C(12)-H(12A) | 104.8 | C(16)-C(23)-H(23B) | 107.3 |
| C(5)-C(13)-C(12) | 116.53(13) | C(12)-C(23)-H(23B) | 107.3 |
| C(5)-C(13)-H(13A) | 108.2 | H(23A)-C(23)-H(23B) | 106.9 |
| C(12)-C(13)-H(13A) | 108.2 | O(1)-C(24)-C(25) | 106.44(16) |
| C(5)-C(13)-H(13B) | 108.2 | O(1)-C(24)-H(24A) | 110.4 |
| C(12)-C(13)-H(13B) | 108.2 | C(25)-C(24)-H(24A) | 110.4 |
| H(13A)-C(13)-H(13B) | 107.3 | O(1)-C(24)-H(24B) | 110.4 |
| C(15)-C(14)-C(2) | 119.55(12) | C(25)-C(24)-H(24B) | 110.4 |
| C(15)-C(14)-H(14A) | 107.4 | H(24A)-C(24)-H(24B) | 108.6 |
| C(2)-C(14)-H(14A) | 107.4 | O(2)-C(25)-C(24) | 108.45(15) |
| C(15)-C(14)-H(14B) | 107.4 | O(2)-C(25)-H(25A) | 110.0 |
| C(2)-C(14)-H(14B) | 107.4 | C(24)-C(25)-H(25A) | 110.0 |
| H(14A)-C(14)-H(14B) | 107.0 | O(2)-C(25)-H(25B) | 110.0 |
| C(20)-C(15)-C(16) | 118.04(14) | C(24)-C(25)-H(25B) | 110.0 |
| C(20)-C(15)-C(14) | 118.23(13) | H(25A)-C(25)-H(25B) | 108.4 |
| C(16)-C(15)-C(14) | 123.72(13) | C(24)-O(1)-C(1) | 108.41(13) |
| C(17)-C(16)-C(15) | 118.19(14) | C(25)-O(2)-C(1) | 108.48(13) |
| C(17)-C(16)-C(23) | 118.08(14) | | |
| C(15)-C(16)-C(23) | 123.72(14) | | |

**Table 4.** Anisotropic displacement parameters ($Å^2 x\ 10^3$) for **ethylene-ketal III-8**. The anisotropic displacement factor exponent takes the form: $-2\pi^2[ h^2 a^{*2} U^{11} + ... + 2 h k a^* b^* U^{12} ]$

| | $U^{11}$ | $U^{22}$ | $U^{33}$ | $U^{23}$ | $U^{13}$ | $U^{12}$ |
|---|---|---|---|---|---|---|
| C(1) | 35(1) | 38(1) | 29(1) | -5(1) | 11(1) | -8(1) |
| C(2) | 29(1) | 33(1) | 33(1) | -3(1) | 12(1) | 0(1) |
| C(3) | 32(1) | 32(1) | 38(1) | 0(1) | 11(1) | 0(1) |
| C(4) | 28(1) | 33(1) | 35(1) | -2(1) | 8(1) | -5(1) |
| C(5) | 28(1) | 38(1) | 33(1) | 0(1) | 5(1) | -4(1) |
| C(6) | 27(1) | 41(1) | 40(1) | 3(1) | 4(1) | 0(1) |
| C(7) | 28(1) | 38(1) | 39(1) | -5(1) | 8(1) | -5(1) |
| C(8) | 32(1) | 36(1) | 34(1) | -2(1) | 9(1) | -7(1) |
| C(9) | 30(1) | 33(1) | 37(1) | 4(1) | 7(1) | -1(1) |
| C(10) | 40(1) | 55(1) | 51(1) | -4(1) | 16(1) | 4(1) |
| C(11) | 45(1) | 56(1) | 38(1) | 3(1) | 14(1) | 0(1) |
| C(12) | 38(1) | 41(1) | 26(1) | 5(1) | 7(1) | -1(1) |
| C(13) | 33(1) | 51(1) | 32(1) | 6(1) | 4(1) | -1(1) |
| C(14) | 30(1) | 35(1) | 30(1) | 0(1) | 7(1) | 2(1) |
| C(15) | 30(1) | 30(1) | 31(1) | -3(1) | 7(1) | -2(1) |
| C(16) | 33(1) | 32(1) | 32(1) | -1(1) | 7(1) | 0(1) |
| C(17) | 36(1) | 36(1) | 38(1) | -3(1) | 4(1) | 6(1) |
| C(18) | 32(1) | 39(1) | 38(1) | -10(1) | 8(1) | 0(1) |
| C(19) | 34(1) | 38(1) | 31(1) | -6(1) | 9(1) | -6(1) |
| C(20) | 34(1) | 34(1) | 31(1) | -1(1) | 6(1) | 2(1) |
| C(21) | 48(1) | 67(1) | 47(1) | -15(1) | 12(1) | 15(1) |
| C(22) | 52(1) | 58(1) | 33(1) | -5(1) | 12(1) | 5(1) |
| C(23) | 43(1) | 35(1) | 34(1) | 5(1) | 8(1) | 5(1) |
| C(24) | 72(1) | 75(2) | 64(1) | -23(1) | 47(1) | -26(1) |
| C(25) | 64(1) | 90(2) | 53(1) | -31(1) | 35(1) | -23(1) |
| O(1) | 40(1) | 43(1) | 35(1) | -4(1) | 17(1) | -11(1) |
| O(2) | 49(1) | 50(1) | 31(1) | -11(1) | 17(1) | -15(1) |

**Table 5.** Hydrogen coordinates ( x $10^4$) and isotropic displacement parameters ($Å^2$x $10^3$) for **ethylene-ketal III-8**.

| | x | y | z | U(eq) |
|---|---|---|---|---|
| H(2A) | 9521 | 7655 | 2252 | 37 |
| H(3A) | 7753 | 6574 | 1985 | 40 |
| H(3B) | 8382 | 6234 | 2793 | 40 |
| H(6A) | 5015 | 10184 | 2407 | 43 |
| H(9A) | 7388 | 6467 | 3693 | 40 |
| H(10A) | 4063 | 10481 | 3336 | 71 |
| H(10B) | 4805 | 10347 | 4129 | 71 |
| H(10C) | 4012 | 8892 | 3817 | 71 |
| H(11A) | 6593 | 6650 | 4719 | 68 |
| H(11B) | 5315 | 6958 | 4538 | 68 |
| H(11C) | 6122 | 8409 | 4834 | 68 |
| H(12A) | 7504 | 11039 | 1181 | 41 |
| H(13A) | 5928 | 10305 | 1468 | 47 |
| H(13B) | 6498 | 8660 | 1302 | 47 |
| H(14A) | 9758 | 8523 | 3411 | 38 |
| H(14B) | 9967 | 10008 | 2915 | 38 |
| H(17A) | 6811 | 13143 | 3166 | 44 |
| H(20A) | 9221 | 9437 | 4406 | 40 |
| H(21A) | 6128 | 13823 | 4181 | 80 |
| H(21B) | 6994 | 13764 | 4927 | 80 |
| H(21C) | 6118 | 12349 | 4734 | 80 |
| H(22A) | 8732 | 9991 | 5514 | 71 |
| H(22B) | 7478 | 10423 | 5440 | 71 |
| H(22C) | 8369 | 11822 | 5607 | 71 |
| H(23A) | 8519 | 12394 | 2159 | 44 |
| H(23B) | 7256 | 12678 | 2094 | 44 |
| H(24A) | 10575 | 9131 | 1179 | 79 |
| H(24B) | 10052 | 10618 | 679 | 79 |
| H(25A) | 8719 | 9199 | 158 | 79 |
| H(25B) | 9430 | 7663 | 485 | 79 |

**Table 6.** Torsion angles [°] for **ethylene-ketal III-8**.

| | |
|---|---|
| O(2)-C(1)-C(2)-C(14) | 167.86(12) |
| O(1)-C(1)-C(2)-C(14) | 53.31(16) |
| C(12)-C(1)-C(2)-C(14) | -68.95(17) |
| O(2)-C(1)-C(2)-C(3) | -59.22(15) |
| O(1)-C(1)-C(2)-C(3) | -173.77(11) |
| C(12)-C(1)-C(2)-C(3) | 63.97(17) |
| C(1)-C(2)-C(3)-C(4) | -76.99(17) |
| C(14)-C(2)-C(3)-C(4) | 55.34(18) |
| C(2)-C(3)-C(4)-C(9) | -113.94(16) |
| C(2)-C(3)-C(4)-C(5) | 63.0(2) |
| C(9)-C(4)-C(5)-C(6) | -1.6(2) |
| C(3)-C(4)-C(5)-C(6) | -178.59(14) |
| C(9)-C(4)-C(5)-C(13) | 175.01(14) |
| C(3)-C(4)-C(5)-C(13) | -2.0(2) |
| C(4)-C(5)-C(6)-C(7) | 2.9(2) |
| C(13)-C(5)-C(6)-C(7) | -173.78(15) |
| C(5)-C(6)-C(7)-C(8) | -1.4(2) |
| C(5)-C(6)-C(7)-C(10) | 175.46(15) |
| C(6)-C(7)-C(8)-C(9) | -1.4(2) |
| C(10)-C(7)-C(8)-C(9) | -178.21(15) |
| C(6)-C(7)-C(8)-C(11) | 175.27(15) |
| C(10)-C(7)-C(8)-C(11) | -1.5(2) |
| C(5)-C(4)-C(9)-C(8) | -1.2(2) |
| C(3)-C(4)-C(9)-C(8) | 175.83(14) |
| C(7)-C(8)-C(9)-C(4) | 2.7(2) |
| C(11)-C(8)-C(9)-C(4) | -173.95(15) |
| O(2)-C(1)-C(12)-C(23) | -168.94(12) |
| O(1)-C(1)-C(12)-C(23) | -54.95(16) |
| C(2)-C(1)-C(12)-C(23) | 67.88(17) |
| O(2)-C(1)-C(12)-C(13) | 57.93(16) |
| O(1)-C(1)-C(12)-C(13) | 171.92(11) |
| C(2)-C(1)-C(12)-C(13) | -65.26(17) |
| C(6)-C(5)-C(13)-C(12) | 116.23(17) |
| C(4)-C(5)-C(13)-C(12) | -60.4(2) |
| C(1)-C(12)-C(13)-C(5) | 78.17(18) |
| C(23)-C(12)-C(13)-C(5) | -53.8(2) |
| C(1)-C(2)-C(14)-C(15) | 71.87(17) |
| C(3)-C(2)-C(14)-C(15) | -60.09(18) |
| C(2)-C(14)-C(15)-C(20) | 129.68(15) |
| C(2)-C(14)-C(15)-C(16) | -51.2(2) |
| C(20)-C(15)-C(16)-C(17) | -2.0(2) |
| C(14)-C(15)-C(16)-C(17) | 178.96(14) |
| C(20)-C(15)-C(16)-C(23) | 176.83(14) |
| C(14)-C(15)-C(16)-C(23) | -2.3(2) |

| | |
|---|---|
| C(15)-C(16)-C(17)-C(18) | 0.7(2) |
| C(23)-C(16)-C(17)-C(18) | -178.17(15) |
| C(16)-C(17)-C(18)-C(19) | 1.2(2) |
| C(16)-C(17)-C(18)-C(21) | -176.45(17) |
| C(17)-C(18)-C(19)-C(20) | -1.7(2) |
| C(21)-C(18)-C(19)-C(20) | 175.91(16) |
| C(17)-C(18)-C(19)-C(22) | -179.66(16) |
| C(21)-C(18)-C(19)-C(22) | -2.0(3) |
| C(18)-C(19)-C(20)-C(15) | 0.4(2) |
| C(22)-C(19)-C(20)-C(15) | 178.38(15) |
| C(16)-C(15)-C(20)-C(19) | 1.5(2) |
| C(14)-C(15)-C(20)-C(19) | -179.41(14) |
| C(17)-C(16)-C(23)-C(12) | -126.45(16) |
| C(15)-C(16)-C(23)-C(12) | 54.8(2) |
| C(1)-C(12)-C(23)-C(16) | -71.80(18) |
| C(13)-C(12)-C(23)-C(16) | 60.3(2) |
| O(1)-C(24)-C(25)-O(2) | -15.7(3) |
| C(25)-C(24)-O(1)-C(1) | 15.8(3) |
| O(2)-C(1)-O(1)-C(24) | -10.17(19) |
| C(12)-C(1)-O(1)-C(24) | -126.11(17) |
| C(2)-C(1)-O(1)-C(24) | 106.29(17) |
| C(24)-C(25)-O(2)-C(1) | 9.4(3) |
| O(1)-C(1)-O(2)-C(25) | 0.4(2) |
| C(12)-C(1)-O(2)-C(25) | 115.73(18) |
| C(2)-C(1)-O(2)-C(25) | -116.27(17) |

## C.2. Sulfone-ketal III-10

A suitable crystal of **sulfone-ketal III-10** was coated with Paratone N oil, suspended in a small fiber loop and placed in a cooled nitrogen gas stream at 173 K on a Bruker D8 SMART APEX CCD sealed tube diffractometer with graphite monochromated MoKα (0.71073Å) radiation. Data was measured using a series of combinations of phi and omega scans with 10 s frame exposures and 0.3º frame widths. Data collection, indexing and initial cell refinements were all carried out using

SMART[3] software. Frame integration and final cell refinements were done using SAINT[4] software. The final cell parameters were determined from least-squares refinement on 3398 reflections. The SADABS[5] program was used to carry out absorption corrections. The structure was solved using Direct methods and difference Fourier techniques (SHELXTL, V6.12).[6] Hydrogen atoms were placed in their expected chemical positions using the HIX command and were included in the final cycles of least-squares with isotropic Uij's related to the riding atom. The C-H distances were fixed at 0.93 Å (aromatic), 0.98 (methane), 0.97 Å ($CH_2$), or 0.96 Å ($CH_3$). All non-hydrogen atoms were refined anisotropically. Scattering factors and anomalous dispersion corrections are taken from the *International Tables for x-ray Crystallography*.[7] Structure solution, refinement, graphics and generation of publication materials were performed using SHELXTL, V6.12 software. Additional details of data collection and structure refinement are given in Tables T1-T6. The crystals were all intimately twinned to some degree so data was collected on one clean sample that contained approximately equal contributions of the two components. The unit cells for each component were determined by using a beta test program written by George Sheldrick called Cell_Now. The reflection data was processed with SAINT, taking into account the overlapping of reflections from the two components and were corrected for absorption effects S9 by using TWINABS, a version of SADABS. The structure was solved using only the data that was generated by component 1, however the final refinements used all the data and included the contributions from both components.

**Table 1.** Crystal data and structure refinement for **sulfone-ketal III-10**.

| | | |
|---|---|---|
| Identification code | sj_s | |
| Empirical formula | C25 H30 O4 S2 | |
| Formula weight | 458.61 | |
| Temperature | 173(2) K | |
| Wavelength | 1.54178 Å | |
| Crystal system | Monoclinic | |
| Space group | P2(1)/n | |
| Unit cell dimensions | a = 24.360(4) Å | α = 90°. |
| | b = 11.319(3) Å | β = 106.799(13)°. |
| | c = 24.615(5) Å | γ = 90°. |
| Volume | 6498(2) $Å^3$ | |
| Z | 12 | |
| Density (calculated) | 1.406 $Mg/m^3$ | |
| Absorption coefficient | 2.479 $mm^{-1}$ | |
| F(000) | 2928 | |
| Crystal size | 0.28 x 0.08 x 0.02 $mm^3$ | |
| Theta range for data collection | 3.03 to 60.01°. | |
| Index ranges | -27<=h<=24, -12<=k<=10, -19<=l<=27 | |
| Reflections collected | 26097 | |
| Independent reflections | 9241 [R(int) = 0.2760] | |
| Completeness to theta = 60.01° | 95.6 % | |
| Absorption correction | Semi-empirical from equivalents | |
| Refinement method | Full-matrix least-squares on $F^2$ | |
| Data / restraints / parameters | 9241 / 0 / 838 | |
| Goodness-of-fit on $F^2$ | 1.006 | |
| Final R indices [I>2sigma(I)] | R1 = 0.0971, wR2 = 0.1817 | |
| R indices (all data) | R1 = 0.3069, wR2 = 0.2561 | |
| Largest diff. peak and hole | 0.300 and -0.312 $e.Å^{-3}$ | |

**Table 2.** Atomic coordinates ( x $10^4$) and equivalent isotropic displacement parameters ($Å^2$x $10^3$) for **sulfone-ketal III-10**. U(eq) is defined as one third of the trace of the orthogonalized $U^{ij}$ tensor.

| | x | y | z | U(eq) |
|---|---|---|---|---|
| C(1) | 4587(5) | 9181(9) | 1420(5) | 61(3) |
| C(2) | 4349(5) | 10009(10) | 1801(5) | 69(3) |
| C(3) | 4059(5) | 9467(11) | 2197(6) | 82(4) |
| C(4) | 4393(6) | 8753(12) | 2700(6) | 73(4) |
| C(5) | 4321(6) | 8990(13) | 3237(7) | 97(5) |
| C(6) | 4636(8) | 8449(16) | 3743(7) | 96(5) |
| C(7) | 5025(8) | 7572(15) | 3713(7) | 96(5) |
| C(8) | 5069(6) | 7304(12) | 3171(7) | 93(4) |
| C(9) | 4776(5) | 7835(12) | 2671(6) | 74(4) |
| C(10) | 4851(5) | 7442(10) | 2123(5) | 69(4) |
| C(11) | 5053(5) | 8290(10) | 1733(5) | 68(3) |
| C(12) | 5618(5) | 8959(10) | 2021(6) | 72(4) |
| C(13) | 5663(6) | 9546(12) | 2578(6) | 77(4) |
| C(14) | 6118(6) | 9229(12) | 3059(7) | 93(4) |
| C(15) | 6180(8) | 9703(15) | 3596(8) | 107(5) |
| C(16) | 5820(8) | 10560(16) | 3656(7) | 101(5) |
| C(17) | 5380(6) | 10947(12) | 3192(7) | 95(5) |
| C(18) | 5308(6) | 10484(12) | 2636(6) | 74(4) |
| C(19) | 4819(6) | 10886(10) | 2158(6) | 87(4) |
| C(20) | 3684(6) | 9374(12) | 427(6) | 101(5) |
| C(21) | 4100(5) | 10235(12) | 352(6) | 99(5) |
| C(22) | 4568(7) | 8816(13) | 4298(6) | 127(6) |
| C(23) | 5415(7) | 6957(15) | 4234(7) | 154(7) |
| C(24) | 5832(7) | 11082(15) | 4218(7) | 140(6) |
| C(25) | 6645(6) | 9250(16) | 4108(7) | 149(7) |
| C(1B) | 1104(5) | 1045(10) | 6424(5) | 64(3) |
| C(2B) | 962(6) | 1910(11) | 6867(5) | 78(4) |
| C(3B) | 729(5) | 1339(10) | 7306(5) | 72(4) |
| C(4B) | 1100(5) | 604(11) | 7781(6) | 69(4) |
| C(5B) | 1102(6) | 830(13) | 8333(6) | 84(4) |
| C(6B) | 1457(7) | 272(13) | 8793(7) | 90(4) |
| C(7B) | 1825(6) | -585(13) | 8713(7) | 86(4) |
| C(8B) | 1825(6) | -897(12) | 8160(7) | 88(4) |
| C(9B) | 1489(5) | -311(12) | 7699(6) | 75(4) |
| C(10B) | 1504(5) | -686(10) | 7121(6) | 79(4) |
| C(11B) | 1612(5) | 198(10) | 6675(5) | 72(4) |
| C(12B) | 2174(5) | 902(10) | 6887(6) | 83(4) |
| C(13B) | 2316(5) | 1482(10) | 7456(6) | 66(3) |
| C(14B) | 2779(5) | 1123(11) | 7893(6) | 75(4) |
| C(15B) | 2919(6) | 1573(13) | 8450(7) | 89(4) |

| | | | | |
|---|---|---|---|---|
| C(16B) | 2560(6) | 2477(13) | 8576(6) | 85(4) |
| C(17B) | 2093(6) | 2833(12) | 8120(7) | 91(4) |
| C(18B) | 1954(5) | 2356(11) | 7564(6) | 77(4) |
| C(19B) | 1433(5) | 2796(10) | 7110(6) | 84(4) |
| C(20B) | 59(5) | 1197(10) | 5620(5) | 83(4) |
| C(21B) | 455(5) | 1837(11) | 5337(6) | 85(4) |
| C(22B) | 1466(6) | 638(13) | 9387(6) | 111(5) |
| C(23B) | 2245(6) | -1128(14) | 9218(6) | 119(5) |
| C(24B) | 2661(5) | 3005(13) | 9140(6) | 108(5) |
| C(25B) | 3428(5) | 1145(13) | 8910(6) | 110(5) |
| C(1C) | 3133(5) | 4204(10) | 1412(6) | 74(4) |
| C(2C) | 2830(5) | 3407(10) | 1726(5) | 74(4) |
| C(3C) | 3230(5) | 2440(10) | 2092(6) | 82(4) |
| C(4C) | 3639(6) | 2855(11) | 2637(6) | 72(4) |
| C(5C) | 3647(6) | 2249(13) | 3135(7) | 96(5) |
| C(6C) | 3998(6) | 2593(14) | 3690(6) | 94(5) |
| C(7C) | 4404(6) | 3502(13) | 3714(6) | 82(4) |
| C(8C) | 4419(6) | 4015(12) | 3216(7) | 97(5) |
| C(9C) | 4042(6) | 3771(12) | 2690(6) | 80(4) |
| C(10C) | 4116(5) | 4453(11) | 2195(6) | 92(5) |
| C(11C) | 3580(5) | 5075(11) | 1802(6) | 79(4) |
| C(12C) | 3315(6) | 5976(10) | 2109(6) | 81(4) |
| C(13C) | 3123(6) | 5578(12) | 2610(7) | 80(4) |
| C(14C) | 3363(6) | 6112(11) | 3150(7) | 80(4) |
| C(15C) | 3236(7) | 5814(13) | 3621(7) | 88(4) |
| C(16C) | 2839(6) | 4894(13) | 3618(7) | 84(4) |
| C(17C) | 2602(6) | 4381(11) | 3082(8) | 88(5) |
| C(18C) | 2725(6) | 4679(12) | 2575(6) | 75(4) |
| C(19C) | 2453(5) | 4044(11) | 2043(6) | 83(4) |
| C(20C) | 2940(6) | 5190(14) | 311(7) | 127(6) |
| C(21C) | 3503(7) | 4453(12) | 467(6) | 111(5) |
| C(22C) | 3941(6) | 1941(14) | 4195(6) | 123(6) |
| C(23C) | 4772(7) | 3837(13) | 4273(6) | 128(6) |
| C(24C) | 2671(6) | 4524(14) | 4101(6) | 120(6) |
| C(25C) | 3494(6) | 6418(14) | 4178(6) | 117(5) |
| O(1) | 5064(4) | 11035(7) | 1025(4) | 97(3) |
| O(2) | 5091(3) | 9101(7) | 602(4) | 85(3) |
| O(3) | 4211(4) | 7341(7) | 722(4) | 93(3) |
| O(4) | 3560(5) | 7927(8) | 1231(5) | 127(4) |
| O(1B) | 1525(4) | 1049(7) | 5540(4) | 99(3) |
| O(2B) | 1359(3) | 3002(7) | 5895(4) | 97(3) |
| O(3B) | 667(4) | -716(7) | 5705(4) | 95(3) |
| O(4B) | 140(4) | -357(7) | 6420(4) | 105(3) |
| O(1C) | 2457(4) | 6163(9) | 1018(5) | 130(4) |
| O(2C) | 2106(4) | 4233(8) | 626(4) | 118(4) |
| O(3C) | 4042(4) | 2918(8) | 1217(5) | 121(4) |

| | | | | |
|---|---|---|---|---|
| O(4C) | 3060(4) | 2451(8) | 661(4) | 109(3) |
| S(1) | 4788(2) | 9929(3) | 846(2) | 76(1) |
| S(2) | 3963(2) | 8286(3) | 955(2) | 84(1) |
| S(1B) | 1184(2) | 1801(3) | 5787(2) | 78(1) |
| S(2B) | 466(2) | 94(3) | 6055(2) | 85(1) |
| S(1C) | 2577(2) | 5021(4) | 843(2) | 90(1) |
| S(2C) | 3461(2) | 3341(3) | 942(2) | 89(1) |

**Table 3.** Bond lengths [Å] and angles [°] for **sulfone-ketal III-10**.

| | | | |
|---|---|---|---|
| C(1)-C(11) | 1.547(14) | C(16)-C(17) | 1.392(18) |
| C(1)-C(2) | 1.551(15) | C(16)-C(24) | 1.497(19) |
| C(1)-S(1) | 1.832(12) | C(17)-C(18) | 1.429(17) |
| C(1)-S(2) | 1.908(11) | C(17)-H(17A) | 0.9500 |
| C(2)-C(3) | 1.492(15) | C(18)-C(19) | 1.483(16) |
| C(2)-C(19) | 1.576(15) | C(19)-H(19A) | 0.9900 |
| C(2)-H(2A) | 1.0000 | C(19)-H(19B) | 0.9900 |
| C(3)-C(4) | 1.505(16) | C(20)-C(21) | 1.455(15) |
| C(3)-H(3A) | 0.9900 | C(20)-S(2) | 1.778(13) |
| C(3)-H(3B) | 0.9900 | C(20)-H(20A) | 0.9900 |
| C(4)-C(5) | 1.408(17) | C(20)-H(20B) | 0.9900 |
| C(4)-C(9) | 1.412(16) | C(21)-S(1) | 1.798(12) |
| C(5)-C(6) | 1.401(18) | C(21)-H(21A) | 0.9900 |
| C(5)-H(5A) | 0.9500 | C(21)-H(21B) | 0.9900 |
| C(6)-C(7) | 1.389(19) | C(22)-H(22A) | 0.9800 |
| C(6)-C(22) | 1.482(18) | C(22)-H(22B) | 0.9800 |
| C(7)-C(8) | 1.402(19) | C(22)-H(22C) | 0.9800 |
| C(7)-C(23) | 1.525(19) | C(23)-H(23A) | 0.9800 |
| C(8)-C(9) | 1.371(16) | C(23)-H(23B) | 0.9800 |
| C(8)-H(8A) | 0.9500 | C(23)-H(23C) | 0.9800 |
| C(9)-C(10) | 1.481(17) | C(24)-H(24A) | 0.9800 |
| C(10)-C(11) | 1.536(15) | C(24)-H(24B) | 0.9800 |
| C(10)-H(10A) | 0.9900 | C(24)-H(24C) | 0.9800 |
| C(10)-H(10B) | 0.9900 | C(25)-H(25A) | 0.9800 |
| C(11)-C(12) | 1.552(14) | C(25)-H(25B) | 0.9800 |
| C(11)-H(11A) | 1.0000 | C(25)-H(25C) | 0.9800 |
| C(12)-C(13) | 1.498(17) | C(1B)-C(11B) | 1.546(14) |
| C(12)-H(12A) | 0.9900 | C(1B)-C(2B) | 1.576(15) |
| C(12)-H(12B) | 0.9900 | C(1B)-S(1B) | 1.845(12) |
| C(13)-C(18) | 1.403(17) | C(1B)-S(2B) | 1.893(11) |
| C(13)-C(14) | 1.415(17) | C(2B)-C(3B) | 1.505(15) |
| C(14)-C(15) | 1.393(19) | C(2B)-C(19B) | 1.511(15) |
| C(14)-H(14A) | 0.9500 | C(2B)-H(2BA) | 1.0000 |
| C(15)-C(16) | 1.34(2) | C(3B)-C(4B) | 1.505(15) |
| C(15)-C(25) | 1.520(19) | C(3B)-H(3B1) | 0.9900 |

| | | | |
|---|---|---|---|
| C(3B)-H(3B2) | 0.9900 | C(24B)-H(24D) | 0.9800 |
| C(4B)-C(5B) | 1.381(16) | C(24B)-H(24E) | 0.9800 |
| C(4B)-C(9B) | 1.456(16) | C(24B)-H(24F) | 0.9800 |
| C(5B)-C(6B) | 1.366(17) | C(25B)-H(25D) | 0.9800 |
| C(5B)-H(5BA) | 0.9500 | C(25B)-H(25E) | 0.9800 |
| C(6B)-C(7B) | 1.372(17) | C(25B)-H(25F) | 0.9800 |
| C(6B)-C(22B) | 1.514(18) | C(1C)-C(2C) | 1.512(16) |
| C(7B)-C(8B) | 1.405(18) | C(1C)-C(11C) | 1.575(15) |
| C(7B)-C(23B) | 1.496(17) | C(1C)-S(2C) | 1.862(13) |
| C(8B)-C(9B) | 1.365(16) | C(1C)-S(1C) | 1.885(12) |
| C(8B)-H(8BA) | 0.9500 | C(2C)-C(19C) | 1.544(16) |
| C(9B)-C(10B) | 1.495(16) | C(2C)-C(3C) | 1.567(15) |
| C(10B)-C(11B) | 1.565(16) | C(2C)-H(2CA) | 1.0000 |
| C(10B)-H(10C) | 0.9900 | C(3C)-C(4C) | 1.497(16) |
| C(10B)-H(10D) | 0.9900 | C(3C)-H(3C1) | 0.9900 |
| C(11B)-C(12B) | 1.539(15) | C(3C)-H(3C2) | 0.9900 |
| C(11B)-H(11B) | 1.0000 | C(4C)-C(5C) | 1.400(17) |
| C(12B)-C(13B) | 1.495(15) | C(4C)-C(9C) | 1.407(16) |
| C(12B)-H(12C) | 0.9900 | C(5C)-C(6C) | 1.439(18) |
| C(12B)-H(12D) | 0.9900 | C(5C)-H(5CA) | 0.9500 |
| C(13B)-C(14B) | 1.375(15) | C(6C)-C(7C) | 1.417(17) |
| C(13B)-C(18B) | 1.400(16) | C(6C)-C(22C) | 1.488(17) |
| C(14B)-C(15B) | 1.410(17) | C(7C)-C(8C) | 1.368(17) |
| C(14B)-H(14B) | 0.9500 | C(7C)-C(23C) | 1.458(17) |
| C(15B)-C(16B) | 1.436(18) | C(8C)-C(9C) | 1.381(17) |
| C(15B)-C(25B) | 1.498(17) | C(8C)-H(8CA) | 0.9500 |
| C(16B)-C(17B) | 1.407(17) | C(9C)-C(10C) | 1.496(17) |
| C(16B)-C(24B) | 1.466(17) | C(10C)-C(11C) | 1.551(15) |
| C(17B)-C(18B) | 1.418(17) | C(10C)-H(10E) | 0.9900 |
| C(17B)-H(17B) | 0.9500 | C(10C)-H(10F) | 0.9900 |
| C(18B)-C(19B) | 1.512(16) | C(11C)-C(12C) | 1.520(16) |
| C(19B)-H(19C) | 0.9900 | C(11C)-H(11C) | 1.0000 |
| C(19B)-H(19D) | 0.9900 | C(12C)-C(13C) | 1.509(17) |
| C(20B)-C(21B) | 1.527(16) | C(12C)-H(12E) | 0.9900 |
| C(20B)-S(2B) | 1.753(11) | C(12C)-H(12F) | 0.9900 |
| C(20B)-H(20C) | 0.9900 | C(13C)-C(18C) | 1.391(17) |
| C(20B)-H(20D) | 0.9900 | C(13C)-C(14C) | 1.421(17) |
| C(21B)-S(1B) | 1.803(11) | C(14C)-C(15C) | 1.328(18) |
| C(21B)-H(21C) | 0.9900 | C(14C)-H(14C) | 0.9500 |
| C(21B)-H(21D) | 0.9900 | C(15C)-C(16C) | 1.420(18) |
| C(22B)-H(22D) | 0.9800 | C(15C)-C(25C) | 1.498(18) |
| C(22B)-H(22E) | 0.9800 | C(16C)-C(17C) | 1.404(17) |
| C(22B)-H(22F) | 0.9800 | C(16C)-C(24C) | 1.427(18) |
| C(23B)-H(23D) | 0.9800 | C(17C)-C(18C) | 1.405(17) |
| C(23B)-H(23E) | 0.9800 | C(17C)-H(17C) | 0.9500 |
| C(23B)-H(23F) | 0.9800 | C(18C)-C(19C) | 1.474(16) |

| | |
|---|---|
| C(19C)-H(19E) | 0.9900 |
| C(19C)-H(19F) | 0.9900 |
| C(20C)-C(21C) | 1.556(17) |
| C(20C)-S(1C) | 1.789(16) |
| C(20C)-H(20E) | 0.9900 |
| C(20C)-H(20F) | 0.9900 |
| C(21C)-S(2C) | 1.740(13) |
| C(21C)-H(21E) | 0.9900 |
| C(21C)-H(21F) | 0.9900 |
| C(22C)-H(22G) | 0.9800 |
| C(22C)-H(22H) | 0.9800 |
| C(22C)-H(22I) | 0.9800 |
| C(23C)-H(23G) | 0.9800 |
| C(23C)-H(23H) | 0.9800 |
| C(23C)-H(23I) | 0.9800 |
| C(24C)-H(24G) | 0.9800 |
| C(24C)-H(24H) | 0.9800 |
| C(24C)-H(24I) | 0.9800 |
| C(25C)-H(25G) | 0.9800 |
| C(25C)-H(25H) | 0.9800 |
| C(25C)-H(25I) | 0.9800 |
| O(1)-S(1) | 1.428(8) |
| O(2)-S(1) | 1.430(8) |
| O(3)-S(2) | 1.426(9) |
| O(4)-S(2) | 1.406(10) |
| O(1B)-S(1B) | 1.440(8) |
| O(2B)-S(1B) | 1.427(8) |
| O(3B)-S(2B) | 1.439(9) |
| O(4B)-S(2B) | 1.452(9) |
| O(1C)-S(1C) | 1.419(9) |
| O(2C)-S(1C) | 1.429(8) |
| O(3C)-S(2C) | 1.463(9) |
| O(4C)-S(2C) | 1.435(9) |

| | |
|---|---|
| C(11)-C(1)-C(2) | 116.2(11) |
| C(11)-C(1)-S(1) | 111.3(8) |
| C(2)-C(1)-S(1) | 114.6(7) |
| C(11)-C(1)-S(2) | 107.1(7) |
| C(2)-C(1)-S(2) | 108.2(8) |
| S(1)-C(1)-S(2) | 97.3(6) |
| C(3)-C(2)-C(1) | 118.5(10) |
| C(3)-C(2)-C(19) | 107.4(11) |
| C(1)-C(2)-C(19) | 112.3(10) |
| C(3)-C(2)-H(2A) | 105.9 |
| C(1)-C(2)-H(2A) | 105.9 |
| C(19)-C(2)-H(2A) | 105.9 |
| C(2)-C(3)-C(4) | 120.8(11) |
| C(2)-C(3)-H(3A) | 107.1 |
| C(4)-C(3)-H(3A) | 107.1 |
| C(2)-C(3)-H(3B) | 107.1 |
| C(4)-C(3)-H(3B) | 107.1 |
| H(3A)-C(3)-H(3B) | 106.8 |
| C(5)-C(4)-C(9) | 116.8(14) |
| C(5)-C(4)-C(3) | 119.0(14) |
| C(9)-C(4)-C(3) | 124.1(13) |
| C(6)-C(5)-C(4) | 124.5(15) |
| C(6)-C(5)-H(5A) | 117.7 |
| C(4)-C(5)-H(5A) | 117.7 |
| C(7)-C(6)-C(5) | 118.1(15) |
| C(7)-C(6)-C(22) | 120.7(17) |
| C(5)-C(6)-C(22) | 121.2(18) |
| C(6)-C(7)-C(8) | 116.5(16) |
| C(6)-C(7)-C(23) | 123.3(16) |
| C(8)-C(7)-C(23) | 120.1(18) |
| C(9)-C(8)-C(7) | 126.6(16) |
| C(9)-C(8)-H(8A) | 116.7 |
| C(7)-C(8)-H(8A) | 116.7 |
| C(8)-C(9)-C(4) | 117.1(14) |
| C(8)-C(9)-C(10) | 121.1(14) |
| C(4)-C(9)-C(10) | 121.7(13) |
| C(9)-C(10)-C(11) | 121.8(10) |
| C(9)-C(10)-H(10A) | 106.9 |
| C(11)-C(10)-H(10A) | 106.9 |
| C(9)-C(10)-H(10B) | 106.9 |
| C(11)-C(10)-H(10B) | 106.9 |
| H(10A)-C(10)-H(10B) | 106.7 |
| C(10)-C(11)-C(1) | 113.4(10) |
| C(10)-C(11)-C(12) | 114.9(10) |
| C(1)-C(11)-C(12) | 109.7(9) |
| C(10)-C(11)-H(11A) | 106.1 |
| C(1)-C(11)-H(11A) | 106.1 |
| C(12)-C(11)-H(11A) | 106.1 |
| C(13)-C(12)-C(11) | 117.1(11) |
| C(13)-C(12)-H(12A) | 108.0 |
| C(11)-C(12)-H(12A) | 108.0 |
| C(13)-C(12)-H(12B) | 108.0 |
| C(11)-C(12)-H(12B) | 108.0 |
| H(12A)-C(12)-H(12B) | 107.3 |
| C(18)-C(13)-C(14) | 117.6(14) |
| C(18)-C(13)-C(12) | 123.0(12) |
| C(14)-C(13)-C(12) | 119.1(15) |
| C(15)-C(14)-C(13) | 122.8(15) |

| | | | |
|---|---|---|---|
| C(15)-C(14)-H(14A) | 118.6 | H(24A)-C(24)-H(24B) | 109.5 |
| C(13)-C(14)-H(14A) | 118.6 | C(16)-C(24)-H(24C) | 109.5 |
| C(16)-C(15)-C(14) | 119.1(16) | H(24A)-C(24)-H(24C) | 109.5 |
| C(16)-C(15)-C(25) | 120.4(18) | H(24B)-C(24)-H(24C) | 109.5 |
| C(14)-C(15)-C(25) | 120.5(18) | C(15)-C(25)-H(25A) | 109.5 |
| C(15)-C(16)-C(17) | 120.7(17) | C(15)-C(25)-H(25B) | 109.5 |
| C(15)-C(16)-C(24) | 123.2(16) | H(25A)-C(25)-H(25B) | 109.5 |
| C(17)-C(16)-C(24) | 115.9(18) | C(15)-C(25)-H(25C) | 109.5 |
| C(16)-C(17)-C(18) | 121.5(15) | H(25A)-C(25)-H(25C) | 109.5 |
| C(16)-C(17)-H(17A) | 119.3 | H(25B)-C(25)-H(25C) | 109.5 |
| C(18)-C(17)-H(17A) | 119.3 | C(11B)-C(1B)-C(2B) | 114.8(10) |
| C(13)-C(18)-C(17) | 117.8(13) | C(11B)-C(1B)-S(1B) | 111.0(9) |
| C(13)-C(18)-C(19) | 121.9(13) | C(2B)-C(1B)-S(1B) | 113.4(8) |
| C(17)-C(18)-C(19) | 119.7(14) | C(11B)-C(1B)-S(2B) | 106.9(8) |
| C(18)-C(19)-C(2) | 122.5(10) | C(2B)-C(1B)-S(2B) | 111.7(8) |
| C(18)-C(19)-H(19A) | 106.7 | S(1B)-C(1B)-S(2B) | 97.5(5) |
| C(2)-C(19)-H(19A) | 106.7 | C(3B)-C(2B)-C(19B) | 113.7(12) |
| C(18)-C(19)-H(19B) | 106.7 | C(3B)-C(2B)-C(1B) | 115.7(10) |
| C(2)-C(19)-H(19B) | 106.7 | C(19B)-C(2B)-C(1B) | 113.2(11) |
| H(19A)-C(19)-H(19B) | 106.6 | C(3B)-C(2B)-H(2BA) | 104.2 |
| C(21)-C(20)-S(2) | 115.1(9) | C(19B)-C(2B)-H(2BA) | 104.2 |
| C(21)-C(20)-H(20A) | 108.5 | C(1B)-C(2B)-H(2BA) | 104.2 |
| S(2)-C(20)-H(20A) | 108.5 | C(4B)-C(3B)-C(2B) | 122.0(11) |
| C(21)-C(20)-H(20B) | 108.5 | C(4B)-C(3B)-H(3B1) | 106.8 |
| S(2)-C(20)-H(20B) | 108.5 | C(2B)-C(3B)-H(3B1) | 106.8 |
| H(20A)-C(20)-H(20B) | 107.5 | C(4B)-C(3B)-H(3B2) | 106.8 |
| C(20)-C(21)-S(1) | 109.4(9) | C(2B)-C(3B)-H(3B2) | 106.8 |
| C(20)-C(21)-H(21A) | 109.8 | H(3B1)-C(3B)-H(3B2) | 106.7 |
| S(1)-C(21)-H(21A) | 109.8 | C(5B)-C(4B)-C(9B) | 116.7(12) |
| C(20)-C(21)-H(21B) | 109.8 | C(5B)-C(4B)-C(3B) | 119.6(13) |
| S(1)-C(21)-H(21B) | 109.8 | C(9B)-C(4B)-C(3B) | 123.6(12) |
| H(21A)-C(21)-H(21B) | 108.2 | C(6B)-C(5B)-C(4B) | 123.5(15) |
| C(6)-C(22)-H(22A) | 109.5 | C(6B)-C(5B)-H(5BA) | 118.3 |
| C(6)-C(22)-H(22B) | 109.5 | C(4B)-C(5B)-H(5BA) | 118.3 |
| H(22A)-C(22)-H(22B) | 109.5 | C(5B)-C(6B)-C(7B) | 119.5(16) |
| C(6)-C(22)-H(22C) | 109.5 | C(5B)-C(6B)-C(22B) | 120.2(15) |
| H(22A)-C(22)-H(22C) | 109.5 | C(7B)-C(6B)-C(22B) | 120.3(15) |
| H(22B)-C(22)-H(22C) | 109.5 | C(6B)-C(7B)-C(8B) | 120.0(13) |
| C(7)-C(23)-H(23A) | 109.5 | C(6B)-C(7B)-C(23B) | 119.3(16) |
| C(7)-C(23)-H(23B) | 109.5 | C(8B)-C(7B)-C(23B) | 120.6(15) |
| H(23A)-C(23)-H(23B) | 109.5 | C(9B)-C(8B)-C(7B) | 121.0(14) |
| C(7)-C(23)-H(23C) | 109.5 | C(9B)-C(8B)-H(8BA) | 119.5 |
| H(23A)-C(23)-H(23C) | 109.5 | C(7B)-C(8B)-H(8BA) | 119.5 |
| H(23B)-C(23)-H(23C) | 109.5 | C(8B)-C(9B)-C(4B) | 119.3(13) |
| C(16)-C(24)-H(24A) | 109.5 | C(8B)-C(9B)-C(10B) | 118.6(13) |
| C(16)-C(24)-H(24B) | 109.5 | C(4B)-C(9B)-C(10B) | 122.0(12) |

| | | | |
|---|---|---|---|
| C(9B)-C(10B)-C(11B) | 122.9(11) | S(2B)-C(20B)-H(20D) | 110.3 |
| C(9B)-C(10B)-H(10C) | 106.6 | H(20C)-C(20B)-H(20D) | 108.5 |
| C(11B)-C(10B)-H(10C) | 106.6 | C(20B)-C(21B)-S(1B) | 110.4(9) |
| C(9B)-C(10B)-H(10D) | 106.6 | C(20B)-C(21B)-H(21C) | 109.6 |
| C(11B)-C(10B)-H(10D) | 106.6 | S(1B)-C(21B)-H(21C) | 109.6 |
| H(10C)-C(10B)-H(10D) | 106.6 | C(20B)-C(21B)-H(21D) | 109.6 |
| C(12B)-C(11B)-C(1B) | 110.2(9) | S(1B)-C(21B)-H(21D) | 109.6 |
| C(12B)-C(11B)-C(10B) | 114.0(11) | H(21C)-C(21B)-H(21D) | 108.1 |
| C(1B)-C(11B)-C(10B) | 113.5(10) | C(6B)-C(22B)-H(22D) | 109.5 |
| C(12B)-C(11B)-H(11B) | 106.2 | C(6B)-C(22B)-H(22E) | 109.5 |
| C(1B)-C(11B)-H(11B) | 106.2 | H(22D)-C(22B)-H(22E) | 109.5 |
| C(10B)-C(11B)-H(11B) | 106.2 | C(6B)-C(22B)-H(22F) | 109.5 |
| C(13B)-C(12B)-C(11B) | 119.2(11) | H(22D)-C(22B)-H(22F) | 109.5 |
| C(13B)-C(12B)-H(12C) | 107.5 | H(22E)-C(22B)-H(22F) | 109.5 |
| C(11B)-C(12B)-H(12C) | 107.5 | C(7B)-C(23B)-H(23D) | 109.5 |
| C(13B)-C(12B)-H(12D) | 107.5 | C(7B)-C(23B)-H(23E) | 109.5 |
| C(11B)-C(12B)-H(12D) | 107.5 | H(23D)-C(23B)-H(23E) | 109.5 |
| H(12C)-C(12B)-H(12D) | 107.0 | C(7B)-C(23B)-H(23F) | 109.5 |
| C(14B)-C(13B)-C(18B) | 118.7(13) | H(23D)-C(23B)-H(23F) | 109.5 |
| C(14B)-C(13B)-C(12B) | 121.2(12) | H(23E)-C(23B)-H(23F) | 109.5 |
| C(18B)-C(13B)-C(12B) | 120.0(11) | C(16B)-C(24B)-H(24D) | 109.5 |
| C(13B)-C(14B)-C(15B) | 124.5(13) | C(16B)-C(24B)-H(24E) | 109.5 |
| C(13B)-C(14B)-H(14B) | 117.8 | H(24D)-C(24B)-H(24E) | 109.5 |
| C(15B)-C(14B)-H(14B) | 117.8 | C(16B)-C(24B)-H(24F) | 109.5 |
| C(14B)-C(15B)-C(16B) | 118.5(13) | H(24D)-C(24B)-H(24F) | 109.5 |
| C(14B)-C(15B)-C(25B) | 122.3(14) | H(24E)-C(24B)-H(24F) | 109.5 |
| C(16B)-C(15B)-C(25B) | 119.3(15) | C(15B)-C(25B)-H(25D) | 109.5 |
| C(17B)-C(16B)-C(15B) | 115.7(14) | C(15B)-C(25B)-H(25E) | 109.5 |
| C(17B)-C(16B)-C(24B) | 121.0(15) | H(25D)-C(25B)-H(25E) | 109.5 |
| C(15B)-C(16B)-C(24B) | 123.3(14) | C(15B)-C(25B)-H(25F) | 109.5 |
| C(16B)-C(17B)-C(18B) | 125.0(14) | H(25D)-C(25B)-H(25F) | 109.5 |
| C(16B)-C(17B)-H(17B) | 117.5 | H(25E)-C(25B)-H(25F) | 109.5 |
| C(18B)-C(17B)-H(17B) | 117.5 | C(2C)-C(1C)-C(11C) | 114.5(11) |
| C(13B)-C(18B)-C(17B) | 117.6(12) | C(2C)-C(1C)-S(2C) | 111.4(8) |
| C(13B)-C(18B)-C(19B) | 122.1(13) | C(11C)-C(1C)-S(2C) | 111.2(9) |
| C(17B)-C(18B)-C(19B) | 120.2(12) | C(2C)-C(1C)-S(1C) | 108.7(9) |
| C(2B)-C(19B)-C(18B) | 116.9(10) | C(11C)-C(1C)-S(1C) | 111.6(8) |
| C(2B)-C(19B)-H(19C) | 108.1 | S(2C)-C(1C)-S(1C) | 98.1(7) |
| C(18B)-C(19B)-H(19C) | 108.1 | C(1C)-C(2C)-C(19C) | 115.4(10) |
| C(2B)-C(19B)-H(19D) | 108.1 | C(1C)-C(2C)-C(3C) | 113.4(11) |
| C(18B)-C(19B)-H(19D) | 108.1 | C(19C)-C(2C)-C(3C) | 113.4(11) |
| H(19C)-C(19B)-H(19D) | 107.3 | C(1C)-C(2C)-H(2CA) | 104.4 |
| C(21B)-C(20B)-S(2B) | 107.2(9) | C(19C)-C(2C)-H(2CA) | 104.4 |
| C(21B)-C(20B)-H(20C) | 110.3 | C(3C)-C(2C)-H(2CA) | 104.4 |
| S(2B)-C(20B)-H(20C) | 110.3 | C(4C)-C(3C)-C(2C) | 116.0(10) |
| C(21B)-C(20B)-H(20D) | 110.3 | C(4C)-C(3C)-H(3C1) | 108.3 |

| | | | |
|---|---|---|---|
| C(2C)-C(3C)-H(3C1) | 108.3 | C(14C)-C(15C)-C(16C) | 120.7(16) |
| C(4C)-C(3C)-H(3C2) | 108.3 | C(14C)-C(15C)-C(25C) | 122.8(16) |
| C(2C)-C(3C)-H(3C2) | 108.3 | C(16C)-C(15C)-C(25C) | 116.4(15) |
| H(3C1)-C(3C)-H(3C2) | 107.4 | C(17C)-C(16C)-C(15C) | 113.7(14) |
| C(5C)-C(4C)-C(9C) | 116.6(13) | C(17C)-C(16C)-C(24C) | 121.5(15) |
| C(5C)-C(4C)-C(3C) | 117.9(13) | C(15C)-C(16C)-C(24C) | 124.7(15) |
| C(9C)-C(4C)-C(3C) | 125.4(13) | C(16C)-C(17C)-C(18C) | 126.9(14) |
| C(4C)-C(5C)-C(6C) | 123.5(15) | C(16C)-C(17C)-H(17C) | 116.6 |
| C(4C)-C(5C)-H(5CA) | 118.3 | C(18C)-C(17C)-H(17C) | 116.6 |
| C(6C)-C(5C)-H(5CA) | 118.3 | C(13C)-C(18C)-C(17C) | 116.4(14) |
| C(7C)-C(6C)-C(5C) | 117.0(13) | C(13C)-C(18C)-C(19C) | 122.5(13) |
| C(7C)-C(6C)-C(22C) | 123.9(14) | C(17C)-C(18C)-C(19C) | 121.1(15) |
| C(5C)-C(6C)-C(22C) | 119.1(16) | C(18C)-C(19C)-C(2C) | 119.8(11) |
| C(8C)-C(7C)-C(6C) | 118.0(13) | C(18C)-C(19C)-H(19E) | 107.4 |
| C(8C)-C(7C)-C(23C) | 124.6(14) | C(2C)-C(19C)-H(19E) | 107.4 |
| C(6C)-C(7C)-C(23C) | 117.4(14) | C(18C)-C(19C)-H(19F) | 107.4 |
| C(7C)-C(8C)-C(9C) | 125.0(15) | C(2C)-C(19C)-H(19F) | 107.4 |
| C(7C)-C(8C)-H(8CA) | 117.5 | H(19E)-C(19C)-H(19F) | 106.9 |
| C(9C)-C(8C)-H(8CA) | 117.5 | C(21C)-C(20C)-S(1C) | 110.4(10) |
| C(8C)-C(9C)-C(4C) | 119.4(14) | C(21C)-C(20C)-H(20E) | 109.6 |
| C(8C)-C(9C)-C(10C) | 117.1(14) | S(1C)-C(20C)-H(20E) | 109.6 |
| C(4C)-C(9C)-C(10C) | 123.3(13) | C(21C)-C(20C)-H(20F) | 109.6 |
| C(9C)-C(10C)-C(11C) | 117.7(11) | S(1C)-C(20C)-H(20F) | 109.6 |
| C(9C)-C(10C)-H(10E) | 107.9 | H(20E)-C(20C)-H(20F) | 108.1 |
| C(11C)-C(10C)-H(10E) | 107.9 | C(20C)-C(21C)-S(2C) | 109.6(10) |
| C(9C)-C(10C)-H(10F) | 107.9 | C(20C)-C(21C)-H(21E) | 109.7 |
| C(11C)-C(10C)-H(10F) | 107.9 | S(2C)-C(21C)-H(21E) | 109.7 |
| H(10E)-C(10C)-H(10F) | 107.2 | C(20C)-C(21C)-H(21F) | 109.7 |
| C(12C)-C(11C)-C(10C) | 113.4(12) | S(2C)-C(21C)-H(21F) | 109.7 |
| C(12C)-C(11C)-C(1C) | 113.9(10) | H(21E)-C(21C)-H(21F) | 108.2 |
| C(10C)-C(11C)-C(1C) | 114.0(10) | C(6C)-C(22C)-H(22G) | 109.5 |
| C(12C)-C(11C)-H(11C) | 104.8 | C(6C)-C(22C)-H(22H) | 109.5 |
| C(10C)-C(11C)-H(11C) | 104.8 | H(22G)-C(22C)-H(22H) | 109.5 |
| C(1C)-C(11C)-H(11C) | 104.8 | C(6C)-C(22C)-H(22I) | 109.5 |
| C(13C)-C(12C)-C(11C) | 118.9(10) | H(22G)-C(22C)-H(22I) | 109.5 |
| C(13C)-C(12C)-H(12E) | 107.6 | H(22H)-C(22C)-H(22I) | 109.5 |
| C(11C)-C(12C)-H(12E) | 107.6 | C(7C)-C(23C)-H(23G) | 109.5 |
| C(13C)-C(12C)-H(12F) | 107.6 | C(7C)-C(23C)-H(23H) | 109.5 |
| C(11C)-C(12C)-H(12F) | 107.6 | H(23G)-C(23C)-H(23H) | 109.5 |
| H(12E)-C(12C)-H(12F) | 107.0 | C(7C)-C(23C)-H(23I) | 109.5 |
| C(18C)-C(13C)-C(14C) | 117.3(14) | H(23G)-C(23C)-H(23I) | 109.5 |
| C(18C)-C(13C)-C(12C) | 122.9(14) | H(23H)-C(23C)-H(23I) | 109.5 |
| C(14C)-C(13C)-C(12C) | 119.7(14) | C(16C)-C(24C)-H(24G) | 109.5 |
| C(15C)-C(14C)-C(13C) | 124.9(15) | C(16C)-C(24C)-H(24H) | 109.5 |
| C(15C)-C(14C)-H(14C) | 117.5 | H(24G)-C(24C)-H(24H) | 109.5 |
| C(13C)-C(14C)-H(14C) | 117.5 | C(16C)-C(24C)-H(24I) | 109.5 |

| | |
|---|---|
| H(24G)-C(24C)-H(24I) | 109.5 |
| H(24H)-C(24C)-H(24I) | 109.5 |
| C(15C)-C(25C)-H(25G) | 109.5 |
| C(15C)-C(25C)-H(25H) | 109.5 |
| H(25G)-C(25C)-H(25H) | 109.5 |
| C(15C)-C(25C)-H(25I) | 109.5 |
| H(25G)-C(25C)-H(25I) | 109.5 |
| H(25H)-C(25C)-H(25I) | 109.5 |
| O(1)-S(1)-O(2) | 116.8(6) |
| O(1)-S(1)-C(21) | 107.7(6) |
| O(2)-S(1)-C(21) | 109.6(6) |
| O(1)-S(1)-C(1) | 112.0(5) |
| O(2)-S(1)-C(1) | 107.9(5) |
| C(21)-S(1)-C(1) | 101.9(6) |
| O(4)-S(2)-O(3) | 114.4(6) |
| O(4)-S(2)-C(20) | 112.3(7) |
| O(3)-S(2)-C(20) | 110.0(7) |
| O(4)-S(2)-C(1) | 114.2(6) |
| O(3)-S(2)-C(1) | 106.5(5) |
| C(20)-S(2)-C(1) | 98.1(6) |
| O(2B)-S(1B)-O(1B) | 117.6(6) |
| O(2B)-S(1B)-C(21B) | 106.3(6) |
| O(1B)-S(1B)-C(21B) | 109.8(6) |
| O(2B)-S(1B)-C(1B) | 112.5(5) |
| O(1B)-S(1B)-C(1B) | 107.5(6) |
| C(21B)-S(1B)-C(1B) | 101.8(6) |
| O(3B)-S(2B)-O(4B) | 119.2(6) |
| O(3B)-S(2B)-C(20B) | 108.5(6) |
| O(4B)-S(2B)-C(20B) | 108.4(6) |
| O(3B)-S(2B)-C(1B) | 105.9(6) |
| O(4B)-S(2B)-C(1B) | 115.1(6) |
| C(20B)-S(2B)-C(1B) | 97.4(5) |
| O(1C)-S(1C)-O(2C) | 118.0(7) |
| O(1C)-S(1C)-C(20C) | 108.3(7) |
| O(2C)-S(1C)-C(20C) | 107.8(8) |
| O(1C)-S(1C)-C(1C) | 112.8(6) |
| O(2C)-S(1C)-C(1C) | 107.3(5) |
| C(20C)-S(1C)-C(1C) | 101.3(6) |
| O(4C)-S(2C)-O(3C) | 115.3(6) |
| O(4C)-S(2C)-C(21C) | 110.4(7) |
| O(3C)-S(2C)-C(21C) | 108.2(7) |
| O(4C)-S(2C)-C(1C) | 108.2(6) |
| O(3C)-S(2C)-C(1C) | 114.6(6) |
| C(21C)-S(2C)-C(1C) | 99.0(6) |

**Table 4.** Anisotropic displacement parameters ($Å^2 x\ 10^3$) for **sulfone-ketal III-10**. The anisotropic displacement factor exponent takes the form: $-2\pi^2[ h^2 a^{*2} U^{11} + ... + 2 h k a^* b^* U^{12} ]$

| | $U^{11}$ | $U^{22}$ | $U^{33}$ | $U^{23}$ | $U^{13}$ | $U^{12}$ |
|---|---|---|---|---|---|---|
| C(1) | 48(7) | 39(7) | 100(11) | -8(7) | 27(7) | -1(6) |
| C(2) | 73(9) | 66(8) | 71(9) | 11(8) | 23(7) | 6(8) |
| C(3) | 82(10) | 79(9) | 97(12) | 3(8) | 45(9) | 5(8) |
| C(4) | 62(9) | 75(10) | 80(12) | 0(8) | 18(8) | -24(8) |
| C(5) | 90(11) | 114(12) | 89(14) | -20(11) | 27(10) | -16(9) |
| C(6) | 109(14) | 99(13) | 77(13) | -9(11) | 20(10) | -42(11) |
| C(7) | 123(15) | 97(12) | 69(13) | 1(10) | 31(11) | -37(11) |
| C(8) | 105(12) | 77(10) | 87(13) | 4(10) | 14(10) | -22(8) |
| C(9) | 55(9) | 75(10) | 83(12) | -4(9) | 7(8) | -9(8) |
| C(10) | 72(9) | 59(8) | 79(10) | -8(7) | 26(8) | -21(7) |
| C(11) | 66(9) | 56(8) | 84(10) | 2(7) | 27(7) | 9(7) |
| C(12) | 71(9) | 64(8) | 82(11) | 9(8) | 21(7) | -2(7) |
| C(13) | 88(11) | 65(9) | 67(11) | 12(8) | 7(9) | -28(8) |
| C(14) | 84(11) | 98(11) | 93(13) | -4(11) | 20(10) | -18(9) |
| C(15) | 118(15) | 89(13) | 105(17) | 13(11) | 17(13) | -8(10) |
| C(16) | 112(14) | 108(14) | 61(12) | 5(10) | -12(10) | -30(11) |
| C(17) | 106(13) | 79(10) | 101(14) | -28(10) | 30(11) | -34(9) |
| C(18) | 75(10) | 55(9) | 88(13) | -11(8) | 16(9) | -12(8) |
| C(19) | 95(11) | 62(9) | 113(13) | -11(9) | 46(9) | -24(8) |
| C(20) | 106(12) | 94(10) | 78(11) | 6(9) | -14(8) | 16(10) |
| C(21) | 69(10) | 98(11) | 127(14) | 39(10) | 21(9) | 1(8) |
| C(22) | 169(16) | 152(14) | 81(13) | -32(10) | 67(12) | -72(12) |
| C(23) | 178(17) | 159(16) | 110(16) | 44(13) | 16(13) | -2(13) |
| C(24) | 156(16) | 178(16) | 70(13) | -21(12) | 7(10) | -32(12) |
| C(25) | 99(13) | 230(20) | 95(15) | 26(14) | -12(10) | -53(12) |
| C(1B) | 51(8) | 76(8) | 59(9) | -10(7) | 7(6) | -11(7) |
| C(2B) | 80(10) | 79(9) | 73(10) | -3(8) | 22(8) | 35(8) |
| C(3B) | 84(10) | 74(9) | 70(10) | 8(7) | 41(8) | 28(7) |
| C(4B) | 52(8) | 78(9) | 73(11) | 0(8) | 11(7) | -7(7) |
| C(5B) | 89(11) | 107(11) | 57(10) | -11(9) | 22(8) | -28(9) |
| C(6B) | 77(11) | 89(12) | 106(15) | 9(10) | 28(10) | -19(9) |
| C(7B) | 70(10) | 91(11) | 85(13) | 14(9) | 1(9) | 7(8) |
| C(8B) | 88(11) | 108(11) | 70(12) | 14(10) | 23(9) | 20(9) |
| C(9B) | 56(9) | 94(11) | 77(12) | -12(9) | 23(8) | -12(8) |
| C(10B) | 75(9) | 73(9) | 86(11) | 22(8) | 20(8) | 26(7) |
| C(11B) | 79(9) | 51(8) | 80(10) | -11(7) | 11(7) | 20(7) |
| C(12B) | 78(10) | 66(9) | 107(13) | -20(8) | 32(8) | 9(8) |
| C(13B) | 68(9) | 56(8) | 69(10) | 14(8) | 13(7) | 7(7) |
| C(14B) | 62(9) | 79(9) | 83(11) | -3(9) | 19(8) | 4(7) |
| C(15B) | 71(11) | 96(11) | 106(14) | 17(10) | 33(10) | -4(9) |

| | | | | | | |
|---|---|---|---|---|---|---|
| C(16B) | 75(11) | 97(11) | 70(11) | -3(9) | 2(8) | -31(9) |
| C(17B) | 98(12) | 97(11) | 91(13) | -21(10) | 46(10) | -12(9) |
| C(18B) | 63(10) | 74(9) | 98(13) | -1(9) | 30(8) | 1(8) |
| C(19B) | 77(10) | 63(8) | 98(12) | -27(8) | 3(8) | 15(8) |
| C(20B) | 67(9) | 73(9) | 88(11) | -2(8) | -14(7) | -17(7) |
| C(21B) | 57(9) | 92(9) | 100(12) | 2(8) | 12(8) | 11(8) |
| C(22B) | 133(13) | 121(12) | 70(12) | 24(10) | 17(10) | 29(10) |
| C(23B) | 100(12) | 162(15) | 97(14) | 14(11) | 30(10) | 6(10) |
| C(24B) | 104(12) | 147(13) | 63(11) | -26(10) | 8(8) | -24(9) |
| C(25B) | 74(10) | 166(14) | 74(11) | 24(10) | -5(8) | 1(9) |
| C(1C) | 74(9) | 49(7) | 94(11) | 5(8) | 16(8) | -5(7) |
| C(2C) | 80(10) | 60(8) | 79(10) | 0(8) | 17(8) | 4(8) |
| C(3C) | 75(9) | 52(8) | 118(13) | 3(8) | 27(9) | -3(7) |
| C(4C) | 73(10) | 58(9) | 91(13) | -4(8) | 32(9) | 2(8) |
| C(5C) | 83(11) | 104(12) | 99(14) | -9(11) | 24(10) | 23(9) |
| C(6C) | 87(11) | 122(13) | 71(12) | 40(10) | 19(9) | 10(10) |
| C(7C) | 73(10) | 88(10) | 72(11) | 22(9) | 0(8) | -1(8) |
| C(8C) | 84(11) | 99(11) | 94(14) | 37(11) | 2(9) | 22(8) |
| C(9C) | 79(10) | 72(10) | 82(12) | 14(9) | 11(9) | 7(8) |
| C(10C) | 55(9) | 90(10) | 134(14) | 24(10) | 31(9) | -7(8) |
| C(11C) | 74(9) | 60(8) | 112(12) | 18(9) | 41(9) | -6(8) |
| C(12C) | 91(11) | 66(9) | 87(12) | 6(8) | 26(9) | -6(8) |
| C(13C) | 80(11) | 71(10) | 88(13) | -2(9) | 24(9) | 14(8) |
| C(14C) | 66(10) | 77(10) | 99(13) | 10(10) | 27(9) | 9(7) |
| C(15C) | 86(12) | 82(11) | 99(14) | 5(10) | 30(10) | 25(9) |
| C(16C) | 93(11) | 72(10) | 100(13) | -31(10) | 49(10) | -2(9) |
| C(17C) | 74(10) | 65(9) | 145(17) | 0(10) | 63(11) | -3(7) |
| C(18C) | 79(10) | 83(10) | 65(10) | -5(8) | 25(8) | 13(8) |
| C(19C) | 66(9) | 92(10) | 104(12) | 12(9) | 46(9) | -2(8) |
| C(20C) | 102(13) | 132(13) | 140(16) | 68(12) | 26(10) | 21(11) |
| C(21C) | 156(15) | 110(11) | 80(12) | 29(9) | 54(10) | 26(11) |
| C(22C) | 106(13) | 172(15) | 92(13) | 11(12) | 28(10) | -23(11) |
| C(23C) | 152(14) | 144(14) | 74(13) | 2(11) | 11(11) | -27(11) |
| C(24C) | 112(13) | 178(15) | 79(12) | -5(11) | 41(10) | -37(11) |
| C(25C) | 106(12) | 154(14) | 95(13) | -16(11) | 35(10) | 10(10) |
| O(1) | 122(8) | 83(6) | 85(7) | 5(5) | 32(5) | -41(6) |
| O(2) | 72(6) | 93(6) | 89(7) | -1(5) | 22(5) | 1(5) |
| O(3) | 83(7) | 90(6) | 102(8) | -28(6) | 20(5) | -15(5) |
| O(4) | 118(9) | 117(8) | 146(11) | 37(7) | 35(8) | -12(6) |
| O(1B) | 86(7) | 102(7) | 123(9) | -26(6) | 50(6) | -3(5) |
| O(2B) | 92(7) | 82(6) | 124(9) | -8(6) | 41(6) | -32(5) |
| O(3B) | 95(7) | 98(6) | 84(7) | -28(6) | 15(5) | -5(5) |
| O(4B) | 108(8) | 94(7) | 117(9) | 33(6) | 37(6) | -7(6) |
| O(1C) | 103(8) | 107(8) | 175(12) | -5(7) | 30(7) | 51(6) |
| O(2C) | 87(7) | 99(7) | 146(10) | 29(7) | -3(6) | -25(6) |
| O(3C) | 98(8) | 100(7) | 173(11) | 16(7) | 53(7) | 27(6) |

| | | | | | | |
|---|---|---|---|---|---|---|
| O(4C) | 110(8) | 84(6) | 130(9) | -28(6) | 32(6) | -13(6) |
| S(1) | 78(2) | 72(2) | 79(3) | 9(2) | 22(2) | 3(2) |
| S(2) | 75(3) | 75(3) | 95(3) | 0(2) | 15(2) | -5(2) |
| S(1B) | 79(3) | 82(3) | 79(3) | 3(2) | 29(2) | -3(2) |
| S(2B) | 78(3) | 76(2) | 99(3) | -4(2) | 20(2) | -12(2) |
| S(1C) | 82(3) | 87(3) | 96(3) | 22(2) | 19(2) | 8(2) |
| S(2C) | 103(3) | 79(3) | 93(3) | 1(2) | 42(2) | 7(3) |

Table 5. Hydrogen coordinates ( x $10^4$) and isotropic displacement parameters ($Å^2$x $10^3$) for **sulfone-ketal III-10**.

| | x | y | z | U(eq) |
|---|---|---|---|---|
| H(2A) | 4053 | 10514 | 1536 | 83 |
| H(3A) | 3750 | 8951 | 1968 | 98 |
| H(3B) | 3869 | 10115 | 2345 | 98 |
| H(5A) | 4040 | 9555 | 3258 | 117 |
| H(8A) | 5328 | 6692 | 3148 | 111 |
| H(10A) | 4478 | 7114 | 1896 | 83 |
| H(10B) | 5125 | 6775 | 2207 | 83 |
| H(11A) | 5134 | 7788 | 1431 | 81 |
| H(12A) | 5939 | 8392 | 2079 | 87 |
| H(12B) | 5673 | 9571 | 1754 | 87 |
| H(14A) | 6392 | 8669 | 3015 | 111 |
| H(17A) | 5121 | 11533 | 3247 | 114 |
| H(19A) | 4984 | 11293 | 1886 | 104 |
| H(19B) | 4614 | 11495 | 2313 | 104 |
| H(20A) | 3514 | 8970 | 60 | 122 |
| H(20B) | 3371 | 9801 | 526 | 122 |
| H(21A) | 3974 | 11042 | 417 | 119 |
| H(21B) | 4127 | 10194 | -41 | 119 |
| H(22A) | 4818 | 8335 | 4600 | 191 |
| H(22B) | 4168 | 8706 | 4295 | 191 |
| H(22C) | 4672 | 9651 | 4365 | 191 |
| H(23A) | 5342 | 7275 | 4577 | 232 |
| H(23B) | 5816 | 7094 | 4250 | 232 |
| H(23C) | 5336 | 6107 | 4209 | 232 |
| H(24A) | 6154 | 10747 | 4515 | 210 |
| H(24B) | 5472 | 10900 | 4302 | 210 |
| H(24C) | 5878 | 11941 | 4205 | 210 |
| H(25A) | 6624 | 9675 | 4448 | 224 |
| H(25B) | 7022 | 9381 | 4050 | 224 |
| H(25C) | 6589 | 8404 | 4156 | 224 |
| H(2BA) | 636 | 2399 | 6635 | 93 |
| H(3B1) | 564 | 1979 | 7484 | 86 |
| H(3B2) | 405 | 831 | 7099 | 86 |
| H(5BA) | 843 | 1405 | 8396 | 101 |
| H(8BA) | 2062 | -1526 | 8107 | 106 |
| H(10C) | 1133 | -1077 | 6940 | 94 |
| H(10D) | 1802 | -1305 | 7178 | 94 |
| H(11B) | 1652 | -295 | 6351 | 87 |
| H(12C) | 2493 | 360 | 6888 | 99 |
| H(12D) | 2169 | 1524 | 6603 | 99 |

| | | | | |
|---|---|---|---|---|
| H(14B) | 3021 | 530 | 7813 | 90 |
| H(17B) | 1852 | 3439 | 8190 | 110 |
| H(19C) | 1266 | 3461 | 7270 | 101 |
| H(19D) | 1564 | 3115 | 6794 | 101 |
| H(20C) | -268 | 841 | 5330 | 100 |
| H(20D) | -93 | 1758 | 5850 | 100 |
| H(21C) | 329 | 2667 | 5260 | 102 |
| H(21D) | 433 | 1453 | 4969 | 102 |
| H(22D) | 1747 | 157 | 9664 | 166 |
| H(22E) | 1085 | 521 | 9436 | 166 |
| H(22F) | 1573 | 1473 | 9445 | 166 |
| H(23D) | 2182 | -814 | 9566 | 179 |
| H(23E) | 2636 | -940 | 9212 | 179 |
| H(23F) | 2193 | -1988 | 9207 | 179 |
| H(24D) | 3009 | 2664 | 9399 | 162 |
| H(24E) | 2333 | 2845 | 9283 | 162 |
| H(24F) | 2711 | 3861 | 9115 | 162 |
| H(25D) | 3446 | 1559 | 9265 | 165 |
| H(25E) | 3779 | 1303 | 8803 | 165 |
| H(25F) | 3393 | 294 | 8964 | 165 |
| H(2CA) | 2551 | 2951 | 1420 | 88 |
| H(3C1) | 2986 | 1814 | 2181 | 98 |
| H(3C2) | 3455 | 2075 | 1859 | 98 |
| H(5CA) | 3408 | 1575 | 3106 | 115 |
| H(8CA) | 4710 | 4584 | 3232 | 117 |
| H(10E) | 4267 | 3906 | 1960 | 110 |
| H(10F) | 4413 | 5063 | 2343 | 110 |
| H(11C) | 3730 | 5552 | 1534 | 95 |
| H(12E) | 3597 | 6621 | 2241 | 97 |
| H(12F) | 2979 | 6324 | 1827 | 97 |
| H(14C) | 3634 | 6727 | 3175 | 96 |
| H(17C) | 2330 | 3768 | 3059 | 106 |
| H(19E) | 2211 | 4619 | 1776 | 99 |
| H(19F) | 2192 | 3447 | 2126 | 99 |
| H(20E) | 2686 | 4924 | -60 | 152 |
| H(20F) | 3031 | 6034 | 277 | 152 |
| H(21E) | 3834 | 4973 | 641 | 133 |
| H(21F) | 3560 | 4099 | 120 | 133 |
| H(22G) | 4208 | 2273 | 4539 | 185 |
| H(22H) | 4031 | 1105 | 4163 | 185 |
| H(22I) | 3548 | 2015 | 4218 | 185 |
| H(23G) | 4671 | 3366 | 4564 | 192 |
| H(23H) | 4719 | 4677 | 4339 | 192 |
| H(23I) | 5174 | 3691 | 4292 | 192 |
| H(24G) | 2889 | 4968 | 4436 | 180 |
| H(24H) | 2748 | 3678 | 4165 | 180 |

| | | | | |
|---|---|---|---|---|
| H(24I) | 2260 | 4673 | 4034 | 180 |
| H(25G) | 3764 | 7024 | 4133 | 176 |
| H(25H) | 3697 | 5836 | 4460 | 176 |
| H(25I) | 3190 | 6788 | 4306 | 176 |

Table 6. Torsion angles [°] for **sulfone-ketal III-10**.

| | |
|---|---|
| C(11)-C(1)-C(2)-C(3) | -60.8(15) |
| S(1)-C(1)-C(2)-C(3) | 167.1(9) |
| S(2)-C(1)-C(2)-C(3) | 59.8(14) |
| C(11)-C(1)-C(2)-C(19) | 65.4(13) |
| S(1)-C(1)-C(2)-C(19) | -66.7(12) |
| S(2)-C(1)-C(2)-C(19) | -174.0(8) |
| C(1)-C(2)-C(3)-C(4) | 68.3(17) |
| C(19)-C(2)-C(3)-C(4) | -60.2(15) |
| C(2)-C(3)-C(4)-C(5) | 131.5(13) |
| C(2)-C(3)-C(4)-C(9) | -49.3(17) |
| C(9)-C(4)-C(5)-C(6) | 6(2) |
| C(3)-C(4)-C(5)-C(6) | -175.2(12) |
| C(4)-C(5)-C(6)-C(7) | -4(2) |
| C(4)-C(5)-C(6)-C(22) | 175.0(13) |
| C(5)-C(6)-C(7)-C(8) | 0(2) |
| C(22)-C(6)-C(7)-C(8) | -178.6(12) |
| C(5)-C(6)-C(7)-C(23) | 176.9(13) |
| C(22)-C(6)-C(7)-C(23) | -2(2) |
| C(6)-C(7)-C(8)-C(9) | 1(2) |
| C(23)-C(7)-C(8)-C(9) | -175.5(12) |
| C(7)-C(8)-C(9)-C(4) | 1(2) |
| C(7)-C(8)-C(9)-C(10) | -178.2(13) |
| C(5)-C(4)-C(9)-C(8) | -3.8(17) |
| C(3)-C(4)-C(9)-C(8) | 177.0(11) |
| C(5)-C(4)-C(9)-C(10) | 175.0(11) |
| C(3)-C(4)-C(9)-C(10) | -4.2(18) |
| C(8)-C(9)-C(10)-C(11) | -122.0(14) |
| C(4)-C(9)-C(10)-C(11) | 59.3(18) |
| C(9)-C(10)-C(11)-C(1) | -73.8(15) |
| C(9)-C(10)-C(11)-C(12) | 53.5(16) |
| C(2)-C(1)-C(11)-C(10) | 59.5(13) |
| S(1)-C(1)-C(11)-C(10) | -166.8(8) |
| S(2)-C(1)-C(11)-C(10) | -61.6(12) |
| C(2)-C(1)-C(11)-C(12) | -70.4(13) |
| S(1)-C(1)-C(11)-C(12) | 63.3(11) |
| S(2)-C(1)-C(11)-C(12) | 168.4(8) |
| C(10)-C(11)-C(12)-C(13) | -48.6(14) |
| C(1)-C(11)-C(12)-C(13) | 80.5(13) |
| C(11)-C(12)-C(13)-C(18) | -64.3(15) |
| C(11)-C(12)-C(13)-C(14) | 122.2(12) |
| C(18)-C(13)-C(14)-C(15) | 8(2) |
| C(12)-C(13)-C(14)-C(15) | -177.9(13) |
| C(13)-C(14)-C(15)-C(16) | -5(2) |
| C(13)-C(14)-C(15)-C(25) | 174.5(13) |

| | |
|---|---|
| C(14)-C(15)-C(16)-C(17) | 2(2) |
| C(25)-C(15)-C(16)-C(17) | -177.6(13) |
| C(14)-C(15)-C(16)-C(24) | 176.8(14) |
| C(25)-C(15)-C(16)-C(24) | -3(3) |
| C(15)-C(16)-C(17)-C(18) | -2(2) |
| C(24)-C(16)-C(17)-C(18) | -177.6(13) |
| C(14)-C(13)-C(18)-C(17) | -8.3(18) |
| C(12)-C(13)-C(18)-C(17) | 178.1(11) |
| C(14)-C(13)-C(18)-C(19) | -179.9(11) |
| C(12)-C(13)-C(18)-C(19) | 6.5(19) |
| C(16)-C(17)-C(18)-C(13) | 5.7(19) |
| C(16)-C(17)-C(18)-C(19) | 177.5(13) |
| C(13)-C(18)-C(19)-C(2) | 51.3(19) |
| C(17)-C(18)-C(19)-C(2) | -120.1(13) |
| C(3)-C(2)-C(19)-C(18) | 61.8(16) |
| C(1)-C(2)-C(19)-C(18) | -70.2(16) |
| S(2)-C(20)-C(21)-S(1) | -1.2(15) |
| C(11B)-C(1B)-C(2B)-C(3B) | -67.7(15) |
| S(1B)-C(1B)-C(2B)-C(3B) | 163.3(9) |
| S(2B)-C(1B)-C(2B)-C(3B) | 54.2(13) |
| C(11B)-C(1B)-C(2B)-C(19B) | 65.9(13) |
| S(1B)-C(1B)-C(2B)-C(19B) | -63.1(12) |
| S(2B)-C(1B)-C(2B)-C(19B) | -172.1(8) |
| C(19B)-C(2B)-C(3B)-C(4B) | -61.5(15) |
| C(1B)-C(2B)-C(3B)-C(4B) | 71.9(16) |
| C(2B)-C(3B)-C(4B)-C(5B) | 129.7(13) |
| C(2B)-C(3B)-C(4B)-C(9B) | -46.9(18) |
| C(9B)-C(4B)-C(5B)-C(6B) | 2.1(19) |
| C(3B)-C(4B)-C(5B)-C(6B) | -174.7(11) |
| C(4B)-C(5B)-C(6B)-C(7B) | -2(2) |
| C(4B)-C(5B)-C(6B)-C(22B) | 175.2(12) |
| C(5B)-C(6B)-C(7B)-C(8B) | -1(2) |
| C(22B)-C(6B)-C(7B)-C(8B) | -178.3(12) |
| C(5B)-C(6B)-C(7B)-C(23B) | 175.3(12) |
| C(22B)-C(6B)-C(7B)-C(23B) | -2(2) |
| C(6B)-C(7B)-C(8B)-C(9B) | 4(2) |
| C(23B)-C(7B)-C(8B)-C(9B) | -172.4(12) |
| C(7B)-C(8B)-C(9B)-C(4B) | -3.7(19) |
| C(7B)-C(8B)-C(9B)-C(10B) | -179.7(12) |
| C(5B)-C(4B)-C(9B)-C(8B) | 0.7(17) |
| C(3B)-C(4B)-C(9B)-C(8B) | 177.4(12) |
| C(5B)-C(4B)-C(9B)-C(10B) | 176.5(11) |
| C(3B)-C(4B)-C(9B)-C(10B) | -6.8(18) |
| C(8B)-C(9B)-C(10B)-C(11B) | -127.9(13) |
| C(4B)-C(9B)-C(10B)-C(11B) | 56.2(17) |
| C(2B)-C(1B)-C(11B)-C(12B) | -65.7(14) |

| | |
|---|---|
| S(1B)-C(1B)-C(11B)-C(12B) | 64.5(12) |
| S(2B)-C(1B)-C(11B)-C(12B) | 169.8(9) |
| C(2B)-C(1B)-C(11B)-C(10B) | 63.5(13) |
| S(1B)-C(1B)-C(11B)-C(10B) | -166.3(9) |
| S(2B)-C(1B)-C(11B)-C(10B) | -61.0(11) |
| C(9B)-C(10B)-C(11B)-C(12B) | 56.2(16) |
| C(9B)-C(10B)-C(11B)-C(1B) | -71.1(15) |
| C(1B)-C(11B)-C(12B)-C(13B) | 81.2(14) |
| C(10B)-C(11B)-C(12B)-C(13B) | -47.8(14) |
| C(11B)-C(12B)-C(13B)-C(14B) | 114.3(13) |
| C(11B)-C(12B)-C(13B)-C(18B) | -61.4(16) |
| C(18B)-C(13B)-C(14B)-C(15B) | 0.0(19) |
| C(12B)-C(13B)-C(14B)-C(15B) | -175.7(12) |
| C(13B)-C(14B)-C(15B)-C(16B) | -1(2) |
| C(13B)-C(14B)-C(15B)-C(25B) | 179.8(12) |
| C(14B)-C(15B)-C(16B)-C(17B) | 0.1(19) |
| C(25B)-C(15B)-C(16B)-C(17B) | 179.7(12) |
| C(14B)-C(15B)-C(16B)-C(24B) | 179.6(12) |
| C(25B)-C(15B)-C(16B)-C(24B) | -1(2) |
| C(15B)-C(16B)-C(17B)-C(18B) | 1(2) |
| C(24B)-C(16B)-C(17B)-C(18B) | -178.6(13) |
| C(14B)-C(13B)-C(18B)-C(17B) | 1.0(18) |
| C(12B)-C(13B)-C(18B)-C(17B) | 176.8(11) |
| C(14B)-C(13B)-C(18B)-C(19B) | -179.5(12) |
| C(12B)-C(13B)-C(18B)-C(19B) | -3.7(19) |
| C(16B)-C(17B)-C(18B)-C(13B) | -2(2) |
| C(16B)-C(17B)-C(18B)-C(19B) | 178.9(13) |
| C(3B)-C(2B)-C(19B)-C(18B) | 57.0(16) |
| C(1B)-C(2B)-C(19B)-C(18B) | -77.6(16) |
| C(13B)-C(18B)-C(19B)-C(2B) | 63.5(18) |
| C(17B)-C(18B)-C(19B)-C(2B) | -117.0(13) |
| S(2B)-C(20B)-C(21B)-S(1B) | -29.6(11) |
| C(11C)-C(1C)-C(2C)-C(19C) | 63.2(15) |
| S(2C)-C(1C)-C(2C)-C(19C) | -169.5(9) |
| S(1C)-C(1C)-C(2C)-C(19C) | -62.5(13) |
| C(11C)-C(1C)-C(2C)-C(3C) | -70.0(13) |
| S(2C)-C(1C)-C(2C)-C(3C) | 57.3(13) |
| S(1C)-C(1C)-C(2C)-C(3C) | 164.3(8) |
| C(1C)-C(2C)-C(3C)-C(4C) | 75.9(15) |
| C(19C)-C(2C)-C(3C)-C(4C) | -58.2(15) |
| C(2C)-C(3C)-C(4C)-C(5C) | 128.1(12) |
| C(2C)-C(3C)-C(4C)-C(9C) | -55.4(17) |
| C(9C)-C(4C)-C(5C)-C(6C) | 6.4(19) |
| C(3C)-C(4C)-C(5C)-C(6C) | -176.7(12) |
| C(4C)-C(5C)-C(6C)-C(7C) | -8(2) |
| C(4C)-C(5C)-C(6C)-C(22C) | 175.5(13) |

| | |
|---|---|
| C(5C)-C(6C)-C(7C)-C(8C) | 3(2) |
| C(22C)-C(6C)-C(7C)-C(8C) | 178.8(14) |
| C(5C)-C(6C)-C(7C)-C(23C) | -178.5(13) |
| C(22C)-C(6C)-C(7C)-C(23C) | -2(2) |
| C(6C)-C(7C)-C(8C)-C(9C) | 4(2) |
| C(23C)-C(7C)-C(8C)-C(9C) | -174.5(14) |
| C(7C)-C(8C)-C(9C)-C(4C) | -6(2) |
| C(7C)-C(8C)-C(9C)-C(10C) | 178.1(13) |
| C(5C)-C(4C)-C(9C)-C(8C) | 0.6(19) |
| C(3C)-C(4C)-C(9C)-C(8C) | -176.0(12) |
| C(5C)-C(4C)-C(9C)-C(10C) | 176.0(12) |
| C(3C)-C(4C)-C(9C)-C(10C) | -1(2) |
| C(8C)-C(9C)-C(10C)-C(11C) | -128.8(14) |
| C(4C)-C(9C)-C(10C)-C(11C) | 55.7(18) |
| C(9C)-C(10C)-C(11C)-C(12C) | 59.6(15) |
| C(9C)-C(10C)-C(11C)-C(1C) | -72.8(16) |
| C(2C)-C(1C)-C(11C)-C(12C) | -64.2(14) |
| S(2C)-C(1C)-C(11C)-C(12C) | 168.4(9) |
| S(1C)-C(1C)-C(11C)-C(12C) | 59.9(13) |
| C(2C)-C(1C)-C(11C)-C(10C) | 67.9(14) |
| S(2C)-C(1C)-C(11C)-C(10C) | -59.5(13) |
| S(1C)-C(1C)-C(11C)-C(10C) | -168.0(9) |
| C(10C)-C(11C)-C(12C)-C(13C) | -57.4(17) |
| C(1C)-C(11C)-C(12C)-C(13C) | 75.0(16) |
| C(11C)-C(12C)-C(13C)-C(18C) | -57.5(19) |
| C(11C)-C(12C)-C(13C)-C(14C) | 120.9(13) |
| C(18C)-C(13C)-C(14C)-C(15C) | 0.1(19) |
| C(12C)-C(13C)-C(14C)-C(15C) | -178.4(13) |
| C(13C)-C(14C)-C(15C)-C(16C) | 1(2) |
| C(13C)-C(14C)-C(15C)-C(25C) | -179.0(12) |
| C(14C)-C(15C)-C(16C)-C(17C) | -1(2) |
| C(25C)-C(15C)-C(16C)-C(17C) | 178.6(11) |
| C(14C)-C(15C)-C(16C)-C(24C) | -179.2(14) |
| C(25C)-C(15C)-C(16C)-C(24C) | 1(2) |
| C(15C)-C(16C)-C(17C)-C(18C) | 0.8(19) |
| C(24C)-C(16C)-C(17C)-C(18C) | 178.9(14) |
| C(14C)-C(13C)-C(18C)-C(17C) | -0.4(17) |
| C(12C)-C(13C)-C(18C)-C(17C) | 178.0(11) |
| C(14C)-C(13C)-C(18C)-C(19C) | -179.0(11) |
| C(12C)-C(13C)-C(18C)-C(19C) | -0.5(19) |
| C(16C)-C(17C)-C(18C)-C(13C) | 0(2) |
| C(16C)-C(17C)-C(18C)-C(19C) | 178.5(12) |
| C(13C)-C(18C)-C(19C)-C(2C) | 56.8(17) |
| C(17C)-C(18C)-C(19C)-C(2C) | -121.6(13) |
| C(1C)-C(2C)-C(19C)-C(18C) | -74.5(16) |
| C(3C)-C(2C)-C(19C)-C(18C) | 58.7(15) |

| | |
|---|---|
| S(1C)-C(20C)-C(21C)-S(2C) | 21.3(14) |
| C(20)-C(21)-S(1)-O(1) | -144.2(10) |
| C(20)-C(21)-S(1)-O(2) | 87.8(12) |
| C(20)-C(21)-S(1)-C(1) | -26.3(12) |
| C(11)-C(1)-S(1)-O(1) | -94.6(8) |
| C(2)-C(1)-S(1)-O(1) | 39.9(11) |
| S(2)-C(1)-S(1)-O(1) | 153.8(5) |
| C(11)-C(1)-S(1)-O(2) | 35.2(9) |
| C(2)-C(1)-S(1)-O(2) | 169.7(8) |
| S(2)-C(1)-S(1)-O(2) | -76.4(6) |
| C(11)-C(1)-S(1)-C(21) | 150.6(9) |
| C(2)-C(1)-S(1)-C(21) | -75.0(10) |
| S(2)-C(1)-S(1)-C(21) | 39.0(7) |
| C(21)-C(20)-S(2)-O(4) | 147.0(12) |
| C(21)-C(20)-S(2)-O(3) | -84.3(12) |
| C(21)-C(20)-S(2)-C(1) | 26.6(13) |
| C(11)-C(1)-S(2)-O(4) | 87.8(9) |
| C(2)-C(1)-S(2)-O(4) | -38.3(10) |
| S(1)-C(1)-S(2)-O(4) | -157.2(6) |
| C(11)-C(1)-S(2)-O(3) | -39.5(10) |
| C(2)-C(1)-S(2)-O(3) | -165.5(8) |
| S(1)-C(1)-S(2)-O(3) | 75.5(6) |
| C(11)-C(1)-S(2)-C(20) | -153.2(9) |
| C(2)-C(1)-S(2)-C(20) | 80.7(9) |
| S(1)-C(1)-S(2)-C(20) | -38.2(7) |
| C(20B)-C(21B)-S(1B)-O(2B) | -121.0(9) |
| C(20B)-C(21B)-S(1B)-O(1B) | 110.7(9) |
| C(20B)-C(21B)-S(1B)-C(1B) | -3.0(10) |
| C(11B)-C(1B)-S(1B)-O(2B) | -104.6(8) |
| C(2B)-C(1B)-S(1B)-O(2B) | 26.3(10) |
| S(2B)-C(1B)-S(1B)-O(2B) | 144.0(5) |
| C(11B)-C(1B)-S(1B)-O(1B) | 26.5(9) |
| C(2B)-C(1B)-S(1B)-O(1B) | 157.4(8) |
| S(2B)-C(1B)-S(1B)-O(1B) | -84.9(6) |
| C(11B)-C(1B)-S(1B)-C(21B) | 141.9(8) |
| C(2B)-C(1B)-S(1B)-C(21B) | -87.2(9) |
| S(2B)-C(1B)-S(1B)-C(21B) | 30.5(7) |
| C(21B)-C(20B)-S(2B)-O(3B) | -61.2(10) |
| C(21B)-C(20B)-S(2B)-O(4B) | 168.0(9) |
| C(21B)-C(20B)-S(2B)-C(1B) | 48.4(9) |
| C(11B)-C(1B)-S(2B)-O(3B) | -48.7(9) |
| C(2B)-C(1B)-S(2B)-O(3B) | -175.1(8) |
| S(1B)-C(1B)-S(2B)-O(3B) | 65.9(6) |
| C(11B)-C(1B)-S(2B)-O(4B) | 85.3(9) |
| C(2B)-C(1B)-S(2B)-O(4B) | -41.1(10) |
| S(1B)-C(1B)-S(2B)-O(4B) | -160.1(5) |

| | |
|---|---|
| C(11B)-C(1B)-S(2B)-C(20B) | -160.4(9) |
| C(2B)-C(1B)-S(2B)-C(20B) | 73.2(10) |
| S(1B)-C(1B)-S(2B)-C(20B) | -45.8(7) |
| C(21C)-C(20C)-S(1C)-O(1C) | 128.0(11) |
| C(21C)-C(20C)-S(1C)-O(2C) | -103.3(11) |
| C(21C)-C(20C)-S(1C)-C(1C) | 9.2(12) |
| C(2C)-C(1C)-S(1C)-O(1C) | 95.9(10) |
| C(11C)-C(1C)-S(1C)-O(1C) | -31.4(11) |
| S(2C)-C(1C)-S(1C)-O(1C) | -148.1(6) |
| C(2C)-C(1C)-S(1C)-O(2C) | -35.7(11) |
| C(11C)-C(1C)-S(1C)-O(2C) | -163.0(9) |
| S(2C)-C(1C)-S(1C)-O(2C) | 80.3(7) |
| C(2C)-C(1C)-S(1C)-C(20C) | -148.5(9) |
| C(11C)-C(1C)-S(1C)-C(20C) | 84.1(11) |
| S(2C)-C(1C)-S(1C)-C(20C) | -32.6(8) |
| C(20C)-C(21C)-S(2C)-O(4C) | 70.9(12) |
| C(20C)-C(21C)-S(2C)-O(3C) | -162.1(11) |
| C(20C)-C(21C)-S(2C)-C(1C) | -42.4(12) |
| C(2C)-C(1C)-S(2C)-O(4C) | 42.5(11) |
| C(11C)-C(1C)-S(2C)-O(4C) | 171.6(8) |
| S(1C)-C(1C)-S(2C)-O(4C) | -71.4(7) |
| C(2C)-C(1C)-S(2C)-O(3C) | -87.6(10) |
| C(11C)-C(1C)-S(2C)-O(3C) | 41.5(10) |
| S(1C)-C(1C)-S(2C)-O(3C) | 158.5(6) |
| C(2C)-C(1C)-S(2C)-C(21C) | 157.5(10) |
| C(11C)-C(1C)-S(2C)-C(21C) | -73.4(10) |
| S(1C)-C(1C)-S(2C)-C(21C) | 43.7(8) |

**C.3. *st*-[$PE_3$]$_2$**

A suitable crystal of ***st*-[$PE_3$]$_2$** was coated with Paratone N oil, suspended in a small fiber loop and placed in a cooled nitrogen gas stream at 173 K on a Bruker D8 SMART APEX CCD sealed tube diffractometer with graphite monochromated MoKα (0.71073Å) radiation. Data was measured using a series of combinations of phi and omega scans with 10 s frame exposures and 0.3º frame widths. Data collection, indexing and initial cell refinements were all carried out using SMART[3] software. Frame integration and final cell refinements were done using SAINT[4] software. The final cell parameters were determined from least-squares refinement on 3398 reflections. The SADABS[5] program was used to carry out absorption corrections. The structure was solved using Direct methods and difference Fourier techniques (SHELXTL, V6.12).[6] Hydrogen atoms were placed in their expected chemical positions using the HIX command and were included in the final cycles of least-squares with isotropic Uij's related to the riding atom. The C-H distances were fixed at 0.93 Å (aromatic), 0.98 (methane), 0.97 Å ($CH_2$), or 0.96 Å ($CH_3$). All non-hydrogen atoms were refined anisotropically. Scattering factors and anomalous dispersion corrections are taken from the *International Tables for x-ray Crystallography*.[7] Structure solution, refinement, graphics and generation of publication materials were performed using SHELXTL, V6.12 software. Additional details of data collection and structure refinement are given in Tables T1-T6. The crystals were all intimately twinned to some degree so data was collected on one clean sample that contained approximately equal contributions of the two components. The unit cells for each component were determined by using a beta test program written by George Sheldrick called Cell_Now. The reflection data was processed with SAINT, taking into account the overlapping of reflections from the two components and were corrected for absorption effects S9 by using TWINABS, a version of SADABS. The structure was solved using only the data that was generated by component 1, however the final refinements used all the data and included the contributions from both components.

**Table 1.** Crystal data and structure refinement for ***st*-[$PE_3$]$_2$**.

| | | |
|---|---|---|
| Identification code | sj_pa | |
| Empirical formula | C57 H46 O2 | |
| Formula weight | 762.94 | |
| Temperature | 293(2) K | |
| Wavelength | 1.54178 Å | |
| Crystal system | Triclinic | |
| Space group | P-1 | |
| Unit cell dimensions | a = 12.3555(8) Å | α = 91.846(6)°. |
| | b = 13.3765(8) Å | β = 107.045(6)°. |
| | c = 14.5765(12) Å | γ = 116.524(5)°. |
| Volume | 2023.0(2) $Å^3$ | |
| Z | 2 | |
| Density (calculated) | 1.252 $Mg/m^3$ | |
| Absorption coefficient | 0.570 $mm^{-1}$ | |
| F(000) | 808 | |
| Crystal size | 0.20 x 0.19 x 0.15 $mm^3$ | |
| Theta range for data collection | 3.23 to 69.26°. | |
| Index ranges | -14<=h<=14, -15<=k<=15, -16<=l<=17 | |
| Reflections collected | 15626 | |
| Independent reflections | 6350 [R(int) = 0.1796] | |
| Completeness to theta = 69.26° | 84.0 % | |
| Absorption correction | Semi-empirical from equivalents | |
| Max. and min. transmission | 0.9194 and 0.8946 | |
| Refinement method | Full-matrix least-squares on $F^2$ | |
| Data / restraints / parameters | 6350 / 0 / 533 | |
| Goodness-of-fit on $F^2$ | 1.018 | |
| Final R indices [I>2sigma(I)] | R1 = 0.0909, wR2 = 0.1882 | |
| R indices (all data) | R1 = 0.1820, wR2 = 0.2191 | |
| Extinction coefficient | 0.0047(3) | |
| Largest diff. peak and hole | 0.303 and -0.256 e.$Å^{-3}$ | |

**Table 2.** Atomic coordinates ( x $10^4$) and equivalent isotropic displacement parameters ($Å^2$x $10^3$) for ***st*-[$PE_3$]$_2$**. U(eq) is defined as one third of the trace of the orthogonalized $U^{ij}$ tensor.

| | x | y | z | U(eq) |
|---|---|---|---|---|
| C(1) | 7743(5) | 6741(4) | 3427(4) | 68(2) |
| C(2) | 9053(5) | 7329(4) | 3500(4) | 72(2) |
| C(3) | 9792(5) | 6753(4) | 3557(4) | 70(2) |
| C(4) | 9247(5) | 5618(4) | 3587(4) | 75(2) |
| C(5) | 7958(5) | 5034(4) | 3571(4) | 67(2) |
| C(6) | 7207(5) | 5594(4) | 3457(4) | 71(2) |
| C(7) | 5814(5) | 4905(4) | 3449(4) | 77(2) |
| C(8) | 4671(5) | 4835(4) | 2588(4) | 75(2) |
| C(9) | 4540(5) | 4379(4) | 1543(5) | 80(2) |
| C(10) | 5755(5) | 4920(4) | 1275(4) | 73(2) |
| C(11) | 6309(6) | 4255(4) | 1087(5) | 77(2) |
| C(12) | 7427(6) | 4747(5) | 863(4) | 77(2) |
| C(13) | 8022(5) | 5887(4) | 862(4) | 75(2) |
| C(14) | 7488(6) | 6563(4) | 1047(4) | 76(2) |
| C(15) | 6337(5) | 6075(4) | 1259(4) | 72(2) |
| C(16) | 5740(5) | 6792(4) | 1455(4) | 77(2) |
| C(17) | 5700(5) | 6980(4) | 2506(4) | 75(2) |
| C(18) | 7006(5) | 7411(4) | 3355(4) | 71(2) |
| C(19) | 4617(6) | 5963(4) | 2670(5) | 78(2) |
| C(20) | 3330(6) | 6177(6) | 3461(6) | 114(3) |
| C(21) | 2613(7) | 5791(8) | 2443(6) | 149(4) |
| C(22) | 9720(5) | 8561(5) | 3566(4) | 76(2) |
| C(23) | 10323(5) | 9567(5) | 3675(5) | 79(2) |
| C(24) | 11121(6) | 10763(5) | 3797(5) | 84(2) |
| C(25) | 10731(6) | 11542(5) | 4031(5) | 91(2) |
| C(26) | 11521(7) | 12700(5) | 4138(5) | 101(2) |
| C(27) | 12730(7) | 13096(5) | 4068(5) | 103(2) |
| C(28) | 13130(7) | 12345(5) | 3886(5) | 112(3) |
| C(29) | 12350(6) | 11184(5) | 3730(5) | 109(2) |
| C(30) | 7427(5) | 3855(4) | 3634(4) | 73(2) |
| C(31) | 7045(5) | 2883(4) | 3725(4) | 71(2) |
| C(32) | 6616(6) | 1700(4) | 3791(5) | 79(2) |
| C(33) | 7509(6) | 1287(5) | 3943(5) | 110(3) |
| C(34) | 7122(7) | 169(5) | 4030(5) | 117(3) |
| C(35) | 5893(7) | -558(5) | 3988(5) | 99(2) |
| C(36) | 5020(6) | -140(5) | 3856(5) | 102(2) |
| C(37) | 5388(6) | 972(5) | 3758(5) | 101(2) |
| C(38) | 8083(6) | 7754(5) | 1050(5) | 84(2) |
| C(39) | 8545(6) | 8761(5) | 1086(5) | 86(2) |
| C(40) | 9011(7) | 9966(5) | 1240(5) | 95(2) |
| C(41) | 10180(7) | 10733(6) | 1166(5) | 114(3) |

| | | | | |
|---|---|---|---|---|
| C(42) | 10585(7) | 11894(6) | 1322(5) | 116(3) |
| C(43) | 9859(9) | 12293(6) | 1531(6) | 123(3) |
| C(44) | 8687(9) | 11561(6) | 1632(7) | 145(4) |
| C(45) | 8272(8) | 10412(6) | 1482(6) | 143(4) |
| C(46) | 5678(6) | 3052(5) | 1097(4) | 77(2) |
| C(47) | 5124(5) | 2051(4) | 1122(4) | 77(2) |
| C(48) | 4400(6) | 877(5) | 1157(5) | 87(2) |
| C(49) | 4833(7) | 109(5) | 1119(5) | 103(2) |
| C(50) | 4109(8) | -1038(5) | 1151(5) | 106(2) |
| C(51) | 2938(8) | -1375(6) | 1243(6) | 131(3) |
| C(52) | 2492(8) | -627(6) | 1320(7) | 162(4) |
| C(53) | 3192(7) | 489(6) | 1286(6) | 135(3) |
| C(54) | 8011(6) | 4018(5) | 653(5) | 102(2) |
| C(55) | 9282(6) | 6436(5) | 656(5) | 104(2) |
| C(56) | 11142(5) | 7381(4) | 3546(5) | 93(2) |
| C(57) | 9998(5) | 4977(4) | 3656(4) | 89(2) |
| O(1) | 3390(4) | 5769(3) | 1949(3) | 86(1) |
| O(2) | 4552(4) | 6218(3) | 3614(3) | 81(1) |

**Table 3.** Bond lengths [Å] and angles [°] for ***st*-[$PE_3$]$_2$**.

| | | | |
|---|---|---|---|
| C(1)-C(6) | 1.382(6) | C(31)-C(32) | 1.444(6) |
| C(1)-C(2) | 1.417(7) | C(32)-C(37) | 1.374(8) |
| C(1)-C(18) | 1.525(6) | C(32)-C(33) | 1.407(7) |
| C(2)-C(3) | 1.422(6) | C(33)-C(34) | 1.375(7) |
| C(2)-C(22) | 1.461(7) | C(34)-C(35) | 1.370(9) |
| C(3)-C(4) | 1.367(6) | C(35)-C(36) | 1.391(8) |
| C(3)-C(56) | 1.501(7) | C(36)-C(37) | 1.373(7) |
| C(4)-C(5) | 1.418(7) | C(38)-C(39) | 1.197(7) |
| C(4)-C(57) | 1.506(6) | C(39)-C(40) | 1.433(7) |
| C(5)-C(6) | 1.411(6) | C(40)-C(41) | 1.387(9) |
| C(5)-C(30) | 1.430(6) | C(40)-C(45) | 1.406(9) |
| C(6)-C(7) | 1.543(7) | C(41)-C(42) | 1.390(8) |
| C(7)-C(8) | 1.555(6) | C(42)-C(43) | 1.326(10) |
| C(8)-C(19) | 1.542(6) | C(43)-C(44) | 1.394(10) |
| C(8)-C(9) | 1.558(7) | C(44)-C(45) | 1.372(8) |
| C(9)-C(10) | 1.524(7) | C(46)-C(47) | 1.210(7) |
| C(10)-C(15) | 1.387(7) | C(47)-C(48) | 1.430(7) |
| C(10)-C(11) | 1.406(7) | C(48)-C(49) | 1.360(7) |
| C(11)-C(12) | 1.384(7) | C(48)-C(53) | 1.418(9) |
| C(11)-C(46) | 1.443(7) | C(49)-C(50) | 1.401(8) |
| C(12)-C(13) | 1.366(7) | C(50)-C(51) | 1.360(9) |
| C(12)-C(54) | 1.517(7) | C(51)-C(52) | 1.356(9) |
| C(13)-C(14) | 1.396(7) | C(52)-C(53) | 1.363(8) |
| C(13)-C(55) | 1.523(7) | | |
| C(14)-C(15) | 1.409(7) | C(6)-C(1)-C(2) | 118.3(4) |
| C(14)-C(38) | 1.425(7) | C(6)-C(1)-C(18) | 123.1(5) |
| C(15)-C(16) | 1.510(6) | C(2)-C(1)-C(18) | 118.5(4) |
| C(16)-C(17) | 1.563(7) | C(1)-C(2)-C(3) | 121.4(4) |
| C(17)-C(19) | 1.510(8) | C(1)-C(2)-C(22) | 121.4(4) |
| C(17)-C(18) | 1.556(7) | C(3)-C(2)-C(22) | 117.1(5) |
| C(19)-O(2) | 1.441(7) | C(4)-C(3)-C(2) | 119.5(5) |
| C(19)-O(1) | 1.471(6) | C(4)-C(3)-C(56) | 120.5(5) |
| C(20)-C(21) | 1.423(9) | C(2)-C(3)-C(56) | 120.0(5) |
| C(20)-O(2) | 1.435(6) | C(3)-C(4)-C(5) | 119.7(5) |
| C(21)-O(1) | 1.368(8) | C(3)-C(4)-C(57) | 121.2(5) |
| C(22)-C(23) | 1.188(6) | C(5)-C(4)-C(57) | 119.1(4) |
| C(23)-C(24) | 1.427(7) | C(6)-C(5)-C(4) | 120.6(4) |
| C(24)-C(25) | 1.398(7) | C(6)-C(5)-C(30) | 121.0(5) |
| C(24)-C(29) | 1.400(8) | C(4)-C(5)-C(30) | 118.4(4) |
| C(25)-C(26) | 1.386(7) | C(1)-C(6)-C(5) | 120.4(5) |
| C(26)-C(27) | 1.382(8) | C(1)-C(6)-C(7) | 121.8(4) |
| C(27)-C(28) | 1.351(8) | C(5)-C(6)-C(7) | 117.7(4) |
| C(28)-C(29) | 1.380(8) | C(6)-C(7)-C(8) | 120.1(5) |
| C(30)-C(31) | 1.197(6) | C(19)-C(8)-C(7) | 110.5(5) |

| | | | |
|---|---|---|---|
| C(19)-C(8)-C(9) | 113.3(5) | C(37)-C(32)-C(33) | 118.4(5) |
| C(7)-C(8)-C(9) | 116.6(5) | C(37)-C(32)-C(31) | 122.8(5) |
| C(10)-C(9)-C(8) | 116.3(5) | C(33)-C(32)-C(31) | 118.7(5) |
| C(15)-C(10)-C(11) | 120.5(6) | C(34)-C(33)-C(32) | 119.3(6) |
| C(15)-C(10)-C(9) | 119.8(5) | C(35)-C(34)-C(33) | 122.1(6) |
| C(11)-C(10)-C(9) | 119.7(5) | C(34)-C(35)-C(36) | 118.4(6) |
| C(12)-C(11)-C(10) | 119.9(5) | C(37)-C(36)-C(35) | 120.3(6) |
| C(12)-C(11)-C(46) | 120.6(5) | C(36)-C(37)-C(32) | 121.5(6) |
| C(10)-C(11)-C(46) | 119.4(6) | C(39)-C(38)-C(14) | 176.2(7) |
| C(13)-C(12)-C(11) | 120.1(5) | C(38)-C(39)-C(40) | 171.2(8) |
| C(13)-C(12)-C(54) | 120.4(6) | C(41)-C(40)-C(45) | 117.5(7) |
| C(11)-C(12)-C(54) | 119.5(5) | C(41)-C(40)-C(39) | 122.9(7) |
| C(12)-C(13)-C(14) | 120.7(6) | C(45)-C(40)-C(39) | 119.7(7) |
| C(12)-C(13)-C(55) | 120.1(5) | C(40)-C(41)-C(42) | 120.5(8) |
| C(14)-C(13)-C(55) | 119.2(5) | C(43)-C(42)-C(41) | 120.9(8) |
| C(13)-C(14)-C(15) | 120.0(5) | C(42)-C(43)-C(44) | 120.9(8) |
| C(13)-C(14)-C(38) | 122.1(6) | C(45)-C(44)-C(43) | 118.9(9) |
| C(15)-C(14)-C(38) | 117.9(5) | C(44)-C(45)-C(40) | 121.2(8) |
| C(10)-C(15)-C(14) | 118.7(5) | C(47)-C(46)-C(11) | 177.8(7) |
| C(10)-C(15)-C(16) | 120.6(5) | C(46)-C(47)-C(48) | 176.2(6) |
| C(14)-C(15)-C(16) | 120.7(5) | C(49)-C(48)-C(53) | 117.3(6) |
| C(15)-C(16)-C(17) | 117.9(5) | C(49)-C(48)-C(47) | 123.4(7) |
| C(19)-C(17)-C(18) | 112.6(5) | C(53)-C(48)-C(47) | 119.2(5) |
| C(19)-C(17)-C(16) | 111.9(5) | C(48)-C(49)-C(50) | 122.7(7) |
| C(18)-C(17)-C(16) | 115.5(5) | C(51)-C(50)-C(49) | 117.6(7) |
| C(1)-C(18)-C(17) | 118.9(4) | C(52)-C(51)-C(50) | 121.5(7) |
| O(2)-C(19)-O(1) | 106.0(5) | C(51)-C(52)-C(53) | 121.0(9) |
| O(2)-C(19)-C(17) | 109.6(5) | C(52)-C(53)-C(48) | 119.7(7) |
| O(1)-C(19)-C(17) | 108.5(5) | C(21)-O(1)-C(19) | 108.3(5) |
| O(2)-C(19)-C(8) | 108.6(5) | C(20)-O(2)-C(19) | 107.7(5) |
| O(1)-C(19)-C(8) | 107.5(4) | | |
| C(17)-C(19)-C(8) | 116.2(5) | | |
| C(21)-C(20)-O(2) | 107.3(6) | | |
| O(1)-C(21)-C(20) | 109.8(6) | | |
| C(23)-C(22)-C(2) | 175.6(6) | | |
| C(22)-C(23)-C(24) | 175.8(6) | | |
| C(25)-C(24)-C(29) | 118.5(6) | | |
| C(25)-C(24)-C(23) | 121.5(6) | | |
| C(29)-C(24)-C(23) | 120.0(5) | | |
| C(26)-C(25)-C(24) | 120.3(6) | | |
| C(27)-C(26)-C(25) | 120.2(6) | | |
| C(28)-C(27)-C(26) | 119.5(6) | | |
| C(27)-C(28)-C(29) | 122.2(7) | | |
| C(28)-C(29)-C(24) | 119.3(6) | | |
| C(31)-C(30)-C(5) | 176.4(6) | | |
| C(30)-C(31)-C(32) | 176.5(7) | | |

**Table 4.** Anisotropic displacement parameters ($Å^2 x\ 10^3$) for ***st*-[$PE_3$]$_2$**. The anisotropic displacement factor exponent takes the form: $-2\pi^2[ h^2 a^{*2} U^{11} + ... + 2 h k a^* b^* U^{12} ]$

| | $U^{11}$ | $U^{22}$ | $U^{33}$ | $U^{23}$ | $U^{13}$ | $U^{12}$ |
|---|---|---|---|---|---|---|
| C(1) | 57(3) | 58(3) | 84(5) | 16(3) | 22(3) | 24(3) |
| C(2) | 59(3) | 57(3) | 96(5) | 15(3) | 28(4) | 23(3) |
| C(3) | 59(3) | 64(3) | 84(5) | 15(3) | 26(3) | 26(3) |
| C(4) | 63(3) | 65(3) | 94(5) | 12(3) | 21(4) | 32(3) |
| C(5) | 63(3) | 58(3) | 76(4) | 16(3) | 20(3) | 29(3) |
| C(6) | 57(3) | 62(3) | 92(5) | 19(3) | 29(3) | 26(3) |
| C(7) | 56(3) | 63(3) | 108(5) | 22(3) | 24(4) | 27(3) |
| C(8) | 61(3) | 55(3) | 103(5) | 16(3) | 28(4) | 24(3) |
| C(9) | 69(4) | 68(3) | 95(5) | 12(4) | 28(4) | 27(3) |
| C(10) | 64(3) | 72(3) | 74(5) | 2(3) | 18(4) | 28(3) |
| C(11) | 73(4) | 65(3) | 89(5) | 5(3) | 30(4) | 31(3) |
| C(12) | 82(4) | 76(4) | 77(5) | 6(3) | 28(4) | 40(3) |
| C(13) | 71(4) | 72(4) | 84(5) | 12(3) | 39(4) | 28(3) |
| C(14) | 69(4) | 68(3) | 84(5) | 12(3) | 31(4) | 25(3) |
| C(15) | 69(4) | 63(3) | 79(5) | 12(3) | 24(4) | 27(3) |
| C(16) | 71(4) | 64(3) | 88(5) | 14(3) | 20(4) | 30(3) |
| C(17) | 75(4) | 52(3) | 84(5) | 5(3) | 16(4) | 28(3) |
| C(18) | 63(3) | 60(3) | 89(5) | 16(3) | 27(4) | 28(3) |
| C(19) | 69(4) | 65(3) | 89(5) | 16(4) | 15(4) | 33(3) |
| C(20) | 78(5) | 112(5) | 160(8) | 15(5) | 36(5) | 57(4) |
| C(21) | 88(6) | 244(11) | 128(8) | -4(7) | 28(6) | 97(7) |
| C(22) | 68(4) | 82(4) | 89(5) | 25(4) | 34(4) | 39(3) |
| C(23) | 70(4) | 65(3) | 105(6) | 28(4) | 33(4) | 32(3) |
| C(24) | 74(4) | 76(4) | 101(6) | 30(4) | 33(4) | 33(3) |
| C(25) | 87(4) | 77(4) | 109(6) | 15(4) | 36(4) | 38(4) |
| C(26) | 112(6) | 78(4) | 117(7) | 22(4) | 44(5) | 47(4) |
| C(27) | 101(6) | 75(4) | 113(6) | 13(4) | 34(5) | 27(4) |
| C(28) | 95(5) | 77(4) | 169(8) | 39(5) | 69(5) | 30(4) |
| C(29) | 89(5) | 76(4) | 158(7) | 30(5) | 52(5) | 31(4) |
| C(30) | 65(3) | 75(4) | 83(5) | 10(3) | 18(3) | 40(3) |
| C(31) | 65(3) | 65(3) | 82(5) | 11(3) | 23(3) | 32(3) |
| C(32) | 78(4) | 53(3) | 95(5) | 9(3) | 19(4) | 29(3) |
| C(33) | 91(5) | 68(4) | 180(8) | 29(4) | 46(5) | 44(4) |
| C(34) | 118(6) | 82(4) | 159(8) | 15(5) | 38(6) | 62(5) |
| C(35) | 113(6) | 72(4) | 130(7) | 32(4) | 58(5) | 48(4) |
| C(36) | 93(5) | 71(4) | 137(7) | 20(4) | 52(5) | 27(4) |
| C(37) | 84(5) | 68(4) | 157(7) | 30(4) | 53(5) | 34(3) |
| C(38) | 79(4) | 86(4) | 94(5) | 18(4) | 41(4) | 40(4) |
| C(39) | 82(4) | 68(4) | 106(6) | 28(4) | 40(4) | 28(3) |
| C(40) | 95(5) | 81(4) | 100(6) | 20(4) | 34(5) | 33(4) |
| C(41) | 118(6) | 91(5) | 116(7) | 19(5) | 46(5) | 32(5) |

| | | | | | | |
|---|---|---|---|---|---|---|
| C(42) | 107(6) | 82(5) | 127(7) | 25(5) | 26(5) | 27(4) |
| C(43) | 137(8) | 87(5) | 147(8) | 38(5) | 48(7) | 54(5) |
| C(44) | 155(9) | 103(6) | 197(10) | 43(7) | 68(8) | 72(6) |
| C(45) | 123(7) | 95(5) | 224(10) | 38(6) | 62(7) | 61(5) |
| C(46) | 81(4) | 82(4) | 77(5) | 12(4) | 34(4) | 43(3) |
| C(47) | 81(4) | 67(3) | 82(5) | 11(3) | 24(4) | 37(3) |
| C(48) | 88(5) | 70(4) | 95(5) | 12(4) | 21(4) | 38(4) |
| C(49) | 122(6) | 86(4) | 113(6) | 21(4) | 57(5) | 49(4) |
| C(50) | 131(7) | 77(4) | 109(6) | 14(4) | 45(6) | 47(5) |
| C(51) | 110(7) | 71(4) | 174(9) | 1(5) | 36(7) | 22(5) |
| C(52) | 99(6) | 86(5) | 249(12) | 21(7) | 22(7) | 24(5) |
| C(53) | 79(5) | 80(5) | 216(10) | 23(6) | 29(6) | 27(4) |
| C(54) | 99(5) | 95(4) | 130(6) | 21(4) | 52(5) | 54(4) |
| C(55) | 112(6) | 99(5) | 121(6) | 31(4) | 73(5) | 47(4) |
| C(56) | 62(4) | 79(4) | 130(6) | 16(4) | 32(4) | 29(3) |
| C(57) | 67(4) | 71(3) | 131(6) | 19(4) | 35(4) | 34(3) |
| O(1) | 68(3) | 87(3) | 100(4) | 13(2) | 22(3) | 39(2) |
| O(2) | 74(3) | 78(2) | 94(3) | 10(2) | 31(3) | 38(2) |

**Table 5.** Hydrogen coordinates ( x $10^4$) and isotropic displacement parameters (Å$^2$x $10^3$) for ***st*-[$PE_3$]$_2$**.

| | x | y | z | U(eq) |
|---|---|---|---|---|
| H(7A) | 5781 | 5213 | 4046 | 93 |
| H(7B) | 5655 | 4131 | 3488 | 93 |
| H(8) | 3894 | 4275 | 2696 | 90 |
| H(9A) | 4243 | 3566 | 1475 | 96 |
| H(9B) | 3878 | 4485 | 1073 | 96 |
| H(16A) | 4863 | 6446 | 999 | 92 |
| H(16B) | 6206 | 7534 | 1306 | 92 |
| H(17A) | 5476 | 7594 | 2529 | 90 |
| H(18A) | 7570 | 8182 | 3312 | 86 |
| H(18B) | 6846 | 7455 | 3965 | 86 |
| H(20A) | 2876 | 5660 | 3831 | 136 |
| H(20B) | 3453 | 6927 | 3672 | 136 |
| H(21A) | 1895 | 5035 | 2331 | 179 |
| H(21B) | 2271 | 6296 | 2203 | 179 |
| H(25A) | 9938 | 11282 | 4114 | 109 |
| H(26A) | 11237 | 13212 | 4258 | 121 |
| H(27A) | 13265 | 13873 | 4145 | 124 |
| H(28A) | 13957 | 12620 | 3865 | 134 |
| H(29A) | 12638 | 10686 | 3582 | 130 |
| H(33A) | 8352 | 1766 | 3983 | 132 |
| H(34A) | 7712 | -102 | 4120 | 140 |
| H(35A) | 5648 | -1312 | 4046 | 119 |
| H(36A) | 4184 | -616 | 3833 | 123 |
| H(37A) | 4793 | 1238 | 3668 | 121 |
| H(41A) | 10697 | 10468 | 1011 | 137 |
| H(42A) | 11376 | 12399 | 1279 | 139 |
| H(43A) | 10136 | 13071 | 1612 | 148 |
| H(44A) | 8195 | 11848 | 1798 | 174 |
| H(45A) | 7487 | 9919 | 1541 | 172 |
| H(49A) | 5643 | 356 | 1069 | 124 |
| H(50A) | 4419 | -1551 | 1112 | 127 |
| H(51A) | 2431 | -2136 | 1253 | 157 |
| H(52A) | 1696 | -880 | 1397 | 195 |
| H(53A) | 2879 | 995 | 1348 | 162 |
| H(54A) | 7474 | 3244 | 684 | 153 |
| H(54B) | 8855 | 4295 | 1130 | 153 |
| H(54C) | 8072 | 4055 | 12 | 153 |
| H(55A) | 9571 | 7236 | 687 | 155 |
| H(55B) | 9147 | 6093 | 16 | 155 |
| H(55C) | 9921 | 6324 | 1134 | 155 |
| H(56A) | 11510 | 6877 | 3604 | 139 |

| | | | | |
|---|---|---|---|---|
| H(56B) | 11651 | 8015 | 4083 | 139 |
| H(56C) | 11128 | 7651 | 2942 | 139 |
| H(57A) | 10849 | 5483 | 3662 | 133 |
| H(57B) | 9569 | 4364 | 3103 | 133 |
| H(57C) | 10056 | 4675 | 4247 | 133 |

**Table 6.** Torsion angles [°] for ***st*-[PE$_3$]$_2$**.

| | |
|---|---|
| C(6)-C(1)-C(2)-C(3) | 2.8(9) |
| C(18)-C(1)-C(2)-C(3) | -179.2(5) |
| C(6)-C(1)-C(2)-C(22) | -174.2(6) |
| C(18)-C(1)-C(2)-C(22) | 3.8(9) |
| C(1)-C(2)-C(3)-C(4) | -2.9(9) |
| C(22)-C(2)-C(3)-C(4) | 174.2(6) |
| C(1)-C(2)-C(3)-C(56) | 174.7(6) |
| C(22)-C(2)-C(3)-C(56) | -8.2(9) |
| C(2)-C(3)-C(4)-C(5) | -0.7(9) |
| C(56)-C(3)-C(4)-C(5) | -178.3(6) |
| C(2)-C(3)-C(4)-C(57) | -179.5(6) |
| C(56)-C(3)-C(4)-C(57) | 2.8(9) |
| C(3)-C(4)-C(5)-C(6) | 4.4(9) |
| C(57)-C(4)-C(5)-C(6) | -176.8(5) |
| C(3)-C(4)-C(5)-C(30) | -178.1(6) |
| C(57)-C(4)-C(5)-C(30) | 0.8(9) |
| C(2)-C(1)-C(6)-C(5) | 0.9(9) |
| C(18)-C(1)-C(6)-C(5) | -177.0(5) |
| C(2)-C(1)-C(6)-C(7) | 176.1(6) |
| C(18)-C(1)-C(6)-C(7) | -1.8(9) |
| C(4)-C(5)-C(6)-C(1) | -4.5(9) |
| C(30)-C(5)-C(6)-C(1) | 178.0(6) |
| C(4)-C(5)-C(6)-C(7) | -179.8(6) |
| C(30)-C(5)-C(6)-C(7) | 2.7(9) |
| C(1)-C(6)-C(7)-C(8) | 58.5(8) |
| C(5)-C(6)-C(7)-C(8) | -126.3(6) |
| C(6)-C(7)-C(8)-C(19) | -75.0(7) |
| C(6)-C(7)-C(8)-C(9) | 56.3(6) |
| C(19)-C(8)-C(9)-C(10) | 80.3(6) |
| C(7)-C(8)-C(9)-C(10) | -49.6(6) |
| C(8)-C(9)-C(10)-C(15) | -61.7(7) |
| C(8)-C(9)-C(10)-C(11) | 115.6(6) |
| C(15)-C(10)-C(11)-C(12) | -1.4(10) |
| C(9)-C(10)-C(11)-C(12) | -178.7(6) |
| C(15)-C(10)-C(11)-C(46) | -179.3(5) |
| C(9)-C(10)-C(11)-C(46) | 3.4(9) |

| | |
|---|---|
| C(10)-C(11)-C(12)-C(13) | 2.6(10) |
| C(46)-C(11)-C(12)-C(13) | -179.5(6) |
| C(10)-C(11)-C(12)-C(54) | -179.5(6) |
| C(46)-C(11)-C(12)-C(54) | -1.6(9) |
| C(11)-C(12)-C(13)-C(14) | -2.7(10) |
| C(54)-C(12)-C(13)-C(14) | 179.5(6) |
| C(11)-C(12)-C(13)-C(55) | 177.5(6) |
| C(54)-C(12)-C(13)-C(55) | -0.3(9) |
| C(12)-C(13)-C(14)-C(15) | 1.5(10) |
| C(55)-C(13)-C(14)-C(15) | -178.7(6) |
| C(12)-C(13)-C(14)-C(38) | -179.9(6) |
| C(55)-C(13)-C(14)-C(38) | -0.1(10) |
| C(11)-C(10)-C(15)-C(14) | 0.2(9) |
| C(9)-C(10)-C(15)-C(14) | 177.5(5) |
| C(11)-C(10)-C(15)-C(16) | 179.6(5) |
| C(9)-C(10)-C(15)-C(16) | -3.1(9) |
| C(13)-C(14)-C(15)-C(10) | -0.2(9) |
| C(38)-C(14)-C(15)-C(10) | -179.0(6) |
| C(13)-C(14)-C(15)-C(16) | -179.6(6) |
| C(38)-C(14)-C(15)-C(16) | 1.6(9) |
| C(10)-C(15)-C(16)-C(17) | 66.9(8) |
| C(14)-C(15)-C(16)-C(17) | -113.7(6) |
| C(15)-C(16)-C(17)-C(19) | -79.1(6) |
| C(15)-C(16)-C(17)-C(18) | 51.5(6) |
| C(6)-C(1)-C(18)-C(17) | -54.6(8) |
| C(2)-C(1)-C(18)-C(17) | 127.6(6) |
| C(19)-C(17)-C(18)-C(1) | 75.7(7) |
| C(16)-C(17)-C(18)-C(1) | -54.6(6) |
| C(18)-C(17)-C(19)-O(2) | 52.9(6) |
| C(16)-C(17)-C(19)-O(2) | -175.0(4) |
| C(18)-C(17)-C(19)-O(1) | 168.2(4) |
| C(16)-C(17)-C(19)-O(1) | -59.7(6) |
| C(18)-C(17)-C(19)-C(8) | -70.6(7) |
| C(16)-C(17)-C(19)-C(8) | 61.5(6) |
| C(7)-C(8)-C(19)-O(2) | -55.5(6) |
| C(9)-C(8)-C(19)-O(2) | 171.6(4) |
| C(7)-C(8)-C(19)-O(1) | -169.7(5) |
| C(9)-C(8)-C(19)-O(1) | 57.4(7) |
| C(7)-C(8)-C(19)-C(17) | 68.6(7) |
| C(9)-C(8)-C(19)-C(17) | -64.4(7) |
| O(2)-C(20)-C(21)-O(1) | -9.6(9) |
| C(1)-C(2)-C(22)-C(23) | 125(9) |
| C(3)-C(2)-C(22)-C(23) | -52(9) |
| C(2)-C(22)-C(23)-C(24) | 63(16) |
| C(22)-C(23)-C(24)-C(25) | -176(10) |
| C(22)-C(23)-C(24)-C(29) | 1(10) |

| | |
|---|---|
| C(29)-C(24)-C(25)-C(26) | 3.5(10) |
| C(23)-C(24)-C(25)-C(26) | -179.5(6) |
| C(24)-C(25)-C(26)-C(27) | -3.6(11) |
| C(25)-C(26)-C(27)-C(28) | 0.6(12) |
| C(26)-C(27)-C(28)-C(29) | 2.5(12) |
| C(27)-C(28)-C(29)-C(24) | -2.5(12) |
| C(25)-C(24)-C(29)-C(28) | -0.6(11) |
| C(23)-C(24)-C(29)-C(28) | -177.6(6) |
| C(6)-C(5)-C(30)-C(31) | -140(11) |
| C(4)-C(5)-C(30)-C(31) | 42(11) |
| C(5)-C(30)-C(31)-C(32) | -87(16) |
| C(30)-C(31)-C(32)-C(37) | -133(10) |
| C(30)-C(31)-C(32)-C(33) | 50(10) |
| C(37)-C(32)-C(33)-C(34) | 1.5(11) |
| C(31)-C(32)-C(33)-C(34) | 178.5(6) |
| C(32)-C(33)-C(34)-C(35) | -0.9(12) |
| C(33)-C(34)-C(35)-C(36) | -0.2(13) |
| C(34)-C(35)-C(36)-C(37) | 0.8(12) |
| C(35)-C(36)-C(37)-C(32) | -0.2(11) |
| C(33)-C(32)-C(37)-C(36) | -0.9(11) |
| C(31)-C(32)-C(37)-C(36) | -177.8(6) |
| C(13)-C(14)-C(38)-C(39) | -157(11) |
| C(15)-C(14)-C(38)-C(39) | 22(11) |
| C(14)-C(38)-C(39)-C(40) | 9(15) |
| C(38)-C(39)-C(40)-C(41) | 147(4) |
| C(38)-C(39)-C(40)-C(45) | -33(5) |
| C(45)-C(40)-C(41)-C(42) | -0.4(12) |
| C(39)-C(40)-C(41)-C(42) | 180.0(6) |
| C(40)-C(41)-C(42)-C(43) | -0.8(12) |
| C(41)-C(42)-C(43)-C(44) | 2.0(14) |
| C(42)-C(43)-C(44)-C(45) | -1.9(15) |
| C(43)-C(44)-C(45)-C(40) | 0.7(14) |
| C(41)-C(40)-C(45)-C(44) | 0.5(13) |
| C(39)-C(40)-C(45)-C(44) | -179.9(7) |
| C(12)-C(11)-C(46)-C(47) | 166(17) |
| C(10)-C(11)-C(46)-C(47) | -16(18) |
| C(11)-C(46)-C(47)-C(48) | 24(25) |
| C(46)-C(47)-C(48)-C(49) | -180(100) |
| C(46)-C(47)-C(48)-C(53) | -3(11) |
| C(53)-C(48)-C(49)-C(50) | 3.3(11) |
| C(47)-C(48)-C(49)-C(50) | -179.8(6) |
| C(48)-C(49)-C(50)-C(51) | -1.2(12) |
| C(49)-C(50)-C(51)-C(52) | -1.3(14) |
| C(50)-C(51)-C(52)-C(53) | 1.5(15) |
| C(51)-C(52)-C(53)-C(48) | 0.7(15) |
| C(49)-C(48)-C(53)-C(52) | -3.0(12) |

| | |
|---|---|
| C(47)-C(48)-C(53)-C(52) | 179.9(7) |
| C(20)-C(21)-O(1)-C(19) | 9.6(9) |
| O(2)-C(19)-O(1)-C(21) | -5.8(7) |
| C(17)-C(19)-O(1)-C(21) | -123.5(6) |
| C(8)-C(19)-O(1)-C(21) | 110.1(6) |
| C(21)-C(20)-O(2)-C(19) | 5.6(7) |
| O(1)-C(19)-O(2)-C(20) | 0.0(6) |
| C(17)-C(19)-O(2)-C(20) | 116.9(5) |
| C(8)-C(19)-O(2)-C(20) | -115.2(5) |

### *C.4. st-[$PE_3$-OHex]$_2$*

A suitable crystal of ***st*-[$PE_3$-OHex]$_2$** was coated with Paratone N oil, suspended in a small fiber loop and placed in a cooled nitrogen gas stream at 173 K on a Bruker D8 SMART APEX CCD sealed tube diffractometer with graphite monochromated MoKα (0.71073Å) radiation. Data was measured using a series of combinations of phi and omega scans with 10 s frame exposures and 0.3º frame widths. Data collection, indexing and initial cell refinements were all carried out using

SMART[3] software. Frame integration and final cell refinements were done using SAINT[4] software. The final cell parameters were determined from least-squares refinement on 3398 reflections. The SADABS[5] program was used to carry out absorption corrections. The structure was solved using Direct methods and difference Fourier techniques (SHELXTL, V6.12).[6] Hydrogen atoms were placed in their expected chemical positions using the HIX command and were included in the final cycles of least-squares with isotropic Uij's related to the riding atom. The C-H distances were fixed at 0.93 Å (aromatic), 0.98 (methane), 0.97 Å ($CH_2$), or 0.96 Å ($CH_3$). All non-hydrogen atoms were refined anisotropically. Scattering factors and anomalous dispersion corrections are taken from the *International Tables for x-ray Crystallography*.[7] Structure solution, refinement, graphics and generation of publication materials were performed using SHELXTL, V6.12 software. Additional details of data collection and structure refinement are given in Tables T1-T6. The crystals were all intimately twinned to some degree so data was collected on one clean sample that contained approximately equal contributions of the two components. The unit cells for each component were determined by using a beta test program written by George Sheldrick called Cell_Now. The reflection data was processed with SAINT, taking into account the overlapping of reflections from the two components and were corrected for absorption effects S9 by using TWINABS, a version of SADABS. The structure was solved using only the data that was generated by component 1, however the final refinements used all the data and included the contributions from both components.

**Table 1.** Crystal data and structure refinement for ***st*-[$PE_3$-OHex]$_2$**.

| | | |
|---|---|---|
| Identification code | sj_c1s | |
| Empirical formula | C81 H94 O6 | |
| Formula weight | 1163.56 | |
| Temperature | 173(2) K | |
| Wavelength | 0.71073 Å | |
| Crystal system | Triclinic | |
| Space group | P-1 | |
| Unit cell dimensions | a = 13.0501(19) Å | α = 85.270(2)°. |
| | b = 13.4975(19) Å | β = 88.528(2)°. |
| | c = 19.190(3) Å | γ = 86.500(2)°. |
| Volume | 3361.7(8) $Å^3$ | |
| Z | 2 | |
| Density (calculated) | 1.149 $Mg/m^3$ | |
| Absorption coefficient | 0.071 $mm^{-1}$ | |
| F(000) | 1256 | |
| Crystal size | 0.27 x 0.23 x 0.22 $mm^3$ | |
| Theta range for data collection | 1.06 to 26.37°. | |
| Index ranges | -16<=h<=16, -16<=k<=16, -23<=l<=23 | |
| Reflections collected | 52272 | |
| Independent reflections | 13744 [R(int) = 0.0548] | |
| Completeness to theta = 26.37° | 99.9 % | |
| Absorption correction | Semi-empirical from equivalents | |
| Max. and min. transmission | 0.9847 and 0.9812 | |
| Refinement method | Full-matrix least-squares on $F^2$ | |
| Data / restraints / parameters | 13744 / 1 / 784 | |
| Goodness-of-fit on $F^2$ | 1.056 | |
| Final R indices [I>2sigma(I)] | R1 = 0.0941, wR2 = 0.2658 | |
| R indices (all data) | R1 = 0.1695, wR2 = 0.3252 | |
| Largest diff. peak and hole | 1.283 and -0.462 e.$Å^{-3}$ | |

Table 2. Atomic coordinates ( x $10^4$) and equivalent isotropic displacement parameters ($Å^2$x $10^3$) for ***st*-[$PE_3$-OHex]$_2$**. U(eq) is defined as one third of the trace of the orthogonalized $U^{ij}$ tensor.

| | x | y | z | U(eq) |
|---|---|---|---|---|
| C(1) | 8040(4) | 6411(3) | 4255(3) | 81(1) |
| C(2) | 7331(3) | 5618(3) | 4533(2) | 53(1) |
| C(3) | 6846(2) | 5047(2) | 4067(2) | 45(1) |
| C(4) | 6177(2) | 4306(2) | 4313(2) | 41(1) |
| C(5) | 5704(3) | 3683(2) | 3801(2) | 43(1) |
| C(6) | 6046(2) | 2563(2) | 3878(2) | 41(1) |
| C(7) | 7226(2) | 2418(2) | 3928(2) | 43(1) |
| C(8) | 7645(2) | 1462(2) | 4305(2) | 43(1) |
| C(9) | 8220(2) | 738(2) | 3949(2) | 44(1) |
| C(10) | 8662(2) | -134(2) | 4314(2) | 47(1) |
| C(11) | 9286(3) | -870(3) | 3919(2) | 59(1) |
| C(12) | 9029(3) | -1161(3) | 5438(2) | 60(1) |
| C(13) | 8541(2) | -259(2) | 5031(2) | 47(1) |
| C(14) | 7950(2) | 462(2) | 5389(2) | 42(1) |
| C(15) | 7495(2) | 1314(2) | 5022(2) | 41(1) |
| C(16) | 6860(2) | 2096(2) | 5394(2) | 44(1) |
| C(17) | 5713(2) | 2269(2) | 5197(2) | 42(1) |
| C(18) | 5312(3) | 3338(2) | 5320(2) | 45(1) |
| C(19) | 5991(2) | 4145(2) | 5030(2) | 41(1) |
| C(20) | 6478(3) | 4710(2) | 5493(2) | 46(1) |
| C(21) | 7145(3) | 5450(3) | 5245(2) | 53(1) |
| C(22) | 7651(3) | 6042(3) | 5761(2) | 72(1) |
| C(23) | 5457(2) | 2002(2) | 4465(2) | 42(1) |
| C(24) | 7068(3) | 5203(2) | 3333(2) | 51(1) |
| C(25) | 7282(3) | 5328(3) | 2721(2) | 54(1) |
| C(26) | 7530(3) | 5426(3) | 1989(2) | 57(1) |
| C(27) | 8218(3) | 6102(3) | 1711(2) | 68(1) |
| C(28) | 8469(4) | 6172(4) | 1003(3) | 83(1) |
| C(29) | 8025(4) | 5571(5) | 565(2) | 89(2) |
| C(30) | 7316(4) | 4915(4) | 848(3) | 92(2) |
| C(31) | 7089(4) | 4845(3) | 1535(2) | 75(1) |
| C(32) | 8959(5) | 6179(8) | -446(3) | 163(4) |
| C(33) | 9046(6) | 5734(6) | -1220(3) | 129(2) |
| C(34) | 9714(5) | 6259(6) | -1636(3) | 123(2) |
| C(35) | 9734(4) | 6001(5) | -2383(3) | 99(2) |
| C(36) | 10343(5) | 6657(5) | -2852(4) | 120(2) |
| C(37) | 10349(4) | 6416(6) | -3602(3) | 123(2) |
| C(38) | 6303(3) | 4534(3) | 6229(2) | 54(1) |
| C(39) | 6153(3) | 4383(3) | 6850(2) | 61(1) |
| C(40) | 5990(3) | 4185(3) | 7584(2) | 60(1) |

| | | | | |
|---|---|---|---|---|
| C(41) | 6637(4) | 4531(4) | 8060(2) | 79(1) |
| C(42) | 6500(5) | 4317(5) | 8764(3) | 96(2) |
| C(43) | 5711(5) | 3748(5) | 9020(3) | 96(2) |
| C(44) | 5055(4) | 3409(5) | 8557(3) | 97(2) |
| C(45) | 5197(4) | 3626(4) | 7850(2) | 82(1) |
| C(46) | 4902(6) | 2966(9) | 10021(3) | 183(5) |
| C(47) | 5135(6) | 2949(11) | 10821(4) | 247(7) |
| C(48) | 4469(8) | 2629(13) | 11230(4) | 284(9) |
| C(49) | 4791(9) | 2667(12) | 12007(4) | 238(7) |
| C(50) | 4087(9) | 2212(10) | 12413(6) | 198(5) |
| C(51) | 3037(8) | 2640(6) | 12508(4) | 153(3) |
| C(52) | 8358(3) | 890(3) | 3205(2) | 50(1) |
| C(53) | 8465(3) | 1042(3) | 2580(2) | 56(1) |
| C(54) | 8637(3) | 1199(3) | 1846(2) | 55(1) |
| C(55) | 8142(3) | 1960(3) | 1437(2) | 68(1) |
| C(56) | 8337(4) | 2101(4) | 725(2) | 76(1) |
| C(57) | 9035(4) | 1453(4) | 409(2) | 72(1) |
| C(58) | 9531(4) | 705(4) | 812(2) | 74(1) |
| C(59) | 9343(3) | 573(3) | 1512(2) | 68(1) |
| C(60) | 8810(5) | 2226(4) | -746(3) | 103(2) |
| C(61) | 9268(5) | 2064(4) | -1488(3) | 99(2) |
| C(62) | 8931(5) | 2802(4) | -2014(3) | 109(2) |
| C(63) | 9290(4) | 2623(4) | -2740(3) | 92(2) |
| C(64) | 8798(5) | 3381(5) | -3281(4) | 115(2) |
| C(65) | 9088(4) | 3247(4) | -4005(3) | 103(2) |
| C(66) | 7814(2) | 337(2) | 6131(2) | 46(1) |
| C(67) | 7686(3) | 283(3) | 6754(2) | 53(1) |
| C(68) | 7482(3) | 258(3) | 7491(2) | 58(1) |
| C(69) | 6761(4) | 928(4) | 7760(2) | 80(1) |
| C(70) | 6537(4) | 908(4) | 8457(3) | 93(2) |
| C(71) | 7025(4) | 201(4) | 8921(2) | 76(1) |
| C(72) | 7752(3) | -469(3) | 8666(2) | 69(1) |
| C(73) | 7981(3) | -438(3) | 7962(2) | 61(1) |
| C(74) | 7151(4) | -490(4) | 10111(2) | 81(1) |
| C(75) | 6657(4) | -310(4) | 10805(2) | 90(2) |
| C(76) | 7040(4) | -1053(4) | 11393(2) | 81(1) |
| C(77) | 6535(4) | -862(4) | 12091(2) | 80(1) |
| C(78) | 6902(4) | -1584(4) | 12686(2) | 88(2) |
| C(79) | 6339(4) | -1392(5) | 13367(3) | 105(2) |
| C(80) | 4716(3) | 601(3) | 4146(2) | 57(1) |
| C(81) | 3886(3) | 1313(3) | 4402(2) | 56(1) |
| O(1) | 5620(2) | 954(2) | 4423(1) | 49(1) |
| O(2) | 4386(2) | 2224(2) | 4351(1) | 50(1) |
| O(3) | 8229(3) | 5539(4) | -131(2) | 139(2) |
| O(4) | 5666(4) | 3574(4) | 9730(2) | 136(2) |
| O(5) | 9287(3) | 1507(3) | -285(2) | 97(1) |

| | | | | |
|---|---|---|---|---|
| O(6) | 6726(3) | 242(3) | 9604(2) | 99(1) |

**Table 3.** Bond lengths [Å] and angles [°] for ***st*-[PE$_3$-OHex]$_2$**.

| | | | |
|---|---|---|---|
| C(1)-C(2) | 1.513(5) | C(17)-H(17) | 1.0000 |
| C(1)-H(1A) | 0.9800 | C(18)-C(19) | 1.509(4) |
| C(1)-H(1B) | 0.9800 | C(18)-H(18A) | 0.9900 |
| C(1)-H(1C) | 0.9800 | C(18)-H(18B) | 0.9900 |
| C(2)-C(21) | 1.383(5) | C(19)-C(20) | 1.404(5) |
| C(2)-C(3) | 1.414(5) | C(20)-C(21) | 1.411(5) |
| C(3)-C(4) | 1.411(4) | C(20)-C(38) | 1.428(5) |
| C(3)-C(24) | 1.433(5) | C(21)-C(22) | 1.510(5) |
| C(4)-C(19) | 1.393(5) | C(22)-H(22A) | 0.9800 |
| C(4)-C(5) | 1.512(4) | C(22)-H(22B) | 0.9800 |
| C(5)-C(6) | 1.545(5) | C(22)-H(22C) | 0.9800 |
| C(5)-H(5A) | 0.9900 | C(23)-O(1) | 1.427(4) |
| C(5)-H(5B) | 0.9900 | C(23)-O(2) | 1.431(4) |
| C(6)-C(23) | 1.523(4) | C(24)-C(25) | 1.200(5) |
| C(6)-C(7) | 1.545(4) | C(25)-C(26) | 1.430(5) |
| C(6)-H(6) | 1.0000 | C(26)-C(31) | 1.378(6) |
| C(7)-C(8) | 1.505(5) | C(26)-C(27) | 1.386(5) |
| C(7)-H(7A) | 0.9900 | C(27)-C(28) | 1.387(6) |
| C(7)-H(7B) | 0.9900 | C(27)-H(27) | 0.9500 |
| C(8)-C(15) | 1.384(5) | C(28)-C(29) | 1.378(7) |
| C(8)-C(9) | 1.407(5) | C(28)-H(28) | 0.9500 |
| C(9)-C(10) | 1.418(5) | C(29)-O(3) | 1.358(6) |
| C(9)-C(52) | 1.435(5) | C(29)-C(30) | 1.389(7) |
| C(10)-C(13) | 1.380(5) | C(30)-C(31) | 1.341(6) |
| C(10)-C(11) | 1.489(5) | C(30)-H(30) | 0.9500 |
| C(11)-H(11A) | 0.9800 | C(31)-H(31) | 0.9500 |
| C(11)-H(11B) | 0.9800 | C(32)-O(3) | 1.415(9) |
| C(11)-H(11C) | 0.9800 | C(32)-C(33) | 1.646(9) |
| C(12)-C(13) | 1.507(5) | C(32)-H(32A) | 0.9900 |
| C(12)-H(12A) | 0.9800 | C(32)-H(32B) | 0.9900 |
| C(12)-H(12B) | 0.9800 | C(33)-C(34) | 1.359(8) |
| C(12)-H(12C) | 0.9800 | C(33)-H(33A) | 0.9900 |
| C(13)-C(14) | 1.416(5) | C(33)-H(33B) | 0.9900 |
| C(14)-C(15) | 1.406(5) | C(34)-C(35) | 1.501(8) |
| C(14)-C(66) | 1.427(5) | C(34)-H(34A) | 0.9900 |
| C(15)-C(16) | 1.515(5) | C(34)-H(34B) | 0.9900 |
| C(16)-C(17) | 1.551(5) | C(35)-C(36) | 1.464(8) |
| C(16)-H(16A) | 0.9900 | C(35)-H(35A) | 0.9900 |
| C(16)-H(16B) | 0.9900 | C(35)-H(35B) | 0.9900 |
| C(17)-C(23) | 1.528(5) | C(36)-C(37) | 1.502(8) |
| C(17)-C(18) | 1.539(5) | C(36)-H(36A) | 0.9900 |

| | | | |
|---|---|---|---|
| C(36)-H(36B) | 0.9900 | C(58)-C(59) | 1.359(6) |
| C(37)-H(37A) | 0.9800 | C(58)-H(58) | 0.9500 |
| C(37)-H(37B) | 0.9800 | C(59)-H(59) | 0.9500 |
| C(37)-H(37C) | 0.9800 | C(60)-O(5) | 1.388(6) |
| C(38)-C(39) | 1.205(5) | C(60)-C(61) | 1.556(7) |
| C(39)-C(40) | 1.425(6) | C(60)-H(60A) | 0.9900 |
| C(40)-C(45) | 1.380(6) | C(60)-H(60B) | 0.9900 |
| C(40)-C(41) | 1.387(6) | C(61)-C(62) | 1.417(8) |
| C(41)-C(42) | 1.367(7) | C(61)-H(61A) | 0.9900 |
| C(41)-H(41) | 0.9500 | C(61)-H(61B) | 0.9900 |
| C(42)-C(43) | 1.379(8) | C(62)-C(63) | 1.492(7) |
| C(42)-H(42) | 0.9500 | C(62)-H(62A) | 0.9900 |
| C(43)-O(4) | 1.363(6) | C(62)-H(62B) | 0.9900 |
| C(43)-C(44) | 1.374(8) | C(63)-C(64) | 1.522(8) |
| C(44)-C(45) | 1.374(6) | C(63)-H(63A) | 0.9900 |
| C(44)-H(44) | 0.9500 | C(63)-H(63B) | 0.9900 |
| C(45)-H(45) | 0.9500 | C(64)-C(65) | 1.453(8) |
| C(46)-O(4) | 1.406(10) | C(64)-H(64A) | 0.9900 |
| C(46)-C(47) | 1.572(10) | C(64)-H(64B) | 0.9900 |
| C(46)-H(46A) | 0.9900 | C(65)-H(65A) | 0.9800 |
| C(46)-H(46B) | 0.9900 | C(65)-H(65B) | 0.9800 |
| C(47)-C(48) | 1.230(11) | C(65)-H(65C) | 0.9800 |
| C(47)-H(47A) | 0.9900 | C(66)-C(67) | 1.200(5) |
| C(47)-H(47B) | 0.9900 | C(67)-C(68) | 1.429(6) |
| C(48)-C(49) | 1.565(11) | C(68)-C(69) | 1.386(6) |
| C(48)-H(48A) | 0.9900 | C(68)-C(73) | 1.393(5) |
| C(48)-H(48B) | 0.9900 | C(69)-C(70) | 1.359(6) |
| C(49)-C(50) | 1.335(12) | C(69)-H(69) | 0.9500 |
| C(49)-H(49A) | 0.9900 | C(70)-C(71) | 1.387(7) |
| C(49)-H(49B) | 0.9900 | C(70)-H(70) | 0.9500 |
| C(50)-C(51) | 1.466(12) | C(71)-O(6) | 1.361(5) |
| C(50)-H(50A) | 0.9900 | C(71)-C(72) | 1.379(7) |
| C(50)-H(50B) | 0.9900 | C(72)-C(73) | 1.374(6) |
| C(51)-H(51A) | 0.9800 | C(72)-H(72) | 0.9500 |
| C(51)-H(51B) | 0.9800 | C(73)-H(73) | 0.9500 |
| C(51)-H(51C) | 0.9800 | C(74)-O(6) | 1.426(6) |
| C(52)-C(53) | 1.205(5) | C(74)-C(75) | 1.496(6) |
| C(53)-C(54) | 1.423(6) | C(74)-H(74A) | 0.9900 |
| C(54)-C(55) | 1.378(6) | C(74)-H(74B) | 0.9900 |
| C(54)-C(59) | 1.392(5) | C(75)-C(76) | 1.521(7) |
| C(55)-C(56) | 1.382(6) | C(75)-H(75A) | 0.9900 |
| C(55)-H(55) | 0.9500 | C(75)-H(75B) | 0.9900 |
| C(56)-C(57) | 1.388(6) | C(76)-C(77) | 1.511(6) |
| C(56)-H(56) | 0.9500 | C(76)-H(76A) | 0.9900 |
| C(57)-C(58) | 1.361(6) | C(76)-H(76B) | 0.9900 |
| C(57)-O(5) | 1.361(5) | C(77)-C(78) | 1.508(7) |

| | |
|---|---|
| C(77)-H(77A) | 0.9900 |
| C(77)-H(77B) | 0.9900 |
| C(78)-C(79) | 1.515(7) |
| C(78)-H(78A) | 0.9900 |
| C(78)-H(78B) | 0.9900 |
| C(79)-H(79A) | 0.9800 |
| C(79)-H(79B) | 0.9800 |
| C(79)-H(79C) | 0.9800 |
| C(80)-O(1) | 1.430(4) |
| C(80)-C(81) | 1.503(5) |
| C(80)-H(80A) | 0.9900 |
| C(80)-H(80B) | 0.9900 |
| C(81)-O(2) | 1.422(4) |
| C(81)-H(81A) | 0.9900 |
| C(81)-H(81B) | 0.9900 |

| | |
|---|---|
| C(2)-C(1)-H(1A) | 109.7 |
| C(2)-C(1)-H(1B) | 109.4 |
| H(1A)-C(1)-H(1B) | 109.5 |
| C(2)-C(1)-H(1C) | 109.4 |
| H(1A)-C(1)-H(1C) | 109.5 |
| H(1B)-C(1)-H(1C) | 109.5 |
| C(21)-C(2)-C(3) | 119.4(3) |
| C(21)-C(2)-C(1) | 120.4(3) |
| C(3)-C(2)-C(1) | 120.2(4) |
| C(4)-C(3)-C(2) | 121.3(3) |
| C(4)-C(3)-C(24) | 119.6(3) |
| C(2)-C(3)-C(24) | 119.0(3) |
| C(19)-C(4)-C(3) | 118.9(3) |
| C(19)-C(4)-C(5) | 121.2(3) |
| C(3)-C(4)-C(5) | 119.9(3) |
| C(4)-C(5)-C(6) | 114.9(3) |
| C(4)-C(5)-H(5A) | 108.5 |
| C(6)-C(5)-H(5A) | 108.5 |
| C(4)-C(5)-H(5B) | 108.5 |
| C(6)-C(5)-H(5B) | 108.5 |
| H(5A)-C(5)-H(5B) | 107.5 |
| C(23)-C(6)-C(5) | 111.9(3) |
| C(23)-C(6)-C(7) | 114.4(3) |
| C(5)-C(6)-C(7) | 110.7(3) |
| C(23)-C(6)-H(6) | 106.4 |
| C(5)-C(6)-H(6) | 106.4 |
| C(7)-C(6)-H(6) | 106.4 |
| C(8)-C(7)-C(6) | 116.7(3) |
| C(8)-C(7)-H(7A) | 108.1 |
| C(6)-C(7)-H(7A) | 108.1 |
| C(8)-C(7)-H(7B) | 108.1 |
| C(6)-C(7)-H(7B) | 108.1 |
| H(7A)-C(7)-H(7B) | 107.3 |
| C(15)-C(8)-C(9) | 119.5(3) |
| C(15)-C(8)-C(7) | 119.1(3) |
| C(9)-C(8)-C(7) | 121.3(3) |
| C(8)-C(9)-C(10) | 121.1(3) |
| C(8)-C(9)-C(52) | 119.1(3) |
| C(10)-C(9)-C(52) | 119.8(3) |
| C(13)-C(10)-C(9) | 119.1(3) |
| C(13)-C(10)-C(11) | 121.5(3) |
| C(9)-C(10)-C(11) | 119.4(3) |
| C(10)-C(11)-H(11A) | 109.4 |
| C(10)-C(11)-H(11B) | 109.4 |
| H(11A)-C(11)-H(11B) | 109.5 |
| C(10)-C(11)-H(11C) | 109.6 |
| H(11A)-C(11)-H(11C) | 109.5 |
| H(11B)-C(11)-H(11C) | 109.5 |
| C(13)-C(12)-H(12A) | 109.4 |
| C(13)-C(12)-H(12B) | 109.6 |
| H(12A)-C(12)-H(12B) | 109.5 |
| C(13)-C(12)-H(12C) | 109.3 |
| H(12A)-C(12)-H(12C) | 109.5 |
| H(12B)-C(12)-H(12C) | 109.5 |
| C(10)-C(13)-C(14) | 119.8(3) |
| C(10)-C(13)-C(12) | 120.5(3) |
| C(14)-C(13)-C(12) | 119.6(3) |
| C(15)-C(14)-C(13) | 120.7(3) |
| C(15)-C(14)-C(66) | 118.9(3) |
| C(13)-C(14)-C(66) | 120.4(3) |
| C(8)-C(15)-C(14) | 119.7(3) |
| C(8)-C(15)-C(16) | 118.6(3) |
| C(14)-C(15)-C(16) | 121.7(3) |
| C(15)-C(16)-C(17) | 117.1(3) |
| C(15)-C(16)-H(16A) | 108.0 |
| C(17)-C(16)-H(16A) | 108.0 |
| C(15)-C(16)-H(16B) | 108.0 |
| C(17)-C(16)-H(16B) | 108.0 |
| H(16A)-C(16)-H(16B) | 107.3 |
| C(23)-C(17)-C(18) | 111.2(3) |
| C(23)-C(17)-C(16) | 115.4(3) |
| C(18)-C(17)-C(16) | 110.8(3) |
| C(23)-C(17)-H(17) | 106.3 |
| C(18)-C(17)-H(17) | 106.3 |
| C(16)-C(17)-H(17) | 106.3 |
| C(19)-C(18)-C(17) | 115.2(3) |

| | | | |
|---|---|---|---|
| C(19)-C(18)-H(18A) | 108.5 | O(3)-C(32)-C(33) | 98.5(7) |
| C(17)-C(18)-H(18A) | 108.5 | O(3)-C(32)-H(32A) | 112.1 |
| C(19)-C(18)-H(18B) | 108.5 | C(33)-C(32)-H(32A) | 112.1 |
| C(17)-C(18)-H(18B) | 108.5 | O(3)-C(32)-H(32B) | 112.1 |
| H(18A)-C(18)-H(18B) | 107.5 | C(33)-C(32)-H(32B) | 112.1 |
| C(4)-C(19)-C(20) | 119.7(3) | H(32A)-C(32)-H(32B) | 109.7 |
| C(4)-C(19)-C(18) | 120.8(3) | C(34)-C(33)-C(32) | 109.6(6) |
| C(20)-C(19)-C(18) | 119.4(3) | C(34)-C(33)-H(33A) | 109.7 |
| C(19)-C(20)-C(21) | 121.2(3) | C(32)-C(33)-H(33A) | 109.7 |
| C(19)-C(20)-C(38) | 119.8(3) | C(34)-C(33)-H(33B) | 109.7 |
| C(21)-C(20)-C(38) | 119.0(3) | C(32)-C(33)-H(33B) | 109.7 |
| C(2)-C(21)-C(20) | 119.4(3) | H(33A)-C(33)-H(33B) | 108.2 |
| C(2)-C(21)-C(22) | 121.1(3) | C(33)-C(34)-C(35) | 113.4(6) |
| C(20)-C(21)-C(22) | 119.5(4) | C(33)-C(34)-H(34A) | 108.9 |
| C(21)-C(22)-H(22A) | 109.5 | C(35)-C(34)-H(34A) | 108.9 |
| C(21)-C(22)-H(22B) | 109.4 | C(33)-C(34)-H(34B) | 108.9 |
| H(22A)-C(22)-H(22B) | 109.5 | C(35)-C(34)-H(34B) | 108.9 |
| C(21)-C(22)-H(22C) | 109.5 | H(34A)-C(34)-H(34B) | 107.7 |
| H(22A)-C(22)-H(22C) | 109.5 | C(36)-C(35)-C(34) | 113.5(6) |
| H(22B)-C(22)-H(22C) | 109.5 | C(36)-C(35)-H(35A) | 108.9 |
| O(1)-C(23)-O(2) | 105.7(2) | C(34)-C(35)-H(35A) | 108.9 |
| O(1)-C(23)-C(6) | 110.4(3) | C(36)-C(35)-H(35B) | 108.9 |
| O(2)-C(23)-C(6) | 107.6(3) | C(34)-C(35)-H(35B) | 108.9 |
| O(1)-C(23)-C(17) | 109.6(3) | H(35A)-C(35)-H(35B) | 107.7 |
| O(2)-C(23)-C(17) | 109.1(3) | C(35)-C(36)-C(37) | 113.9(5) |
| C(6)-C(23)-C(17) | 114.1(3) | C(35)-C(36)-H(36A) | 108.8 |
| C(25)-C(24)-C(3) | 178.2(4) | C(37)-C(36)-H(36A) | 108.8 |
| C(24)-C(25)-C(26) | 177.2(4) | C(35)-C(36)-H(36B) | 108.8 |
| C(31)-C(26)-C(27) | 117.6(4) | C(37)-C(36)-H(36B) | 108.8 |
| C(31)-C(26)-C(25) | 120.8(3) | H(36A)-C(36)-H(36B) | 107.7 |
| C(27)-C(26)-C(25) | 121.6(4) | C(36)-C(37)-H(37A) | 109.3 |
| C(26)-C(27)-C(28) | 120.9(4) | C(36)-C(37)-H(37B) | 109.8 |
| C(26)-C(27)-H(27) | 119.5 | H(37A)-C(37)-H(37B) | 109.5 |
| C(28)-C(27)-H(27) | 119.5 | C(36)-C(37)-H(37C) | 109.4 |
| C(29)-C(28)-C(27) | 119.9(4) | H(37A)-C(37)-H(37C) | 109.5 |
| C(29)-C(28)-H(28) | 120.0 | H(37B)-C(37)-H(37C) | 109.5 |
| C(27)-C(28)-H(28) | 120.0 | C(39)-C(38)-C(20) | 179.8(5) |
| O(3)-C(29)-C(28) | 125.9(5) | C(38)-C(39)-C(40) | 178.7(4) |
| O(3)-C(29)-C(30) | 115.6(5) | C(45)-C(40)-C(41) | 117.3(4) |
| C(28)-C(29)-C(30) | 118.4(4) | C(45)-C(40)-C(39) | 121.5(4) |
| C(31)-C(30)-C(29) | 121.1(5) | C(41)-C(40)-C(39) | 121.1(4) |
| C(31)-C(30)-H(30) | 119.5 | C(42)-C(41)-C(40) | 121.2(5) |
| C(29)-C(30)-H(30) | 119.5 | C(42)-C(41)-H(41) | 119.4 |
| C(30)-C(31)-C(26) | 122.0(4) | C(40)-C(41)-H(41) | 119.4 |
| C(30)-C(31)-H(31) | 119.0 | C(41)-C(42)-C(43) | 120.7(5) |
| C(26)-C(31)-H(31) | 119.0 | C(41)-C(42)-H(42) | 119.7 |

| | | | |
|---|---|---|---|
| C(43)-C(42)-H(42) | 119.7 | C(53)-C(52)-C(9) | 178.3(4) |
| O(4)-C(43)-C(44) | 126.1(6) | C(52)-C(53)-C(54) | 177.3(4) |
| O(4)-C(43)-C(42) | 115.0(6) | C(55)-C(54)-C(59) | 117.2(4) |
| C(44)-C(43)-C(42) | 118.9(5) | C(55)-C(54)-C(53) | 123.1(3) |
| C(43)-C(44)-C(45) | 120.1(5) | C(59)-C(54)-C(53) | 119.7(4) |
| C(43)-C(44)-H(44) | 119.9 | C(54)-C(55)-C(56) | 121.7(4) |
| C(45)-C(44)-H(44) | 119.9 | C(54)-C(55)-H(55) | 119.1 |
| C(44)-C(45)-C(40) | 121.7(5) | C(56)-C(55)-H(55) | 119.1 |
| C(44)-C(45)-H(45) | 119.1 | C(55)-C(56)-C(57) | 119.5(4) |
| C(40)-C(45)-H(45) | 119.1 | C(55)-C(56)-H(56) | 120.3 |
| O(4)-C(46)-C(47) | 100.9(8) | C(57)-C(56)-H(56) | 120.3 |
| O(4)-C(46)-H(46A) | 111.6 | C(58)-C(57)-O(5) | 115.8(4) |
| C(47)-C(46)-H(46A) | 111.6 | C(58)-C(57)-C(56) | 119.0(4) |
| O(4)-C(46)-H(46B) | 111.6 | O(5)-C(57)-C(56) | 125.1(5) |
| C(47)-C(46)-H(46B) | 111.6 | C(59)-C(58)-C(57) | 121.3(4) |
| H(46A)-C(46)-H(46B) | 109.4 | C(59)-C(58)-H(58) | 119.3 |
| C(48)-C(47)-C(46) | 116.3(10) | C(57)-C(58)-H(58) | 119.3 |
| C(48)-C(47)-H(47A) | 108.2 | C(58)-C(59)-C(54) | 121.3(4) |
| C(46)-C(47)-H(47A) | 108.2 | C(58)-C(59)-H(59) | 119.3 |
| C(48)-C(47)-H(47B) | 108.2 | C(54)-C(59)-H(59) | 119.3 |
| C(46)-C(47)-H(47B) | 108.2 | O(5)-C(60)-C(61) | 106.9(5) |
| H(47A)-C(47)-H(47B) | 107.4 | O(5)-C(60)-H(60A) | 110.3 |
| C(47)-C(48)-C(49) | 111.1(11) | C(61)-C(60)-H(60A) | 110.3 |
| C(47)-C(48)-H(48A) | 109.4 | O(5)-C(60)-H(60B) | 110.3 |
| C(49)-C(48)-H(48A) | 109.4 | C(61)-C(60)-H(60B) | 110.3 |
| C(47)-C(48)-H(48B) | 109.4 | H(60A)-C(60)-H(60B) | 108.6 |
| C(49)-C(48)-H(48B) | 109.4 | C(62)-C(61)-C(60) | 114.1(5) |
| H(48A)-C(48)-H(48B) | 108.0 | C(62)-C(61)-H(61A) | 108.7 |
| C(50)-C(49)-C(48) | 107.4(11) | C(60)-C(61)-H(61A) | 108.7 |
| C(50)-C(49)-H(49A) | 110.2 | C(62)-C(61)-H(61B) | 108.7 |
| C(48)-C(49)-H(49A) | 110.2 | C(60)-C(61)-H(61B) | 108.7 |
| C(50)-C(49)-H(49B) | 110.2 | H(61A)-C(61)-H(61B) | 107.6 |
| C(48)-C(49)-H(49B) | 110.2 | C(61)-C(62)-C(63) | 115.3(5) |
| H(49A)-C(49)-H(49B) | 108.5 | C(61)-C(62)-H(62A) | 108.4 |
| C(49)-C(50)-C(51) | 122.8(12) | C(63)-C(62)-H(62A) | 108.4 |
| C(49)-C(50)-H(50A) | 106.6 | C(61)-C(62)-H(62B) | 108.4 |
| C(51)-C(50)-H(50A) | 106.6 | C(63)-C(62)-H(62B) | 108.4 |
| C(49)-C(50)-H(50B) | 106.6 | H(62A)-C(62)-H(62B) | 107.5 |
| C(51)-C(50)-H(50B) | 106.6 | C(62)-C(63)-C(64) | 112.0(5) |
| H(50A)-C(50)-H(50B) | 106.6 | C(62)-C(63)-H(63A) | 109.2 |
| C(50)-C(51)-H(51A) | 109.3 | C(64)-C(63)-H(63A) | 109.2 |
| C(50)-C(51)-H(51B) | 110.4 | C(62)-C(63)-H(63B) | 109.2 |
| H(51A)-C(51)-H(51B) | 109.5 | C(64)-C(63)-H(63B) | 109.2 |
| C(50)-C(51)-H(51C) | 108.7 | H(63A)-C(63)-H(63B) | 107.9 |
| H(51A)-C(51)-H(51C) | 109.5 | C(65)-C(64)-C(63) | 115.6(5) |
| H(51B)-C(51)-H(51C) | 109.5 | C(65)-C(64)-H(64A) | 108.4 |

| | |
|---|---|
| C(63)-C(64)-H(64A) | 108.4 |
| C(65)-C(64)-H(64B) | 108.4 |
| C(63)-C(64)-H(64B) | 108.4 |
| H(64A)-C(64)-H(64B) | 107.4 |
| C(64)-C(65)-H(65A) | 109.5 |
| C(64)-C(65)-H(65B) | 109.5 |
| H(65A)-C(65)-H(65B) | 109.5 |
| C(64)-C(65)-H(65C) | 109.4 |
| H(65A)-C(65)-H(65C) | 109.5 |
| H(65B)-C(65)-H(65C) | 109.5 |
| C(67)-C(66)-C(14) | 176.7(4) |
| C(66)-C(67)-C(68) | 176.6(4) |
| C(69)-C(68)-C(73) | 117.5(4) |
| C(69)-C(68)-C(67) | 120.4(4) |
| C(73)-C(68)-C(67) | 122.1(4) |
| C(70)-C(69)-C(68) | 121.7(4) |
| C(70)-C(69)-H(69) | 119.1 |
| C(68)-C(69)-H(69) | 119.1 |
| C(69)-C(70)-C(71) | 120.4(5) |
| C(69)-C(70)-H(70) | 119.8 |
| C(71)-C(70)-H(70) | 119.8 |
| O(6)-C(71)-C(72) | 125.8(4) |
| O(6)-C(71)-C(70) | 115.3(5) |
| C(72)-C(71)-C(70) | 119.0(4) |
| C(73)-C(72)-C(71) | 120.2(4) |
| C(73)-C(72)-H(72) | 119.9 |
| C(71)-C(72)-H(72) | 119.9 |
| C(72)-C(73)-C(68) | 121.2(4) |
| C(72)-C(73)-H(73) | 119.4 |
| C(68)-C(73)-H(73) | 119.4 |
| O(6)-C(74)-C(75) | 108.0(4) |
| O(6)-C(74)-H(74A) | 110.1 |
| C(75)-C(74)-H(74A) | 110.1 |
| O(6)-C(74)-H(74B) | 110.1 |
| C(75)-C(74)-H(74B) | 110.1 |
| H(74A)-C(74)-H(74B) | 108.4 |
| C(74)-C(75)-C(76) | 113.2(5) |
| C(74)-C(75)-H(75A) | 108.9 |
| C(76)-C(75)-H(75A) | 108.9 |
| C(74)-C(75)-H(75B) | 108.9 |
| C(76)-C(75)-H(75B) | 108.9 |
| H(75A)-C(75)-H(75B) | 107.8 |
| C(77)-C(76)-C(75) | 112.6(5) |
| C(77)-C(76)-H(76A) | 109.1 |
| C(75)-C(76)-H(76A) | 109.1 |
| C(77)-C(76)-H(76B) | 109.1 |
| C(75)-C(76)-H(76B) | 109.1 |
| H(76A)-C(76)-H(76B) | 107.8 |
| C(78)-C(77)-C(76) | 113.9(5) |
| C(78)-C(77)-H(77A) | 108.8 |
| C(76)-C(77)-H(77A) | 108.8 |
| C(78)-C(77)-H(77B) | 108.8 |
| C(76)-C(77)-H(77B) | 108.8 |
| H(77A)-C(77)-H(77B) | 107.7 |
| C(77)-C(78)-C(79) | 111.9(5) |
| C(77)-C(78)-H(78A) | 109.2 |
| C(79)-C(78)-H(78A) | 109.2 |
| C(77)-C(78)-H(78B) | 109.2 |
| C(79)-C(78)-H(78B) | 109.2 |
| H(78A)-C(78)-H(78B) | 107.9 |
| C(78)-C(79)-H(79A) | 109.1 |
| C(78)-C(79)-H(79B) | 109.7 |
| H(79A)-C(79)-H(79B) | 109.5 |
| C(78)-C(79)-H(79C) | 109.6 |
| H(79A)-C(79)-H(79C) | 109.5 |
| H(79B)-C(79)-H(79C) | 109.5 |
| O(1)-C(80)-C(81) | 102.4(3) |
| O(1)-C(80)-H(80A) | 111.3 |
| C(81)-C(80)-H(80A) | 111.3 |
| O(1)-C(80)-H(80B) | 111.3 |
| C(81)-C(80)-H(80B) | 111.3 |
| H(80A)-C(80)-H(80B) | 109.2 |
| O(2)-C(81)-C(80) | 101.8(3) |
| O(2)-C(81)-H(81A) | 111.4 |
| C(80)-C(81)-H(81A) | 111.4 |
| O(2)-C(81)-H(81B) | 111.4 |
| C(80)-C(81)-H(81B) | 111.4 |
| H(81A)-C(81)-H(81B) | 109.3 |
| C(23)-O(1)-C(80) | 107.9(2) |
| C(81)-O(2)-C(23) | 108.3(2) |
| C(29)-O(3)-C(32) | 118.1(5) |
| C(43)-O(4)-C(46) | 117.6(6) |
| C(57)-O(5)-C(60) | 120.6(4) |
| C(71)-O(6)-C(74) | 118.9(4) |

**Table 4.** Anisotropic displacement parameters ($Å^2 x\ 10^3$) for ***st*-[$PE_3$-OHex]$_2$**. The anisotropic displacement factor exponent takes the form: $-2\pi^2[ h^2 a^{*2} U^{11} + ... + 2 h k a^* b^* U^{12} ]$

| | $U^{11}$ | $U^{22}$ | $U^{33}$ | $U^{23}$ | $U^{13}$ | $U^{12}$ |
|---|---|---|---|---|---|---|
| C(1) | 73(3) | 68(3) | 104(4) | 1(2) | -6(3) | -33(2) |
| C(2) | 43(2) | 45(2) | 73(3) | -4(2) | -8(2) | -8(2) |
| C(3) | 39(2) | 40(2) | 57(2) | -3(2) | -3(2) | -2(1) |
| C(4) | 37(2) | 35(2) | 50(2) | -6(1) | 0(1) | -1(1) |
| C(5) | 43(2) | 41(2) | 45(2) | 0(2) | -5(2) | -6(1) |
| C(6) | 43(2) | 43(2) | 38(2) | -5(1) | -2(1) | -8(1) |
| C(7) | 43(2) | 43(2) | 44(2) | -5(2) | 5(2) | -5(1) |
| C(8) | 37(2) | 43(2) | 49(2) | -8(2) | 1(2) | -6(1) |
| C(9) | 33(2) | 44(2) | 58(2) | -12(2) | -1(2) | -7(1) |
| C(10) | 35(2) | 42(2) | 66(3) | -12(2) | -1(2) | -6(1) |
| C(11) | 48(2) | 50(2) | 80(3) | -15(2) | -3(2) | 0(2) |
| C(12) | 48(2) | 44(2) | 88(3) | -5(2) | -9(2) | -5(2) |
| C(13) | 35(2) | 41(2) | 66(3) | -3(2) | -9(2) | -9(1) |
| C(14) | 35(2) | 40(2) | 54(2) | -3(2) | -6(2) | -8(1) |
| C(15) | 34(2) | 43(2) | 48(2) | -7(2) | -4(1) | -7(1) |
| C(16) | 50(2) | 39(2) | 43(2) | -4(1) | -3(2) | -5(2) |
| C(17) | 45(2) | 40(2) | 41(2) | -1(1) | 6(1) | -6(1) |
| C(18) | 41(2) | 47(2) | 45(2) | -6(2) | 5(2) | -2(2) |
| C(19) | 37(2) | 34(2) | 51(2) | -7(1) | -1(2) | 1(1) |
| C(20) | 45(2) | 41(2) | 53(2) | -11(2) | -6(2) | 5(2) |
| C(21) | 47(2) | 43(2) | 70(3) | -13(2) | -16(2) | -4(2) |
| C(22) | 75(3) | 60(2) | 86(3) | -15(2) | -30(2) | -13(2) |
| C(23) | 40(2) | 38(2) | 50(2) | -4(2) | 1(2) | -5(1) |
| C(24) | 45(2) | 38(2) | 68(3) | 1(2) | 1(2) | -9(2) |
| C(25) | 54(2) | 48(2) | 60(3) | 1(2) | 3(2) | -13(2) |
| C(26) | 57(2) | 55(2) | 58(2) | -3(2) | 2(2) | -9(2) |
| C(27) | 71(3) | 78(3) | 57(3) | -6(2) | 10(2) | -20(2) |
| C(28) | 75(3) | 105(4) | 67(3) | 8(3) | 13(2) | -14(3) |
| C(29) | 78(3) | 135(5) | 52(3) | -15(3) | -2(2) | 9(3) |
| C(30) | 90(4) | 115(4) | 75(4) | -26(3) | -7(3) | -13(3) |
| C(31) | 88(3) | 75(3) | 66(3) | -10(2) | -1(2) | -18(2) |
| C(32) | 98(5) | 330(12) | 51(3) | 37(5) | 12(3) | 5(6) |
| C(33) | 124(6) | 167(7) | 96(5) | 6(4) | -15(4) | -21(5) |
| C(34) | 88(4) | 183(7) | 106(5) | -41(5) | 8(4) | -27(4) |
| C(35) | 82(4) | 120(5) | 99(4) | -27(3) | -8(3) | -10(3) |
| C(36) | 80(4) | 106(5) | 177(7) | -11(4) | -16(4) | -26(3) |
| C(37) | 72(4) | 185(7) | 110(5) | 27(5) | -26(3) | -42(4) |
| C(38) | 58(2) | 47(2) | 57(3) | -17(2) | -12(2) | 6(2) |
| C(39) | 67(3) | 57(2) | 62(3) | -16(2) | -13(2) | 8(2) |
| C(40) | 69(3) | 66(3) | 47(2) | -14(2) | -11(2) | 16(2) |
| C(41) | 87(3) | 88(3) | 64(3) | -23(2) | -14(2) | 12(3) |

| | | | | | | |
|---|---|---|---|---|---|---|
| C(42) | 105(4) | 126(5) | 60(3) | -36(3) | -24(3) | 26(4) |
| C(43) | 80(4) | 148(5) | 56(3) | -18(3) | -5(3) | 39(4) |
| C(44) | 73(3) | 153(5) | 63(3) | 0(3) | -2(3) | 9(3) |
| C(45) | 67(3) | 119(4) | 60(3) | -13(3) | -7(2) | 4(3) |
| C(46) | 125(6) | 343(14) | 65(4) | 25(6) | 30(4) | 44(7) |
| C(47) | 112(6) | 520(20) | 82(5) | 55(9) | 14(5) | 65(9) |
| C(48) | 153(9) | 600(30) | 81(6) | 16(10) | -6(6) | 55(13) |
| C(49) | 204(11) | 430(20) | 80(6) | 9(8) | -46(6) | -42(13) |
| C(50) | 163(9) | 304(14) | 126(8) | 47(8) | -78(7) | -53(10) |
| C(51) | 178(8) | 138(6) | 153(7) | -49(5) | 12(6) | -45(6) |
| C(52) | 42(2) | 48(2) | 62(3) | -17(2) | 3(2) | -3(2) |
| C(53) | 48(2) | 58(2) | 63(3) | -18(2) | 2(2) | -7(2) |
| C(54) | 52(2) | 62(2) | 55(2) | -22(2) | 3(2) | -6(2) |
| C(55) | 69(3) | 72(3) | 64(3) | -18(2) | 4(2) | 4(2) |
| C(56) | 93(3) | 71(3) | 66(3) | -9(2) | -10(2) | -4(2) |
| C(57) | 86(3) | 76(3) | 57(3) | -21(2) | 3(2) | -9(3) |
| C(58) | 74(3) | 92(3) | 58(3) | -25(2) | 5(2) | 9(3) |
| C(59) | 67(3) | 78(3) | 59(3) | -20(2) | -3(2) | 7(2) |
| C(60) | 169(6) | 67(3) | 76(4) | -8(3) | -6(4) | -16(3) |
| C(61) | 146(5) | 79(3) | 75(4) | -24(3) | -3(3) | 4(3) |
| C(62) | 149(5) | 70(3) | 111(5) | -18(3) | 45(4) | -23(3) |
| C(63) | 103(4) | 81(3) | 96(4) | -31(3) | 42(3) | -32(3) |
| C(64) | 99(4) | 87(4) | 158(6) | -25(4) | -11(4) | 17(3) |
| C(65) | 67(3) | 103(4) | 137(5) | -6(4) | -8(3) | 4(3) |
| C(66) | 38(2) | 44(2) | 57(3) | -1(2) | -10(2) | -6(2) |
| C(67) | 49(2) | 54(2) | 56(3) | 0(2) | -12(2) | -10(2) |
| C(68) | 54(2) | 66(2) | 54(2) | -1(2) | -11(2) | -12(2) |
| C(69) | 81(3) | 94(3) | 59(3) | 5(2) | -6(2) | 13(3) |
| C(70) | 92(4) | 113(4) | 69(3) | -5(3) | 4(3) | 24(3) |
| C(71) | 83(3) | 96(4) | 50(3) | 0(2) | -5(2) | -13(3) |
| C(72) | 73(3) | 78(3) | 56(3) | -1(2) | -13(2) | -6(2) |
| C(73) | 66(3) | 67(3) | 52(3) | -3(2) | -12(2) | -10(2) |
| C(74) | 95(3) | 95(4) | 54(3) | 4(2) | -8(2) | -22(3) |
| C(75) | 97(4) | 109(4) | 64(3) | -2(3) | -4(3) | -25(3) |
| C(76) | 92(3) | 101(4) | 52(3) | -4(2) | 1(2) | -26(3) |
| C(77) | 83(3) | 93(3) | 65(3) | -9(3) | 3(2) | -21(3) |
| C(78) | 88(3) | 115(4) | 60(3) | 4(3) | 4(2) | -7(3) |
| C(79) | 104(4) | 143(5) | 62(3) | 6(3) | 12(3) | 22(4) |
| C(80) | 61(2) | 47(2) | 65(3) | -5(2) | -11(2) | -14(2) |
| C(81) | 49(2) | 50(2) | 71(3) | -2(2) | -5(2) | -18(2) |
| O(1) | 48(1) | 39(1) | 60(2) | -5(1) | -1(1) | -10(1) |
| O(2) | 39(1) | 45(1) | 68(2) | -4(1) | -3(1) | -9(1) |
| O(3) | 101(3) | 262(6) | 53(2) | -21(3) | 9(2) | 3(3) |
| O(4) | 130(4) | 227(5) | 44(2) | -15(3) | -2(2) | 52(4) |
| O(5) | 133(3) | 110(3) | 48(2) | -14(2) | 13(2) | -5(2) |
| O(6) | 111(3) | 126(3) | 58(2) | -4(2) | 3(2) | 4(2) |

**Table 5.** Hydrogen coordinates ( x $10^4$) and isotropic displacement parameters (Å$^2$x $10^3$) for ***st*-[$PE_3$-OHex]$_2$**.

| | x | y | z | U(eq) |
|---|---|---|---|---|
| H(1A) | 7748 | 7068 | 4363 | 122 |
| H(1B) | 8123 | 6393 | 3747 | 122 |
| H(1C) | 8711 | 6283 | 4473 | 122 |
| H(5A) | 5878 | 3953 | 3321 | 52 |
| H(5B) | 4947 | 3751 | 3860 | 52 |
| H(6) | 5860 | 2285 | 3434 | 49 |
| H(7A) | 7522 | 2460 | 3447 | 52 |
| H(7B) | 7474 | 2980 | 4164 | 52 |
| H(11A) | 9991 | -925 | 4086 | 88 |
| H(11B) | 9288 | -647 | 3419 | 88 |
| H(11C) | 8989 | -1521 | 3989 | 88 |
| H(12A) | 8709 | -1759 | 5315 | 89 |
| H(12B) | 8931 | -1094 | 5941 | 89 |
| H(12C) | 9765 | -1217 | 5323 | 89 |
| H(16A) | 7189 | 2737 | 5303 | 52 |
| H(16B) | 6890 | 1910 | 5903 | 52 |
| H(17) | 5324 | 1818 | 5533 | 51 |
| H(18A) | 4628 | 3461 | 5107 | 54 |
| H(18B) | 5220 | 3387 | 5830 | 54 |
| H(22A) | 8381 | 6084 | 5636 | 108 |
| H(22B) | 7581 | 5710 | 6232 | 108 |
| H(22C) | 7319 | 6714 | 5750 | 108 |
| H(27) | 8522 | 6524 | 2010 | 82 |
| H(28) | 8948 | 6635 | 820 | 100 |
| H(30) | 6987 | 4510 | 551 | 110 |
| H(31) | 6611 | 4380 | 1714 | 91 |
| H(32A) | 9621 | 6103 | -201 | 196 |
| H(32B) | 8701 | 6886 | -474 | 196 |
| H(33A) | 9289 | 5023 | -1169 | 155 |
| H(33B) | 8362 | 5784 | -1435 | 155 |
| H(34A) | 10413 | 6133 | -1447 | 148 |
| H(34B) | 9524 | 6979 | -1623 | 148 |
| H(35A) | 10018 | 5306 | -2403 | 119 |
| H(35B) | 9021 | 6034 | -2551 | 119 |
| H(36A) | 11059 | 6613 | -2688 | 144 |
| H(36B) | 10067 | 7352 | -2823 | 144 |
| H(37A) | 10738 | 5780 | -3649 | 184 |
| H(37B) | 10670 | 6943 | -3898 | 184 |
| H(37C) | 9642 | 6366 | -3749 | 184 |
| H(41) | 7185 | 4925 | 7894 | 95 |
| H(42) | 6954 | 4562 | 9080 | 116 |

| | | | | |
|---|---|---|---|---|
| H(44) | 4501 | 3024 | 8726 | 117 |
| H(45) | 4738 | 3386 | 7536 | 98 |
| H(46A) | 4976 | 2291 | 9854 | 219 |
| H(46B) | 4205 | 3263 | 9916 | 219 |
| H(47A) | 5781 | 2539 | 10911 | 297 |
| H(47B) | 5257 | 3637 | 10929 | 297 |
| H(48A) | 4352 | 1933 | 11141 | 341 |
| H(48B) | 3817 | 3032 | 11150 | 341 |
| H(49A) | 5477 | 2325 | 12081 | 286 |
| H(49B) | 4822 | 3367 | 12120 | 286 |
| H(50A) | 4381 | 2092 | 12885 | 238 |
| H(50B) | 4026 | 1549 | 12237 | 238 |
| H(51A) | 3051 | 3210 | 12792 | 229 |
| H(51B) | 2601 | 2142 | 12742 | 229 |
| H(51C) | 2761 | 2863 | 12048 | 229 |
| H(55) | 7655 | 2399 | 1649 | 82 |
| H(56) | 7996 | 2637 | 455 | 91 |
| H(58) | 10019 | 266 | 599 | 89 |
| H(59) | 9700 | 43 | 1779 | 81 |
| H(60A) | 8941 | 2901 | -616 | 124 |
| H(60B) | 8059 | 2156 | -736 | 124 |
| H(61A) | 10026 | 2052 | -1469 | 119 |
| H(61B) | 9082 | 1406 | -1620 | 119 |
| H(62A) | 9167 | 3451 | -1899 | 131 |
| H(62B) | 8171 | 2853 | -2003 | 131 |
| H(63A) | 9123 | 1946 | -2843 | 110 |
| H(63B) | 10046 | 2657 | -2772 | 110 |
| H(64A) | 8043 | 3357 | -3231 | 138 |
| H(64B) | 8978 | 4054 | -3175 | 138 |
| H(65A) | 9835 | 3265 | -4064 | 155 |
| H(65B) | 8754 | 3782 | -4311 | 155 |
| H(65C) | 8871 | 2602 | -4128 | 155 |
| H(69) | 6414 | 1414 | 7450 | 95 |
| H(70) | 6043 | 1382 | 8626 | 112 |
| H(72) | 8095 | -954 | 8979 | 83 |
| H(73) | 8490 | -898 | 7794 | 74 |
| H(74A) | 7903 | -439 | 10132 | 97 |
| H(74B) | 7019 | -1166 | 9984 | 97 |
| H(75A) | 5904 | -345 | 10770 | 107 |
| H(75B) | 6791 | 370 | 10921 | 107 |
| H(76A) | 6904 | -1734 | 11279 | 97 |
| H(76B) | 7792 | -1019 | 11430 | 97 |
| H(77A) | 6667 | -178 | 12201 | 96 |
| H(77B) | 5783 | -897 | 12052 | 96 |
| H(78A) | 7647 | -1526 | 12745 | 106 |
| H(78B) | 6798 | -2272 | 12571 | 106 |

| | | | | |
|---|---|---|---|---|
| H(79A) | 6419 | -702 | 13470 | 158 |
| H(79B) | 6625 | -1846 | 13747 | 158 |
| H(79C) | 5608 | -1499 | 13323 | 158 |
| H(80A) | 4607 | -92 | 4331 | 69 |
| H(80B) | 4751 | 636 | 3629 | 69 |
| H(81A) | 3278 | 1356 | 4100 | 68 |
| H(81B) | 3673 | 1118 | 4890 | 68 |

**Table 6.** Torsion angles [°] for ***st*-[PE$_3$-OHex]$_2$**.

| | |
|---|---|
| C(21)-C(2)-C(3)-C(4) | -0.2(5) |
| C(1)-C(2)-C(3)-C(4) | -179.7(3) |
| C(21)-C(2)-C(3)-C(24) | -178.0(3) |
| C(1)-C(2)-C(3)-C(24) | 2.5(5) |
| C(2)-C(3)-C(4)-C(19) | 0.5(5) |
| C(24)-C(3)-C(4)-C(19) | 178.3(3) |
| C(2)-C(3)-C(4)-C(5) | -177.7(3) |
| C(24)-C(3)-C(4)-C(5) | 0.1(5) |
| C(19)-C(4)-C(5)-C(6) | -63.4(4) |
| C(3)-C(4)-C(5)-C(6) | 114.7(3) |
| C(4)-C(5)-C(6)-C(23) | 81.0(3) |
| C(4)-C(5)-C(6)-C(7) | -47.8(4) |
| C(23)-C(6)-C(7)-C(8) | 26.6(4) |
| C(5)-C(6)-C(7)-C(8) | 154.0(3) |
| C(6)-C(7)-C(8)-C(15) | -69.5(4) |
| C(6)-C(7)-C(8)-C(9) | 113.1(3) |
| C(15)-C(8)-C(9)-C(10) | -1.1(5) |
| C(7)-C(8)-C(9)-C(10) | 176.3(3) |
| C(15)-C(8)-C(9)-C(52) | 179.0(3) |
| C(7)-C(8)-C(9)-C(52) | -3.6(4) |
| C(8)-C(9)-C(10)-C(13) | -1.3(5) |
| C(52)-C(9)-C(10)-C(13) | 178.6(3) |
| C(8)-C(9)-C(10)-C(11) | -178.5(3) |
| C(52)-C(9)-C(10)-C(11) | 1.4(4) |
| C(9)-C(10)-C(13)-C(14) | 2.2(4) |
| C(11)-C(10)-C(13)-C(14) | 179.4(3) |
| C(9)-C(10)-C(13)-C(12) | -178.0(3) |
| C(11)-C(10)-C(13)-C(12) | -0.9(5) |
| C(10)-C(13)-C(14)-C(15) | -0.8(4) |
| C(12)-C(13)-C(14)-C(15) | 179.4(3) |
| C(10)-C(13)-C(14)-C(66) | 179.6(3) |
| C(12)-C(13)-C(14)-C(66) | -0.1(4) |
| C(9)-C(8)-C(15)-C(14) | 2.5(4) |
| C(7)-C(8)-C(15)-C(14) | -175.0(3) |
| C(9)-C(8)-C(15)-C(16) | -179.1(3) |

| | |
|---|---|
| C(7)-C(8)-C(15)-C(16) | 3.5(4) |
| C(13)-C(14)-C(15)-C(8) | -1.6(4) |
| C(66)-C(14)-C(15)-C(8) | 178.0(3) |
| C(13)-C(14)-C(15)-C(16) | -180.0(3) |
| C(66)-C(14)-C(15)-C(16) | -0.4(4) |
| C(8)-C(15)-C(16)-C(17) | 63.7(4) |
| C(14)-C(15)-C(16)-C(17) | -117.9(3) |
| C(15)-C(16)-C(17)-C(23) | -25.7(4) |
| C(15)-C(16)-C(17)-C(18) | -153.2(3) |
| C(23)-C(17)-C(18)-C(19) | -82.0(3) |
| C(16)-C(17)-C(18)-C(19) | 47.6(4) |
| C(3)-C(4)-C(19)-C(20) | -0.8(5) |
| C(5)-C(4)-C(19)-C(20) | 177.3(3) |
| C(3)-C(4)-C(19)-C(18) | -177.8(3) |
| C(5)-C(4)-C(19)-C(18) | 0.3(5) |
| C(17)-C(18)-C(19)-C(4) | 63.9(4) |
| C(17)-C(18)-C(19)-C(20) | -113.1(3) |
| C(4)-C(19)-C(20)-C(21) | 0.8(5) |
| C(18)-C(19)-C(20)-C(21) | 177.9(3) |
| C(4)-C(19)-C(20)-C(38) | -178.8(3) |
| C(18)-C(19)-C(20)-C(38) | -1.7(5) |
| C(3)-C(2)-C(21)-C(20) | 0.2(5) |
| C(1)-C(2)-C(21)-C(20) | 179.7(3) |
| C(3)-C(2)-C(21)-C(22) | 179.8(3) |
| C(1)-C(2)-C(21)-C(22) | -0.7(6) |
| C(19)-C(20)-C(21)-C(2) | -0.5(5) |
| C(38)-C(20)-C(21)-C(2) | 179.1(3) |
| C(19)-C(20)-C(21)-C(22) | 179.9(3) |
| C(38)-C(20)-C(21)-C(22) | -0.4(5) |
| C(5)-C(6)-C(23)-O(1) | 167.1(2) |
| C(7)-C(6)-C(23)-O(1) | -66.0(3) |
| C(5)-C(6)-C(23)-O(2) | 52.3(3) |
| C(7)-C(6)-C(23)-O(2) | 179.1(2) |
| C(5)-C(6)-C(23)-C(17) | -68.9(3) |
| C(7)-C(6)-C(23)-C(17) | 58.0(4) |
| C(18)-C(17)-C(23)-O(1) | -166.6(2) |
| C(16)-C(17)-C(23)-O(1) | 66.2(3) |
| C(18)-C(17)-C(23)-O(2) | -51.2(3) |
| C(16)-C(17)-C(23)-O(2) | -178.5(2) |
| C(18)-C(17)-C(23)-C(6) | 69.1(3) |
| C(16)-C(17)-C(23)-C(6) | -58.2(4) |
| C(4)-C(3)-C(24)-C(25) | -119(12) |
| C(2)-C(3)-C(24)-C(25) | 59(12) |
| C(3)-C(24)-C(25)-C(26) | 90(14) |
| C(24)-C(25)-C(26)-C(31) | 30(9) |
| C(24)-C(25)-C(26)-C(27) | -150(8) |

| | |
|---|---|
| C(31)-C(26)-C(27)-C(28) | -1.4(7) |
| C(25)-C(26)-C(27)-C(28) | 178.4(4) |
| C(26)-C(27)-C(28)-C(29) | 0.6(7) |
| C(27)-C(28)-C(29)-O(3) | -177.5(5) |
| C(27)-C(28)-C(29)-C(30) | 1.1(8) |
| O(3)-C(29)-C(30)-C(31) | 176.8(5) |
| C(28)-C(29)-C(30)-C(31) | -2.0(8) |
| C(29)-C(30)-C(31)-C(26) | 1.2(8) |
| C(27)-C(26)-C(31)-C(30) | 0.5(7) |
| C(25)-C(26)-C(31)-C(30) | -179.3(4) |
| O(3)-C(32)-C(33)-C(34) | 178.9(6) |
| C(32)-C(33)-C(34)-C(35) | -172.0(6) |
| C(33)-C(34)-C(35)-C(36) | 172.0(6) |
| C(34)-C(35)-C(36)-C(37) | -178.8(5) |
| C(19)-C(20)-C(38)-C(39) | -17(100) |
| C(21)-C(20)-C(38)-C(39) | 163(100) |
| C(20)-C(38)-C(39)-C(40) | 90(100) |
| C(38)-C(39)-C(40)-C(45) | -88(21) |
| C(38)-C(39)-C(40)-C(41) | 91(21) |
| C(45)-C(40)-C(41)-C(42) | 0.7(7) |
| C(39)-C(40)-C(41)-C(42) | -178.0(4) |
| C(40)-C(41)-C(42)-C(43) | 0.0(8) |
| C(41)-C(42)-C(43)-O(4) | 179.1(4) |
| C(41)-C(42)-C(43)-C(44) | -0.8(8) |
| O(4)-C(43)-C(44)-C(45) | -179.0(5) |
| C(42)-C(43)-C(44)-C(45) | 0.9(8) |
| C(43)-C(44)-C(45)-C(40) | -0.1(8) |
| C(41)-C(40)-C(45)-C(44) | -0.7(7) |
| C(39)-C(40)-C(45)-C(44) | 178.1(4) |
| O(4)-C(46)-C(47)-C(48) | 166.5(13) |
| C(46)-C(47)-C(48)-C(49) | -179.2(11) |
| C(47)-C(48)-C(49)-C(50) | -173.4(14) |
| C(48)-C(49)-C(50)-C(51) | -70.5(17) |
| C(8)-C(9)-C(52)-C(53) | 12(13) |
| C(10)-C(9)-C(52)-C(53) | -168(13) |
| C(9)-C(52)-C(53)-C(54) | 135(11) |
| C(52)-C(53)-C(54)-C(55) | -156(8) |
| C(52)-C(53)-C(54)-C(59) | 23(9) |
| C(59)-C(54)-C(55)-C(56) | -0.1(6) |
| C(53)-C(54)-C(55)-C(56) | 179.1(4) |
| C(54)-C(55)-C(56)-C(57) | 1.1(7) |
| C(55)-C(56)-C(57)-C(58) | -1.5(7) |
| C(55)-C(56)-C(57)-O(5) | 179.5(4) |
| O(5)-C(57)-C(58)-C(59) | -179.8(4) |
| C(56)-C(57)-C(58)-C(59) | 1.1(7) |
| C(57)-C(58)-C(59)-C(54) | -0.2(7) |

| | |
|---|---|
| C(55)-C(54)-C(59)-C(58) | -0.3(6) |
| C(53)-C(54)-C(59)-C(58) | -179.6(4) |
| O(5)-C(60)-C(61)-C(62) | -174.3(5) |
| C(60)-C(61)-C(62)-C(63) | -175.3(5) |
| C(61)-C(62)-C(63)-C(64) | 173.4(5) |
| C(62)-C(63)-C(64)-C(65) | -178.6(5) |
| C(15)-C(14)-C(66)-C(67) | -19(6) |
| C(13)-C(14)-C(66)-C(67) | 161(6) |
| C(14)-C(66)-C(67)-C(68) | 39(11) |
| C(66)-C(67)-C(68)-C(69) | -10(7) |
| C(66)-C(67)-C(68)-C(73) | 169(6) |
| C(73)-C(68)-C(69)-C(70) | -0.6(7) |
| C(67)-C(68)-C(69)-C(70) | 178.6(4) |
| C(68)-C(69)-C(70)-C(71) | -0.6(8) |
| C(69)-C(70)-C(71)-O(6) | -178.9(5) |
| C(69)-C(70)-C(71)-C(72) | 1.1(8) |
| O(6)-C(71)-C(72)-C(73) | 179.5(4) |
| C(70)-C(71)-C(72)-C(73) | -0.4(7) |
| C(71)-C(72)-C(73)-C(68) | -0.7(6) |
| C(69)-C(68)-C(73)-C(72) | 1.2(6) |
| C(67)-C(68)-C(73)-C(72) | -178.0(3) |
| O(6)-C(74)-C(75)-C(76) | 179.5(4) |
| C(74)-C(75)-C(76)-C(77) | 179.9(4) |
| C(75)-C(76)-C(77)-C(78) | -179.7(4) |
| C(76)-C(77)-C(78)-C(79) | -177.3(4) |
| O(1)-C(80)-C(81)-O(2) | 36.9(4) |
| O(2)-C(23)-O(1)-C(80) | 11.8(3) |
| C(6)-C(23)-O(1)-C(80) | -104.2(3) |
| C(17)-C(23)-O(1)-C(80) | 129.3(3) |
| C(81)-C(80)-O(1)-C(23) | -30.3(3) |
| C(80)-C(81)-O(2)-C(23) | -30.9(4) |
| O(1)-C(23)-O(2)-C(81) | 13.0(3) |
| C(6)-C(23)-O(2)-C(81) | 130.9(3) |
| C(17)-C(23)-O(2)-C(81) | -104.9(3) |
| C(28)-C(29)-O(3)-C(32) | -0.3(9) |
| C(30)-C(29)-O(3)-C(32) | -178.9(6) |
| C(33)-C(32)-O(3)-C(29) | 171.7(5) |
| C(44)-C(43)-O(4)-C(46) | 2.2(9) |
| C(42)-C(43)-O(4)-C(46) | -177.6(6) |
| C(47)-C(46)-O(4)-C(43) | 179.0(6) |
| C(58)-C(57)-O(5)-C(60) | 178.4(5) |
| C(56)-C(57)-O(5)-C(60) | -2.5(7) |
| C(61)-C(60)-O(5)-C(57) | -179.3(4) |
| C(72)-C(71)-O(6)-C(74) | -3.1(7) |
| C(70)-C(71)-O(6)-C(74) | 176.8(4) |
| C(75)-C(74)-O(6)-C(71) | -177.0(4) |

# VITA

## Subodh Prakash Jagtap

Subodh Jagtap was born in Nasik, Maharashtra, India. He attended Institute of Chemical Technology (erstwhile UDCT), University of Mumbai, where he received a Bachelor of Technology (B. Tech) in Paint Technology (Polymer and Surface Coating Division). In 2007, he joined Georgia Institute of Technology pursuing a doctorate degree in polymer chemistry. His research was concentrated on the design and synthesis of π-stacked conjugated oligomers and polymers for organic electronic applications. He was a part of a bioengineering project to develop bioimplants. He defended his thesis in February, 2012. He will be taking a position at The Dow Chemical Company starting from April, 2012. In his spare time, he enjoys watching and playing sports (Cricket, Lawn-Tennis), watching movies, and spending time with his wife, Sayali.